AN INVESTIGATION INTO THE SOURCES, CYCLING AND ATTENUATION OF NITRATE IN AN AGRICULTURAL LOWLAND CATCHMENT USING STABLE ISOTOPES OF NITROGEN AND OXYGEN IN NITRATE

Sarah Katrina Wexler
October 2010

A thesis presented to the School of Environmental Sciences,
University of East Anglia,
in candidate for the degree of Doctor of Philosophy

ABSTRACT

A catchment-scale approach has been used to investigate sources, cycling and attenuation of nitrogen contamination which results in decreasing nitrate concentrations in a river downstream. Analysis of $\delta^{15}N_{NO3}$ and $\delta^{18}O_{NO3}$ from catchment water samples using the denitrifier method, with solute and isotope mass-balance modelling, was employed to characterise the dominant influences which result in high nitrate concentrations seen in the River Wensum, an agricultural lowland catchment with an area of 570 km^2 in East Anglia, eastern England. Nitrate isotopic composition and concentration demonstrate the effects of microbial cycling on source nitrate and riverine nitrogen export. Microbially mediated denitrification is responsible for the trend of decreasing nitrate concentration observed in the river. Primarily occurring in the hyporheic sediments, but also in-stream, denitrification is estimated to remove 883 kg/day of nitrate-nitrogen by the catchment outlet, representing 42% of the potential riverine nitrate load. Estimated removal rates of 372 kg/day and 511 kg/day for the mid and lower Wensum river respectively represent 27% and 25% of the within-reach nitrate-nitrogen load. In the mid Wensum, mass-balance isotope modelling suggests that in-stream removal accounts for up to a quarter of the within-reach reduction in load, while in the lower Wensum a strong influence is seen from denitrification in groundwater-fed lakes adjacent to the river. The nitrate removal via hyporheic and in-stream denitrification provides a natural attenuation mechanism which has significance for environmental regulators, and is an important process for the mitigation of global fixed nitrogen enrichment. At the catchment scale, the solute and isotope mass-balance mixing modelling approach is recommended to characterise the dominant influences on riverine nitrate concentrations and quantify denitrification within the river valley.

ACKNOWLEDGEMENTS

I thank my supervisors Kevin Hiscock and Paul Dennis, for their continued support and advice. Kevin had the belief in me to enable me to study for a PhD, and has been a continued source of encouragement, inspiration ans scientific understanding. My work in the stable isotope lab, overseen by Paul, relied on and his expert knowledge, and his experience, kindness, enthusiasm, and deep scientific insight throughout my project have been invaluable. I also wish to thank the Environment Agency for the CASE sponsorship, and for responding to my numerous data requests.

I thank the technical support staff Lix Claxton, Jenny Stevenson, Kim Wright, Graham Chilvers, Simon Ellis, John Brindle, Rob Utting, Paul Disdale, Emily Sear, Emma Hooper, and Judith Mayne for their help, time, and patience throughout my lab and field work.

I am completely indebted to Alison Bateman, the unsung hero of the stable isotope lab. Without her I doubt the denitrifier method would have ever got off the ground. She was always calm, patient and very wise, and a great pleasure to work with. Thanks area also due to Gareth Lee for help with the microbiology lab work, Jan Kaiser, for advice and hands-on input with setting up the method. I also thank Laura Bristow, Alina Marca and Simon Kelly for working with me in the stable isotope lab, Alex Baker for help with the aerosol sampling, and Tobi Kreuger for advice on modelling. Finally, thank you to Chris Adams, Sian Loveless, and Stuart Vinen for proof reading my chapters.

TABLE OF CONTENTS

Page

LIST OF FIGURES

Page

1. INTRODUCTION

2. STABLE ISOTOPES: THEORY AND APPLICATIONS

3. METHODS

4. RESULTS

5. DISCUSSION

LIST OF TABLES

1. INTRODUCTION

Over the last century there has been dramatic perturbation of the global reactive nitrogen budget which has lead to a doubling of reactive nitrogen in the environment. The amount of reactive nitrogen of anthropogenic origin now equals that derived from natural terrestrial nitrogen fixation, and is predicted to exceed it by 2020 (Figure 1.1) (Millennium Ecosystem Assessment, 2005). The majority of anthropogenic fixation comes from fertiliser production and industrial processes. Inputs from these sources increased sharply after 1960, mainly due to greater ammonia production by the Haber Bosch process. It has been estimated that 100 teragrams (Tg) of nitrogen were fixed in this way in the year 2000, 80% of which was used as agricultural fertiliser (Galloway *et al.*, 2003). This reflects changes over the last 50 years in agricultural practices to increase food production both in response to population increase and for food security. Sources of reactive nitrogen from enhanced biological nitrogen fixation in agriculture and from fossil fuel combustion through both fixation of atmospheric nitrogen during combustion, and the release of sequestered organic nitrogen within the fossil fuel, also increased to 33 Tg and 25 Tg respectively in the year 2000 (Galloway *et al.*, 2003).

Anthropogenic nitrogen fixation results from activities which benefit humankind, from increased food production, to development through access to energy and industrialisation. However, there are problems associated with the accumulation of reactive nitrogen in the environment. These include: enhanced production of ozone in the troposphere which causes respiratory and cardiac disease (Wolfe and Patz, 2002, Galloway *et al.*, 2003); increased production of nitrous oxide, a potent greenhouse gas with high radiative forcing produced from denitrification which is stimulated by the increased availability of reactive nitrogen; destruction, catalyzed by nitrous oxide, of the protective layer of stratospheric ozone, (nitrous oxide has recently been identified as the single most important ozone-depleting emission) (Ravishankara *et al.*, 2009); increased aquatic biomass productivity leading to hypoxia, eutrophication, and a loss of species diversity (Vitousek *et al.*, 1997, Hornung, 1999, Cole *et al.*, 2006); and acidification of terrestrial water bodies from atmospheric deposition of oxides of nitrogen (Vitousek *et al.*, 1997, Driscoll *et al.*, 2001).

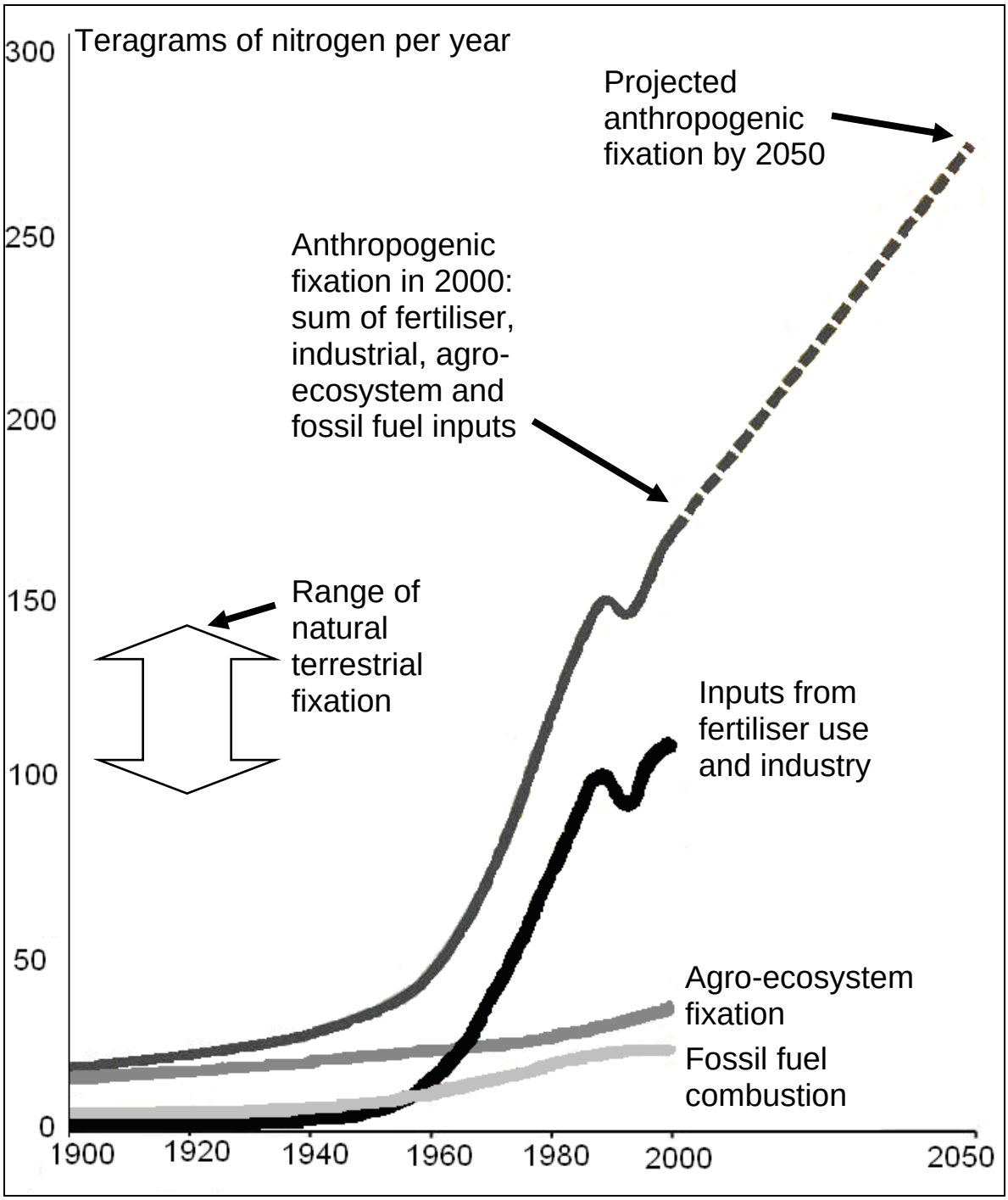

Figure 1.1 Anthropogenically derived reactive nitrogen inputs since 1900 (Tg), showing the range expected from natural terrestrial reactive nitrogen fixed by bacteria. The falling off of anthropogenic fixation in the early 1990s is attributable to a temporary decrease in fertiliser use, mainly in Europe. (Millennium Ecosystem Assessment, 2005, Rekacewicz *et al.*, 2005)

A result of the doubling of reactive nitrogen in the terrestrial environment is the transport of this increased nitrogen loading through the landscape to rivers, and ultimately to the oceans. Green *et al.* (2004) modelled preindustrial and contemporary global nitrogen loading with riverine export using reactive nitrogen load and spatially distributed hydrological attributes in a nutrient flux model and estimated that in Europe, the total loading has increased almost six-fold, from 4.5 Tg per annum to 26.2 Tg per annum. The largest increase from preindustrial to contemporary global riverine nitrogen flux was seen in Europe, North America and southeast Asia (Figure 1.2). However, the mean global percentage of the total terrestrial load exported was 18% (range 0% to 100%), indicating a great capacity for nitrogen transformation, storage, and removal, within the environment before the nitrogen loading reaches the river mouth.

Reactive nitrogen may be transformed through assimilation into biomass, resulting in short-term storage and increased residence time prior to riverine export. Of greater significance to the global reactive nitrogen budget is its removal through denitrification. This is because the majority of reactive nitrogen is returned to the atmosphere in the form of unreactive N_2 gas, although as mentioned above, the small proportion of N_2O produced alongside molecular nitrogen has significant detrimental effects. While some of the removal and storage of reactive nitrogen occurs within the landscape, a significant proportion is thought to occur within rivers and groundwater (Figure 1.3) (Seitzinger *et al.*, 2006). Multiple factors are thought to control the efficiency with which nitrogen is removed from the landscape, and from surface and groundwaters (Wade *et al.*, 2005).

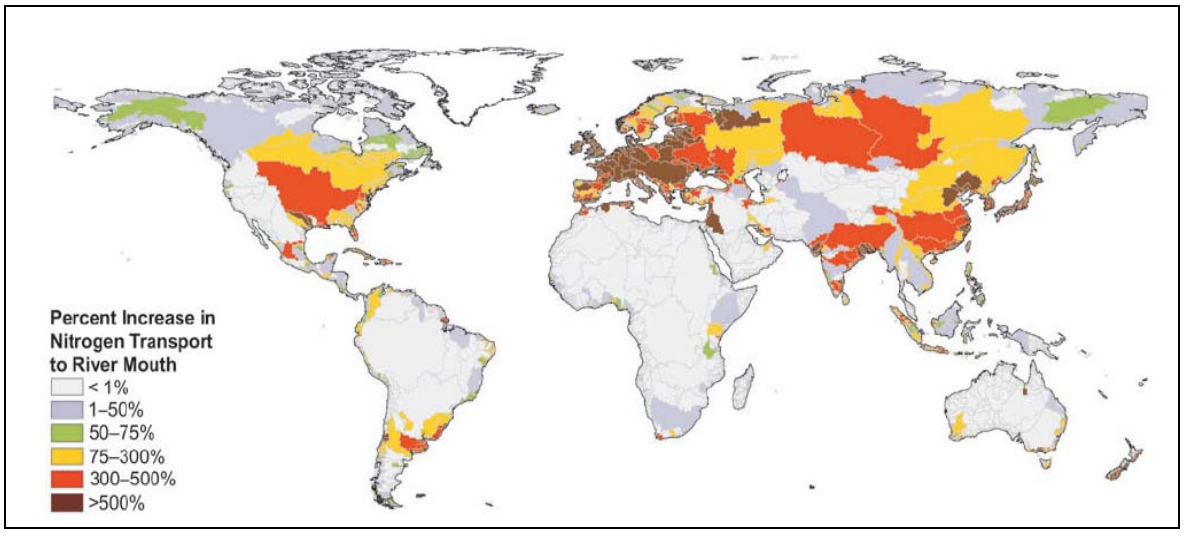

Figure 1.2 Percentage increase of preindustrial to contemporary global riverine total nitrogen flux, showing Europe with over 500% increase (Millennium Ecosystem Assessment, 2005, after Green *et al*, 2004).

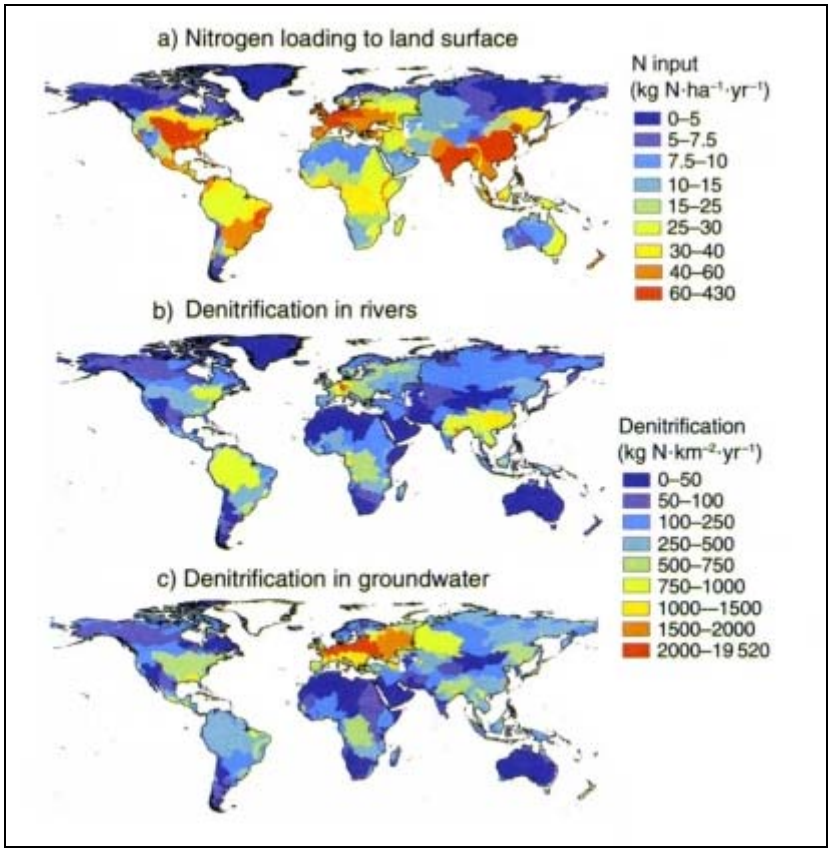

Figure 1.3 a) Nitrogen loading to land surface (kg N/ha/yr) and denitrification (kg N/km^2/yr) in rivers (b) and groundwater (c), from Seitzinger *et al.* (2006).

1.1 RESEARCH AIM AND OBJECTIVES

Aim:

- To identify sources, cycling and removal processes of nitrate contamination in a lowland agricultural river, which cause high concentrations of riverine nitrate that are observed to decrease downstream.

Main Objectives:

- To set up the denitrifier method for the analysis of $\delta^{15}N_{NO3}$ and $\delta^{18}O_{NO3}$ (Sigman *et al.*, 2001, Casciotti *et al.*, 2002), with the denitrifier group in the Stable Isotope Laboratory at UEA for use with freshwater samples.

- To apply the denitrifier method at the catchment scale to characterise the nitrate dynamics in the study river.

Further Objectives:

To investigate:

- Spatial, flow related and seasonal trends in nitrate isotopic composition and concentration at river sampling locations along river reach transects which may correlate to decreasing nitrate concentrations observed in the study river;
- Locations where concentrated sources of nitrate, which may be identifiable through their isotopic composition, enter the river via drainage ditches.

In addition, to identify:

- The nitrate isotopic composition and concentration of groundwater from the Chalk which supplies baseflow to the river;
- Nitrate source isotopic composition in fertiliser, manure, sewage, atmospheric dry deposition and precipitation.

1.2 BACKGROUND

A prerequisite to this study is an understanding of the catchment characteristics and physical parameters which influence the passage of nitrogen through the catchment. A major transport pathway of nitrogen from land to river is the drainage of rainfall through infiltration to the soil, and along shallow flowpaths in the unsaturated and saturated zones, or via drainage ditches to the river. Infiltration also recharges groundwater, which reaches the river as baseflow. Key controls on these processes are the climate, soil type, vegetation, hydrology, hydrogeology and hydrochemistry of the catchment. These are influenced by geology, topography, and geomorphology, and modified by anthropogenic land use. Chapter 1 introduces these key controls and characteristics in the study catchment.

The study location comprises the Wensum catchment in central Norfolk, East Anglia which has an area of 570 km^2 and is drained by The Wensum river which is approximately 75 km long (Figure 1.4). East Anglia is one of the most productive agricultural regions in Britain, and, as such, is particularly prone to problems of diffuse pollution caused by nitrogen fertilisers and manure, as well as sewage effluent, leached soil nitrogen, and atmospheric inputs, which enter the river in runoff and baseflow.

.

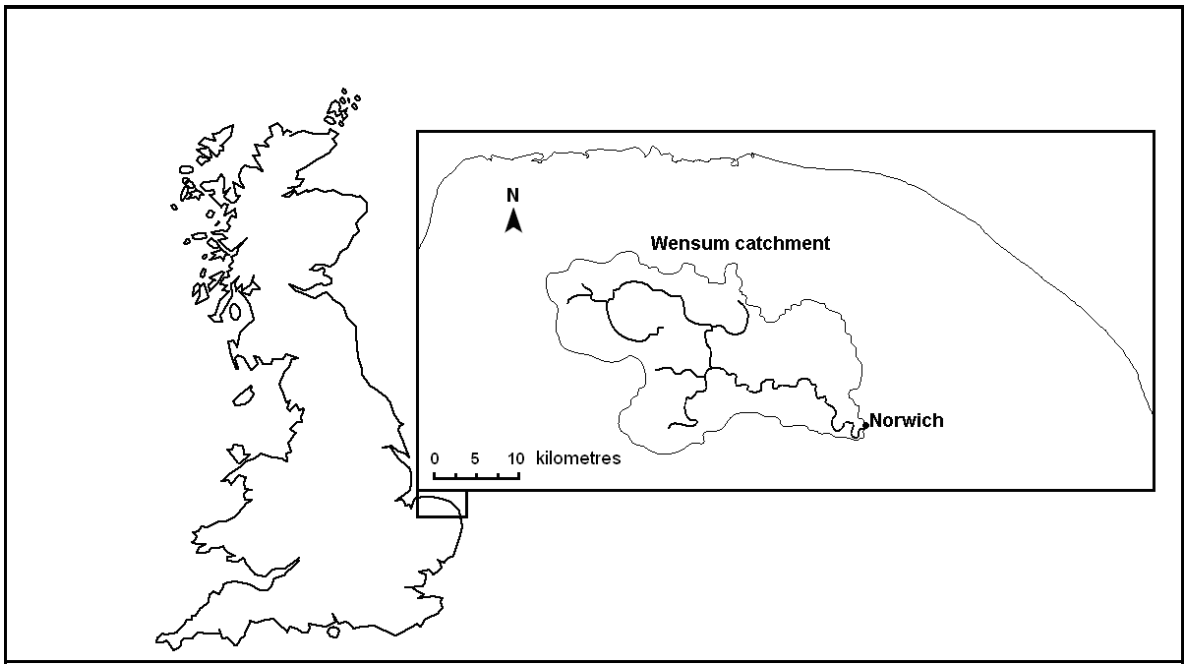

Figure 1.4 Location of Wensum study catchment, Norfolk, East Anglia, UK.

Nitrate contamination has increased with the intensification of agricultural practice and the greater use of fertilisers over the past fifty years. This trend has been particularly marked in East Anglia where the flat terrain in combination with lowland drainage has supported the use of intensive agricultural techniques.

The river Wensum was given whole river Site of Special Scientific Interest (SSSI) status in 1993 as one of the best examples of a naturally-enriched calcareous lowland river, and 381 hectares within the central catchment are designated a Special Area of Conservation. The Wensum converges with the Yare past the city of Norwich and flows into the southern Broads, part of the Broads National Park, a protected wetland habitat and an essential feeding ground for many species of water birds. The catchment falls within the Broadland rivers region of the Anglian River Basin District Management Plan (Environment Agency, 2009a), which aims to improve the ecological, biological and chemical status of rivers, water bodies and groundwater by 2015 in response to the European Water Framework Directive (2000/60/EC: Council of European Communities, 2000), through the implementation of a range of measures including advising and incentivising farmers towards best practice, with potential to increase regulatory controls. Despite its ecological importance and protected status, the Wensum river has high nitrate concentrations, with mean concentrations in the upper

reaches of the river commonly exceeding 35 mg/L nitrate (Environment Agency, 2009b). Although nitrate concentrations are high in the River Wensum, decreasing concentrations are observed downstream, reaching 26 mg/L by the catchment outlet at Costessey (Environment Agency, 2009b).

In addition to the ecological impacts of high nitrate concentration, its presence in recharging groundwater threatens the long-term quality of groundwater reserves for future generations. The nitrate concentration in water for public supply is controlled by legislation and can necessitate costly treatment if concentrations exceed the permissible drinking water limit of 50 mg/L as set out in the EU Drinking Water Directive (98/83/EC: Council of European Communities, 1998). This limit is set using the precautionary principle, due to on-going debate over possible adverse health effects linked to nitrate consumption, including, type one diabetes in children, methaemoglobinaemia in infants, cancer and reproductive effects (Ward *et al.*, 2005). Major public supply boreholes are situated in the catchment, and the river Wensum supplies water for the city of Norwich.

Nitrate is one of the few contaminants to have been legislated for specifically by the European Union, in the Directive of Diffuse Pollution by Nitrates, also known as the EC Nitrates Directive (91/676/EEC: Council of European Communities, 1991). Nitrate pollution is now covered by the European Water Framework Directive (2000/60/EC: Council of European Communities, 2000) which requires that good ecological and chemical status is achieved in surface waters and groundwaters by 2015.

In England, regulation of nitrate contamination falls under the 2008 Nitrate Pollution and Prevention Regulations (Statutory Instrument 2008/2349). The key tool of these regulations is the designation, by Defra, of Nitrate Vulnerable Zones (NVZs), where rules apply concerning measures aimed at reducing agricultural nitrogen loss to water in accordance with the EC Nitrates Directive. The Nitrates Directive uses a concentration of 50 mg/L NO_3^- to identify polluted surface and groundwaters including waters in which concentrations could reach 50 mg/L if preventative action is not taken. The directive also includes lakes, estuaries, coastal waters which are eutrophic or could

become so without preventative action. The first NVZs were designated in 1996 with further areas added in 2002 and 2008 (Defra: Water Quality Division, 2008). Now approximately 70% of the land in England has NVZ designation. The methodology used to identify NVZs was revised by the Environment Agency in 2008 and is based on the monitoring and modelling of water quality. The modelling work included an assessment of the agricultural nitrogen load for catchments in England and Wales, expressed as confidence in predicted water quality, with a quality failure above 50 mg/L NO_3^- (Figure 1.5). This assessment shows a predicted failure in water quality throughout the study area including the Wensum catchment. This appears to be in conflict with the observed decrease in nitrate concentration downstream observed in the River Wensum.

As a result of the revised assessment much of the study area is now a designated NVZ (Figure 1.6). Measures included in the NVZ rules for farmers are a limit on livestock manure nitrogen application of 170 kg/ha/year, the prohibition of the spreading of high-nitrogen-content organic manures and inorganic nitrogen fertiliser for set times per year, and requirements for adequate slurry storage, as well as responsibilities for planning and record keeping (Defra, 2009a). Other initiatives underway in the study catchment aimed at protecting water quality include the English Catchment Sensitive Farming Delivery Initiative which encourages farmers to take action voluntarily to prevent diffuse water pollution (Environment Agency, 2009c), as well as inclusion of nitrogen control measures in the cross-compliance necessary for Single Payment Scheme eligibility (Defra, 2009b).

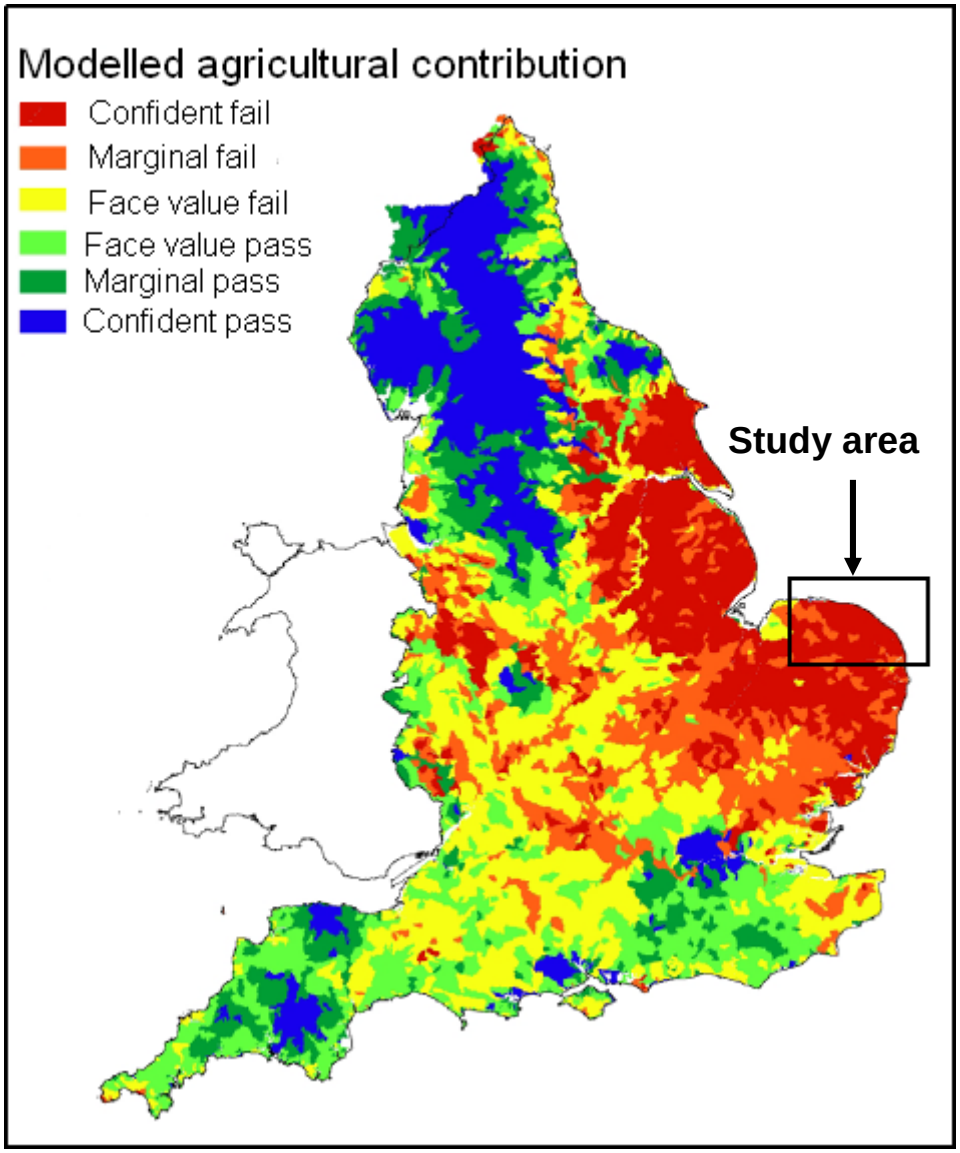

Figure 1.5 Environment Agency model output showing predicted water quality failure due to nitrate concentrations > 50 mg/L from agricultural nitrogen loading, showing study area (adapted from Defra: Water Quality Division, 2008).

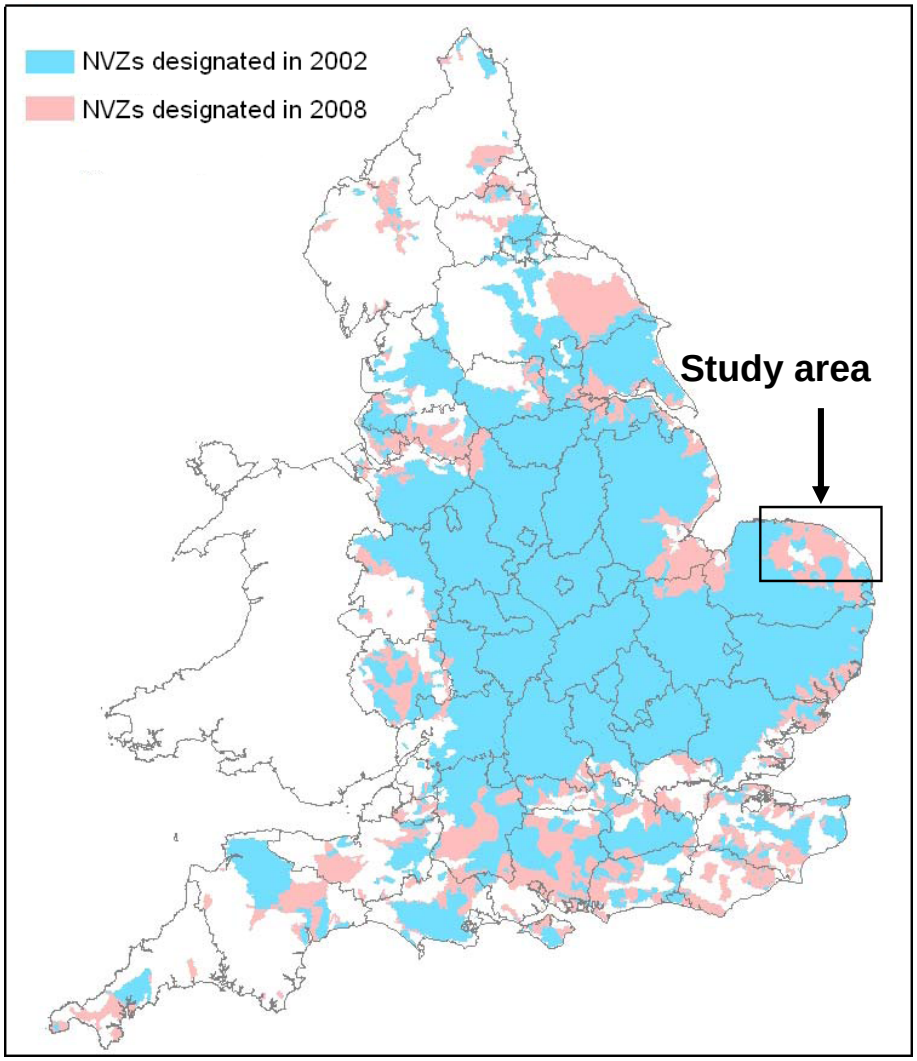

Figure 1.6 Map of NVZ designated areas in England (2002 and 2008) showing study area (adapted from Defra: Water Quality Division, 2008).

1.3 REGIONAL GEOLOGY

The study area is underlain by the Chalk, the dominant solid geology of Norfolk. The Chalk is a white, fine grained, fissured limestone of very high carbonate fraction, deposited during the Upper Cretaceous. The nomenclature used to describe the lithostratigraphy of the Chalk in England has evolved as research has progressed, and is now divided into the Southern Province, the Transitional Province and the Northern Province. Much of East Anglia, including the study catchment, falls within the Transitional Province, with North Norfolk within the Northern Province. The current

nomenclature used by the British Geological Survey is presented in Table 1.1 (Hopson, 2005). The Chalk reaches a thickness of 470 m in east Norfolk, tilting at an angle of approximately 1^{o} east-north-east. The maximum elevation of the Chalk is found near the limit of its western extent, at 95 m above sea level. At Great Yarmouth in the east its minimum elevation is -154 m below sea level (Moorlock *et al.*, 2002). The Chalk is separated unconformably from Lower Cretaceous and Jurassic deposits by Carstone, a ferruginous sandstone, overlain in south Norfolk by the Gault Formation comprising grey mudstones (Arthurton *et al.*, 1994). In east Norfolk the Chalk is overlain by Tertiary deposits comprising the Lower London Tertiaries, which are overlain by the London Clay Formation. The Chalk in much of Norfolk is overlain by unconsolidated Pleistocene sediments including the Crag in eastern Norfolk (Figure 1.7).

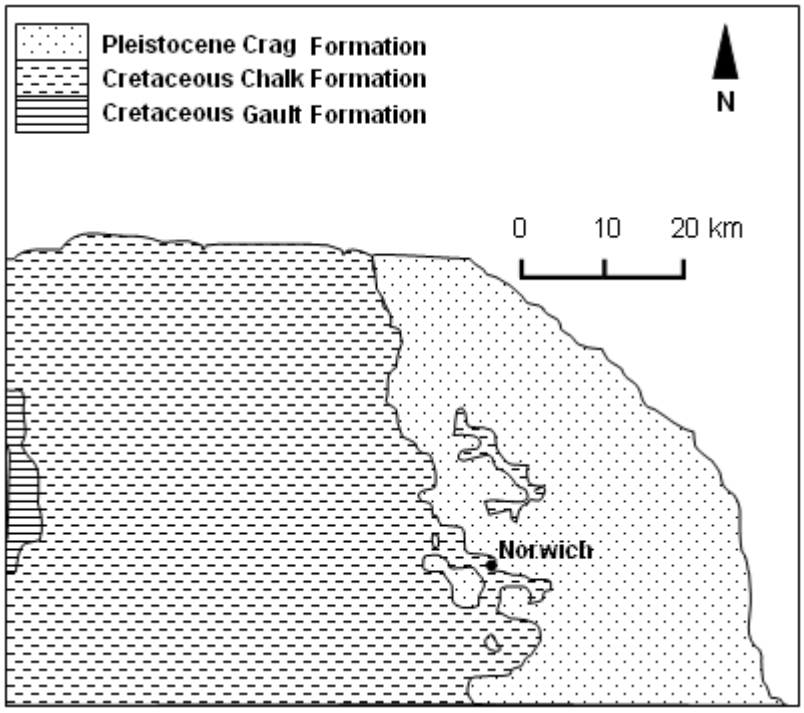

Figure 1.7 Regional solid geology (after Chatwin, 1961).

The early unconsolidated Pleistocene sediments comprise the Crag Group which is made up of non-glacial sediments of interbedded marine gravels, shelly sands, silts and clays (Moorlock *et al.*, 2002). The three members of this group are the Red Crag which marks the beginning of the Quaternary and is coarse grained and poorly sorted with oxidised ferruginous concretions, and the overlying sediments of the Wroxham Crag and the Norwich Crag. The Norwich Crag is finer grained and better sorted than the

Wroxham Crag, which contains more quartz. The Crag is thicker to the east and absent in places near its western extent. Its westerly limit is located just within the Wensum catchment near Norwich. To the east, the Crag is separated from the Chalk by the London Clay Formation. The Crag is overlain in east Norfolk by the Corton Formation, a grey-brown clay rich till with gravel and flint clasts, and in north Norfolk by the Cromer Forest Bed Formation which comprises non-glacial freshwater and estuarine deposits with a high organic content (Arthurton *et al.*, 1994).

Unconsolidated sediments from the mid-Pleistocene form the dominant surface geology of Norfolk comprising two formations formed during the Anglian glaciation. The stratigraphy has recently been revised to comprise The Lowestoft and Overstrand Formations (Moorlock *et al.*, 2000). The former originated during the British Ice Advance and is a calcareous clay with flint, chalk, and limestone clasts previously referred to as the Chalky Boulder Clay. The Lowestoft Till Formation forms a plateau which covers much of East Anglia, reaching thicknesses of up to 40 m, with its southern limit north of London. The Overstrand Formation, limited to north Norfolk, is a non-calcareous sandy brown clay with flint clasts (Moorlock *et al.*, 2002).

These sediments were deposited in the mid Pleistocene during a series of ice advances of Scandinavian and British origins. Subsequent glacial-interglacial cycling created early valley forms from periglacial processes. These gentle valleys are still a feature of Norfolk topography though now dry. Increased fluvial activity in response to warming created sections of river terracing from sediments supplied through slope erosion. The Devensian marks the final glacial stage in Britain, depositing the Holkam Till, a sandy clay with chalk and flint clasts, in north Norfolk. During the Holocene, peats, clays and alluvium were deposited, and soils were formed (Moorlock *et al.*, 2000) (Table 1.1).

Table 1.1 Geological succession of Norfolk (excluding north Norfolk) from the Cretaceous (adapted from Arthurton *et al.*, 1994, Moorlock *et al.*, 2000, , 2002, Hopson, 2005)

Era	Period	Epoch	Stratigraphy	Deposits	Ice advances
Cenozoic	Quaternary	Holocene		Peats, clays, alluvium, coverloam, head, river terrace deposits	Devensian
		Pleistocene	Overstrand Formation	Brown sandy non-calcareous clays with flints	Scandinavian
			Lowestoft Till Formation	Calcareous clay till with chalk clasts and flints	British
			Corton Formation	Grey-brown silty-clayey sand with flints	Scandinavian
			Cromer Forest Bed Formation	Sandy clay with gravel, high organic content	
			Wroxham Crag Formation	High quartz content marine shelly sands, marine and freshwater clays and gravels	
			Norwich Crag Formation	Fine-grained marine shelly sands, marine and freshwater clays and gravels	
			Red Crag Formation	Coarse-grained marine shelly sands, marine and freshwater clays and gravels	
	Tertiary	Palaeogene	London Clay Formation	Fine-grained marine clay	
			Lower London Tertiaries	Marine sands, silts and clays	**Chalk sub-groups**
Mezozoic	Cretaceous		Portsdown Chalk Formation	White chalk with marl seams and flint bands	White Chalk sub-group (previously Upper Chalk)
			Culver Chalk Formation	Soft white chalk with flint seams	
			Newhaven Chalk Formation	Soft to medium-hard white chalk with marl seams and flint bands	
			Seaford Chalk Formation	Firm white chalk with semi-continuous tabular flint seams	
			Lewes Nodular Chalk Formation	Very hard nodular chalk with soft to medium chalks and marls	
			New Pit Chalk Formation	Hard chalk with marl seams and flints	White Chalk sub-group (previously Middle Chalk)
			Holywell Nodular Chalk Formation	Hard nodular chalk with thin marls and shell debris	
			Zig Zag Chalk Formation	Firm grey chalk with marly chalks	Grey Chalk sub-group (previously Lower Chalk)
			West Melbury Marly Chalk Formation	Soft grey marly chalk with hard grey limestone	
			Gault Formation	Grey mudstone	
			Carstone	Ferruginous sandstone	

1.4 HYDROGEOLOGY

The regional hydrogeology of Norfolk is dominated by the Upper Chalk, a major aquifer and a valuable groundwater resource. It has dual porosity due to extensive fracturing and fissuring developed by solutional weathering in the upper 80 - 100 m of the microporous Chalk matrix. Below this, fissuring is less frequent and closed by pressure from the overburden (Hiscock, 2005). The Chalk matrix has a low intrinsic permeability, with its aquifer yield due to the high secondary permeability resulting from the fractures and fissures. The Upper Chalk reaches a thickness of nearly 400 m in the east. In an extensive area of Norfolk the Chalk is overlain by the confining clay-rich Lowestoft Till plateau, the thickness of which affects the potentiometric surface of the Chalk. The Lowestoft Till is thin or absent in west Norfolk, exposing the Chalk in places. It is also absent in north-east Norfolk where the upper stratigraphy comprises the Crag, overlain by glacial clays sands and gravels, with the London Clay Formation to the east, which separates the Crag from the Chalk (Moseley *et al.*, 1976). With its intergranular permeability the Crag is a locally important aquifer in north-east Norfolk.

In the Wensum catchment, the dominant hydrogeology is the Chalk which is mainly confined by the Lowestoft Till in the interfluves (the land between two river valleys) (Figure 1.8). However, there are significant outcrops of Chalk to the west of the catchment and the Chalk in the river valley has been exposed in places by erosion. Recharge to the Chalk in the interfluves is limited by the low permeability of the till, though Toynton (1979) suggested that although a low permeability aquitard, the till may allow recharge to the Chalk through preferential flow channels as a result of its spatially varied thickness and the presence of sandy strata. There are broad, deep areas of glacial sand and gravel deposits surrounding the river channel in the Wensum valley, in hydraulic continuity with the Chalk (Moseley *et al.*, 1976). The westerly most extent of the Crag is located within the catchment to the east, and Crag deposits have also been exposed along the river channel here.

Transmissivity and storativity of the Chalk in Norfolk show a high degree of spatial variation resulting from the distribution of overlying Pleistocene deposits (Hiscock *et*

al., 1996). Where the Chalk is confined under the till, fissuring is poorly developed, resulting in transmissivities of less than 100 m^2/day, whereas where fissuring is more prevalent in the valleys and where the Chalk outcrops transmissivities can reach 2000 m^2/day. Mean transmissivity and storativity of the Chalk in the Wensum catchment have been calculated as 685 $\pm$ 260 m^2/day and 0.064 $\pm$ 0.029 respectively (Toynton, 1979).

The Wensum catchment contains significant groundwater resources and groundwater is licensed for abstraction both at high volume for public supply, and at a smaller scale for uses including business, farming and irrigation, and domestic supply. Based on maximum volumes licensed by the Environment Agency for abstraction, up to 45 million cubic metres of groundwater are abstracted from the Wensum catchment each year.

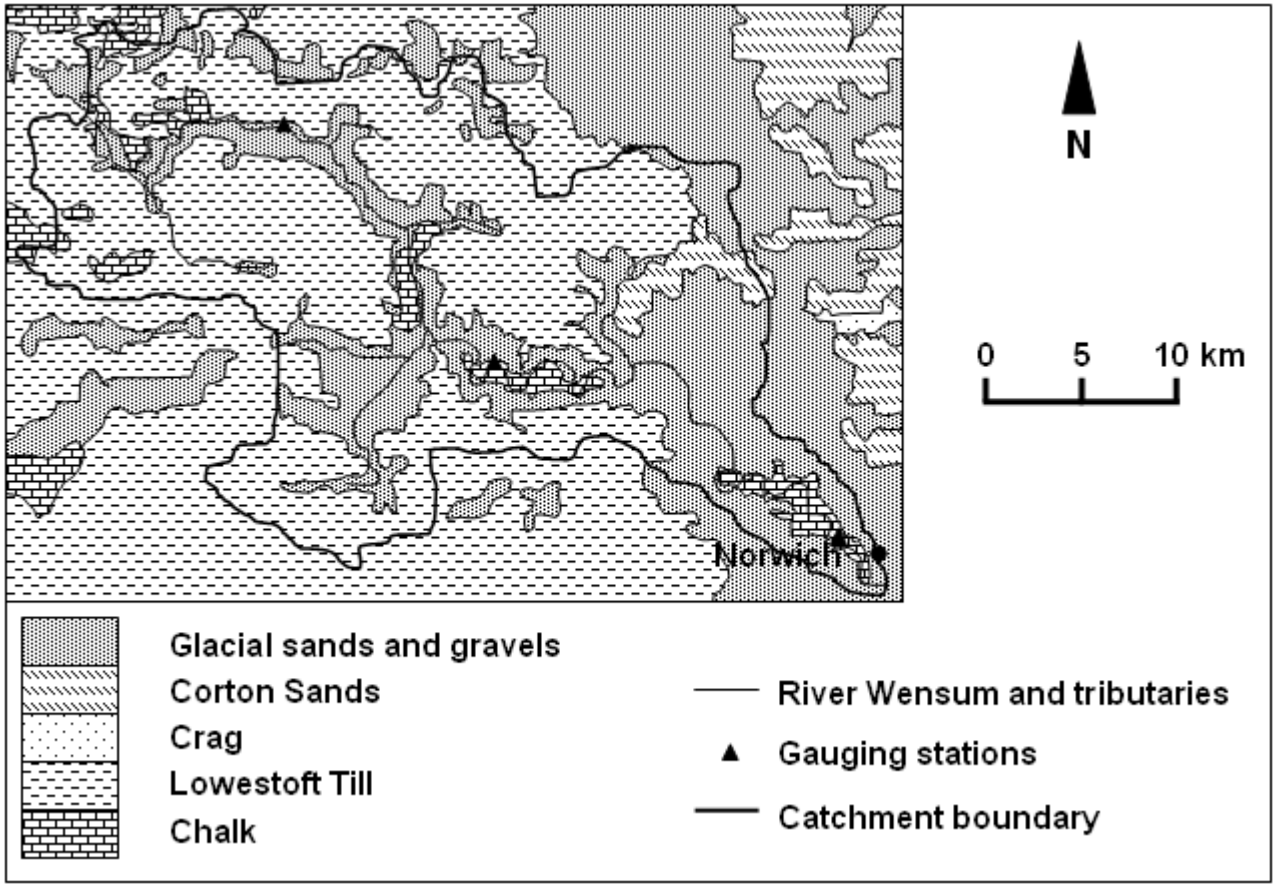

Figure 1.8 Location map showing surface geology of the Wensum catchment (adapted from Moseley *et al.*, 1976).

1.5 HYDROLOGY

A river's baseflow index (BFI) is used as a descriptor of a catchment's characteristics, expressing the proportion of river flow which derives from stored shallow and deep groundwater as opposed to rainfall runoff. It is defined as the ratio of the smoothed minimum mean daily flow to the mean daily flow of the total recorded hydrograph for that river (Shaw, 1994). The Wensum is a meandering lowland river with a high BFI which indicates that a large proportion of its flow is derived from groundwater inputs (Table 1.2). A high BFI supports flow in dry periods, and also implies a reduced range of flow conditions (low flashiness). In addition it suggests that groundwater chemistry will have a strong influence on river water chemistry. The Wensum becomes tidal at Norwich, downstream of the study area. Flooding can occur as a result of heavy rainfall and also due to tidal surges and high tides (Environment Agency, 2006).

There are operational Environment Agency gauging stations on the Wensum at Fakenham, Swanton Morley and Costessey Mill, which marks the downstream limits of the study area (Figure 1.8). The greatest proportional flow increase downstream is seen in the mid river reach, where mean flow increases threefold between Fakenham and Swanton Morley (approximately 25 km), in comparison to a 1.5 fold increase in the lower river reach between Swanton Morley and Costessey (approximately 30 km), (Table 1.2). The baseflow index decreases slightly from the upper catchment to the catchment outlet, indicating an increasing proportion of surface accretion.

There are ten wastewater treatment plants in the catchment (Figure 1.9). Two major sources of effluent discharge occur from the works at Fakenham on the upper river, and at East Dereham in the southern catchment (via the Wendling Beck tributary which converges with the Wensum before Swanton Morley). The works at Fakenham are licensed to discharge effluent for a population equivalent of 13 493, at a rate of 180 litres per capita per day, which gives an effluent discharge of 0.028 $m^3 s^{-1}$, or 3.2% of the mean river flow at Fakenham (Table 1.2). The discharge licence at East Dereham represents an effluent discharge of 0.036 $m^3 s^{-1}$, or 1.4 % of the mean river flow at Swanton Morley. The other wastewater sources are minor sewage treatment works of the smaller towns and villages which release treated effluent into the rivers. In addition

rural dwellings are often served by septic tank systems which may leak septic effluent which reaches the river network.

Significant volumes of groundwater and surface water are abstracted in the catchment (Table 1.2). Major abstraction licences for public supply are held by Anglian water for groundwater abstraction and surface water abstraction from the river at Costessey pits, just beyond the gauging station at Costessey Mill. The majority of abstraction licences are for smaller volumes, used for domestic supply and spray irrigation.

Table 1.2 Flow data, discharges and abstractions for the Wensum catchment with flow data for specific Environment Agency gauging stations on the River Wensum (Entec, 2007, Marsh and Hannaford, 2008, Centre for Ecology and Hydrology, 2009, Environment Agency, 2009d, Environment Agency, 2009e).

Catchment	**Wensum**		
Gauging station	**Fakenham 34011 (TF 919294)**	**Swanton Morley 34014 (TG 020184)**	**Costessey Mill 34004 (TG 177128)**
Catchment area (km^2)	162	398	571
Mean flow ($m^3 s^{-1}$)	0.87	2.64	4.04
Base Flow Index (BFI)	0.83	0.75	0.74
Effluent volume[a] ($m^3 s^{-1}$)	0.028	0.036	-
Groundwater abstractions (Ml/d)	33.0[b]		
Surface water abstractions (Ml/d)	46.4[b]		

[a] Effluent discharge volumes are calculated based on the population served by the wastewater works, with each person producing 180 litres of effluent per day.
[b] Abstractions for the Wensum catchment are estimated from long-term averages 1970-2003

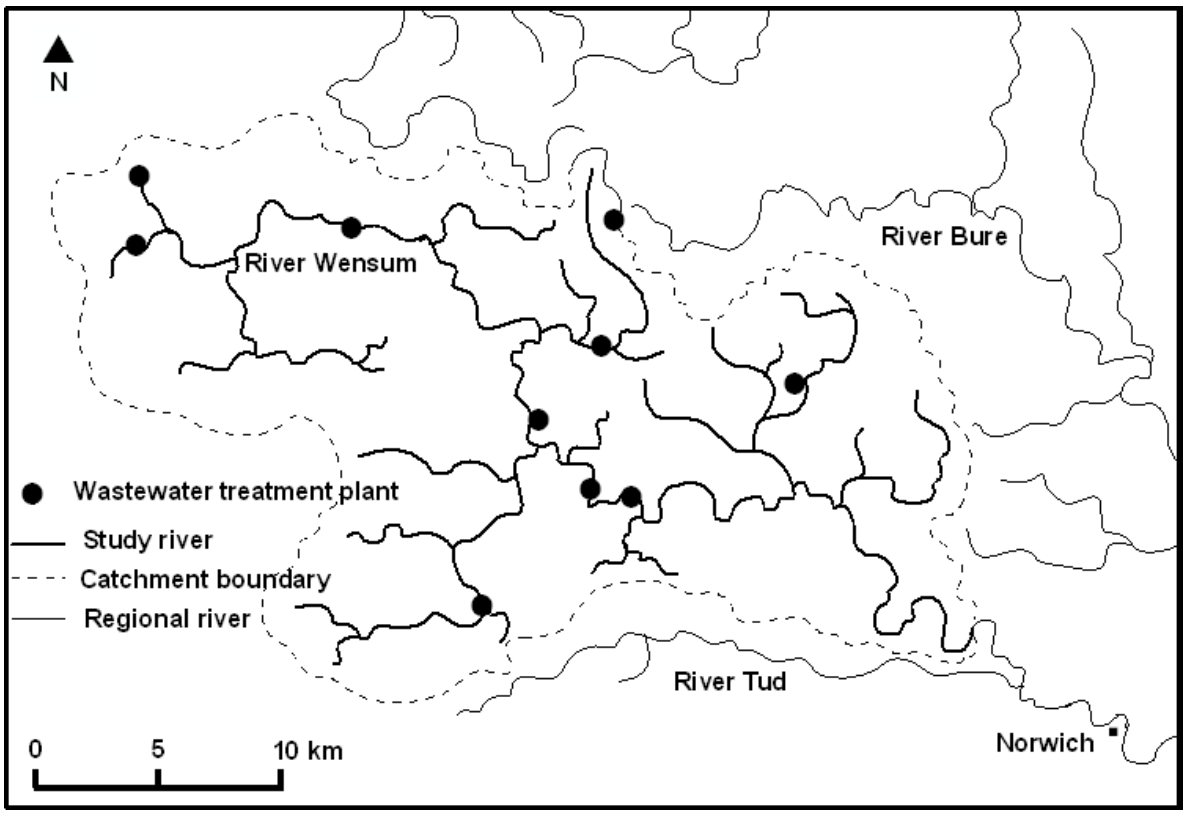

Figure 1.9 Location of wastewater treatment plants in the Wensum catchment.

The Wensum valley contains significant gravel deposits and series of groundwater-fed lakes have been created from disused gravel pits adjacent to the river, with two networks of lakes located in the mid river between Fakenham and Swanton gauging stations, and a further three networks in the lower river between Swanton and Costessey Mill gauging stations. These are mostly now used for recreational fishing.

1.6 HYDROCHEMISTRY

The hydrochemistry of the Wensum catchment is influenced by the Chalk, resulting in Ca-HCO_3 dominated catchment waters of neutral pH. An investigation into major ion concentrations at the river Wensum catchment outlet (Edwards, 1973), found a large range in concentrations of nitrate and sulphate which correlated positively with flow, showing higher concentrations with higher flows and a mean value of 22 mg/L nitrate with a range of 13 to 43 mg/L (Table 1.3). Nitrate concentrations in the Chalk groundwater have a high degree of spatial variability, ranging from below the limit of detection to 62 mg/L at different locations (Hiscock, 1993). Riverine concentrations of nitrate, sodium, potassium, calcium, chloride, bicarbonate, and sulphate are

encompassed by the greater ranges found in Chalk groundwater in Norfolk, while riverine concentrations of magnesium and silica can be below the range normally found in Chalk groundwater. The high degree of spatial variability in solute concentrations in the Chalk has been attributed to the age of the groundwater and the permeability and distribution of different overlying deposits (Hiscock, 1993). Groundwater from the Norfolk Chalk in the river valleys which is exposed or overlain by a thin layer of permeable deposits, has been found to have high concentrations of nitrate, while the Chalk on the interfluves has nitrate concentrations below the limit of detection (Hiscock, 1993).

Table 1.3 Major ion concentrations (mg/L) of the Wensum river at the catchment outlet sampled under baseflow and highflow conditions, and Chalk groundwater in Norfolk (from Edwards, 1973, Hiscock, 1993).

	Wensum river		**The Chalk**
Major ion	**Concentration range (mg/L)**	**Mean concentration (mg/L)**	**Concentration range (mg/L)**
Na^+	29 - 36	33	18 - 93
K^+	4.2 - 5.0	3.8	1.4 - 15.8
Ca^+	110 - 140	130	70 - 175
Mg^{2+}	2.5 - 6.7	4.5	4.6 - 15.9
Si	0.7 - 6.3	3.3	4.5 - 10.3
Cl^-	33 - 57	42	24 - 149
HCO_3^-	243 - 320	290	211 - 449
NO_3^-	13 - 43	22	0 - 62
SO_4^{2-}	36 - 102	48	4 - 133

1.7 CLIMATE

East Anglia is one of the driest counties in Britain. Annual rainfall statistics from the UK Met Office for East Anglia 1961-1990 show an average rainfall of 601 mm per annum, with 114 days a year of rainfall exceeding 1 mm (Met Office, 2009). Most rain falls from October to December, with these statistics showing anomalously low rainfall in February, and fairly high rainfall maintained through the summer months. The 30-year average of annual sunshine hours is 1499 hours, which is towards the higher end of the range for Britain. Mean monthly minimum temperatures are lowest in January and February (0.6 0^oC), and July and August have the highest mean monthly maximum temperatures (21.1 0^oC). There are, on average 51 days of air frost a year.

Catchment-specific annual average rainfall statistics (1961-1990) show that the Wensum catchment has a slightly higher 30-year average than the East Anglian mean, receiving 672 mm of rainfall (Centre for Ecology and Hydrology, 2009). Average groundwater recharge, as effective rainfall to the East Anglian region is around 140 mm per year (Yusoff *et al.,* 2002), though recharge to exposed Chalk may be higher, but considerably lower where there are overlying clay-rich deposits.

1.8 TOPOGRAPHY AND GEOMORPHOLOGY

The topography of Norfolk is gently undulating with elevation rarely reaching 100 metres above sea level. The highest elevations are to the north and west of the Wensum catchment. As a result of the low relief the Wensum river has a low channel gradient (< 0.001) and has relatively low energy. The river has a locally stepped bed profile arising from numerous hydraulic controls in the form of mills and weirs. River bed substrates are mostly stable and in usual flow conditions the rivers do not mobilise an active gravel supply (Sear *et al.,* 2006). However, fine sediments from field and drainage ditch erosion accumulate in the gravels of the riverbed.

1.9 SOIL

The predominant soil type in the study catchment is loam, which is particularly suitable for arable farming of cereals, sugar beet, potatoes and vegetables (Mackney *et al.*, 1983). Loam soils provide optimal moisture retention and drainage, avoiding waterlogging due to the balance of sand silt and clay fractions in the soil. However, drainage may be affected by the depth of the loam, the permeability of subsoils, and the height of the watertable. Soil drainage affects nutrient retention time, so uptake potential by plants and soil biota, and speed of leaching. Low permeability subsoils may bring about shallow lateral flowpaths, while water-logging may allow localised denitrification to occur in temporary anaerobic conditions. The study catchment soils are of mixed fertility and are usually amended with fertilisers.

The soils of the Wensum catchment comprise freely draining loams in the north west of the catchment, with an increasing clay fraction and poorer permeability in the central catchment and interfluves, and well drained sandy soils in the lower catchment. The

upper river valley soils are quick draining loam with sand, giving way to peat soils which are close to the water table in the lower river valley (National Soil Resources Institute, 2009) (Table 1.4).

Table 1.4 Soil characteristics of the study catchments (adapted from National Soil Resources Institute, 2009)

Wensum catchment	**Soil Characteristics**
Area:	
North west upper catchment	Freely draining, slightly acid loamy and sandy soils.
Central catchment north and south	Slightly acid loamy and clayey soils with impeded drainage.
North and south interfluves	Slowly permeable seasonally wet slightly acid but base-rich loamy and clayey soils.
Lower catchment north and south	Freely draining slightly acid sandy soils with low fertility.
River valley (upper and mid)	Loamy and sandy soils with naturally high groundwater and a peaty surface.
River valley (lower)	Fen peat soils with naturally high groundwater.

1.10 LAND USE

East Anglia contains some of England's best agricultural land resulting from the loam soils and a gentle topography. The study river passes through farmland so is directly impacted by agricultural activity. The Agricultural and Horticultural Census for 2005 recorded that over 85% of land in Norfolk was being used for farming (Defra, 2006). Of this 66% was used for growing crops or left fallow. Cereal crop cultivation was the largest single land use category, followed by sugar beet and oil seed rape, horticulture and potatoes, while livestock, dairy, pig and poultry operations together also represented almost 22% of farms.

Within the study area there are several small towns, the largest of which is Dereham with a population of approximately 17 000 (Office for National Statistics, 2005). In addition to these towns there are numerous villages and isolated rural dwellings, connected by a road network which is drained to the river via drainage ditches.

1.11 SUMMARY

In summary, the anthropogenic perturbation of the global reactive nitrogen budget has lead to a doubling of reactive nitrogen in the environment, which has resulted in a host of effects, from increased greenhouse gas emissions to a loss of species diversity. This research, which aims to identify sources and removal processes of nitrogen contamination in a river draining a lowland agricultural catchment, can form the basis for a monitoring tool with which to evaluate the success of regulatory measures, as well as providing insights into nitrogen transport and removal processes, which in turn can inform the development of future control measures. The ecologically sensitive catchment drained by the River Wensum is impacted by the high degree of agricultural land use, much of which is put to arable farming, and the discharge of effluent from wastewater treatment works, which together result in high nitrate concentrations in the Wensum river, although the observed decrease in nitrate concentration in the river downstream conflicts with a predicted failure in water quality modelled for the study area. Due to the gentle topography in the catchment and the distribution of permeable soils, rainfall may lead to the leaching of nitrate in runoff. Whether this runoff reaches the river or recharges groundwater will be influenced by the distribution of geological strata within the catchment, in particular, the low permeability Lowestoft Till Formation. In this baseflow dominated river, the hydrochemistry of the Chalk groundwater supporting flow will influence riverine hydrochemistry, including the concentration and isotopic composition of nitrate.

1.12 THESIS OUTLINE

This chapter introduces the key controls and characteristics of the study catchment. Chapter 2 presents stable isotope theory and its application to the nitrogen cycle and nitrate source identification, and discusses catchment case studies where the nitrate dual-isotope method has been used, drawing conclusions which are relevant to this research design. Chapter 3 gives an account of the research design and methods, including the set up the denitrifier method (Sigman *et al.*, 2001, Casciotti *et al.*, 2002) and method development experiments. Chapter 4 presents results of isotopic and hydrochemical and analysis of samples collected in the Wensum catchment. Chapter 5 presents the discussion and interpretation of the results. Conclusions are presented in Chapter 6.

2. STABLE ISOTOPES: THEORY AND APPLICATIONS

2.1 STABLE ISOTOPE THEORY

2.1.1 Stable Isotope Ratios

Isotopes are atoms of a particular element which are differentiated by their atomic mass due to the fact that they have the same number of protons but a different number of neutrons in their nuclei. Stable isotopes are those which do not undergo radioactive decay. In the natural environment the lightest isotope is usually the super-abundant form while heavier isotopes of the same element, with one or more extra neutrons, are rare in comparison. Nitrogen has two stable isotopes: the lighter, super-abundant ^{14}N (with a nucleus comprising seven protons and seven neutrons); and the heavier, rarer ^{15}N (with a nucleus comprising seven protons and eight neutrons). The natural abundances of these two isotopes in air, expressed as percentages are ^{14}N: 99.636 %, ^{15}N: 0.364 % (De Laeter *et al.*, 2003). Oxygen has three stable isotopes ^{16}O, ^{17}O and ^{18}O, each with eight protons and eight, nine and ten neutrons respectively in their nuclei. Their natural abundances in ocean water are ^{16}O: 99.757 %, ^{17}O: 0.038 %, ^{18}O: 0.205 % (De Laeter *et al.*, 2003). Stable isotope ratios of bulk elements are measured using isotope ratio mass spectrometers (IRMS). Isotope ratios are defined as the ratio of the heavy isotope to the light isotope, relative to the isotope standard, which for nitrogen is Air and for oxygen is Vienna Standard Mean Ocean Water (VSMOW). Isotope ratios are expressed in delta (δ) notation. δ is expressed according to the recent recommendations from the International Union of Pure and Applied Chemistry Inorganic Chemistry Division Commission on Isotopic Abundances and Atomic Weights (IUPAC) (Coplen, 2008) as:

$$\delta = \frac{\left(R_{Sample}\right)}{\left(R_{S\tan dard}\right)} - 1 \qquad \text{Equation 2.1}$$

where R is the ratio of the heavy to the light isotope in the sample and the standard.

δ values are reported in parts per thousand denoted by the permil (‰) sign, so δ values are multiplied by 1000. The δ value of the standard is zero, so a positive δ value shows

that the sample has more of the rare heavy isotope than the standard, and a negative δ value indicates that the sample has less of the heavy isotope than the standard. In this thesis negative δ values are expressed with a negative sign (-), and positive values have no sign. In order to compare environmental samples with each other, capital Δ can be used to describe absolute differences in isotopic composition. For example, the difference in isotopic composition of two nitrate compounds with $\delta^{15}N_{NO3}$ -5 ‰ and $\delta^{15}N_{NO3}$ 5‰ can be expressed as $\Delta^{15}N = 10$ ‰.

2.1.2 Stable Isotope Fractionation

2.1.2.1 Mass Dependent Effects and Equilibrium and Kinetic Fractionation

Due to the difference in the number of neutrons in their nuclei, isotopes of the same element have different atomic masses. This can give rise to physiochemical isotope effects, meaning that, for example molecules containing heavy isotopes may have different physical properties (e.g. density, temperature, boiling and melting points, vapour pressure and viscosity) to those containing light isotopes of the same element. This can result in mass-dependent equilibrium fractionation which preferentially partitions molecules containing heavy or light isotopes into different phases (Hoefs, 2004). As the thermodynamic properties of an atom depend upon its mass, isotopes have different thermodynamic thresholds resulting from their different vibrational frequencies in the ground state (at 0 K). Heavier isotopes have a lower vibrational frequency which results in a lower zero point energy than their isotopically lighter counterparts. This means that chemical bonds involving heavier isotopes are marginally stronger than those involving lighter isotopes.

Isotopic fractionation occurs as a result of both equilibrium and kinetic processes (Hoefs, 2004). In equilibrium fractionation the process is controlled by the Gibbs free energy change of the isotope exchange reaction, expressed by the equilibrium fractionation factor. The equilibrium fractionation factor (α) is equal to the equilibrium rate constant $K_{eqb,}$ and controlled by the Gibbs free energy change in the relationship:

$$\alpha = K_{eq} = e^{(-\Delta G/RT)} \qquad \text{Equation 2.2}$$

where ΔG is the Gibbs free energy change of the isotope exchange reaction, R is the universal gas constant, and T is absolute temperature.

For an equilibrium exchange reaction A ↔ B, the equilibrium fractionation factor $\alpha_{a\text{-}b}$ can be expressed:

$$\alpha_{a\text{-}b} = R_A / R_B \qquad \text{Equation 2.3}$$

where R_A and R_B are the isotope ratios of the partitions A and B (Coplen *et al.,* 2000).

Kinetic effects result from faster reaction rates associated with molecules containing the lighter isotopes. Non-equilibrium mass-dependent kinetic fractionation is caused by this propensity of isotopes to react at slightly different rates, and supports the preferential uptake of one isotope over the other during irreversible one-way biological processes, resulting in isotopic fractionation. The majority of fractionating processes affecting the isotopes of nitrate are biologically mediated kinetic fractionations, and are influenced by parameters which control the mediating organism's activity, such as Eh, temperature, pH and moisture, as well as the concentration of the substrate and reaction rates.

The kinetic fractionation factor of the product with respect to the reactant substrate ($\alpha_{P\text{-}S}$) is expressed as:

$$\alpha_{P\text{-}S} = R_P / R_S \qquad \text{Equation 2.4}$$

where R_P refers to the isotope ratio of the newly formed product form, and R_S is that of the residual substrate (Kendall, 1998).

Gibbs free energy change associated with isotopic fractionation is typically in the order of a few Joules/mol. Therefore, in general, α has a value close to 1. A more convenient way of expressing fractionation is in the deviation of α from 1 which is expressed as the isotope enrichment factor (ε), defined as:

$$\varepsilon = \alpha - 1 \qquad \text{Equation 2.5}$$

ε values are reported in parts per thousand, denoted by the permil (‰) sign. For kinetic fractionation, subscripts are used to clarify that the enrichment factor refers to the isotopic enrichment of the product with respect to the substrate ($\varepsilon_{P\text{-}S}$). If $\varepsilon > 0$ it shows enrichment of the heavy isotope in the product with respect to the substrate. Conversely if $\varepsilon < 0$ it represents depletion of the heavy isotope relative to the substrate (Kendall, 1998). Equilibrium and kinetic isotopic fractionation can be modelled using Rayleigh equations.

2.1.2.2 Rayleigh Fractionation

As fractionation proceeds the fractionation of the residual substrate increases in an exponential relationship. If all the reactant is used up, the eventual isotopic composition of the final product is the same as that of the original substrate. Progressive fractionation is described by Rayleigh equations which were developed to describe unidirectional first-order reactions in well mixed systems, with the fractionation occurring under a constant fractionation factor. Under these conditions the isotopic composition of the product evolves in parallel to that of the substrate. Kinetic fractionation is not in fact in equilibrium, but if back reactions do not occur and there is a finite reservoir of the compound a Rayleigh equation can be used to describe it (Mariotti *et al.*, 1988):

$$\delta_S = \delta_{S0} + \varepsilon_{P\text{-}S} \times \ln (C/C_0) \qquad \text{Equation 2.6}$$

where δ_S refers to the isotopic composition of the substrate at time t, δ_{S0} refers to the initial isotopic composition of the substrate, C is the concentration of the substrate at time t, C_0 is the original concentration and ε is the isotope enrichment factor. This Rayleigh equation has been used to characterise denitrification in terrestrial water (Mariotti *et al.*, 1988, Cey *et al.*, 1999, Fukada *et al.*, 2004, Deutsch *et al.*, 2005).

2.1.2.3 Fractionation in the Nitrogen Cycle

The nitrogen cycle enables this essential nutrient to be removed from air for incorporation into the amino acids of living organisms. Atmospheric nitrogen is fixed by microorganisms including bacteria, fungi and archaea, which convert it using the nitrogenase enzyme to ammonia for incorporation into organic molecules.

Anthropogenic fixation of atmospheric nitrogen now exceeds microbial fixation (Galloway *et al.*, 2003). Industrially fixed nitrogen is primarily used for the production of fertilisers, and enhanced fixation during crop cultivation can also be considered an anthropogenic fixation pathway. In addition to these sources a small amount of nitrogen is fixed by lightening (Drapcho *et al.*, 1983). Fixed nitrogen is cycled through living and dead biomass, in organic and inorganic forms. Nitrogen in dead biomass is made available once more for assimilation by living organisms through remineralisation of organic-N to ammonium. Some of this ammonium may instead undergo oxidation via nitrification to produce nitrite and nitrate. Nitrogen is returned to the atmosphere when nitrate undergoes stepwise reduction during microbial denitrification producing molecular nitrogen and a very small amount of nitrous oxide. All steps of the nitrogen cycle occur in the terrestrial biosphere including aquatic environments, and are mediated by microorganisms mostly living in soil and sediments. Alongside the cycling of nitrogen originating from microbially mediated fixation in the terrestrial biosphere, is the cycling of nitrogen inputs from other sources, including artificial fertiliser, atmospheric deposition and precipitation, as well as concentrated sources of nitrogen in manure and sewage. The various stages in the nitrogen cycle cause isotopic fractionation of varying magnitudes. In order for isotopic fractionation to be apparent in the isotopic composition of remaining substrate pool, it must be well mixed. As a result of the variety of parameters affecting fractionation in natural environments, fractionation factors for particular processes show variation, especially where fractionation is significant (Figure 2.1; Table 2.1).

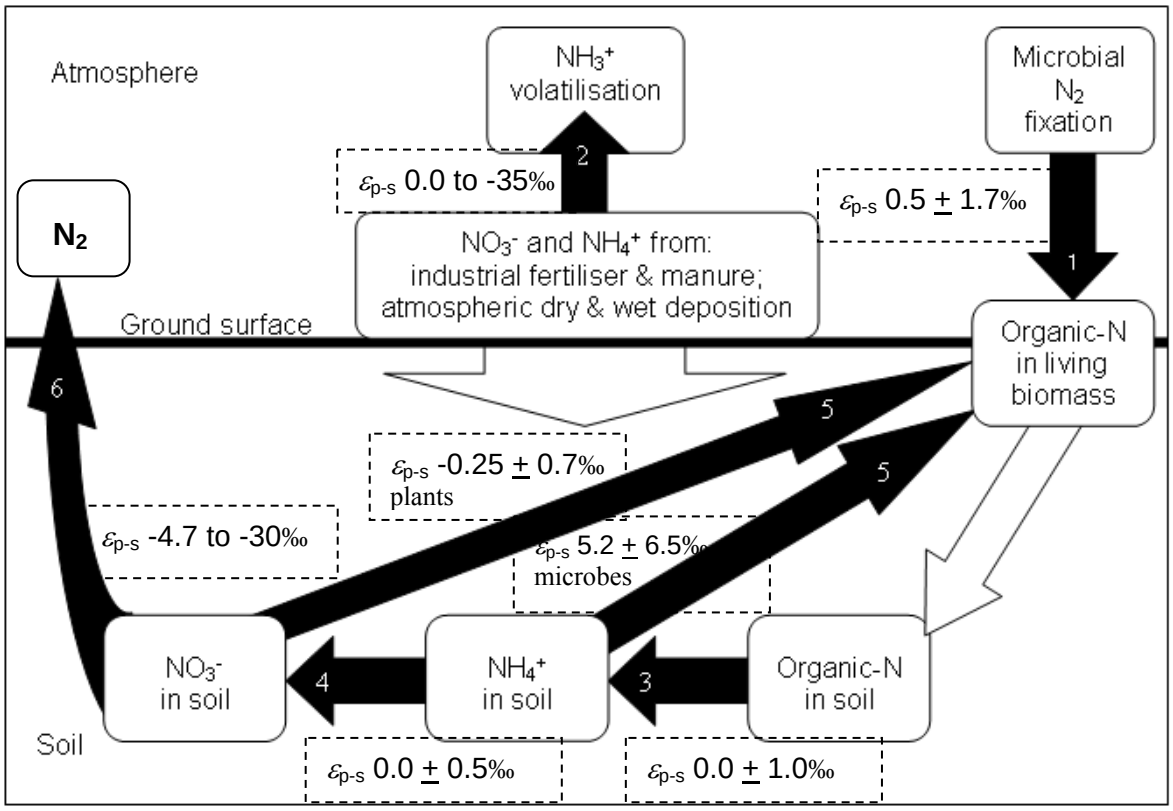

Figure 2.1 Simplified representation of the nitrogen cycle. Black numbered arrows indicate processes which incur isotopic fractionation: 1 microbial N_2 fixation; 2 ammonia volatilisation; 3 mineralisation of soil organic nitrogen; 4 nitrification; 5 nitrate and ammonium assimilation by plants and micro-organisms; 6 denitrification. Process numbers correspond to Table 2.1 and explanatory text below. Nitrogen isotope enrichment factors associated with each fractionating process are included in boxes.

Table 2.1 Ranges of ^{15}N isotope enrichment factors ($\varepsilon_{P\text{-}S}$ ‰) for isotopically fractionating processes in the nitrogen cycle. Numbers correlate to arrows depicting processes in Figure 2.1. Note that the enrichment factor subscript ($_{P\text{-}S}$) refers to the isotopic enrichment of the product with respect to the substrate. For clarity the product and substrate nitrogen species are included in the table. (Sources: Delwiche and Steyn, 1970, Fegin *et al.*, 1974, Mariotti *et al.*, 1980, Mariotti *et al.*, 1981, Vogel *et al.*, 1981, Heaton, 1986, Hubner, 1986, Mariotti *et al.*, 1988, Hogberg, 1997, Deutsch *et al.*, 2005, Kendall *et al.*, 2007).

Process	**Isotope enrichment factor $\varepsilon_{P\text{-}S}$ ‰**	**Product (P)**	**Substrate (S)**
1. Fixation of N_2 (microbial)	0.5 ± 1.7	organic N	atmospheric N_2
2. Volatilisation of NH_3^+	0.0 to - 35	$NH_3^+{}_{(gas)}$	$NH_4^+{}_{(aq)}$
3. Mineralisation of soil organic nitrogen	0.0 ± 1.0	NH_4^+	organic N
4. Nitrification (bacterial): NH_4^+ limited Nitrification (bacterial): NH_4^+ abundant	0.0 ± 0.5 - 14 to - 35	NO_3^-	NH_4^+
5. Assimilation: plants Assimilation: microbial	- 0.25 ± 0.7 5.2 ± 6.5	organic N	NH_4^+ and NO_3^-
6. Denitrification	- 4.7 to - 30	N_2 (N_2O)	NO_3^-

Investigations into isotopic fractionation factors associated with different processes in the nitrogen cycle have determined that some processes incur negligible fractionation, while others lead to a significant level of isotope fractionation.

1. Fixation:

Microbially-mediated nitrogen fixation produces a slight isotopic fractionation which oscillates around zero (Fogel and Cifuentes, 1993, Hogberg, 1997). A review by Hubner (1986) found $\varepsilon_{P\text{-}S}$ 0.5 $\pm$ 1.7 ‰ (n = 24) in studies of nitrogen fixation by azotobacter and various legumes. In terms of quantity, microbially mediated nitrogen fixation is matched by anthropogenic fixation of atmospheric nitrogen, for example for use as agricultural fertilisers. The industrial production of ammonium involves near quantitative conversion so produces ammonium with an isotopic composition close to zero (Heaton, 1986). Urea and nitrate are the other main nitrogen species produced industrially for fertilizers. A review of nitrogen fertilizer isotopic composition (Hubner, 1986) found mean values of $\delta^{15}N_{NH4+}$ - 0.9 $\pm$ 1.9 ‰ (n = 39) for ammonium fertilizer, with a similarly narrow range for industrially-produced urea ($\delta^{15}N_{NH4+}$ 0.2 $\pm$ 1.3 ‰ n = 8), and a slightly broader range for nitrate fertilizer ($\delta^{15}N_{NO3}$ 2.8 $\pm$ 1.8 ‰ n = 28), though the range of $\delta^{15}N$ of these species is wider if it includes natural salt deposits and products from laboratory chemical suppliers.

2. Ammonia volatilisation:

Ammonia volatilisation from soils is often significant after fertiliser and manure applications when ammonium concentrations are high and much of this ammonium is unadsorbed, and is enhanced by warm and windy conditions on moist alkaline soils (Killham, 1994). It is a major cause of economic loss to farmers as over 50% of nitrogen fertiliser can be lost in this way (Royal Society, 1983, Yang *et al.*, 2003). Volatilisation of ammonia leads to a combination of equilibrium and kinetic isotopic fractionations. Under acid to neutral pH, the system does not support ammonia volatilisation as it is controlled by ammonia $\leftrightarrow$ ammonium equilibrium which, below pH 9 vastly favours ammonium. This equilibrium in fact involves two stages: the equilibrium between dissolved ammonia and ammonium; and that between dissolved and gaseous ammonia. This latter equilibrium is controlled by the availability of dissolved ammonia from the

former (Johnson, 2004). When volatilisation occurs, there may also be diffusion towards the site of volatilisation which causes kinetic fractionation (Hogberg, 1997).

Ammonia volatilisation can occur as a result of urea hydrolysis. Mediated by urease, urea hydrolysis leads to transient bicarbonate formation and a temporary rise in pH. This shifts the ammonia$\leftrightarrow$ammonium equilibrium to favour ammonia, which is subsequently volatilised. This loss of ammonia from the system lowers pH preventing further volatilisation. Although a transient effect, the isotope fractionation associated with it can be significant with an $\varepsilon_{P\text{-}S}$ ($NH_3^+{}_{(gas)}$ - $NH_4^+{}_{(aq)}$) of -25 to -35 ‰, and can result in isotopically enriched bulk residual ammonium which may go on to be nitrified, retaining its heavy $\delta^{15}N$ (Heaton *et al.*, 1997, Kendall *et al.*, 2007).

In addition to the isotopic fractionation of ammonium from volatilisation, a fractionation arising from ion exchange in clay soils giving rise to an $\varepsilon_{P\text{-}S}$ of -1 to -7 ‰, has been reported (where ε_P refers to ammonium exchanged onto the clay ion exchanger and ε_S to the ammonium in solution) as a function of the concentration of ammonium in solution and the cation exchange capacity (CEC) of the soil (Karamanos and Rennie, 1978).

3. Mineralisation:

When dead biomass is decomposed by microorganisms, organic nitrogen is remineralised to ammonium. This causes negligible fractionation, with an $\varepsilon_{P\text{-}S}$ of approximately 0 ± 1‰ (Hogberg, 1997, Kendall *et al.*, 2007).

4. Nitrification:

Ammonium is converted to nitrate by nitrifying microorganisms. Recent genomic sequencing suggests that some soil archaea may be chemoautotrophic nitrifiers (Schleper *et al.*, 2005), and that ammonium oxidising archaea may outnumber bacterial ammonium oxidisers (Leininger *et al.*, 2006). Nevertheless, to date, the nitrification pathway best characterised is that mediated in soils in two distinct steps by the chemoautotrophic bacteria *Nitrosomonas*, which oxidises ammonium to nitrite via hydroxylamine, and by *Nitrobacter*, which oxidises this nitrite to nitrate (Killham, 1994). Where ammonium concentrations are at background levels ammonium production from the remineralisation of organic nitrogen is the rate limiting step and

fractionation due to nitrification is likely to be negligible ($\varepsilon_{P\text{-}S}$ 0 $\pm$ 0.5 ‰), meaning that nitrate produced via the remineralisation-nitrification pathway has an isotopic composition very close to that of the soil organic nitrogen (Heaton, 1986, Kendall *et al.*, 2007). However, under conditions where ammonium is not limited, the slower of the two reactions, the oxidation of ammonium to nitrite, is likely to be the rate-limiting step (Kendall, 1998). Isotopic fractionation occurs during this step, meaning that when ammonium is abundant, for example after fertiliser application, large fractionations can develop between the ammonium substrate pool which becomes progressively enriched, and nitrite and end product nitrate which are increasingly isotopically light, leading to $\varepsilon_{P\text{-}S}$ -14 to -35 ‰ (Fegin *et al.*, 1974, Mariotti *et al.*, 1981). High concentrations of ammonium are usually quickly restored to background concentrations via rapid assimilation and nitrification. This means that large fractionations are a temporary effect seen in recently fertilised soils or disturbed soils in which remineralisation has been stimulated, and that, when background concentrations are restored, ammonium production from remineralisation becomes the rate limiting step.

The above discussion concerns the fractionation of nitrogen in nitrate produced via nitrification. In addition to this, the two oxidation steps during nitrification of ammonium by *Nitrosomonas* and *Nitrobacter* incorporate three oxygen atoms into product nitrate, and their origin determines the $\delta^{18}O$ of the resulting nitrate. Laboratory culture studies have indicated that two of these oxygen atoms are sourced from water and one from oxygen. In the first step, the oxidation of ammonium to nitrite, two oxygen atoms are incorporated: the first as ammonium is oxidised to hydroxylamine; and the second as the hydroxylamine is oxidised to nitrite. It has been shown that the first oxidation incorporates oxygen from dissolved oxygen (Hollocher *et al.*, 1981) and that the second oxygen atom is derived from water (Andersson and Hooper, 1983). The single oxidation step which converts nitrite to nitrate uses water as the oxygen source (Aleem *et al.*, 1965, Kumar *et al.*, 1983, Hollocher, 1984, DiSpirito and Hooper, 1986). Thus oxygen in nitrate from nitrification is expected to comprise two oxygen atoms from water and one from dissolved oxygen (Kendall *et al.*, 2007). If it is assumed that ambient H_2O and O_2 are the oxygen sources, and that no fractionation occurs during incorporation, the $\delta^{18}O$ of nitrate resulting from nitrification can be represented by the equation (Kendall *et al.*, 2007):

$$\delta^{18}O_{NO3} = {}^{2}/_{3} (\delta^{18}O_{H2O}) + {}^{1}/_{3} (\delta^{18}O_{O2}) \qquad \text{Equation 2.7}$$

The $\delta^{18}O_{H2O}$ of modern groundwater in East Anglia is within the range $\delta^{18}O_{H2O}$ -7.0 to -7.5 ‰ (Feast *et al.*, 1998, Darling and Talbot, 2003) and the accepted value for $\delta^{18}O_{O2}$ of air is 23.5‰ (Kroopnick and Craig, 1972), which suggests a $\delta^{18}O_{NO3}$ of 2.8 to 3.2 ‰ for nitrate produced via microbially-mediated nitrification in East Anglia. However, it has been suggested that oxygen exchange may occur between nitrite and water during both the *Nitrosomonas* and *Nitrobacter* mediated oxidation steps (Andersson and Hooper, 1983, Kool *et al.*, 2007). This would result in a proportionally larger contribution from water to the final oxygen isotopic composition of bulk nitrate produced via nitrification and a lighter oxygen isotopic composition. Conversely, if nitrate is produced through heterotrophic nitrification, thought to occur at a slow rate, mediated by fungi in acid woodland soils, it appears that fewer than two oxygen atoms from water are incorporated, resulting in a higher than predicted $\delta^{18}O_{NO3}$ (Mayer *et al.*, 2001, Spoelestra *et al.*, 2007).

5. Assimilation:

Nitrogen assimilation usually refers to the uptake of ammonium by living organisms. Nitrate and nitrite may also be taken-up via assimilatory reduction during which the compound is converted to ammonium within the cell. Plant uptake of ammonium appears to result in negligible kinetic isotopic fractionation (e.g. $\varepsilon_{P\text{-}S}$ -0.25 $\pm$ 0.7 ‰, n=38, Hubner, 1986, based on an interpretation of data from Mariotti *et al.*, 1980), though where roots have a mycorrhizal association, this may cause fractionation of the ammonium during transfer to the plant (Hogberg, 1997). Fractionation resulting from assimilation by soil and freshwater microorganisms is significant and varied, and likely to be dependent on the concentration of the nitrogen substrate and the growth rate of the organism, for example $\varepsilon_{P\text{-}S}$ 5.2 $\pm$ 6.5 ‰ was reported by Delwiche and Steyn (1970). Importantly, where the substrate assimilated is nitrate or nitrite, any isotope effects associated with uptake will fractionate both the nitrogen and oxygen isotopes of the residual substrate. The relationship between the nitrogen and oxygen enrichment factors where both isotopes of a compound are fractionated simultaneously is known as the fractionation ratio. Field studies of assimilation using both N and O isotopes of nitrate are lacking to date. However, a laboratory single strain culture study of four marine phytoplankton species suggested that $\varepsilon_{P\text{-}S}{}^{15}N_{NO3} = \varepsilon_{P\text{-}S}{}^{18}O_{NO3}$, giving a fractionation

ratio of O:N of 1 (Granger *et al.*, 2004). The applicability of these findings to the soil and freshwater environment is not yet clear. Biomass production in soil and freshwater environments has a seasonal cycle which will result in high levels of nitrogen assimilation in spring and summer and low to negligible levels in autumn and winter (Weisse, 1991, Lloyd and Taylor, 1994, McCulloch *et al.*, 2007).

6. Denitrification:

Denitrification is the microbially-mediated step-wise reduction of nitrate with an end product of molecular nitrogen and a small proportion of nitrous oxide, which effectively returns molecular nitrogen to the atmosphere completing the nitrogen cycle:

$$NO_3^- \rightarrow NO_2^- \rightarrow NO \rightarrow N_2O \rightarrow N_2 \qquad \text{Equation 2.8}$$

It is carried out by a broad range of facultative anaerobic bacteria which may either be heterotrophic or autotrophic. Denitrification has been found to occur in temperatures as low as 0^oC with rates slowing below 5^oC (Holtan-Hartwig *et al.*, 2002).

Facultative anaerobic bacteria switch from aerobic to anaerobic respiration under low oxygen conditions when a labile organic carbon source is available, successively using NO_3^-, NO_2^-, and N_2O as electron acceptors, (NO acts as an intermediary). With respect to environmental research into the nitrogen cycle, a useful kinetic isotopic fractionation of the denitrification pathway is the reduction of nitrate to nitrite, mediated by a dissimilatory nitrate reductase, and useful because it alters the isotopic composition of the residual nitrate pool, causing $\delta^{15}N_{NO3}$ to increase exponentially as concentration decreases (Equation 2.6). Denitrification occurs under anaerobic conditions (including in anaerobic microsites when macro conditions are aerobic), in soils, sediments, groundwaters and surface waters, generally when the concentration of dissolved oxygen falls below 0.5 mg/l (Hubner, 1986, Zumft, 1997).

Isotopic fractionation due to denitrification is highly variable ($\varepsilon_{P\text{-}S}$ $^{15}N_{NO3}$ -4.7 to -30 ‰) (Mariotti *et al.*, 1981, Vogel *et al.*, 1981, Mariotti *et al.*, 1988). It shows an inverse relation with denitrification rate, meaning that the slowest denitrification rates cause the greatest isotopic enrichments. For example, Vogel *et al.* (1981) calculated an $\varepsilon_{P\text{-}S}$ $^{15}N_{NO3}$ of -30 ± 6 ‰ for denitrified groundwater in which the oldest recharge water was ^{14}C

dated as 27 000 years old, indicating that extremely slow denitrification had caused a calculated reduction in concentration of up to 86 mg/L NO_3^- over a period of 15 000 years (Heaton *et al.*, 1983). In contrast, Deutsch *et al.* (2005) found an $\varepsilon_{P\text{-}S}\ ^{15}N_{NO3}$ of -5.9 ‰ in drain water from an agricultural field over a six-month summer and autumn period, coupled with a drop in nitrate concentration of over 62 mg/L NO_3^- indicative of rapid denitrification.

In the same way that assimilation affects both the nitrogen and oxygen isotopic composition of the residual nitrate during partial removal by a fractionating process, denitrification causes fractionation of oxygen isotope ratios of nitrate in tandem with those of nitrogen. There is much empirical data from field studies in various terrestrial environments which suggests a denitrification fractionation ratio of O:N in the range of 0.4 to 0.6, indicating that $\varepsilon_{P\text{-}S}{}^{15}N_{NO3} \approx 2 \times \varepsilon_{P\text{-}S}{}^{18}O_{NO3}$ (Böttcher *et al.*, 1990, Aravena and Robertson, 1998, Cey *et al.*, 1999, Lehmann *et al.*, 2003, Fukada *et al.*, 2004, Deutsch *et al.*, 2005, Petitta *et al.*, 2009). Some of these studies involved analysis of samples using the silver nitrate off-line sealed glass tube combustion method. It has been suggested that this method may lead to an artificially low fractionation ratio due to scale compression (a reduction in the range of oxygen isotope ratios) as a result of oxygen exchange with the SiO_2 of the glass combustion tubes (Revesz and Bohlke, 2002), though Kendall *et al.* (2007) note that a number of studies used variations of both the sealed tube and pyrolysis methods and found a similar denitrification fractionation ratio of 0.5 to 0.7.

The studies referred to above describe field based research into denitrification. Recent laboratory studies have been carried out using single strains of denitrifying bacteria grown in culture media including two strains isolated from soil, which produced a fractionation ratio of 1, and a freshwater photosynthetic denitrifier which produced a ratio of 0.6 (Granger *et al.*, 2008). This variation appears to be attributable to a difference in the nitrate reductase used by the bacteria examined. There are two dissimilatory nitrate reductases (for energy production), the respiratory and the periplasmic, as well as an assimilatory nitrate reductase (to incorporate nitrogen into cells), and some denitrifiying organisms contain all three (Warnecke-Eberz and Friedrich, 1993, Zumft, 1997). If a difference in fractionation ratio can be caused by

different nitrate reductases, it suggests that denitrification in the field, carried out by a diverse microbial community, will produce a composite fractionation ratio.

The bacterial diversity of denitrification is broad, and includes autotrophic sulphur, hydrogen and iron oxidisers, denitrifying photosynthetic bacteria, as well as diazotrophs (nitrogen fixers) which can denitrify and fix nitrogen at the same time. Aerobic denitrification has also been identified in various organisms which can activate denitrification genes under high concentrations of dissolved oxygen (Zumft, 1997). Denitrification is not limited to bacteria and is also carried out by archaea and fungi (Michalski and Nicholas, 1984, Killham, 1994, Zumft, 1997).

There are likely to be other pathways by which nitrate is cycled or removed within a catchment environment, which can encompass a wide variety of physiochemical conditions. Among these are the dissimilatory nitrate reduction to ammonium (DNRA) during which, in carbon-rich anoxic conditions, where there is a high labile carbon to nitrate ratio, heterotrophic fermentative soil bacteria reduce nitrate by using it as an electron acceptor for respiration, producing ammonium (Tiedje, 1988). Another pathway is nitrifier denitrification during which ammonia is oxidised to nitrite then reduced to nitrous oxide and molecular nitrogen by autotrophic nitrifiers (Wrage *et al.*, 2001). Although likely to incur kinetic isotope fractionations, little is know of the isotope effects associated with these processes.

2.1.3 Source Nitrate Dual-Isotope Signatures

Much effort has been made in recent years to identify the isotopic composition of nitrate from different sources (e.g. Kendall, 1998). For technical reasons, research was initially limited to analysis of $\delta^{15}N_{NO3}$, and as a consequence more data exist for $\delta^{15}N_{NO3}$ than for $\delta^{18}O_{NO3}$, though this initial imbalance is now being addressed. The expected range of nitrate source isotopic composition is well constrained for industrially-produced nitrate fertiliser, which can be analysed before any microbial interference, and for atmospheric nitrate in precipitation and dry and wet deposition, which although encompassing a large range, is well differentiated from other sources by its isotopically heavy $\delta^{18}O_{NO3}$ (Figure 2.2; Table 2.2). However, one of the limitations of using literature compilations to attribute ranges of isotopic composition to the other nitrate

sources is the ubiquitous microbial colonisation of the natural environment wherever nitrogen occurs.

If a microbial community is utilising a nitrogen source *in situ*, it is likely that ongoing isotopic fractionation is altering the original isotopic composition of the source (Anisfeld *et al.*, 2007). This is particularly true for sewage and manure, where nitrate is produced from nitrification of ammonium derived from the remineralisation of urea (Killham, 1994). Prior to nitrification, the $\delta^{15}N_{NH4}$ of these waste products will become progressively enriched in ^{15}N if volatilisation of ammonia occurs (Section 2.1.2.3), potentially leading to a broad range of nitrification product $\delta^{15}N_{NO3}$. The $\delta^{18}O_{NO3}$ of nitrate produced through chemoautotrophic bacterial nitrification can be predicted locally (Equation 2.6), and has a narrow range (Figure 2.2; Table 2.2), though it is possible that at a small spatial and temporal scale, $\delta^{18}O_{H2O}$ sourced directly from precipitation rather than from bulk soil water may provide the water-source oxygen, producing a wider range of $\delta^{18}O_{NO3}$. However, $\delta^{18}O_{NO3}$ in nitrification-product manure and sewage may show an influence from the isotopic composition of source water in the waste which could have undergone metabolic fractionation. In addition, subsequent evaporation of water from the waste could affect the isotopic composition of the nitrification source water. Both these effects would lead to a heavier than predicted $\delta^{18}O_{NO3}$ of nitrate produced from nitrification of ammonium in manure and sewage. Both these effects would lead to a heavier than predicted $\delta^{18}O_{NO3}$ of nitrate produced from nitrification of ammonium in manure and sewage.

In addition to the potentially wide range of $\delta^{15}N_{NO3}$ resulting from volatilisation of waste-product ammonia prior to nitrification, under favourable circumstances, denitrification within manure or sewage can cause the isotopic enrichment of both isotopes of nitrate in parallel, resulting in the wide range of values reported in the literature (Shearer *et al.*, 1974a, Heaton, 1986, Kendall, 1998, Anisfeld *et al.*, 2007). Denitrification will affect the isotopic composition of nitrate formed from nitrification of remineralised soil organic matter in pristine soils in a similar way (Figure 2.2, Table 2.2). Soil may also contain nitrate from nitrification of ammonium from other sources (e.g. atmospheric and fertiliser sources) and this may also undergo denitrification. For clarity, nitrate from sources after these microbial fractionations is not included in Figure 2.2 and Table 2.2. In fact, fertiliser ammonium nitrified by chemoautotrophic bacteria in

the soil is likely to produce a $\delta^{15}N_{NO3}$ close to 0 ‰ (Kendall *et al.*, 2007), while atmospheric ammonium from dry deposition and precipitation is likely to produce a range of $\delta^{15}N_{NO3}$ almost identical to that of atmospheric nitrate although the nitrogen isotopic composition of dry deposition and precipitation differ (Heaton *et al.*, 1997).

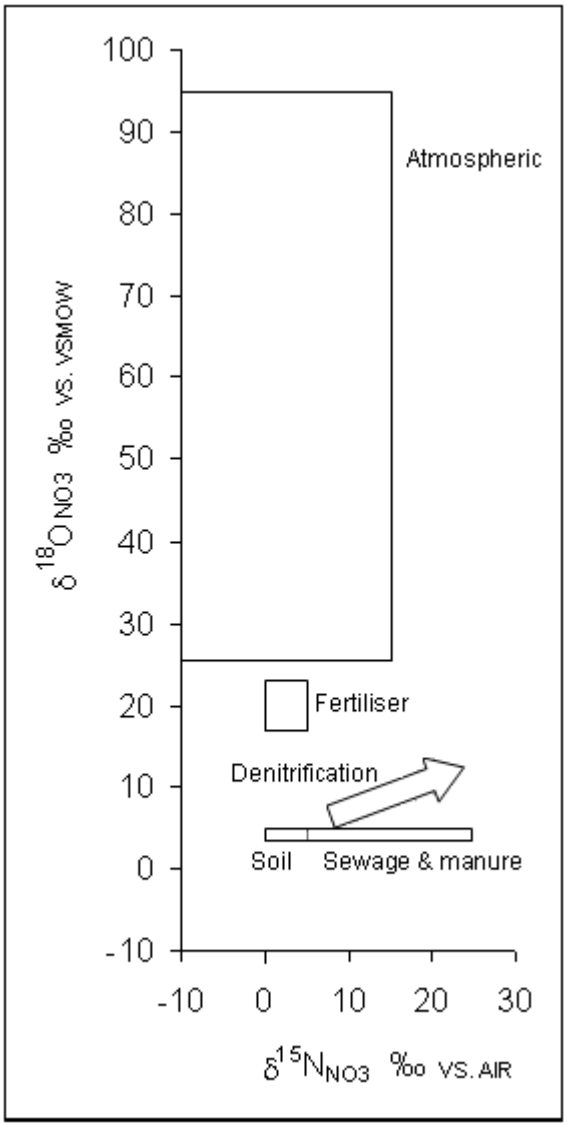

Figure 2.2 Expected ranges of $\delta^{15}N_{NO3}$ (‰) and $\delta^{18}O_{NO3}$ (‰) of nitrate sources. Arrow represents isotopic fractionation due to denitrification based on a fractionation ratio of O:N of 0.5. "Soil" refers to nitrate from pristine soil. The $\delta^{18}O_{NO3}$ of soil, sewage and manure nitrate is based on predicted values for bulk chemoautotrophic bacterial nitrification in East Anglia using Equation 2.6. Literature values for substrates themselves rather than soils or groundwaters impacted by substrates have been used where possible. (Sources: Shearer *et al.*, 1974a, Heaton, 1986, Hubner, 1986, Amberger and Schmidt, 1987, Fogg *et al.*, 1998, Kendall, 1998, Anisfeld *et al.*, 2007, Kendall *et al.*, 2007). Note that Kendall *et al.,* (2007) found that atmospheric nitrate samples prepared with the denitrified method showed a lower limit on the range of $\delta^{18}O_{NO3}$ values of > 60‰, and suggested that atmospheric $\delta^{18}O_{NO3}$ values from previous studies below 60‰ may have been an artefact of the sealed glass tube method, leading to an overestimation of the range by expanding the lower limit.

Table 2.2 Expected ranges of $\delta^{15}N_{NO3}$ (‰) and $\delta^{18}O_{NO3}$ (‰) of nitrate sources ($\delta^{15}N_{NH4}$ not included). The $\delta^{18}O_{NO3}$ of soil, sewage and manure nitrate are based on predicted values for bulk chemoautotrophic bacterial nitrification in East Anglia using Equation 2.6. Literature values for substrates themselves, rather than soils or groundwaters impacted by substrates, have been used where possible. (Sources: Shearer *et al.*, 1974a, Heaton, 1986, Hubner, 1986, Amberger and Schmidt, 1987, Fogg *et al.*, 1998, Kendall, 1998, Anisfeld *et al.*, 2007, Kendall *et al.*, 2007).

Nitrate source	**$\delta^{15}N_{NO3}$ ‰ vs. AIR**	**$\delta^{18}O_{NO3}$ ‰ vs. VSMOW**
Atmospheric (dry deposition and precipitation)	-10 to 15	25 to 95
Industrial fertiliser	0 to 5	17 to 23
Sewage and manure (nitrified NH_4^+)	5 to 25	3 ± 0.2
Pristine soil (nitrified NH_4^+ from mineralised SOM)	0 to 5	3 ± 0.2

2.2 NITRATE DUAL-ISOTOPE RESEARCH

The development of nitrate stable isotope research began in the 1970s with the use of $\delta^{15}N$ to identify sources of nitrate contamination in the terrestrial environment (Kohl *et al.*, 1971, Black and Waring, 1977, Kreitler, 1979). Soon after this, investigations began to focus on processes which alter the $\delta^{15}N_{NO3}$ source signature through isotopic fractionation (Mariotti *et al.*, 1981, Mariotti *et al.*, 1988). Later, source and process identification was greatly enhanced by the development of techniques which enable the measurement of $\delta^{18}O_{NO3}$ so that the both nitrogen and oxygen isotopes of nitrate can be measured (Amberger and Schmidt, 1987, Chang *et al.*, 1999, Silva *et al.*, 2000, Casciotti *et al.*, 2002).

2.2.1 Denitrification in Surface Water Sediments and the Groundwater-Surface Water Interface

The isotopic effects of denitrification in groundwater has been well characterised (Mariotti *et al.*, 1988, Böttcher *et al.*, 1990, Aravena and Robertson, 1998, Fukada *et al.*, 2004, Petitta *et al.*, 2009). Two studies using submerged sediment cores taken from surface water environments aimed to clarify the isotopic effect of denitrification in surface waters as part of larger studies investigating nitrogen cycling dynamics in the Seine (Sebilo *et al.*, 2003) and in a first order stream (Kellman, 2004). The laboratory methods used were not identical, making direct comparison problematic. Nevertheless, the results of the two studies are somewhat conflicting. Sebilo *et al.* (2003) found a slow rate of nitrate removal coupled with minor isotopic enrichment of $\delta^{15}N_{NO3}$ from cores of undisturbed sediment overlain by continuously oxygenated water, in comparison to cores of an agitated anaerobic slurry formed from the same sediment which demonstrated a higher removal rate with greater isotopic enrichment (denitrification rates were not reported). The initial nitrate concentration in the water from both experiments was approximately 30 ml/L NO_3^-. Sebilo *et al.* (2003) suggested that in the oxygenated cores, denitrification was limited to the anaerobic sediments where the rate-limiting step was the molecular diffusion of nitrate through the sediments along a concentration gradient caused by nitrate removal from the denitrifying bacteria, which would cause a negligible, diffusion-related isotopic fractionation.

Kellman (2004) carried out a two-staged experiment, first investigating the correlation between nitrate removal rate, nitrate concentration, and dissolved oxygen concentration in two sets of cores of undisturbed sediment overlain by low and high nitrate concentration water, (approximately 9 mg/L NO_3^- and 30 ml/L NO_3^- respectively) which was continuously artificially oxygenated in the first set of cores, but not in the second set in which anaerobic conditions developed over time. The results showed no difference in nitrate removal rate between the oxygenated and non-oxygenated cores and a higher removal rate in the cores overlain by water with a high concentration of nitrate. Thus, nitrate removal rate was seen to be affected by nitrate concentration but not dissolved oxygen concentration in the water. Kellman (2004) ascribed these results to the fact that denitrification in the cores was unaffected by levels of dissolved oxygen because it occurred in the anaerobic sediment rather than the overlying water. Next, cores overlain with high nitrate concentration water were tested for nitrate removal and $\delta^{15}N_{NO3}$ over time, without being artificially oxygenated. Both a high nitrate removal rate and significant isotopic enrichment of $\delta^{15}N_{NO3}$ were seen from these cores, in contrast to the findings of Sebilo *et al.* (2003), with the results of Kellman's study producing a range of nitrate removal of 4 to 15 mg m^2/hour. This apparent contradiction reflects a continuing uncertainty as to whether or not sedimentary denitrification in streams and rivers will impart a similar isotopic effect to that seen in groundwater environments; in other words, whether it is controlled by diffusion or advection. It is likely that both advection and diffusion-controlled denitrification occur, and depend on variations in riverbed conditions.

The investigation into the isotopic effect of in-stream riverine denitrification through experiments with submerged sediment cores is likely to have involved denitrification in the uppermost anaerobic layer of the cores. In addition to denitrification in the riverbed surface sediments, denitrification often occurs in the hyporheic zone removing nitrate from river water when it is diverted through flow channels within the sediments below the river bed and through meander bends (Figure 2.3). The hyporheic zone represents the interface between groundwater and surface water within the fluvial sediments below a river, and is a reactive zone characterised by redox and temperature gradients, which has a supply of organic carbon from the river and supports intense microbial activity, including denitrification (Boulton *et al.*, 1998). The geochemical definition of the hyporheic zone is of a mixing zone between surface water and deep-sourced

groundwater, while hydrologists define it as subsurface region containing flowpaths that originate and terminate in the stream (Gooseff, 2010). Hyporheic zone depths of over 5 metres can occur where river valleys have been filled by gravel deposits (Buss *et al.*, 2009).

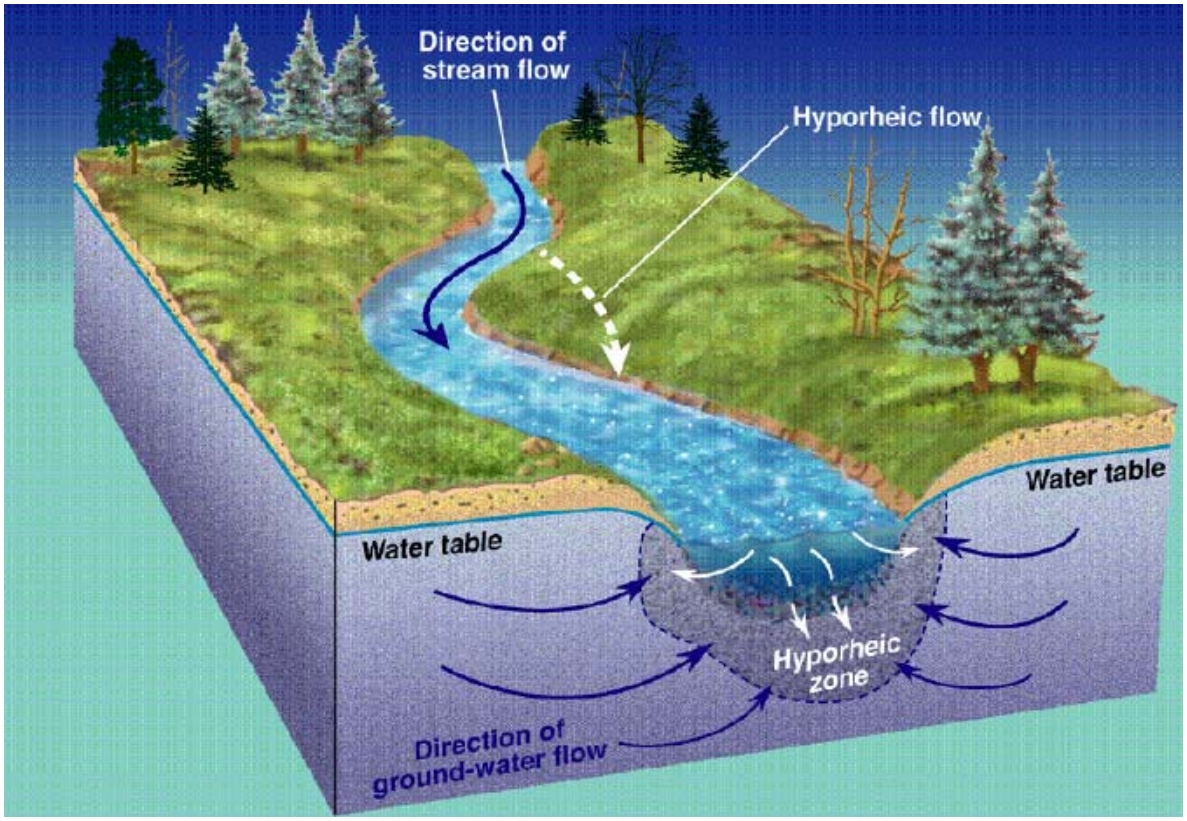

Figure 2.3 Conceptual model of the relationship between the hyporheic zone and river and groundwater flow paths (Buss *et al.*, 2009).

The hyporheic zone has been found to support denitrification rates of 28 to 64 mg per hour per cubic metre of sediments (Sheibley *et al.*, 2003). A study by Hinkle *et al.* (2001) in a small area (15 km^2) using isotopes of water and $\delta^{15}N_{NO3}$ with chloride concentrations found that nitrate from groundwater advecting into the hyporheic zone was almost totally removed, while, nitrate from stream water circulating through the hyporheic sediments saw a reduction in nitrate concentration. However, a multiple regression analysis by Smith *et al.* (2009) into the natural attenuation potential of nitrate at the groundwater-surface water interface across the UK under baseflow conditions, using the variables of the organic carbon fraction, the sediment permeability and thickness, and the baseflow index, places the study area in Norfolk in the lowest band, suggesting that hyporheic denitrification there is not significant.

A number of studies have quantified riverine denitrification rates using a variety of techniques including the use of natural abundance stable isotope ratios, the acetylene block technique, the measurement of N_2:Ar ratios, nitrogen mass balance and modelling, producing a range of rates spanning two orders of magnitude, from 2 mg/m^2/hour to 222 mg/m^2/hour riverine nitrate-nitrogen removal relative to streambed area, with up to 778 mg/m^2/hour measured in a wetland environment (Sjodin *et al.*, 1997, Laursen and Seitzinger, 2002, Kellman, 2004, Royer *et al.*, 2004, Laursen and Seitzinger, 2005, Hernandez and Mitsch, 2006, Pina-Ochoa and Alvarez-Cobelas, 2006).

With respect to the reduction in riverine nitrogen loads attributable to denitrification in the river corridor, two large-scale modelling studies and one field-based study using the acetylene block technique suggest rates of 20% to 45% riverine nitrogen removal (Alexander *et al.*, 2000, Kemp and Dodds, 2002, Seitzinger *et al.*, 2006). However, the overall efficiency of riverine nitrate removal has been found to decline with rising nitrate concentrations, such that a greater proportion of nitrate is removed at lower concentrations (Kemp and Dodds, 2002, Mulholland *et al.*, 2008).

2.2.2 Catchment Research

There have been a number of field scale investigations using $\delta^{15}N_{NO3}$ and $\delta^{18}O_{NO3}$ to identify sources and transformations of nitrate along short flowpath transects from fields or woods and riparian zones to first order streams using study areas of a few km^2. The advantage of this small scale is that it is possible to characterise the study site hydrological system with confidence. Moreover a single main source of nitrate can usually be identified and tracked along the transect and processes such as nitrate assimilation or denitrification can be inferred from changes in nitrate concentration and isotopic composition over short distances (Cey *et al.*, 1999, Clement *et al.*, 2003, Kellman and Hillaire-Marcel, 2003, Kellman, 2004, Deutsch *et al.*, 2005, Deutsch *et al.*, 2006).

A number of studies in small and very small sub-catchments (1.5 ha to 19 km^2) and urban environments have shown that atmospheric nitrate from snow melt and precipitation during storms can be identified using $\delta^{15}N_{NO3}$ and $\delta^{18}O_{NO3}$ when a strong

pulse occurs (Burns and Kendall, 2002, Cambell *et al.*, 2002, Silva *et al.*, 2002, Sickman *et al.*, 2003, Pardo *et al.*, 2004). However, in general, the studies found a lower than expected proportion of nitrate with an atmospheric isotopic signature in stormflow. This was interpreted to be the result of isotope effects caused by rapid microbial cycling in the soil.

In contrast to the application of the nitrate dual-isotope technique to very small field sites, there have been a number of geographically large-scale studies in which samples were collected from groups of larger rivers at their catchment outlets, in an effort to correlate nitrate isotopic composition with land use and nitrate source, and to investigate microbial cycling (Battaglin *et al.*, 2001, Chang *et al.*, 2002, Mayer *et al.*, 2002, Johannsen *et al.*, 2008).

A study undertaken by Mayer *et al.* (2002) aimed to identify nitrate sources and denitrification using $\delta^{15}N_{NO3}$ and $\delta^{18}O_{NO3}$ from samples taken at the outlets of 16 medium and large-sized catchments in the north-eastern United States, which had been shown in a previous study to support a high level of nitrogen retention and removal (Boyer *et al.*, 2002). Perhaps as a result of the low frequency of sampling in relation to the large geographical scale of the study and the decision to limit sampling to catchment outlets, it was not possible to identify nitrate sources and evidence of denitrification was not found. The narrow range of $\delta^{15}N_{NO3}$ and $\delta^{18}O_{NO3}$ seen in the samples implied that nitrate isotopic composition had been homogenised by the time flow exited the catchments, and probably comprised a mix of sources and fractionations due to microbial cycling. However, significant relationships were found between high $\delta^{15}N_{NO3}$ values and those catchments with a higher percentage of urban or agricultural land use and higher mean nitrate concentrations. Lower $\delta^{15}N_{NO3}$ values were seen in the highly forested catchments where nitrate concentrations were lower, and was attributed to nitrate from an original soil organic nitrogen source. In general, the outcomes of this study reflect those of the other geographically ambitious studies in that although some relationship between $\delta^{15}N_{NO3}$ and $\delta^{18}O_{NO3}$ and land use is retained at catchment outlets, a more detailed interpretation is hindered by the homogenised nature of nitrate isotopic composition by the time it is exported from the catchment in river water.

Recently, dual-isotopes of nitrate have been used to investigate sources and cycling of nitrogen in medium-sized catchments (200 to 700 km^2), by Anisfeld *et al.* (2007) in two mixed-land use catchments in Connecticut, and Buda and DeWalle (2009) in a mixed-land use catchment in Pennsylvania. These studies developed approaches from the earlier research at small field sites aimed at identifying atmospheric inputs in streamflow mentioned above. A third study by Petitta *et al.* (2009) on an agricultural plain in central Italy investigated complex groundwater and surface water interactions which affect seasonal nitrate dynamics.

Anisfeld *et al.* (2007) described a mass balance source apportionment approach which utilised $\delta^{15}N_{NO3}$ and $\delta^{18}O_{NO3}$ from baseflow and stormflow samples from two rivers draining urban/agricultural catchments, with analyses of sewage, precipitation and soil nitrate samples. Soil nitrate was defined in this study as any nitrate resulting from nitrification in the soil, including that which originates from ammonium of atmospheric and fertiliser sources. Atmospheric nitrate, identifiable by its enriched $\delta^{18}O_{NO3}$, was found to contribute <10% during baseflow and up to 50% during stormflow with a high correlation between the proportion of atmospheric nitrate and flow, although Anisfeld *et al.* (2007) stress that this does not include contributions from other nitrogen species in atmospheric deposition which may have been nitrified in the soil and leached to the rivers. The wide range of isotopic composition found in sewage effluent in this study confounded its source apportionment, and this in turn impacted the apportionment of soil nitrate which was calculated by a difference method. Interestingly, when examined together, the isotopic composition of sewage effluent which was collected from a number of treatment works showed evidence of denitrification, seen in isotopic enrichment of both isotopes with a fractionation ratio of 0.56 and a decrease in nitrate concentration, suggesting that denitrification was occurring in wastewater works where it was not an engineered process, as well as in those plants where it was. Anisfeld *et al.* (2007) recommended the use of $\delta^{15}N_{NO3}$ and $\delta^{18}O_{NO3}$ for source identification at the local scale while highlighting the limits of source apportionment where isotopic fractionation has occurred.

Buda and DeWalle (2009) investigated changes in nitrate source and movement during storm events using hydrograph separation with $\delta^{18}O_{H2O}$ and $\delta^{18}O_{NO3}$ to elucidate

transport pathways of event and pre-event water and atmospheric nitrate. The study areas, all within one catchment, included an upland forested site with shallow soils on sandstone and shale bedrock, and agricultural and urban lowland sites underlain by karstic carbonate geology. Stormflow response at the upland forested site showed a storm-size modulated response. Smaller storms showed very large inputs of atmospheric nitrate with an isotopic mass-balance and hydrograph separation indicating that the proportion of event nitrate was larger than the proportion of event water in stream discharge. This might suggest that dry deposition had been flushed from vegetated surfaces contributing to the atmospheric signal in the early part of the storm. This phenomenon of dry deposition wash-off was also seen at an urban site, which also indicated overland flow over impermeable surfaces. At the forested site, larger storms resulted in a different signal, resulting from the flushing of nitrate stored in the soil via shallow flowpaths. The stormflow response at the lowland agricultural site suggested a stable piston-flow effect across the magnitude of storms, which flushed stored nitrate into the river via groundwater flowpaths. Through utilising the difference in isotope mass balance given by the oxygen isotopes of nitrate and water this study enabled detailed interpretation of the response of three study sites representing different environments to nitrate inputs from storm events.

Petitta *et al.* (2009) investigated seasonally influenced nitrate dynamics and groundwater/surface water interactions in irrigation channels within an agricultural area which occupies the bed of a large drained lake underlain by a carbonate aquifer in central Italy. The study used analysis of major ions, DOC and physical parameters alongside $\delta^{15}N_{NO3}$, $\delta^{18}O_{NO3}$, $\delta^{2}H_{H2O}$ and $\delta^{18}O_{H2O}$ from samples taken from irrigation channels and groundwater to characterise the interplay between seasonal variations in sources of flow to the channels and nitrate sources, expressed in a three-staged conceptual model. The model shows an annual cycle which begins with manure applications to the agricultural land in early winter, nitrate from which is carried in runoff to the channels in winter and spring rains which also flush out shallow nitrate-rich groundwater water from the lacustrine deposits, resulting in high nitrate concentrations of mixed source in channel water. In early summer when the channels start to be used for irrigation, discharge from artesian springs on the edge of the plain is at a maximum bringing diluting low-nitrate waters to the irrigation channels, and adding a third source of nitrate. At the end of the irrigation season, water is mainly sourced

from the high-nitrate shallow aquifer once more, raising nitrate concentrations in the channel. The model is supported by isotopic and hydrochemical fingerprinting of nitrate and water sources. Enriched $\delta^{15}N_{NO3}$ and $\delta^{18}O_{NO3}$ alongside high DOC concentrations suggest that denitrification occurs in the shallow groundwater of the lacustrine deposits. This study is interesting for its complex seasonal hydrological characterisation based on the differentiation of water and nitrate sources using stable isotopes and hydrochemistry.

The interpretations presented in the literature discussed here can be combined into a conceptual model to depict processes which affect the isotopic composition of nitrate during transport through a catchment to a river (Figure 2.4). Impermeable surfaces can enable atmospheric nitrate from precipitation and wash off to reach the river isotopically unaltered, while nitrate from sewage effluent and agricultural runoff during storms may also reach the river without major isotopic alteration. Infiltration will carry nitrogen inputs from the surface into the soil zone where intense microbial nitrogen-cycling activity will alter the isotopic composition of nitrate which may then either reach the river via subsurface flowpaths or be carried in recharge to groundwater. Nitrate in groundwater may be isotopically altered further if conditions in the aquifer or the hyporheic zone support denitrification, reaching the river in baseflow. In addition to the above processes, nitrate transported in river water may have its isotopic composition further modified by fractionating in-stream removal processes (assimilation and denitrification).

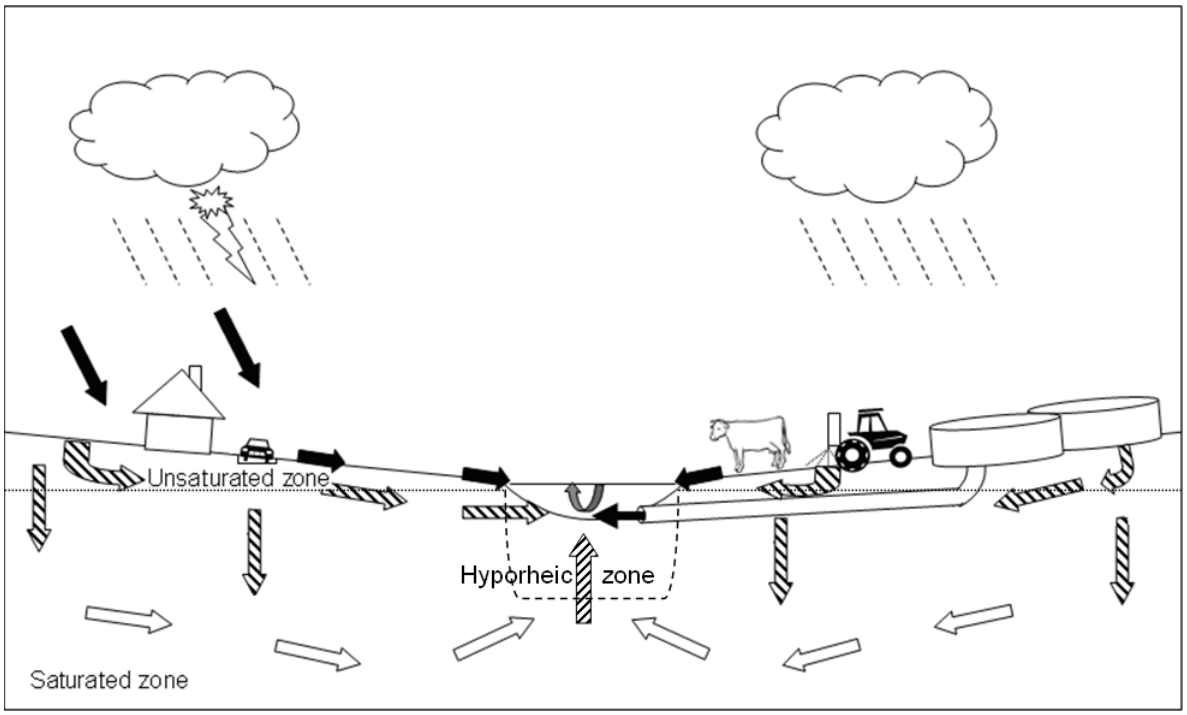

Figure 2.4 Conceptual model of dissolved nitrogen transport through a catchment to a river, showing pathways in which the isotopic composition of nitrate may be altered due to microbially-mediated fractionating processes. Black arrows: isotopically unaltered source nitrate; hatched arrows: nitrate with an isotopic composition resulting from fractionation in the soil and unsaturated zone; white arrows: groundwater nitrate which may undergo further fractionation; grey arrow: nitrate which may undergo fractionation in-stream.

2.3 SUMMARY

Stable isotope theory has been discussed and the ^{15}N isotope fractionations associated with nitrogen cycling have been described. The wide range of ^{15}N fractionations reported in the literature for the process of nitrification have been presented, and a narrow range of $\delta^{18}O_{NO3}$ in nitrate produced via nitrification has been predicted for the region of East Anglia. The wide range of isotope fractionations which affect $\delta^{15}N_{NO3}$ and $\delta^{18}O_{NO3}$ during denitrification has been discussed, along with the O:N fractionation ratio expected as denitrification progresses. The nitrate dual-isotope ranges of sources of nitrate reported in the literature have been set out, including data relevant to agricultural catchments. A conceptual model has been presented to show processes incurring isotope fractionations of $\delta^{15}N_{NO3}$ and $\delta^{18}O_{NO3}$ as nitrate is transported through a catchment to a river.

Nitrate dual-isotope catchment studies have been discussed and inform the study design used in this research into the Wensum catchment in East Anglia. The importance of

scale and resolution in study design has been shown, and the importance of collecting data from headwaters to the catchment outlet, especially if source apportionment is to be attempted, as isotope fractionations mask the original isotopic signature of source nitrate. In particular, the importance of sampling during different flow conditions and at a variety of temporal and spatial scales has been noted, and the use of other hydrochemical and isotopic tracers in conjunction with $\delta^{15}N_{NO3}$ and $\delta^{18}O_{NO3}$ to support interpretations of the dual-isotopes of nitrate.

3. METHODS

In this chapter the research design and field sampling protocols are described for the various sample types collected, including the methods used for sample preparation and storage. This is followed by an explanation of the denitrifier method for the analysis of $\delta^{15}N_{NO3}$ and $\delta^{18}O_{NO3}$, which includes details of the data reduction methodology and experiments carried out during the setting up and development of the method. The techniques used for the analysis of $\delta^{18}O_{H2O}$ and $\delta^{2}H_{H2O}$ are briefly outlined, followed by a description of field measurements and further hydrochemical analysis techniques. Finally, the equations used to model results are presented. The precision and reproducibility of each analysis method are presented in each section, and detailed supplementary information is supplied in Appendix 1. In accordance with the conventions of freshwater hydrochemistry, concentrations of major and minor ions and trace elements are reported in mg/L and μg/L. For the dissolved nitrogen species (nitrate, nitrite, ammonium, and dissolved organic nitrogen) concentrations are reported in μM as this enables a better understanding of stochiometry within the nitrogen cycle.

3.1 RESEARCH DESIGN

The two focal points of this research were the interest expressed by the CASE partner, the Environment Agency in the cause of the decreasing concentration of nitrate seen in the Wensum river downstream, and the setting up of the denitrifier method (Sigman *et al.*, 2001, Casciotti *et al.*, 2002) with the denitrifier group in the Stable Isotope Laboratory for the measurement of stable isotopes of $\delta^{15}N_{NO3}$ and $\delta^{18}O_{NO3}$. Thus, the collection of field samples for the analysis of nitrate isotopic composition was the main objective of the field work. These samples were collected from the study river, tributaries and drains, and from groundwater which supplies baseflow to the river. In addition to these samples, a small number of samples from sources of nitrate to the catchment were collected (precipitation, dry deposition, agricultural nitrate fertiliser from two local suppliers, wastewater effluent, cattle and poultry manure). The purpose of these samples was to confirm that their nitrate dual-isotopic composition was within the ranges reported in the literature. The precipitation samples were collected during

storms which occurred on days prior to river sampling. All samples were analysed for $\delta^{15}N_{NO3}$ and $\delta^{18}O_{NO3}$ of nitrate using the denitrifier method.

Consideration was given to the feasibility of including analysis of the concentration and isotopic composition of other nitrogen species from river water as part of this research. These species include the other dissolved inorganic nitrogen (DIN) species nitrite and ammonium, as well as dissolved organic nitrogen (DON) and suspended particulate nitrogen (SPN). Concentrations of nitrate, nitrite, and ammonium were routinely measured by liquid ion chromatography. However, due to time and resource constraints, and because concentrations of ammonium and nitrite were consistently very low in comparison to nitrate (usually < 1 % of DIN), the isotopic analysis of nitrite and ammonium was not pursued. DON concentrations were measured in some of samples. Later in the research sample sets were not analysed for DON due to technical difficulties with the instrument. Although $\delta^{15}N$ of high molecular weight DON has been used in conjunction with other parameters (C: N ratio, $\delta^{13}C$, ^{13}C NMR, flow data) to elucidate differing DOM signals between rivers (Duan *et al.*, 2007), the benefits to this study were not clear and for this reason, alongside the technical, resource, and time constraints, the approach was not attempted in this study. $\delta^{15}N$ of SPN has not been found to be a useful tool to differentiate SPN sources in river water (Kendall *et al.*, 2001). For this reason $\delta^{15}N_{SPN}$ was not measured. The measurement of concentrations of nitrate and the other major ions and trace elements was carried out routinely. In addition measurements of $\delta^{18}O_{H2O}$ and $\delta^{2}H_{H2O}$ were carried out for groundwater samples and selected river samples.

Potential sampling sites on the river Wensum, its tributaries, and the drains draining into it were selected through consulting OS maps using the criteria of an even spatial distribution along the river, and safe access to site. Drains were selected for sampling if they were close to river sampling locations and large enough to suggest that flow was not ephemeral. Following identification of sampling locations on the maps, a reconnaissance trip was made to the catchment and, after some sites were discounted due to poor access, the feasibility of carrying out a full spatial sampling survey of headwater to catchment outlet within one day was tested (Figure 3.1). Sampling regimes

were designed to include spatial and temporal elements. These included full river transects (headwater to catchment outlet), shorter transects of a higher spatial resolution, surveys which included tributaries and drains, repeated sampling at selected river locations, and the use of automatic water samplers simultaneously sited at two locations a distance apart on the river.

The Environment Agency Register of Current Licensed Groundwater Abstractions (commonly known as the borehole register) was consulted to identify suitable boreholes from which to take samples within the catchment. Grid references were exported to a GIS map of the catchment and this was used to select Chalk boreholes sited in the interfluves and the river valley. The borehole owners were approached by letter. All positive responses lead to samples being collected during the recharge season in February 2008. Where permission for a second visit was obtained, follow-up samples were taken at the end of the summer in August 2008. Borehole samples were all taken from irrigation boreholes which were sited on farms, golf courses and garden nurseries (Figure 3.1).

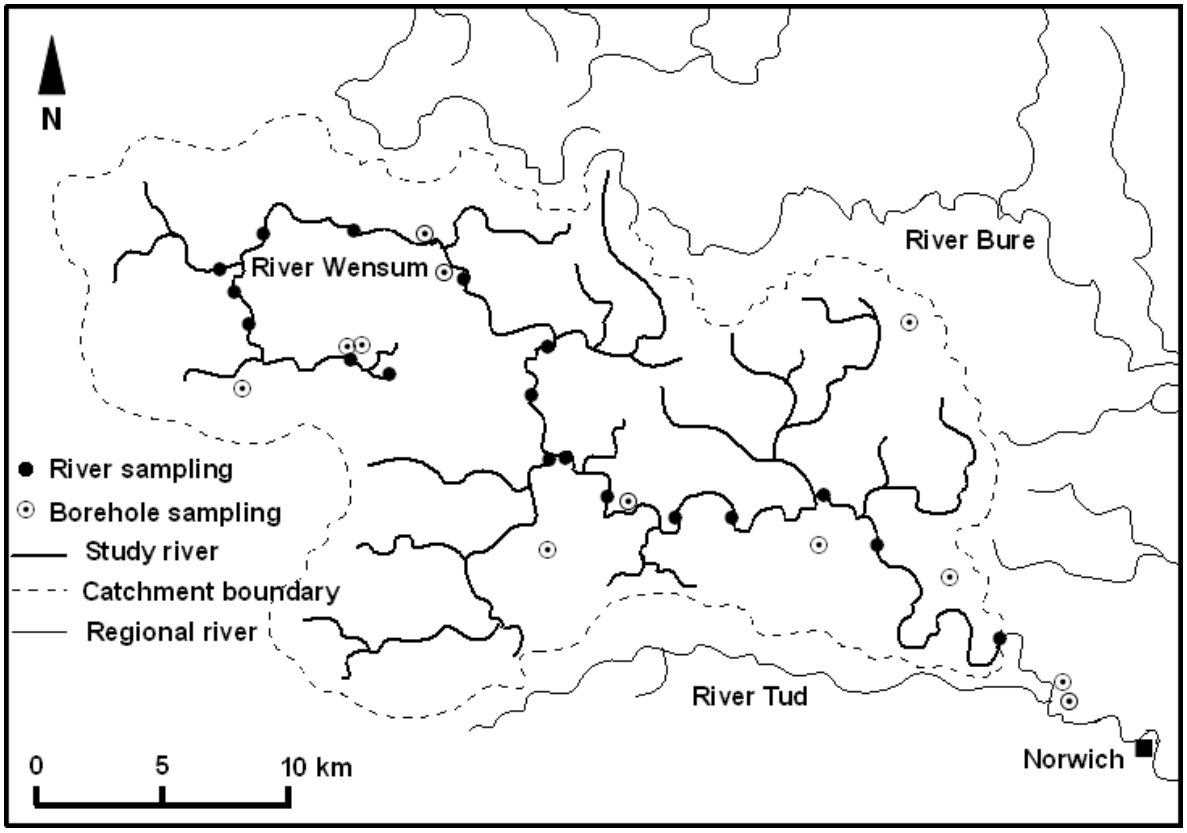

Figure 3.1 Main river and groundwater sampling locations in the Wensum catchment.

3.2 SAMPLE COLLECTION

3.2.1 River Water

Samples were collected from the Wensum river and its tributaries and drains between February 2007 and September 2009. The majority of samples were collected manually, using a sampling bucket suspended from access bridges on a rope. The bucket was rinsed by filling it then emptying it onto the bank three times. The sample was taken on the fourth filling and sub-sampled into a smaller similarly rinsed bucket. Vinyl gloves were worn during sampling. Field measurements of pH, Eh, dissolved oxygen (DO), electrical conductivity (EC) and temperature were made with the remaining sample in the bucket using electronic field meters which were calibrated on the day of use. The field meters were left to stabilise while the samples were filtered. From the sub-sampling bucket, a 50 ml tube was rinsed and filled with unfiltered water for alkalinity titration. Next, a 50 ml syringe was flushed three times with sample water then fitted with a 0.22 μm cellulose acetate filter unit. 15 ml of sample water was pushed through the syringe to waste to rinse the filter unit. Water was filtered directly into polystyrene screw-cap tubes which were first rinsed three times with a few ml of filtered sample water. Two 50 ml tubes were filled leaving 15 ml of headspace, for nitrate isotopic analysis. These samples were frozen within 12 hours in a -20^{o}C freezer. Samples were removed from the freezer 24 hours prior to isotopic analysis and thawed out at room temperature. An additional two 15 ml tubes were filled for water isotope and major ion analysis without leaving headspace. Back in the laboratory, a 0.2 ml subsample was taken from the major ion tubes and added to a tube containing 9 ml deionised water which had been pre-acidified by the addition of 0.8 ml concentrated nitric acid to pH ~ 2, for trace element analysis. These samples were stored in the 4^{o}C cold store and the samples for water isotope analysis were sealed with parafilm and stored upside-down to ensure a gas tight seal. Prior to isotopic analysis samples were removed from the cold store and brought to room temperature over 24 hours.

Automatic water samplers (Epic) were used on one occasion. Samples are collected in 24 x 500 ml HDPE bottles via a hosepipe suspended in the river. All components coming into contact with sample water were pre-cleaned in 5% Decon. Samples were

collected using the field protocol outlined above. Two samplers programmed to sample at hourly intervals for 24 hours were sited at Fakenham gauging station (TG 919294) and Swanton Morley gauging station (TG 020184) as a major storm was unfolding. The samples were prepared using the field protocol outlined above.

3.2.2 Groundwater

All of the boreholes sampled had fixed submersible pumps, with most discharging through irrigation hoses. Pumps were switched on and left to pump to waste for 15 minutes to flush before samples were collected in a bucket and prepared using the field protocol. The odour and colour of the sample were noted. Although the preferred method to measure well head parameters was to use a flow cell, borehole owners wished for the samples to be taken as quickly as possible to minimise interruption to their work. For this reason, pH, Eh, DO, EC and temperature were measured from borehole samples in the bucket. This compromise was felt to be acceptable because well head parameters are less relevant to this study than the less transient hydrochemistry of groundwater which is likely to be retained in baseflow to the rivers. Three groundwater samples had to be discounted. Two samples from one location collected in spring and autumn were discarded after it was discovered that the samples were collected after ion exchange treatment. Another sample was discarded because it was likely that contamination had occurred. Of the remaining groundwater samples, one had a nitrate concentration below the measurement limit for isotopic analysis.

3.2.3 Nitrate Sources

Precipitation was collected in large Decon washed plastic boxes on an event basis from a garden in Norwich, filtered on collection through a pre-rinsed 50 ml plastic syringe fitted with a 0.22 μm cellulose acetate filter unit into aliquots, one for liquid ion chromatography stored at 4^{o}C, one for water isotope analysis sealed with parafilm and stored upside-down at 4^{o}C, and the third, frozen at -20^{o}C for subsequent nitrate isotopic analysis. Dry deposition aerosol samples were collected over a ten-day period in summer 2008 using a three-stage cascade impact aerosol sampler on the roof of the Environmental Sciences building at the University of East Anglia, (Baker, 2004), calibrated and set at a flow rate of 1 m^3/min, and fitted with two slotted filters on plates

3 and 4, and one back-up filter, all Whatman 41 cellulose filters. Filters were changed once a day, and used filters were folded inwards and frozen at -20^{o}C for later preparation. During preparation, the edge was cut off all filters, and the filter folded into quarters. These quarters were cut into small pieces directly into 50 ml tubes. Quarters from the two slotted filters were combined in one tube to represent aerosol size < 1 micron diameter, and the back-up filter was cut into a different tube to represent aerosol size > 1 micron diameter. The 1 micron cut-off represents the boundary between larger mechanically generated particles and smaller particles produced in the atmosphere from gases (Baker *et al.*, 2007). 20 ml of deionised water was added to each tube and the tubes were sonicated at room temperature for 1 hour. A 20 ml plastic syringe was rinsed three times with deionised water, and 4 ml of sample water was pushed through the syringe to waste to rinse the 0.22 μm cellulose acetate filter unit. Aliquots of the filtered samples were analysed by liquid ion chromatography for concentrations of NO_3^- and NO_2^- and the remaining sample aliquots were frozen for subsequent isotopic analysis. Filter blanks were analysed alongside samples.

Sewage effluent and suspensions of cattle and chicken manure in deionised water were filtered through pre-flushed 0.22 μm cellulose acetate filter units into 50 ml pre-rinsed tubes. Aliquots were taken for liquid ion chromatography, and the remaining split was frozen. The waste was autoclaved before disposal. The nitrate fertiliser samples were dissolved in deionised water, aliquots measured by liquid ion chromatography, and the remaining fraction frozen until isotopic analysis.

3.2.4 Flow and Precipitation Data

Flow data (daily mean flow and 15-minute sampling interval) from gauging stations on the Wensum at Fakenham, Swanton Morley and Costessey Mill were kindly supplied by the Environment Agency. Daily precipitation data for Norfolk from the Met Office Midas Land Surface Observation Data was acquired from the British Atmospheric Data Centre.

3.3 ANALYSIS OF N AND O ISOTOPES OF NITRATE

3.3.1 Sample Analysis

NO_3^- was converted to N_2O using the denitrifier method (Sigman *et al.*, 2001, Casciotti *et al.*, 2002) and its isotopic composition measured against a laboratory cylinder N_2O reference gas on a Europa Geo 20:20 continuous flow gas chromatograph isotope ratio mass spectrometer (GCIRMS), with a TG II prep system which uses Valco valves to control carrier gas circulation, a customised Gilson autosampler, and an open split interface (Rockmann *et al.*, 2003). Conversion of dissolved NO_3^- to a gas (N_2O) was necessary to enable isotopic analysis on the Geo 20:20. N_2O was extracted and purified from sample vials before isotopic analysis. The purge and trap and extraction and purification system on the Geo relies on the different freezing and boiling points of N_2O, N_2, He, H_2O and CO_2 (Appendix 1). N_2O from sample vials was purged for 500 seconds from headspace with helium using a double needle, and trapped in a cryogenic trap consisting of a steel loop immersed in liquid nitrogen (LN_2), then cryo-focussed into a second steel loop immersed in LN_2. Before the steel loops, the helium carrier gas-headspace gas mixture was cleaned by passing it through a reverse flow Nafion drier and a magnesium perchlorate trap to remove H_2O, a Carbosorb trap to remove CO_2 and a Supelco F trap to remove volatile organic compounds (Kaiser *et al.*, 2007). A stationary loop immersed in a dry-ice/ ethanol trap was placed in-line between the two LN_2 traps, to further remove H_2O cryogenically, with the trap removed at the end of the analysis to allow H_2O to be purged to waste. After cryofocussing the N_2O passed through a Varian Poraplot/Q pre-column to separate any further compounds which might cause interference. This column was back-flushed after the N_2O has passed through it. The N_2O then passed through a HP-PLOT/Q GC column which was kept at 30^oC in a GC oven. This enabled separation of CO_2 creating a short delay between passing the CO_2 and N_2O peaks to the mass spectrometer via the open split. This was necessary because CO_2 causes isobaric interference at masses 44, 45 and 46, the masses measured for N_2O. N_2O reference gas from a cylinder was injected directly into the open split before the sample N_2O (Figure 3.2 and 3.3). Efficiency was maximised by purging and trapping the subsequent sample while the initial sample was purified and analysed.

The Geo 20:20 mass spectrometer measures masses 44, 45, and 46. In the mass spectrometer source, a heated filament produces electrons which bombard the N_2O molecules and ionise them to form N_2O^+. The ions are focused and accelerated along a flight tube through the magnetic sector where ions of a higher mass (incorporating the heavy isotopes) travel on a trajectory with a larger radius than those of a lower mass. This enables ions of masses 44, 45, and 46 to be collected in separate Faraday cups and the signals amplified. The 45/44 and 46/44 ratios are calculated by the Sercon Callisto operational software.

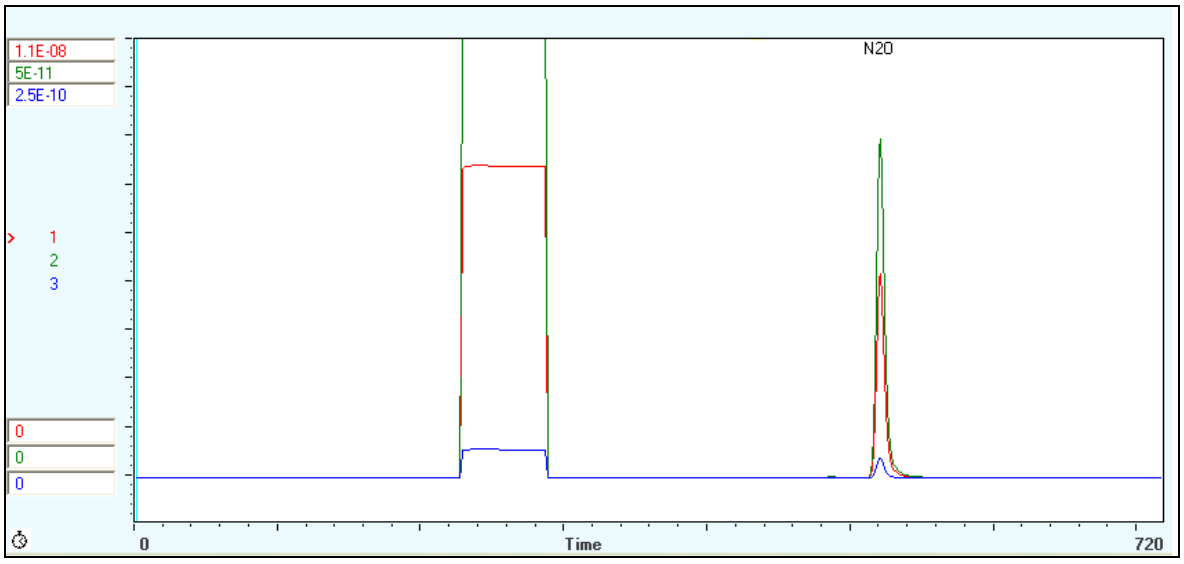

Figure 3.2 Trace from Sercon Callisto software showing N_2O reference gas peak (square top) and sample peak analysed on the Geo 20:20 GCIRMS.

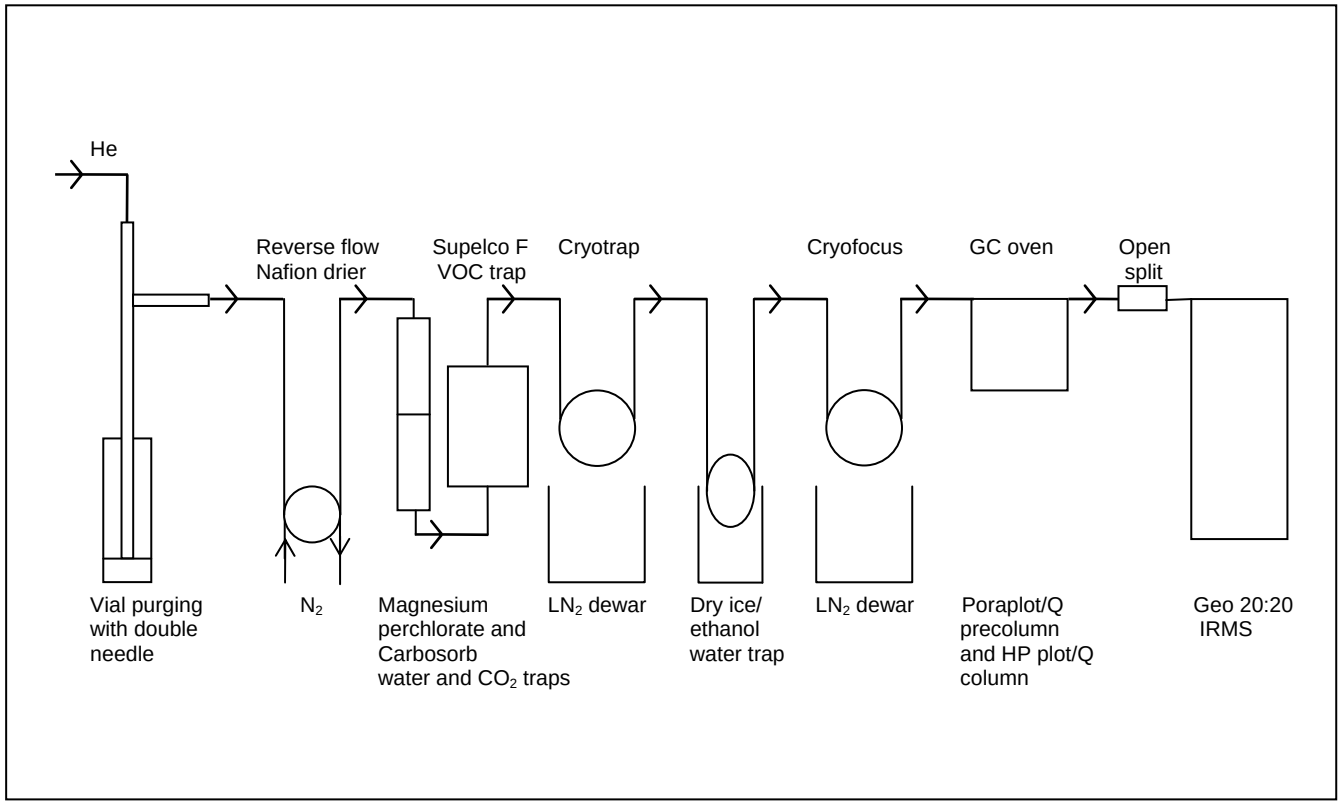

Figure 3.3 Schematic of N_2O extraction and purification line on the Geo 20:20 GCIRMS.

3.3.2 Day to Day Running, Routine Maintenance and Troubleshooting on the Geo 20:20

Set up and operation of the Geo 20:20 were controlled by the Sercon Callisto software. Before analysis, mass scans were carried out to check background levels of N_2, O_2, Ar, CO_2, and, using the on screen controls to manipulate the open split so that it was configured a) with He flow through the main length of the prep line to the GC flowing to waste, to measure backgrounds from the short distance of line after the GC, through the open split to the mass spectrometer; and b) so that He flow through the GC went to the MS, to measure backgrounds from the whole prep line beyond the double needle. These were compared day to day to monitor for any increase in background levels which could indicate a leak in the prep line. Following this, the mass spectrometer high voltage was tuned to N_2O by taking out the line from the GC to the open split and putting in the N_2O reference gas line using the on screen controls, and scanning voltage across the N_2O mass range (approximately 2700-2750 volts). Next the Nafion drier N_2 flow rate was turned up to 120 ml/ min, the LN_2 and dry/ice ethanol traps filled, and the carrier gas helium flow rate checked using a digital flow meter connected to an exit port at the back of the TGII. The sample run list was then written, and a set up file selected or adjusted. The set up file contained parameters which controlled the Gilson autosampler and TGII prep system, such as purge needle maximum depth and centring, purge time, the time at which valves were thrown, and the standard gas used. During a run, the LN_2 dewar was refilled approximately every four hours. After running for four hours or more, ice developed on the steel loops of the cryotrap and cryofocus. This acted to insulate the inside of the steel capillaries from the cold when the loops were immersed in LN_2, resulting in loss of sample from the trap. To prevent this, the loops were defrosted with a hand-held warm air drier when they were removed from the LN_2 dewar during the run.

If an increase in background levels was detected during the initial scans, valves and connections were examined using a helium detector, to detected low levels of leaking helium carrier gas. If the helium detector failed to detect a leak, valves and joint connections were sprayed with cylinder argon with the MS high voltage tuned to mass

40, so that any argon drawn into the line through a leak would be seen in a rise in background levels. If a leak was found, connection joints were tightened or remade with new ferrules.

Through day to day running, N_2O beam areas, which represent yield, from vials filled with 20 ppm N_2O were monitored for any decrease which could indicate the first signs of needle port blockage. The needle was prone to block after approximately 10 days of analysis runs through the formation of a white precipitate in the upper ports derived from the sodium hydroxide amended bacterial culture. To prevent this, once a week the needle was removed and flushed with deionised water using a syringe and blown dry with cylinder argon. Remounting the needle necessitated adjusting the settings of the automatic sampler needle depth and centring, and carrying out a background level scan with the needle in a vial to check for any leaks around the needle fittings.

Occasionally, interference appeared in the N_2O peaks from sample vials which could not be attributed to leaks. It was suspected that the interference was caused by the GC HP-PLOT/Q GC column retaining water or other compounds which were then slowly released. When this occurred, the column was reconditioned by baking it at 200^oC for 24 hours in the GC oven.

3.3.3 Sample Preparation

The denitrifier method is based on the conversion of nitrate and nitrite to nitrous oxide through the biochemical activity of a naturally occurring single strain bacterial denitrifier, *Pseudomonas aureofaciens* (ATCC #13985). This bacterium is a facultative anaerobe which, under low oxygen conditions, uses nitrate and nitrite as electron acceptors during anaerobic respiration. However, because this particular strain lacks nitrous oxide reductase activity, the usual denitrification pathway is truncated at the nitrous oxide step:

$$NO_3^- \rightarrow NO_2^- \rightarrow NO \rightarrow N_2O \,||\, (N_2 \text{ not produced}) \qquad \text{Equation 3.1}$$

The method used in this research, as developed by Sigman *et al.* (2001) and Casciotti *et al*. (2002), with minor adaptations, is described in brief here. The full laboratory protocol is included in Appendix 1. A freeze dried pellet of *Pseudomonas aureofaciens* was resuspended in nutrient-enriched Tryptic Soy Broth media (TSB) and cultured on nutrient-enriched Tryptic Soy Agar (TSA) plates to derive single colonies of bacterial culture. These single colonies were used to inoculate tubes of TSB and the culture was snap frozen in LN_2 in 1.5 ml aliquots as working stock, and stored in a - 80^{o}C freezer. Thereafter, working stock was used to inoculate TSA plates, from which single colonies were taken to inoculate tubes of TSB to grow on the culture. This culture was then used to inoculate pre-prepared sealed bottles of TSB. After six to ten days' incubation time the bacterial culture in the bottles was concentrated sevenfold by centrifuging to separate off the supernatant, and resuspending in a small volume of "nitrate free" TSB which had not been amended with nitrate. To this concentrated culture, antifoam was added to avoid excessive bubbling during purging, and 3 ml of culture concentrate was transferred to analysis vials. Vials were capped with rubber-butyl stoppers and crimp sealed to make a gas tight seal which allowed insertion and removal of needles without compromising the seal. Vials were purged with helium to remove oxygen and create anaerobic conditions within the vial, then transferred to a shaker table to encourage the conversion of any residual nitrate in the culture solution to nitrous oxide via anaerobic respiration. Vials were purged a second time to remove any such nitrous oxide from the headspace while keeping conditions in the vial anaerobic. Vials were then injected with a volume of sample which contained 20 nanomoles of nitrate. Sigman *et al.* (2001) recommend that injection volumes should not be more than five times the volume of the culture solution in the vial to ensure quantitative conversion of NO_3^- to N_2O. For the majority of samples this was not an issue as injection volumes were between 20 μL and 100 μL with a mean value close to 50 μL. Batches of international and laboratory nitrate standards using 50 μL injections of 400 μM concentration were prepared at the same time, and further vials were left with no nitrate injection, to be analysed as bacterial blanks. Vials were left inverted overnight to enable the bacterial culture to covert nitrate to nitrous oxide, then the bacteria were lysed by injecting each vial with 0.2 ml of a 6 molar sodium hydroxide solution. Experiments confirmed that after sodium hydroxide injection, vials in an inverted position could be left for at least a week before analysis

without any loss of headspace gas, change in the isotopic value of standards, or increase in blank size.

International nitrate isotope calibration standards of accepted isotopic compositions which encompass the expected isotopic values of the samples were processed and analysed alongside samples, with isotopic measurements made relative to a cylinder reference gas using reference gas δ values set to 0.00 ‰. In this research, three international nitrate standards with isotopic compositions reported in Bohlke *et al.* (2003) were used (Table 3.1). Nitrogen isotopic composition is reported relative to air, and oxygen isotopic composition relative to VSMOW (Vienna Standard Mean Ocean Water).

Table 3.1 Isotopic composition of international nitrate reference standards used in this study reported in Bohlke *et al*.(2003). Precision: $\delta^{15}N_{NO3} \pm 0.1$ ‰, $\delta^{18}O_{NO3} \pm 0.3$ ‰ and O $\delta^{17}O_{NO3} \pm 0.3$ ‰.

Isotopic composition of international nitrate references (Bohlke *et al.*, 2003).	**$\delta^{18}O_{NO3}$ ‰** vs. VSMOW	**$\delta^{15}N_{NO3}$ ‰** vs. AIR	**$\delta^{17}O_{NO3}$ ‰** vs. VSMOW
Reference standard			
USGS 34 KNO_3	- 27.9	- 1.8	- 14.8
USGS 35 $NaNO_3$	57.5	2.7	51.5
IAEA N3 KNO_3	25.6	4.7	13.2

There are three sources of error inherent in the denitrifier method. The first is the isotopic fractionation of oxygen in product N_2O caused by the fact that five out of six oxygen atoms are lost during the conversion of NO_3^- to N_2O, which uses two molecules of NO_3^- to produce one molecule of N_2O:

$$2NO_3^- \rightarrow 2NO_2^- \rightarrow 2NO \rightarrow N_2O \qquad \text{Equation 3.2}$$

During this reduction pathway, isotopically light oxygen atoms are preferentially selected as electron acceptors and lost from the product, leading to an isotopic enrichment in N_2O oxygen of approximately $\Delta^{18}O_{N2O} = 40$ ‰. Although this effect cannot be accurately determined without calibrating the cylinder reference gas N_2O, by setting the reference gas δ values to 0.00 ‰, the stability of this effect can be monitored within and between bacterial batches using the international standards to monitor the

consistency of the method. If the NO_3^- is quantatively reduced to N_2O there is no net fractionation of nitrogen isotopes as all nitrogen atoms are retained in the product.

The second error is caused by oxygen exchange with water which occurs during denitrification. Tests comparing oxygen exchange from NO_3^- standards to that from NO_2^- standards found no additional exchange with the NO_3^- standards suggesting that the exchange takes place at the $2NO_2^- \rightarrow 2NO$ step (Sigman *et al.*, 2001, Casciotti *et al.*, 2002). The international nitrate standards span a wide isotopic range for $\delta^{18}O_{NO3}$ of 85.4 ‰ (USGS 34 $\delta^{18}O_{NO3}$ -27.9 ‰ to USGS 35 $\delta^{18}O_{NO3}$ 57.5 ‰). The effect of oxygen exchange with water on this range is to shrink it by modifying the oxygen isotopic composition of the USGS standards with addition of oxygen of an isotopic composition within the range of the standards (the deionised water from our laboratory has $\delta^{18}O_{H2O}$ -6.9 ‰, within the standard range). This scale compression is useful as it can be used to quantify the fraction of N_2O oxygen derived from the original nitrate standards using Equation 3.3 (Coplen *et al.*, 2004):

$$O_{NO3R} = \frac{[((1+\delta^{18}O_{N2O}\text{-USGS35})/ (1+\delta^{18}O_{N2O}\text{-USGS34})) -1]}{[((1+\delta^{18}O_{NO3}\text{-USGS35})/ (1+\delta^{18}O_{NO3}\text{-USGS34})) -1]} \qquad \text{Equation 3.3}$$

where O_{NO3R} is the oxygen fraction from the nitrate standards retained in the N_2O product; $\delta^{18}O_{N2O}$-USGS35 and $\delta^{18}O_{N2O}$-USGS34 are the measured isotopic composition of N_2O from these standards relative to the reference gas; and $\delta^{18}O_{NO3}$-USGS35 and $\delta^{18}O_{NO3}$-USGS34 are the accepted values of these nitrate standards.

The third source of error is the N_2O blank from bacterial vials (which were not injected with NO_3^-). This is the only effect which can influence both measured $\delta^{15}N_{N2O}$ and $\delta^{18}O_{N2O}$. Sigman *et al.* (2001) and Casciotti *et al.* (2002) found that the bacterial blank represented 5% of the N_2O produced from a standard, which, assuming complete conversion of NO_3^- to N_2O is equivalent to 0.5 nanomoles of N_2O. Due to the wide variability in measured isotopic composition of the bacterial blank, numerically correcting for the blank effect, based on measurements from a the small number of blanks included in each analysis could lead to additional error. For this reason the blank

effect is corrected implicitly by calibrating to standards which also contain a contribution from the bacterial blank. The oxygen exchange calculations using Equation 3.3 also includes the effects of any isotopic scale compression from the bacterial blank.

The three effects of isotopic fractionation of oxygen, oxygen exchange with water, and the bacterial N_2O blank should be consistent within a bacterial batch, meaning that the effects can be monitored for each analysis run to check that the method is working consistently. These effects on measured $\delta^{18}O_{N2O}$ can be approximated by the following mass balance equation (Casciotti *et al.*, 2002), which is based on the assumption that oxygen exchange with water does not incur isotopic fractionation:

$$\delta^{18}O_{N2O}\text{measured} = (\delta^{18}\text{Otrue} + \varepsilon)\, s\, (1 - x) + \delta^{18}O_{H2O}\, s\, x + \delta^{18}O_b\, b \quad \text{Equation 3.4}$$

where all $\delta^{18}O$ values are relative to VSMOW and: δ^{18}Otrue is the true oxygen isotopic composition of the nitrate standard; ε is the net isotopic fractionation from preferential removal of five out of six oxygen atoms; s is the amount of sample nitrate added (mol); x is the fraction of oxygen atoms in product N_2O which originate from oxygen exchange with water; $\delta^{18}O_{H2O}$ is the isotopic composition of oxygen in the water; $\delta^{18}O_b$ is the isotopic composition of oxygen in the blank; and $_b$ is the amount of N_2O in the blank (mol).

There are two further factors which need to be taken into account with the denitrifier method. The first is that *Pseudomonas aureofaciens* denitrifies both NO_3^- and NO_2^-, so the measured isotopic composition of samples which contain both compounds will represent N_2O derived from $NO_3^- + NO_2^-$. The effect of this has been investigated by Casciotti and McIlvin (2007), who concluded that if the molar amount of NO_2^- represents less than 1% of the combined molar amount of $NO_3^- + NO_2^-$, it can be ignored as it will have a negligible effect on the isotopic composition of product N_2O (i.e. within measurement error). The authors suggest that if the concentration of NO_2^- is high enough to interfere with the isotopic composition of product N_2O it can be removed using the ascorbic acid method (Granger *et al.*, 2006). In this study, concentrations of NO_2^- were consistently less than 1 % so no action was taken.

Finally, a correction is necessary for the ^{17}O contribution to mass 45, the mass which is usually attributed to ^{15}N (Equation 3.5):

N_2O at m/z 45: $^{14+15+16}_{N\ N\ O}$ or $^{14+14+17}_{N\ N\ O}$ Equation 3.5

There is a mass dependent relationship between $\delta^{17}O$ and $\delta^{18}O$ which is expressed by the formula $\delta^{17}O = 0.5279\ \delta^{18}O$ (Barkan and Luz, 2005), enabling correction of results for the mass dependent ^{17}O contribution to mass 45.

Kinetic and equilibrium isotope fractionations are caused by the different atomic masses of the isotopes and are therefore mass dependent (Chapter 2). Isotopic fractionation which is not controlled by isotope mass difference is called mass-independent fractionation. If the relationship between $\delta^{17}O$ and $\delta^{18}O$ diverges from the mass-dependent formula above due to incorporation of additional mass-independently fractionated ^{17}O, the sample is said to contain a ^{17}O anomaly. NO_3^- of atmospheric origin often contains a ^{17}O anomaly which is thought to derive from mass-independent fractionation of ^{17}O during the formation of tropospheric ozone which is then transferred to atmospheric NO_3^- during the oxidation of NO_x by ozone in the atmosphere (Michalski and Xu, 2010). The $NaNO_3$ standard USGS 35 contains mass-independently fractionated ^{17}O and the contribution of this ^{17}O anomaly to mass 45 requires correction before calibration curves for $\delta^{15}N$ are made. Although anomalous ^{17}O could also affect mass 46 (in the form of 14+15+17) this is a very rare configuration and its contribution would be too small to affect measured values within expected precisions (Bohlke *et al.*, 2003).

An equation devised by McIlvin and Altabet (2005) can be used to correct for the ^{17}O contribution at mass 45, whether it is caused by mass dependent or mass independent fractionations:

$$\delta^{15}N_{N2Osample} = \delta^{45}N_{N2Osample}\,[1 + {}^{17}R_{std}/\,(2\,{}^{15}R_{std})] - \delta^{17}O_{NO3}\,[{}^{17}R_{std}/\,(2\,{}^{15}R_{std})]$$

Equation 3.6

where $^{17}R_{std}$ and $^{15}R_{std}$ are the $^{15}N/^{14}N$ and $^{17}O/^{16}O$ ratios of the N_2O reference gas as measured by the IRMS, and $\delta^{17}O_{NO3}$ refers to the total $\delta^{17}O$ of the sample or standard, including any contribution from a ^{17}O anomaly. The ^{17}O anomaly of the USGS 35 standard has been measured as $\Delta^{17}O$ 20.87 ‰ (Kaiser *et al.*, 2007) such that $\delta^{17}O_{N2O}$ USGS 35 = ($\delta^{18}O_{N2O}$ x 0.5279) + 20.87 ‰. In order to correct the ^{17}O anomaly in samples containing atmospheric NO_3^-, it is necessary to measure $\delta^{17}O_{N2O}$. However, this was not within the scope of this study. Instead a range of values for the ^{17}O anomaly from precipitation of $\Delta^{17}O$ = 17 ‰ to 31 ‰ presented in Kaiser *et al.* (2007) was used to correct atmospheric samples to calculate maximum and minimum $\delta^{15}N_{NO3}$ values for atmospheric samples.

Theoretically, if accurate amounts and isotopic values can be determined for isotopic fractionation due to preferential oxygen loss, oxygen exchange with water, and the bacterial blank, a numerical correction for these factors is possible. However, there are inherent difficulties in this, due to problems in obtaining accurate values for each parameter in each analysis run, such as the true isotopic composition of the bacterial blank. Instead, by correcting for the ^{17}O anomaly of USGS 35 and forming a calibration curve from the measured values of the international nitrate standards with respect to the N_2O reference gas and their accepted values, these effects can be corrected robustly, avoiding propagation of errors associated with the quantification of all the error-causing parameters. Moreover, in each analysis run, four or five sets of the three international standards are included, meaning that inherent corrections in the calibration are based on twelve to sixteen measurements.

3.3.4 Data Reduction

The data reduction methodology used in this research involves drift correction, ^{17}O correction, ^{17}O anomaly correction for USGS 35, quantification of the percentage of oxygen retained and the relative size of the bacterial blank, creation of calibration curves, and checking the curves with a laboratory standard (SIL-TF). Further details are provided in Appendix 1.

The N_2O reference gas pulse analysed before each sample vial N_2O peak (Figure 3.3) was used to correct measured values from sample vials for drift from the mass spectrometer. This reference gas was 99.999% volume N_2O, purity grade 5 (Aire Liquide). Figures 3.4a and b show a typical pattern of drift seen during a 10 hour analysis run. It was not clear what caused this phenomenon, and patterns of drift varied from day to day. In order for drift corrections to be made, measured isotope ratios of the reference gas pulses and the sample vials were converted to δ values using the equation $\delta = ((R_{sample}/ R_{standard}) - 1) \times 1000$ (‰). For the reference gas pulses $R_{standard}$ refers to the ratios of the first N_2O reference gas pulse in the analysis run, set to 0.0 ‰, and R_{sample} refers to the ratios of the subsequent pulses. The Callisto software did not enable the use of a reference gas pulse as the reference for sample vials. Instead a sample vial purged with 20 ppm N_2O (BOC) (30 ml/ min for 15 minutes) was used. So, measured isotope ratios of sample vials were converted to δ values using $R_{standard}$ from the vial purged with 20 ppm N_2O in the first position in the analysis run. Each analysis run started with at least four 20 ppm N_2O vials. If either the first reference gas pulse or the first 20 ppm vial ratios appeared anomalous, the subsequent position was selected as the reference. Drift correction was undertaken against the reference gas pulse, working on the assumption that the pattern of drift seen in the reference gas also affected sample vials. For drift correction reference gas δ values were subtracted from sample δ values. In addition to the reference gas pulse which was injected directly in-line before the MS, further sample vials purged with 20 ppm N_2O were scattered throughout the analysis run in order to monitor the performance of the extraction and purification line (Figures 3.4a and b).

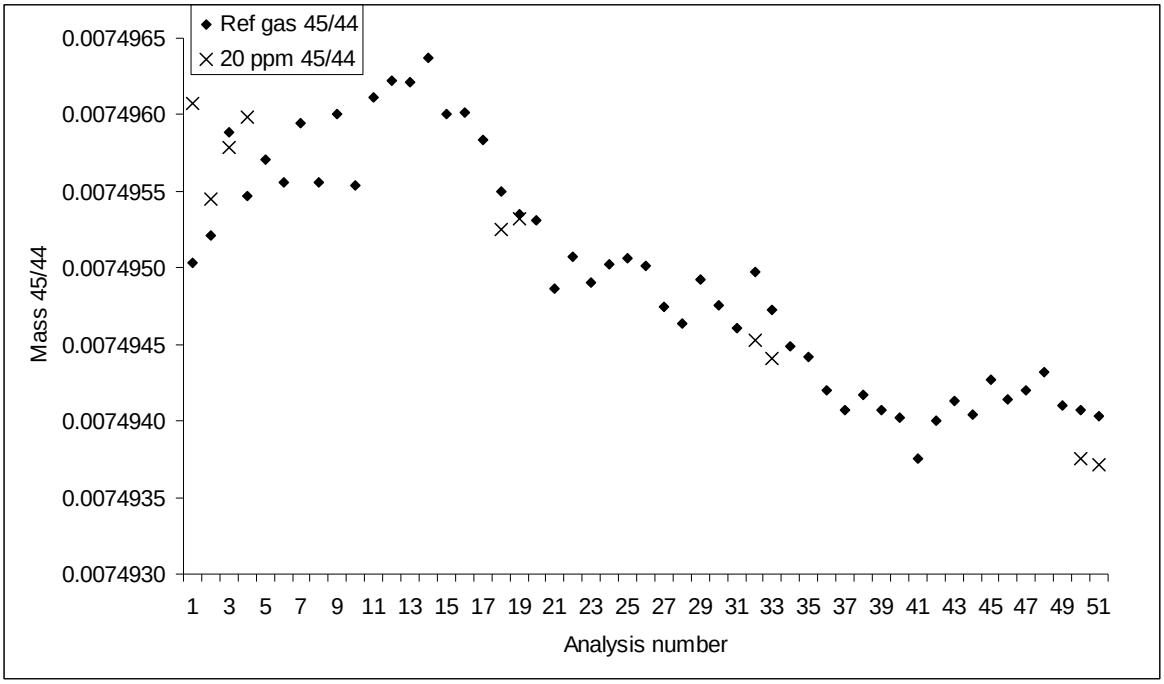

Figure3.4a Ratios of N_2O mass 45/44 of reference gas N_2O pulses and 20 ppm N_2O purged sample vials in a 51-sample analysis run. Range of drift is equivalent to approximately $\pm$ 0.2‰.

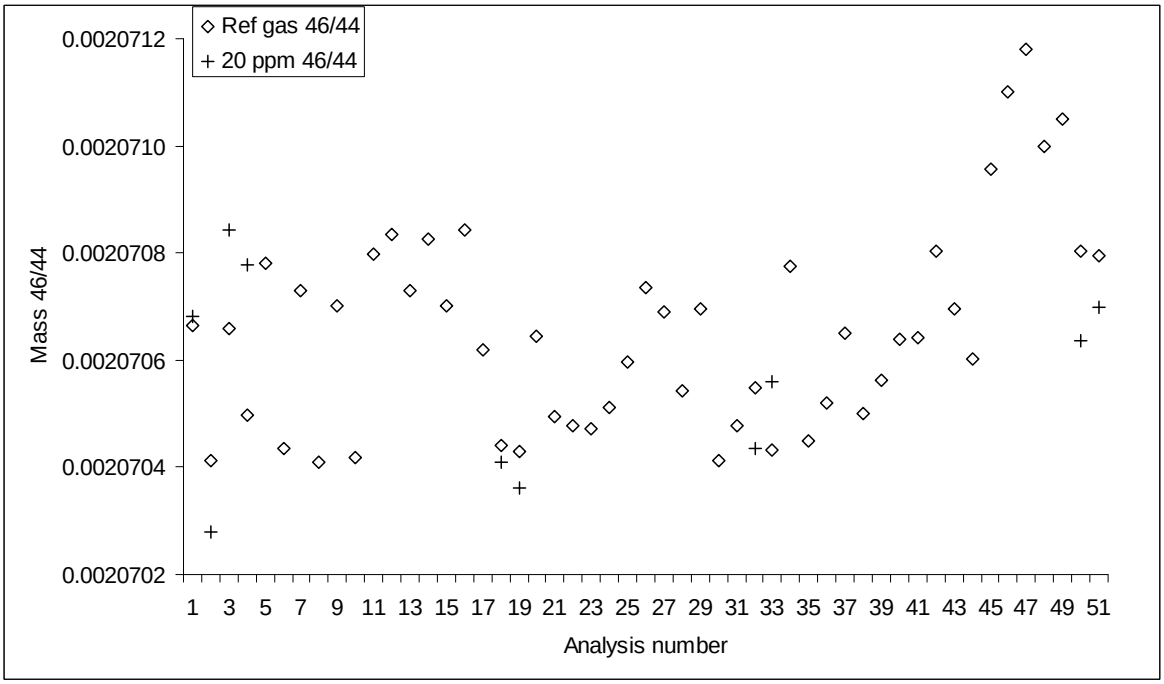

Figure 3.4b Ratios of N_2O mass 46/44 of reference gas N_2O pulses and 20 ppm N_2O purged sample vials in a 51-sample analysis run. Range of drift is equivalent to approximately $\pm$ 0.2‰.

Following drift correction, the mass dependent ^{17}O correction was made for all samples using Equation 3.6 (McIlvin and Altabet, 2005), with $\delta^{17}O_{N2O}$ ‰ = ($\delta^{18}O_{N2O}$ x 0.528) ‰, and the ^{17}O anomaly of the USGS 35 standard was corrected using $\delta^{17}O_{N2O}$ =

($\delta^{18}O_{N2O}$ x 0.528) + 20.87 ‰ (Kaiser *et al.*, 2007). Once correction for drift and ^{17}O had been carried out, the performance of the denitrifier culture and data consistency with previous analysis runs was checked by calculating the percentage of oxygen retained from the NO_3^- standards and the size of the bacterial blank relative to the standards using equations set out above.

The mean percentage of oxygen retained (i.e. sourced from the original nitrate molecule as opposed to oxygen from water via oxygen exchange, or from the N_2O blank), across 28 analysis runs was 96% with a range of 92% to 98%. The mean beam area of the N_2O blank across the analysis runs, was smaller than the 5% reported by Sigman *et al.* (2001) and Casciotti *et al.* (2002), representing 1.4 $\pm$ 0.7 % of the mean beam area of N_2O from the calibration standards from all analyses.

Calibration curves were made using x,y plots of the mean corrected δ_{N2O} values from each of the three international NO_3^- standards against their accepted δ_{NO3} values for nitrogen and oxygen, and best fit equations from these curves were used to calibrate measured values from sample vials in an Excel spreadsheet. However, the $\delta^{15}N_{NO3}$ range of the international standards is rather narrow, and does not encompass the more enriched nitrogen isotopic composition expected from samples impacted with agricultural nitrogen (Chapter 2). For this reason, a KNO_3 laboratory standard, SIL-TF, with an enriched $\delta^{15}N_{NO3}$ was analysed with each batch, and calibrated to the international reference standards, giving an isotopic composition of $\delta^{15}N_{NO3}$ 13.3 $\pm$ 0.1 ‰ and $\delta^{18}O_{NO3}$ 29.2 $\pm$ 0.1 ‰ (n = 80). As this isotopic composition had not been verified independently, it could not be used with the same confidence as the international standards. Instead, after the analysis work had been completed and the SIL-TF isotopic composition calculated from the full data set, a second series of calibration curves were created including SIL-TF, to verify the use of the international standards to calibrate for an extended range of $\delta^{15}N_{NO3}$ and as an extra indicator of the performance of the calibration standards (Figures 3.5a-d) (Appendix 1).

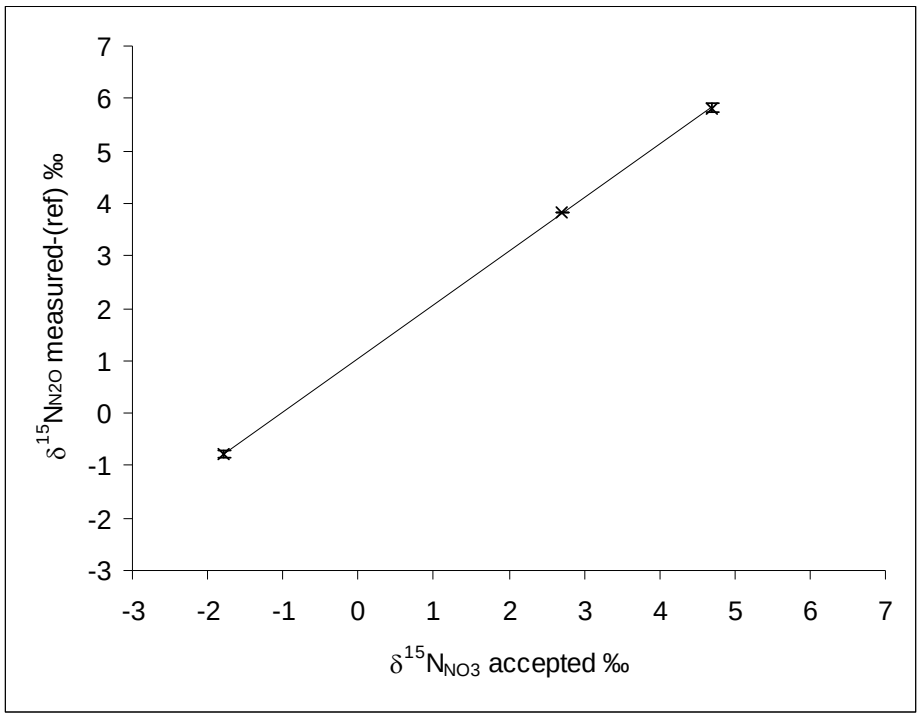

Figure 3.5a Example of calibration curve for $\delta^{15}N_{N2O}$ (‰) (relative to reference gas) versus $\delta^{15}N_{NO3}$ (‰) (accepted) for the three international standards IAEA-N3, USGS 34, AND USGS 35 from an analysis run using four replicates for each standard (error bars represent $\pm$ 1 standard deviation from the mean).

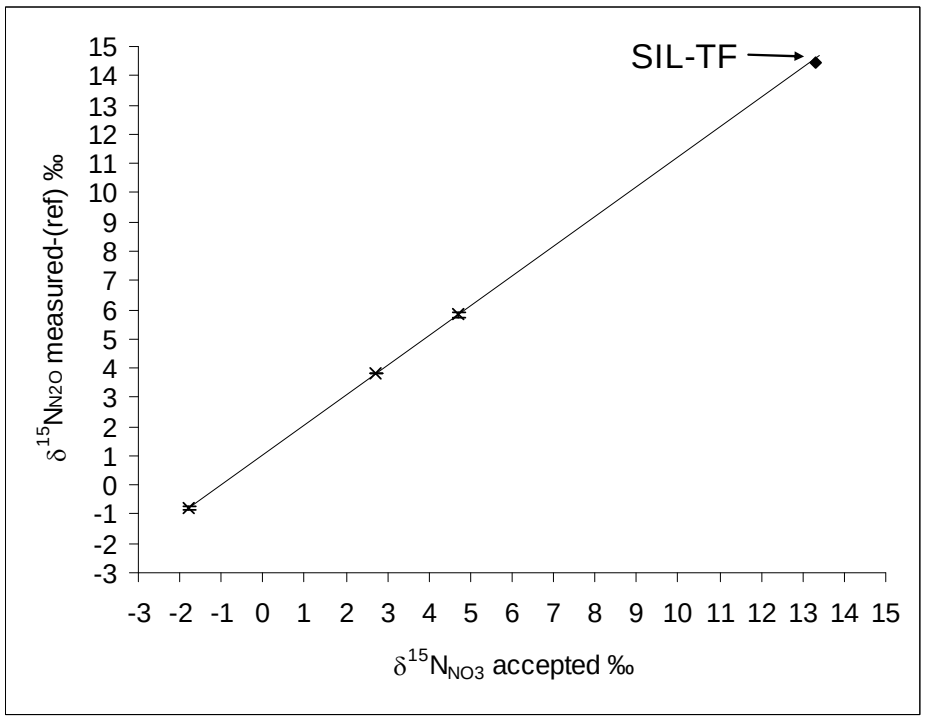

Figure 3.5b Example of calibration curve for $\delta^{15}N_{N2O}$ (‰) (relative to reference gas) versus $\delta^{15}N_{NO3}$ (‰) (accepted) for the three international standards IAEA-N3, USGS 34, AND USGS 35 with best fit line extended, and laboratory standard SIL-TF, from an analysis run using four replicates for each standard (error bars represent $\pm$ 1 standard deviation from the mean).

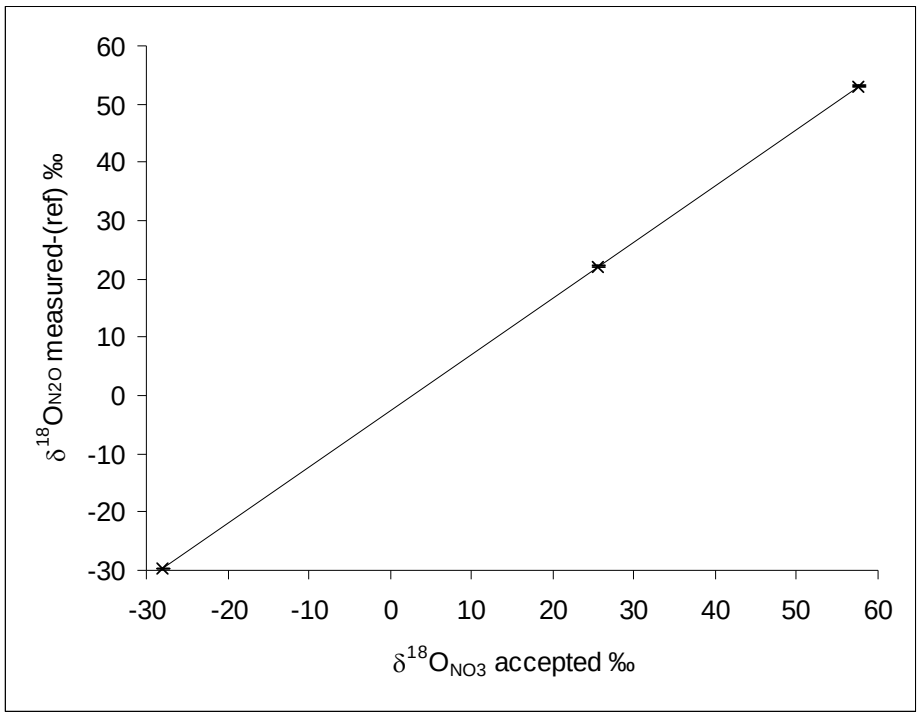

Figure 3.5c Example of calibration curve for $\delta^{18}O_{N2O}$ (‰) (relative to reference gas) versus $\delta^{18}O_{NO3}$ (‰) (accepted) for the three international standards IAEA-N3, USGS 34, AND USGS 35 from an analysis run using four replicates for each standard (error bars represent $\pm$ 1 standard deviation from the mean).

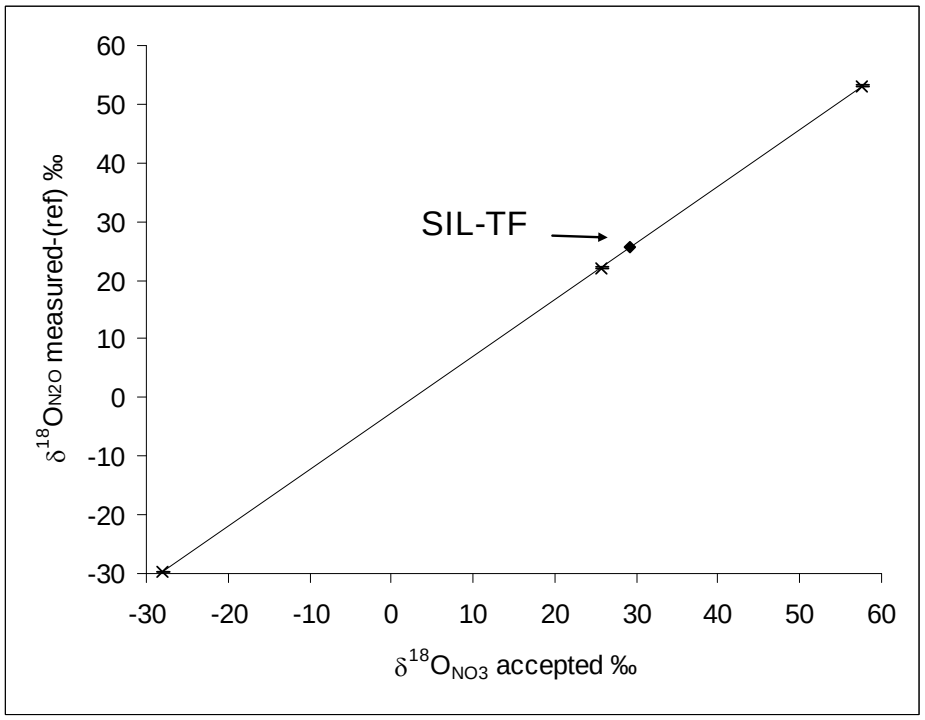

Figure 3.5d Example of calibration curve for $\delta^{18}O_{N2O}$ (‰) (relative to reference gas) versus $\delta^{18}O_{NO3}$ (‰) (accepted) for the three international standards IAEA-N3, USGS 34, AND USGS 35 and laboratory standard SIL-TF from an analysis run using four replicates for each standard (error bars represent $\pm$ 1 standard deviation from the mean).

3.3.5 Precision

Analysis runs included the three international NO_3^- standards and SIL-TF in sets of four or five replicates depending on the number of samples in the run. The standard concentration was 400 μM NO_3^- and an injection volume of 50 μL was used to inject 20 nanomoles NO_3^-. The mean within-run precision based on one standard deviation from the means of replicate standard analyses was $\pm$ 0.11 ‰ for $\delta^{15}N_{NO3}$ and $\pm$ 0.14 ‰ for $\delta^{18}O_{NO3}$. Uncertainty is expressed in all data plots throughout this thesis using the within run analytical precision. Between run precision, from analysis of five samples each analysed a total of six times in six different analysis runs across the analysis period and based on the poorest reproducibility seen for each isotope was $\pm$ 0.23 ‰ for $\delta^{15}N_{NO3}$ and $\pm$ 0.28 ‰ for $\delta^{18}O_{NO3}$. Therefore, the overall confidence in the measured $\delta^{15}N_{NO3}$ and values is $\delta^{15}N_{NO3}$ $\pm$ 0.2 ‰ and $\delta^{18}O_{NO3}$ $\pm$ 0.3 ‰.

To calibrate the small number of samples with very low NO_3^- concentration (< 1 μM) which required injection volumes of 10 ml, the three international NO_3^- standards and SIL-TF were analysed at a concentration of 0.4 μM with an injection volume of 10 ml to inject 4 nanomoles NO_3^-. Within run precision based on one standard deviation from the means of replicate standard analyses was $\pm$ 0.64 ‰ for $\delta^{15}N_{NO3}$ and $\pm$ 0.75 ‰ for $\delta^{18}O_{NO3}$. However, because of the possibility of error caused by residual NO_3^- in the deionised water used to make up these standards, samples were also calibrated to standards of 400 μM NO_3^- and an injection volume of 10 μL to inject 4 nanomoles NO_3^-. The maximum difference in calibrated $\delta^{15}N_{NO3}$ and $\delta^{18}O_{NO3}$ values from the two standard sets was used to quantify the uncertainty due to calibration, which was $\pm$ 0.98 ‰ for $\delta^{15}N_{NO3}$ and $\pm$ 3.06 ‰ for $\delta^{18}O_{NO3}$.

3.3.6 Methods development

3.3.6.1 Extraction and Purification Line

Double needles for the automatic water sampler were made to our specifications. Once sample vials had been purchased, rack plates were designed to modify the Gilson autosampler rack in order to hold the maximum number of vials. The selection of the best GC column to separate the CO_2 and N_2O peaks was made through a process of trial

and error, with various columns tried until the HP-PLOT/Q GC was found to perform best. First the Nafion drier, and then the dry ice/ ethanol water trap were fitted in response to interferences seen in the N_2O trace, which we attributed to water. The Supelco F trap was fitted in response to an interference seen with high volume samples. Optimal flow rates were found through a process of trial and error for the helium carrier gas and N_2O reference gases.

3.3.6.2 N_2O Yield

Work began with the denitrifier group to set up the laboratory culturing protocol in early 2007. Initial tests on N_2O yield were carried out using a laboratory KNO_3 standard SIL-1. This standard was later analysed for isotopic composition which was found to be close to that of the international standard IAEA N3, so in later isotopic tests SIL-1 was discarded and IAEA N3 used instead. While we were working to set up the laboratory culturing protocol we were also working on the extraction and purification line on the Europa Geo 20:20 GCIRMS for nitrous oxide analysis from aqueous samples. Once we had established the denitrifier culturing protocol in the laboratory, the Geo 20:20 was not ready, so initial tests were carried out on a Shimadzu GC 8A gas chromatograph with an electron capture detector (ECD), calibrated by manually injecting 0.1, 0.3 and 0.5 ml of 995 ppm cylinder nitrous oxide. For the lower end of the calibration, 21 ml vials filled with outside air were purged with an assumed approximate concentration of 0.3 ppm N_2O (Khalil *et al.*, 2002), and the system blank was measured. This calibration was used to quantify the percentage of NO_3^- to N_2O conversion and recovery from 20 nanomole laboratory nitrate standard injections (SIL-1), and to quantify the procedural bacterial blank from 3 ml of bacterial culture (Figure 3.6). Stoichiometrically, the *Pseudomonas aureofaciens* denitrification pathway produces half the number of moles of N_2O product as those of NO_3^- substrate used, so 100% conversion and recovery should produce 10 nanomoles of N_2O. Results showed over 100% NO_3^- to N_2O recovery, with a mean of 11.3 $\pm$ 1.5 nanomoles of nitrous oxide (n = 16). The blank was approximately 1 % of the standard or 0.12 $\pm$ 0.05 nanomoles (n = 19). The remaining 10% above the expected yield may have been due to carry-over from the previous sample, or due to inaccuracies in the calibration. Taken together, the results from the bacterial standards and bacterial blank indicated that the culturing protocol was working successfully.

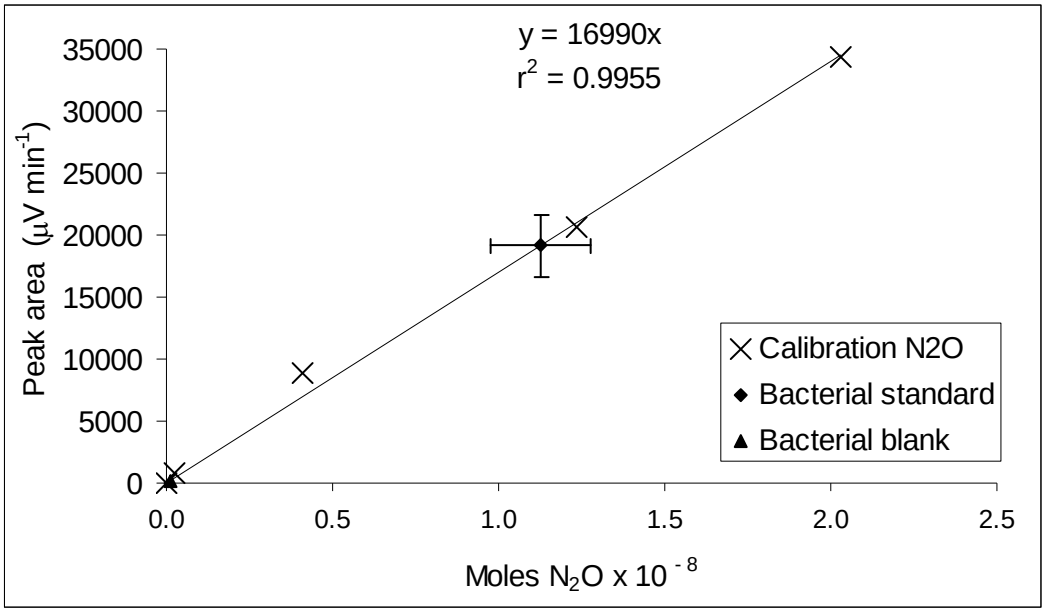

Figure 3.6 N_2O concentration calibration curve (peak area $\mu V\ min^{-1}$ versus moles $N_2O\ x10^{-8}$) showing concentration produced by the bacterial standard (SIL-1) and 3 ml bacterial blank. Error bars represent $\pm$ 1 standard deviation.

3.3.6.3 Headspace versus Liquid Purging

The nitrous oxide purge and trap extraction line on the Geo used a Gilson autosampler which we adapted to take 86 glass vials of 21 ml volume. A double needle with a lower port leading from the inner needle and an upper port leading from the outer needle was inserted through the rubber-butyl stopper of the sample vial. During purging, helium flowed out of the lower port creating pressure in the vial and forcing helium and headspace gas out through the upper port to the cryogenic trapping system of the TG II. Initially, I planned for the lower port to be submerged in the culture liquid in the sample vial during purging, but due to the length of needle shaft taken by the sharp tip which pierces the stopper, it was not possible for the engineers to site the lower port far enough down to guarantee that it would be submerged. In fact, at maximum needle depth, the lower port fell on, just below, or just above the meniscus of the culture liquid (Figure 3.7). This was due both to the small variations in liquid volume (usual range 3.0 to 3.1 ml) from minor variations in injection volumes of high-nitrate-concentration samples, and the day to day manipulation of the autosampler rack plates. Attempting to purge vials with the needle in the liquid could have led to additional sources of error due to differences in purging efficiency between submerged and non-submerged purging, and because of isotopic fractionation associated with gaseous and dissolved N_2O partitioning, so I decided to use headspace purging for all high-nitrate-concentration

samples. Theoretically, if NO_3^- calibration standards undergo identical treatment and analysis as samples, and match them closely in concentration and injection volume, any differences between the true isotopic composition of the total N_2O in sample vials, and that which is measured by headspace sampling or from incomplete purging should be corrected in the calibration (Morkved *et al.*, 2007). However, in order to better understand the system and so potential sources of error, I investigated headspace subsample isotopic composition and that of total N_2O in a sample vial.

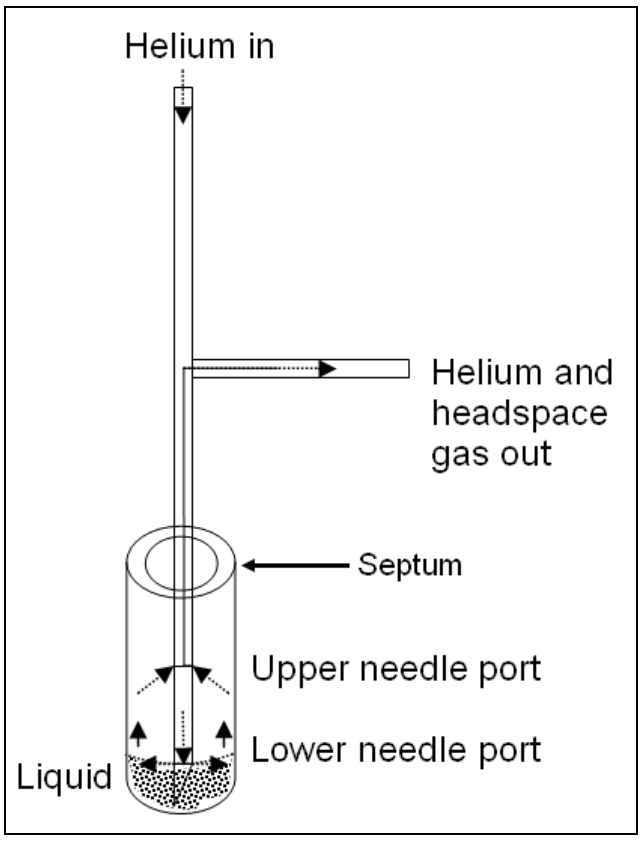

Figure 3.7 Schematic of sample vial containing 3 ml liquid during helium purging with double needle on Gilson autosampler showing lower needle port on meniscus.

At equilibrium, in the closed system of the vial, N_2O partitions between the headspace and the liquid. This partitioning is controlled by the ratio of liquid to headspace, temperature and pressure, and is described by the Ostwald coefficient (Wilhelm *et al.*, 1977), which expresses the ratio between moles of gas per litre of water and moles of gas per litre of gas in a closed system at equilibrium. At 20^{o}C and 101.325 kPa the Ostwald coefficient has been determined empirically to be 0.6788 (Wilhelm *et al.*, 1977) (Figure 3.8).

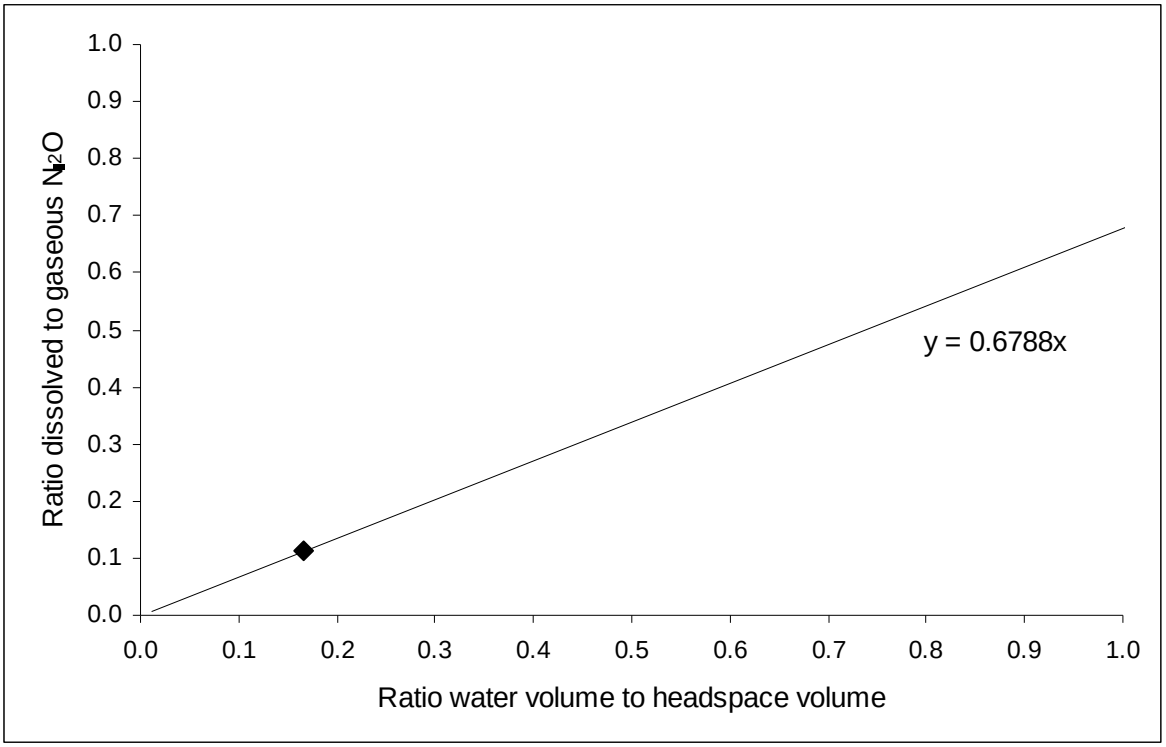

Figure 3.8 Ostwald coefficient shown as slope of the ratio of water volume to headspace volume versus the ratio of dissolved to gaseous N_2O in a closed system at equilibrium (Wilhelm *et al.*, 1977). Filled diamond represents conditions in sample vial used in this research.

Based on the assumption that the aqueous bacterial solution has similar properties to water, the Ostwald coefficient predicts that in a 21 ml sample vial with 3 ml liquid at 20°C and 101.325 kPa approximately 90 % of the N_2O will be in the headspace and 10 % dissolved in the liquid (Figure 3.8). The calculation was checked against a calculation with the temperature dependent Henry's law constant and mass balance equations using a method from Hudson (2004) (Appendix 1).

Equilibrium isotopic fractionation is associated with N_2O liquid/ headspace partitioning, and has been determined empirically by Inoue and Mook (1994), who found gaseous to dissolved equilibrium isotope enrichment factors of $\varepsilon^{15}N_{N2O}$ -0.75 ‰ and $\varepsilon^{18}O_{N2O}$ - 1.06 ‰ over a temperature range of 0°C to 44.6°C. Thus in our system before purging, we could expect the isotopic composition of N and O in N_2O in the liquid to be 0.75 ‰ and 1.06 ‰ heavier than in the headspace.

An isotope mass balance equation can be used to represent the isotopic composition of total bulk N_2O in the vial ($\delta_{totalN2O}$) from the mass balance of headspace and dissolved N_2O (Equation 3.7).

$$\delta_{totalN2O} = ((\ mol_{hsN2O}\ x\ \delta_{hsN2O}) + (\ mol_{lqN2O}\ x\ \delta_{lqN2O})) / (mol_{hsN2O} + mol_{lqN2O})$$

Equation 3.7

where subscripts $_{hs}$ and $_{lq}$ refer to the headspace (gaseous) and liquid (dissolved) fractions of N_2O.

Based on the isotope equilibrium fractionation and the gaseous to dissolved ratio of N_2O in the sample vial, Equation 3.7 can be used to predict the isotopic composition of headspace and dissolved N_2O (Appendix 1). If the isotopic composition of total bulk N_2O in the vial (δ_{total}) is set at 0 ‰ for both $\delta^{15}N_{totalN2O}$ and $\delta^{18}O_{totalN2O}$, at equilibrium the isotopic composition of headspace N_2O will be $\delta^{15}N_{hsN2O}$ - 0.075 ‰ and $\delta^{18}O_{hsN2O}$ - 0.106 ‰, and that of dissolved N_2O will be $\delta^{15}N_{lqN2O}$ 0.675 ‰ and $\delta^{18}O_{lqN2O}$ 0.954 ‰. Due to the greater proportion of N_2O in the headspace than the liquid, headspace N_2O isotopic composition is close to that of the total bulk isotopic composition while the isotopic composition of the smaller dissolved fraction is heavier than that of the bulk N_2O. Thus at a first approximation the error associated with subsampling the headspace is approximately - 0.1 ‰ for both N and O.

When N_2O is removed from the headspace through purging, the headspace/ liquid equilibrium partitioning is perturbed, and N_2O is evaded from the liquid into the headspace, leading to kinetic isotopic fractionation. For dissolved N_2O evading into headspace the kinetic isotope enrichment factors have been determined empirically as $\varepsilon_{g\text{-}l}{}^{15}N_{N2O}$ -0.70 ‰ and $\varepsilon_{g\text{-}l}{}^{18}O_{N2O}$ -1.9 ‰ (Inoue and Mook, 1994). This means that dissolved gas leaving the liquid during vial purging will be 0.70 ‰ and 1.9 ‰ lighter for N and O respectively than that left behind in the liquid, so at the start of purging the N_2O evaded from the liquid will have an isotopic composition of $\delta^{15}N_{lqN2O}$ -0.025 ‰ and $\delta^{18}O_{lqN2O}$ -0.946 ‰. As more N_2O is evaded into headspace from the liquid, the isotopic composition of the diminishing pool of N_2O in the liquid will become increasingly heavy, along with the isotopic composition of the N_2O evolved into the

headspace, which will be offset from the isotopic composition of N_2O in the liquid by the N and O kinetic isotope enrichment factors (Mariotti *et al.*, 1981).

The potential error associated with limited purging or headspace subsampling from a starting point of equilibrium fractionation followed by kinetic effects during purging should be negligible for $\delta^{15}N_{lqN2O}$, but for $\delta^{18}O_{N2O}$ could be larger than the initial figure of - 0.106 ‰ suggested by equilibrium fractionation, leading initially to a lighter measured value for $\delta^{18}O_{N2O}$ than the true value. With increasing purging the liquid-purged N_2O will have an increasingly heavy oxygen isotopic composition so this effect will decrease. Overall the effect of purging an increasing fraction of the liquid (either directly, or from headspace purging which evades the dissolved fraction in to headspace) will be to bring the bulk sample isotopic composition closer to the true composition of the N_2O.

In order to explore the theoretical calculations empirically, vials filled with 50 % deionised water and purged with 20 ppm N_2O were tested using headspace and liquid purging. The Ostwald coefficient predicts that in these vials 32 % of total N_2O will be dissolved in the water. 10.5 ml deionised water was pipetted into vials which were then crimp sealed, purged with helium for 15 minutes then purged with 20 ppm N_2O for 15 minutes. Two sets of vials containing ten replicates each were prepared. One set was analysed using headspace purging while the other was analysed using liquid purging. Included at the start of each run was a 20 ppm filled vial with no water, used as the reference with an isotopic composition set at 0.0 ‰. The experimental design assumed that the same amount of N_2O would be purged from both sets of vials so that a direct comparison between the isotopic composition of headspace and liquid purged vials could be made. However, results showed a 40 % increase in beam area between the headspace and liquid purged vials, indicating that headspace purging does not succeed in evading all dissolved N_2O from the liquid in this experimental set up (Figure 3.9). This meant that a differential mass spectrometer response to N_2O amount may have influenced measured isotopic composition so that a direct comparison of the isotopic composition of the two sets of vials was not robust. Notwithstanding this, the headspace purged vials had lighter $\delta^{15}N_{N2O}$ and $\delta^{18}O_{N2O}$ values than the 0.00 ‰ of the reference, supporting the trend of the theoretical calculations, though with both values lighter than

those predicted at equilibrium. In the case of $\delta^{18}O_{N2O}$ this could indicate the kinetic effects of an initial contribution from isotopically light dissolved N_2O evolved during headspace purging from the liquid. The liquid purged vials had a heavier isotopic composition than the headspace purged vials, which was also closer to 0.00 ‰, demonstrating the predicted effect of purging the liquid in bringing the overall sample isotopic composition closer to the true composition the N_2O. In addition, the $\delta^{18}O_{N2O}$ from the liquid purged vials was lighter than the reference, which again could indicate the initial purging of dissolved N_2O with isotopically light oxygen expected during kinetic fractionation. These results indicated that minor differences in measured isotopic composition are seen between headspace and liquid purged vials. However, due to differences in N_2O yield between the headspace and liquid purged vials, and the possibility that this would affect mass spectrometer response, it was not possible to attribute this solely to headspace/ liquid partitioning isotopic fractionation.

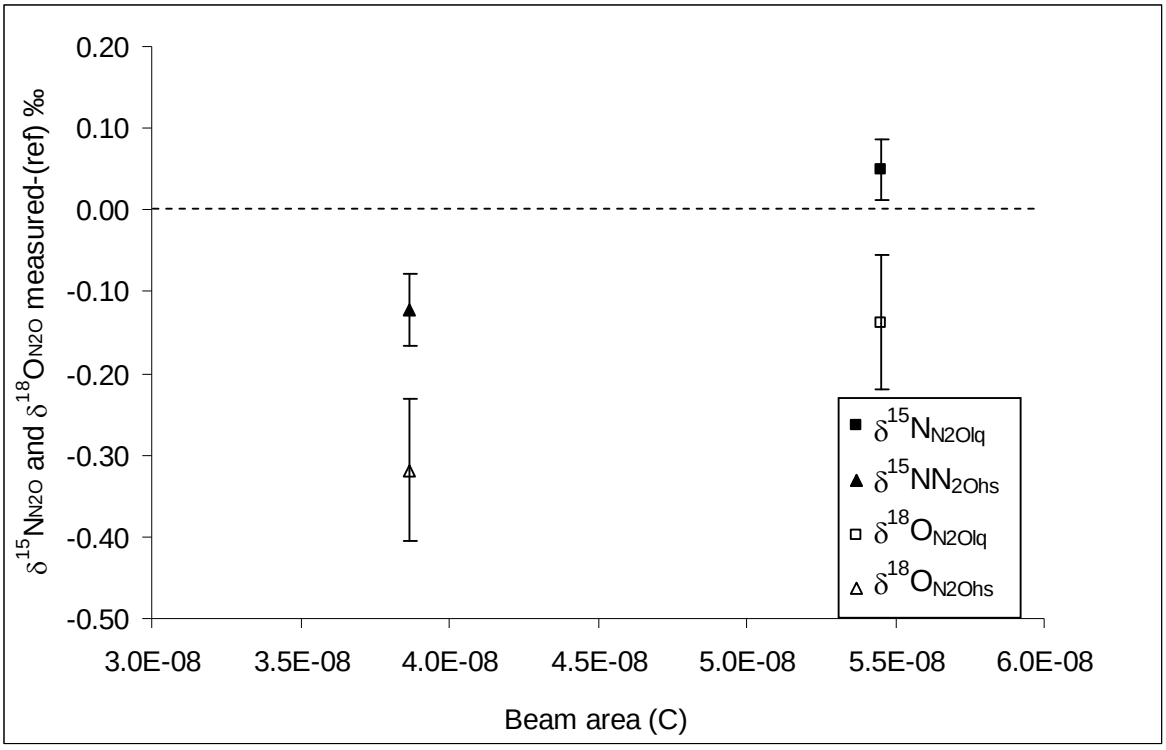

Figure 3.9 $\delta^{15}N_{N2O}$ (‰) and $\delta^{18}O_{N2O}$ (‰) (relative to reference gas) versus beam area (coulomb) of 21 ml sample vials filled with: i) 10.5 ml deionised water + 20 ppm N_2O, headspace purged; ii) and 10.5 ml deionised water + 20 ppm N_2O, liquid purged. Reference gas $\delta^{15}N_{N2O}$ and $\delta^{18}O_{N2O}$ set at 0.0 ‰, indicated by dotted line. Error bars represent $\pm$ 1 standard deviation from the mean (n=10 for each set).

3.3.6.4 Mass Spectrometer Response to N_2O Concentration

To investigate the mass spectrometer response to N_2O concentration bacterial sample vials were injected with different volumes of a laboratory 400 μM KNO_3 standard SIL-1 (injection volumes: 12.5, 25, 50, 100, and 200 μL). Results showed a linear response of the mass spectrometer in beam area (representing amount of N_2O) to injection volume (Figure 3.10). The isotopic composition became heavier with higher injection volumes for both isotopes, with $\delta^{15}N_{N2O}$ showing a near linear response, while the $\delta^{18}O_{N2O}$ response suggested a power function (Figure 3.11a and b). This response might indicate a non-linear relationship between oxygen exchange with water and NO_3^- concentration though the reason for this is not clear. The change in measured isotopic composition with beam area confirmed a differential mass spectrometer response to N_2O concentration, the importance of accurate liquid ion chromatography of samples prior to isotopic analysis in order to inject sample vials with a consistent amount of NO_3^-, and the necessity of calibrating to standards injected with the same amount of NO_3^- as the samples.

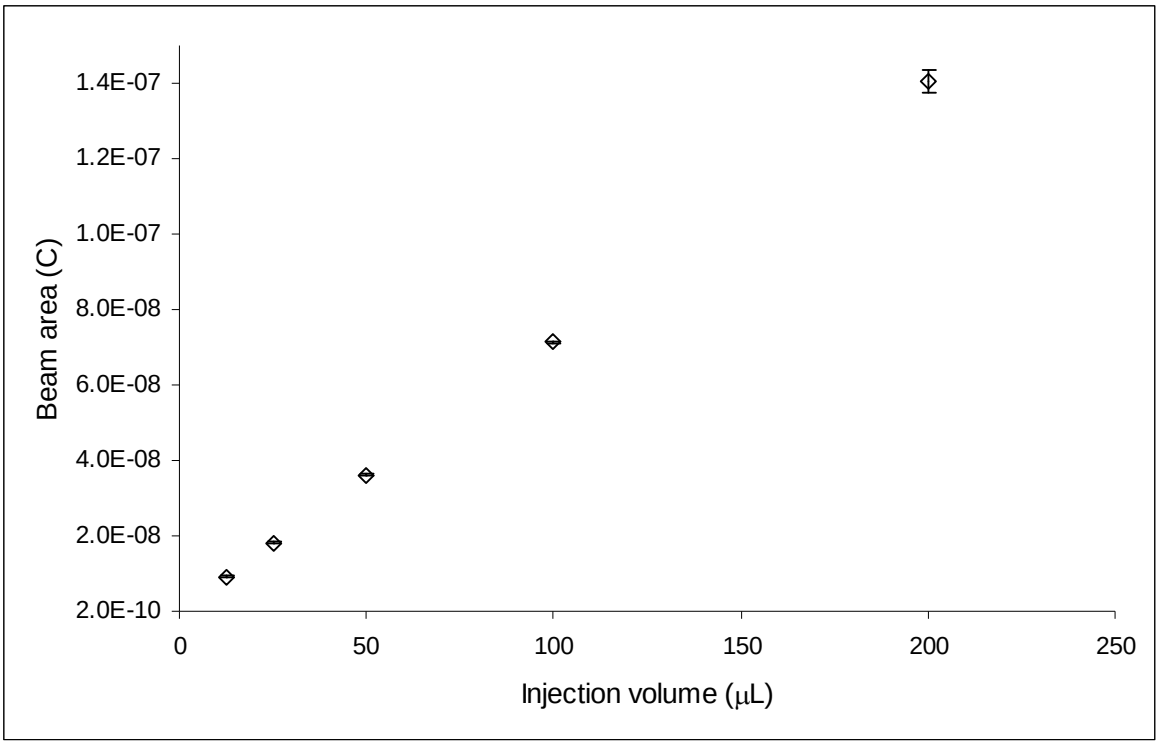

Figure 3.10 Beam area (coulomb) versus injection volume of 400 μM laboratory KNO_3 standard SIL-1 (in triplicate) injected into vials containing 3 ml of bacterial culture. Error bars represent ± 1 standard deviation from the mean.

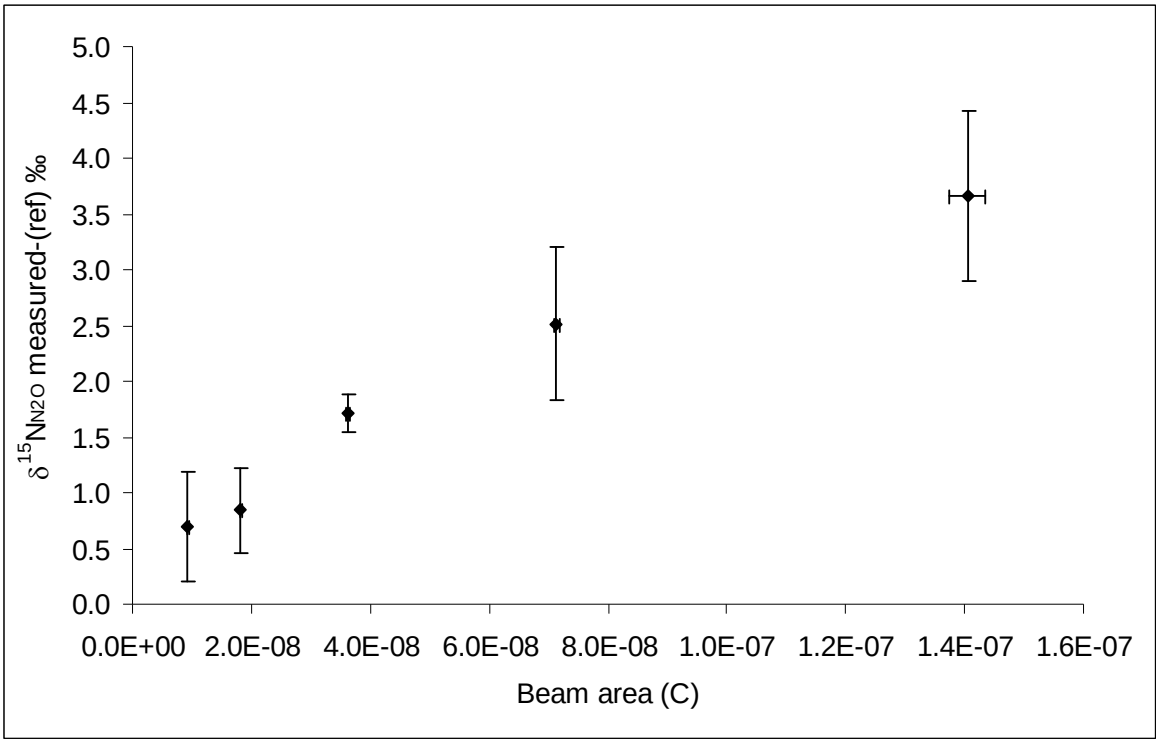

Figure 3.11a $\delta^{15}N_{N2O}$ (‰) (relative to reference gas) versus beam area (coulomb) for different injection volumes of 400 μM laboratory KNO_3 standard SIL-1 (in triplicate). Error bars represent $\pm$ 1 standard deviation from the mean.

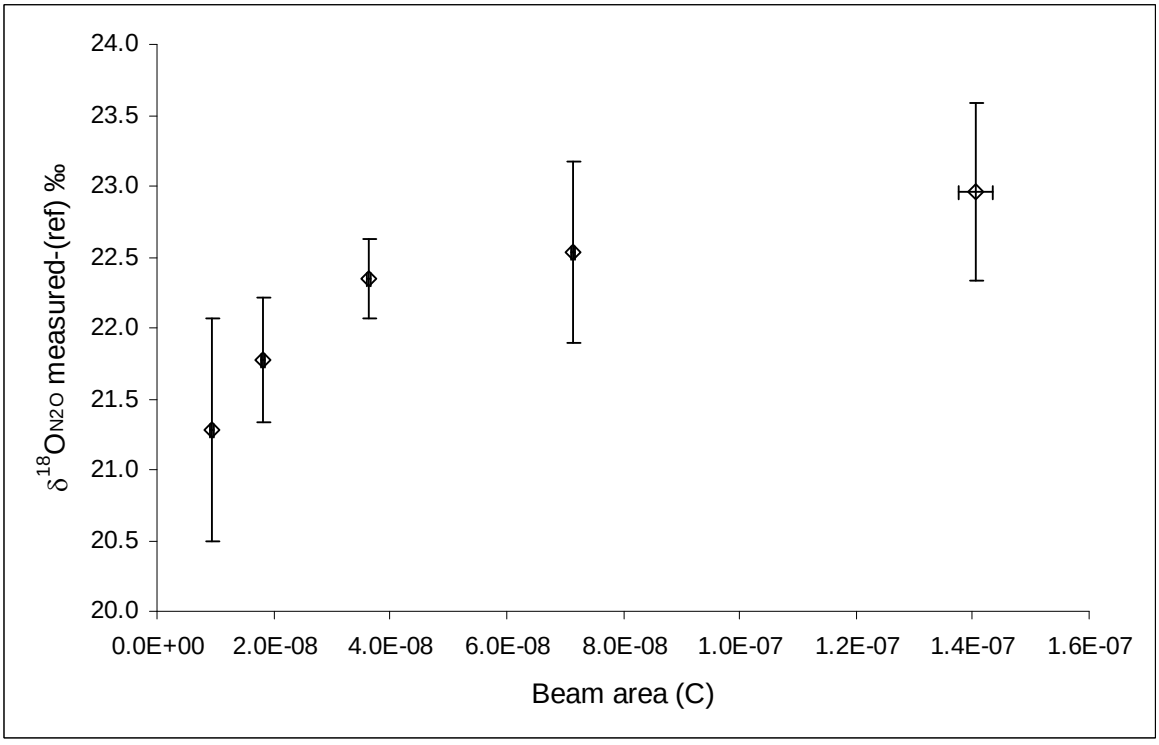

Figure 3.11b $\delta^{18}O_{N2O}$ ‰ (relative to reference gas) versus beam area (coulomb) for different injection volumes of 400 μM laboratory KNO_3 standard SIL-1 (in triplicate). Error bars represent $\pm$ 1 standard deviation from the mean.

3.3.6.5 Purging Efficiency

Next, tests were carried out on purging efficiency using headspace purging of vials containing 3 ml of bacterial solution (the usual volume used in this research), to identify the purge time which would capture the maximum quantity of N_2O. A vial was prepared using the denitrifier method and injected with 50 μL of 400 μM laboratory KNO_3 standard (SIL-1). The vial was then purged repeatedly, and the beam area (representing amount of N_2O) was noted (Figure 3.12). Results showed that approximately 88 % of N_2O was purged from a vial containing 3 ml of liquid in 210 seconds, 95 % in 460 seconds and 98 % by 630 seconds. However, there is a potential for error inherent in this test of leakage from the rubber butyl stopper with repeated piercing by the autosampler needle.

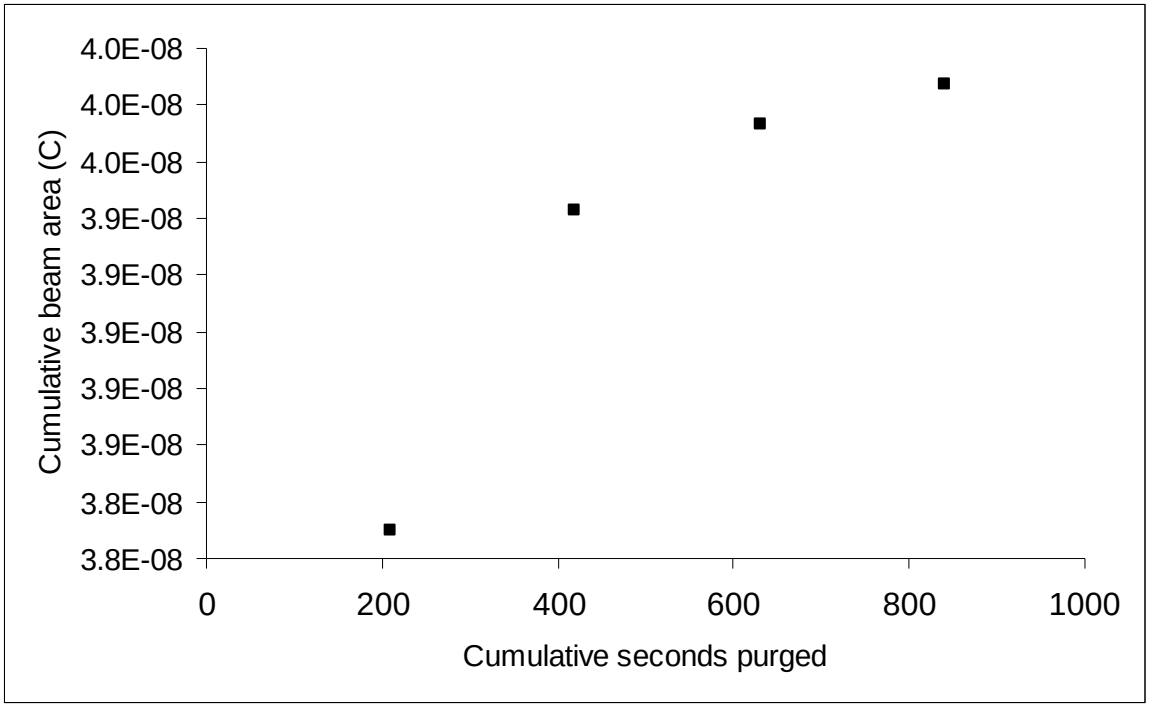

Figure 3.12 Cumulative beam area (coulomb) versus cumulative seconds purged for repeated purging of the same standard vial containing 3 ml of bacterial culture injected with 50 μL of 400 μM laboratory KNO_3 standard SIL-1.

To further examine purging efficiency and to test whether N_2O was lost from the trap with longer purge times, individual vials were purged (in triplicate) for 70, 420, 630 and 840 seconds. This overcame the problem inherent in the previous test. Variations seen in beam areas and isotopic composition with purge time are difficult to interpret with respect to expected kinetic fractionation effects and mass spectrometer response to N_2O

concentration (Figure 3.13 and Figure 3.14). This may indicate that differences seen in beam areas and isotopic composition are within the normal range of variability, and not attributable to purge time. This is supported by the fact that the 420 and 840 second purges produced very similar results in beam areas and isotopic composition. Due to time constraints the experiments were not repeated and a purge time of 500 seconds was used as it was likely to purge over 95 % of the N_2O from the vial without losing it from the cryogenic trap.

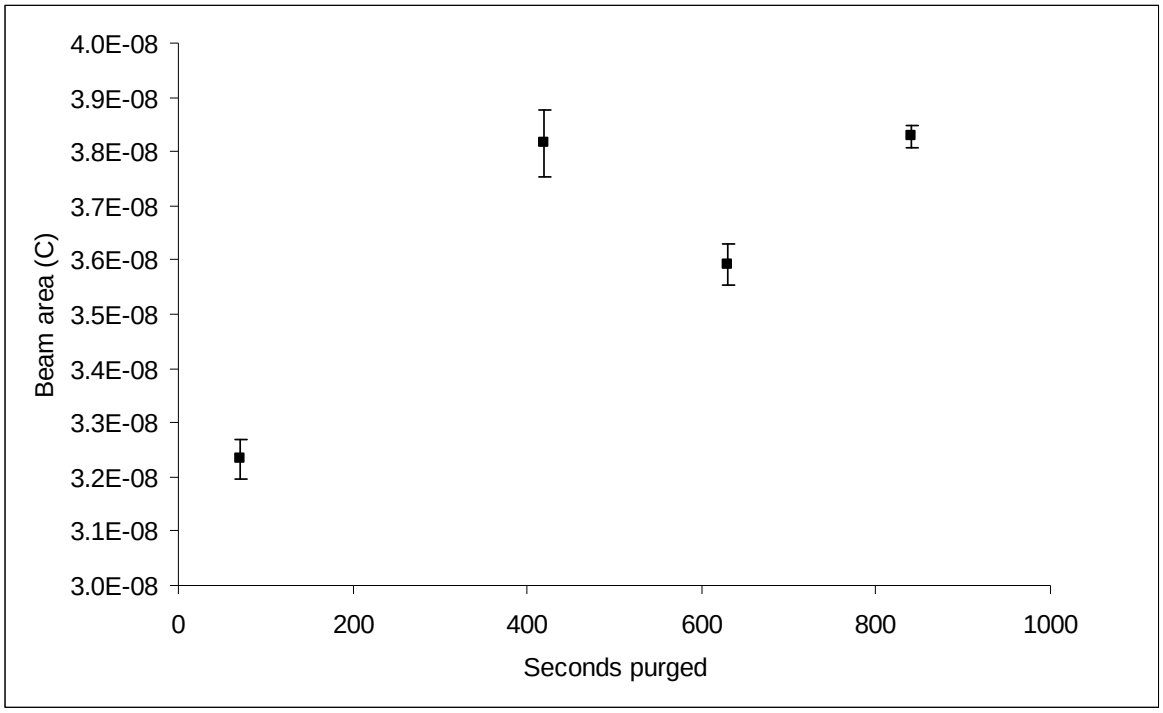

Figure 3.13 Beam area (C) versus seconds purged for different purge times of standard vials containing 3 ml of bacterial culture injected with 50 μL of 400 μM laboratory KNO_3 standard SIL-1 (in triplicate). Error bars represent $\pm$ 1 standard deviation from the mean.

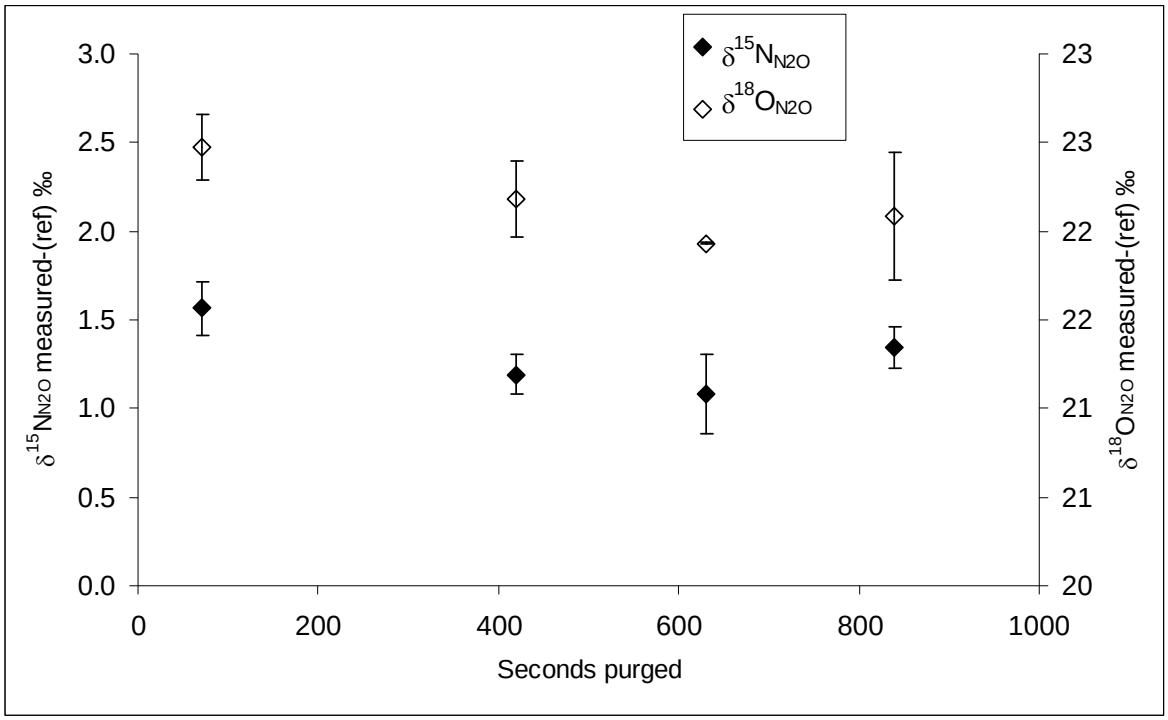

Figure 3.14 $\delta^{15}N_{N2O}$ (‰) and $\delta^{18}O_{N2O}$ (‰) (relative to reference gas) versus seconds purged for different purge times of standard vials containing 3 ml of bacterial culture injected with 50 µL of 400 µM laboratory KNO_3 standard (in triplicate). Error bars represent $\pm$ 1 standard deviation from the mean.

3.3.6.6 Concentration and Volume Effects

Following this test, isotope effects were investigated by injecting sets of calibration standards of different concentrations and volumes. NO_3^- from the three international standards was injected in triplicate using: a) the usual injection volume and concentration used in this research of 50 µL of 400 µM concentration (amount 20 nanomoles); b) varying the volume, with 10 ml of 2 µM concentration (amount 20 nanomoles); c) varying the amount, with 10 µL of 400 µM concentration (amount 4 nanomoles), and d) varying both the amount and the volume, with 10 ml of 0.4 µM concentration (amount 4 nanomoles). Due to the technical constraints of the needle mentioned above, all 50 µL and 10 µL injections were headspace purged and all 10 ml injections were liquid purged. As expected, there were variations in beam area across the data sets. Interestingly, the high volume liquid-purged sets produced smaller beam areas than their low volume headspace-purged counterparts, and injections containing a larger amount of NO_3^- produced larger beam areas (Table 3.2).

Table 3.2 Beam areas (coulomb) and isotopic range across standards (‰) produced by standard injections with varied concentrations and volumes. For comparison, the isotopic range of the international standards is 6.5 ‰ for $\delta^{15}N_{NO3}$ and 85.4 ‰ for $\delta^{18}O_{NO3}$.

Beam areas of standard injections of different volumes and amounts (C)				
Amount NO_3^-/ injection volume	**50 µL / 20 nanomoles**	**10 mL / 20 nanomoles**	**50 µL / 4 nanomoles**	**10 mL / 4 nanomoles**
Mean	4.04×10^{-8}	3.61×10^{-8}	8.90×10^{-9}	7.71×10^{-9}
One standard deviation	1.48×10^{-9}	2.12×10^{-9}	5.6×10^{-10}	1.08×10^{-9}
Isotopic range $^{15}N_{N2O}$ ‰	6.3	6.3	5.7	5.7
Isotopic range $^{18}O_{N2O}$ ‰	83.0	78.2	72.0	64.9

However, the expected trend of heavier isotopic composition with larger beam area was not found. Instead, for $\delta^{15}N_{N2O}$ a reverse trend was seen, with the data set with the lowest beam area showing the heaviest isotopic composition (Figure 3.15a). This could indicate a blank with a $\delta^{15}N_{N2O}$ heavier than that of the standards with an increased contribution at high injection volumes and/or low amounts of NO_3^-. A minor reduction in isotopic range is seen in all standard sets, with the high injection volumes and/or low amount sets showing the largest reduction in range (Table 3.2). The small magnitude of this scale compression is likely to be due to the fact that the isotopic range of $\delta^{15}N_{NO3}$ standards is narrow (6.5 ‰).

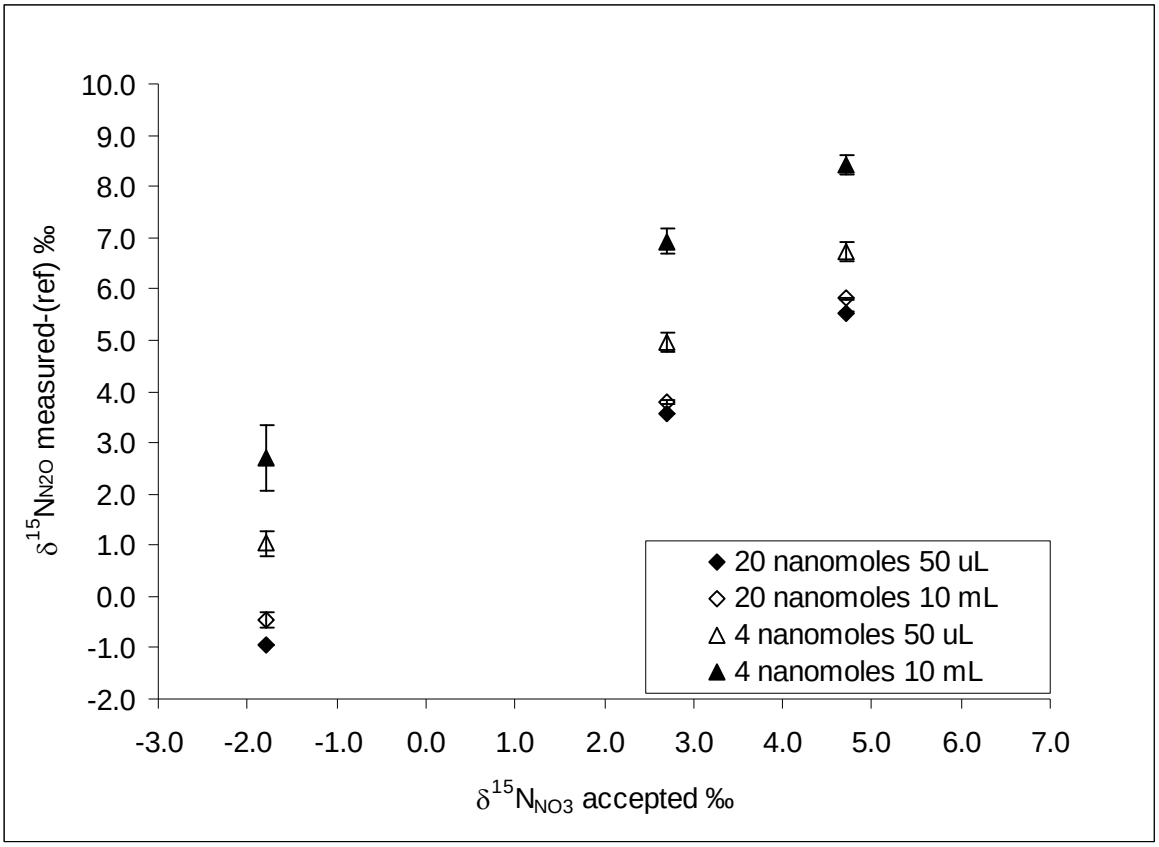

Figure 3.15a $\delta^{15}N_{N2O}$ (‰) (relative to reference gas) versus $\delta^{15}N_{NO3}$ (‰) (accepted) for different amounts and injection volumes of international NO_3^- standards (left to right USGS 34, USGS 35, IAEA N3). Error bars represent $\pm$ 1 standard deviation of the mean from triplicate analyses.

For $\delta^{18}O_{N2O}$ the reverse trend of a lighter isotopic composition with larger beam area was not seen (Table 3.2, Figure 3.15b, presented in separate plots for clearer visualisation). A greater reduction in isotopic range was seen for $\delta^{18}O_{N2O}$ than for $\delta^{15}N_{N2O}$, which is likely to be attributable to the wide isotopic range covered by the standards (85.4 ‰). The scale compression is most prominent in the sample set with the lowest amount of NO_3^- and the highest volume (4 nanomoles in 10 ml injections). This is likely in part to be due to an increased relative contribution from the blank as seen in $\delta^{15}N_{N2O}$ in this set. In addition, oxygen exchange calculations (Equation 3.3), which include any isotopic scale compression from the blank contribution, show NO_3^- oxygen retention of 76% for this standard set in comparison to 98% for the 20 nanomole/ 50 μL standards, suggesting that the reduced isotopic range seen in the low concentration/ high volume set may also be caused by enhanced oxygen exchange with water which has a $\delta^{18}O_{H2O}$ within the range of the standards though the reason for this is not clear. It was not possible to verify the isotopic effects of oxygen exchange with mass balance

calculations because of lack of knowledge of the true isotopic composition of the N_2O reference gas, the true fractionation of $\delta^{18}O_{N2O}$ due to the preferential removal of 5 out of 6 oxygen atoms, and the true $\delta^{18}O_{N2O}$ of the blank.

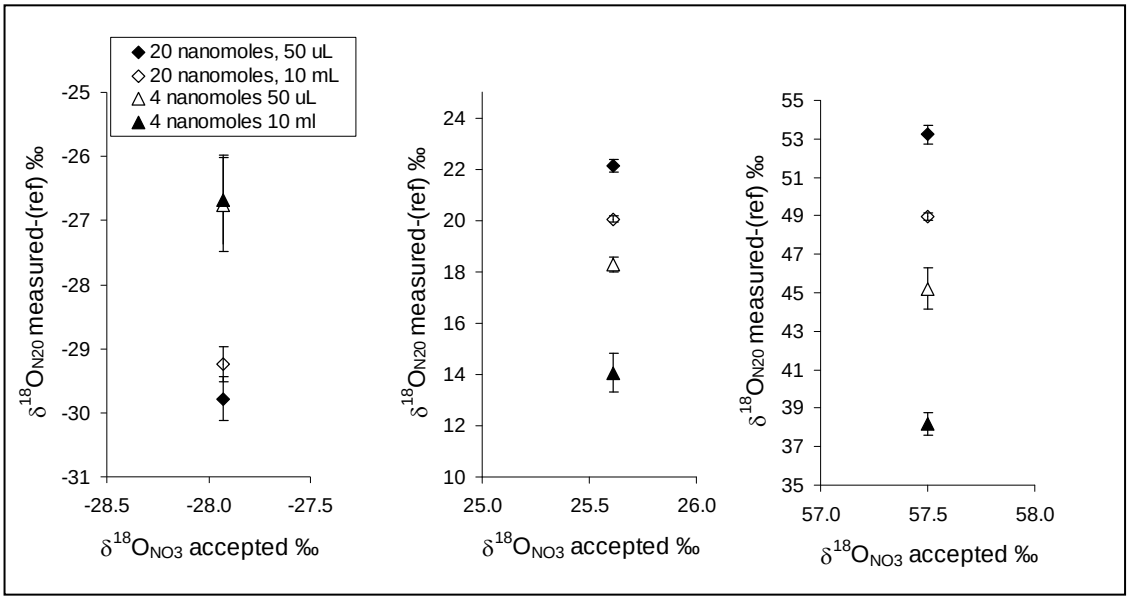

Figure 3.15b $\delta^{18}O_{N2O}$ (‰) (relative to reference gas) versus $\delta^{18}O_{NO3}$ (‰) (accepted) for different amounts and injection volumes of international NO_3^- standards (left to right USGS 34, USGS 35, IAEA N3). Error bars represent $\pm$ 1 standard deviation of the mean from triplicate analyses.

3.3.6.7 Size of the Bacterial Blank and Reliability of Isotopic Measurement

A wide range of measured isotopic composition was seen across the 3 ml bacterial culture blank data set (n=49) collated from all analysis runs (Figure 3.16; Table 3.3), with a smaller variation in beam area. The mean beam area of the blank data set represented 1.4 $\pm$ 0.7 % of the mean beam area of the calibration standards collated from all analyses (n=364), which is equivalent to 0.14 $\pm$ 0.07 nanomoles N_2O. Variations in isotopic composition of the blanks did not correlate to variations in blank beam area. Multiple blanks within the same analysis run produced similar measured isotopic composition often but not consistently, suggesting that isotopic measurement at beam areas < 1.3 x 10^{-9} coulombs, the maximum beam area of the blank, was not reliable. This meant that correcting for the blank contribution to samples and standards numerically (using mass balance) would not be robust, and supported instead the implicit correction through the use of the standard calibration curve.

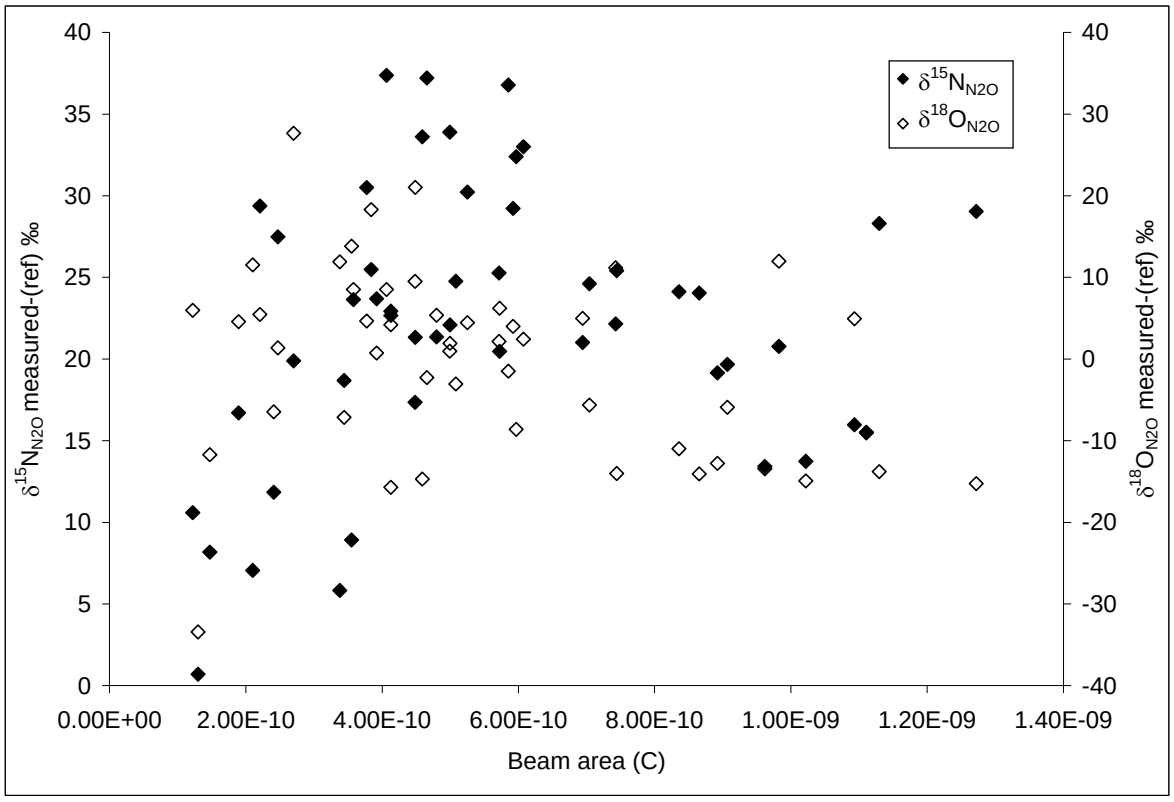

Figure 3.16 $\delta^{18}O_{N2O}$ (‰) and $\delta^{18}O_{NO3}$ (‰) (relative to reference gas) versus beam area (coulomb) of 3 ml bacterial blanks (n=49) measured through the analysis period (headspace purged).

Table 3.3 Range of measured $\delta^{15}N_{N2O}$ (‰), $\delta^{18}O_{N2O}$ (‰) and beam area (coulomb) of 3 ml bacterial blanks measured over analysis period.

Isotopic composition of 3 ml bacterial blanks (n=49)	**$\delta^{15}N_{N2O\ measured\text{-}(ref)}$ ‰**	**$\delta^{18}O_{N2O\ measured\text{-}(ref)}$ ‰**	**Beam area (C)**
Mean	22.2	- 0.3	5.6×10^{-10}
1 standard deviation	8.5	11.5	2.9×10^{-10}
Minimum	0.7	-33.4	1.2×10^{-10}
Maximum	37.4	27.6	1.3×10^{-9}

3.3.6.8 $\delta^{15}N_{N2O}$ of the Bacterial Blank

In response to the fact that reliable isotopic measurement of the bacterial blank was not possible, a different approach was used to infer the value of the blank $\delta^{15}N_{N2O}$. Differences between the accepted $\delta^{15}N_{NO3}$ values of the international standards, the $\delta^{15}N_{N2O}$ measured values of 3 ml standards (50 µL injections of 400 µM concentration, amount 20 nanomoles) and 13 ml low concentration standards (10 ml injections of 0.4 µM concentration, amount 4 nanomoles) (Figure 3.15a), and the beam areas of the standards and bacterial blanks from the two sets were used provide insights about $\delta^{15}N_{N2O}$ of the bacterial blank (Table 3.4).

Table 3.4 Beam areas (coulomb) produced by standard injections and blanks with varied concentrations and volumes (d.i.w. refers to deionised water).

Beam areas of standard injections and blanks of different volumes and amounts (C)				
	Amount NO_3^-/ injection volume	**Mean beam area**	**Amount NO_3^-/ injection volume**	**Mean beam area**
Standard	4 nanomoles /10 ml (concentration 0.4 μM)	7.71×10^{-9} $\pm$ 1.08×10^{-9}	20 nanomoles /50 μL (concentration 400 μM)	4.04×10^{-8} $\pm$ 1.48×10^{-9}
Blank	3 ml bacterial culture solution + 10 ml d.i.w.	1.70×10^{-9} $\pm$ 3.45×10^{-12}	3 ml bacterial culture solution	2.67×10^{-9} $\pm$ 7.65×10^{-11}
	Blank as % of standards	22 %	**Blank as % of standards**	0.7 %

Using a mass balance approach, based on the assumption of a consistent $\delta^{15}N_{N2O}$ for the blank contribution from the bacterial solution and of no other interference affecting measured $\delta^{15}N_{N2O}$ of the standards, $\delta^{15}N_{N2O}$ of the blank was calculated using the difference in relative beam area between the blanks and standards of the two sets:

$$\delta^{15}N_{N2OS13ml} = (\delta^{15}N_{N2OS3ml} \times (1-(ba_{13mlblanks/}\ ba_{13mlstds}) + (ba_{3mlblanks/}\ ba_{3mlstds})) + (\delta^{15}N_{N2Ob} \times ((ba_{13mlblanks/}\ ba_{13mlstds}) - (ba_{3mlblanks/}\ ba_{3mlstds}))$$

Equation 3.8a

Therefore:

$$\delta^{15}N_{N2Ob} = \frac{\delta^{15}N_{N2OS13ml} - ((\delta^{15}N_{N2OS3ml} \times (1-(ba_{13mlblanks/}\ ba_{13mlstds}) + (ba_{3mlblanks/}\ ba_{3mlstds}))}{((ba_{13mlblanks/}\ ba_{13mlstds}) - (ba_{3mlblanks/}\ ba_{3mlstds}))}$$

Equation 3.8b

where: $\delta^{15}N_{N2OS13ml}$ and $\delta^{15}N_{N2OS3ml}$ are the measured isotopic compositions relative to the reference gas of the 13 ml and 3 ml standard sets respectively; $\delta^{15}N_{N2Ob}$ is the isotopic composition of the blank relative to the reference gas, and $ba_{13mlblanks/}\ ba_{13mlstds}$ and $ba_{3mlblanks/}\ ba_{3mlstds}$ are the proportional beam areas of the blanks relative to the beam areas of standard sets of the same volumes. Solving Equation 3.8b for the three international standards gives a measured value (with respect to the reference gas) of $\delta^{15}N_{N2Ob}$ 18.1 $\pm$ 1.7 ‰. Although the 3 ml standards and blanks were headspace purged and those with a volume amendment of 10ml were liquid purged, this discrepancy should not be significant as the calculation is based on the difference between blanks and standards of the same volume. It is not clear what caused the increase in N_2O yield

of the 13 ml blanks relative to the 3 ml blanks. However, the 13 ml blank was amended with 10 ml deionised water, to replicate the 10 ml standard injection. Liquid ion chromatography showed that deionised water sometimes contained NO_3^- concentrations up to 0.04 μM, depending on the condition of the filter packs. This is equivalent to 0.4 nanomoles in 10 ml deionised water, or 10 % of the NO_3^- injected into in the 13ml, 4 nanomole standards. Calibration of $\delta^{15}N_{N2Ob}$ to the 13 ml standard set gives a value of $\delta^{15}N_{NO3}$ 15.4 $\pm$ 1.7 ‰, representing $\delta^{15}N_{NO3}$ of source NO_3^- if the blank is caused by NO_3^-contamination from deionised water.

As blanks amended with 10 ml deionised water gave larger beam area than 3 ml blanks (Table 3.4) it was thought that isotopic measurement of these blanks might be more reliable than that of the 3 ml blanks. However, blanks amended with 10 ml deionised water analysed in different analysis runs produced a wide range of measured isotopic composition between runs ($\delta^{15}N_{N2O}$ 7.5 to 17.2 ‰; $\delta^{18}O_{N2O}$ -3.1 to -13.9 ‰ n = 6), although duplicate blanks within runs gave consistent isotopic measurement (within 0.4 ‰ for both isotopes). An increase in blank size with deionised water amended bacterial blanks was also found by Sigman *et al.* (2001) who suggested that it may be attributable to residual NO_3^- in the deionised water or to the release of sorbed N_2O from the bacterial culture. It is possible that both sources contribute to the blank and account for the variation seen.

3.3.6.9 Analysis of Samples with Very Low NO_3^- Concentration

In this research a small number of samples had very low NO_3^- concentration (< 0.5 μM NO_3^-). Most of these samples were analysed twice over the analysis period. Paired samples analysed in different runs giving beam areas of > 3.0 x 10^{-9} coulombs produced $\delta^{15}N_{N2O}$ and $\delta^{18}O_{N2O}$ measured values within 0.9 ‰ of each other over an isotopic range of $\delta^{15}N_{N2O}$ 2.2 to 12.9 ‰ and $\delta^{18}O_{N2O}$ 1.1 to 22.8 ‰, suggesting that isotopic measurements of these low concentration samples were reliable.

The between-run reproducibility seen from low concentration samples contrasts with the variability seen in the isotopic composition of high volume bacterial blanks between runs. This suggests that the measured isotopic composition of the low concentration

samples is derived from NO_3^- in the sample water rather than from enhanced blank effects from high injection volumes. Due to the fact that samples of very low NO_3^- concentration represented only a very small proportion of the research, further experiments were not undertaken with high volume blanks and low concentration samples.

3.3.7 Water Isotopes: Oxygen

$\delta^{18}O_{H2O}$ was analysed on a Europa Sira II dual inlet isotope ratio mass spectrometer (IRMS) using the CO_2-H_2O equilibration method (Epstein and Mayeda, 1953), based on the equilibration equation which dominates at near neutral pH:

$$CO_{2(g)} \leftrightarrow CO_{2(aq)} + OH^- \leftrightarrow HCO_3^- \qquad \text{Equation 3.9}$$

Following equilibration, headspace CO_2 was analysed on the IRMS which measures masses 44, 45 and 46. A ^{17}O correction was made (Craig, 1957) and values reported with respect to VPDB (Vienna Pee Dee Belemnite). The working reference gas isotopic composition was calibrated to NBS-19 (TS-limestone) with respect to VPDB. Samples were also calibrated against internal water standards which were placed in the run (North Sea water and Norwich tap water). The $\delta^{18}O_{H2O}$ of the internal standards was determined by direct measurement against the international references for $\delta^{18}O_{H2O}$, VSMOW and SLAP (Standard Light Antarctic Precipitation). $\delta^{18}O_{CO2PDB}$ values produced by the IRMS analysis were converted to $\delta^{18}O_{H2O}$ relative to VSMOW using equation Equation 3.10 (Coplen *et al.*, 1983):

$$\delta^{18}O_{VSMOW} = \delta^{18}O_{VPDB} \times 1.03086 + 30.86 \qquad \text{Equation 3.10}$$

The within run precision of $\delta^{18}O_{H2O}$ analysis was $\pm$ 0.06 ‰ and the between run precision was $\pm$ 0.1 ‰.

3.3.8 Water isotopes: Hydrogen

δ^2H_{H2O} was measured on a Thermo Finnigan Delta XP Plus GCIRMS (continuous flow), using pyrolysis. The 0.1 μL sample was injected onto hot glassy carbon at 1400°C, and reacted to produce CO and H_2. Peaks were separated in a GC, and the H_2 isotopic composition was analysed at masses 2 and 3, with the results reported on the VSMOW-SLAP scale. Standards of VSMOW, and SLAP were included in the run for calibration. The reference GISP (Greenland Ice Sheet Precipitation) was included in the run to monitor data accuracy and precision. The within run precision of δ^2H_{H2O} analysis was $\pm$ 0.5 ‰ and the between run precision was $\pm$ 1.3 ‰.

3.4 HYDROCHEMICAL ANALYSIS

3.4.1 Major Ions: Liquid Ion Chromatography

Cl^-, NO_2^-, NO_3^-, SO_4^{2-}, PO_4^{3-} and NH_4^+ concentrations were measured by liquid ion chromatography using a Dionex ICS 2000 (for the anions) and a Dionex DX 600 (for NH_4^+). Two sets of mixed standards were prepared, one for the calibration of dissolved inorganic nitrogen (DIN), comprising KNO_3, $NaNO_2$ and NH_4Cl, and one for Cl^-, SO_4^{2-} and PO_4^{3-} comprising NaCl, K_2SO_4 and KH_2PO_4. Standard concentration ranges were developed to encompass the expected concentration ranges of the samples. Limits of detection were derived from analysis of deionised water blanks (usually 10 to 15 in each run), and calculated as three times the standard deviation of the blanks. Precisions for all analytes were calculated as one standard deviation of triplicate analyses of samples with typical concentration ranges, and expressed as a percentage of the mean concentration of the analyte (Table 3.5).

Table 3.5 Precision, limit of detection (LOD) and analytical instrument used, for compounds and elements analysed.

Compound or element measured	Precision	Limit of detection	Instrument
NO_3^-	+/- 2 %	1.0 µM	Dionex ICS 2000
NO_2^-	+/- 2 %	0.5 µM	Dionex ICS 2000
NH_4^+	+/- 5 %	0.5 µM	Dionex DX 600
DON	+/- 2 %	0.5 µM	Thermalox TN
Cl^-	+/- 3 %	0.07 mg/L	Dionex ICS 2000
SO_4^{2-}	+/- 2 %	0.02 mg/L	Dionex ICS 2000
PO_4^{3-}	+/- 4 %	0.01 mg/L	Dionex ICS 2000
Na	+/- 3 %	0.1 mg/L	Varian Vista ICPAES
K	+/- 3 %	0.05 mg/L	Varian Vista ICPAES
Mg	+/- 3 %	0.03 mg/L	Varian Vista ICPAES
Ca	+/- 3 %	0.3 mg/L	Varian Vista ICPAES
Si	+/- 3 %	0.07 mg /L	Varian Vista ICPAES
Sr	+/- 3 %	0.01 mg/L	Varian Vista ICPAES
Fe	+/- 3 %	0.6 µg/L	Varian Vista ICPAES
Al	+/- 3 %	0.7 µg/L	Varian Vista ICPAES
Zn	+/- 3 %	0.3 µg/L	Varian Vista ICPAES
Mn	+/- 3 %	0.01 µg/L	Varian Vista ICPAES
Cu	+/- 3 %	0.02 µg/L	Varian Vista ICPAES
B	+/- 3 %	0.03 µg/L	Varian Vista ICPAES
HCO_3^-	+/- 3 %	-	Titration

The calculated ionic balance error was 4% based on all the samples for which analysis of all eight major ions was carried out (HCO_3^-; Cl^-; SO_4^{2-}; NO_3^-;Ca^{2+}; Na^+; K^+, Mg^{2+}), indicating that analyses of major anions and cations are consistent.

3.4.2 DON: Total Nitrogen Difference Method

A cross calibration was carried out between the two liquid ion chromatographs and the Thermalox TN using individual KNO_3, $NaNO_2$ and NH_4Cl standard sets and a mixed DIN standard set (KNO_3 + $NaNO_2$ + NH_4Cl) which spanned the concentration ranges expected in samples, to test the precision and reproducibility between the ion chromatographs and the Thermolux TN. The good precision obtained for the separate DIN species on the three instruments and total DIN on the Thermalox TN (r^2 0.99) provided the basis for the use of the difference method for DON analysis. Mixed DIN standards were used routinely on the three instruments during sample analysis. For DON analysis, the Thermalox TN was used to measure total dissolved nitrogen (TDN) of the filtered samples and the concentration of DON was calculated with the difference

method based on the assumption that particulate nitrogen had been removed by 0.22 μm filtering, using the following equation:

$$[DON] = [TDN] - ([NO_3^-] + [NO_2^-] + [NH_4^+]) \quad \text{Equation 3.11}$$

On most occasions both the liquid ion chromatography and DON analysis, using an Analytical Sciences Thermalox TN instrument, were carried out within a few days of sampling.

3.4.3 Major Ions and Trace Elements: ICP-AES

Concentrations of Na, K, Mg, Ca, Si, Sr and the trace elements Fe, Al, Zn, Mn, Cu, Ni, B, Cd, Co, and Cr were measured in all samples using inductively coupled plasma atomic emission spectrometry (ICP-AES). Concentrations of Cd, Co, Cr, and Ni were consistently below the limit of detection for the instrument so results for these elements are not presented. Limits of detection were calculated as three times the standard deviation of triplicate blanks (deionised water). Procedural blanks were included in each analysis to quantify the blank contribution from nitric-acid-amended deionised water. The procedural blank comprised a tube containing 9 ml of deionised water amended with 0.8 ml concentrated nitric acid. Sample concentrations were corrected by subtracting concentrations of the procedural blank.

3.4.4 Total Alkalinity

Sample pH measured within the range pH 6.9 to 7.6, below the range at which carbonate forms. For this reason carbonate alkalinity was not measured using phenolphthalein indicator. Bicarbonate alkalinity was measured by titrating 10 ml of unfiltered sample with 0.01 M HCl and three drops of BDH 4.5 indicator to a grey endpoint. Titrations were performed in triplicate, within 48 hours of sample collection.

3.5 EQUATIONS USED IN MODELS

The interpretation of the data in Chapter 5, Discussion, uses calculations of isotope enrichment factors and mass balance solute and isotope modelling. Isotope enrichment factors are calculated using Equation 3.12 from Mariotti *et al.* (1988):

$$\varepsilon_{P\text{-}S} = \delta_t - \delta_0 / \ln (Ct/C_0) \qquad \text{Equation 3.12}$$

where δ_t refers to the isotopic composition of the nitrate at time t (after the effects of denitrification), δ_0 refers to the initial isotopic composition of the nitrate (before the effects of denitrification), Ct is the concentration of the nitrate at time t (after the effects of denitrification), C_0 is the original nitrate concentration (before the effects of denitrification).

Solute mass balance modelling uses the mass-balance equation:

$$C_{mixed} = \frac{(C_a \times v_a) + (C_b \times v_b)}{(v_a) + (v_b)} \qquad \text{Equation 3.13}$$

Where C_a and C_b denote the concentration of the end members a and b, and v_a and v_b denote their respective volumes. Any number of end members can be added to the model.

Isotope mass balance modelling uses the mass-balance equation:

$$\delta_{mixed} = \frac{(C_a \times v_a \times \delta_a) + (C_b \times v_b \times \delta_b)}{(C_a \times v_a) + (C_b \times v_b)} \qquad \text{Equation 3.14}$$

Where C_a and C_b denote the concentration of the end members a and b, v_a and v_b denote their respective volumes, and δ_a and δ_b denote the respective isotopic values of the end members. Any number of end members can be added to the model.

3.6 SUMMARY

The research design, including the choice of sampling locations, field sampling protocols and field measurement methods were described, together with information as to how samples were prepared for storage, and storage temperatures. Following this, analysis methodology was presented with precision data for each analysis type. First, the denitrifier method for the analysis of stable isotopes of nitrate was described, and the data reduction methodology set out, including corrections for drift and the contribution from the isotope ^{17}O at mass 45. This was followed by a description of denitrifier method development experiments, including investigations of N_2O yield, headspace versus liquid purging, purge efficiency, mass spectrometer response to N_2O amount, concentration and volume effects, and the nitrogen isotopic composition of the bacterial blank, which together demonstrated that the method was set up with care and was working successfully. Next, water isotope analysis techniques were outlined, and hydrochemical analysis methods described. Finally, equations used in models in later chapters were presented.

4. RESULTS

4.1 SAMPLE COLLECTION

Samples were collected between February 2007 and September 2009 from the Wensum river, its tributaries, drains, and Chalk groundwater, across all seasons and flow conditions in spatial and temporal surveys (Table 4.1; Figures 4.1 and 4.2). As the research progressed an increasing number of locations were identified and sampled in the catchment, and one-off individual high-resolution spatial sampling campaigns were carried out after initial results identified potential areas of interest. The result of this is that the sample data set has a non-uniform pattern, as some key locations, such as gauging station sites, were sampled during most surveys, while other locations, such as tributary branches, were sampled only once. The location and date for individual sample collection is show in grid form in Tables 4.2 and 4.3. Borehole samples were collected during winter, with a second survey in summer during which three repeat samples were collected, and two samples from new locations. Full results are presented in Appendix 2.

Nitrate source samples were collected from event precipitation, dry deposition, sewage effluent, manure and fertiliser (Table 4.1). One event precipitation sampled comprised snowfall; all the other precipitation events were rainfall.

Two samples of sewage effluent were collected. The first was from the works at Bylaugh which discharge secondary treated effluent into a tributary of the Wensum. The sample was taken from the effluent discharge outlet. It was not possible to gain access to further wastewater treatment works within the Wensum catchment during the sampling period. A second sample was taken from the works at North Walsham (outside the Wensum catchment), which no longer discharges effluent to a river. This primary treated effluent is discharged via a pipeline offshore. The sample was taken at the point the effluent is discharged into the pipeline.

Table 4.1 Summary of samples collected between February 2007 and September 2009.

Wensum catchment sampling

Sampling date	Season	Sampling design	Number of samples
14/02/2007	Winter	River and tributary spatial survey	16
17/04/2007	Spring	River and tributary spatial survey	10
19-24/04/2007	Spring	Lower river temporal survey (twice daily for six days)	60
18/07/2007	Summer	River and tributary spatial survey	18
18-19/07/2007	Summer	Lower river temporal survey (twice daily for two days)	20
11/12/2007	Winter	River, tributary and drain spatial survey	15
06/04/2008	Spring	River, tributary and drain spatial survey	26
14/09/2008	Autumn	River, tributary and drain spatial survey	25
16/11/2008	Winter	Mid-river high resolution spatial survey	24
12-13/12/2008	Winter	24 hour temporal survey at gauging stations	48
27/05/2009	Spring	Southern catchment tributaries spatial survey	10
25/09/2009	Autumn	River and tributary spatial survey	16
05/02/2008	Winter	Borehole sampling	11
24/08/2009	Summer	Borehole sampling	5
		Total	**304**

Nitrate source sampling

Sampling date	Sample type	Sampling location
16/07/2007	Event precipitation (rain)	Norwich
17/07/2007	Event precipitation (rain)	Norwich
10/12/2007	Event precipitation (rain)	Norwich
05/04/2008	Event precipitation (snow)	Norwich
31/07/2008	Event precipitation (rain)	Norwich
01/08/2008	Event precipitation (rain)	Norwich
17-27/07/2008	Dry deposition	Norwich
19/07/2007	Sewage works effluent	Bylaugh works
01/08/2008	Sewage works effluent	North Walsham works
10/08/2008	Cattle and chicken manure	Central Norfolk

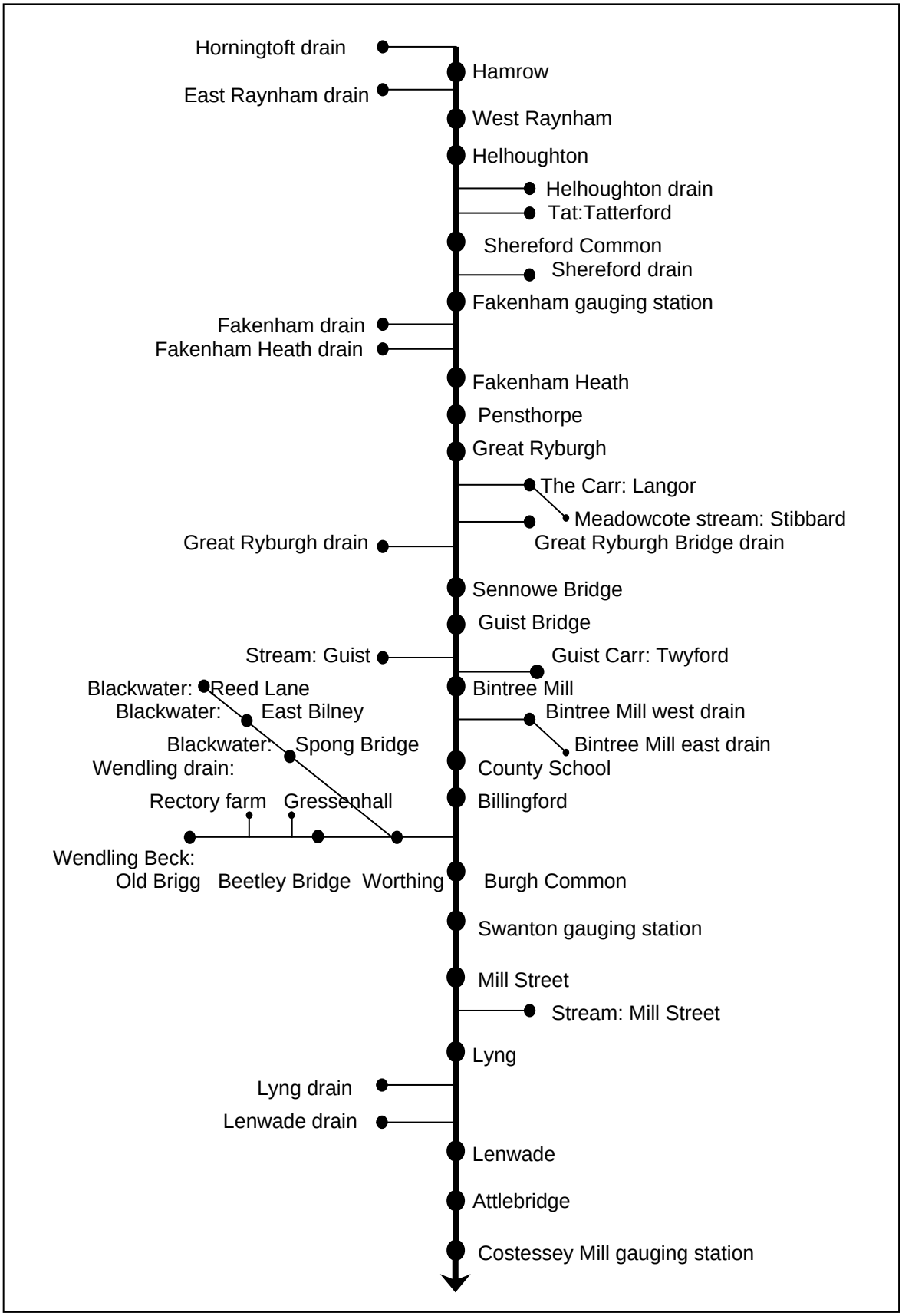

Figure 4.1 Schematic of all sampling locations on the Wensum river, tributaries and drains (not to scale).

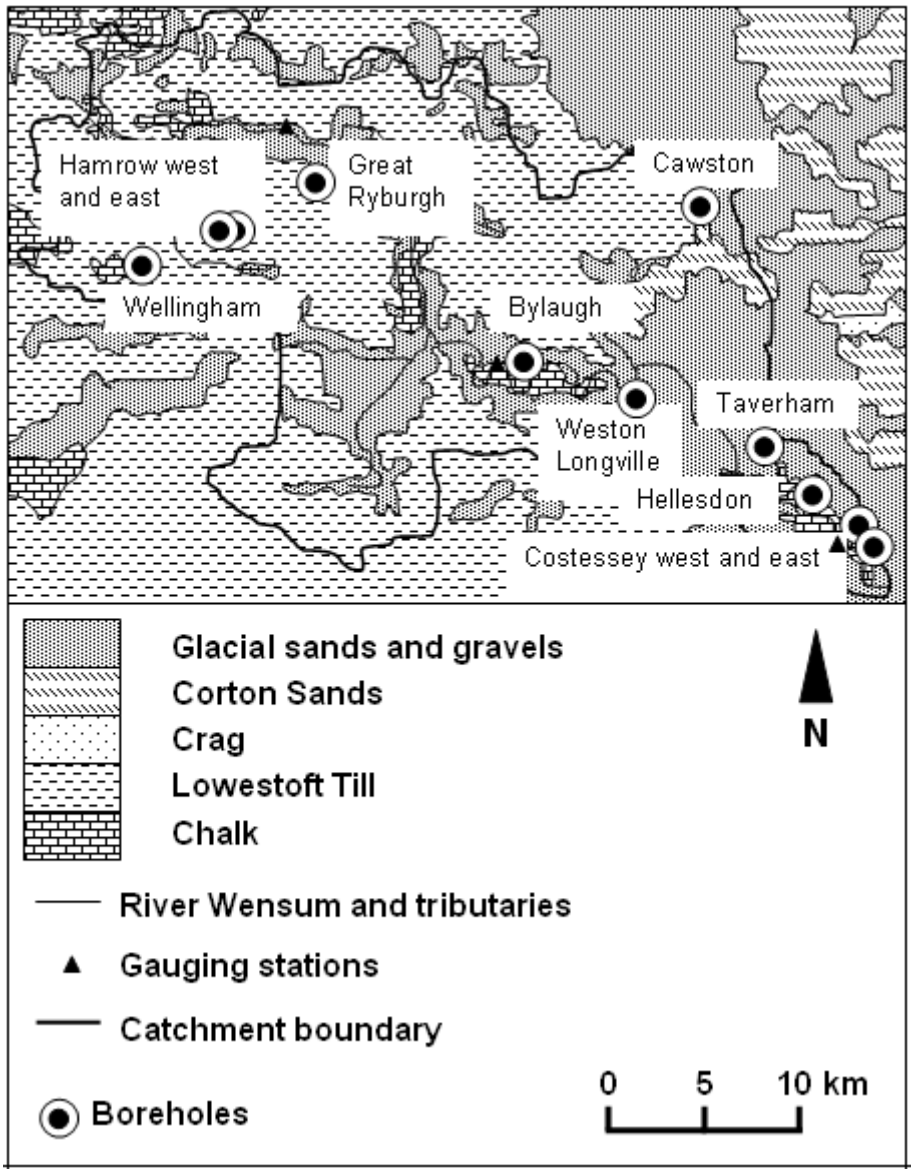

Figure 4.2 Location map showing surface geology of the Wensum catchment, with Chalk borehole locations and names (adapted from Moseley *et al.*, 1976).

Table 4.2 Grid showing Wensum river locations where samples were collected during spatial sampling campaigns (boxes with crosses).

Wensum river sampling locations	Sampling date								
	14/02/2007	17/04/2007	18/07/2007	11/12/2007	06/04/2008	14/09/2008	16/11/2008	27/05/2009	25/09/2009
Hamrow	x		x		x	x			dry
West Raynham	x		x		x	x			x
Helhoughton	x		x		x	x			x
Shereford Common				x	x	x			x
Fakenham GS	x	x	x	x	x	x	x	x	x
Fakenham Heath							x		
Pensthorpe							x		
Great Ryburgh	x		x	x	x	x	x		x
Sennowe Bridge							x		
Guist Bridge							x		
Bintree Mill	x		x	x	x	x	x		x
County School						x	x		x
Billingford	x		x		x	x	x		x
Burgh Common							x		
Swanton GS	x	x	x		x	x	x	x	x
Mill Street	x	x	x	x	x	x	x		x
Lyng		x	x	x	x	x			x
Lenwade	x	x	x	x	x	x			x
Attlebridge		x	x		x	x			x
Costessey Mill GS	x	x	x	x	x	x			x

Table 4.3 Grid showing Wensum tributary and drain locations where samples where collected during spatial sampling campaigns (boxes with crosses).

Wensum tributary and drain sampling locations	Sampling date								
	14/02/2007	17/04/2007	18/07/2007	11/12/2007	06/04/2008	14/09/2008	16/11/2008	27/05/2009	25/09/2009
Horningtoft drain	x	x	x		x	dry			
East Raynham drain					x	dry			
Helhoughton drain					x	x			
Tat: Tatterford	x		x		x	x			x
Shereford drain				x	x	x			
Fakenham drain	x	x	x	x	x	x	x		
Fakenham Heath drain							x		
The Carr: Langor							x		
Meadowcote stream: Stibbard							x		
Great Ryburgh bridge drain						x	x		
Great Ryburgh drain				x	x	x	x		
Stream: Guist							x		
Guist Carr: Twyford							x		
Bintree west drain				x	x	x	x		
Bintree east drain							x		
Blackwater: Reed Lane								x	
Blackwater: East Bilney									
Blackwater: Spong Bridge								x	
Wendling Beck: Old Brigg								x	
Wendling drain: Rectory Farm								x	
Wendling drain: Gressenhall								x	
Wendling Beck: Beetley Bridge								x	
Wendling Beck: Worthing	x		x		x	x	x	x	x
Stream: Mill Street	x	x	x	x	x	x	x		
Lyng drain				x	x	x			
Lenwade drain				x	x	dry			

4.2 RIVER FLOW

Daily mean flow at each gauging station on sampling days is shown in Table 4.4. The categorisation of high, medium and low flow conditions are derived from 10-year daily mean flow for the period 1990-2000 (Entec, 2007). River samples were collected to include all flow conditions. However, due to the fact that there was a two to four week delay until flow gauging data became available, surface water samples were collected according to season and observation of antecedent flow and weather conditions. This meant that high flow sampling did not always occur during peak flow (Figures 4.3 and Figure 4.4 a-j).

Table 4.4 Daily mean flow at gauging stations on the Wensum river on sampling days.

River Wensum gauging stations Daily mean flow (m^3 s^{-1})				
	Fakenham (034011)	Swanton Morley (034014)	Costessey Mill (034004)	Flow condition
Sampling date				
14/02/2007	1.38	5.46	8.31	High
17/04/2007	0.66	2.08	2.95	Low
19-24/04/2007	0.61	1.98	2.70	Low
18/07/2007	1.85	4.96	7.27	High
18-19/07/2007	1.82	4.59	7.39	High
11/12/2007	2.78	6.68	9.33	High
06/04/2008	1.72	3.96	6.22	High/medium
14/09/2008	0.57	2.07	3.64	Low
16/11/2008	0.61	3.12	5.34	Low/ medium
12-13/12/2008	1.21	5.05	8.29	High
27/05/2009	0.66	1.99	3.24	Low
25/09/2009	0.19	0.88	1.55	Low (extreme)

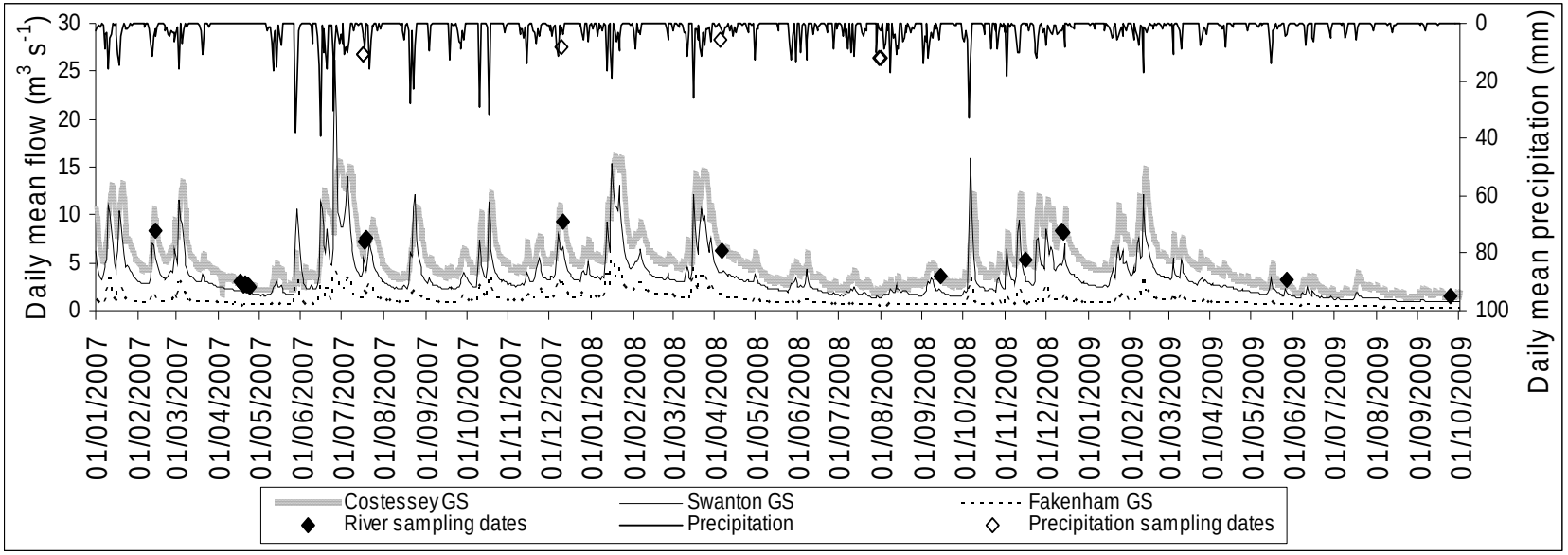

Figure 4.3 Lower x axis: daily mean flow ($m^3 s^{-1}$) from 1/1/2007 to 1/10/2009 from gauging stations on the River Wensum at Fakenham (034011), Swanton Morley (034014) and Costessey Mill (034004), showing river sampling dates. Upper x axis: daily mean precipitation data for Norfolk (mm) (UK Meteorological Office, 2010), showing precipitation sampling dates for samples collected in Norwich.

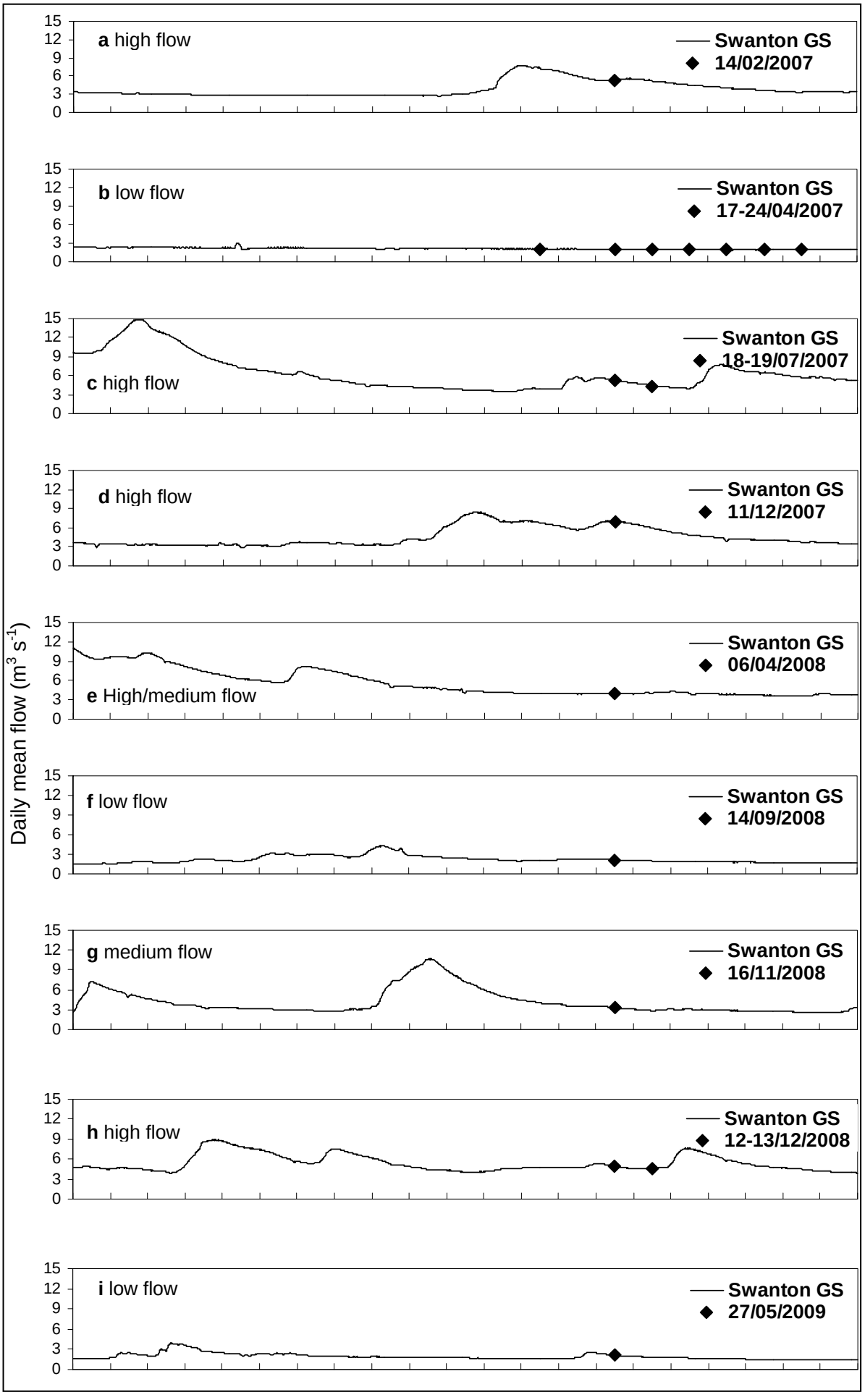
Daily mean flow ($m^3 s^{-1}$)
0
3
6
9
12
15
a high flow
Swanton GS
14/02/2007
b low flow
Swanton GS
17-24/04/2007
c high flow
Swanton GS
18-19/07/2007
d high flow
Swanton GS
11/12/2007
e High/medium flow
Swanton GS
06/04/2008
f low flow
Swanton GS
14/09/2008
g medium flow
Swanton GS
16/11/2008
h high flow
Swanton GS
12-13/12/2008
i low flow
Swanton GS
27/05/2009

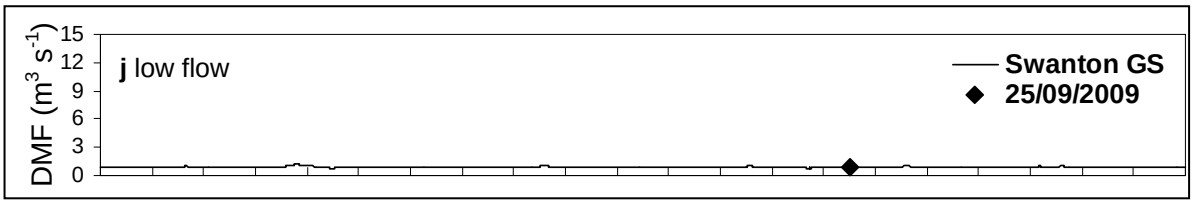

Figure 4.4a-j Daily mean flow (m^3 s^{-1}) with sampling dates at Swanton Morley gauging station on the River Wensum for 14 days leading up to sampling and 7 days after sampling, for each sample survey.

4.3 WENSUM CATCHMENT NO_3^-

A summary of results from nitrate isotopic analysis and liquid ion chromatography of samples from the Wensum catchment is presented in Table 4.5 and Figure 4.5 to Figure 4.8. The isotopic composition of nitrate from across the catchment covers a broad range, ($\delta^{15}N_{NO3}$ 2.5 to 17.5 ‰; $\delta^{18}O_{NO3}$ 0.3 to 30.0 ‰), with a wide range seen also in nitrate concentration (< 1 to 1365 μM NO_3^-). Samples from the River Wensum show a fairly homogeneous nitrate isotopic composition and concentration, and mean values which fall between those of the valley groundwater and the tributaries and drains. The tributary and drain sample subset shows greater heterogeneity than the river sample subset, encompassing the values of the river samples. All groundwater samples collected were from the Chalk. Due to a clear delineation between two groups of Chalk groundwater samples of with respect to nitrate concentration, groundwater from the boreholes in the Chalk in the Wensum valley is also referred to as valley groundwater, and groundwater from the Chalk on the interfluves and valley margins is also referred to as low-nitrate groundwater. Valley groundwater has the lightest isotopic composition and the highest mean nitrate concentration of all the sample subsets, while low-nitrate groundwater in interfluves and valley margins has the lowest nitrate concentration (< 1 μM NO_3^-) and the heaviest oxygen isotope composition. One low-nitrate groundwater sample had a concentration of nitrate too low to allow isotopic analysis (Great Ryburgh A) This sample is not included in the nitrate isotopic data but is included in the presentation of groundwater hydrochemistry.

Table 4.5 Mean ± one standard deviation, maxima and minima of NO_3^- concentration (μM), $\delta^{15}N_{NO3}$ (‰) and $\delta^{18}O_{NO3}$ (‰) of samples from the Wensum catchment (n = 169; where repeated temporal samples were taken, one data set only is included).

Wensum catchment		**NO_3^- concentration μM**	**$\delta^{15}N_{NO3}$ ‰ AIR**	**$\delta^{18}O_{NO3}$ ‰ VSMOW**
Tributary and drain water (n = 64)	Mean ± 1 standard deviation	499 ± 263	10.2 ± 2.8	4.5 ± 1.8
	Maximum	1365	17.5	9.6
	Minimum	20	6.3	1.6
Wensum river water (n = 105)	Mean ± 1 standard deviation	471 ± 111	10.1 ± 1.2	4.4 ± 0.7
	Maximum	757	14.8	7.5
	Minimum	288	7.8	3.0
Valley groundwater (n = 5)	Mean ± 1 standard deviation	973 ± 215	6.9 ± 1.4	1.2 ± 1.2
	Maximum	1314	9.2	3.3
	Minimum	786	5.8	0.3
Low-nitrate groundwater[a] (n = 5)	Mean ± 1 standard deviation	<1	5.9 ± 2.4	21.1 + 9.7
	Maximum	< 1	8.3	30.0
	Minimum	< 1	2.5	8.2

[a] Due to uncertainties with the calibration of low concentration samples there is an associated error of ± 1.0 ‰ for $\delta^{15}N_{NO3}$, and ± 3.1 for $\delta^{18}O_{NO3}$.

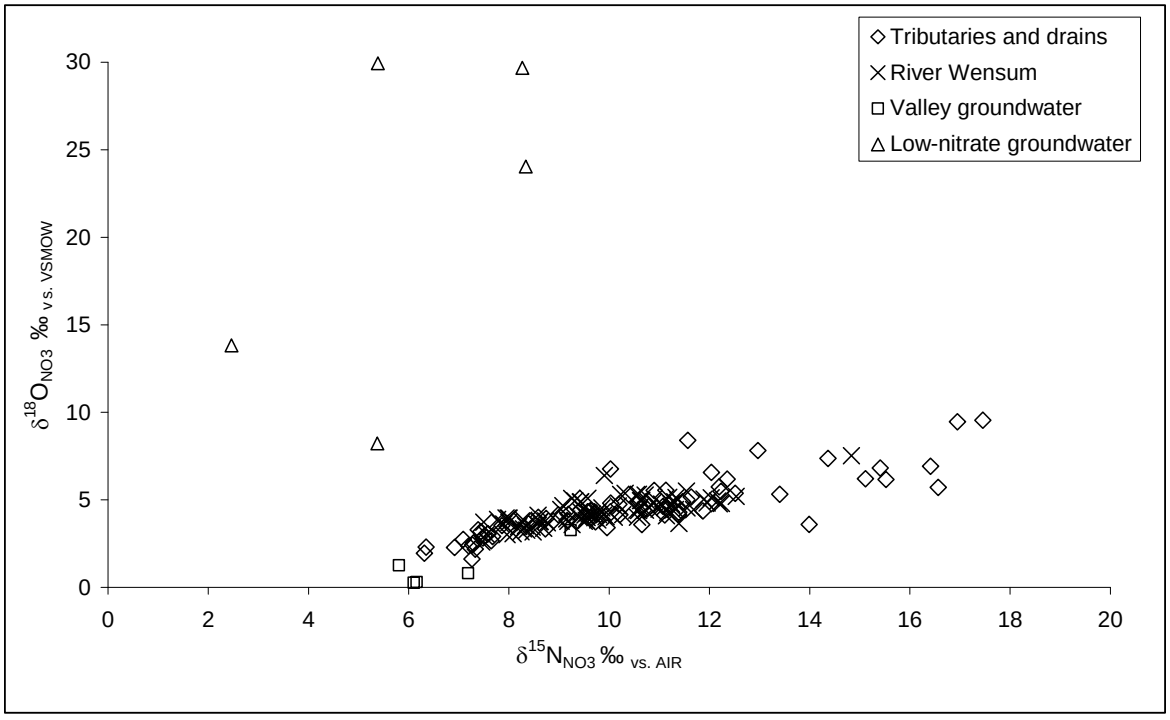

Figure 4.5 $\delta^{18}O_{NO3}$ (‰) versus $\delta^{15}N_{NO3}$ (‰) of samples from the Wensum catchment. Error: $\delta^{15}N_{NO3}$ and $\delta^{18}O_{NO3}$ ± 0.1‰ for River Wensum, tributaries and drains, and valley groundwater samples; $\delta^{15}N_{NO3}$ ± 1.0 ‰ and $\delta^{18}O_{NO3}$ ± 3.1‰ for low-nitrate groundwater.

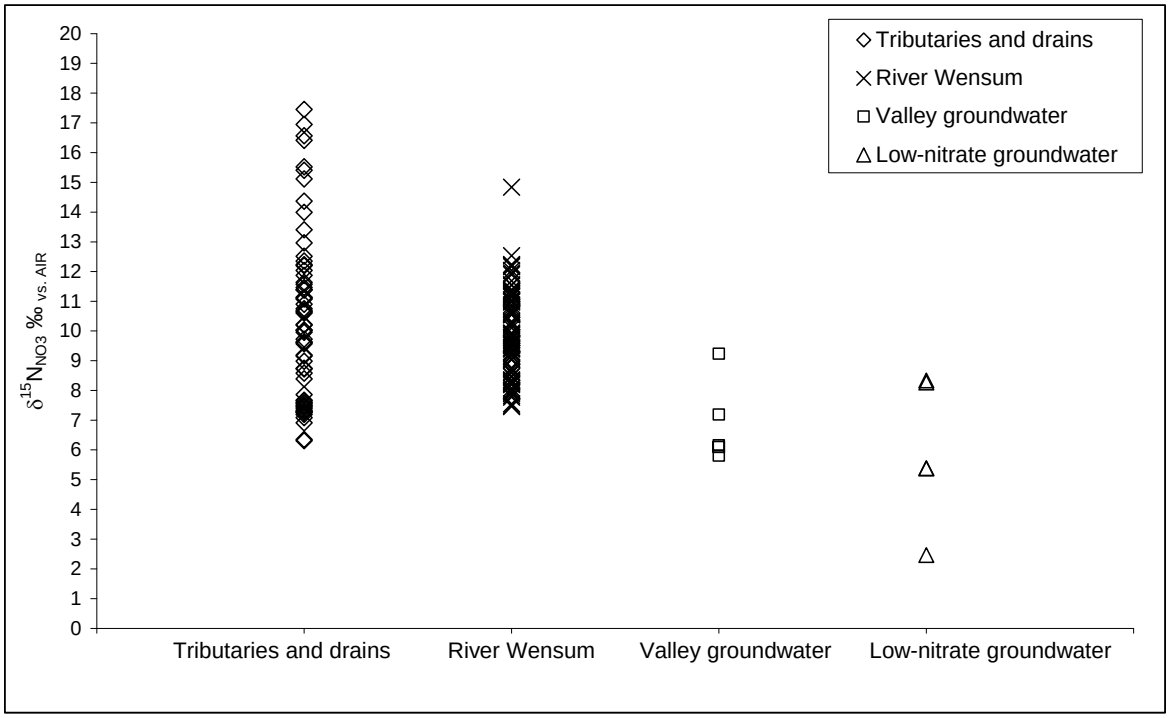

Figure 4.6 $\delta^{15}N_{NO3}$ (‰) of samples from the Wensum catchment. Error: $\delta^{15}N_{NO3} \pm 0.1$‰ for River Wensum, tributaries and drains, and valley Chalk groundwater samples; $\delta^{15}N_{NO3} \pm 1.0$ ‰ for low-nitrate groundwater.

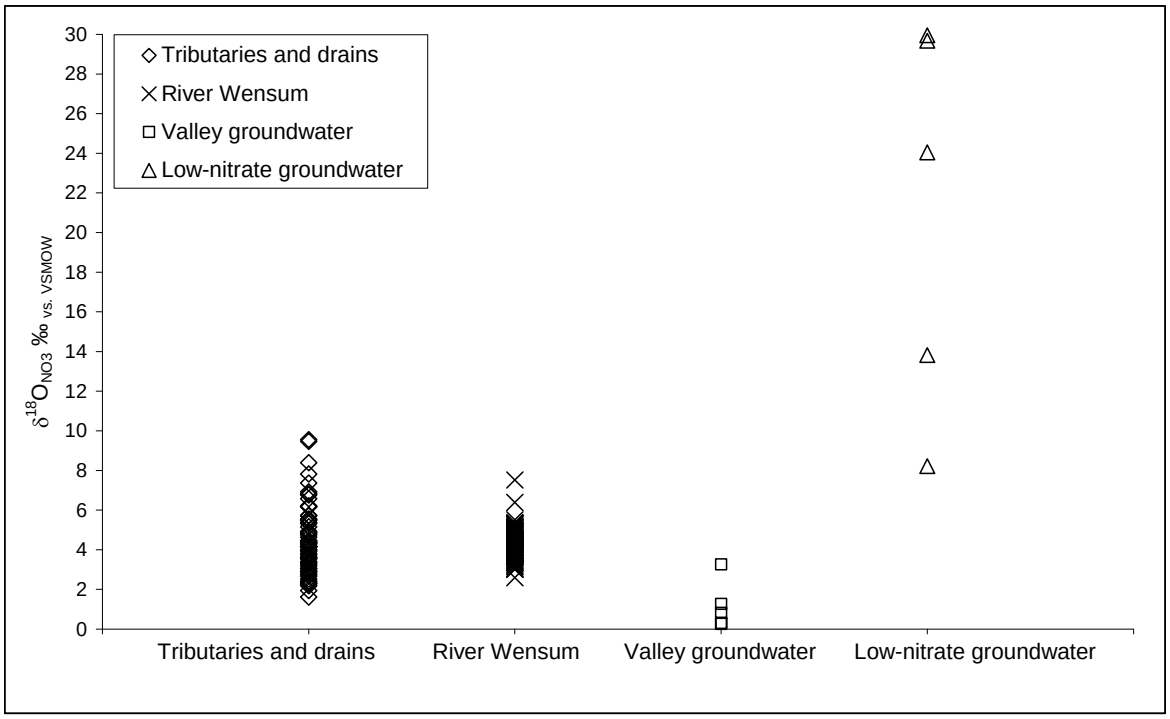

Figure 4.7 $\delta^{18}O_{NO3}$ (‰) of samples from the Wensum catchment. Error: $\delta^{18}O_{NO3} \pm 0.1$‰ for River Wensum, tributaries and drains, and valley Chalk groundwater samples; $\delta^{18}O_{NO3} \pm 3.1$‰ for low-nitrate groundwater.

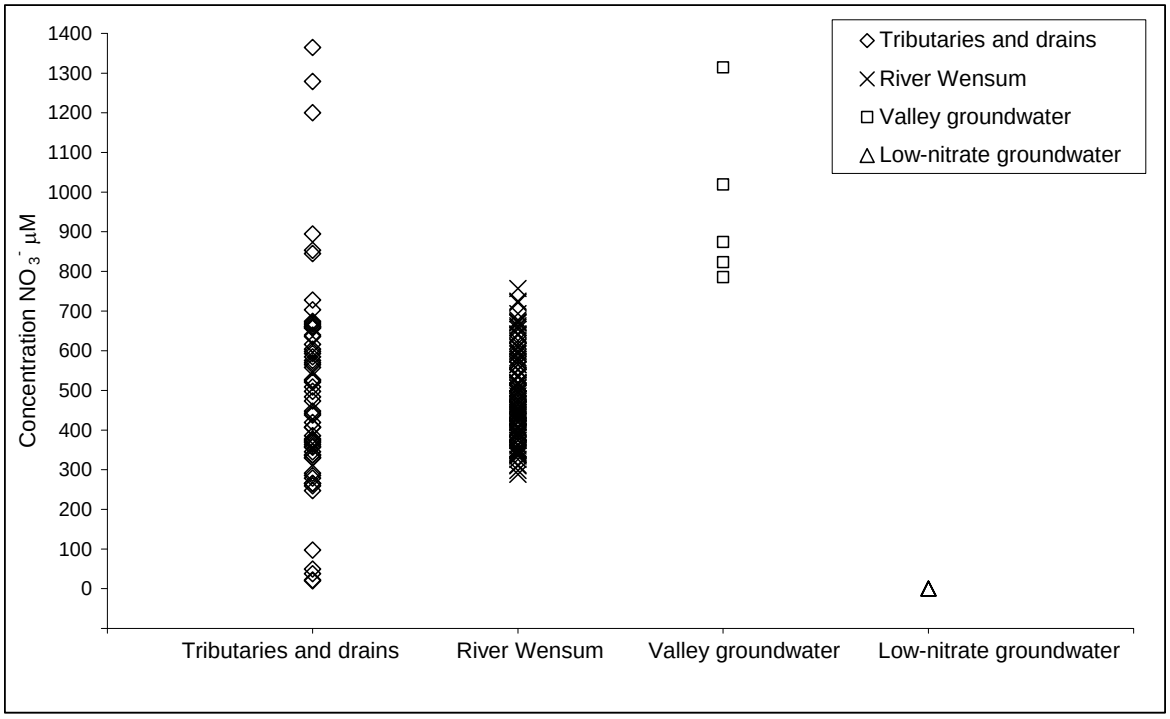

Figure 4.8 Concentration NO_3^- (µM) of samples from the Wensum catchment.

4.3.1 Wensum Spatial Surveys

Mean values with location for all spatial survey sampling sites on the Wensum river from the headwaters at Hamrow to the catchment outlet at Costessey Mill gauging station of $\delta^{15}N_{NO3}$, $\delta^{18}O_{NO3}$ and NO_3^- concentration with one standard deviation are shown in Figures 4.9 to 4.11. Where no standard deviation is shown, the location was sampled once only. Although these samples were collected across all seasons and flow conditions there is a high degree of homogeneity in nitrate isotopic composition and concentration at each sampling location beyond the uppermost sampling site at Hamrow, which, in contrast, shows a high level of variation in all parameters. The evolution of $\delta^{18}O_{NO3}$ from Hamrow to Costessey Mill mirrors that of $\delta^{15}N_{NO3}$, though displaying a slightly reduced range. Fakenham gauging station has nitrate of the lightest isotopic composition. In the mid river reach from Fakenham to Swanton, nitrate isotopic composition becomes increasingly heavy. In the lower river, from Swanton to Costessey, the isotopic composition of nitrate stabilises. NO_3^- concentration shows an inverse trend to isotopic composition, with concentration decreasing beyond Hamrow to Lyng, after which concentration becomes more stable. Single samples from Fakenham Heath and Burgh Common do not conform to these trends, showing a heavier $\delta^{15}N_{NO3}$ coupled with an increase in NO_3^- concentration.

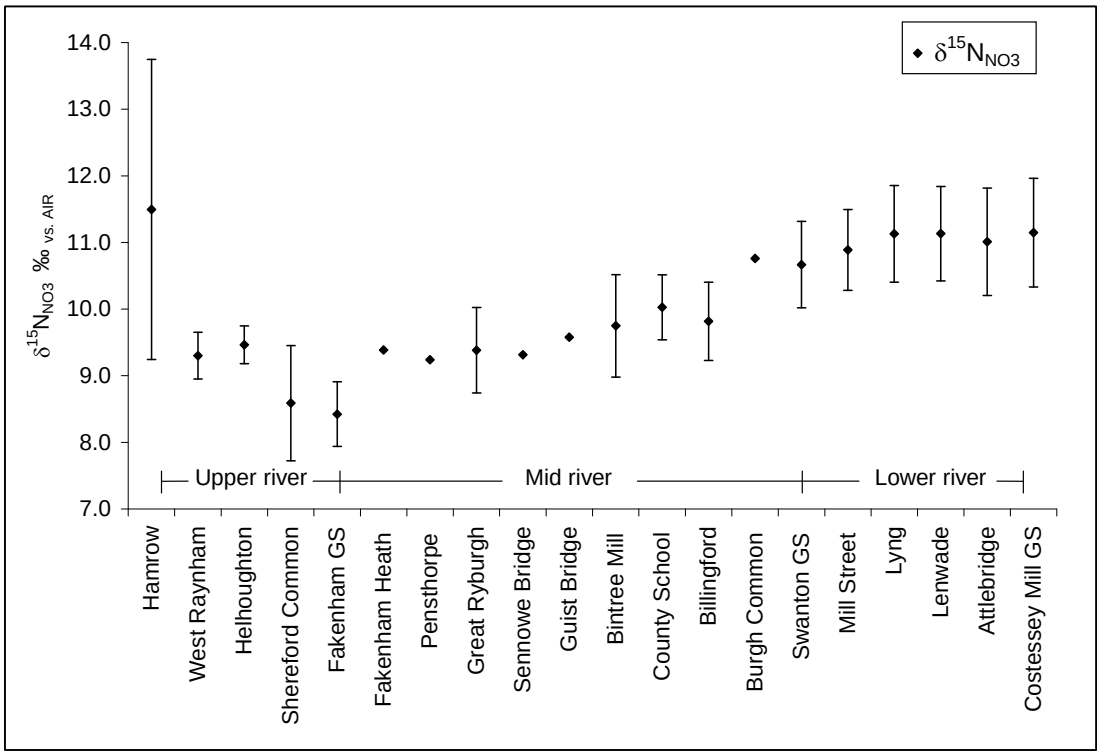

Figure 4.9 Mean $\delta^{15}N_{NO3}$ (‰) $\pm$ 1 standard deviation of nitrate from all sampling locations along the River Wensum headwater (Hamrow) to catchment outlet (Costessey GS) from samples collected between 14/02/2007 and 25/09/2009. GS denotes gauging station location. Locations with no error bars were sampled once only.

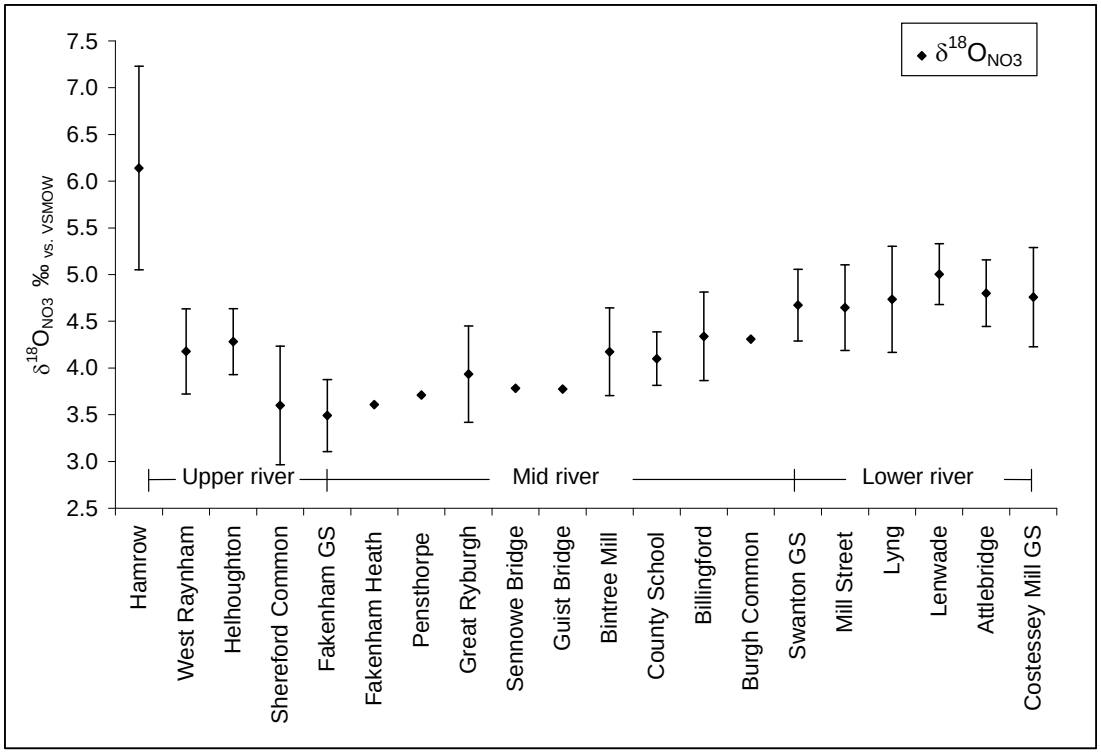

Figure 4.10 Mean $\delta^{18}O_{NO3}$ (‰) $\pm$ 1 standard deviation of nitrate from all sampling locations along the River Wensum headwater (Hamrow) to catchment outlet (Costessey GS) from samples collected between 14/02/2007 and 25/09/2009. GS denotes gauging station location. Locations with no error bars were sampled once only.

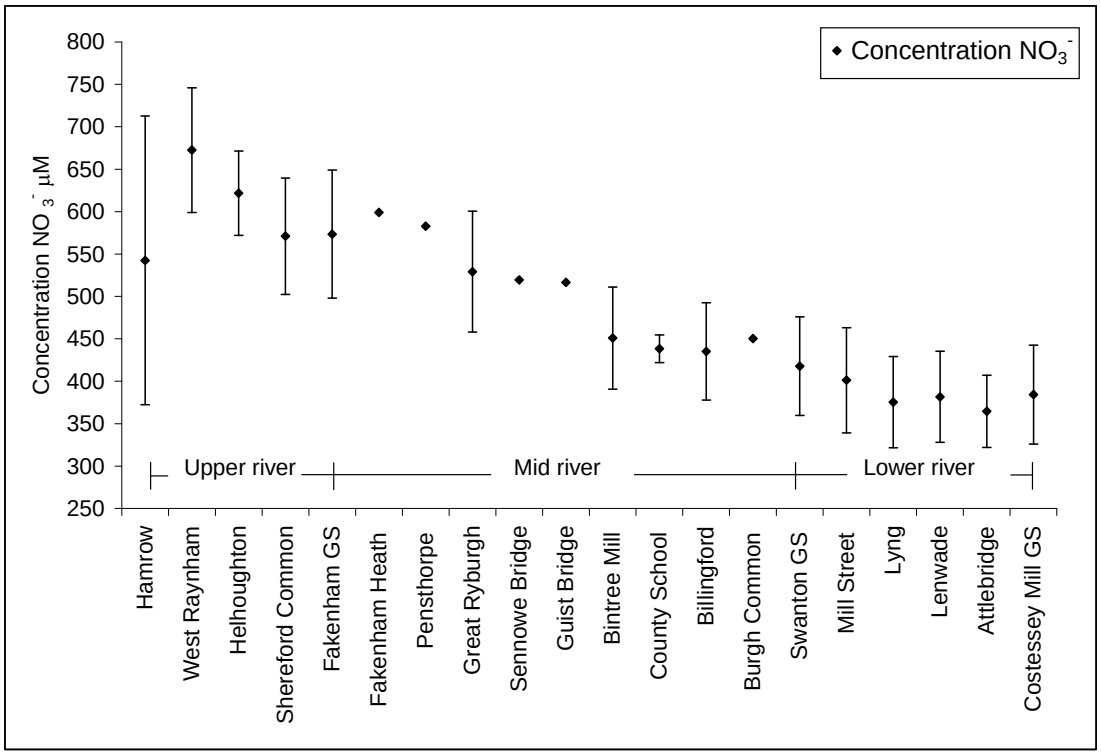

Figure 4.11 Concentration NO_3^- (µM) $\pm$ 1 standard deviation from all sampling locations along the River Wensum headwater (Hamrow) to catchment outlet (Costessey GS) from samples collected between 14/02/2007 and 25/09/2009. GS denotes gauging station location. Locations with no error bars were sampled once only.

The median and range of $\delta^{15}N_{NO3}$, $\delta^{18}O_{NO3}$ and NO_3^- concentration are used to present Wensum tributary and drain samples because of the variability and range of measured values (Figures 4.12 to 4.14). Where no range is shown, the location was sampled once only. Unlike the river samples, consistent parallels or inverse trends between $\delta^{15}N_{NO3}$, $\delta^{18}O_{NO3}$ and nitrate concentration are not seen. Of those sites sampled more than once, locations with the most variation in $\delta^{15}N_{NO3}$ and $\delta^{18}O_{NO3}$ are Shereford drain (n = 3), Great Ryburgh drain (n = 4), Bintree west drain (n = 4), and the Wendling Beck tributary at Worthing (n = 7). NO_3^- concentration also shows a large range at these locations in addition to Horningtoft drain (n = 4), and Lenwade drain (n = 2).

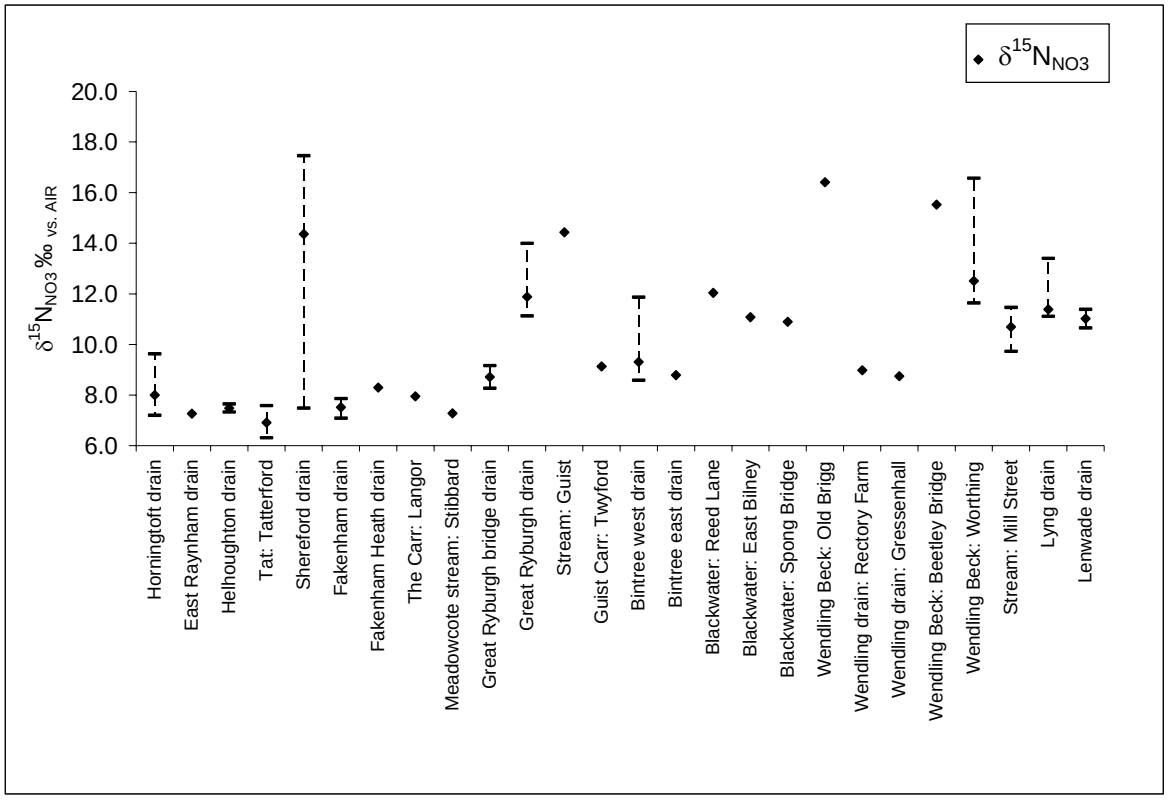

Figure 4.12 Median $\delta^{15}N_{NO3}$ (‰) with range of nitrate from Wensum tributary and drain sampling locations for samples collected between 14/02/2007 and 25/09/2009.

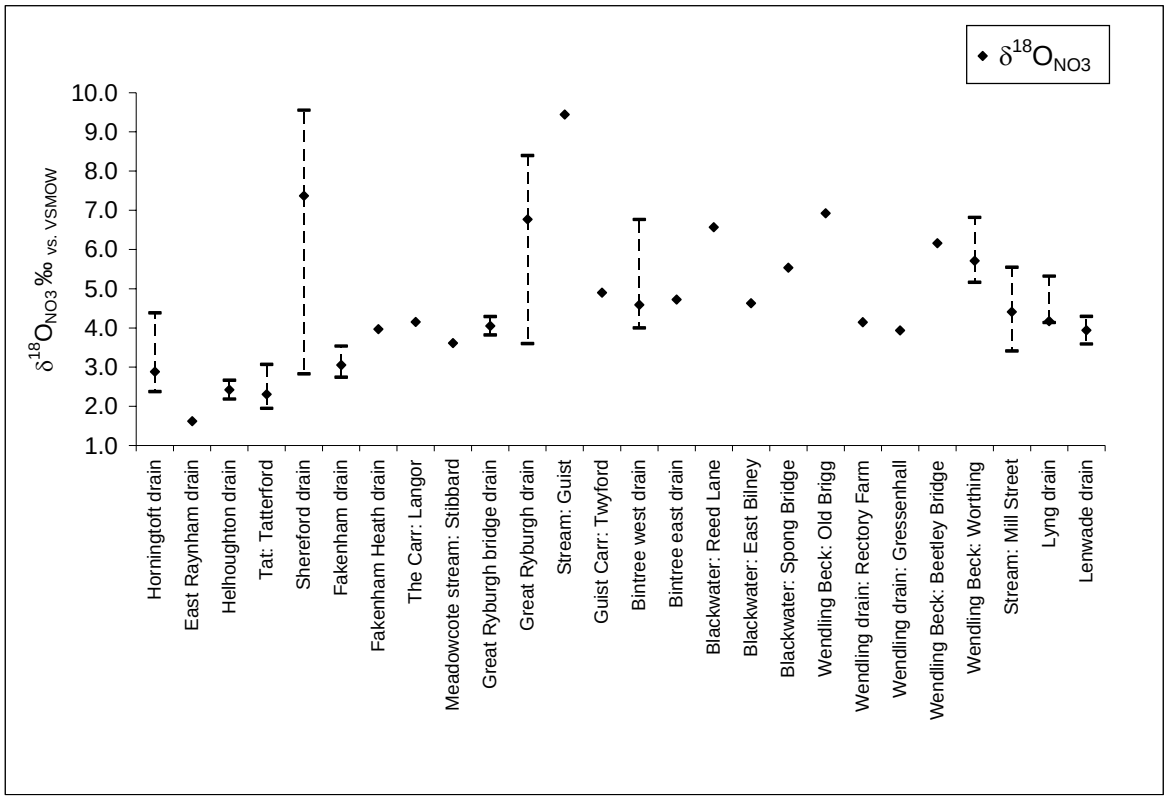

Figure 4.13 Median $\delta^{18}O_{NO3}$ (‰) with range of nitrate from Wensum tributary and drain sampling locations for samples collected between 14/02/2007 and 25/09/2009.

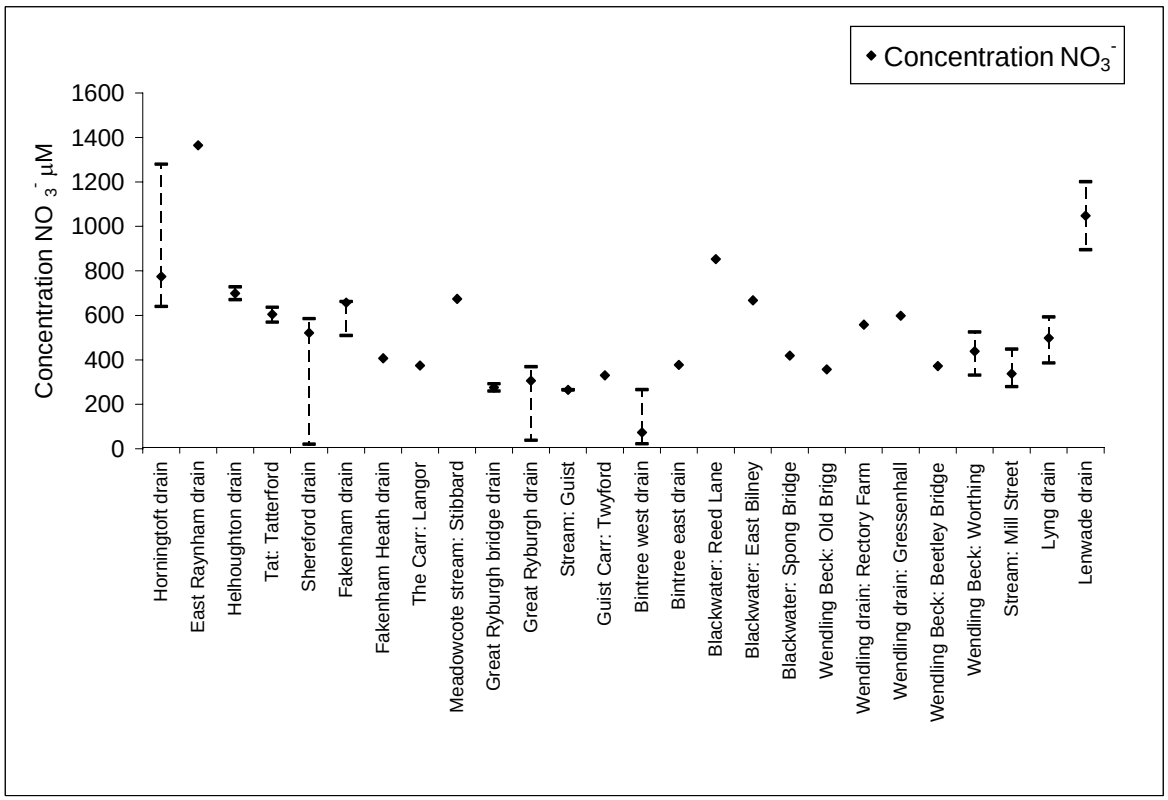

Figure 4.14 Median concentration NO_3^- (µM) with range of nitrate from Wensum tributary and drain sampling locations for samples collected between 14/02/2007 and 25/09/2009.

4.3.2 Wensum Temporal Surveys

The spring low-flow lower river temporal sample set (samples collected twice daily a.m.; 19-24/04/2007; n = 60) shows minor variation in $\delta^{15}N_{NO3}$, $\delta^{18}O_{NO3}$ and NO_3^- concentration between duplicate samples collected 60 to 90 minutes apart on the same day, with some variation falling within the measurement error. Variation between days is also small, but greater than the within day variation, suggesting that the data represent true, though minor variations in $\delta^{15}N_{NO3}$, $\delta^{18}O_{NO3}$ and NO_3^- concentration over the six-day period (Figures 4.15 to 4.17). The overall trend in $\delta^{15}N_{NO3}$ and $\delta^{18}O_{NO3}$ is of decreasing values from Swanton gauging station to Mill Street, then increasing values to Attlebridge ($\delta^{15}N_{NO3}$) and Lenwade ($\delta^{18}O_{NO3}$). NO_3^- concentration decreases between Swanton and Attlebridge, though concentrations are level at Lyng where concentration across samples shows homogeneity.

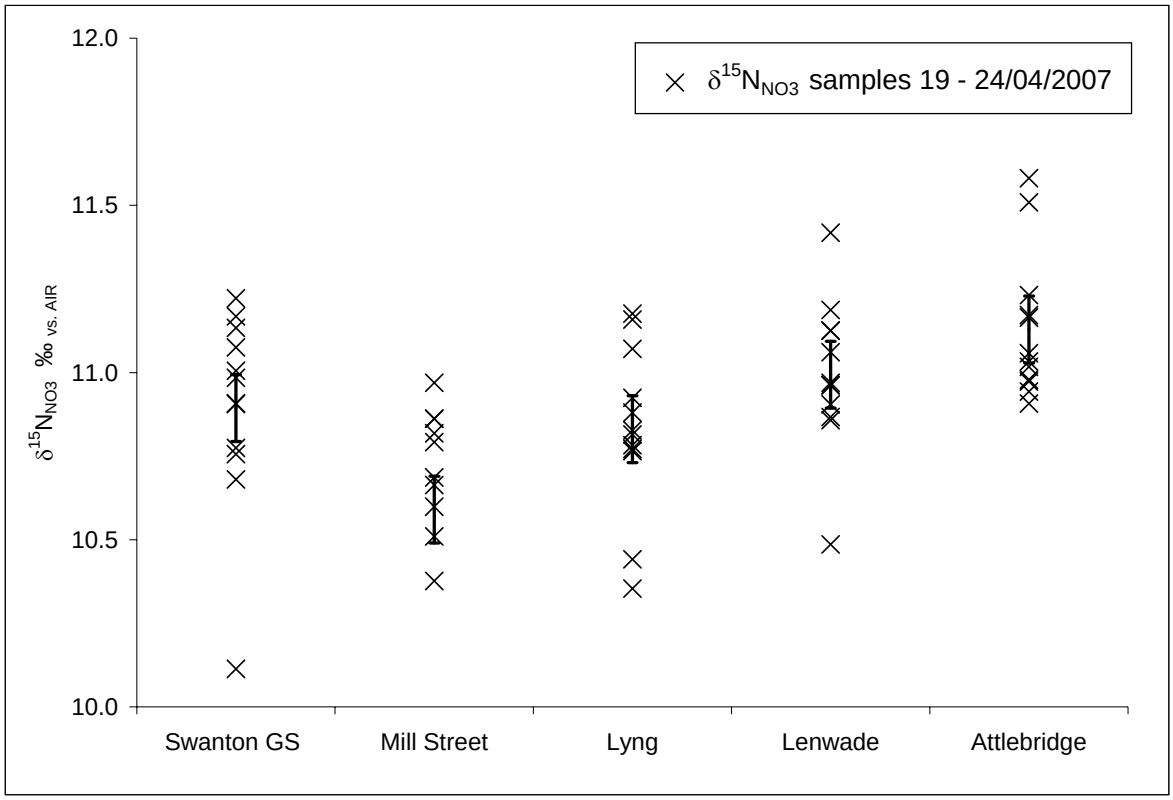

Figure 4.15 $\delta^{15}N_{NO3}$ (‰) of lower river temporal samples collected 19-24/04/2007, with error bars representing measurement error ($\pm$ 0.1‰) around the mean value from each location.

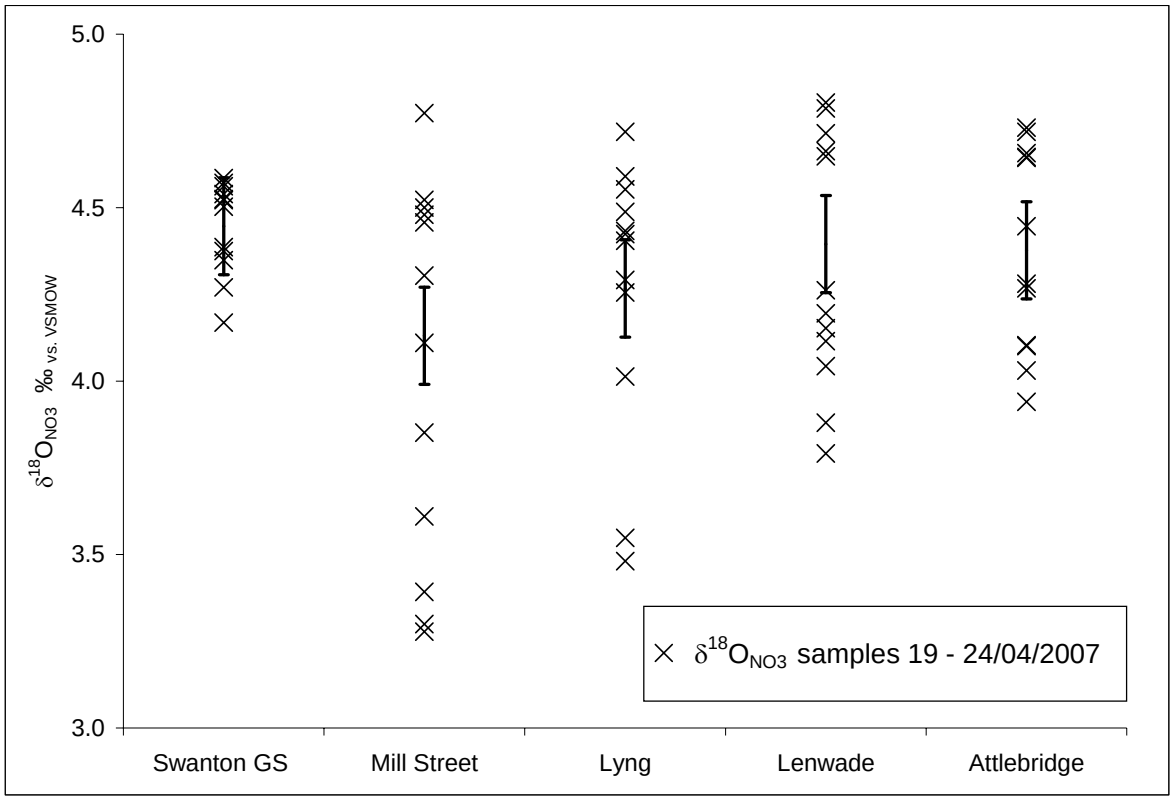

Figure 4.16 $\delta^{18}O_{NO3}$ (‰) of lower river temporal samples collected 19-24/04/2007, with error bars representing measurement error ($\pm$ 0.1‰) around the mean value from each location.

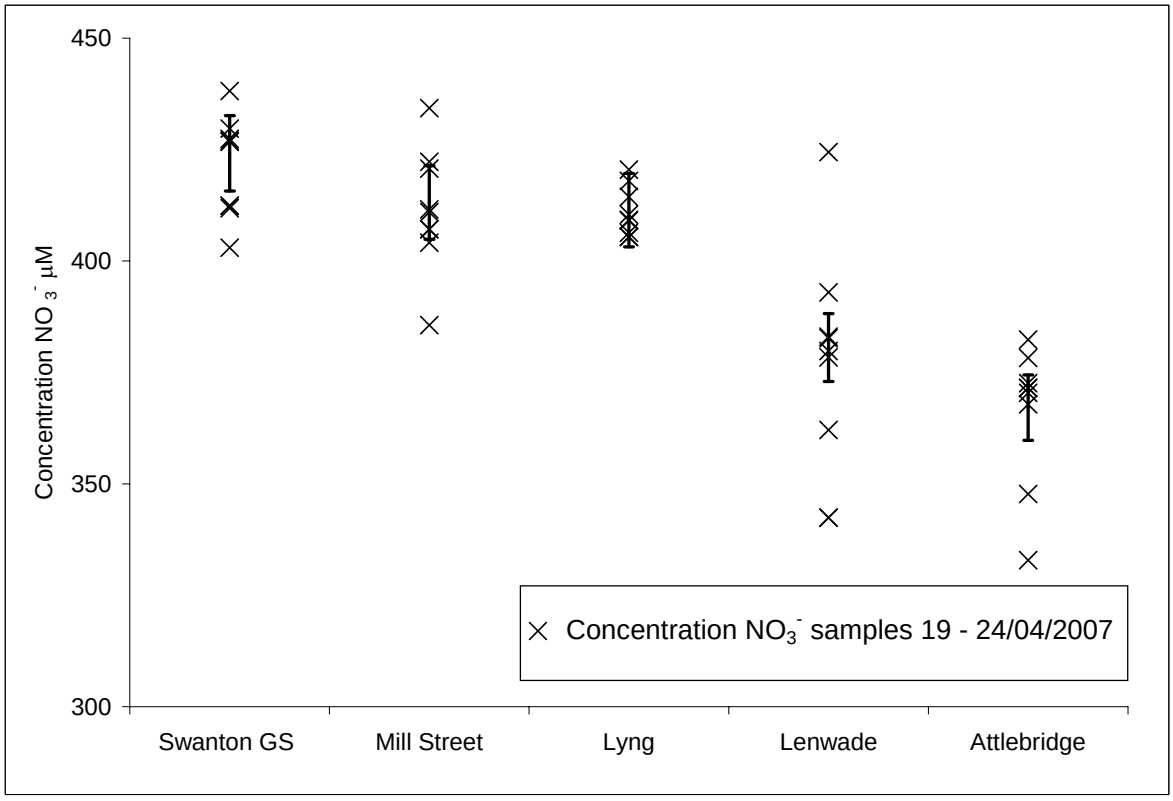

Figure 4.17 NO_3^- (µM) of lower river temporal samples collected 19-24/04/2007, with error bars representing measurement error ($\pm$ 2%) around the mean value from each location.

The time series of 15-minute flow data from Swanton gauging station for the same period shows fluctuating low flow which decreases over the first five days, corresponding to a slight decrease in NO_3^- concentration (Figure 4.18).

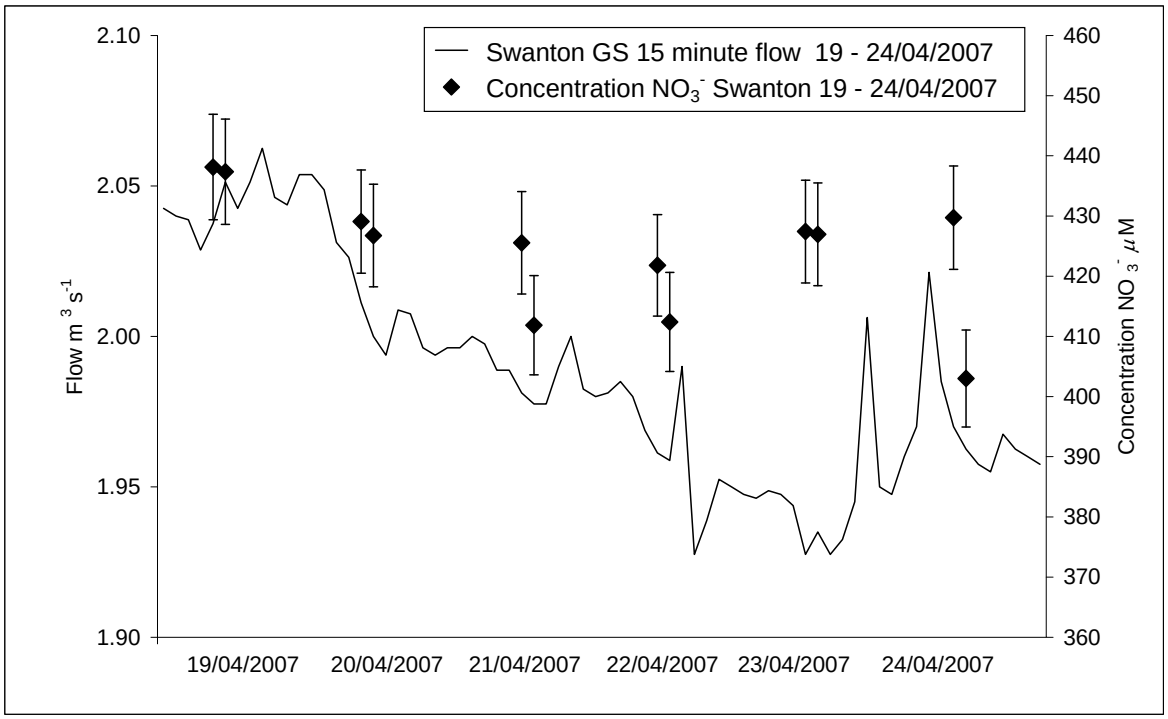

Figure 4.18 15-minute flow at Swanton Morley gauging station (GS) (m^3 s^{-1}) for the period 19-24/04/2007 with concentration NO_3^- (μM) at Swanton gauging station of paired daily samples.

The summer high flow lower river temporal sample set (samples collected twice daily a.m., 18-19/07/2007, n = 20) shows little variation in $\delta^{15}N_{NO3}$, $\delta^{18}O_{NO3}$ and NO_3^- concentration across the two-day period. What variation there is largely falls within the measurement error (Figures 4.19 to 4.21). During this period decreasing flow is seen in 15-minute flow data for Swanton gauging station, while at Costessey Mill gauging station flow increases, indicating the passing of a flood peak through the catchment (Figure 4.22).

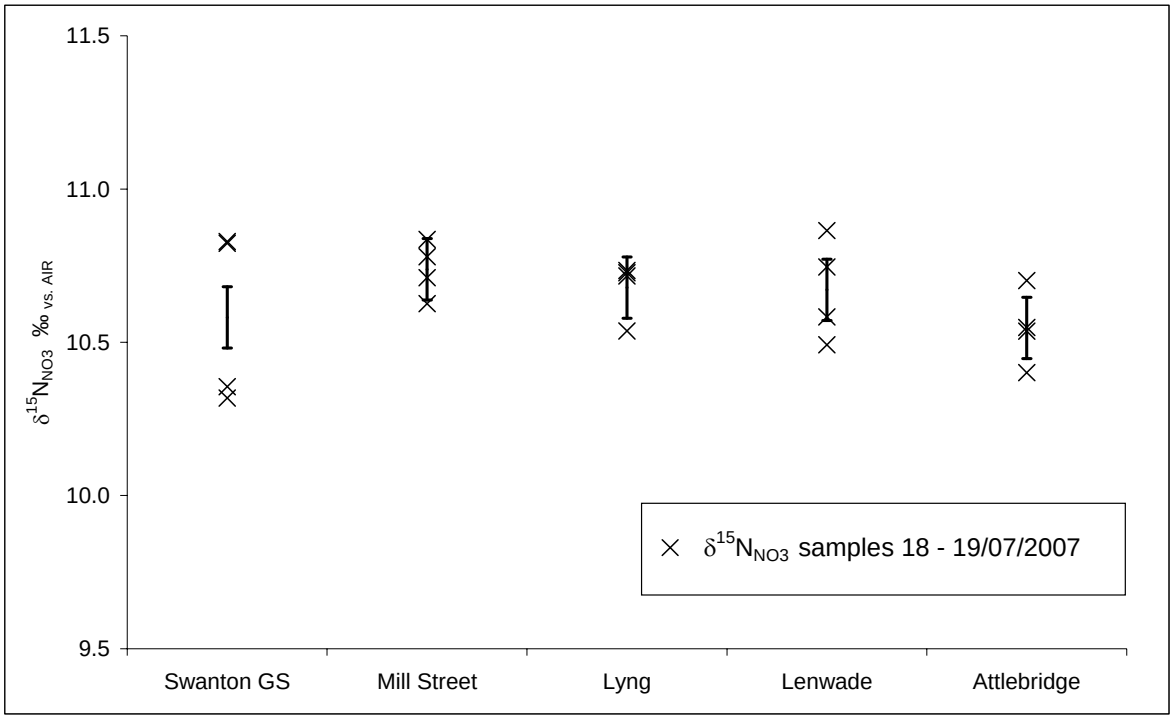

Figure 4.19 $\delta^{15}N_{NO3}$ (‰) of lower river temporal samples collected 18-19/07/2007, with error bars representing measurement error ($\pm$ 0.1‰) around the mean value from each location.

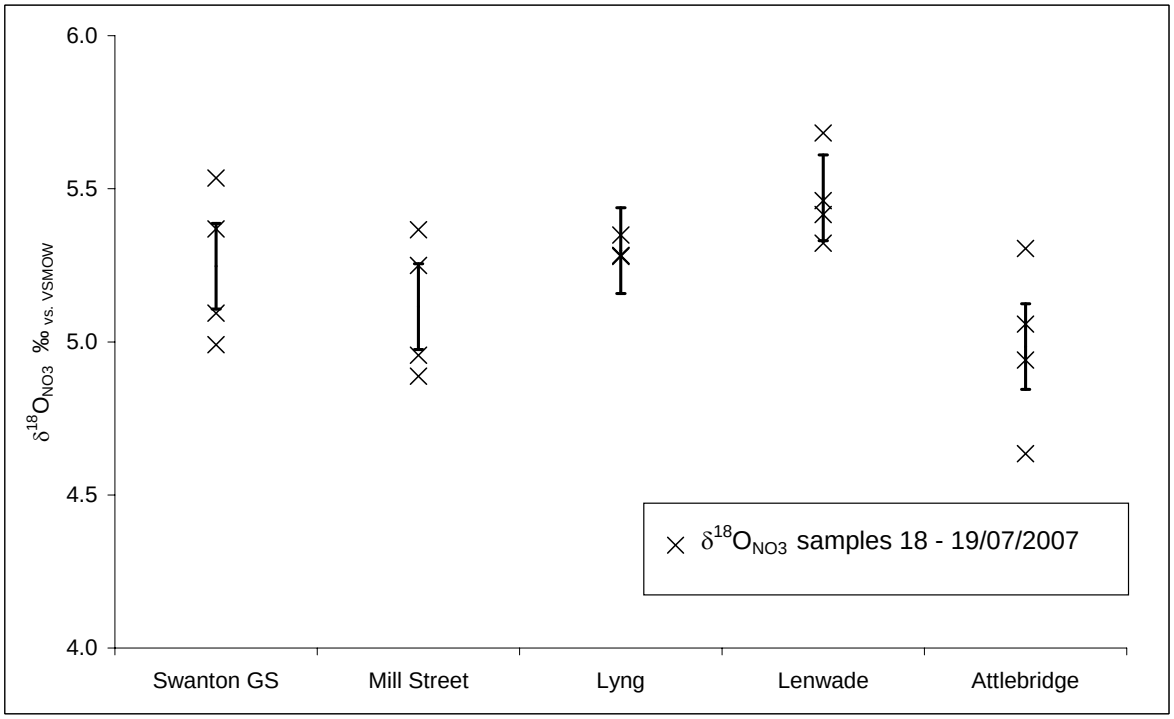

Figure 4.20 $\delta^{18}O_{NO3}$ (‰) of lower river temporal samples collected 18-19/07/2007, with error bars representing measurement error ($\pm$ 0.1‰) around the mean value from each location.

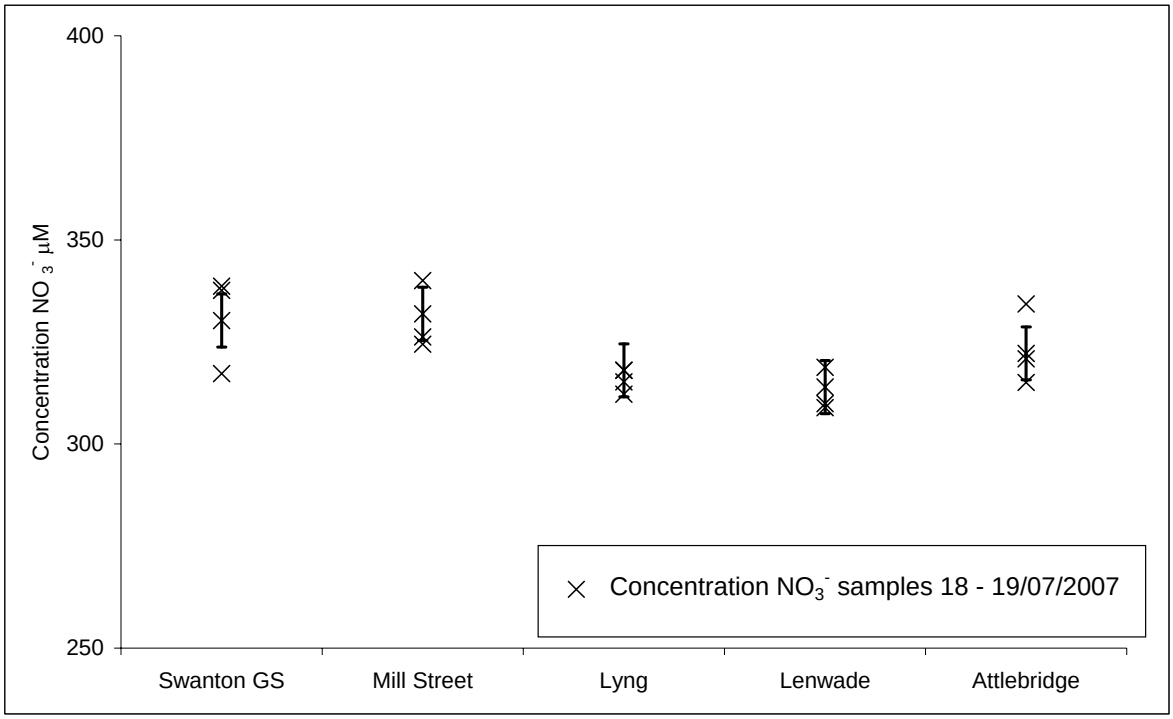

Figure 4.21 NO_3^- (µM) of lower river temporal samples collected 18-19/07/2007, with error bars representing measurement error (± 2%) around the mean value from each location.

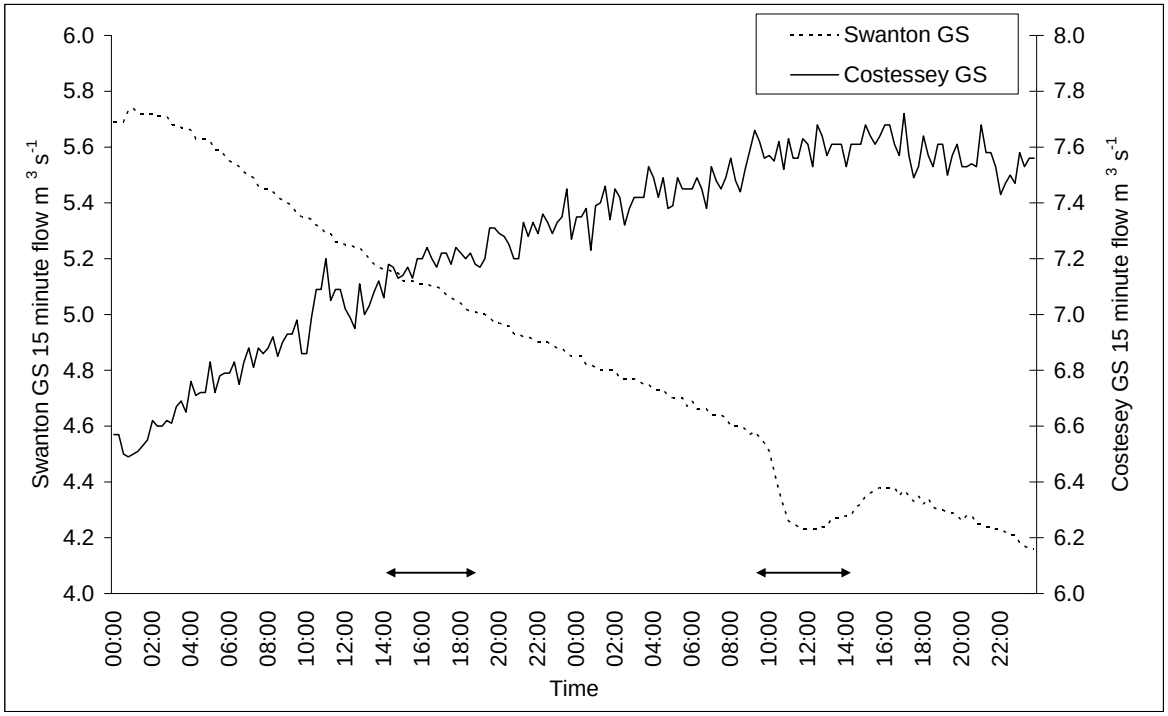

Figure 4.22 15 minute flow at Swanton Morley and Costessey Mill gauging stations (GS) (m^3 s^{-1}) for the period 18-19/07/2007 with arrows indicating sampling periods.

The hourly samples collected during winter from the gauging stations at Fakenham and Swanton (12-13/12/2008, n = 48) show a heavier isotopic composition in the Swanton

samples than in those from Fakenham (Figures 4.23 and 4.24). NO_3^- concentration is lower at Swanton than at Fakenham (Figure 4.25). NO_3^- concentration at both gauging station rises over the first twelve hours of sampling, then decreases in the final four hours at Fakenham, but is maintained at Swanton. Flow, which is high, slowly decreases over much of the 24-hour period, rapidly increasing through the final five hours (Figures 4.26 and 4.27). Flow gauging at Fakenham is of poorer resolution than at Swanton, containing interpolated values. This explains the blocky patter of flow in Figure 4.23.

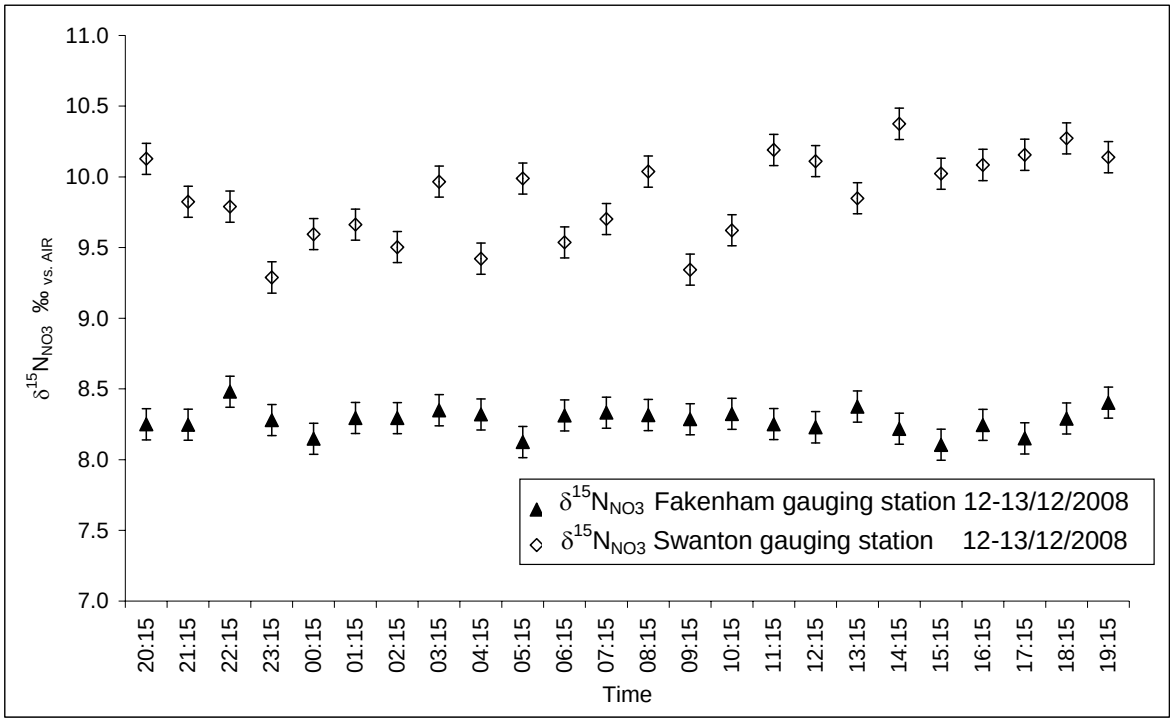

Figure 4.23 $\delta^{15}N_{NO3} \pm 0.1$ (‰) time series of hourly samples collected at Fakenham gauging station and Swanton Morley gauging station 12-13/12/2008.

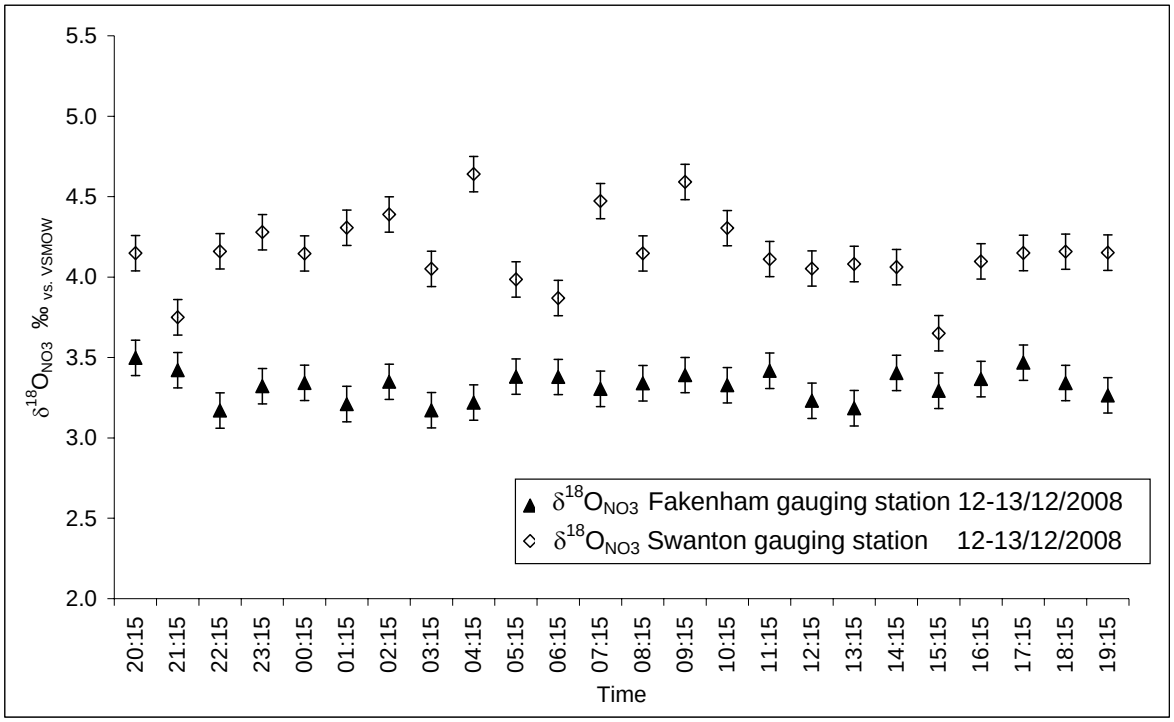

Figure 4.24 $\delta^{18}O_{NO3} \pm 0.1$ (‰) time series of hourly samples collected at Fakenham gauging station and Swanton Morley gauging station 12-13/12/2008.

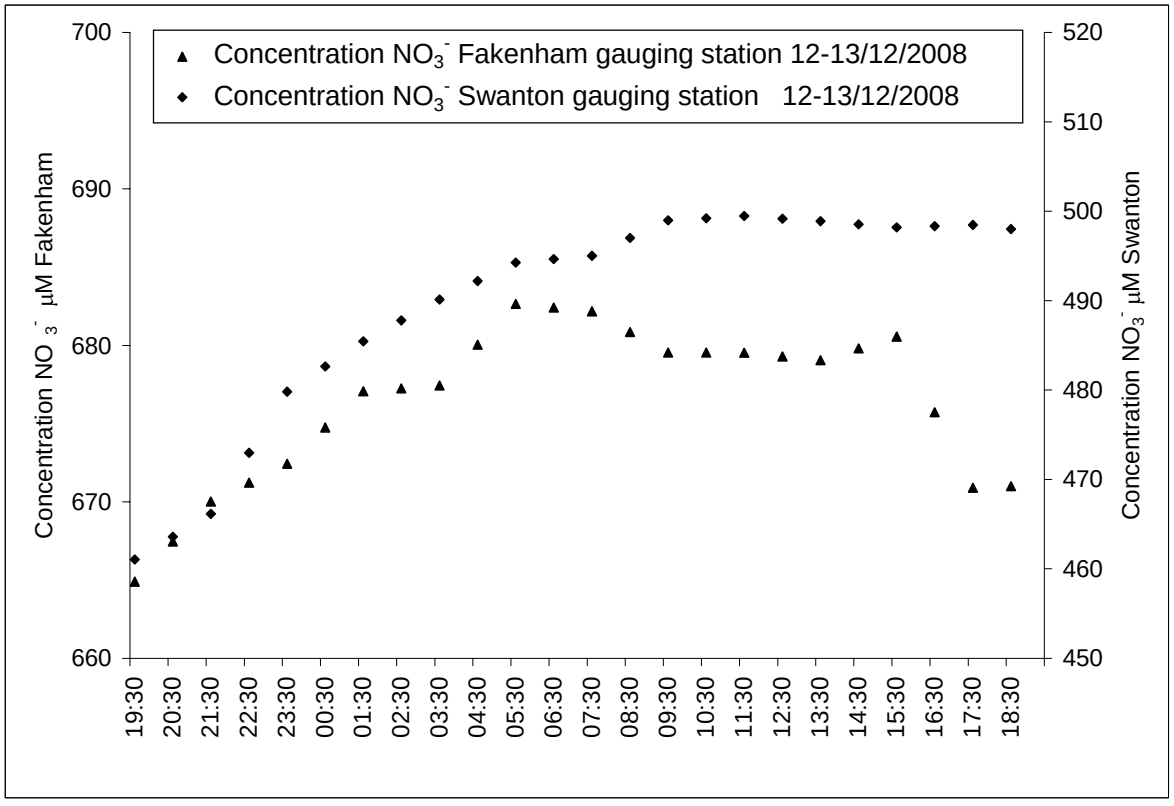

Figure 4.25 Concentration NO_3^- (µM) time series of hourly samples collected at Fakenham and Swanton Morley gauging stations 12-13/12/2008, (note different scales on y axes).

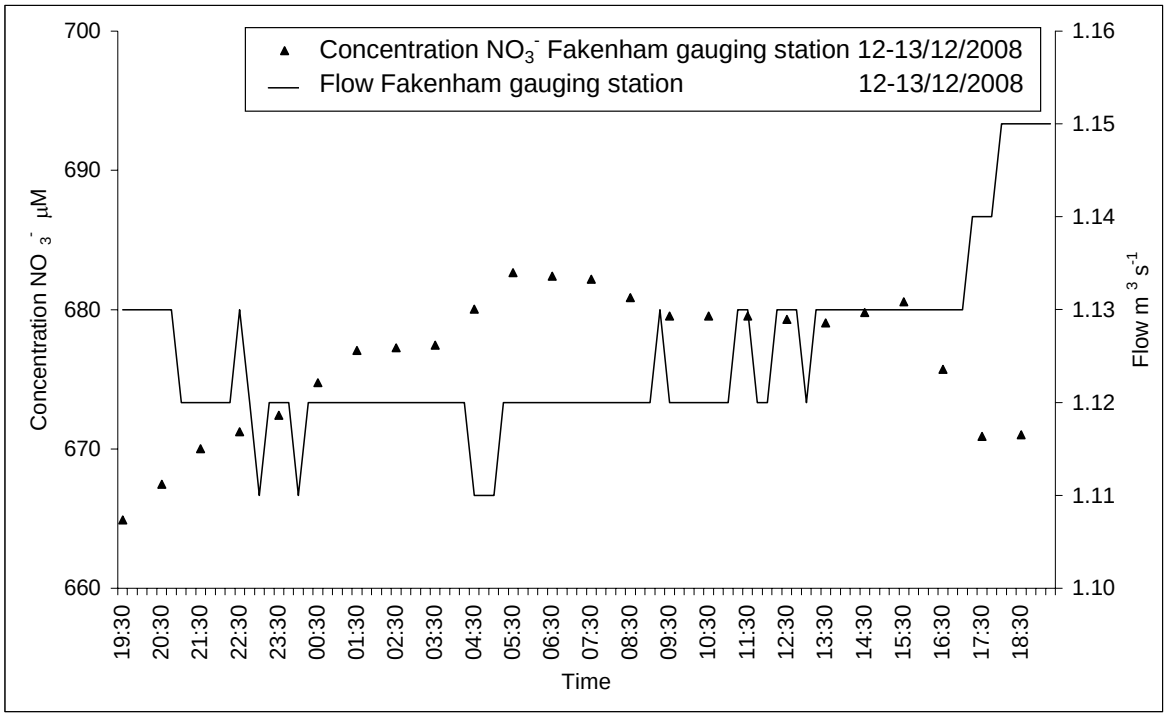

Figure 4.26 Concentration NO_3^- (µM) time series of hourly samples collected at Fakenham gauging station 12-13/12/2008, showing 15-minute flow (m^3 s^{-1}) at Fakenham gauging station

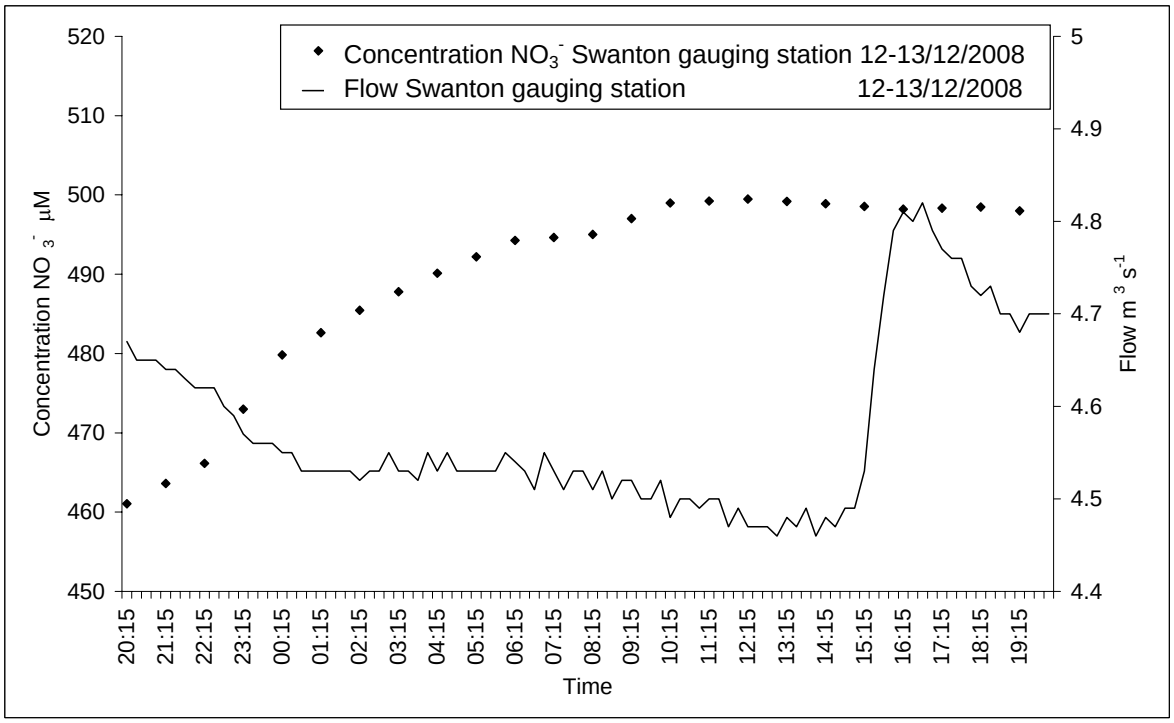

Figure 4.27 Concentration NO_3^- (µM) time series of hourly samples collected at Swanton Morley gauging station 12-13/12/2008, showing 15-minute flow (m^3 s^{-1}) at Swanton Morley gauging station

4.3.3 Chalk Groundwater

Valley groundwater samples from Chalk boreholes in the Wensum valley have a narrow range of $\delta^{15}N_{NO3}$ and $\delta^{18}O_{NO3}$ and high NO_3^- concentrations (Figure 4.28). These Chalk boreholes are overlain by sands and gravels and superficial deposits (borehole logs are included in Appendix 2).

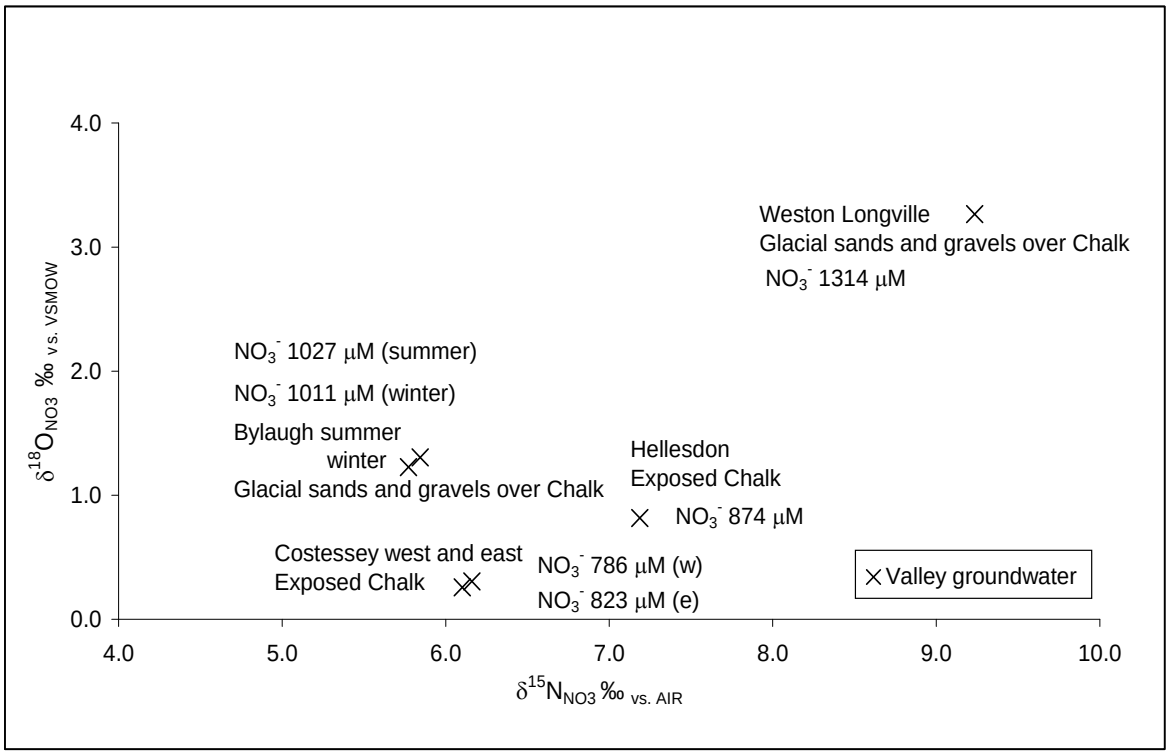

Figure 4.28 Valley Chalk groundwater $\delta^{18}O_{NO3}$ (‰) versus $\delta^{15}N_{NO3}$ (‰) with sampling location. Error: $\delta^{15}N_{NO3}$ and $\delta^{18}O_{NO3}$ $\pm$ 0.1‰.

Groundwater samples from the Chalk on the interfluves and valley margins (low-nitrate groundwater), with NO_3^- concentration high enough to allow isotopic measurement (though below 1 μM NO_3^-) have slightly lower $\delta^{15}N_{NO3}$ in comparison to the surface water catchment samples, with very high $\delta^{18}O_{NO3}$ values (Figure 4.29). The samples from Taverham, Great Ryburgh, and Hamrow west show the heaviest oxygen isotopic composition, with the sample from Hamrow east showing the lightest nitrogen isotopic composition. These Chalk boreholes are overlain by the Lowestoft Till and sands and gravels. (Borehole logs are included in Appendix 2).

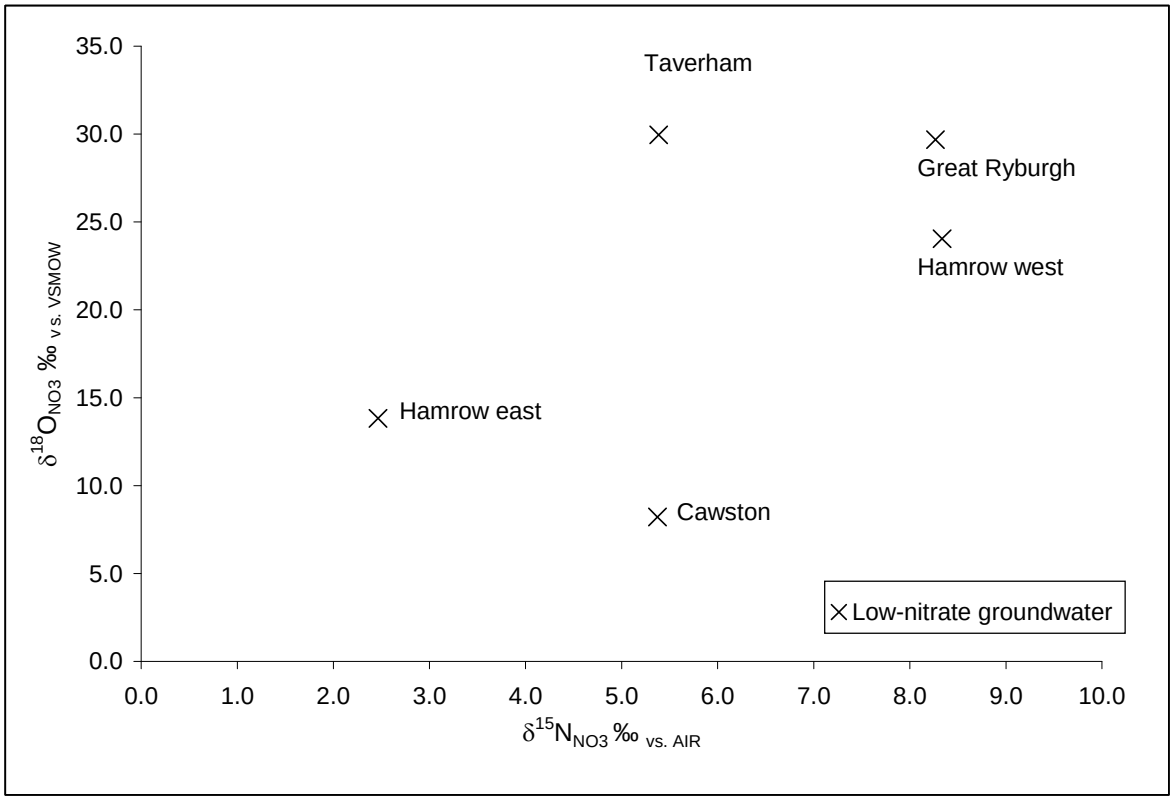

Figure 4.29 Low-nitrate Chalk groundwater $\delta^{18}O_{NO3}$ (‰) versus $\delta^{15}N_{NO3}$ (‰) with sampling location. Error $\pm$ 1.0 ‰ for $\delta^{15}N_{NO3}$ and $\pm$ 3.1 ‰ for $\delta^{18}O_{NO3}$.

4.4 WENSUM CATCHMENT HYDROCHEMISTRY

In cases where results from the analysis of various hydrochemical parameters presented here are not included in the interpretation of sources and cycling of catchment nitrate presented in Chapter 5, Discussion, an interpretation of the data is included in the following text.

4.4.1 Wensum Field Parameters

The Wensum catchment is a $CaCO_3$ dominated system due to the strong influence of the Chalk, with high concentrations of major ions resulting from land use and geology. Mean concentrations of total dissolved solids (TDS) for the river, and tributary and drain, samples are close to 600 mg/L, indicating fairly high concentrations of major ions, with a greater range in values seen in the tributary and drain sample set than in the river samples, which is likely to reflect variations in source inputs from runoff. Mean

electrical conductivity (EC) for these surface water samples is in the range 650-700 μS min^{-1}, in fairly good agreement with the TDS calculation, and again the tributary and drain samples have a greater range of EC. Mean pH is close to neutral, reflecting the strong influence of $CaCO_3$, with a slightly greater range in the tributary and drain samples than in the river samples. Mean redox potential in the river, and tributary and drain samples indicates oxidising conditions, while dissolved oxygen (DO) concentrations indicate conditions at or near oxygen saturation. The range of temperature of surface water samples is 6.0 to 15°C.

The borehole samples have slightly lower TDS than surface water, with a mean EC of 650 μS min^{-1}, which may reflect a slightly lower influence of solutes entrained in runoff. The mean pH of the groundwater is neutral with a narrow range. Eh of the borehole samples is lower than that of the surface water samples, with the lowest measurement, from a borehole sample on the interfluve under the Lowestoft Till indicating a shift to more reducing conditions. A similar pattern is seen in concentrations of DO which are below saturation. Temperature shows a reduced range in comparison to surface water, of 8.4 to 12°C (Table 4.6a-c).

Table 4.6a Field parameters (pH, Eh, DO, and EC) and calculated TDS for Wensum river samples showing mean, one standard deviation, minima and maxima.

Wensum river samples					
Parameter	**Mean**	**One standard deviation**	**Minimum**	**Maximum**	**n**
TDS mg/L	598	72	497	785	-
EC μS min^{-1}	700	100	500	800	76
pH	7.2	0.4	6.5	8.0	84
Eh mV	184	27	104	256	84
DO %	97	8	79	114	70
T °C	12.4	2.3	7.5	15.0	66

Table 4.6b Field parameters (pH, Eh, DO, and EC) and calculated TDS for Wensum tributary and drain samples showing mean, one standard deviation, minima and maxima.

Wensum tributary and drain samples					
Parameter	**Mean**	**One standard deviation**	**Minimum**	**Maximum**	**n**
TDS mg/L	612	122	335	913	-
EC μS min^{-1}	650	100	500	900	25
pH	7.3	0.4	6.0	8.0	30
Eh mV	174	41	71	245	30
DO %	89	19	48	118	18
T °C	11.0	3.9	6.0	15.0	12

Table 4.6c Field parameters (pH, Eh, DO, and EC) and calculated TDS for Wensum Chalk borehole samples showing mean, one standard deviation, minima and maxima.

Wensum borehole samples					
Parameter	**Mean**	**One standard deviation**	**Minimum**	**Maximum**	**n**
TDS mg/L	527	157	310	769	-
EC µS min^{-1}	650	100	450	850	16
pH	7.0	0.1	6.7	7.2	16
Eh mV	75	41	-22	113	16
DO %	60	16	26	76	16
T ^{o}C	10.5	1.0	8.4	12.0	16

4.4.2 TDN Concentrations in Wensum Surface Water

The major species of total dissolved nitrogen in Wensum river water and tributary and drain water is nitrate (> 80 %) with a significant proportion of DON (> 18%). Nitrite and ammonium comprise a negligible fraction of total dissolved nitrogen (< 2 % together), though concentrations in tributary and drain water are almost double those in river water (Table 4.7; Figure 4.30). This is likely to be due to the close proximity of tributaries and drains to sources of contamination from fields, and could also reflect nitrogen cycling within the soil or drains. Although mean concentrations of nitrate are similar in the river samples and the tributary and drain samples, the concentration range of nitrate in the tributary and drain samples is greater than that of the river samples, again reflecting source contamination and nitrogen cycling (20 to1365 µM NO_3^- vs. 228 to 757 µM NO_3^-).

Table 4.7 Concentrations of dissolved nitrogen (µM NO_3^-, NO_2^-, NH_4^+, DON) in samples from the Wensum river, tributary and drains, showing mean, one standard deviation, minima and maxima.

Wensum river dissolved nitrogen concentrations					
Dissolved nitrogen species	**Mean**	**One standard deviation**	**Minimum**	**Maximum**	**n**
NO_3^- µM	475	115	288	757	105
NO_2^- µM	1.8	1.6	<LOD	7.4	105
NH_4^+ µM	2.6	3.9	<LOD	21.4	105
DON µM	109	46	51	195	34
Wensum tributary and drain dissolved nitrogen concentrations					
Dissolved nitrogen species	**Mean**	**One standard deviation**	**Minimum**	**Maximum**	**n**
NO_3^- µM	499	263	20	1365	64
NO_2^- µM	2.7	2.6	<LOD	14.7	64
NH_4^+ µM	4.8	5.4	<LOD	21.4	64
DON µM	112	90	30	467	22

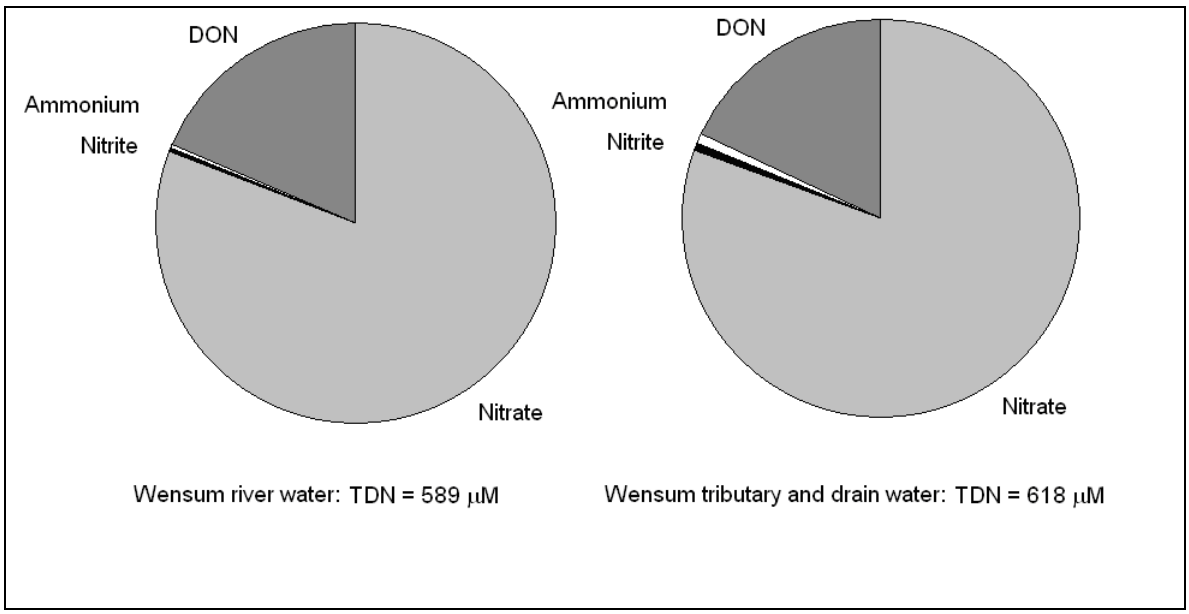

Figure 4.30 Relative proportions in Wensum river water and tributary and drain water of mean concentrations of the four dissolved nitrogen species: nitrate; nitrite; ammonium and DON, showing TDN.

The spatial distribution of nitrate concentration with location from headwaters to catchment outlet in Wensum river samples shows an overall gradual decreasing trend, with wide variation across sample sets at each location (Figure 4.31). In contrast nitrite concentration increases downstream (Figure 4.32). Concentrations of ammonium suggest a similar pattern (Figure 4.33), while DON concentrations appear to be evenly distributed across locations, although the ammonium and DON data sets are smaller than those of nitrate and nitrite, and may not represent the spatial distribution of these species well (Figure 4.34).

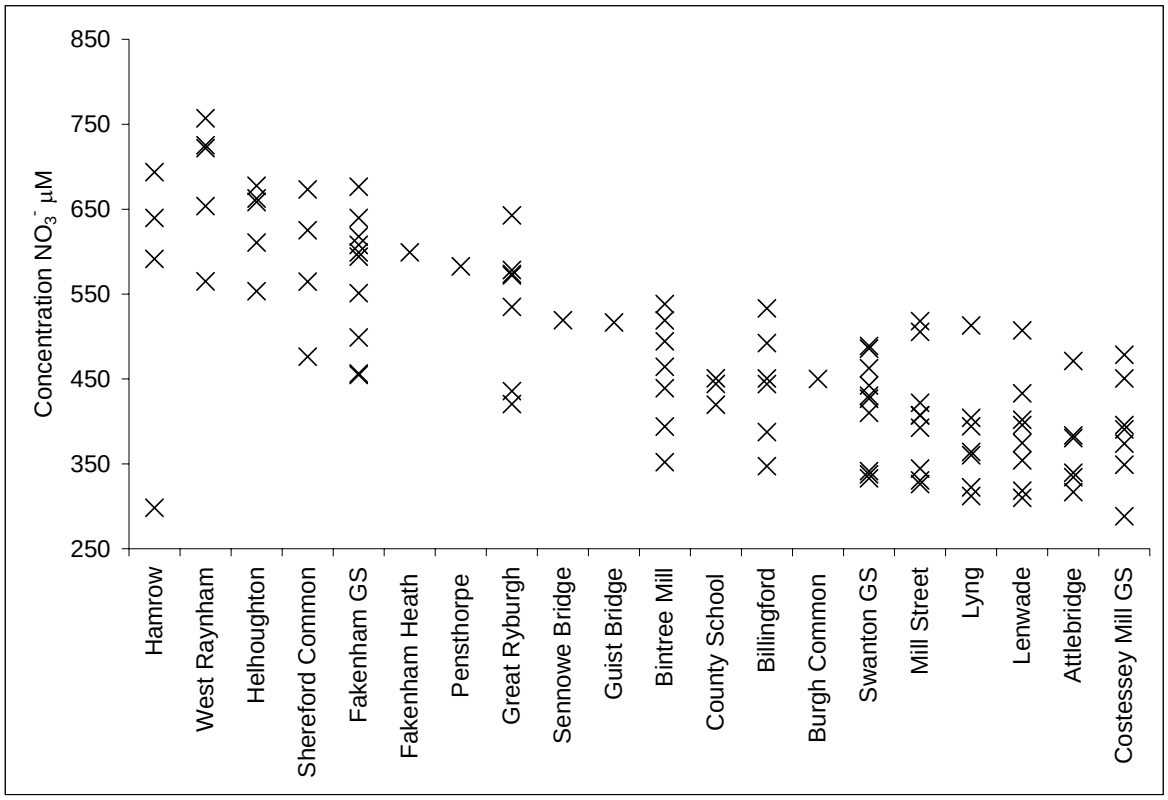

Figure 4.31 Concentration NO_3^- (µM) of Wensum river samples collected between 14/02/2007 and 25/09/2009.

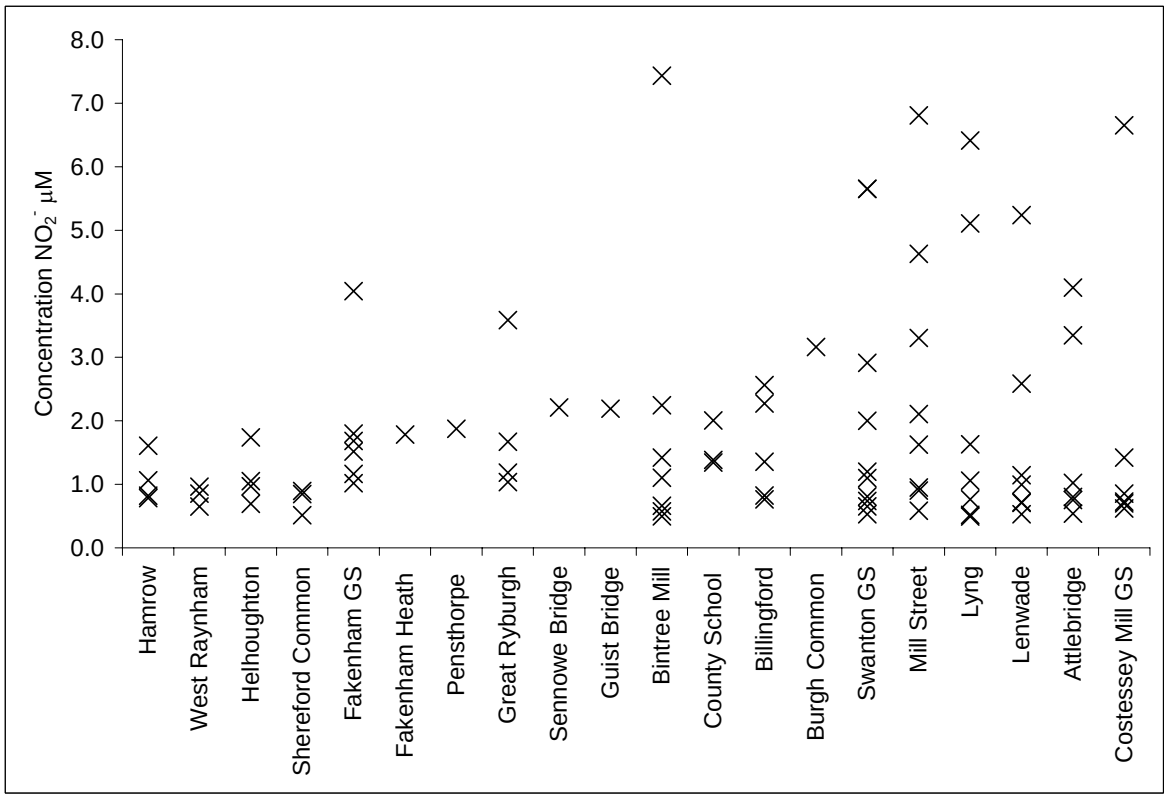

Figure 4.32 Concentration NO_2^- (µM) of Wensum river samples collected between 14/02/2007 and 25/09/2009.

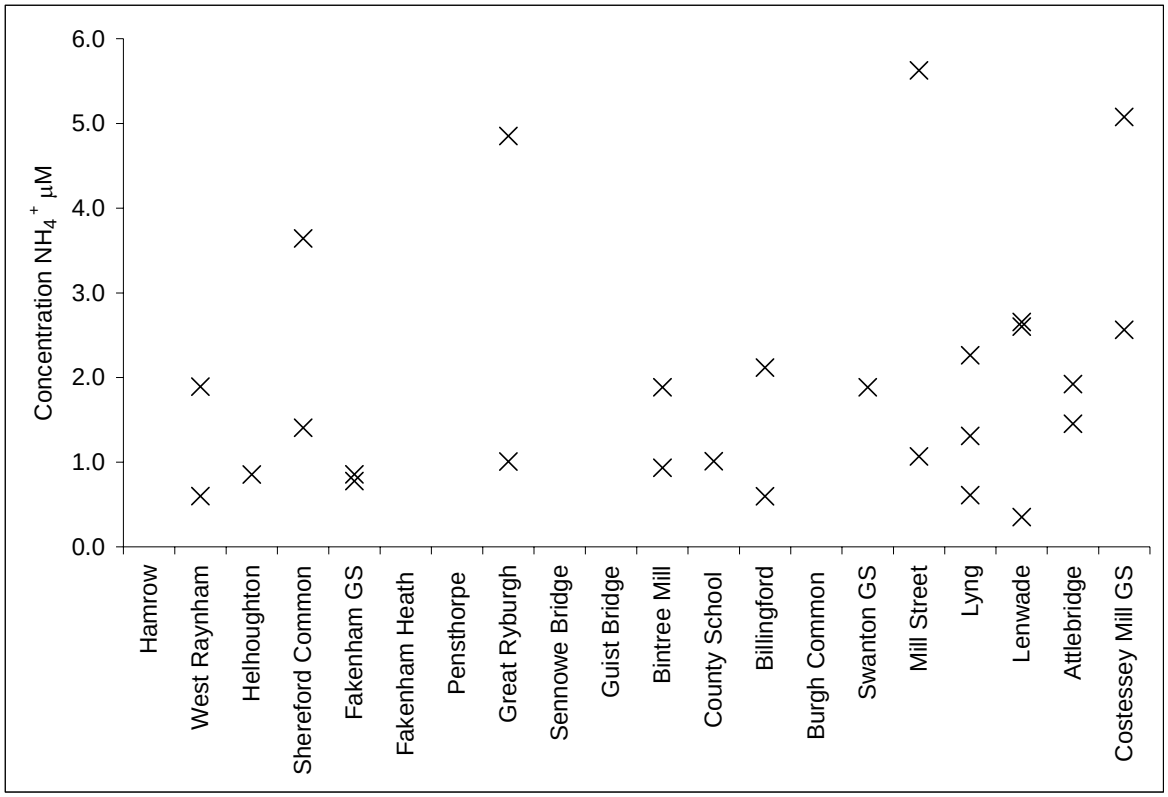

Figure 4.33 Concentration NH_4^+ (µM) of Wensum river samples collected between 14/02/2007 and 25/09/2009. For better visualisation a concentration spike of 21.4 µM at Helhoughton has been excluded.

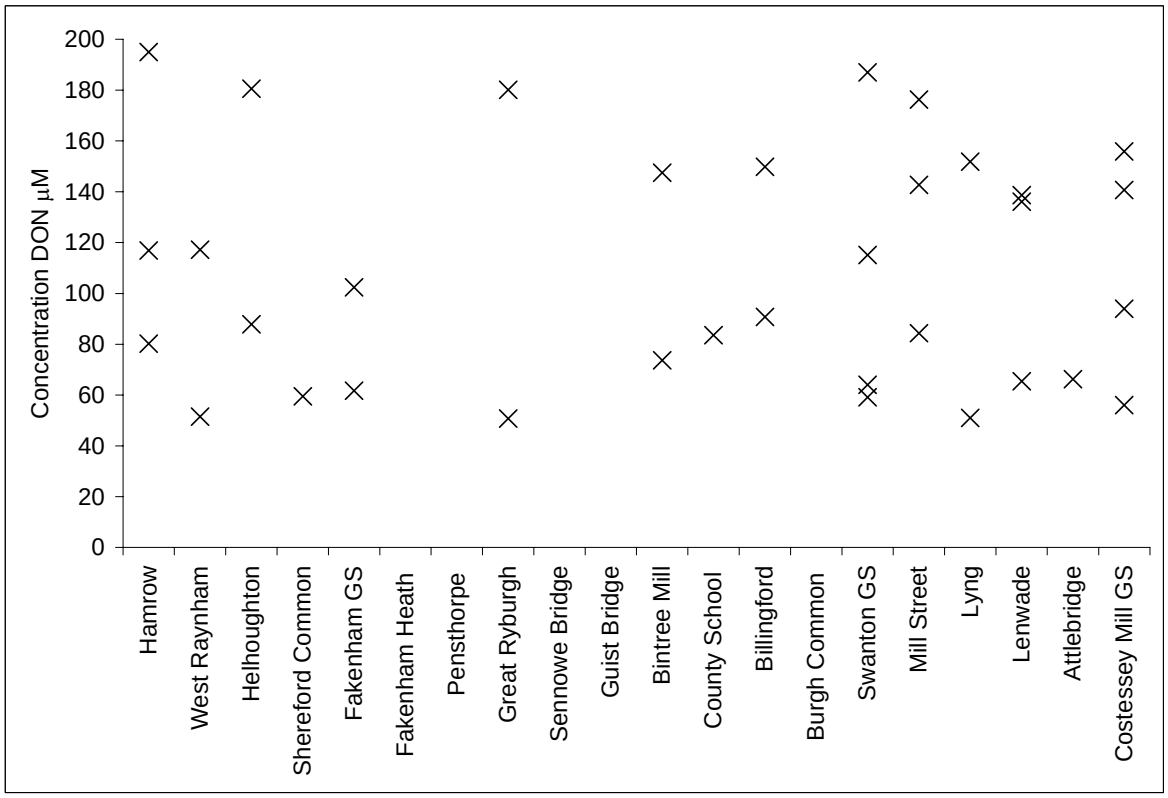

Figure 4.34 Concentration DON (µM) of Wensum river samples collected between 14/02/2007 and 25/09/2009.

4.4.3 Major and Minor Ion and Trace Element Concentrations in Wensum Surface Water

The suite of major anions in Wensum catchment waters comprises bicarbonate, chloride, sulphate, and nitrate, while the major cations comprise calcium, sodium, potassium and magnesium. Overall, there is moderate variation in concentrations of major and minor ions and trace elements across location and sample sets (Tables 4.8a and b). However, concentration spikes are seen in trace elements and major ions in both the river and the tributary and drain samples (Table 4.9). In the Wensum river, the majority of spikes occur in the mid-river high resolution spatial survey (16/11/2008), when flow conditions were low in the upper catchment at Fakenham, and medium at Swanton and Costessey Mill. Concentration spikes in the tributary and drain samples are more evenly distributed across sample sets and are likely to reflect localised and transient mobilisation of solutes in drainage waters.

Table 4.8a Concentrations of major and minor ions and trace elements in samples from the Wensum river, showing mean, one standard deviation, minima and maxima.

Wensum river solute concentrations					
Compound or element measured	**Mean**	**One standard deviation**	**Minimum**	**Maximum**	**n**
Cl^- mg/L	41	7	31	74	102
SO_4^{2-} mg/L	39	9	22	57	102
PO_4^{3-} mg/L	0.13	0.07	<LOD	0.34	102
Na mg/L	23.0	3.3	15.5	30.9	89
K mg/L	3.5	1.4	1.3	7.7	89
Mg mg/L	3.4	0.5	2.4	5.8	89
Ca mg/L	122	12	105	162	89
Si mg /L	2.1	1.0	0.6	4.4	89
Sr mg/L	0.3	0.1	0.2	0.6	16
Fe µg/L	1.0	0.4	<LOD	2.1	89
Al µg/L	1.0	0.5	<LOD	4.2	89
Zn µg/L	1.1	2.8	<LOD	22.5	89
Mn µg/L	0.16	0.08	0.05	0.70	89
Cu µg/L	0.09	0.06	<LOD	0.30	89
B µg/L	0.80	0.82	0.19	6.36	89
HCO_3^- mg /L	336	32	302	401	28

Table 4.8b Concentrations of major and minor ions and trace elements in samples from the Wensum tributaries and drains, showing mean, one standard deviation, minima and maxima.

Wensum tributary and drain solute concentrations					
Compound or element measured	**Mean**	**One standard deviation**	**Minimum**	**Maximum**	**n**
Cl^- mg/L	44	13	27	92	64
SO_4^{2-} mg/L	43	13	20	79	64
PO_4^{3-} mg/L	0.22	0.41	<LOD	1.81	64
Na mg/L	24.9	8.6	13.5	63.8	62
K mg/L	4.1	4.2	0.6	27.8	62
Mg mg/L	3.9	1.1	2.4	8.1	62
Ca mg/L	120	22	36	157	62
Si mg /L	2.1	1.0	0.2	6.1	62
Sr mg/L	0.3	0.0	0.2	0.3	20
Fe µg/L	1.1	0.6	<LOD	3.8	62
Al µg/L	0.36	0.65	0.03	4.78	62
Zn µg/L	1.0	0.6	<LOD	4.7	62
Mn µg/L	0.9	0.9	<LOD	5.3	62
Cu µg/L	0.08	0.07	<LOD	0.32	62
B µg/L	0.83	1.08	<LOD	6.89	62
HCO_3^- mg /L	342	42	234	401	16

Table 4.9 Concentration spikes of major and minor ions, and trace elements in samples from the Wensum river, tributaries and drains, showing data set, location, flow condition and mean concentration.

Wensum river solute concentration spikes					
Data set	**Sample location**	**Compound or element measured**	**Spike**	**Mean**	**Flow condition**
18/07/2007	Helhoughton	NH_4^+ µM	21.4	2.6	High
6/4/2008	Swanton GS	Al µg/L	4.2	1.0	high-medium
16/11/2008	Pensthorpe	Zn µg/L	22.5	1.1	Low-medium
	Pensthorpe	B µg/L	6.4	0.80	
	Bintree Mill	PO_4^{3-} mg/L	0.34	0.13	
	Mill Street	Mg mg/L	5.8	3.4	
	Mill Street	Mn µg/L	0.70	0.16	
25/09/2009	Great Ryburgh	Cl^- mg/L	71	41	Low
	Bintree Mill	Cl^- mg/L	74	41	
Wensum tributary and drain solute concentration spikes					
14/02/2007	Tat: Tatterford	B µg/L	6.9	0.83	High
	Wendling Beck: Worthing	DON	467	112	
18/07/2007	Mill Street: stream	NO_2^- µM	14.7	2.7	High
11/12/2007	Shereford drain	NH_4^+ µM	21.4	4.8	High
	Shereford drain	Mn µg/L	4.8	0.9	
	Lenwade drain	Cl^- mg/L	92	44	
		Na mg/L	45	24.9	
6/4/2008	Bintree west drain	Fe µg/L	3.8	1.1	
		Al µg/L	4.7	0.36	
		Zn µg/L	5.3	1.0	high-medium
14/09/2008	Great Ryburgh bridge drain	PO_4^{3-} mg/L	1.8	0.22	
		K mg/L	27.8	4.1	Low

Mean concentrations of sulphate, chloride, and sodium with location from headwaters to the catchment outlet in Wensum river samples show a large increase in concentration after Fakenham gauging station, followed by a slight decrease before Swanton gauging station, with a ratio of sodium to chloride of 0.58 $\pm$ 0.06. This reduction from the molecular ratio of 0.65 in NaCl is likely to indicate some retention of sodium within catchment soils and sediments as a result of ion exchange and adsorption (Figure 4.35). Magnesium shows a trend of gradually increasing concentration, which may reflect an increasing contribution from surface accretion downstream while potassium shows a sudden increase in concentration at Bintree Mill, which may be due to a local contamination source (Figure 4.36). Mean concentrations of calcium shows an overall decreasing trend downstream, reflecting a slightly reduced influence from Chalk groundwater downstream, with an initial dip in concentration at Shereford (Figure 4.37). Concentrations of phosphate suggest an increase downstream (Figure 4.38). Mean concentrations of trace elements with location do not show any spatial trends so are not presented in figures.

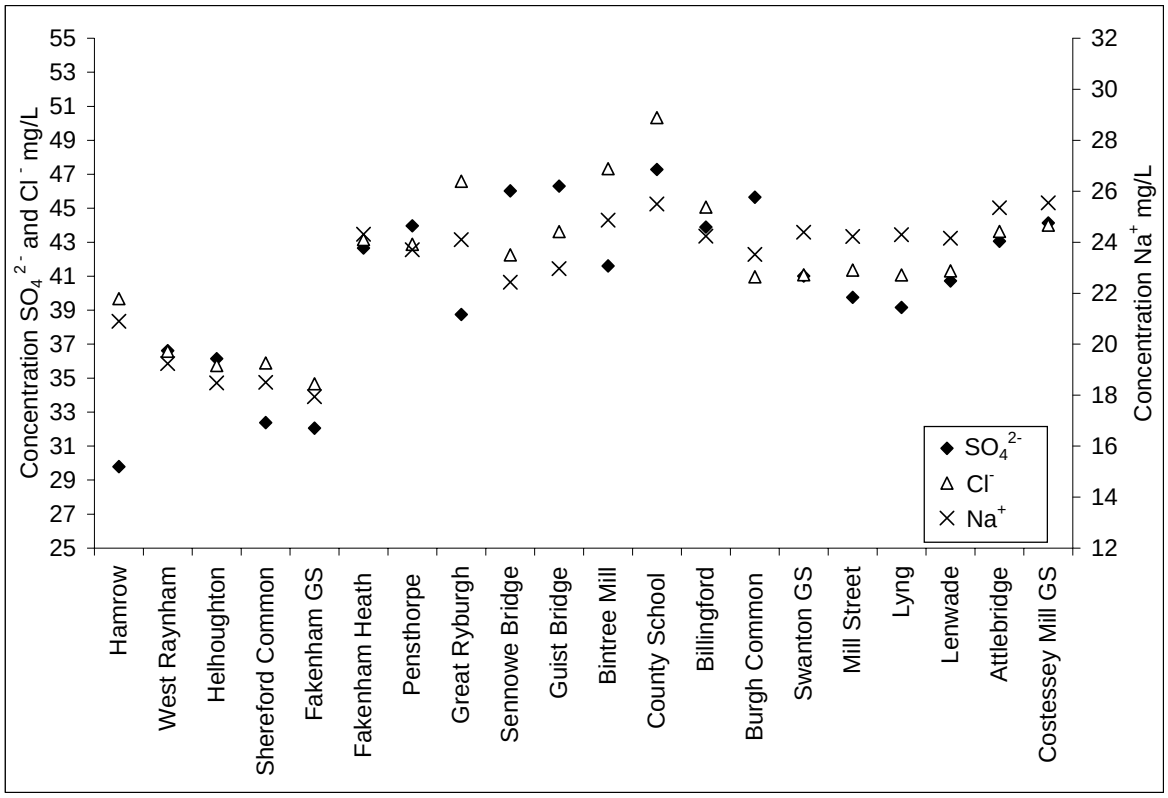

Figure 4.35 Mean concentrations of SO_4^{2-}, Cl^-, and Na^+ (mg/L) of Wensum river samples with location, from samples collected between 14/02/2007 and 25/09/2009.

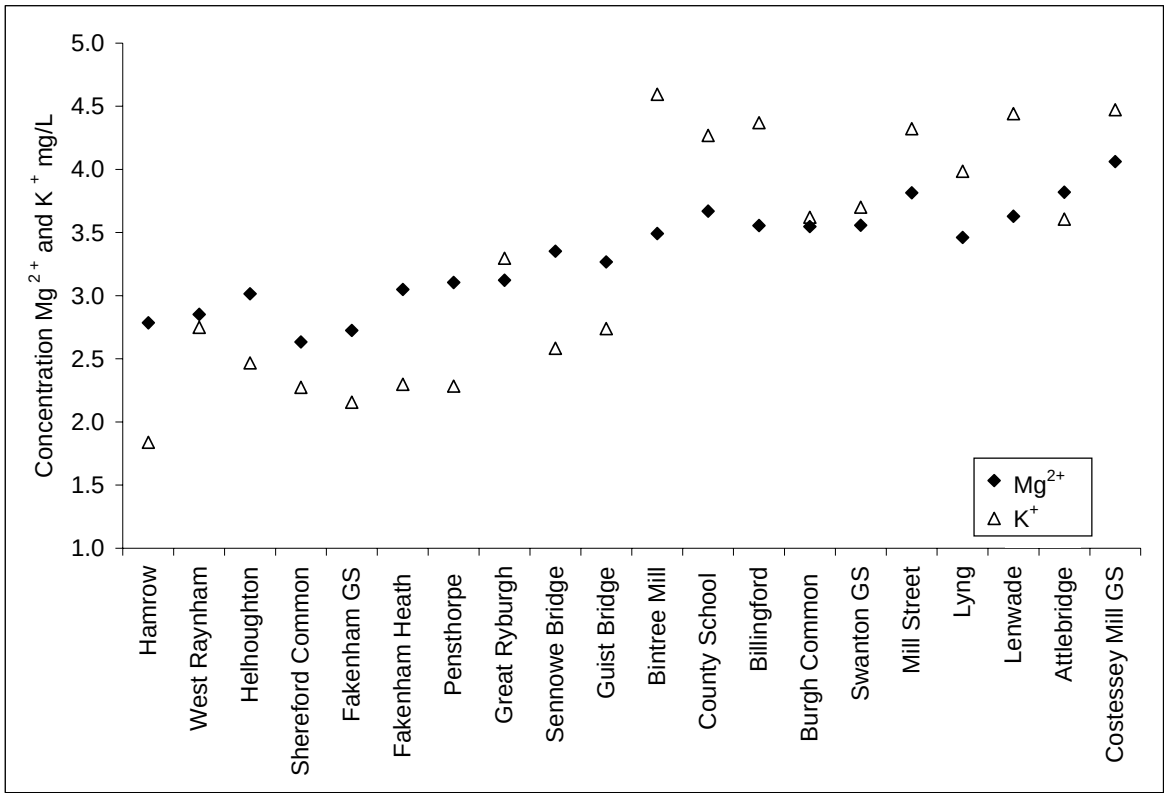

Figure 4.36 Mean concentrations of Mg^{2+} and K^{+} (mg/L) of Wensum river samples with location, from samples collected between 14/02/2007 and 25/09/2009.

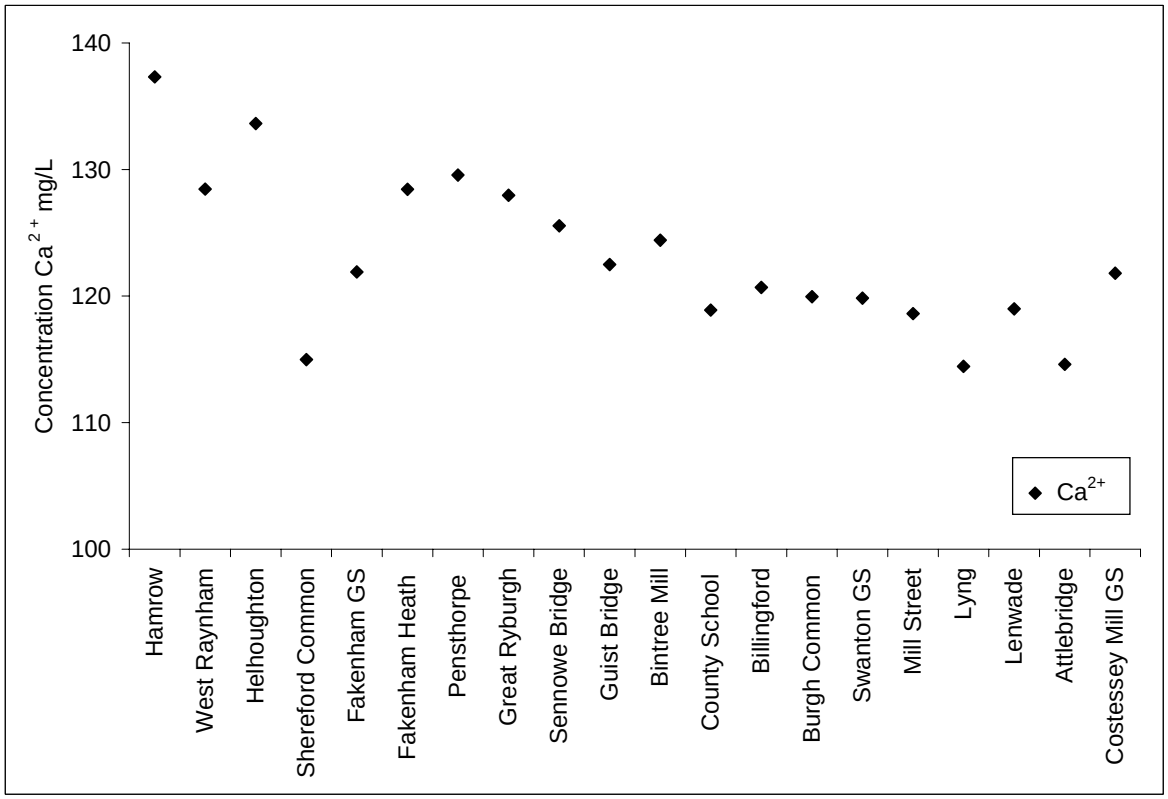

Figure 4.37 Mean concentrations of Ca^{2+} (mg/L) of Wensum river samples with location, from samples collected between 14/02/2007 and 25/09/2009.

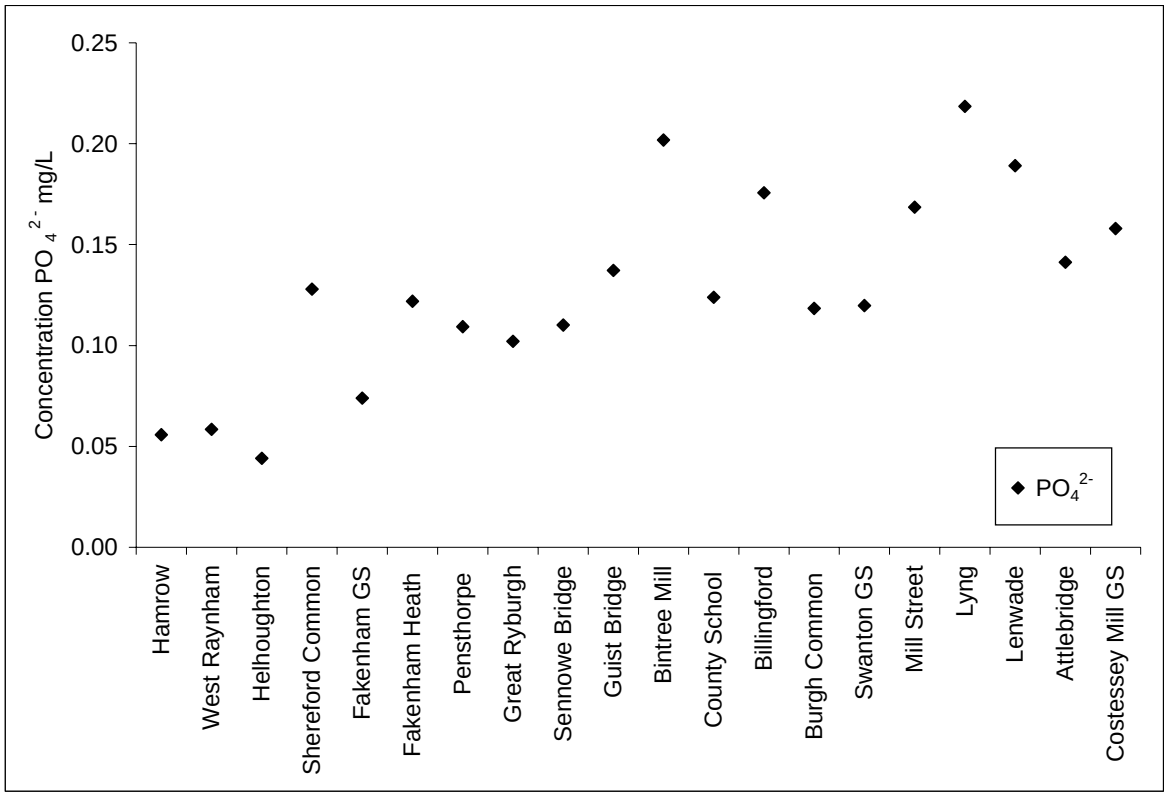

Figure 4.38 Mean concentrations of PO_4^{2-} (mg/L) of Wensum river samples with location, from samples collected between 14/02/2007 and 25/09/2009.

4.4.4 TDN Concentrations in Chalk Groundwater

Wensum catchment low-nitrate Chalk groundwater had total dissolved nitrogen concentrations at the limit of detection. Three samples from the valley Chalk with high nitrate concentrations, (874 to 1314 μM NO_3^-), had very small amounts of DON, equivalent to < 2 % of the total dissolved nitrogen (Table 4.10). The difference between surface and groundwater DON concentrations suggests that either DON is removed from recharge waters during infiltration to the Chalk, or that the DON concentrations seen in surface water samples are generated from nitrogen cycling in-stream.

4.4.5 Major and Minor Ion and Trace Element Concentrations in Chalk Groundwater

Mean concentrations of major and minor ions and trace elements in the Wensum catchment Chalk groundwater samples are similar to those of surface water samples. Minor differences are apparent in the groundwater mean sulphate concentration which is higher than that of surface water, and in calcium, bicarbonate and potassium mean

concentrations in groundwater which are lower than those of the surface water (Table 4.10). The difference in sulphate may be attributable to the influence of sulphate reduction on surface water concentrations. Proportional major anion and cation concentrations in milliequivalents per litre (meq/L) of these samples are presented in Figure 4.39. Bicarbonate and calcium concentrations are highest in the low-nitrate Chalk groundwater samples to the west of the catchment (Hamrow and Wellingham), with lower concentrations of both ions seen in samples from the east of the catchment (Hellesdon and Costessey). Concentrations of sulphate and sodium are also highest in these samples from the east, and lowest in the west catchment low-nitrate Chalk groundwater samples. Magnesium and potassium concentrations show a similar pattern

Table 4.10 Concentrations of major and minor ions, trace elements and DON in samples from the Wensum Chalk boreholes showing mean, one standard deviation, minima and maxima.

Wensum groundwater solute concentrations					
Dissolved nitrogen species	**Mean**	**One standard deviation**	**Minimum**	**Maximum**	**n**
NO_3^- µM	449	520	0.50	1314	13
NO_2^- µM	< LOD	-	-	-	-
NH_4^+ µM	< LOD	-	-	-	-
DON µM	15	2	<LOD	16	13
Compound or element measured	**Mean**	**One standard deviation**	**Minimum**	**Maximum**	**n**
Cl^- mg/L	39	20	17	75	13
SO_4^{2-} mg/L	47	26	8	78	13
PO_4^{3-} mg/L	0.05	0.03	<LOD	0.08	13
Na mg/L	23.1	13.3	11.1	49.3	13
K mg/L	1.7	0.9	0.5	3.1	13
Mg mg/L	4.5	1.7	2.1	7.7	13
Ca mg/L	103	17	67	129	13
Si mg /L	2.6	0.3	2.1	3.1	13
Sr mg/L	0.7	1.0	0.2	4.0	13
Fe µg/L	2.75	3.28	<LOD	9.72	13
Al µg/L	0.77	0.05	0.69	0.85	13
Zn µg/L	1.12	1.22	<LOD	3.91	13
Mn µg/L	0.28	0.26	0.02	0.65	13
Cu µg/L	0.07	0.05	<LOD	0.19	13
B µg/L	0.49	0.23	<LOD	1.08	13
HCO_3^- mg /L	277	46	215	347	13

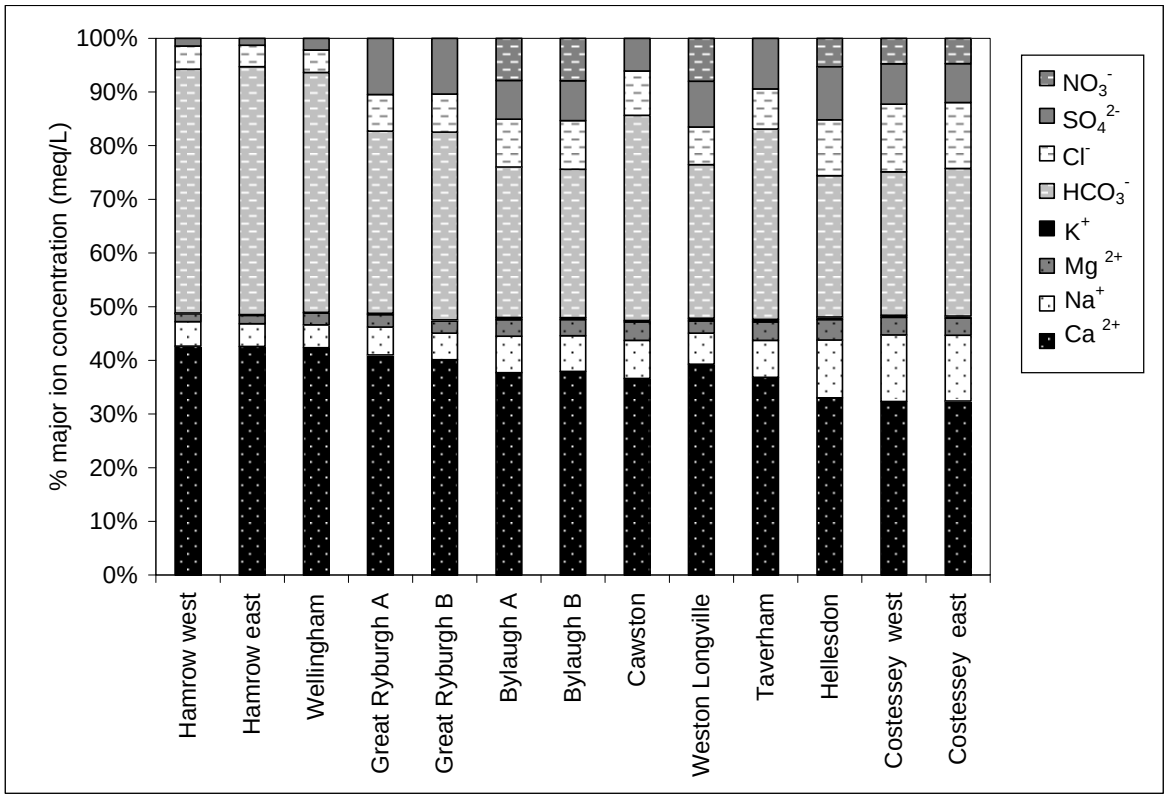

Figure 4.39 Concentrations of major ions (meq/L) presented as a percentage of total major ion concentration for the thirteen Chalk borehole samples from the Wensum catchment. Suffixes A and B refer to paired samples, where A was collected in winter and B in summer.

Trace element concentrations show a varied pattern across the Chalk groundwater samples (Figure 4.40). There are high concentrations of iron in the great Ryburgh A and Hamrow west samples, and of zinc in the samples from Bylaugh A and B (winter and summer paired samples). Boron concentrations are highest at Hamrow east, and copper concentrations are highest at Bylaugh (sample A). Manganese concentrations are highest in the samples from the west of the catchment (Hamrow, Wellingham and Great Ryburgh), and aluminium concentrations are similar across all samples.

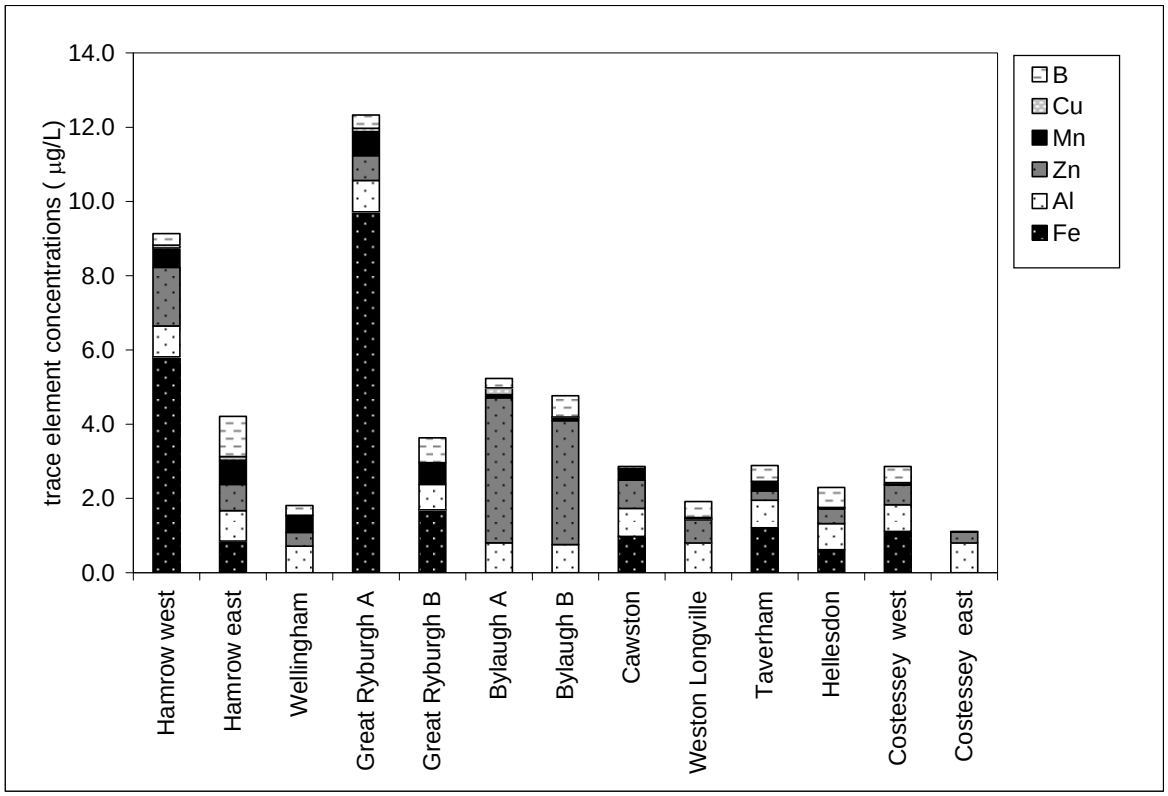

Figure 4.40 Concentrations of trace elements (µg/L) for thirteen Chalk borehole samples from the Wensum catchment. Suffixes A and B refer to paired samples, where A was collected in spring and B in autumn.

4.5 WENSUM CATCHMENT $\delta^{18}O_{H2O}$

The analysis of $\delta^{18}O_{H2O}$ of selected samples from the Wensum catchment shows that the tributary and drain data set has the largest range of isotopic composition, encompassing the range of Wensum river samples. The low-nitrate and valley Chalk groundwater samples are not differentiated from each other, and have a lower mean and range of $\delta^{18}O_{H2O}$ than the surface water samples, though the range of groundwater $\delta^{18}O_{H2O}$ overlaps the ranges of values from the other two data sets (Table 4.11, Figure 4.41).

Table 4.11 Mean $\pm$ one standard deviation, maxima and minima of $\delta^{18}O_{H2O}$ (‰) of samples from the Wensum catchment. Error $\pm$ 0.06 ‰.

Wensum catchment $\delta^{18}O_{H2O}$ ‰ VSMOW					
	Mean	**One standard deviation**	**Minimum**	**Maximum**	**n**
Tributary and drain water (n = 10)	-6.7	0.4	-7.4	-6.0	10
Wensum river water (n = 86)	-6.8	0.2	-7.2	-6.3	86
Valley and low-nitrate Chalk groundwater (n = 13)	-7.3	0.2	-7.5	-7.0	13

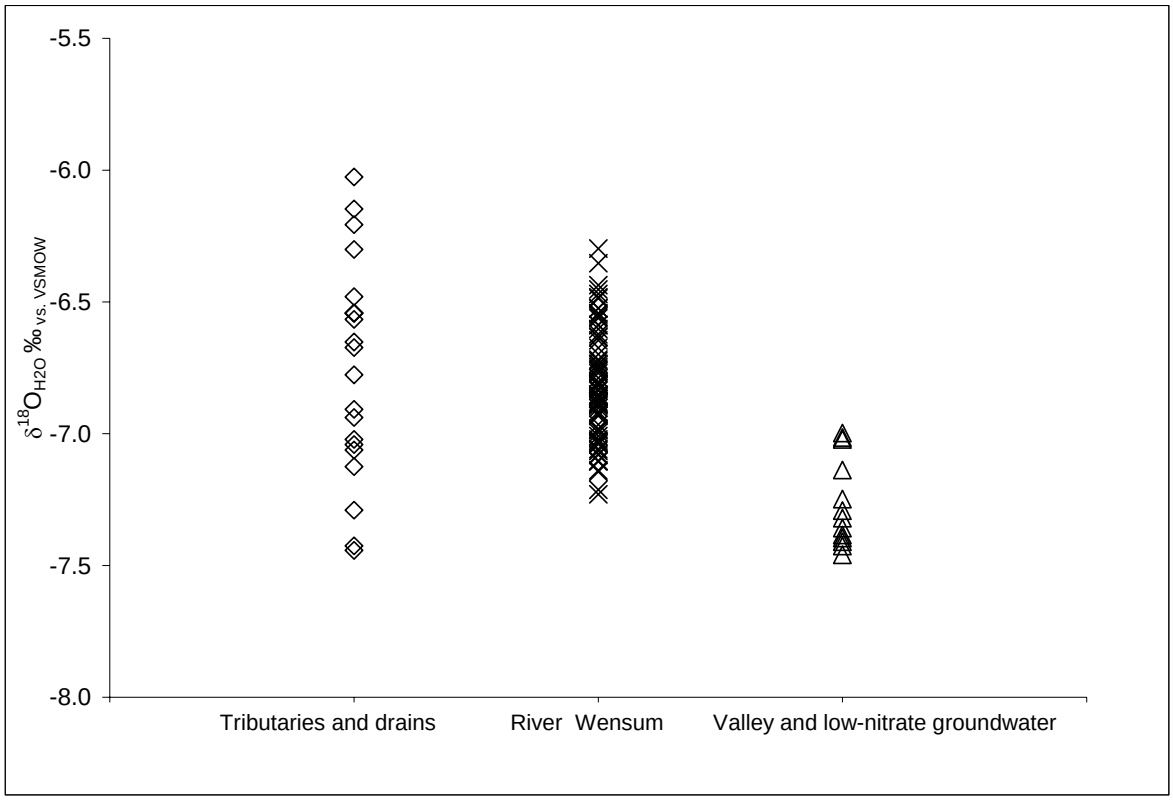

Figure 4.41 $\delta^{18}O_{H2O}$ (‰) of samples from the Wensum catchment. Error $\pm$ 0.06 ‰.

There is no clear differentiation in $\delta^{18}O_{H2O}$ with location of Wensum river samples, which shows a wide range of values at single locations across sample dates, or in the small number of tributary and drain samples which were analysed for $\delta^{18}O_{H2O}$ (Figure 4.42 and 4.43). However, a spatial trend is visible in the Chalk groundwater samples, which show a heavier isotopic composition in the low-nitrate samples from the west of the catchment (Hamrow west and east, and Wellingham), with isotopically lighter samples from the middle of the catchment (Great Ryburgh A and B, and Bylaugh A and B), and with the lightest isotopic composition seen in the samples from the east of the catchment (Taverham, Hellesdon, and Costessey west and east). In addition, the two mid catchment locations where seasonally paired samples were collected (Great Ryburgh A and B, and Bylaugh A and B) show an isotopic difference of $\Delta^{18}O_{H2O}$ = 0.1‰, with the isotopically lighter samples collected in winter and the heavier in summer (Figure 4.44). This may reflect seasonal differences in the isotopic composition of recharge.

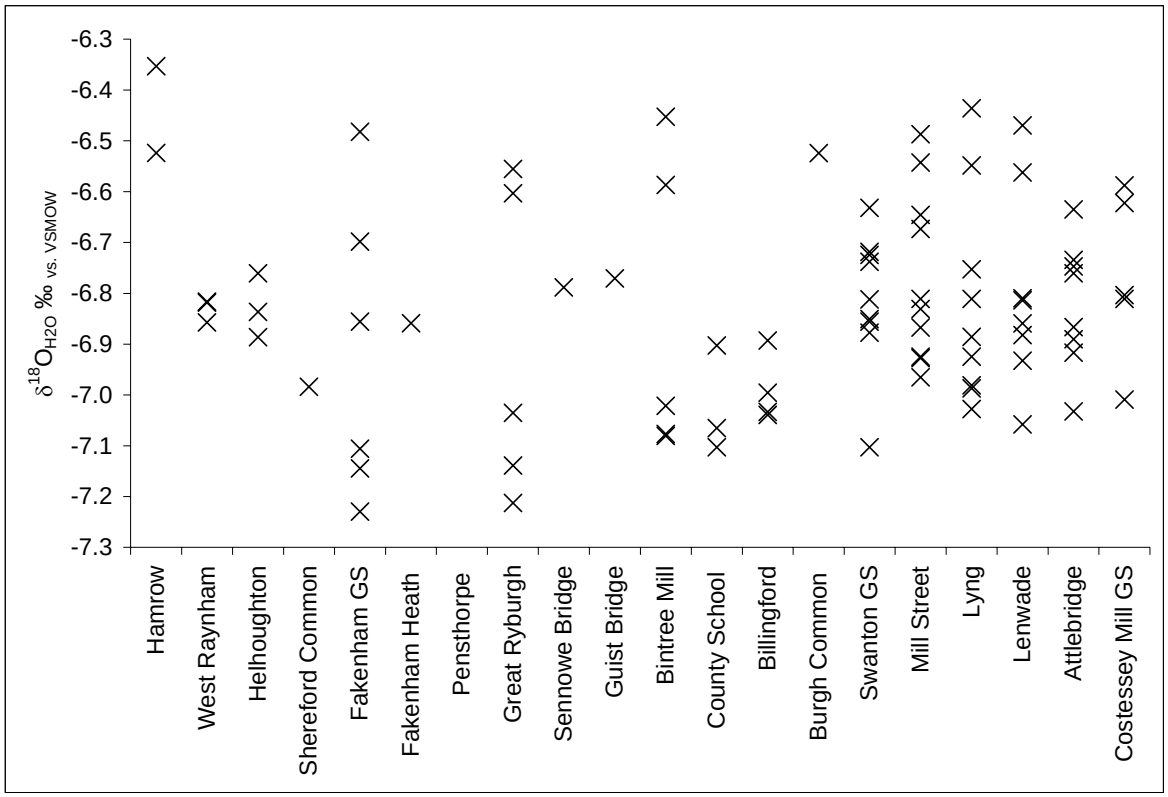

Figure 4.42 $\delta^{18}O_{H2O}$ (‰) of Wensum river samples with location, from samples collected between 14/02/2007 and 25/09/2009. Error $\pm$ 0.06‰.

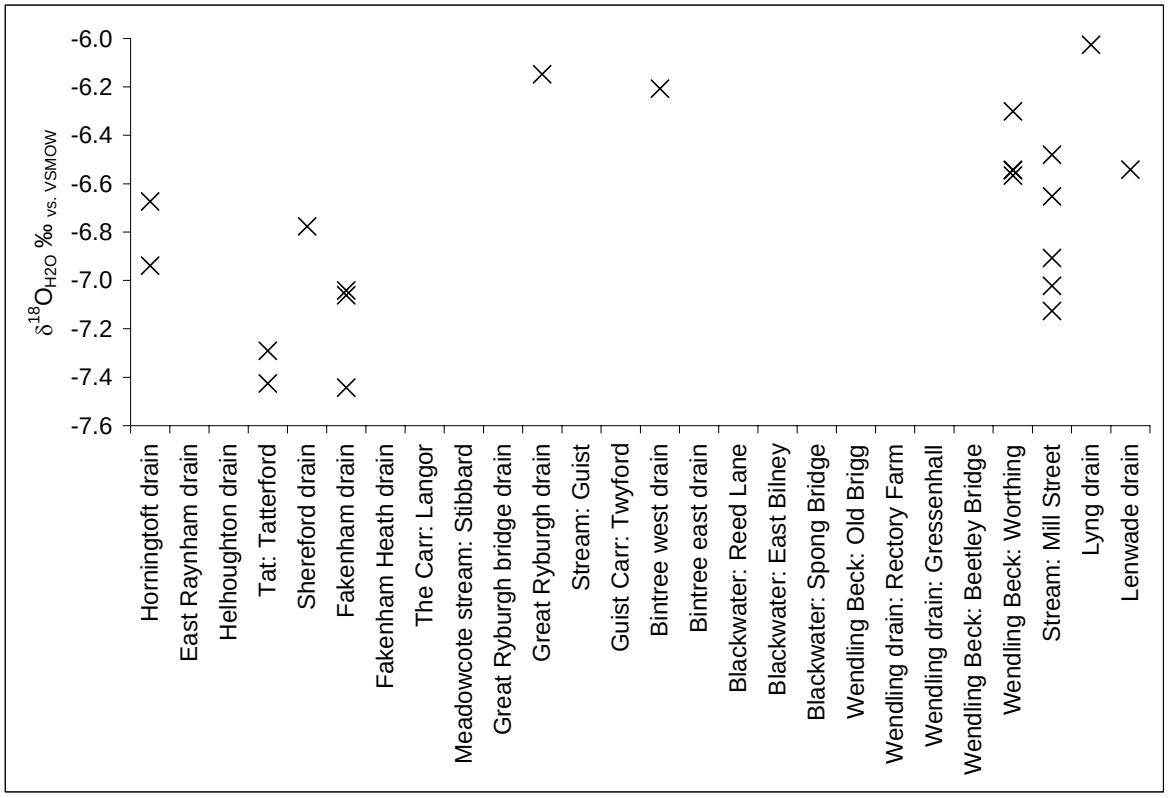

Figure 4.43 $\delta^{18}O_{H2O}$ (‰) of Wensum tributary and drain samples with location, from samples collected between 14/02/2007 and 25/09/2009. Error $\pm$ 0.06 ‰.

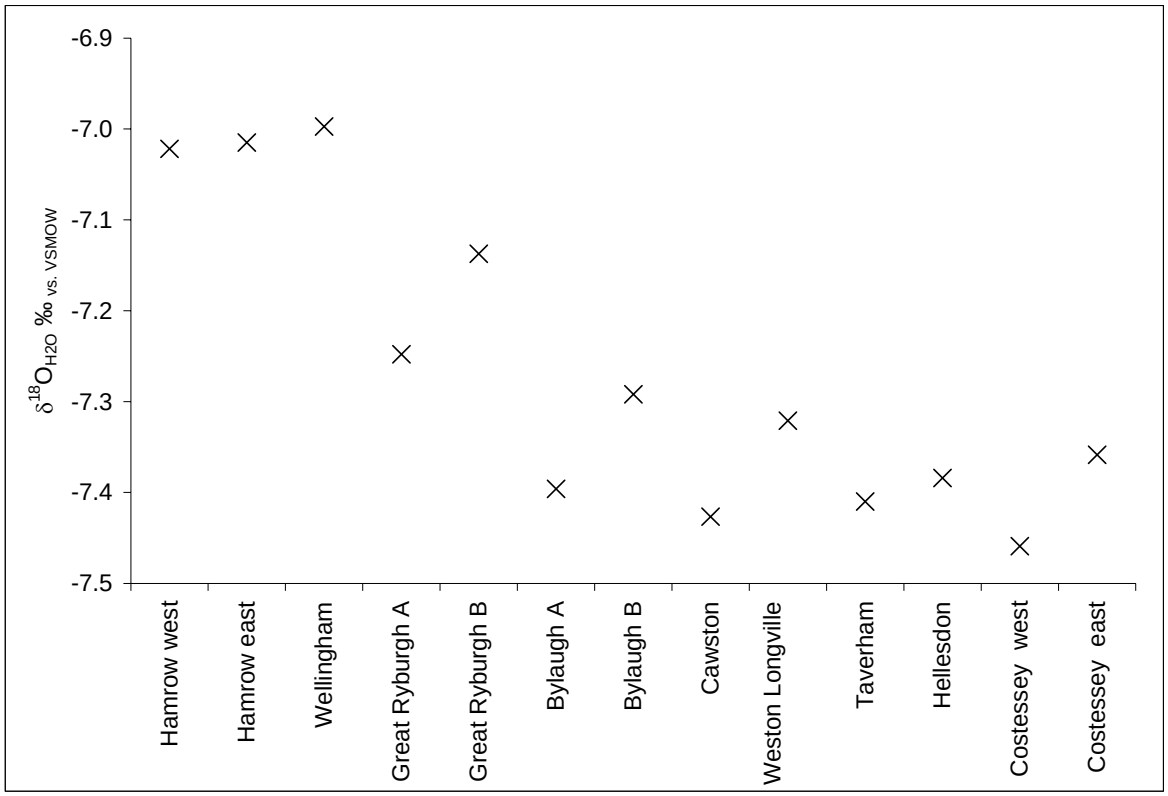

Figure 4.44 $\delta^{18}O_{H2O}$ (‰) of Wensum catchment low-nitrate and valley Chalk groundwater samples with location, Suffixes A and B refer to paired samples, where A was collected in winter and B in summer. Error $\pm$ 0.06 ‰.

4.6 NO_3^- SOURCES

A summary of results from the isotopic analysis of nitrate and liquid ion chromatography of nitrate source samples is presented in Table 4.12 and Figures 4.45 to 4.47. Of the nitrate sources analysed, sewage effluent has the highest $\delta^{15}N_{NO3}$ value, with two dry deposition samples also showing a high $\delta^{15}N_{NO3}$. The $\delta^{15}N_{NO3}$ of precipitation and dry deposition are broadly overlapping and show fairly wide ranges, with two precipitation samples showing the lowest $\delta^{15}N_{NO3}$ of all nitrate sources analysed. The $\delta^{15}N_{NO3}$ of fertiliser falls near the middle of the range of nitrate sources. The range of $\delta^{18}O_{NO3}$ of the nitrate sources is broad, spanning $\Delta^{18}O_{NO3}$ = 86 ‰. The heaviest oxygen isotopic composition is seen in dry deposition samples, with $\delta^{18}O_{NO3}$ of precipitation showing slightly lighter but overlapping values. The $\delta^{18}O_{NO3}$ of the fertiliser samples is lower than any of the atmospheric samples. Wastewater effluent has the lowest $\delta^{18}O_{NO3}$ values of all the nitrate sources analysed. The $\delta^{18}O_{NO3}$ values of the two manure samples ($\delta^{18}O_{NO3}$ 29.2 and 32.3 ‰) are considerably higher than values reported in the literature which are all below $\delta^{18}O_{NO3}$ 15 ‰ (Kendall *et al.,* 2007),

although most studies report the expected $\delta^{18}O_{NO3}$ in manure based on the assumption of nitrification of ammonium sourcing two oxygen molecules from water and one from air (Equation 2.7), with a possible effect of evaporation and/ or denitrification within the manure leading to a slight increase in $\delta^{18}O_{NO3}$ values (Wassenaar, 1995). The two direct measurements presented here could indicate the effects of evaporation and localised denitrification, although the relatively low $\delta^{15}N_{NO3}$ values do not suggest significant denitrification. Other possible reasons for the very high $\delta^{18}O_{NO3}$ values could be that isotopic fractionation of oxygen has occurred during the oxidation of ammonium to nitrate favouring the inclusion of heavier oxygen atoms, or that nitrification source-water within the manure was isotopically heavy, perhaps as a result of metabolic processes. In addition the values may reflect the inclusion of more than one third of oxygen atoms from air. Finally it is possible that cross contamination occurred with the USGS 35 standard ($\delta^{18}O_{NO3}$ 51.5 ‰) in the laboratory during preparation, though it is not clear how this could have occurred. Due to the apparently anomalous $\delta^{18}O_{NO3}$ values of these two manure samples, they will not be included in further discussions of the results.

Table 4.12 Mean ± one standard deviation, maxima and minima of NO_3^- concentration (μM), $\delta^{15}N_{NO3}$ (‰) and $\delta^{18}O_{NO3}$ (‰) of nitrate source samples (where two samples were collected the standard deviation has not been calculated. Samples which were prepared in the laboratory to dissolve nitrate do not display a value for concentration (e.g. dry deposition, fertiliser and manure samples).

Nitrate sources		**NO_3^- concentration μM**	**$\delta^{15}N_{NO3}$ ‰ AIR**	**$\delta^{18}O_{NO3}$ ‰ VSMOW**
Precipitation (n = 6)	Mean ± 1 standard deviation	45 ± 52	-0.8 ± 4.8 [a]	57.1 ± 10.8
	Maximum	146	5.3 [a]	66.5
	Minimum	10	-7.3 [a]	37.5
Dry deposition (n = 27)	Mean ± 1 standard deviation	-	2.9 ± 3.9 [a]	73.2 ± 6.1
	Maximum	-	9.5 [a]	85.3
	Minimum	-	-4.5 [a]	60.6
Wastewater effluent (n = 2)	Mean	1786	12.0	1.0
	Maximum	1928	13.9	2.7
	Minimum	1644	10.1	-0.7
Ammonium nitrate fertiliser (n = 2)	Mean	-	3.4	23.8
	Maximum	-	4.3	24.4
	Minimum	-	2.6	23.3
Cattle manure (n=1)	-	-	7.3	29.2
Chicken manure (n=1)	-	-	7.0	32.3

[a] Due to the uncertainty of the true value of the ^{17}O anomalies of the precipitation and dry deposition samples there is an associated error of ± 0.4 ‰ for $\delta^{15}N_{NO3}$.

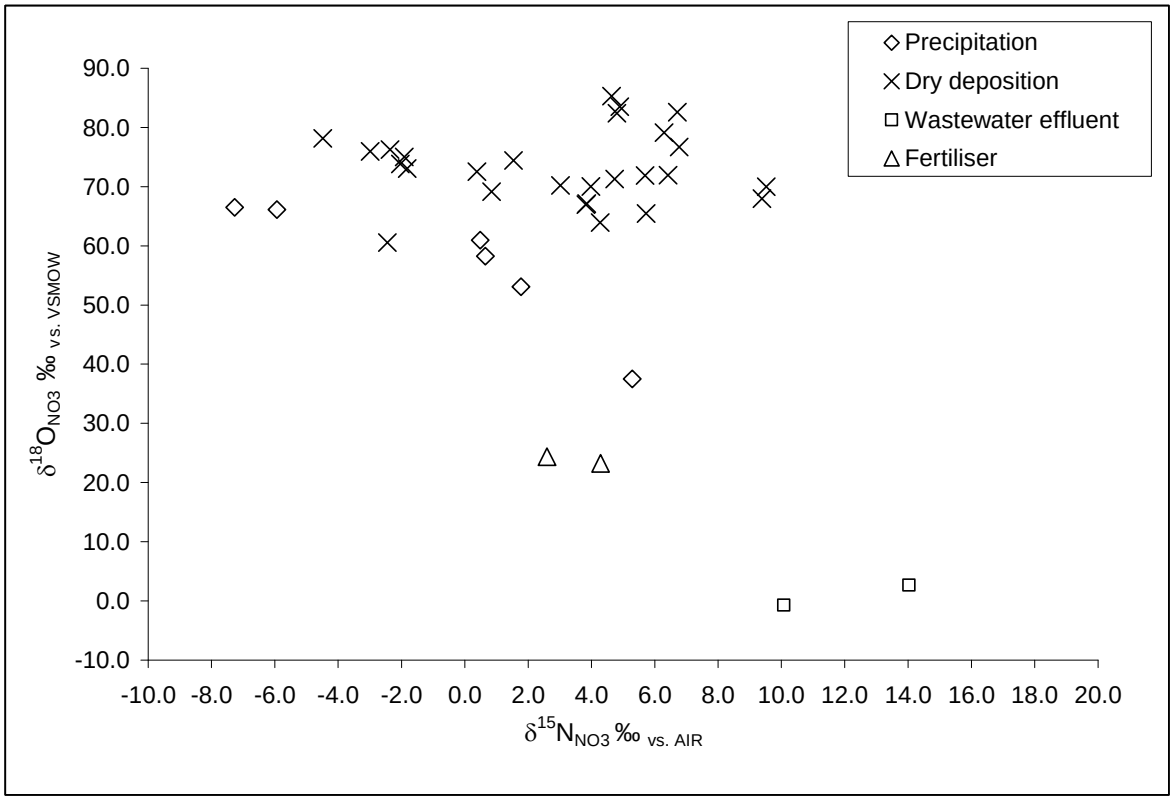

Figure 4.45 $\delta^{18}O_{NO3}$ (‰) versus $\delta^{15}N_{NO3}$ (‰) of nitrate source samples. Error: $\delta^{15}N_{NO3}$ and $\delta^{18}O_{NO3}$ $\pm$ 0.1‰. Additional error of $\delta^{15}N_{NO3}$ $\pm$ 0.4 ‰ for precipitation and dry deposition samples due to the uncertainty of the true value of the ^{17}O anomaly.

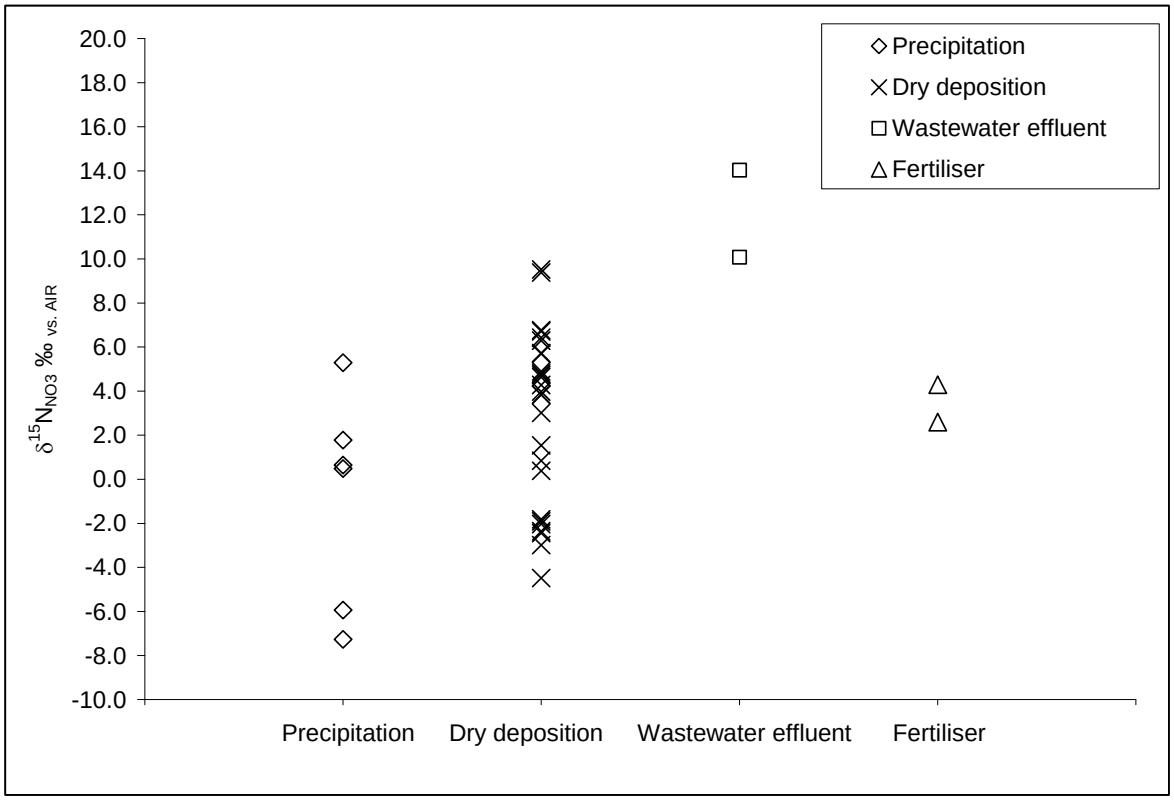

Figure 4.46 $\delta^{15}N_{NO3}$ (‰) of nitrate source samples. Error: $\delta^{15}N_{NO3}$ and $\delta^{18}O_{NO3}$ $\pm$ 0.1‰. Additional error of $\delta^{15}N_{NO3}$ $\pm$ 0.4 ‰ for precipitation and dry deposition samples due to the uncertainty of the true value of the ^{17}O anomaly.

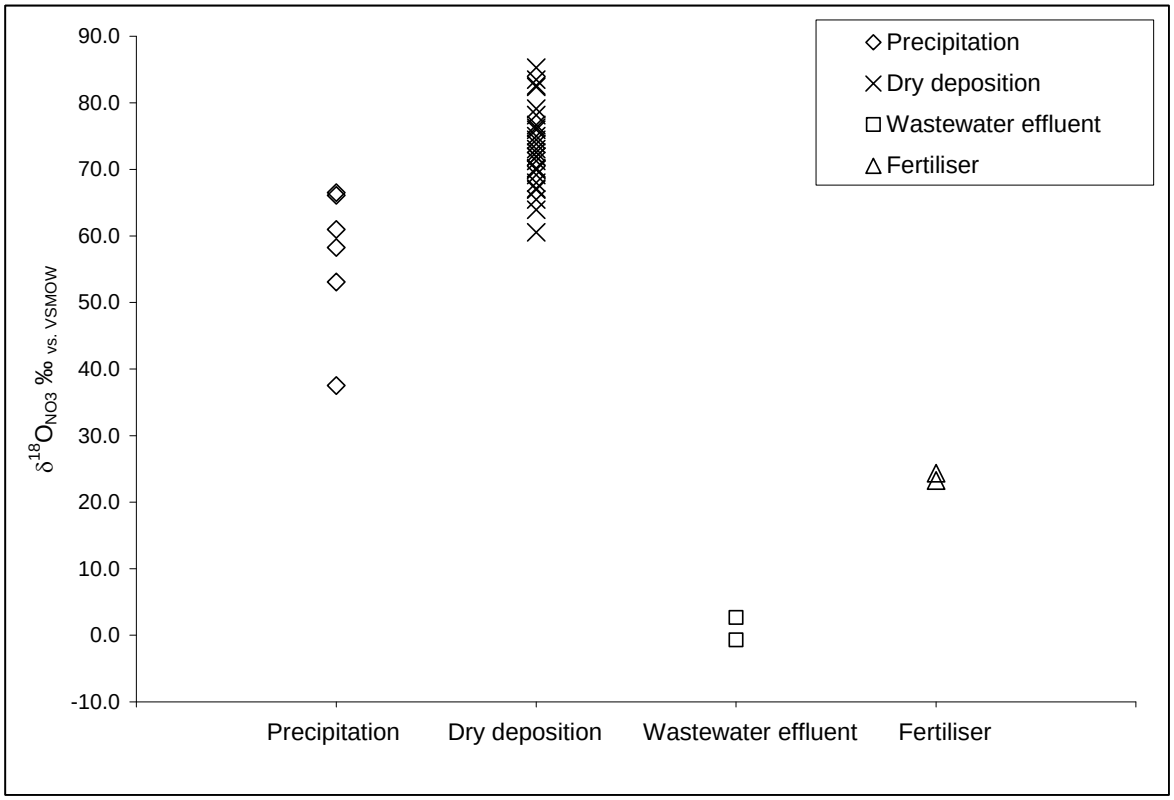

Figure 4.47 $\delta^{18}O_{NO3}$ (‰) of nitrate source samples. Error: $\delta^{18}O_{NO3} \pm 0.1$‰.

The dry deposition aerosol samples showed almost equal proportions of aerosols collected in the two size brackets either side of the one micron cut off representing the boundary between larger mechanically generated particles and smaller particles produced in the atmosphere, with 51% at the larger particle size and 49% at the smaller size. The isotopic composition of the aerosol size group below one micron diameter was slightly lighter but with the isotopic variation of each size group overlapping (Figure 4.48).

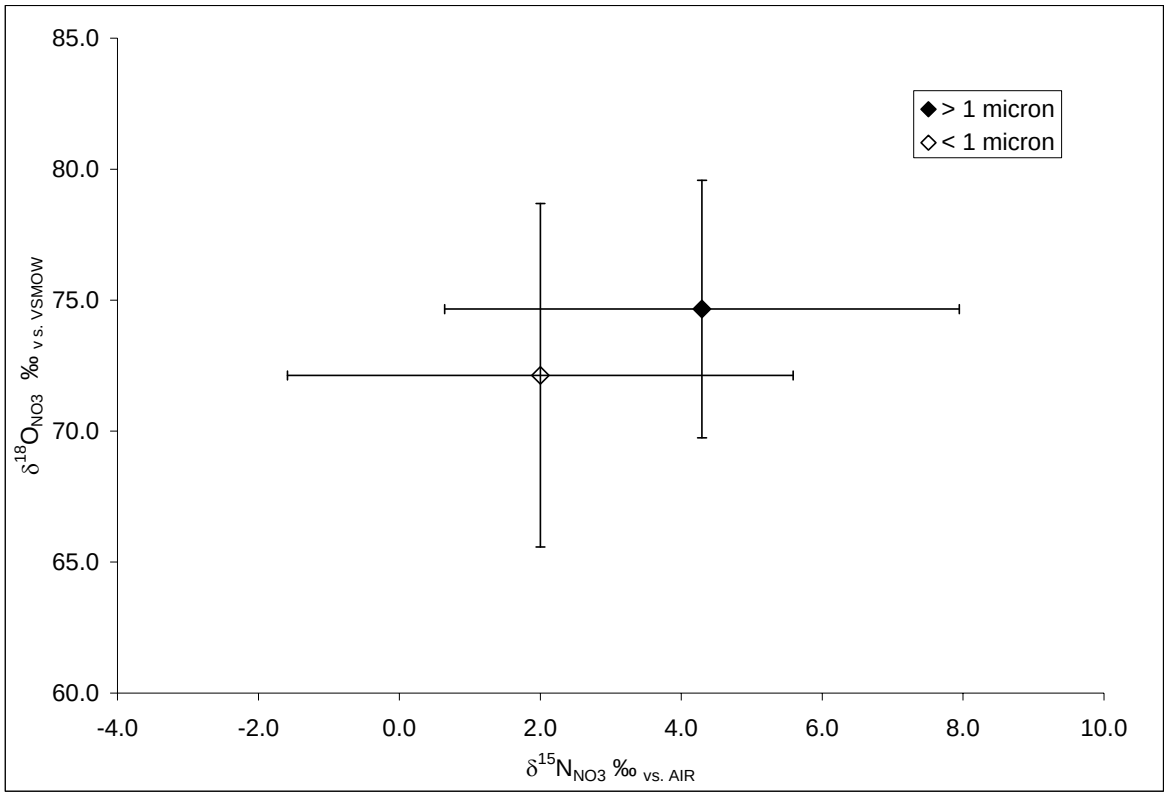

Figure 4.48 $\delta^{18}O_{NO3}$ (‰) versus $\delta^{15}N_{NO3}$ (‰) of dry deposition aerosol samples according to size. Error: $\delta^{15}N_{NO3} \pm 0.4$ ‰ due to the uncertainty of the true value of the ^{17}O anomaly, and $\delta^{18}O_{NO3} \pm 0.1$‰.

4.7 NO_3^- SOURCE HYDROCHEMISTRY

4.7.1 TDN Concentrations of Precipitation and Wastewater Effluent

Analysis of total dissolved nitrogen concentrations was carried out on precipitation and wastewater effluent samples (Table 4.13). The relative proportion of dissolved nitrogen species in precipitation show TDN split between DON (45%), nitrate (29%), and ammonium (25%), with a negligible amount of nitrite (<1%) (Table 4.13, Figure 4.49). In contrast, wastewater effluent TDN comprises mainly nitrate (96%), with DON below the limit of detection, and relatively small proportions of nitrite and ammonium (2% both). This reflects the fact that wastewater ammonium has undergone engineered near-quantitative nitrification within the sewage works.

Table 4.13 Concentrations of major and minor ions and trace elements in samples of precipitation and wastewater effluent showing mean, one standard deviation, minima and maxima.

Nitrate source solute concentrations									
Precipitation solute concentrations						**Wastewater effluent solute concentrations**			
Dissolved nitrogen species	**Mean**	**1 st. dev.**	**Min.**	**Max.**	**n**	**Mean**	**Min.**	**Max.**	**n**
NO_3^- µM	45	52	10	146	6	1786	1644	1928	2
NO_2^- µM	1.2	0.7	<LOD	2.1	6	37.5	34.3	40.7	2
NH_4^+ µM	38.7	45.3	<LOD	117.2	6	31.0	1.1	60.8	2
DON µM	68	73	<LOD	151	6	< LOD	-	-	-
Compound or element measured	**Mean**	**1 st. dev.**	**Min.**	**Max.**	**n**	**Mean**	**Min.**	**Max.**	**n**
Cl^- mg/L	3.7	4.8	1.1	13.4	6	193	128	258	2
SO_4^{2-} mg/L	2.2	1.3	1.0	4.3	6	95	94	96	2
PO_4^{3-} mg/L	0.4	-	<LOD	-	6	20.4	<LOD	-	2
Na mg/L	2.1	1.7	0.9	5.4	6	143	85	200	2
K mg/L	0.6	0.4	0.2	1.4	6	16.6	15.7	17.5	2
Mg mg/L	0.3	0.3	0.1	0.9	6	7.7	5.7	9.7	2
Ca mg/L	3.1	2.3	1.0	6.0	6	110	97	123	2
Si mg /L	0.12	-	<LOD	-	6	5.2	3.0	7.5	2
Fe µg/L	0.9	0.1	<LOD	1.0	6	1.1	1.1	1.1	2
Al µg/L	0.8	0.1	<LOD	0.9	6	0.9	0.8	1.0	2
Zn µg/L	0.9	0.5	<LOD	1.7	6	0.4	0.3	0.6	2
Mn µg/L	0.04	0.02	<LOD	0.06	6	0.12	0.08	0.16	2
Cu µg/L	0.10	0.04	<LOD	0.15	6	0.15	<LOD	-	2
B µg/L	0.89	0.85	<LOD	1.84	6	1.90	1.53	2.28	2

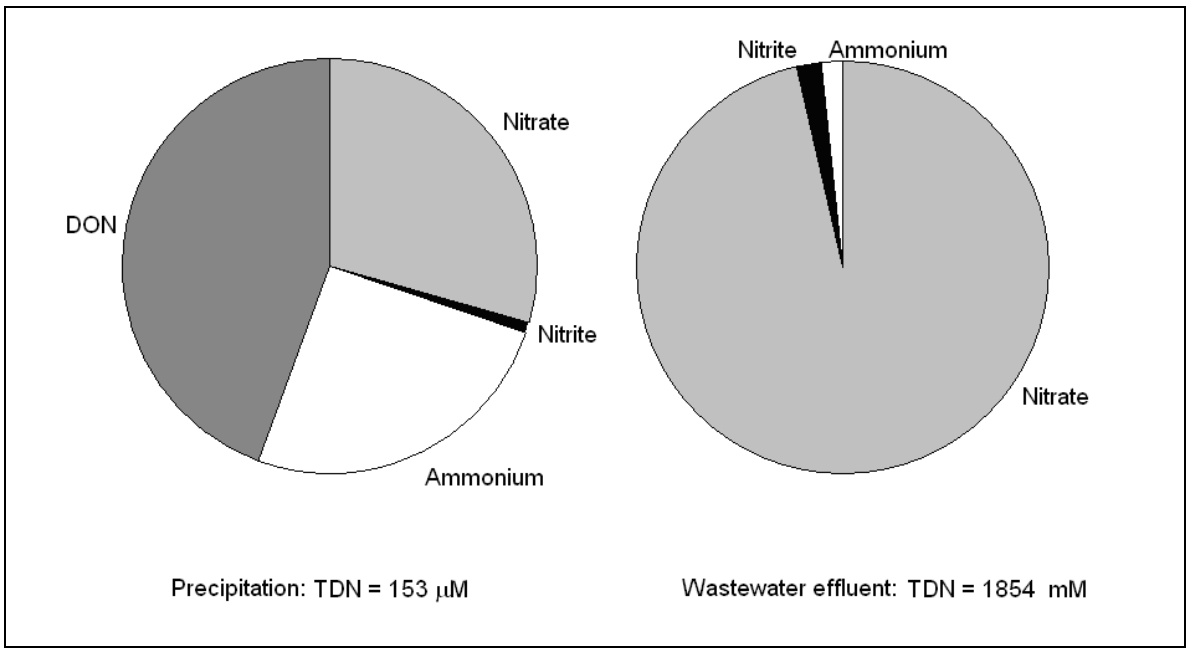

Figure 4.49 Relative proportions in precipitation and wastewater effluent samples of mean concentrations of the four dissolved nitrogen species: nitrate; nitrite; ammonium and DON, showing TDN.

4.7.2 Major and Minor Ion and Trace Element Concentrations of Precipitation and Wastewater Effluent

Concentrations of chloride, sulphate, phosphate, and sodium are high in wastewater effluent, with chloride, sodium, and phosphate concentrations showing a wide range (Table 4.13). In precipitation, concentrations of chloride, sodium and sulphate are relatively high in comparison to the concentrations of the other solutes, which could reflect the influence of marine air masses on precipitation hydrochemistry.

4.7.3 $\delta^{18}O_{H2O}$ of Precipitation and Wastewater Effluent

The $\delta^{18}O_{H2O}$ of the single wastewater effluent sample analysed was -7.2 ‰. Three precipitation samples were analysed for $\delta^{18}O_{H2O}$, giving a mean value of - 4.9 $\pm$ 1.5 ‰ which is lighter than the mean value of all catchment water samples (-6.9 ‰), and a range of $\delta^{18}O_{H2O}$ -6.4 to -3.4 ‰, which just overlaps the heaviest end of the range of $\delta^{18}O_{H2O}$ seen in catchment water samples.

4.8 PAIRED ANALYSIS OF CATCHMENT $\delta^{18}O_{H2O}$ and $\delta^{2}H_{H2O}$

The small number of samples analysed for both $\delta^{18}O_{H2O}$ and $\delta^{2}H_{H2O}$ suggest a local meteoric water line for Norfolk, similar to the world meteoric water line (WMWL) (Craig, 1961) but with a slope which is less steep (Figure 4.50). The deviation from the WMWL is likely to arise as a result of fractionation due to evaporation of surface waters, and variations in deuterium excess resulting from different conditions in precipitation source regions as a result of seasonal changes (Dansgaard, 1964, Darling *et al.*, 2003, Darling and Talbot, 2003). Deuterium excess is caused by variations in atmospheric humidity during the formation of water vapour.

The two sample subsets show some isotopic differentiation. The water isotopic composition of the Wensum river samples are from the low flow sample set (14/09/2008), and show some overlap with the catchment groundwater isotopic composition at the lighter end of the isotopic range of the river samples, with the isotopically heavier river samples clearly differentiated from the groundwater samples. The isotopic range in the river low flow sample set could represent mixing of Chalk baseflow with shallow groundwater from residual runoff. However, the number of samples analysed in each sample subset is small, and these apparent isotopic differentiations might not be borne out with a larger sample set.

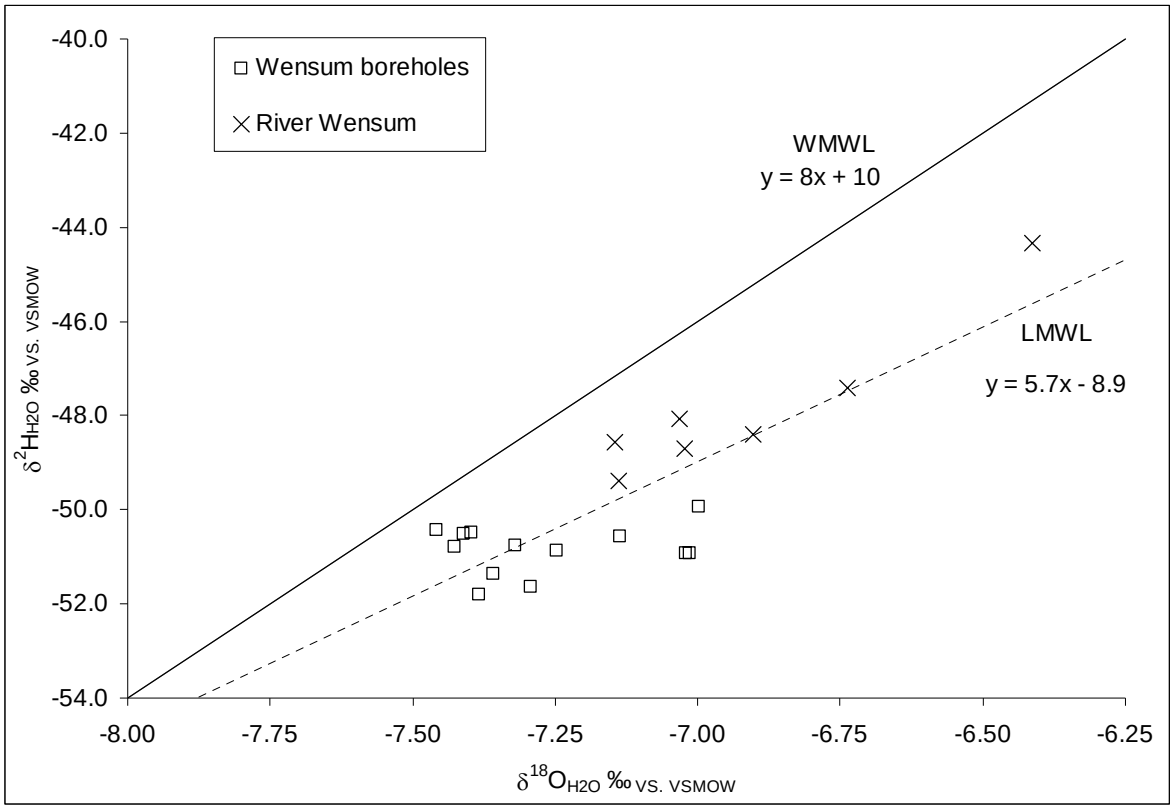

Figure 4.50 δ^2H_{H2O} (‰) versus $\delta^{18}O_{H2O}$ (‰) of samples from the Wensum river (14/09/2008), and catchment Chalk boreholes, showing world meteoric water line (WMWL: filled line) and local meteoric water line for Norfolk from these data (LMWL: dashed line) including regression equations for both lines. Error $\delta^{18}O_{H2O}$ $\pm$ 0.06 ‰; δ^2H_{H2O} $\pm$ 1.3 ‰.

4.9 SUMMARY

In this chapter, results of the research have been described and presented in figures and tables. Data concerning location, sampling date, type, and sample survey design have been presented along with information about river flow before and during sampling. Results from the analysis of samples collected in the Wensum catchment have been presented. First, a summary of results of the analysis of $\delta^{15}N_{NO3}$, $\delta^{18}O_{NO3}$ and nitrate concentration was presented for samples from the catchment, with data divided into the subgroups of river samples, tributary and drain samples, and groundwater samples, and a further division of surface water samples between spatial surveys and temporal surveys. Results of the analyses of further parameters of catchment hydrochemistry were presented, with descriptions of physical parameters, the composition of total dissolved nitrogen, and concentrations of major and minor ions and trace elements, again divided into the sample groupings of river, tributary and drain, and groundwater.

Results from the analysis of $\delta^{18}O_{H2O}$ for selected catchment samples were presented at the end of this section. The nitrate dual isotopic composition of source samples was then described, and results from the hydrochemical analysis of precipitation and wastewater effluent samples were presented, including the composition of total dissolved nitrogen, concentrations of major and minor ions and trace elements, and $\delta^{18}O_{H2O}$. Finally, the results of paired analysis of $\delta^{18}O_{H2O}$ and $\delta^{2}H_{H2O}$ for selected samples from catchment surface water and groundwater were presented in relation to the World Meteoric Water Line. The results presented in Chapter 4 are interpreted in the following chapter, Discussion to investigate nitrate sources to the Wensum catchment and attenuation within it, and to determine the cause of the observed decrease in nitrate concentrations downstream.

5. DISCUSSION

This chapter addresses the research question set out in the Introduction, to identify sources, pathways and removal processes of nitrate contamination which cause high concentrations of nitrate in the River Wensum that are observed to decrease downstream. The data presented in the previous chapter, Results, will be discussed with reference to the review of isotope fractionations in the nitrogen cycle from Chapter 2. Supplementary information for this chapter is included in Appendix 3.

Over 340 samples were analysed for nitrate isotopic composition from the Wensum catchment surface waters and groundwaters, and from direct nitrate sources in order to elucidate the sources, cycling and attenuation of nitrate within the Wensum catchment. With the exception of a small number of solid samples of direct nitrate sources, the samples collected were aqueous, and solute concentrations and water isotopic composition were measured to aid the understanding of the dynamics of catchment nitrate transport.

The results are discussed in the following order: first, the isotopic composition of direct nitrate sources and their overall relationship to catchment water nitrate isotopic composition is explored, followed by an examination of the isotopic composition of low-nitrate Chalk groundwater and valley Chalk groundwater. This is followed by a discussion of the use of solute concentrations and oxygen isotopes of water as tracers. Following this there is an overview of the Wensum catchment samples. Next are detailed examinations of the upper, mid, and lower Wensum river reaches, including the tributaries and drains within each reach. In these chapter sections, mass-balance mixing models are used to elucidate the data. The river reach examinations focus on spatial and temporal trends in nitrate concentration decrease, flow condition, and season, using mean and individual data sets, and utilising hydrochemical data where relevant. These sections also include discussions of the results from temporal sampling. Conclusions from this chapter concerning the sources, cycling, and attenuation of nitrate within the Wensum catchment are presented in the following chapter.

5.1 THE ISOTOPIC COMPOSITION OF DIRECT SOURCE NO_3^- AND ITS RELATIONSHIP TO CATCHMENT WATER NO_3^-

The analyses of the small number of samples of direct nitrate sources to the catchment, from dry deposition, precipitation, fertiliser, and wastewater effluent from sewage works, confirm that their nitrate isotopic composition is within the ranges reported in the literature (Shearer *et al.*, 1974a, Heaton, 1986, Hubner, 1986, Amberger and Schmidt, 1987, Fogg *et al.*, 1998, Kendall, 1998, Anisfeld *et al.*, 2007, Kendall *et al.*, 2007). All atmospheric and fertiliser nitrate samples have considerably higher $\delta^{18}O_{NO3}$ values than $\delta^{15}N_{NO3}$ values, giving a ratio of $\delta^{18}O_{NO3}$ to $\delta^{15}N_{NO3} > 1$ with a wide range of $\delta^{18}O_{NO3}$ values (23.3 to 85.3 ‰) (Figure 5.1). Wastewater effluent from sewage works (also referred to as wastewater effluent or effluent) has rather low $\delta^{18}O_{NO3}$ values, giving a ratio of $\delta^{18}O_{NO3}$ to $\delta^{15}N_{NO3} < 1$. The pattern of high $\delta^{18}O_{NO3}$ values in atmospheric and fertiliser nitrate is in contrast to the catchment water samples from the Wensum which have a ratio of $\delta^{18}O_{NO3}$ to $\delta^{15}N_{NO3} < 1$, and a much smaller range of $\delta^{18}O_{NO3}$ values (0.3 to 9.6 ‰). However, the low-nitrate groundwater samples do not conform to this pattern and have higher $\delta^{18}O_{NO3}$ values than $\delta^{15}N_{NO3}$ values. Two inferences can be made from this. Firstly, that the oxygen isotopic composition of atmospheric and fertiliser nitrate is not visible in catchment water nitrate, and secondly, that the low-nitrate groundwater samples contain some nitrate of atmospheric or fertiliser origin.

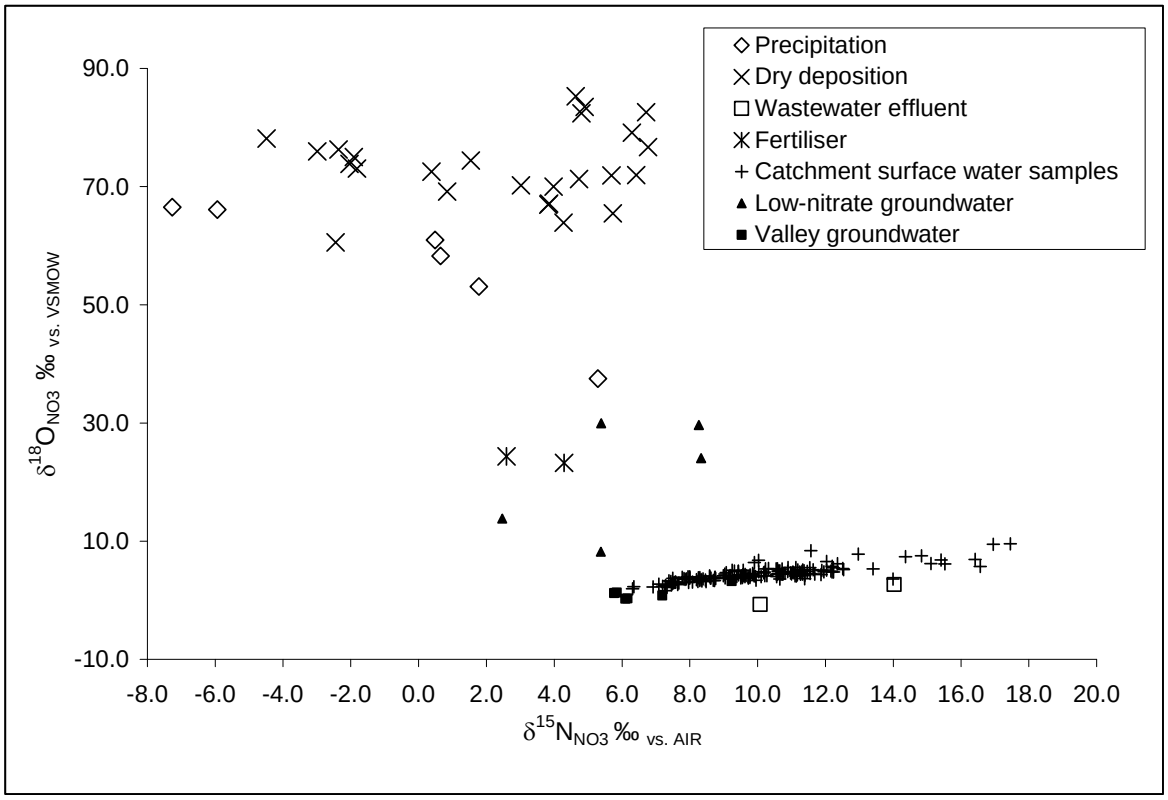

Figure 5.1 $\delta^{18}O_{NO3}$ (‰) versus $\delta^{15}N_{NO3}$ (‰) of nitrate source and catchment surface and Chalk groundwater samples. Error: $\delta^{15}N_{NO3}$ and $\delta^{18}O_{NO3}$ $\pm$ 0.1‰. Additional error of $\delta^{15}N_{NO3}$ $\pm$ 0.4 ‰ for precipitation and dry deposition samples due to the uncertainty of the true value of the ^{17}O anomaly.

The first inference suggests that atmospheric and fertiliser nitrate sources lose their original isotopic composition via microbially mediated reduction. Most atmospheric dry and wet deposition will occur to the land surface, the majority of which is put to agricultural use in this catchment, while fertiliser is also applied directly to fields, meaning that this reduction is likely to be mediated in agricultural soils. It is probable that it occurs during assimilation by the soil biota and plants which reduce the nitrate to ammonium. Ammonium subsequently released from living or dead organisms, alongside ammonium from these sources which is not assimilated, is then nitrified in the soil. The high proportions of DON and ammonium found in precipitation samples suggests that the cycling of these nitrogen species may comprise a significant proportion of nitrate derived from cycling of atmospheric source nitrogen in the soil, while ammonium-nitrate fertiliser will provide a direct source of ammonium for nitrification. Thus, when fertiliser and atmospheric nitrogen "reappears" as nitrate after cycling through assimilation, remineralisation and nitrification, it has a $\delta^{18}O_{NO3}$ value which reflects nitrification in the soil. This finding is supported by evidence of very rapid nitrate cycling in agricultural soils (Burger and Jackson, 2004). It is possible that very

small amounts of atmospheric nitrate escape transformation but that the isotopic composition is swamped by that of post-nitrification nitrate. With the spatial resolution of sampling used in this study it is unlikely that such nitrate would have been sampled.

The $\delta^{15}N_{NO3}$ of nitrate originating from fertiliser and atmospheric sources after cycling may reflect the effects of isotopic fractionation. Assimilation of source nitrogen by the soil biota can cause significant and variable fractionation, leading to higher values of $\delta^{15}N$ incorporated in to biomass (Delwiche and Steyn, 1970). These values will be transferred to nitrate after remineralisation and nitrification resulting in a heavier $\delta^{15}N$ of soil nitrate in comparison to that of the original nitrogen source. In addition, denitrification within the soil leads to gaseous losses of isotopically light nitrogen and an increase in $\delta^{15}N_{NO3}$ of the remaining soil nitrate. Thus the soil nitrogen pool, including nitrate, is likely to reflect a heavier $\delta^{15}N$ than that of the original nitrogen sources. Remineralisation and nitrification produce negligible isotopic fractionation if ammonium concentrations are at background levels (Heaton, 1986, Kendall *et al.*, 2007). However, high concentrations of ammonium can lead to high levels of isotopic fractionation during nitrification, resulting in lower values of $\delta^{15}N_{NO3}$ until ammonium concentrations are restored to background levels by the activity of the biota. This may be the case following ammonium fertiliser applications which create temporarily high concentrations of ammonium, and may incur additional fractionation due to ammonia volatilisation (Heaton, 1986, Kendall *et al.*, 2007). Together, these fractionations will lead to an increase in $\delta^{15}N_{NO3}$ values. The mean $\delta^{15}N_{NO3}$ of fertiliser and atmospheric sources analysed, before these fractionations is $\delta^{15}N_{NO3}$ 2.3 $\pm$ 4.2 ‰. It is not possible to predict exactly the size of the increase in $\delta^{15}N_{NO3}$ as the fractionations are variable.

Expected values for $\delta^{18}O_{NO3}$ originating from fertiliser and atmospheric sources after cycling in the biota can be predicted. Analysis of $\delta^{18}O_{H2O}$ from the Wensum catchment during this research provided a range of $\delta^{18}O_{H2O}$ from catchment waters from the Wensum of -7.5 to -6 ‰, which, when used in Equation 2.7 (Chapter 2) predicts a range of $\delta^{18}O_{NO3}$ for nitrified ammonium of $\delta^{18}O_{NO3}$ 2.8 to 3.8 ‰ (Appendix 3). Therefore, we would expect nitrate which originates from atmospheric and fertiliser sources and has been cycled and nitrified, but has not been affected by any further isotopic fractionation due to denitrification or assimilation, to have an oxygen isotopic

composition in the range $\delta^{18}O_{NO3}$ 2.8 to 3.8 ‰ and a mean $\delta^{15}N_{NO3}$ equal to or higher than 2.3 ± 4.2 ‰ (Figure 5.2).

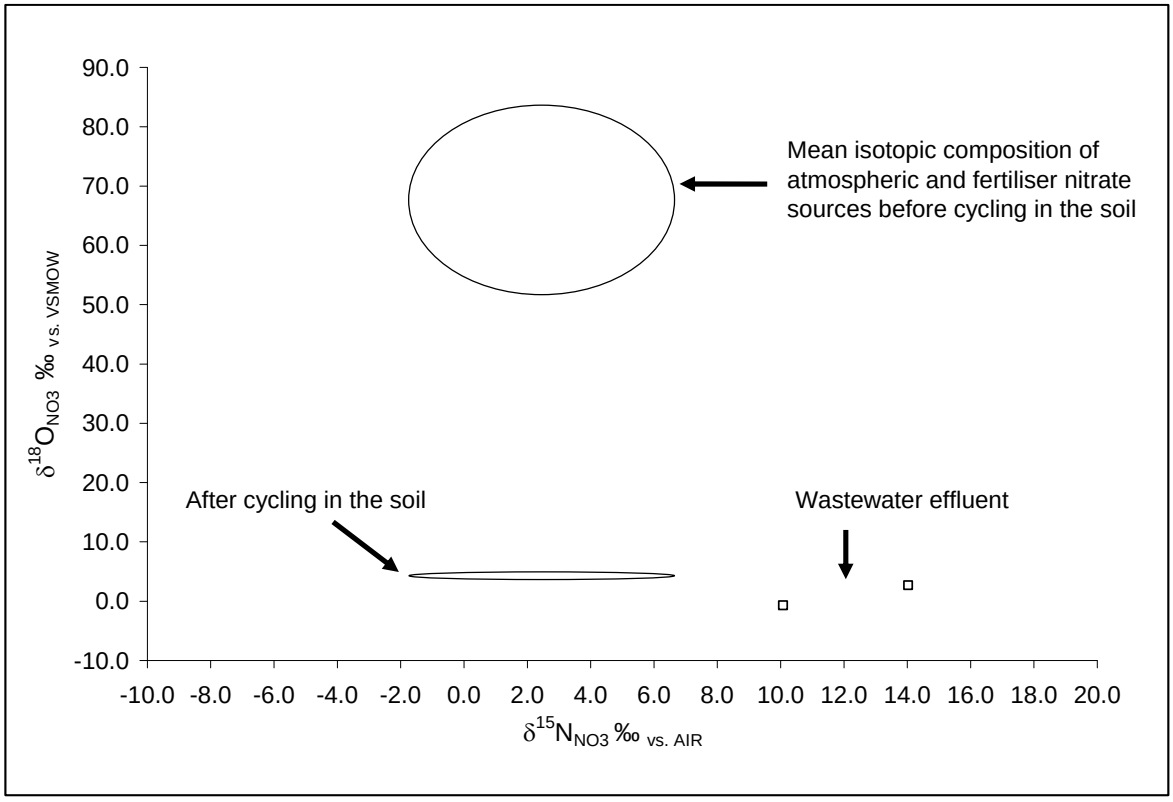

Figure 5.2 Mean isotopic composition ± one standard deviation of atmospheric and fertiliser nitrate, and that predicted after cycling in East Anglian soils. The isotopic composition of wastewater effluent is included for comparison.

Wastewater undergoes an artificial form of nitrogen cycling involving nitrification of ammonium. The $\delta^{18}O_{NO3}$ values of these samples (2.9 and -0.7), are close to the range predicted for nitrification in East Anglia ($\delta^{18}O_{NO3}$ 2.8 to 3.8 ‰). The sample with $\delta^{18}O_{NO3}$ 2.9 ‰ is from primary treated effluent which does not involve engineered nitrification but is likely to be conducive to its occurrence, while the sample with $\delta^{18}O_{NO3}$ -0.7 ‰ is from secondary treated effluent which involves a treatment step of oxidation of ammonium to nitrate. The lower than predicted $\delta^{18}O_{NO3}$ value of this sample could be due to oxygen exchange occurring between nitrite and water during nitrification, as suggested in the literature (Andersson and Hooper, 1983, Kool *et al.*, 2007). The $\delta^{15}N_{NO3}$ values of these samples (10.1 and 14.0 ‰) are in the range of literature values (Fogg *et al.*, 1998, Anisfeld *et al.*, 2007, Kendall *et al.*, 2007), and may reflect isotopic fractionation resulting from ammonia volatilisation and nitrification under high concentrations of ammonium. Unlike the other nitrate sources analysed, effluent from wastewater works is discharged directly into tributaries feeding the

Wensum and because of this, its nitrate isotopic composition might be more successfully used as a tracer of effluent inputs to the catchment. An input of wastewater effluent would be expected to raise the $\delta^{15}N_{NO3}$ value of nitrate in the river while lowering or leaving unchanged the $\delta^{18}O_{NO3}$ value, subject to the isotopic composition of riverine nitrate.

For the isotopic composition of manure, the assumption will be made of nitrification-derived nitrate, with a nitrogen isotopic composition within the range seen in the literature, which is indistinguishable from that of wastewater effluent, and a narrow range of $\delta^{18}O_{NO3}$ values predicted from nitrification calculations.

In summary, when nitrate from atmospheric, fertiliser, manure and effluent nitrate appears as catchment surface water and valley Chalk groundwater nitrate its oxygen isotopic composition reflects the fact that it has been cycled and nitrified. Catchment nitrate will also include nitrate from the soil nitrogen pool which is likely to reflect a heavier $\delta^{15}N$ than that of the original nitrogen sources due to assimilation and denitrification fractionations. Due to the fact that all the major sources of nitrogen to the catchment are cycled and nitrified in this way, the resulting isotopic composition of nitrate originally from atmospheric deposition, precipitation, fertiliser, manure, and wastewater effluent may not be distinguishable from each other at the catchment scale.

Figure 5.3 presents the expected range of isotopic composition of nitrate originating from these sources after cycling and nitrification in East Anglia, (rectangle) with dashed arrows indicating the possible extension of the oxygen isotopic range due to exchange of oxygen atoms between nitrite and water during nitrification, and uncertainty as to the extent of the increase in $\delta^{15}N_{NO3}$ due to isotopic fractionation. Included in the figure are the isotopic compositions of samples from the Wensum catchment, excluding low-nitrate groundwater.

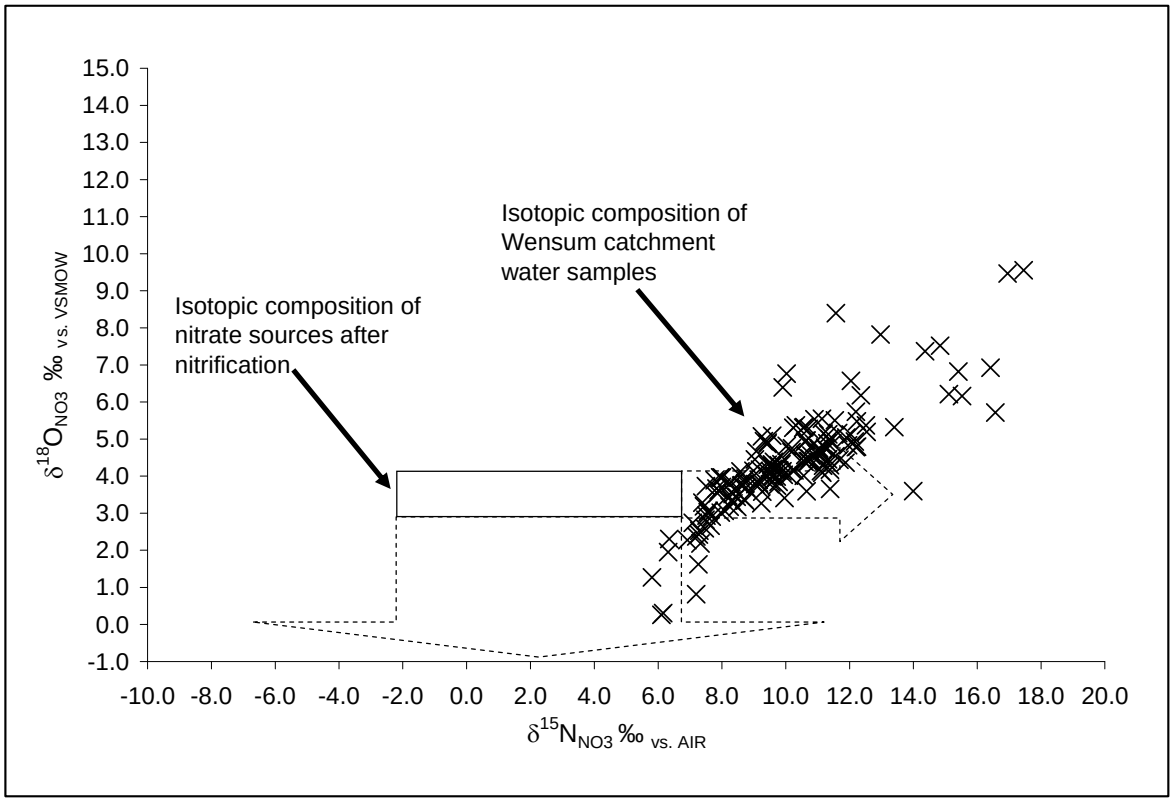

Figure 5.3 Expected range of isotopic composition of nitrate sources after nitrification (rectangle). Dashed arrows indicate extension of oxygen isotopic range due to oxygen exchange with water, and uncertainty of the range of fractionation of $\delta^{15}N_{NO3}$. Included in the figure are the isotopic compositions of samples from the Wensum catchment, excluding low-nitrate groundwater.

It is interesting that although many of the catchment water samples are contained within the source rectangle's extending arrows, a number of samples are differentiated by a heavier oxygen isotopic composition than the range predicted for nitrate sources. A possible explanation for this is that it reflects a mix of a small amount of atmospheric or fertiliser nitrate which has escaped nitrification with a larger amount of source nitrate which has been cycled and nitrified, although the catchment samples do not indicate a simple mixing of the two sources (Figure 5.4). However, if this were the case we would expect some samples collected close to sites of source nitrate deposition or application, for example from field drains, to display a trace of the original source isotopic composition resulting from a mix of nitrate from the two sources. This would lead to variation in the ratio of $\delta^{18}O_{NO3}$ to $\delta^{15}N_{NO3}$. The ratio of $\delta^{18}O_{NO3}$ to $\delta^{15}N_{NO3}$ of catchment water samples falls within a tight range ($\delta^{18}O_{NO3}$: $\delta^{15}N_{NO3}$ 0.4 $\pm$ 0.1), and no sample has a $\delta^{18}O_{NO3}$ value greater than its $\delta^{15}N_{NO3}$ value. For these reasons, this theory will not be explored further, and the assumption of near quantitative cycling of contemporary atmospheric and fertiliser nitrate will be made.

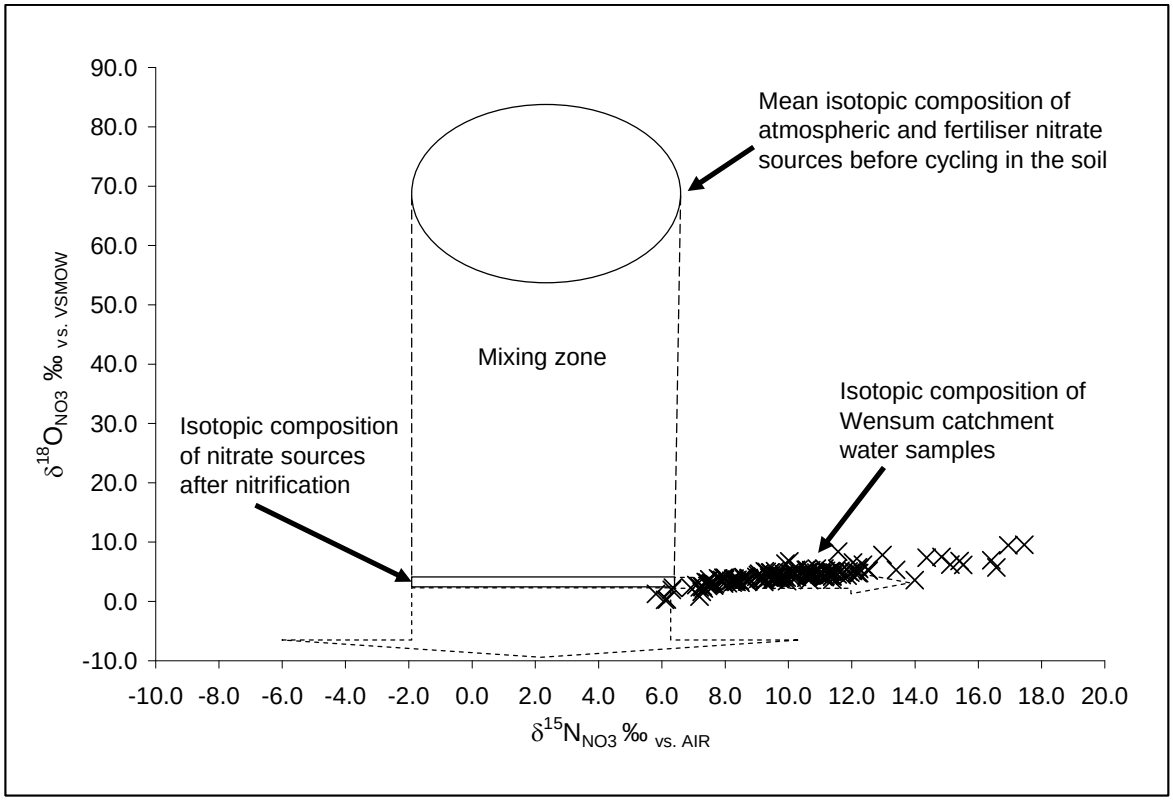

Figure 5.4 Mean isotopic composition ± one standard deviation of atmospheric and fertiliser nitrate and expected range of isotopic composition of nitrate sources after nitrification (rectangle). Dashed arrows indicate extension of isotopic range due to oxygen exchange with water, and uncertainty of the range of fractionation of $\delta^{15}N_{NO3}$. A zone of mixing is delineated by dashed lines between the two ranges. Included in the figure are the isotopic compositions of surface water samples from the Wensum catchment excluding low-nitrate groundwater.

In fact, the catchment water samples with a heavier oxygen isotopic composition also have a heavy nitrogen isotopic composition which may suggest a fractionating process, such as denitrification, which affects both nitrogen and oxygen isotope ratios of nitrate. This theory will be examined in detail later in this chapter.

The second inference from Figure 5.1 is that the low-nitrate groundwater samples contain nitrate of atmospheric or fertiliser origin. Low-nitrate groundwater has the lowest concentration of all catchment water samples (< 1 μM NO_3^-), and high $\delta^{18}O_{NO3}$ values ($\delta^{18}O_{NO3}$ 8.2 to 30.0 ‰) with a ratio of $\delta^{18}O_{NO3}$ to $\delta^{15}N_{NO3}$ > 1 (Figure 5.5). Although a plot of these samples suggests an association between $\delta^{18}O_{NO3}$ and $\delta^{15}N_{NO3}$, the correlation is poor (r^2 0.33) and the slope of the best fit line of $\delta^{15}N_{NO3}$ versus $\delta^{18}O_{NO3}$ is 2.3, which is unlike the slope produced by fractionating processes such as

denitrification and assimilation, and does not suggest that such a process is occurring in these groundwaters. This is corroborated by Feast *et al.* (1998) who found no evidence from measurements of $\delta^{15}N_{NO3}$ that denitrification was occurring in the Chalk groundwaters of the neighbouring Bure catchment. The very low nitrate concentration, therefore, appears to be caused by a very low level of nitrate reaching the groundwater, or of subsequent dilution. These samples were collected from two hydrogeological settings. In this catchment the Lowestoft Till covers the Chalk in the interfluves, acting as an effective aquitard within which denitrification occurs, providing double protection from nitrate contamination (Feast *et al.*, 1998). An influence from the Lowestoft Till is also seen in the clayey interfluve soils which have a low permeability, which is likely to develop waterlogging and anaerobic conditions conducive to denitrification (National Soil Resources Institute, 2009). On the edge of the valley where the Lowestoft Till has been partially eroded, denitrification occurs within the clay-rich Pleistocene sediments, and the overlying soils, protecting the underlying Chalk effectively (Hiscock, 1993). Thus Chalk groundwater in the Wensum catchment has been protected from contemporary nitrate contamination by overlying clay-rich deposits which support denitrification. This means it is highly unlikely that the low-concentration nitrate is derived from a fertiliser source. In addition, its isotopic composition suggests that it is not residual nitrate from denitrification in the overlying glacial deposits as might be expected. This raises the question of how the nitrate reached these groundwaters without undergoing denitrification. A possible explanation is that it was carried in recharge infiltrating slowly through the glacial deposits at a time when environmental conditions did not support denitrification, perhaps when temperatures were around $0^{o}C$, at the end of the last glacial maximum. This hypothesis is supported by findings from Hiscock (1993) who, using carbon dating, suggested that Chalk groundwater in the interfluves of north Norfolk is in the region of 10 000 years old.

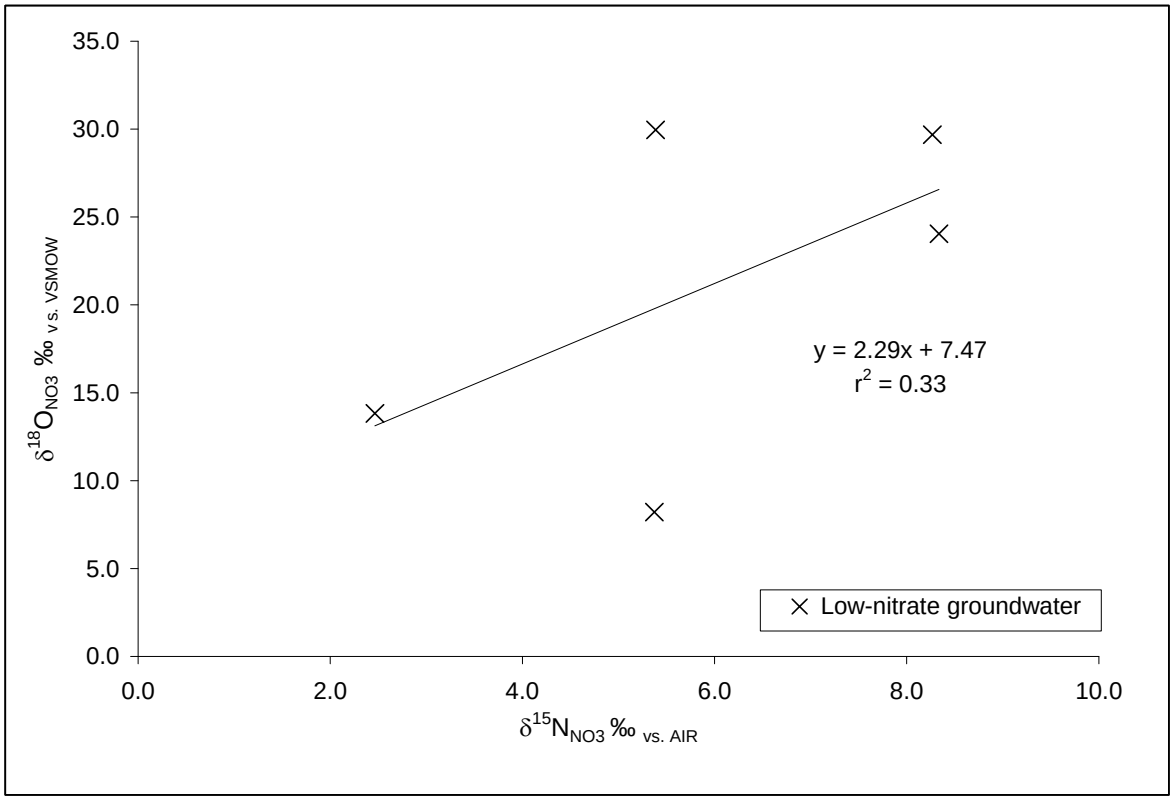

Figure 5.5 $\delta^{18}O_{NO3}$ (‰) versus $\delta^{15}N_{NO3}$ (‰) of low-nitrate Chalk groundwater samples from the Wensum catchment. Error: $\delta^{15}N_{NO3} \pm 1.0$ ‰ and $\delta^{18}O_{NO3} \pm 3.1$‰.

Hiscock *et al.* (1996) calculated an expected range of $\delta^{18}O_{H2O}$ of groundwater between -6.5 and -7.5 ‰ in the Norfolk Chalk where recharge is attributable to modern recharge weighted towards a winter precipitation input. A lighter isotopic composition was found in older confined Chalk groundwater. Interestingly, the $\delta^{18}O_{H2O}$ of the low-nitrate groundwater samples in this research all fall within the range suggested for modern recharge (range $\delta^{18}O_{H2O}$ -7.0 to -7.5 ‰). Although the water isotope data appear to refute the theory of palaeo-nitrate in these samples, a possible explanation for this apparent discrepancy is that these groundwaters are being replenished by modern recharge which infiltrates slowly through the Lowestoft Till and Pleistocene deposits, allowing quantitative denitrification of contemporary nitrate to occur. The water isotopic composition would thus be a mix of old water with a light isotopic composition and modern water of a heavier isotopic composition, bringing it within the range of modern recharge while diluting the concentration of palaeo-nitrate. The $\delta^{18}O_{NO3}$ value of this palaeo-nitrate may suggest a mix of atmospheric and terrestrial sources as it is not as high as contemporary atmospheric sources.

Given the possible palaeo origins of the low-nitrate groundwaters, and the fact that contemporary nitrate does not appear to be reaching them, the nitrate isotopic composition of these groundwaters will not be included in further discussions of catchment water nitrate. In fact, isotopic mass-balance calculations show that a mixing of the low-nitrate groundwater with high nitrate valley Chalk groundwater or river water has virtually no effect on the isotopic composition of the high concentration end member, though clearly concentration is affected. For example, mixing three parts of interfluve water with one part valley Chalk groundwater, using mean values for each, leaves $\delta^{18}O_{NO3}$ and $\delta^{15}N_{NO3}$ unchanged within measurement limits, but reduces concentration from 973 μM NO_3^- to 244 μM NO_3^- (Appendix 3). Therefore, in discussions of catchment water nitrate, low-nitrate groundwater will be treated as a "nitrate free" diluting component.

Valley Chalk groundwater, has some of the highest nitrate concentrations seen in the catchment (786 to 1314 μM NO_3^-). High concentrations of nitrate in groundwater from the exposed Chalk in the river valleys in north Norfolk were also found by Hiscock (1993). These valley Chalk groundwater samples also have the lightest isotopic composition of catchment water samples (Figure 5.6). A plot of $\delta^{15}N_{NO3}$ versus $\delta^{18}O_{NO3}$ of catchment surface water samples (r^2 0.68) gives a slope of 0.49 and shows the valley Chalk groundwater samples sitting at the base of the line and slightly offset from it due to low $\delta^{18}O_{NO3}$ values (Figure 5.6). If the slope of the line implies a fractionating process such as denitrification across all catchment samples, the isotopic composition of valley Chalk groundwater represents the least fractionated/ denitrified nitrate. Valley Chalk groundwater nitrate $\delta^{18}O_{NO3}$ values suggest that it is a product of nitrification of ammonium which supplies "new" oxygen ($\delta^{18}O_{NO3}$ 0.3 to 3.3 ‰). Valley Chalk groundwater nitrate $\delta^{15}N_{NO3}$ values (6.9 $\pm$ 1.4 ‰) are within the expected range for nitrification of ammonium from sources of anthropogenic origin.

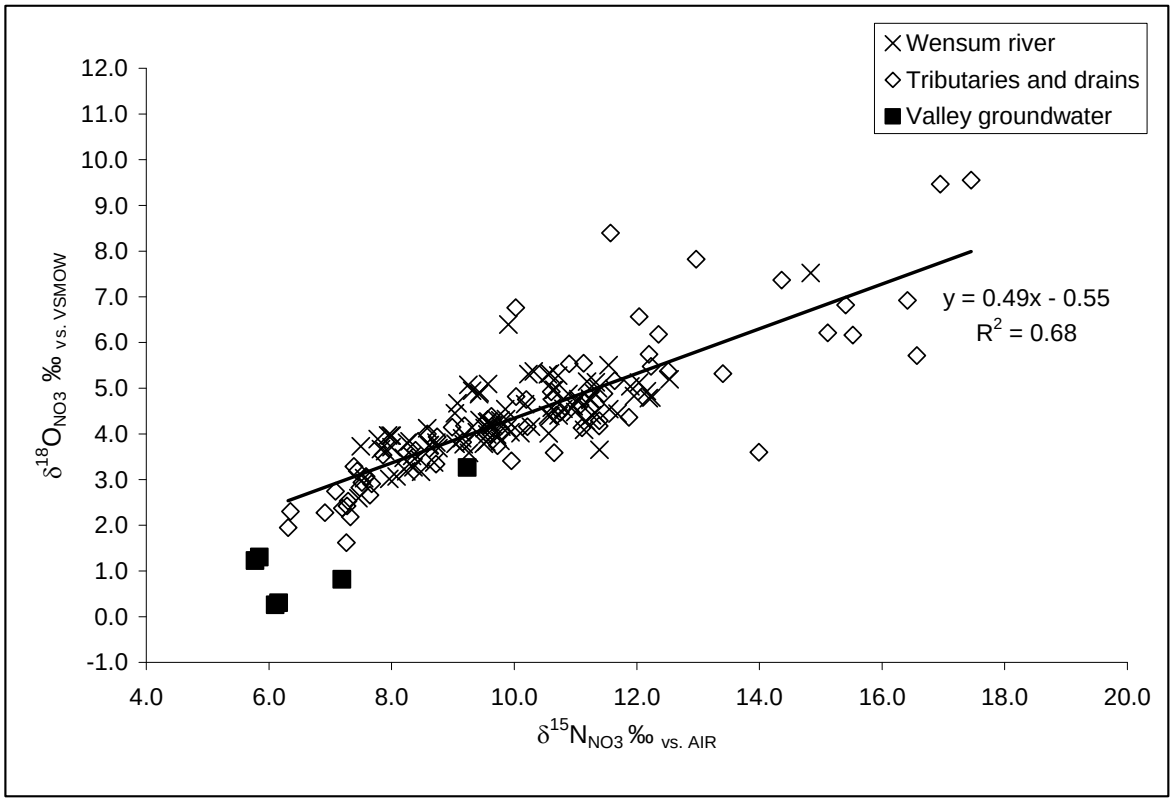

Figure 5.6 $\delta^{18}O_{NO3}$ (‰) versus $\delta^{15}N_{NO3}$ (‰) of valley Chalk groundwater samples with river, and tributary and drain samples from the Wensum catchment. Error: $\delta^{15}N_{NO3}$ and $\delta^{18}O_{NO3}$ $\pm$ 0.1 ‰. Best fit line catchment surface water samples only.

In relation to source nitrate isotopic composition after nitrification, the majority of valley Chalk groundwater samples fit within the range predicted for $\delta^{15}N_{NO3}$ and within the extension of the $\delta^{18}O_{NO3}$ range due to oxygen exchange with water (Figure 5.7). Thus both the nitrogen and oxygen isotopic composition of valley Chalk groundwater nitrate suggest that it derives from nitrification, and that it has not undergone significant subsequent isotopic fractionation from denitrification. The occurrence of this valley Chalk groundwater nitrate in the Chalk only where the Lowestoft Till is thin and patchy, or absent along the Wensum valley, suggests that recharge waters carry leached nitrate rapidly from the soil directly into the Chalk in these areas, with infiltration unimpeded by the clay-rich till. This rapid transport enables the nitrate to avoid denitrification in the shallow saturated zone or the Lowestoft Till, and suggests that the well drained loam soils in the valley do not support significant denitrification under normal conditions. The concentration of nitrate in valley Chalk groundwater and its isotopic composition confirm that significant denitrification does not occur within the Chalk itself, perhaps because a source of organic carbon is lacking. Therefore, when valley Chalk groundwater enters the river as baseflow, it is effectively an indirect source of nitrate

originating from atmospheric, fertiliser, manure and possibly effluent sources. The isotopic composition of valley Chalk groundwater, representing the product of cycled and nitrified sources of nitrogen to the catchment, constrains the predicted range of bulk cycled source nitrate in areas of the catchment with freely draining soils to $\delta^{15}N_{NO3}$ to 5.8 to 9.2 ‰. These areas include the north-west upper catchment, the river valley and the lower catchment north and south, and exclude the interfluves where the soil composition is clayey reflecting the influence of the underlying till.

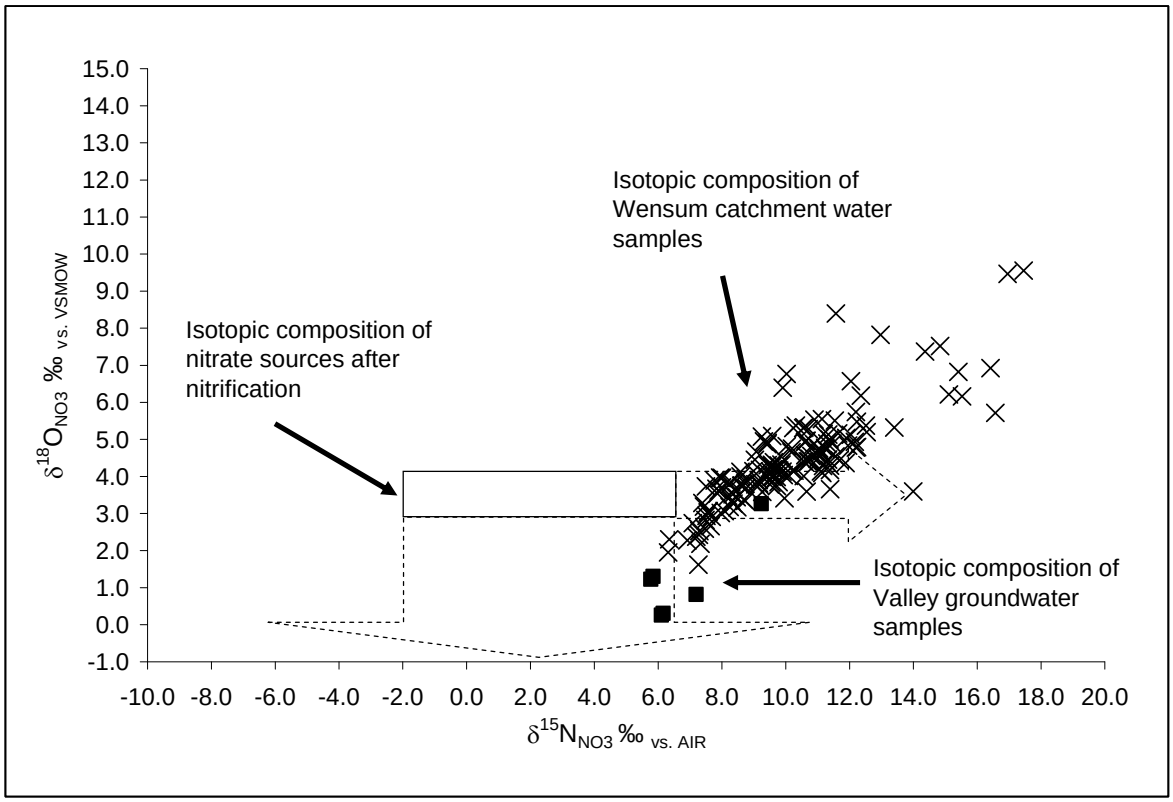

Figure 5.7 Expected range of isotopic composition of nitrate sources after nitrification (rectangle). Dashed arrows indicate extension of oxygen isotopic range due to oxygen exchange with water, and uncertainty of the range of fractionation of $\delta^{15}N_{NO3}$. Included in the figure are the isotopic compositions of surface water samples from the Wensum catchment (crosses), and valley Chalk groundwater (filled boxes).

In summary, it seems that all the major sources of nitrate to the catchment undergo cycling and nitrification, with the resulting isotopic composition forming a narrow range. This means that fertiliser and atmospheric inputs cannot be traced using their very heavy oxygen isotopic composition. Catchment surface water nitrate isotopic composition suggests that it originates from cycled and nitrified source nitrogen, but reflects further fractionations which may be attributable to denitrification. Low-nitrate groundwater may contain very low concentrations of palaeo-nitrate of atmospheric

origin and will act to dilute river water nitrate concentrations if it contributes to baseflow. Valley Chalk groundwater nitrate isotopic composition suggests that it originates from the major sources of nitrate after they have undergone cycling and nitrification.

5.2 WENSUM CATCHMENT: SOLUTE CONCENTRATIONS AND WATER ISOTOPIC COMPOSITION AS TRACERS AND MARKERS OF DIRECT AND INDIRECT SOURCES OF NO_3^-

This section discusses the hydrochemical composition of precipitation, wastewater effluent and groundwater as possible tracers, outlining their effect on river water hydrochemical composition. The water isotopic composition of catchment samples is briefly discussed.

5.2.1 Wastewater Effluent and Precipitation Solute Concentrations in Relation to the Wensum River

The hydrochemical analyses of the two wastewater effluent samples suggest compounds which might be useful tracers of effluent. High concentrations of nitrate, nitrite, ammonium and phosphate found in the effluent samples could potentially act as tracers, although these nutrients are likely to be utilised quickly within river water. High concentrations of chloride, sulphate, sodium and potassium in wastewater could act as tracers as they are considerably higher than those found in river water. $\delta^{18}O_{H2O}$ of wastewater is not distinguishable from that of catchment water.

Due to the small sample size (two effluent samples) calculations of solute load attributable to wastewater effluent were not attempted. It is possible that solute concentrations in effluent vary with flow condition due to the dilutional effects from storm runoff which may pass through the wastewater works, and solute concentrations may vary between works as a result of the mix of domestic and industrial wastewater and differences in processing within the plant.

The hydrochemical analyses of the five precipitation samples show considerably lower concentrations of major ions than those found in the Wensum river, meaning that pure

precipitation would be expected to have a diluting effect on river water major ion concentrations. However, runoff generated by precipitation will entrain dissolved constituents from the soil before reaching the river, so it is questionable whether significant dilution of major ion concentrations in river water occurs from precipitation. Three of the precipitation samples have ammonium concentrations above 20 μM NH_4^+, with one above 100 μM NH_4^+. The very high ammonium concentration may be due to contamination from splash-back rather than from the precipitation itself. Ammonium from precipitation is likely to be assimilated or nitrified in the soil before reaching the river making ammonium an unlikely tracer of precipitation input to river water. Trace element concentrations in the five rain samples are similar to those found in river water, so are not useful tracers.

In summary, the most reliable hydrochemical tracers of effluent are likely to be chloride, sulphate, sodium and potassium. However, it must be noted that high concentrations of these constituents are not exclusive to human waste may also indicate inputs from manure and agricultural runoff, and runoff from roads during winter (Hem, 1985). In addition if samples are collected close to an effluent source before nutrients are utilised by the biota, high concentrations of nitrate, nitrite, ammonium and phosphate may indicate an effluent or manure input. Precipitation may have the effect of minor dilution on river water solute concentrations if runoff does not entrain solutes.

5.2.2 Wensum Catchment Chalk Groundwater Solute Concentrations in Relation to the Wensum River

The purpose of collecting groundwater samples from the valley and interfluves within the Wensum catchment was to support the interpretation of the isotopic composition of nitrate from catchment samples and the discussion of sources and cycling of nitrate inputs to the Wensum river. Therefore, Chalk groundwater hydrochemistry is discussed here with respect to its function of supplying baseflow to the Wensum river. For a detailed discussion of the groundwater hydrochemistry of Norfolk see Hiscock (1993), Hiscock *et al.*(1996), Feast *et al.*(1997), and Feast *et al.* (1998).

Concentrations of calcium and bicarbonate reflect the fact that Chalk groundwaters are of a Ca-HCO_3 type (Hiscock, 1993). As would be expected, the Wensum river is of the

same hydrochemical type, and concentrations of calcium and bicarbonate in groundwater samples from the Wensum catchment will not be discussed further. Magnesium also does not show any differentiation in concentration between groundwater and river water. It was decided not to attempt to use trace elements as groundwater tracers due to the fact that measurements from boreholes will reflect trace element solubility controlled by redox conditions within the aquifers which will not necessarily be maintained along the flowpath to the river.

The three low-nitrate borehole samples on the interfluve are adjacent to the uppermost river sampling locations in the west of the catchment (Hamrow east and west, Wellingham), and have the lowest concentrations of the major ions sulphate, chloride, sodium, and potassium of all the boreholes. In comparison to river water concentrations, these borehole samples have lower concentrations of sulphate, chloride, sodium, and potassium. Therefore, if interfluve Chalk groundwater from the Chalk is supplying baseflow the Wensum river, the effect on concentrations of the major ions would be that of dilution.

The next borehole, at Great Ryburgh, also produced low-nitrate groundwater although it is close to the edge of the river valley. Its hydrochemistry is also is more similar to that of the valley boreholes indicating that it is likely to be on the margin of the Lowestoft Till, protected by denitrification in the till and Pleistocene deposits from nitrate contamination (Hiscock, 1993), but subject to high concentrations of sulphate and mid range concentrations of the other major ions. In relation to Wensum river water hydrochemistry, concentrations of sulphate are higher in the Great Ryburgh borehole than maximum riverine concentrations. Concentrations of chloride, sodium, and potassium are similar to minimum riverine concentrations.

Further downstream, the borehole at Bylaugh is in the valley close to the river, and between river sampling locations of Swanton Morley and Mill Street. Despite its very high nitrate concentrations (> 1000 μM NO_3^-), concentrations of chloride, sodium, and potassium from this borehole are very similar to the riverine means.

East of the Bylaugh borehole is the borehole at Weston Longville, again in the valley and with a very high nitrate concentration (> 1300 μM NO_3^-). The sample from this

borehole has a high sulphate concentration which is above maximum concentrations found in the river. Concentrations of chloride, sodium, and potassium are very similar to the borehole at Bylaugh, with the major ions close to the riverine means.

North of the Weston Longville borehole is the northern catchment low-nitrate groundwater borehole at Cawston. Concentrations of major ions from this borehole are low, with chloride, sodium and potassium at lower concentrations than minimum concentrations of riverine samples.

Further east from Weston Longville and Cawston is the low-nitrate groundwater borehole at Taverham on the north-western outskirts of Norwich. Its concentration of sulphate is just above the range seen in the Wensum river, with concentrations of chloride, sodium and potassium similar to or below the riverine means. This hydrochemical profile is very similar to the borehole at Great Ryburgh, and may also suggest a location on the margin of the Lowestoft Till.

The final three valley boreholes in the east at Hellesdon and Costessey have a similar hydrochemistry, with high nitrate concentrations (786 to 823 μM NO_3^-), and concentrations of sulphate, chloride and sodium above the maximum concentrations found in the river.

In summary, three hydrochemical groups are seen (Table 5.1). The first corresponds to groundwater from the Chalk in the interfluves and has concentrations of sulphate, chloride, sodium, and potassium lower than minimum concentrations in the Wensum river, and nitrate below the limit of detection. The group include the boreholes at Hamrow east and west, Wellingham and Cawston. A baseflow contribution from this groundwater type would be expected to dilute concentrations of the major ions.

The second type corresponds to groundwater from the valley edge where the Lowestoft Till has been partially eroded, but denitrification in the remaining till and the Pleistocene sediments results in nitrate concentrations below the limit of detection. Concentrations of sulphate at or above the maximum concentrations found in the river are seen in this groundwater type, with concentrations of chloride, sodium, and potassium close to the riverine mid range. A baseflow contribution from this water type

would be shown by an increase in sulphate concentrations in the river with a decrease in nitrate. This group includes the boreholes at Great Ryburgh and Taverham.

The third groundwater type corresponds to groundwater from the valley and has high to very high nitrate concentrations and concentrations of sulphate, chloride, and sodium values corresponding to riverine means in the middle catchment, to values above the maximum concentrations found in the river in the east of the catchment, with concentrations of potassium close to the riverine mean across these samples. This group includes the boreholes at Bylaugh, Weston Longville, Hellesdon, and Costessey east and west. A baseflow contribution from this groundwater type would be expected to increase riverine concentrations of nitrate throughout the catchment, and in the east of the catchment towards Norwich, also to increase concentrations of sulphate, chloride, and sodium.

Table 5.1 Concentration ranges of solutes determined to be useful Chalk groundwater tracers for the three hydrochemical groups, including ranges for Wensum river samples for comparison.

Group	NO_3^- µM	SO_4^{2-} mg/L	Cl^- mg/L	Na^+ mg/L	K^+ mg/L
Group 1 interfluve Chalk boreholes:	0.5	8 to 27	18 to 27	11 to 15	0.5 to 0.9
Group 2 valley edge Chalk boreholes:	0.5	46 to 76	27 to 37	16 to 18	1.4 to 2.1
Group 3 valley Chalk boreholes:	786 to 1314	44 to 78	40 to 75	20 to 50	1.9 to 3.1
Wensum river mean, standard deviation, and range:	475 ± 115 288 to 757	39 ± 9 22 to 57	41± 7 31 to 74	23 ± 3 16 to 31	3.5 ± 1.4 1.3 to 7.7

These inferences must be used with slight caution, as, with the exception of chloride, none of these potential groundwater tracers are expected to behave in a conservative manner, and concentrations in baseflow may be altered during advection through the sediments below the riverbed, affected by processes such as reduction, adsorption, and ion exchange.

5.2.3 Wensum Catchment $\delta^{18}O_{H2O}$

$\delta^{18}O_{H2O}$ of the three precipitation samples analysed shows a level of variation ($\delta^{18}O_{H2O}$ -6.4 to -3.4 ‰) which is to be expected from individual rainfall events. Eames (2008) found a mean value of $\delta^{18}O_{H2O}$ from precipitation in East Anglia of -7.1‰, with a range

of $\delta^{18}O_{H2O}$ -12.1‰ to -2.6 ‰. It is possible that an input of precipitation to the soil with a $\delta^{18}O_{H2O}$ value different from that of bulk soil water could lead to transient localised variations in $\delta^{18}O_{NO3}$ values of nitrate from nitrification, though the bulk $\delta^{18}O_{NO3}$ of nitrate from nitrification in the soil will reflect the $\delta^{18}O_{H2O}$ of bulk soil. Due to the small number of precipitation samples collected, baseflow separation using $\delta^{18}O_{H2O}$ was not attempted. The mean $\delta^{18}O_{H2O}$ of Wensum catchment groundwater samples is lower than that of river samples (-7.3 $\pm$ 0.2‰ versus 6.8 $\pm$ 0.3 ‰), suggesting that a low $\delta^{18}O_{H2O}$ in the river could indicate that baseflow addition is occurring, although the range of groundwater $\delta^{18}O_{H2O}$ overlaps both the river and tributary and drain $\delta^{18}O_{H2O}$ ranges.

5.3 OVERVIEW OF WENSUM CATCHMENT NO_3^- CONCENTRATION AND ISOTOPIC COMPOSITION

There is a consistent relationship between $\delta^{15}N_{NO3}$ and $\delta^{18}O_{NO3}$ in samples from the Wensum catchment, (Wensum river, tributaries and drains, and valley Chalk groundwater), such that higher values of $\delta^{15}N_{NO3}$ are coupled with higher values of $\delta^{18}O_{NO3}$. When plotted together, the Wensum catchment data show a slope of 0.53 indicating the fractionation ratio of O:N, (r^2 0.70), and when calculated using an equal weighting of Wensum surface water to Wensum valley Chalk groundwater, the slope is 0.74 (r^2 0.82) (Figure 5.5). The relationship between $\delta^{15}N_{NO3}$ and nitrate concentration shows much scatter resulting in a low correlation (r^2 0.14). However, overall, there is an inverse relationship between isotope ratios and nitrate concentration showing an association of lower nitrate concentrations with nitrate of a heavier isotopic composition, (Figure 5.8). Together, these markers suggest that denitrification is occurring across catchment waters, with the fractionation ratio in good agreement with literature values from field studies of rapid denitrification (Mariotti *et al.*, 1980, Mariotti *et al.*, 1988, Böttcher *et al.*, 1990, Aravena and Robertson, 1998, Cey *et al.*, 1999, Lehmann *et al.*, 2003, Fukada *et al.*, 2004, Deutsch *et al.*, 2005, Petitta *et al.*, 2009). Nitrate is not the only dissolved nitrogen species found in catchment waters. DON in surface water samples comprises 18% of TDN, and a significant proportion of nitrogen is likely to be present in particulate form in surface water. Despite this, the coherent pattern seen in the nitrate isotopic composition and concentration of catchment water

samples suggests that a process such as denitrification forms a vector through the data, influencing nitrate isotopic composition and concentration.

Denitrification causes an exponential increase in the $\delta^{15}N_{NO3}$ of the residual nitrate with decreasing nitrate concentrations. There is a diagnostic which uses this relationship to separate the effects of denitrification from those of mixing in of a water type with low nitrate concentration and a heavy isotopic composition. This is to plot $\delta^{15}N_{NO3}$ against the natural log of nitrate concentration values, which should show a linear relationship if denitrification is occurring and a curve if mixing is occurring, and to plot $\delta^{15}N_{NO3}$ against the reciprocal of concentration values, which should show, conversely, a linear relationship if mixing is occurring and a curve if denitrification is occurring (Mariotti *et al.*, 1988, Kendall *et al.*, 2007). However, when these data are plotted in this way, a significant relationship is not shown ($r^2 = 0.33$), in addition to the fact that the points do not sit closely together to form either a line or a curve (Figures 5.9 and 5.10). This could mean that although denitrification is occurring, as suggested by the slope of Figure 5.6, it is not appropriate to treat catchment data together as a single flowpath along which the process takes place. Additionally, it could imply that an element of mixing is taking place, of denitrified waters with less denitrified waters from different water sources within the catchment.

Isotopic enrichment with a decrease in nitrate concentration can also be caused by assimilation (uptake), which stores assimilated nitrogen temporarily in biomass rather than removing it to the atmosphere as is the case with denitrification. Due to the paucity of studies into the dual-isotopic effects of assimilation on nitrate isotopic composition in the field it is not possible to distinguish denitrification from assimilation at the catchment scale based on isotopic composition alone. It is likely that the isotopic and concentration markers across all data discussed here are in part caused by assimilation. It may be possible to clarify which process is dominant using sampling season, as assimilation rates are likely to be much higher in spring and summer and are sensitive to cold temperatures, while denitrification can occur all year round and down to temperatures of 5^{o}C without rates being greatly affected (Holtan-Hartwig *et al.*, 2002, McCulloch *et al.*, 2007). The temperature range measured from surface water samples was 6.0 to 15^{o}C, and that of groundwater, 8.4 to 12^{o}C. Thus, if assimilation is causing significant temporary removal of nitrate in spring and summer, an increase in

concentration and a lessening or loss of the trend of isotopic enrichment would be expected in winter, whereas if the dominant process is denitrification, the signal will be visible all year round without much seasonal fluctuation.

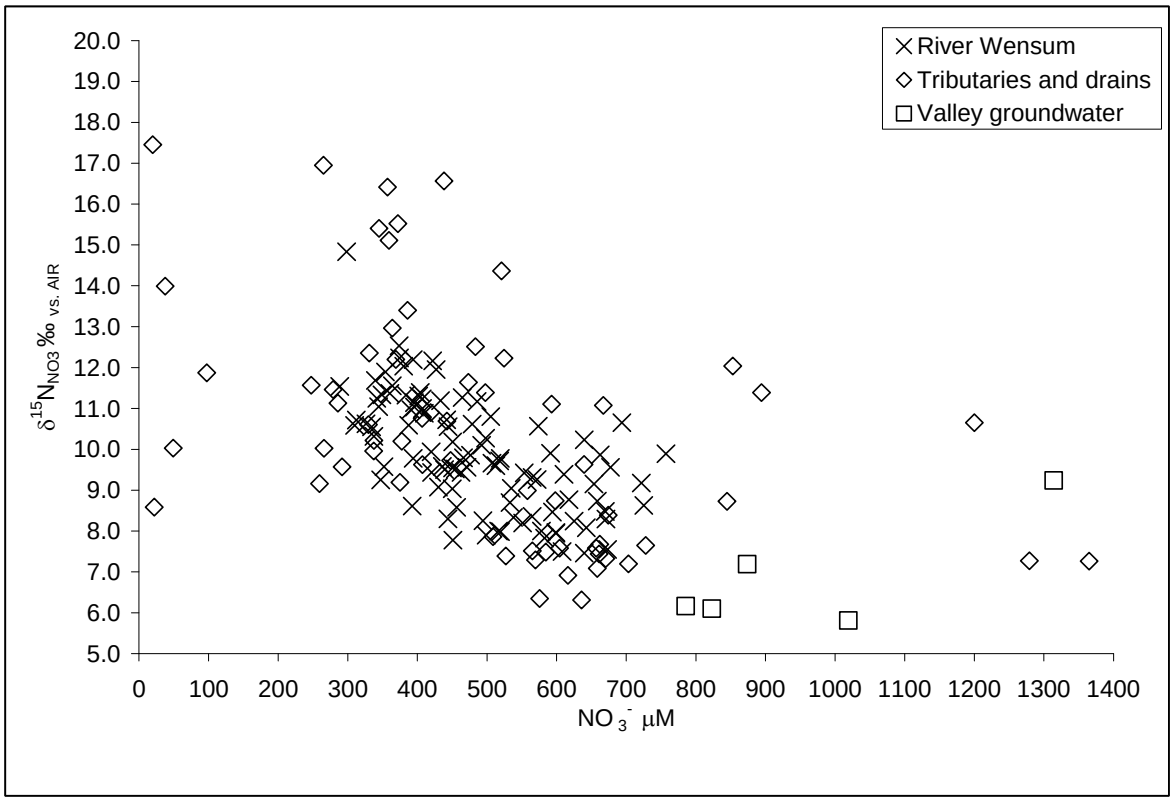

Figure 5.8 $\delta^{15}N_{NO3}$ (‰) versus concentration NO_3^- (µM) of samples from the Wensum catchment. Error: $\delta^{15}N_{NO3}$ and $\delta^{18}O_{NO3}$ $\pm$ 0.1‰.

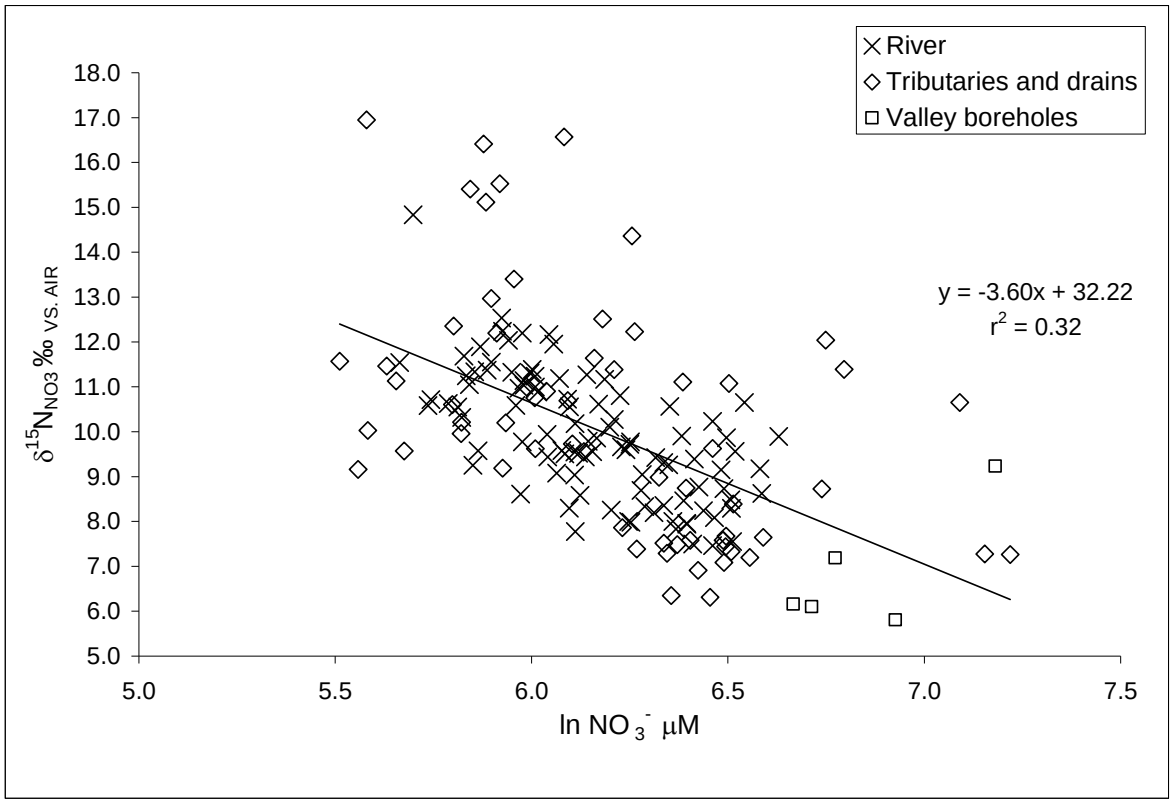

Figure 5.9 $\delta^{15}N_{NO3}$ (‰) versus the natural log of concentration NO_3^- (µM) of samples from the Wensum catchment. Error: $\delta^{15}N_{NO3}$ and $\delta^{18}O_{NO3}$ $\pm$ 0.1‰. ‰. Note low correlation indicating a lack of a significant relationship.

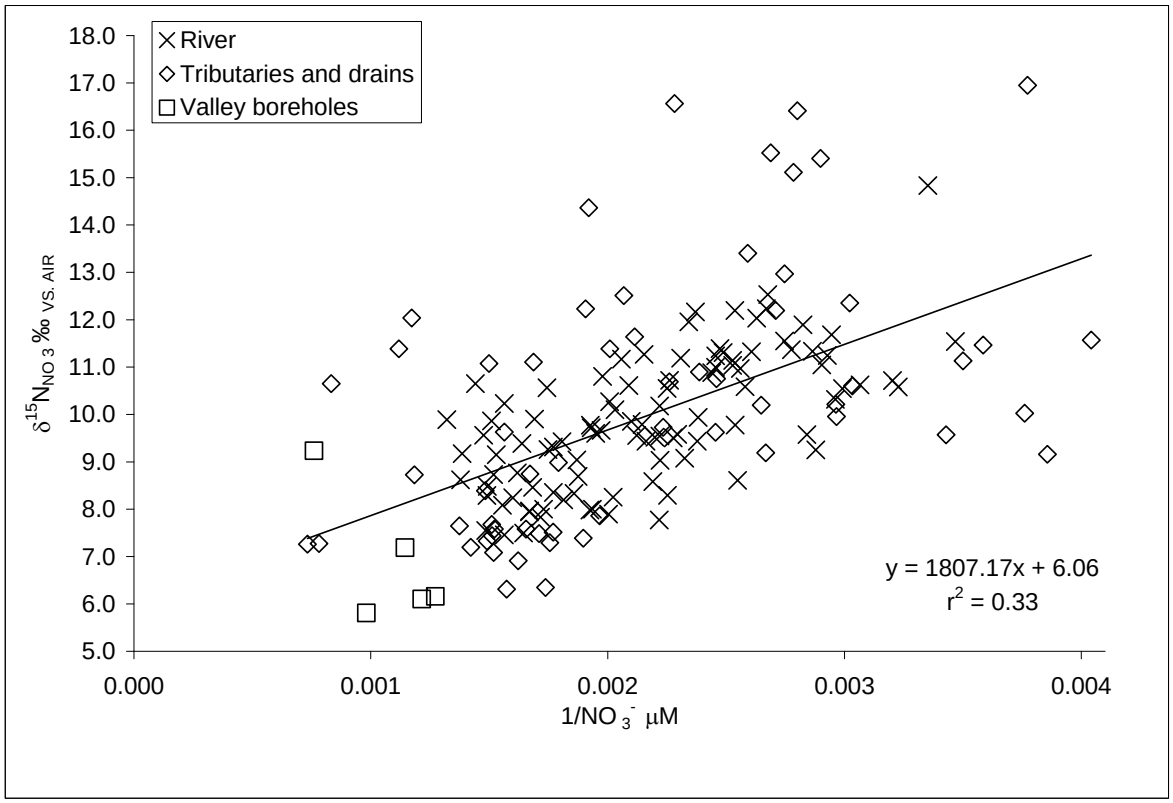

Figure 5.10 $\delta^{15}N_{NO3}$ (‰) versus the reciprocal of concentration NO_3^- (µM) of samples from the Wensum catchment. Error: $\delta^{15}N_{NO3}$ and $\delta^{18}O_{NO3}$ $\pm$ 0.1‰. ‰. Note low correlation indicating a lack of a significant relationship.

A possible signal of temporal denitrification in the middle and lower catchment is found in correlations of export of nitrate, sulphate, and chloride with daily mean flow (Figures 5.11a-c to 5.13a-c) (Appendix 3). Overall export of these solutes at the three gauging stations show high correlations with flow. This linear relationship, which indicates that concentration remains stable with changes in flow, may demonstrate the effect of piston flow whereby runoff, rather than entering the river directly, enters shallow groundwater displacing well mixed groundwater into the river. However, the sample set from 18/07/2007 shows anomalously low export of nitrate and sulphate at the three gauging stations, such that when this data set is removed, correlations between daily mean flow and nitrate-nitrogen and sulphate export improve. A small improvement in correlation is also seen in the chloride export data (Figures 5.11a-c), which is likely to indicate a minor effect of dilution due to the high-flow conditions, with the highest effect at Fakenham and the lowest at Costessey. The percentage by which the chloride load has been reduced due to high-flow dilution can be calculated from the divergence from the best fit lines for chloride on 18/07/2007. This shows a reduction in the expected chloride load of 17% at Fakenham gauging station, 12% at Swanton, and 7% at Costessey. After accounting for this dilution, nitrate and sulphate export is still lower than expected (Table 5.2). In the month leading up to sampling on 18/07/2007 there was severe flooding resulting from a prolonged series of storms (Figure 5.14), which may have lead to enhanced denitrification and sulphate reduction. Potential for microbially mediated nitrate and sulphate reduction can increase as a result of flooding through the development of anaerobic conditions in saturated soils which have a ready supply of organic carbon (Baker and Vervier, 2004, Lloyd *et al.*, 2004, Hernandez and Mitsch, 2006). On the sampling day, flooding had receded and flow was not overbank at most locations, meaning that runoff from the latest storm (16-18/07/2007) would have reached the river after passing through saturated soils in previously flooded areas, enabling enhanced denitrification to occur. Using the linear regression equations of the best fit lines from plots of daily mean flow versus export load for each gauging station with the 18/07/2007 data set excluded, the expected load for the flow on 18/07/2007 can be calculated. Correcting for the percentage loss accounted for by dilution gives the percentage attributable to microbial reduction of nitrate and sulphate (Table 5.2). Nitrate removal shows an increasing trend through the catchment, reaching 30% by Costessey, while sulphate removal is highest by Swanton (17%). This difference in the removal of the two solutes could be attributable to spatial heterogeneities in redox conditions in the

flooded soils, as microbially mediated nitrate and sulphate reduction occurs under different redox conditions. Reduction of nitrate can occur in pH neutral soils over a range of redox potential from + 420 mV to - 205 mV, while sulphate reduction at neutral pH is limited to a redox potential below -220 mV (Killham, 1994).

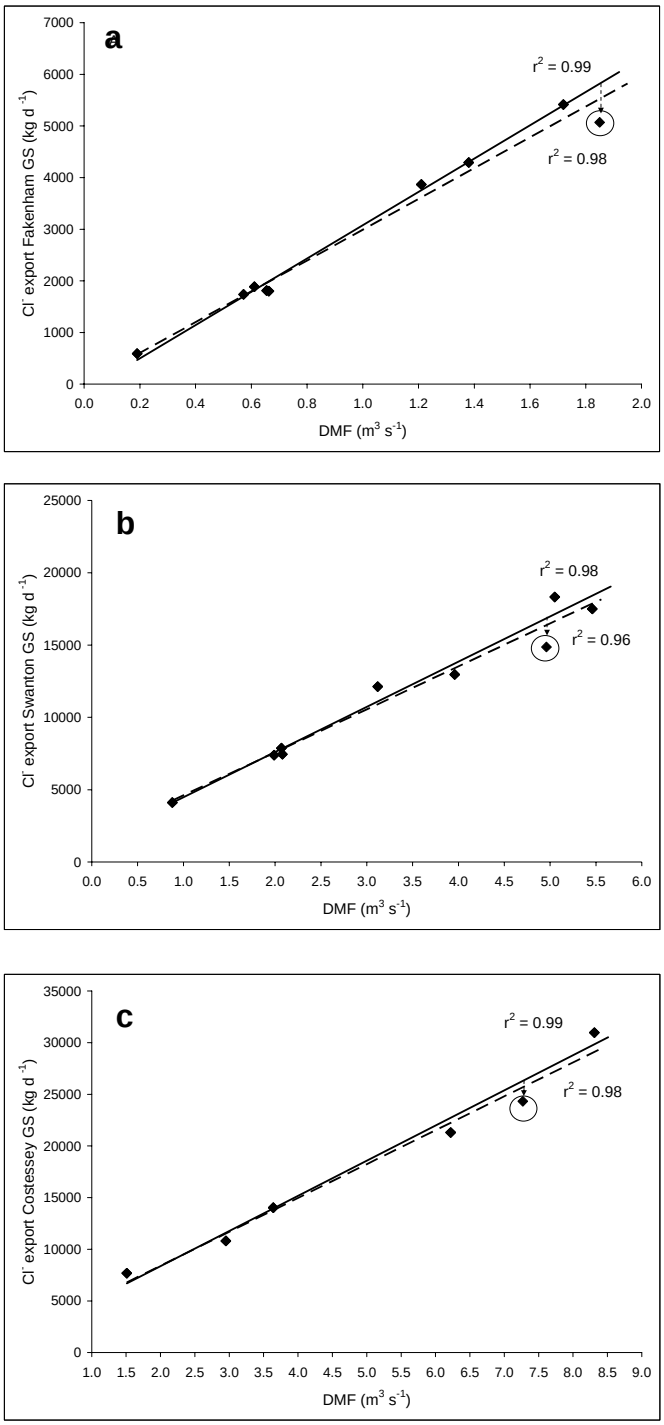

Figure 5.11a-c
Chloride export (kg/day) versus daily mean flow (DMF) ($m^3 s^{-1}$) at Fakenham (a), Swanton (b), and Costessey (c) gauging stations. Arrow and circle shows point from data set 18/07/2007. Dashed line represents linear regression with all data sets, solid line, with 18/07/2007 excluded.

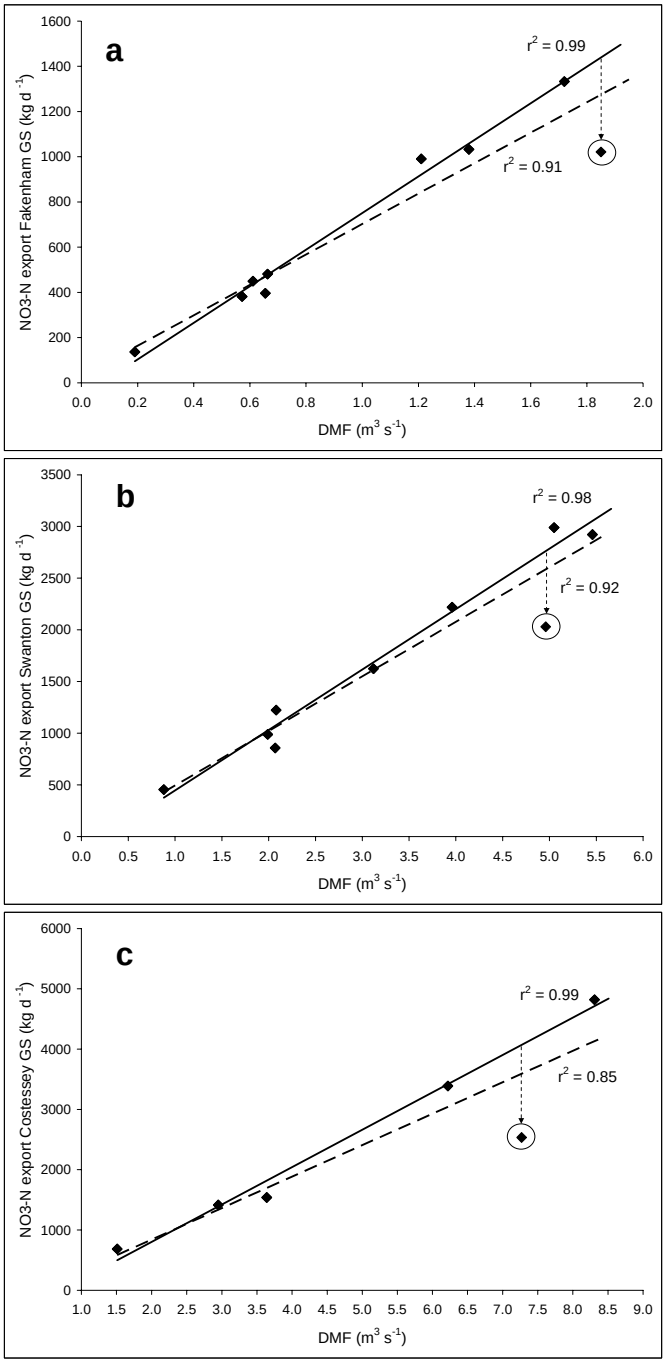

Figure 5.12a-c Nitrate-nitrogen export (kg/day) versus daily mean flow (DMF) (m^3 s^{-1}) at Fakenham (a), Swanton (b), and Costessey (c) gauging stations. Arrow and circle shows point from data set 18/07/2007. Dashed line represents linear regression with all data sets, solid line, with 18/07/2007 excluded.

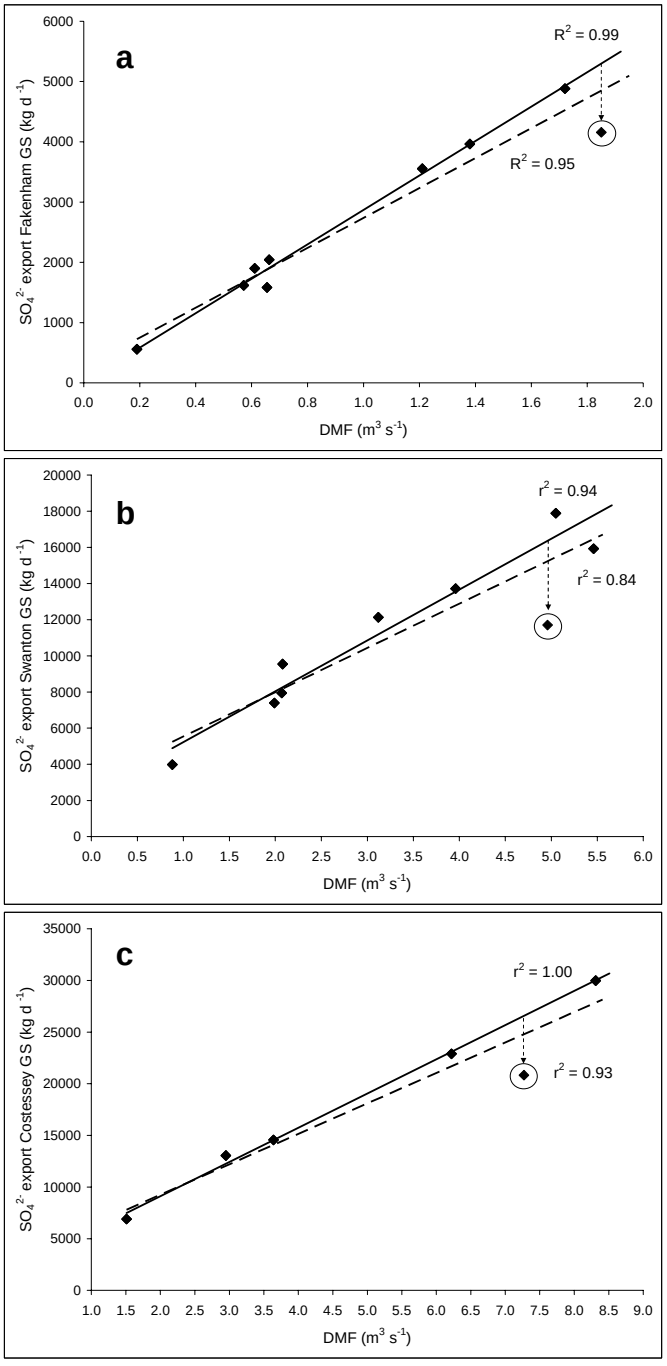

Figure 5.13a-c Sulphate export (kg/day) versus daily mean flow (DMF) (m^3 s^{-1}) at Fakenham (a), Swanton (b), and Costessey (c) gauging stations. Arrow and circle shows point from data set 18/07/2007. Dashed line represents linear regression with all data sets, solid line, with 18/07/2007 excluded.

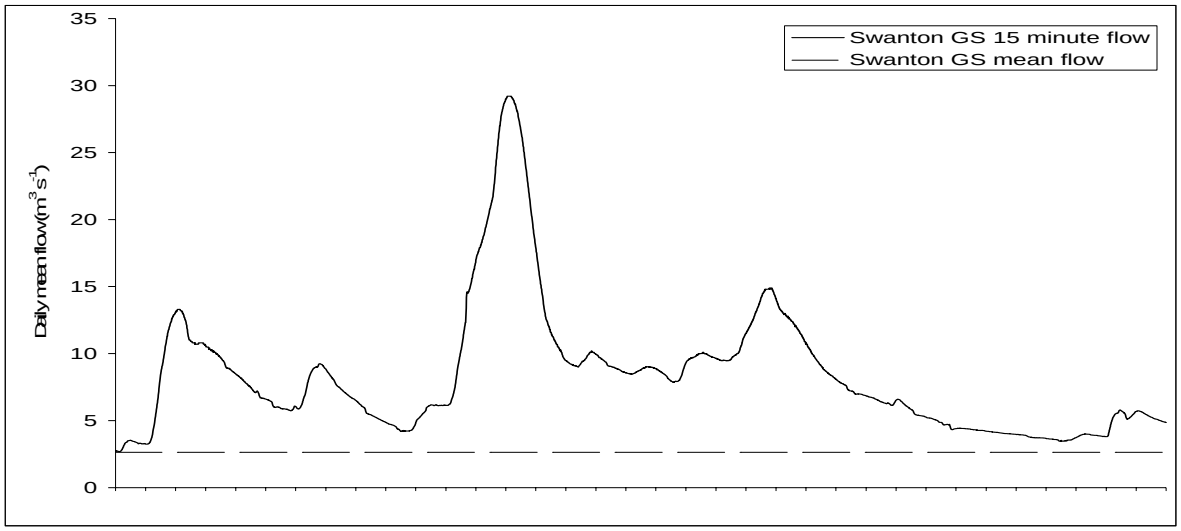

Figure 5.14 Daily mean flow ($m^3 s^{-1}$) at Swanton gauging station for the month preceding sampling on 18/07/2007 showing storm flow with line showing mean flow at Swanton.

Table 5.2 Expected and measured export of nitrate-nitrogen, chloride and sulphate (kg/day) at Fakenham, Swanton and Costessey gauging stations on 18/07/2007, with best fit lines for export versus flow correlations, percentage due to dilution, and percentage removal after dilution correction.

18/07/2007	**NO3-N export (kg/day)**			
Gauging station	**Expected**	**Measured**	**Percentage difference**	**Percentage removal after accounting for dilution**
Fakenham GS	1439	1021	29%	12%
Swanton GS	2761	2029	27%	15%
Costessey GS	4069	2534	38%	30%
	SO_4^{2-} export (kg/day)			
	Expected	**Measured**	**Percentage difference**	**Percentage removal after accounting for dilution**
Fakenham GS	5298	4157	22%	4%
Swanton GS	16362	11704	28%	17%
Costessey GS	26572	20835	22%	14%
	Cl^- export (kg/day)			
	Expected	**Measured**	**Percentage difference due to dilution**	
Fakenham GS	6113	5070	17%	
Swanton GS	16863	14870	12%	
Costessey GS	26300	24327	7%	
Linear regression equations for solute export versus daily mean flow excluding 18/07/2007 data				
Fakenham GS	nitrate-nitrogen export (kg/d) =(809.52 x DMF) -58.6			
	sulphate export (kg/d) = (2857.10 x DMF) + 12.8			
	chloride export (kg/d)= (3227.50 x DMF) + 142.2			
Swanton GS	nitrate-nitrogen export (kg/d) = (584.82 x DMF) - 139.4			
	sulphate export (kg/d) = (2811.60 x DMF) + 2416.2			
	chloride export (kg/d)= (3129.30 x DMF) + 1342.1			
Costessey GS	nitrate-nitrogen export (kg/d) = (619.86 x DMF) -437.14			
	sulphate export (kg/d) = (3313.70 x DMF) + 2481.4			
	chloride export (kg/d) = (3404.90 x DMF) + 1546.0			

In summary, the relationship between Wensum catchment nitrate $\delta^{15}N_{NO3}$ and $\delta^{18}O_{NO3}$ and nitrate concentration suggests that denitrification is occurring, although, due to the fact that mixing is also taking place, it is not possible to confirm denitrification using the usual diagnostic. Correlations of daily mean flow with solute load indicate a transient period of enhanced denitrification in riparian soils after flooding lead to anaerobic conditions.

Further elucidation of the dynamics affecting nitrate concentration and removal can be gained by closer examination of groundwater and surface water samples with river reach, flow condition, and season, in conjunction with data sets from individual sampling campaigns, and hydrochemical data.

5.4 WENSUM RIVER NO_3^- CONCENTRATION AND ISOTOPIC COMPOSITION

5.4.1 Upper Wensum River

A primary focus of this research was to investigate the causes of decreasing concentrations of nitrate downstream in the study rivers. Therefore, a useful starting point for the interpretation of river data is to identify where the nitrate concentration decrease occurs along the river length; whether it is consistent or variable, and if variable whether it is associated with flow condition and/ or season.

There is wide variation in nitrate concentration at Hamrow, the uppermost sampling site on the upper Wensum river. Downstream beyond Hamrow a decrease in nitrate concentration is seen in all data sets between West Raynham and Fakenham (Table 5.3; Figure 5.15). A comparison of the three high-flow data sets from winter, summer and spring does not show a clear seasonal pattern in relation to concentration reduction or mean concentration. The two low-flow data sets are both from autumn, so it is not possible to look for seasonal differences between them. Although both these sets show a similar reduction in concentration, one set has a low mean concentration and the other high. Comparing the high-flow sets with the low-flow sets again shows no clear flow related pattern with respect to concentration decrease or mean concentration. This suggests that any seasonal or flow related influences on nitrate concentration in the upper river may be overwritten by other factors. These could include local agricultural

activity such as fertiliser and manure applications, ploughing, irrigation, as well as variations in the volume and dilution of wastewater effluent discharge. Even though a seasonal influence is not seen in nitrate concentration, as a result of the large range of flow conditions represented by these data, nitrate-nitrogen export at Fakenham shows considerable differentiation between high and low-flow conditions (Table 5.3).

Table 5.3 Reduction in concentration NO_3^- (μM) mean concentration, and nitrate-nitrogen export with flow condition and season in the upper Wensum river between West Raynham and Fakenham gauging station.

Sampling date and season	**Flow condition and daily mean flow Fakenham GS ($m^3 s^{-1}$)**	**Reduction in concentration NO_3^- (μM) West Raynham - Fakenham GS**	**Mean concentration NO_3^- (μM) West Raynham - Fakenham GS**	**NO3-N export (kg/day) at Fakenham GS**
14/02/2007 winter	High (1.38)	139	683	1032
18/07/2007 summer	High (1.85)	135	542	1021
06/04/2008 spring	High (1.72)	86	667	1332
14/09/2008 autumn	Low (0.57)	102	563	382
25/09/2009 autumn	Extreme low (0.19)	128	655	137

Concentrations of chloride in the upper Wensum samples do not appear to correlate with those of nitrate (r^2 0.12), although as with nitrate, a wide range of chloride concentrations are seen across sampling dates at Hamrow (Figure 5.16).

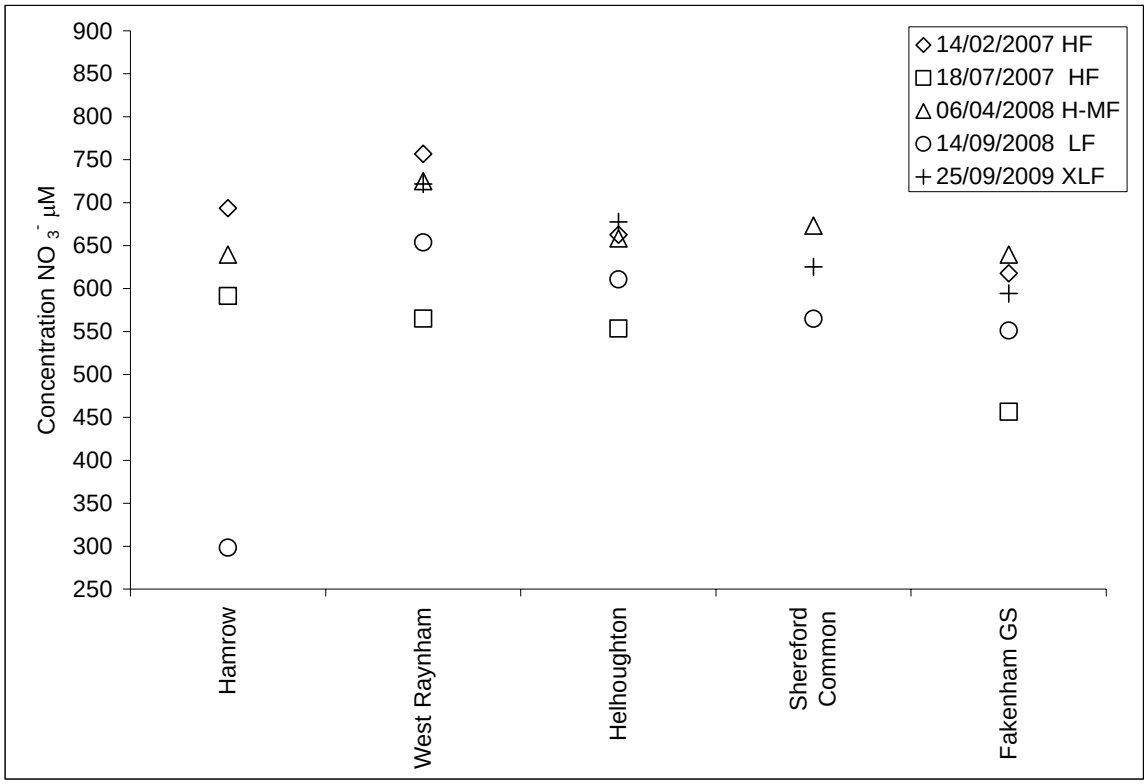

Figure 5.15 Concentration NO_3^- (µM) of samples from the upper Wensum river showing individual data sets with location. Legend includes flow conditions: HF (high-flow); H-MF (high to medium flow with high-flow in upper Wensum); LF (low-flow); XLF (extreme low-flow).

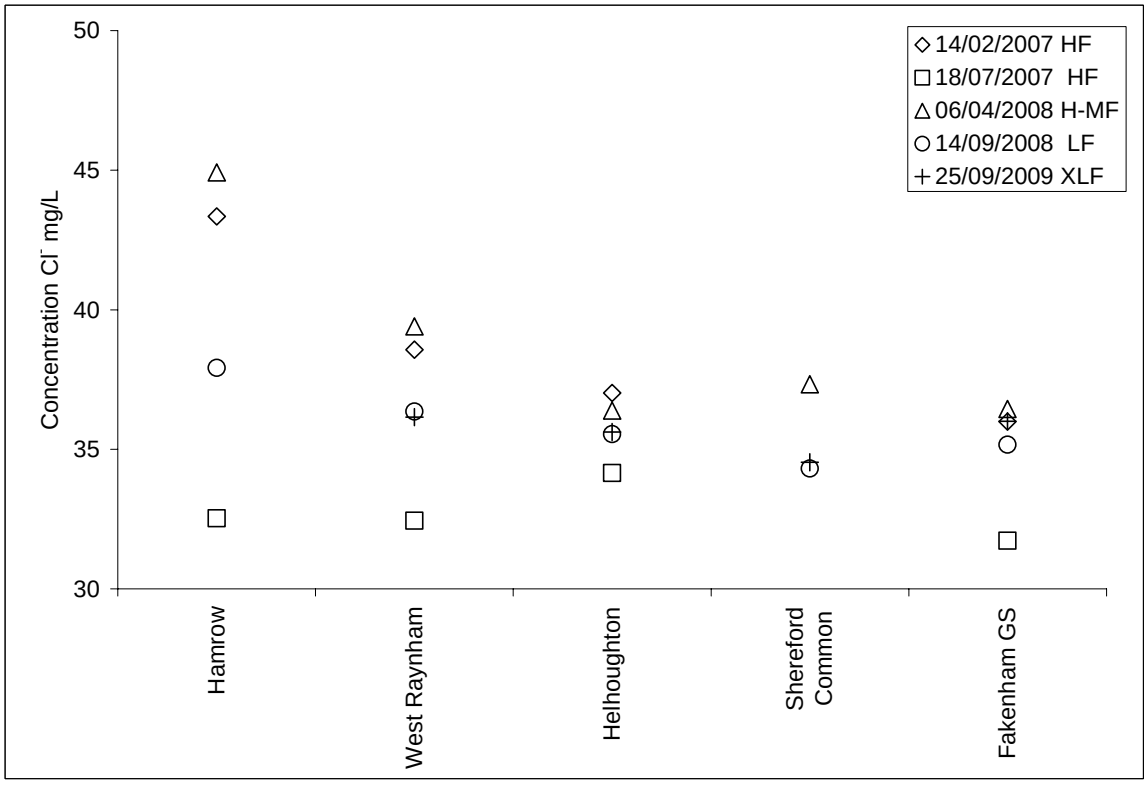

Figure 5.16 Concentration Cl^- (mg/L) of samples from the upper Wensum river showing individual data sets with location. Legend includes flow conditions.

To summarise, beyond the high variation in concentration in headwaters at Hamrow, the upper Wensum river sample sets show a consistent pattern of decreasing concentration between West Raynham and Fakenham gauging station, but this does not appear to be associated with flow condition or season. Overall variations in nitrate concentration across sample sets in this reach do not show an association with flow or season, and do not appear to be closely associated with chloride concentrations.

The isotopic composition of nitrate from the five upper Wensum sampling locations is presented in Figures 5.17 and 5.18. There is evidence of a temporal flow-related denitrification marker at Hamrow during low flow in autumn (14/09/2008). This sample has the heaviest isotopic composition and also the lowest nitrate concentration of all upper Wensum river samples ($\delta^{15}N_{NO3}$ 14.8‰; $\delta^{18}O_{NO3}$ 7.5‰; 298 μM NO_3^-). In addition, an inverse pattern is seen in concentrations of nitrate and chloride, meaning that dilution is unlikely to be the cause of the low nitrate concentration. The combination of enrichment in ^{15}N and ^{18}O with a low nitrate concentration suggests that denitrification may have caused the lower concentration at Hamrow on this date. The isotope enrichment factors $\varepsilon_{P\text{-}S}{}^{15}N_{NO3}$ and $\varepsilon_{P\text{-}S}{}^{18}O_{NO3}$ can be calculated for comparison with literature values, based on the assumption of a temporal denitrification vector at Hamrow between this sample date and the mean values at Hamrow from the other sample sets using Equation 3.12 (Chapter 3) (Appendix 3). This can also be used to determine whether the fractionation ratio of O:N suggests denitrification.

Calculations using Equation 3.12 give values of $\varepsilon_{P\text{-}S}{}^{15}N_{NO3}$ -5.8 ‰ and $\varepsilon_{P\text{-}S}{}^{18}O_{NO3}$ of -2.4 ‰, with a fractionation ratio of O:N of 0.41. Both the enrichment factors and the fractionation ratio are in very good agreement with literature values of rapid denitrification, indicating that the nitrate sampled at Hamrow on 14/09/2008 carries the isotopic markers of denitrification (Mariotti *et al.*, 1980, Mariotti *et al.*, 1988, Böttcher *et al.*, 1990, Aravena and Robertson, 1998, Cey *et al.*, 1999, Lehmann *et al.*, 2003, Fukada *et al.*, 2004, Deutsch *et al.*, 2005, Petitta *et al.*, 2009).

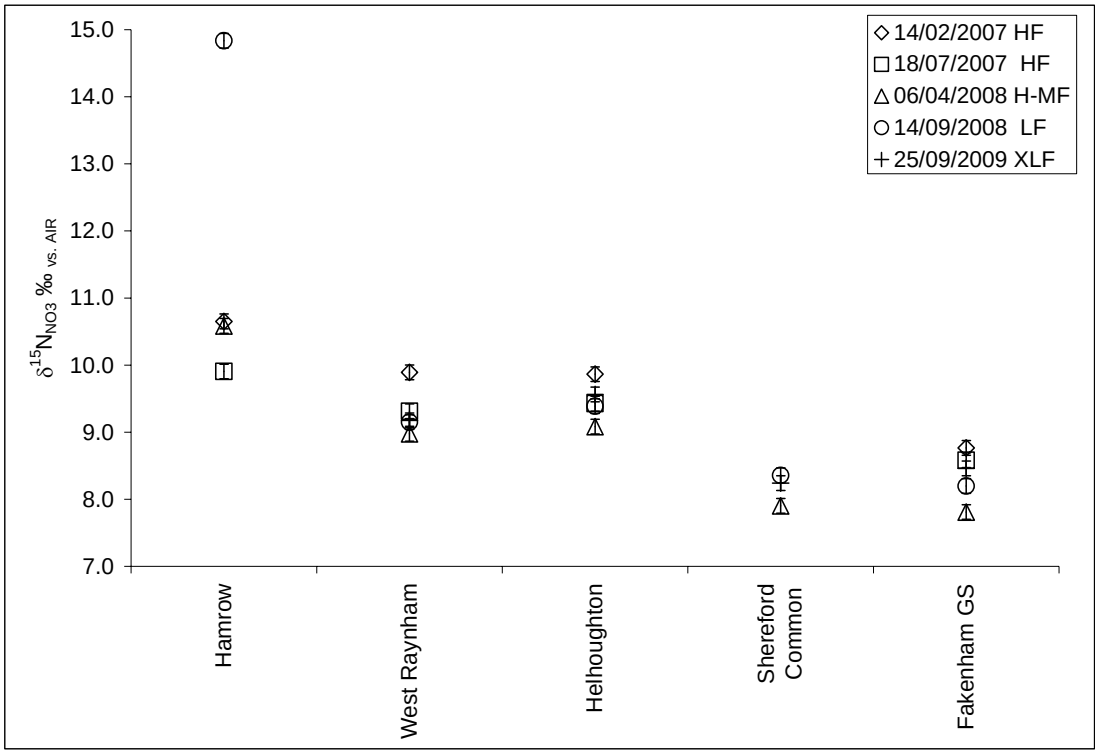

Figure 5.17 $\delta^{15}N_{NO3}$ (‰) of samples from the upper Wensum river showing individual data sets with location. Legend includes flow conditions.

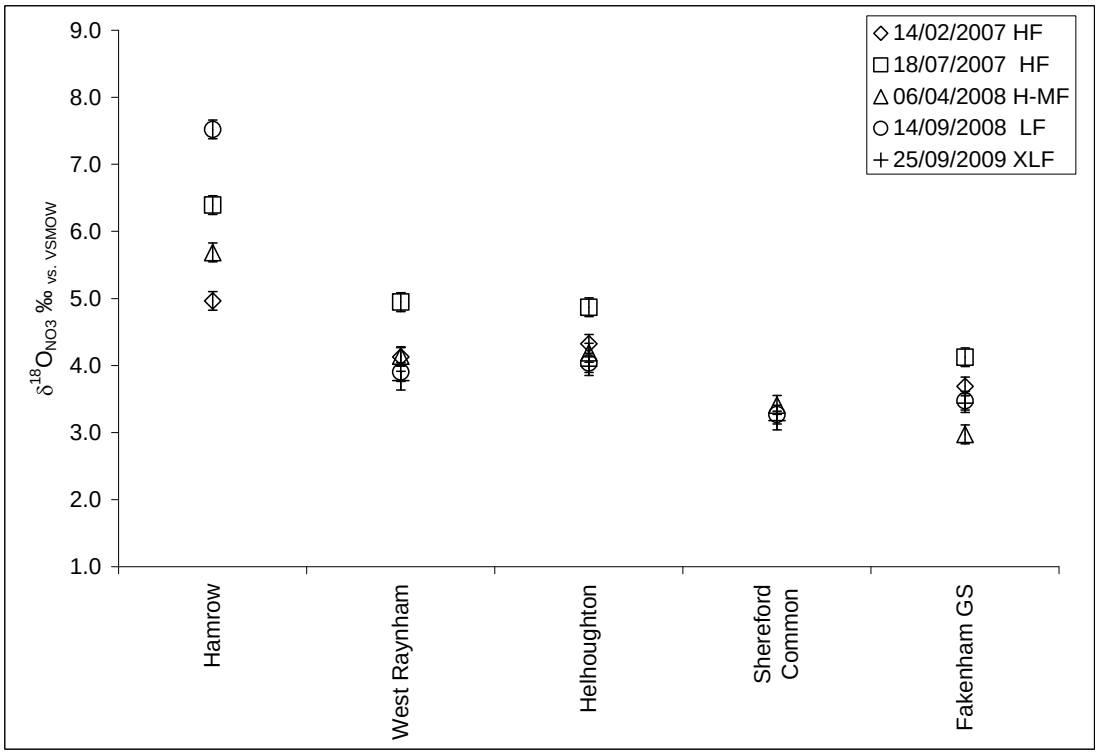

Figure 5.18 $\delta^{18}O_{NO3}$ (‰) of samples from the upper Wensum river showing individual data sets with location. Legend includes flow conditions.

The fact that flow was sustained through all sampling campaigns at Hamrow except during extreme low-flow (25/09/2009) suggests that it is supported by baseflow. This is

likely to be from shallow groundwater in fluvial deposits rather than from the Chalk which has nitrate concentrations below the measurement limit here. It is likely that the denitrification markers seen at Hamrow are attributable to denitrification in shallow fluvial deposits, which is enhanced during drier periods. This could occur as a result of increased residence time of water in the fluvial deposits during low-flow conditions which allow anaerobic conditions conducive to denitrification to develop. During medium and high-flow conditions the quick circulation of runoff entraining dissolved oxygen could confine denitrification to the lower layer of the fluvial deposits and supply baseflow mainly from water which has not undergone denitrification (Figure 5.19).

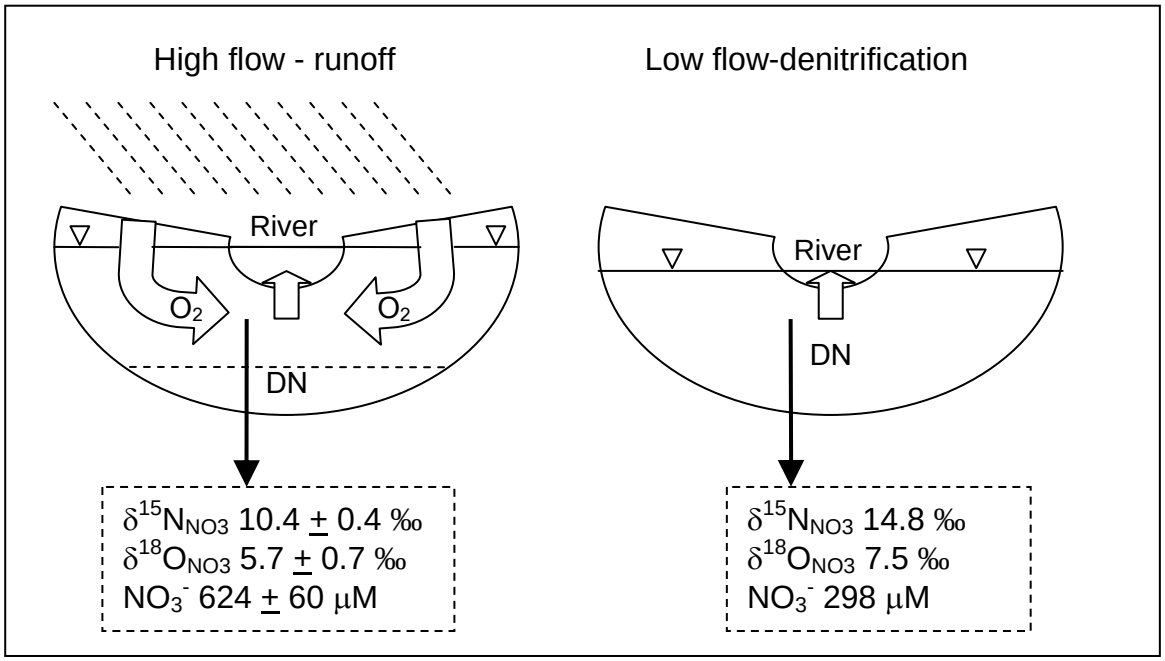

Figure 5.19 Conceptual model of the relationship between denitrification and flow condition in the fluvial deposits which supply baseflow at Hamrow in the upper Wensum. DN refers to the zone of denitrification.

Beyond Hamrow, $\delta^{15}N_{NO3}$ and $\delta^{18}O_{NO3}$ of the upper Wensum river samples show a low level of variation across sample dates from West Raynham to Fakenham gauging station ($\delta^{15}N_{NO3} \pm < 0.4‰$; $\delta^{18}O_{NO3} \pm < 0.5‰$) (Figures 5.17 and 5.18). Although nitrate concentration falls between West Raynham and Fakenham, the isotope data do not suggest a spatial trend of denitrification in this reach, as no corresponding increase in $\delta^{15}N_{NO3}$ and $\delta^{18}O_{NO3}$ is seen, suggesting that the concentration reduction is due to dilution. However, isotopic variation with location in $\delta^{15}N_{NO3}$ across data sets appears to be mirrored by that of $\delta^{18}O_{NO3}$. This is most noticeable in the decrease in both values at Shereford Common, after the confluence with the Tat.

Of the samples from the tributaries and drains feeding into the upper Wensum river, the most significant contribution to flow comes from the Tat tributary which converges with the upper Wensum before Shereford Common (Figure 5.20). The Tat drains the sub-catchment to the north-west where the Lowestoft Till is thin and there are areas of exposed Chalk. Although there are two wastewater effluent sources to the upper reaches of the Tat, the isotopic composition of Tat nitrate does not appear to reflect this as $\delta^{15}N_{NO3}$ values are not particularly high. Nitrate concentrations in the Tat at Tatterford are notably stable (600 $\pm$ 28 μM NO_3^-) and flow was maintained across the five sampling dates suggesting that a stable source of baseflow supports it. The isotopic composition of nitrate from the Tat samples is also homogeneous across flow conditions ($\delta^{15}N_{NO3}$ 6.9 $\pm$ 0.6‰; $\delta^{18}O_{NO3}$ 2.4 $\pm$ 0.4‰), and very close to the mean isotopic composition of the valley Chalk groundwater ($\delta^{15}N_{NO3}$ 6.7 $\pm$ 1.3‰; $\delta^{18}O_{NO3}$ 1.2 $\pm$ 1.1‰). The Chalk is exposed or near the surface in the Tat sub-catchment, and so subject to nitrate contamination, with an expected nitrate concentration and isotopic composition similar to valley Chalk groundwater (it was not possible to sample the groundwater in the Tat sub-catchment). Together these factors suggest that the Chalk in the Tat sub catchment is the most likely source of baseflow to the Tat. The homogeneity of isotopic composition and concentration of nitrate in this small tributary may be explained through the lack of overlying deposits and a rapid water table response in the exposed Chalk during storms, such that it continues to be the predominant source of flow to the Tat under high-flow conditions (Figure 5.21). A direct recharge mechanism is likely, enabling nitrate in recharge to the exposed west-catchment Chalk to escape denitrification in the saturated zone. Although the nitrate isotopic composition from the Tat is very similar to that of valley Chalk groundwater, reflecting the predicted range of bulk cycled source nitrate from freely draining loamy and sandy soils in this part of the catchment, and the recharge mechanism appears to be similar, concentrations of nitrate, sulphate, and chloride are lower in this tributary than those of the closest valley borehole at Bylaugh. This may be due to the more diffuse nature of recharge through the exposed Chalk in the west as opposed to recharge from runoff which is channelled into the river valley, collecting a higher solute load on its way.

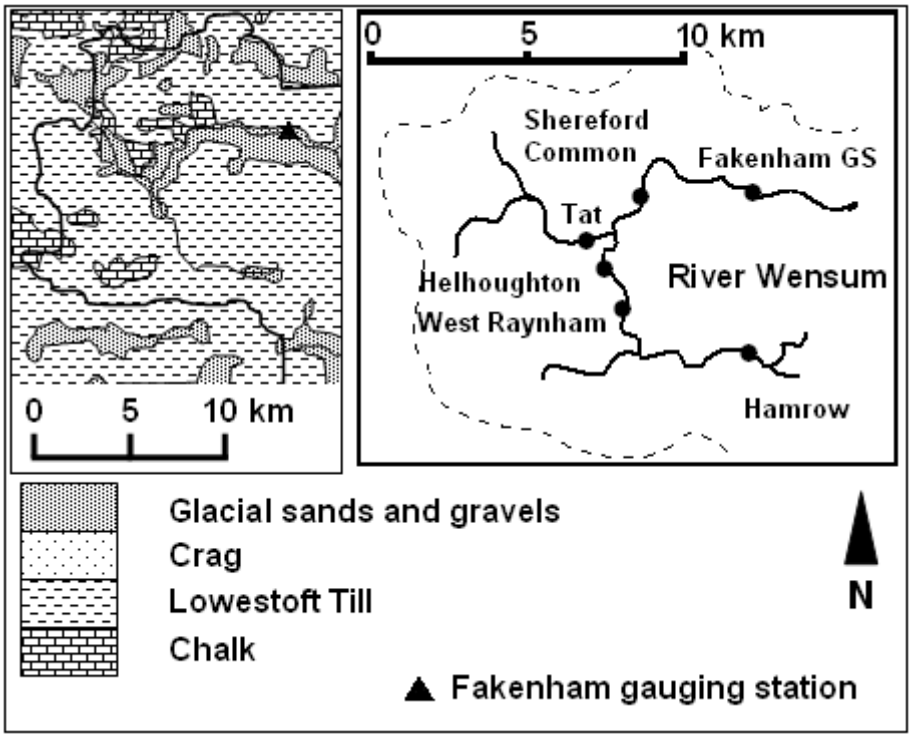

Figure 5.20 Location of upper Wensum sampling sites and Tat tributary with inset of surface geology (adapted from Moseley *et al.*, 1976).

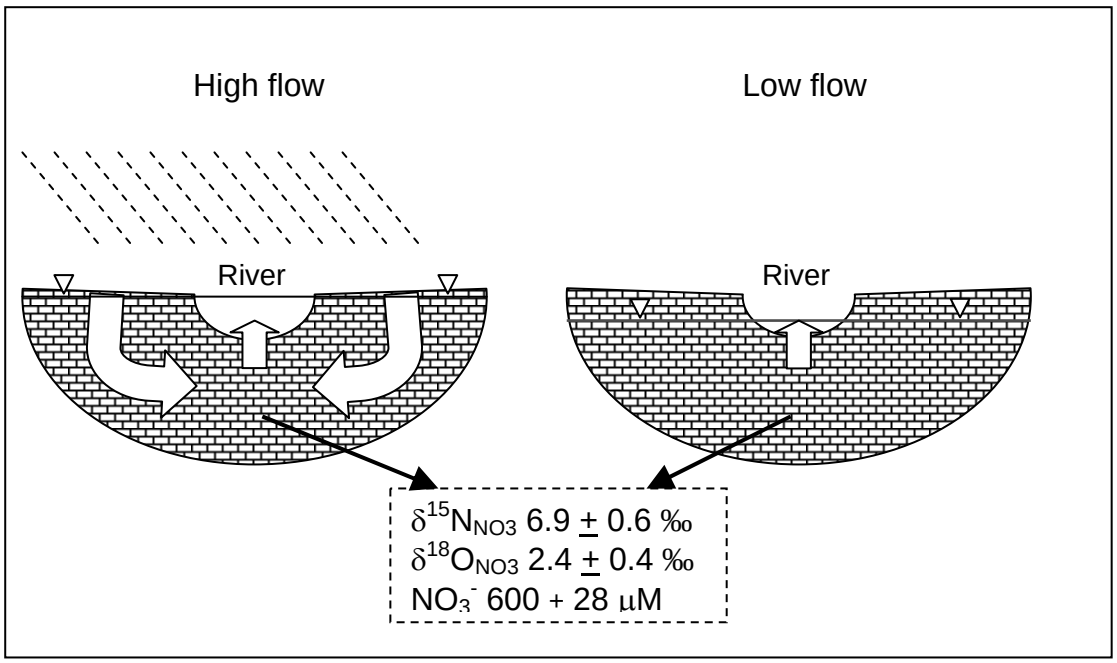

Figure 5.21 Conceptual model of the relationship between recharge to the exposed Chalk and baseflow to the Tat tributary in the Wensum west catchment.

The isotopic composition of nitrate and concentrations of nitrate, chloride, sulphate and sodium from the upper Wensum sampling locations beyond Hamrow to Fakenham gauging station can be modelled using a two member mass-balance mixing model and adjusting concentration of the first end member (Equations 3.13 and 3.14, Chapter 3).

This model was used to reproduce measured values from the five sample sets containing samples from the upper Wensum locations (Appendix 3)

The first end member represents partially denitrified shallow groundwater from the fluvial deposits, and uses the measured isotopic composition at Hamrow for the sampling date modelled. During late autumn 2009 there was no flow at Hamrow (25/09/2009). For this data set the model uses West Raynham as the first member, working on the assumption that the water table of the exposed Chalk will have receded during the dry period, such that flow at West Raynham on this date is likely to be supplied from the fluvial deposits. The second end member represents exposed Chalk baseflow and uses measured values from the Tat for each sample date. The proportional flow increase from Hamrow to Fakenham across the five data sets is from 1.4 to 3.0, which also represents the mixing ratio of exposed Chalk baseflow to baseflow from the fluvial deposits. In order to model the measured variations in solute concentrations through sampling locations, it was necessary to include concentration variations of the first end member representing shallow groundwater from the fluvial deposits, proportionally the same for all solutes (Appendix 3). A model of mean values across the five data sets was also attempted, but failed to reproduce measured values, which suggests that solute concentrations at these upper Wensum locations are controlled by localised spatial and temporal variations. Figures 5.22a-f show the model output for the data set 06/04/2008 (Appendix 3).

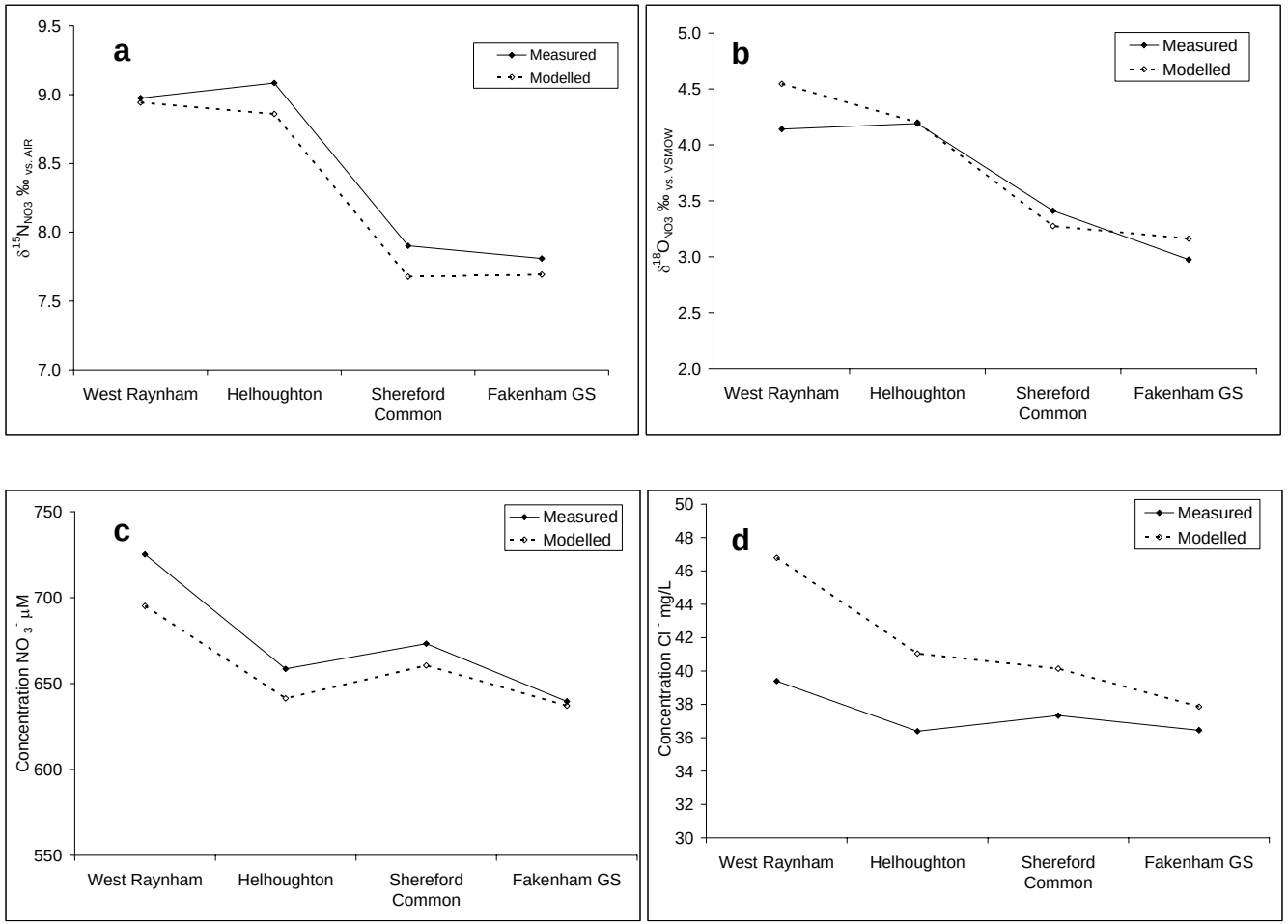

Figure 5.22a-d Measured and modelled values of a) $\delta^{15}N_{NO3}$ (‰); b) $\delta^{18}O_{NO3}$ (‰); c) concentration NO_3^- (µM); and d) concentration Cl^- (mg/L) for Wensum upper river locations West Raynham to Fakenham gauging station on 06/04/2008.

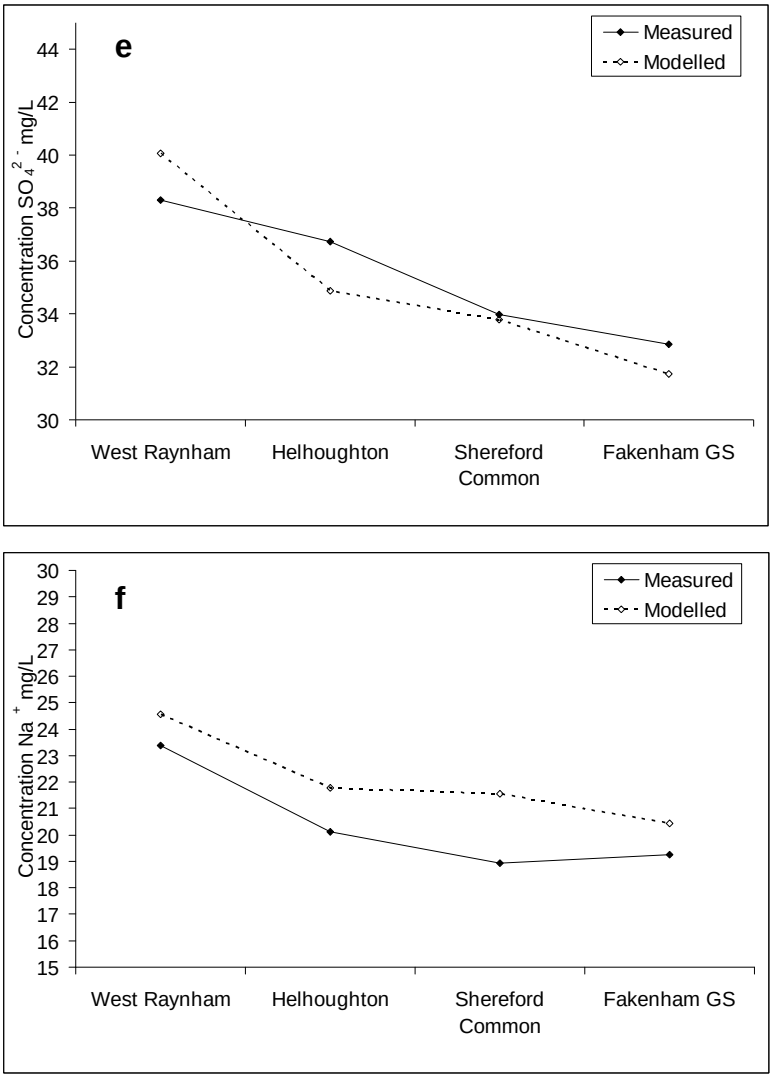

Figure 5.22e-f Measured and modelled values of e) SO_4^{2-} (mg/L) and f) Na^+ (mg/L) for Wensum upper river locations West Raynham to Fakenham gauging station on 06/04/2008.

The model output suggests that a conceptual model of two member mixing of shallow groundwater baseflow from the fluvial deposits, with baseflow from the exposed Chalk, goes some way to representing the hydrological system in the upper river which results in the isotopic composition and concentration of nitrate measured on different dates. The necessity to include concentration variations of the first end member can be explained by the likelihood that in the upper Wensum spatial and temporal variation in concentrations of major ions in shallow groundwater exist due to the influence of localised contamination by sources such as wastewater effluent and manure, which have high concentrations of these solutes.

In order to test the possibility that interfluve Chalk groundwater also contributes to flow in the upper Wensum, concentrations of the solutes determined to be potentially useful

markers of low-nitrate groundwater (sulphate, chloride, sodium, and potassium) were modelled using a three member mass-balance mixing model. The model used the same first two end members as the two member model, with the third member using mean concentrations from the western catchment low-nitrate groundwater boreholes (Hamrow east and west and Wellingham). The effect of including the third member was of dilution of all solutes. Overall, the model output from the two member model was closer to the measured values than the three member model, suggesting that Chalk baseflow from the interfluves is not contributing to flow in the upper Wensum (Appendix 3).

In summary, modelling of nitrate isotopic composition and solute concentrations in the upper Wensum suggests a hydrological system in which shallow groundwater baseflow from the fluvial deposits is augmented by baseflow from the exposed Chalk in the western catchment downstream. This baseflow appears to be recharged directly enabling nitrate in runoff to escape denitrification. There is potential for temporal denitrification in the fluvial deposits during dry conditions when recharge circulation is absent and residence times of this shallow groundwater increase.

5.4.2 Upper Wensum Tributaries and Drains

The samples from the drains feeding into the upper Wensum river at Horningtoft, East Raynham, Helhoughton, and Shereford contribute minor amounts of flow. The high concentrations in Horningtoft drain during winter high flow (14/02/2007) and in East Raynham drain during spring high-medium flow (06/04/2008) are likely to be caused by localised sources of contamination mobilised in runoff (Figure 5.23 contained within squares). This is supported by the fact that high concentrations of chloride are seen in both these samples (Figure 5.24 contained within squares). The isotopic composition of these two samples is relatively low ($\delta^{15}N_{NO3}$ 7.3 ‰ both; $\delta^{18}O_{NO3}$ 2.4 ‰ and 1.6 ‰ respectively), and similar to that of nitrate in the Tat tributary and valley Chalk groundwater, suggesting nitrate from nitrified ammonium which has escaped significant denitrification (Figure 5.25 and 5.26 contained within squares). These drains may be responsible in part for the high nitrate concentrations seen in the river at Hamrow and West Raynham on these dates.

One sample has a heavy isotopic composition, from Shereford drain on 06/04/2008, which may result from isotopic fractionation which may result from isotopic fractionation due to denitrification or assimilation (Figures 5.25 and 5.26 contained within ovals). This is supported by the fact that the nitrate concentration in this sample is low and the chloride concentration is high (Figure 5.23 and 5.24 contained within ovals). However, due to the fact that this site was sampled only twice it is not possible to calculate a mean nitrate isotopic composition and concentration in order to determine the isotope enrichment factors to corroborate this theory.

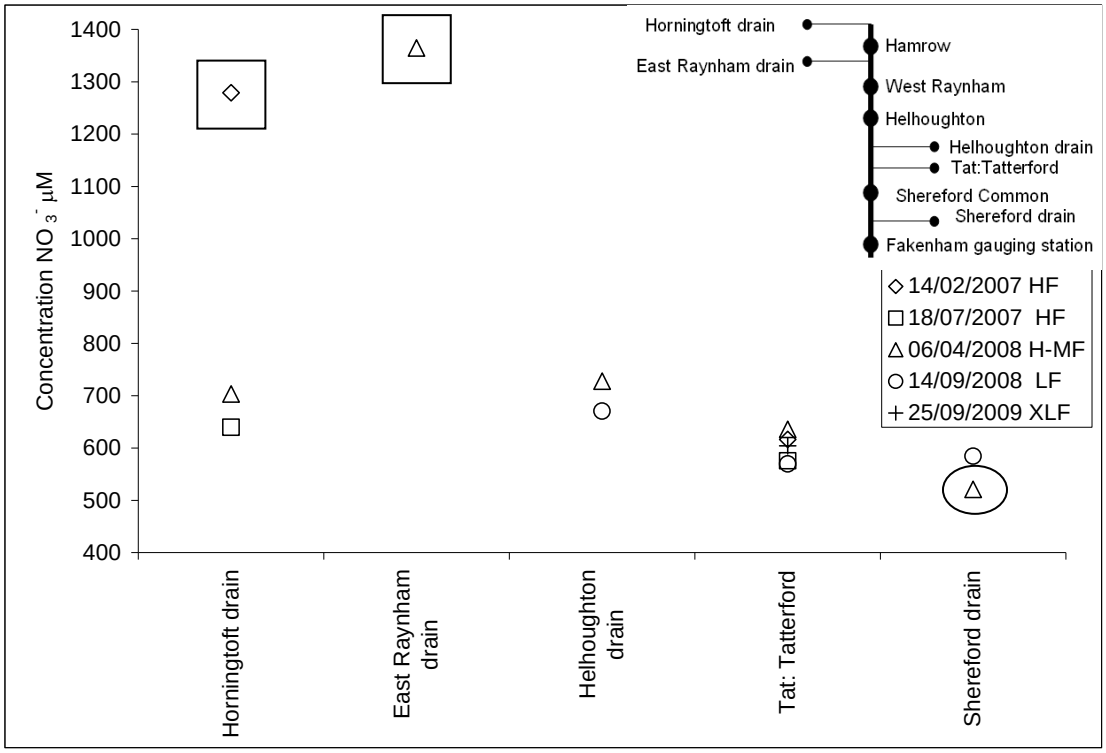

Figure 5.23 Concentration NO_3^- (µM) of samples from the upper Wensum tributaries and drains showing individual data sets with location. Legend includes flow conditions. Squares and oval show samples referred to in the text.

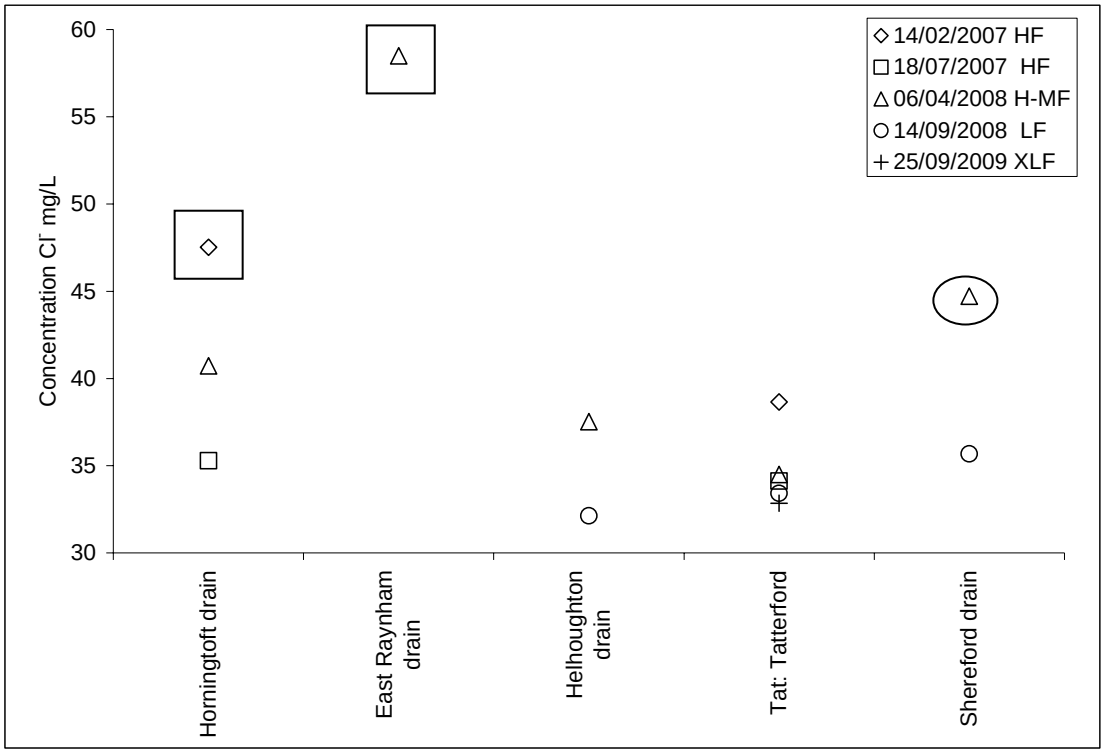

Figure 5.24 Concentration Cl^- (mg/L) of samples from the upper Wensum tributaries and drains showing individual data sets with location. Legend includes flow conditions. Squares and oval show samples referred to in the text.

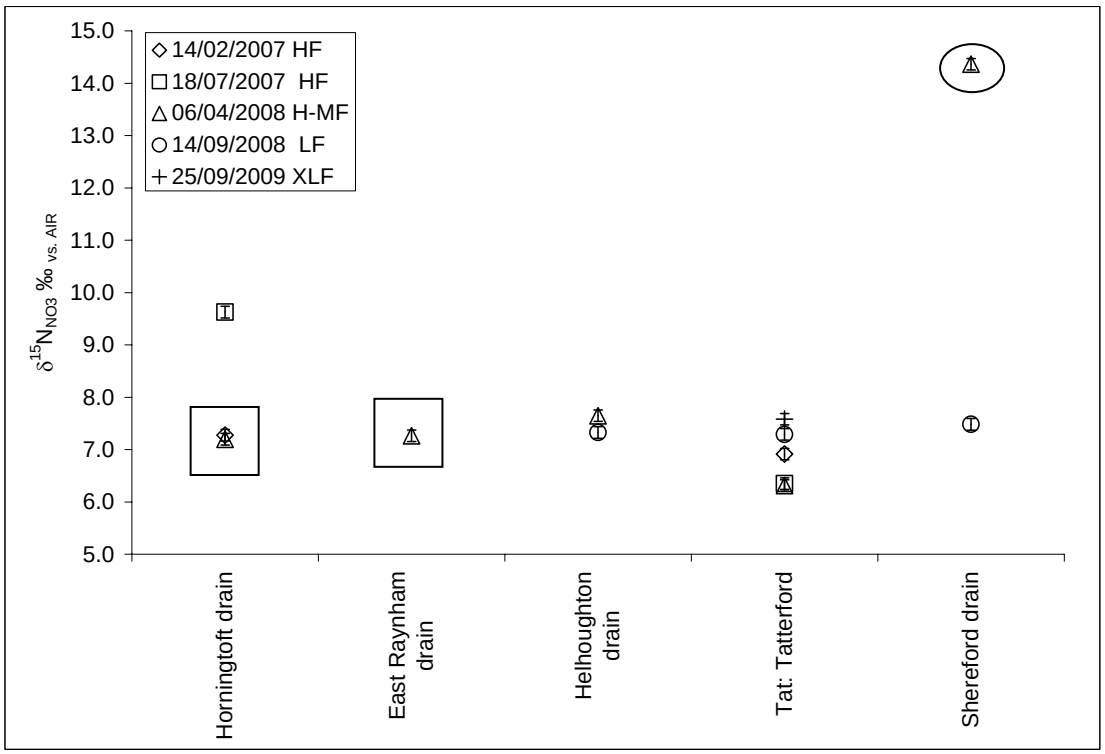

Figure 5.25 $\delta^{15}N_{NO3}$ (‰) of samples from the upper Wensum tributaries and drains showing individual data sets with location. Legend includes flow conditions. Error ($\pm$ 0.1 ‰) is represented by error bars. Squares and oval show samples referred to in the text.

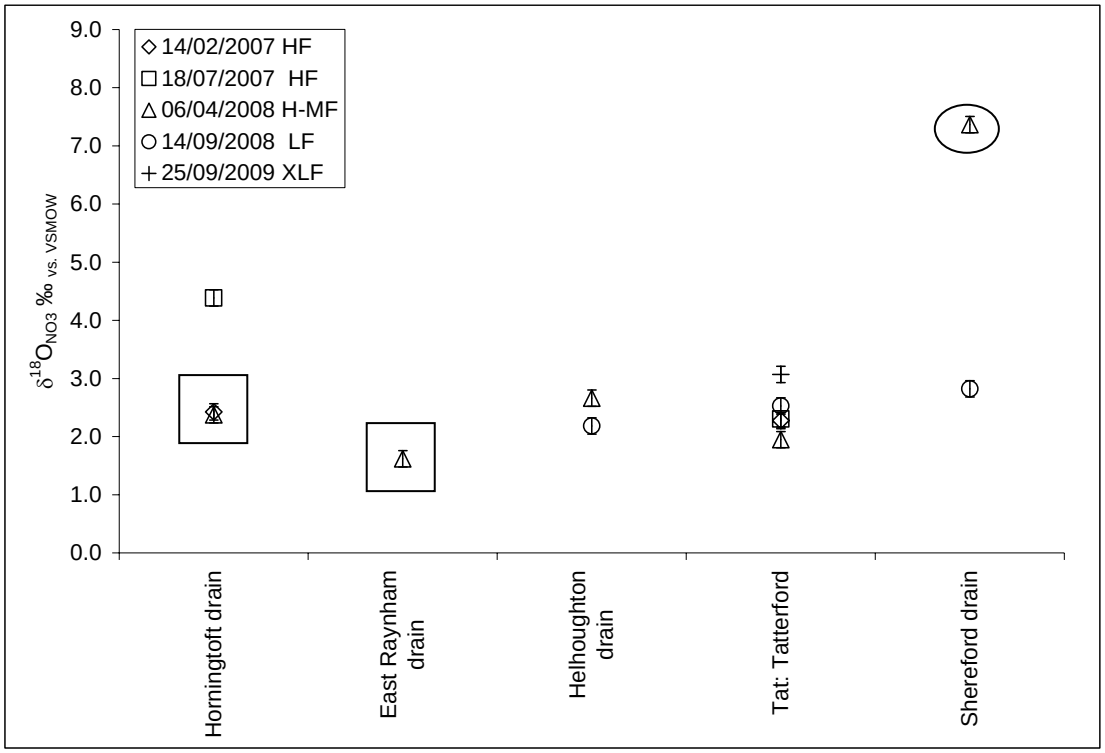

Figure 5.26 $\delta^{18}O_{NO3}$ (‰) of samples from the upper Wensum tributaries and drains showing individual data sets with location. Legend includes flow conditions. Error (± 0.1 ‰) is represented by error bars. Squares and oval show samples referred to in the text.

In summary, samples from the upper Wensum tributaries and drains indicate that baseflow from the exposed Chalk, which receives nitrate from nitrification in the western catchment, supports flow in the Tat tributary, resulting in a homogeneous nitrate concentrations and isotopic composition across flow conditions. In contrast, samples from three upper catchment drains show the effects of temporal and localised sources of nitrate contamination and denitrification.

5.4.3 Mid Wensum River

In the mid river reach between Fakenham and Swanton Morley gauging stations there is a consistent decrease in nitrate concentration across nine data sets (Figure 5.27; Table 5.4). Of these sets, six sets also include samples from the five main sampling locations in this reach. No pattern is seen between the decrease in nitrate concentration with the upstream concentration at Fakenham, the flow condition, season, or the mean concentration in the reach. In conjunction with the concentration decrease from Fakenham to Swanton an increase in $\delta^{15}N_{NO3}$ and $\delta^{18}O_{NO3}$ values is seen (Figure 5.28).

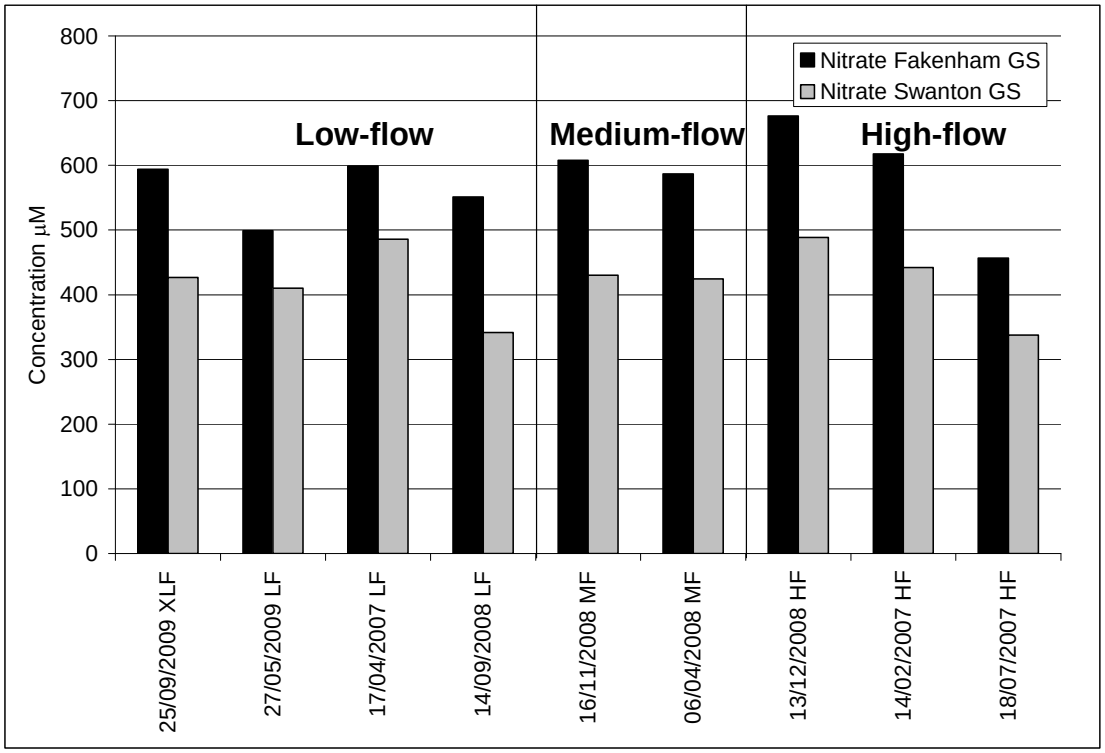

Figure 5.27 Concentration NO_3^- (µM) of samples from the upper Wensum gauging station at Fakenham and the mid Wensum gauging station at Swanton for individual data sets, showing a consistent concentration decrease downstream. X axis labels include flow conditions: HF (high-flow); MF (medium flow); LF (low-flow); XLF (extreme low-flow).

Table 5.4 Reduction in concentration and mean concentration NO_3^- (µM) with flow condition and season in the mid Wensum river between Fakenham and Swanton Morley gauging stations.

Sampling date and season	Flow condition and daily mean flow Swanton GS ($m^3 s^{-1}$)	Reduction in concentration NO_3^- (µM) Fakenham GS - Swanton GS	Mean concentration NO_3^- (µM) Fakenham GS - Swanton GS
14/02/2007 winter	High (5.46)	176	550
17/04/2007 spring	Low (2.08)	113	599
18/07/2007 summer	High (4.96)	119	394
06/04/2008 spring	Medium (3.96)	177	588
14/09/2008 autumn	Low (2.07)	210	467
16/11/2008 winter	Medium (3.12)	178	524
12-13/12/2008 winter	High (5.05)	188	676
27/05/2009 spring	Low (1.99)	89	499
25/09/2009 autumn	Extreme low (0.88)	167	505

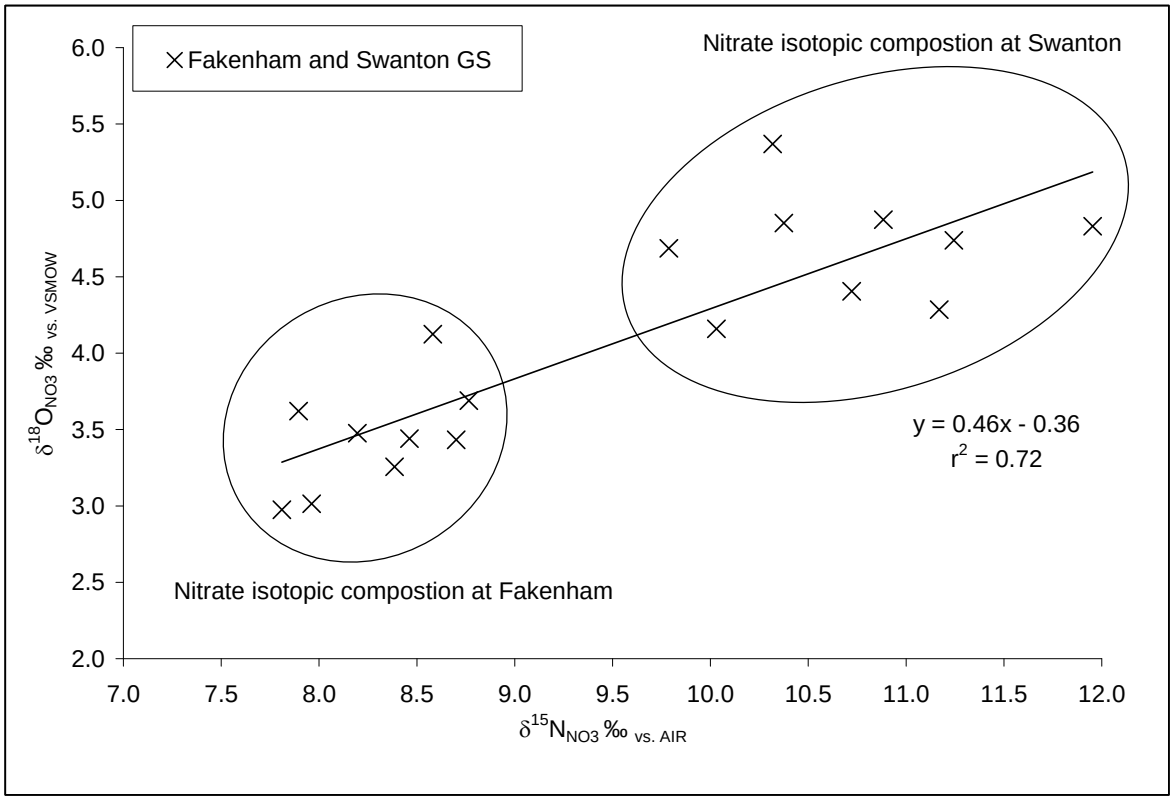

Figure 5.28 $\delta^{18}O_{NO3}$ (‰) versus $\delta^{15}N_{NO3}$ (‰) of samples from the mid Wensum gauging stations at Fakenham and Swanton. Error: $\delta^{15}N_{NO3}$ and $\delta^{18}O_{NO3}$ $\pm$ 0.1‰.

Samples from the five main mid river reach sampling locations show an incremental increase in $\delta^{15}N_{NO3}$ and $\delta^{18}O_{NO3}$ values downstream coupled with a decrease in nitrate concentration, indicating that the change in nitrate isotopic composition and concentration between Fakenham and Swanton occurs gradually over the 25 km reach rather than at a single location (Figures 5.29 to 5.31).

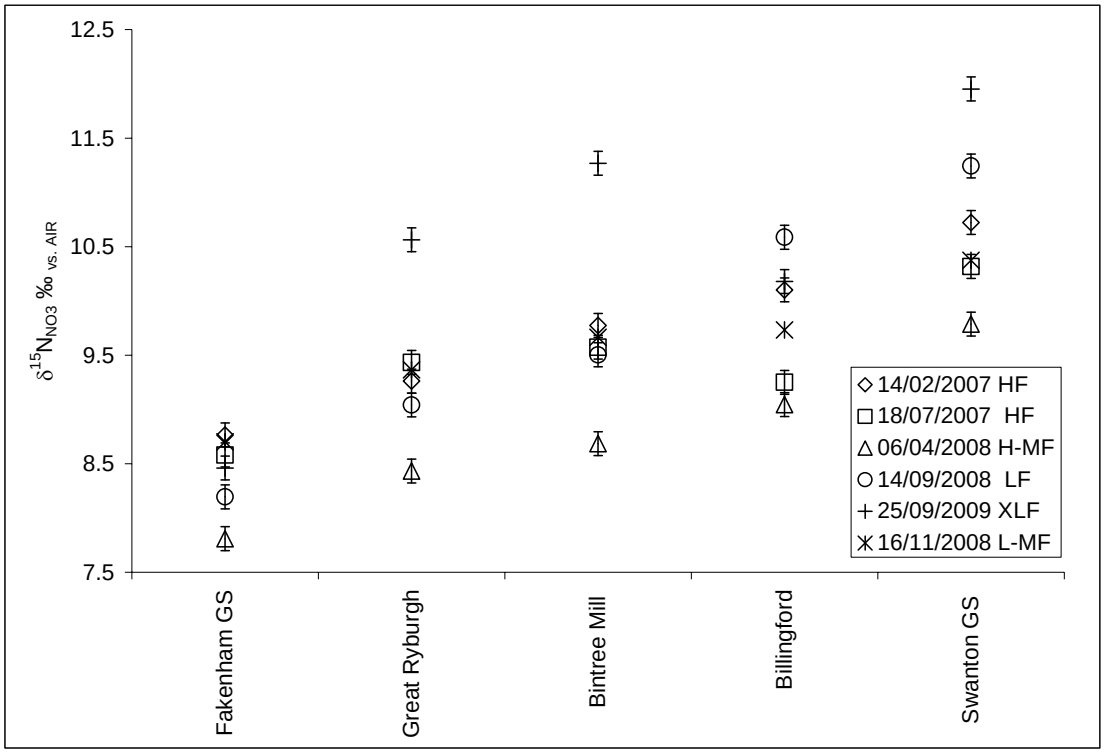

Figure 5.29 $\delta^{15}N_{NO3}$ (‰) of samples from the mid Wensum river showing individual data sets with location. Legend includes flow conditions. Measurement error (± 0.1 ‰) is represented by error bars.

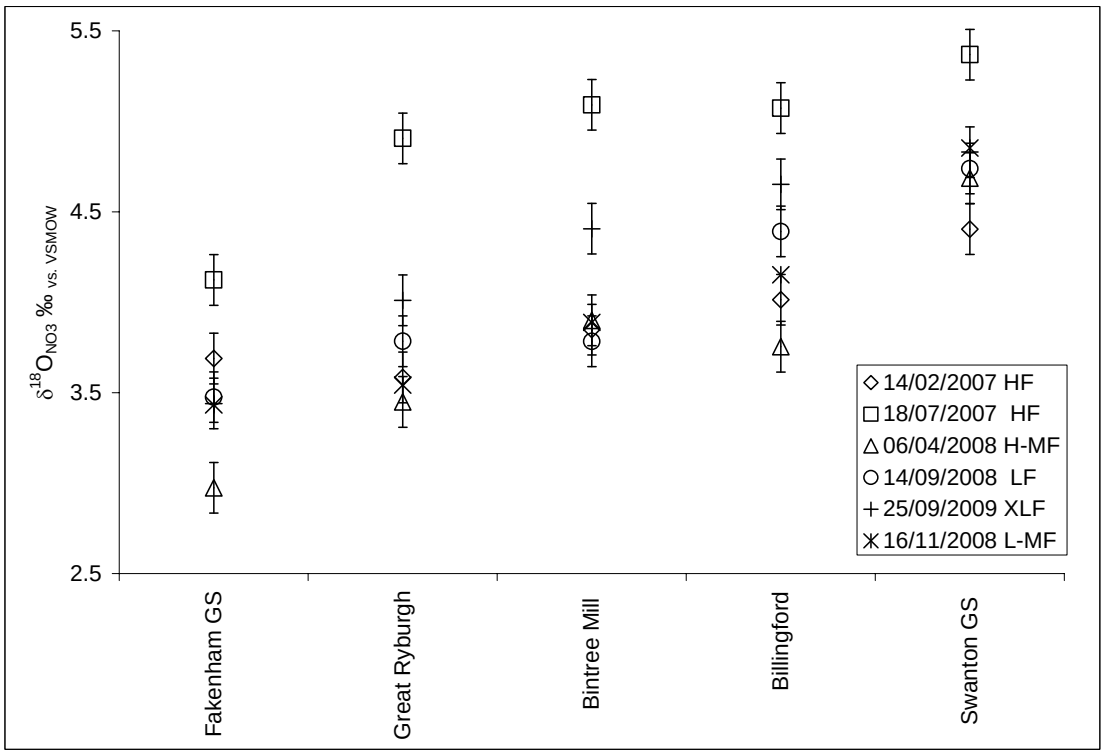

Figure 5.30 $\delta^{18}O_{NO3}$ (‰) of samples from the mid Wensum river showing individual data sets with location. Legend includes flow conditions. Measurement error (± 0.1 ‰) is represented by error bars.

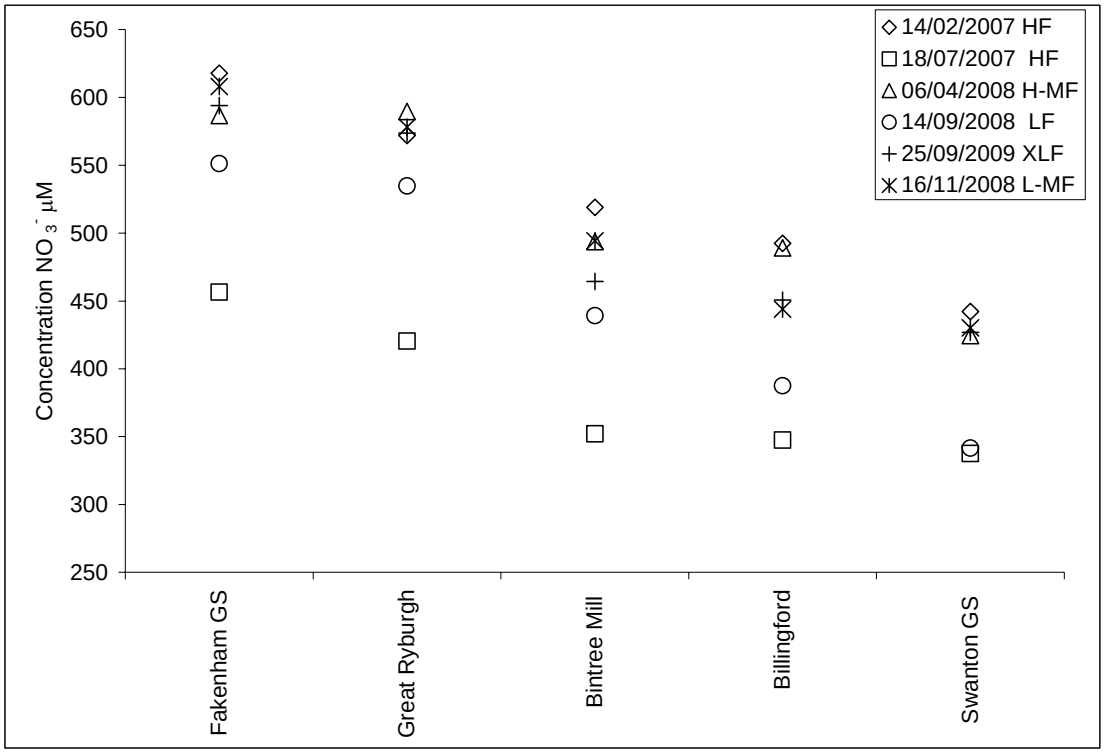

Figure 5.31 Concentration NO_3^- (µM) of samples from the mid Wensum river showing individual data sets with location. Legend includes flow conditions.

To test the possibility that these trends are caused by in-stream denitrification of river water, isotope enrichment factors and fractionation ratios were calculated for the nine data sets (Table 5.5). Most show good agreement with literature values for fractionation ratios from 0.4 to 0.6 (Mariotti *et al.*, 1980, Mariotti *et al.*, 1988, Böttcher *et al.*, 1990, Aravena and Robertson, 1998, Cey *et al.*, 1999, Lehmann *et al.*, 2003, Fukada *et al.*, 2004, Deutsch *et al.*, 2005, Petitta *et al.*, 2009).

Table 5.5 Isotope enrichment factors and fractionation ratios calculated between the mid Wensum gauging stations at Fakenham and Swanton for individual data sets.

Sampling date	Flow condition	Season	$\varepsilon_{P\text{-}S}{}^{15}N_{NO3}$	$\varepsilon_{P\text{-}S}{}^{18}O_{NO3}$	Fractionation ratio O:N
14/02/2007	high	winter	-5.9	-2.1	0.37
17/04/2007	low	spring	-15.3	-6.1	0.40
18/07/2007	high	summer	-5.8	-4.1	0.72
06/04/2008	medium	spring	-6.1	-5.3	0.87
14/09/2008	low	autumn	-6.4	-2.6	0.41
16/11/2008	medium	winter	-4.8	-4.1	0.85
12-13/12/2008	high	winter	-5.0	-2.7	0.55
27/05/2009	low	spring	-15.2	-6.4	0.42
25/09/2009	extreme low	autumn	-10.6	-4.2	0.40

However, when $\delta^{15}N_{NO3}$ from the five main sampling locations is plotted against the natural log of concentration and the reciprocal of concentration, the linear regression r^2 values, which are all above 0.80, are almost identical, meaning that this is not a useful diagnostic with these data to differentiate the effects of mixing from denitrification. This is not surprising, as mixing is definitely occurring in this reach, from baseflow and surface water accretion which results in the increase in flow between the two gauging stations.

If the trends seen are simply due to mixing, this would imply an increasing proportion downstream of a water type with nitrate of a heavy isotopic composition and reasonably low concentration. In the mid river reach it is expected that an increasing amount of baseflow will be advecting into the river, as well as accretion from tributaries and drains, together resulting in the flow increase seen by Swanton gauging station. However, it is not clear which of these sources could be responsible for a mixing trend which would result in the isotopic composition of nitrate seen. Baseflow from low-nitrate groundwater will have a negligible affect on riverine nitrate isotopic composition, although acting to dilute nitrate concentrations, while tributary and drain nitrate overall has a nitrate concentration and isotopic composition similar to that seen at Swanton. Valley Chalk groundwater nitrate is of high concentration with a light isotopic composition. Although tributary and drain accretion will reduce the riverine nitrate concentration and increase its isotopic composition to some extent, it is not at a low enough concentration or of a heavy enough isotopic composition to bring about the nitrate concentration and isotopic composition seen at Swanton. This means that there is no obvious end member responsible for the mixing trend. Moreover, the very high nitrate concentration of the valley Chalk groundwater is puzzling, given the decrease in concentration in this reach, and its baseflow index of 0.75. A possible explanation is that denitrification occurs to the valley Chalk groundwater as it flows vertically through the hyporheic sediments below the riverbed. There are significant glaciofluvial sand and gravel deposits which are up to five metres deep in the river valley. The optimal matrix to support denitrification is a mix of gravel and fine sediment with a good supply of organic matter, and anaerobic conditions (Hedin *et al.*, 1998). These sand and gravel deposits are likely to contain both organic matter and fine sediment via the riverbed and from runoff, and are likely to develop anaerobic conditions below the riverbed where

oxygen levels are low under the uppermost layer of sediments. This environment may support denitrification as valley Chalk groundwater advects up through the hyporheic sediments before reaching the river.

In addition to denitrification in the hyporheic zone, denitrification may occur in lakes. There are two areas in the mid catchment where gravel has been extracted adjacent to the river, and the disused gravel pits have been allowed to flood with groundwater to form lakes up to 5 metres deep. These are at Pensthorpe Park between Fakenham and Great Ryburgh, and Sennowe Park, between Great Ryburgh and Bintree Mill. Denitrification can be significant in lakes (Lehmann *et al.*, 2003) and is controlled by the development of anaerobic conditions at depth, and the residence time of the water. Groundwater infiltrating into these lakes may, therefore, undergo significant denitrification. Two lakes at Pensthorpe Park were sampled in winter 2008 and found to have very low nitrate concentrations and a heavy isotopic composition, which supports this hypothesis (Moon Lake 31 μM NO_3^-, $\delta^{15}N_{NO3}$ 14.4‰, $\delta^{18}O_{NO3}$ 5.2‰; Dark Mere 25 μM NO_3^-, $\delta^{15}N_{NO3}$ 10.6‰, $\delta^{18}O_{NO3}$ 3.8‰). These lakes do not have a surface water connection with the river. However, it is likely that water contained within them contributes to river flow via shallow circulation (Figure 5.32).

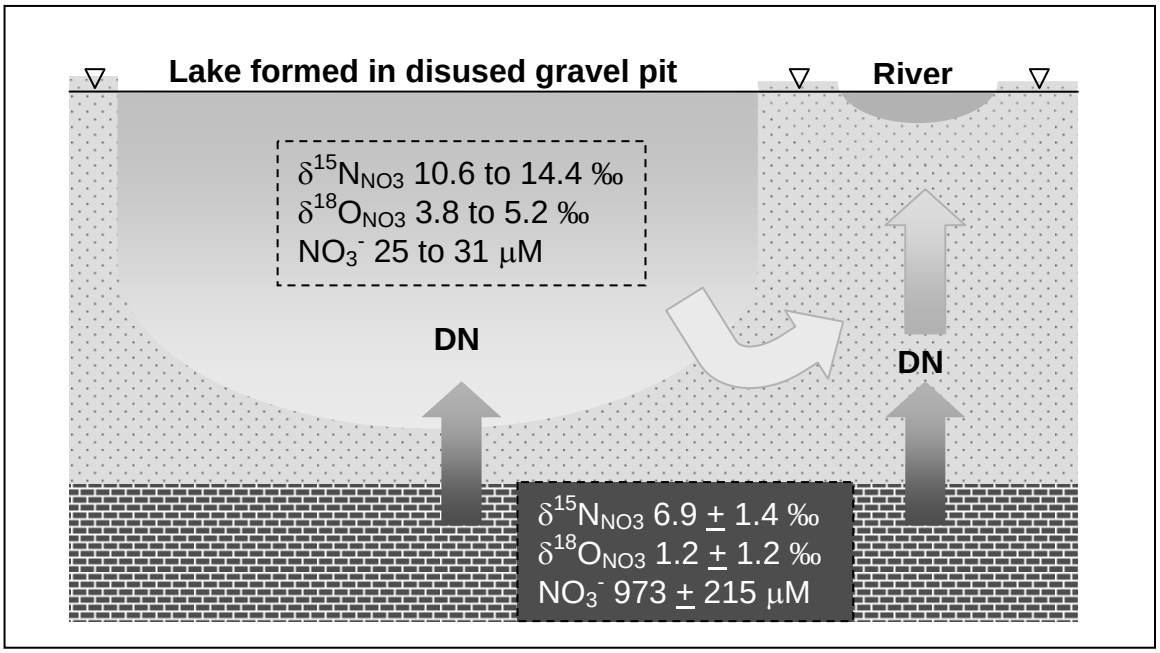

Figure 5.32 Conceptual model of denitrification (DN) in valley Chalk groundwater-fed lake adjacent to river and within the sand and gravel deposits below the river, with colour gradient from dark to light indicating high to low nitrate concentration resulting from denitrification.

In order to investigate the possibility of denitrification of the valley Chalk groundwater end member further, a four-member mass-balance solute mixing model was used to reproduce mean concentrations of chloride, sulphate, sodium, potassium, and nitrate at the five locations from Fakenham to Swanton gauging stations using Equation 3.13 (Chapter 3). There is a trend between the two gauging stations of an increase in concentration by Swanton of these solutes which could be caused by an increasing contribution downstream from eastern catchment valley Chalk groundwater. Interestingly, a flow related response is also seen, with the highest downstream increase in concentrations of chloride, sulphate and sodium in the low-flow data sets, with minor increases of chloride and sulphate in the high-flow sets (Figures 5.33 to 5.36). This could indicate a stronger hydrochemical signal from valley Chalk groundwater baseflow during low-flow along with reduced dilution of wastewater effluent which also has high concentrations of these solutes. Concentrations of potassium do not show this trend.

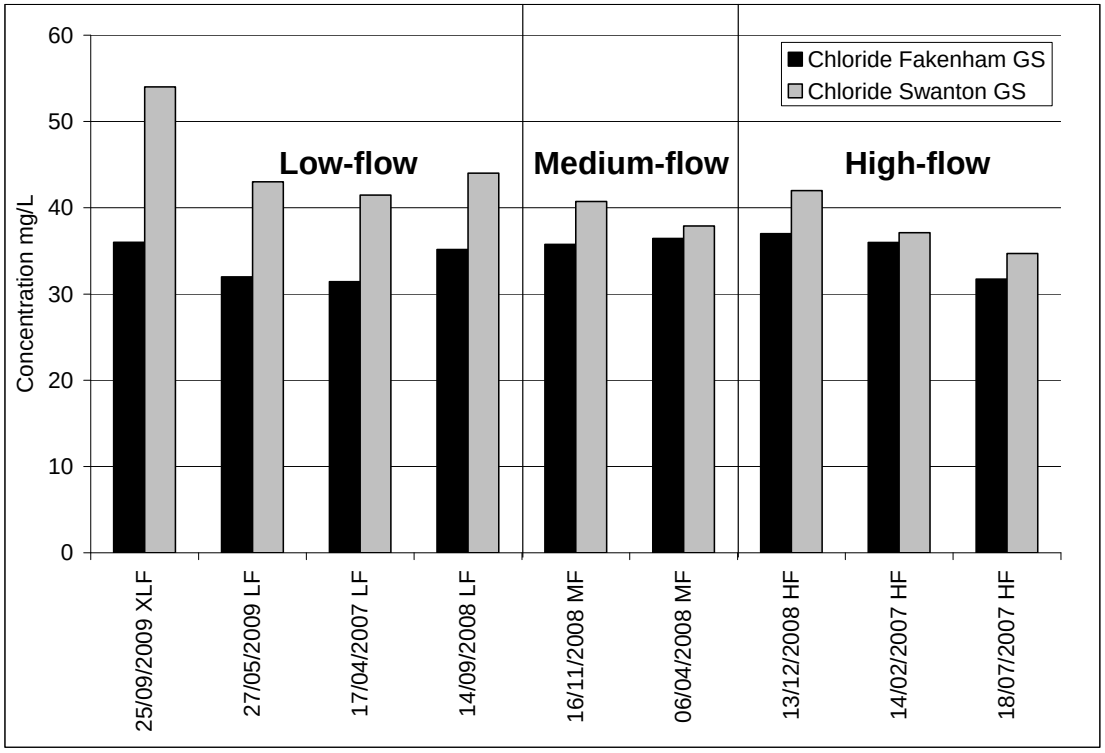

Figure 5.33 Chloride concentrations (mg/L) of samples from the upper Wensum gauging station at Fakenham and the mid Wensum gauging station at Swanton for individual data sets. Labels include flow conditions.

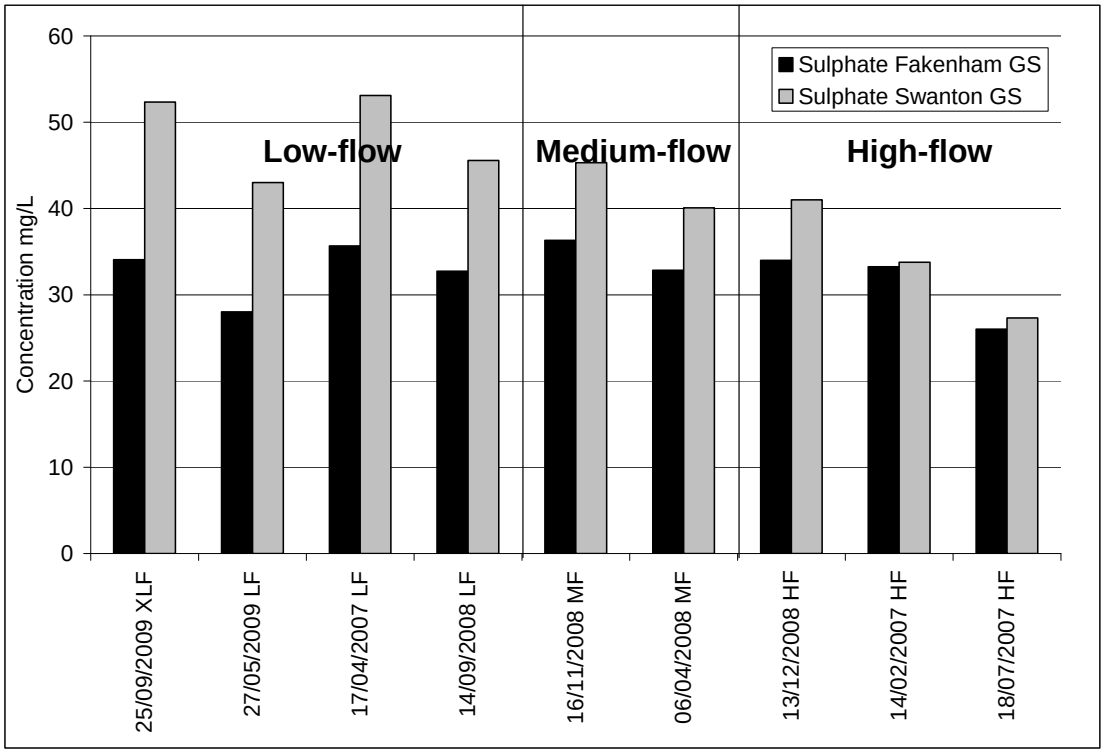

Figure 5.34 Sulphate concentrations (mg/L) of samples from the upper Wensum gauging station at Fakenham and the mid Wensum gauging station at Swanton for individual data sets. Labels include flow conditions.

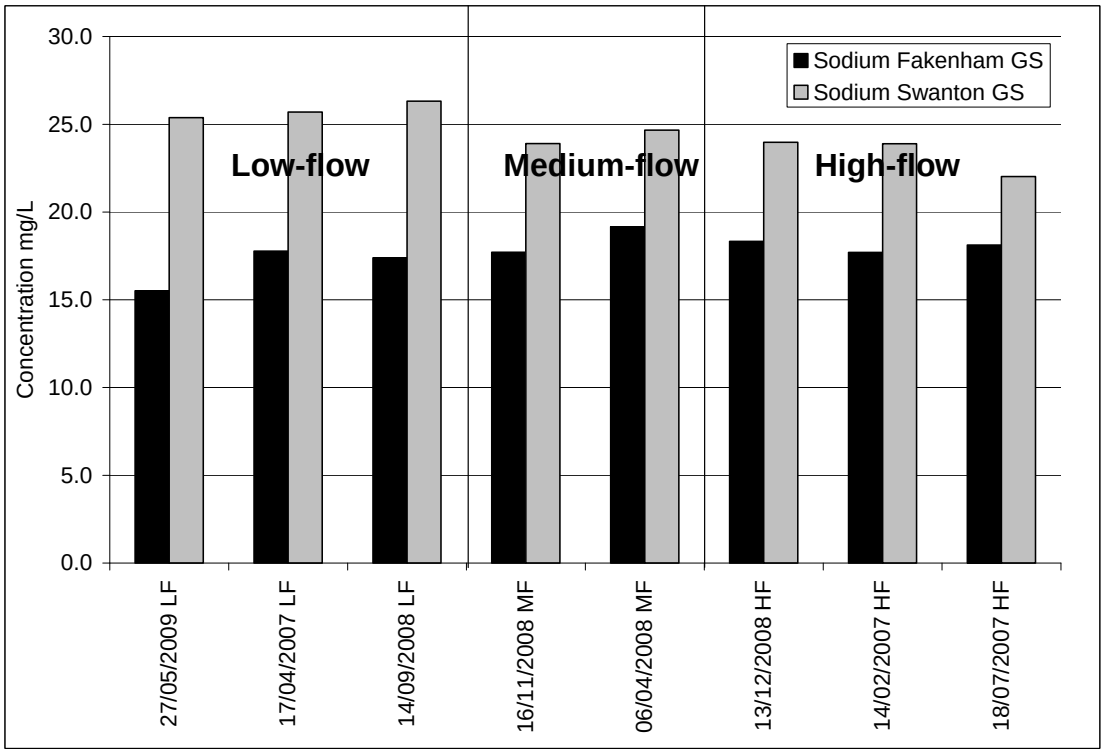

Figure 5.35 Sodium concentrations (mg/L) of samples from the upper Wensum gauging station at Fakenham and the mid Wensum gauging station at Swanton for individual data sets. Labels include flow conditions.

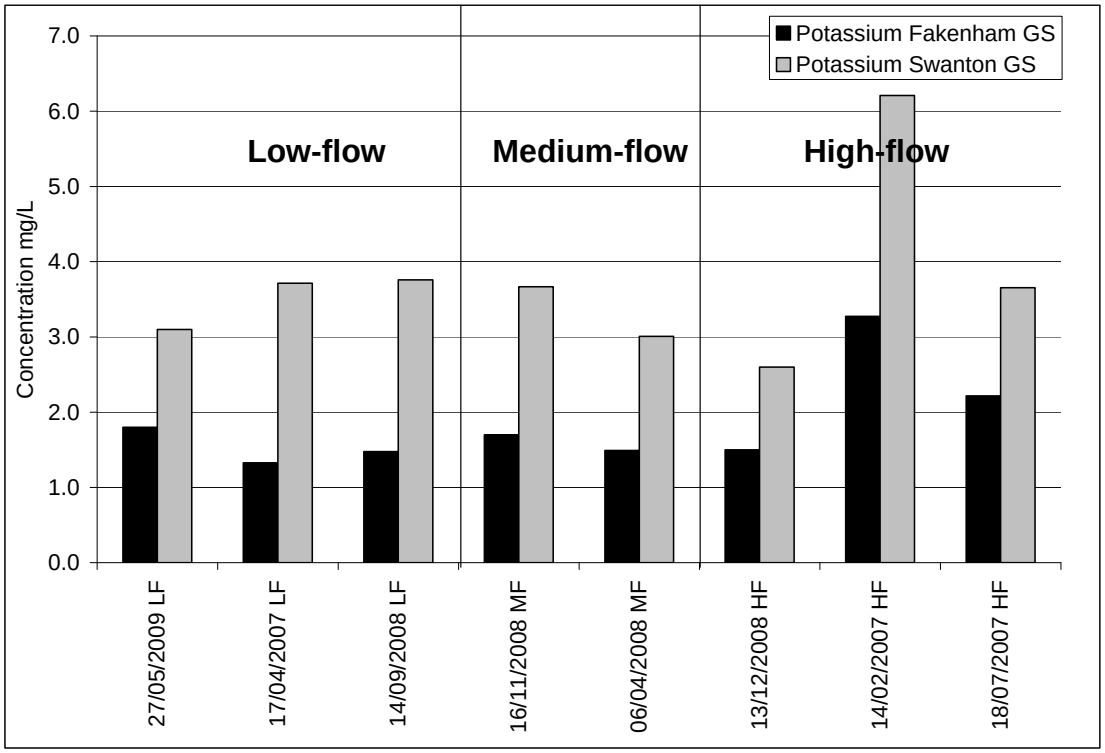

Figure 5.36 Potassium concentrations (mg/L) of samples from the upper Wensum gauging station at Fakenham and the mid Wensum gauging station at Swanton for individual data sets. Labels include flow conditions.

For the model of mean flow conditions, the mean proportional flow increase by Swanton, relative to flow at Fakenham gauging station was used (2.23 $m^3 s^{-1}$), and flow was modelled to increase in equal increments (0.56 $m^3 s^{-1}$) across the five locations. The simplifying assumption of a constant ratio between baseflow inputs and surface water accretion from tributaries of 0.75 to 0.25 was made, based on the baseflow index in this reach of 0.75 (Appendix 3). Within the additional flow at each location attributable to baseflow, a proportion was sourced from valley Chalk groundwater and the remaining fraction from interfluve Chalk groundwater. The ratio of valley to interfluve Chalk groundwater was increased downstream, and used to calibrate the model to concentrations of chloride. At Great Ryburgh, 100% baseflow was supplied by valley Chalk groundwater, at Bintree Mill 90%, with 10% from interfluve Chalk groundwater, at Billingford, the ratio was 75% to 25%, and finally at Swanton gauging station the model used 55% valley Chalk groundwater to 45% interfluve Chalk groundwater. The model reproduced concentrations of chloride and sodium well, with some overestimation of sulphate (Figure 5.37a-c). However, nitrate concentrations were significantly overestimated (Figure 5.37d).

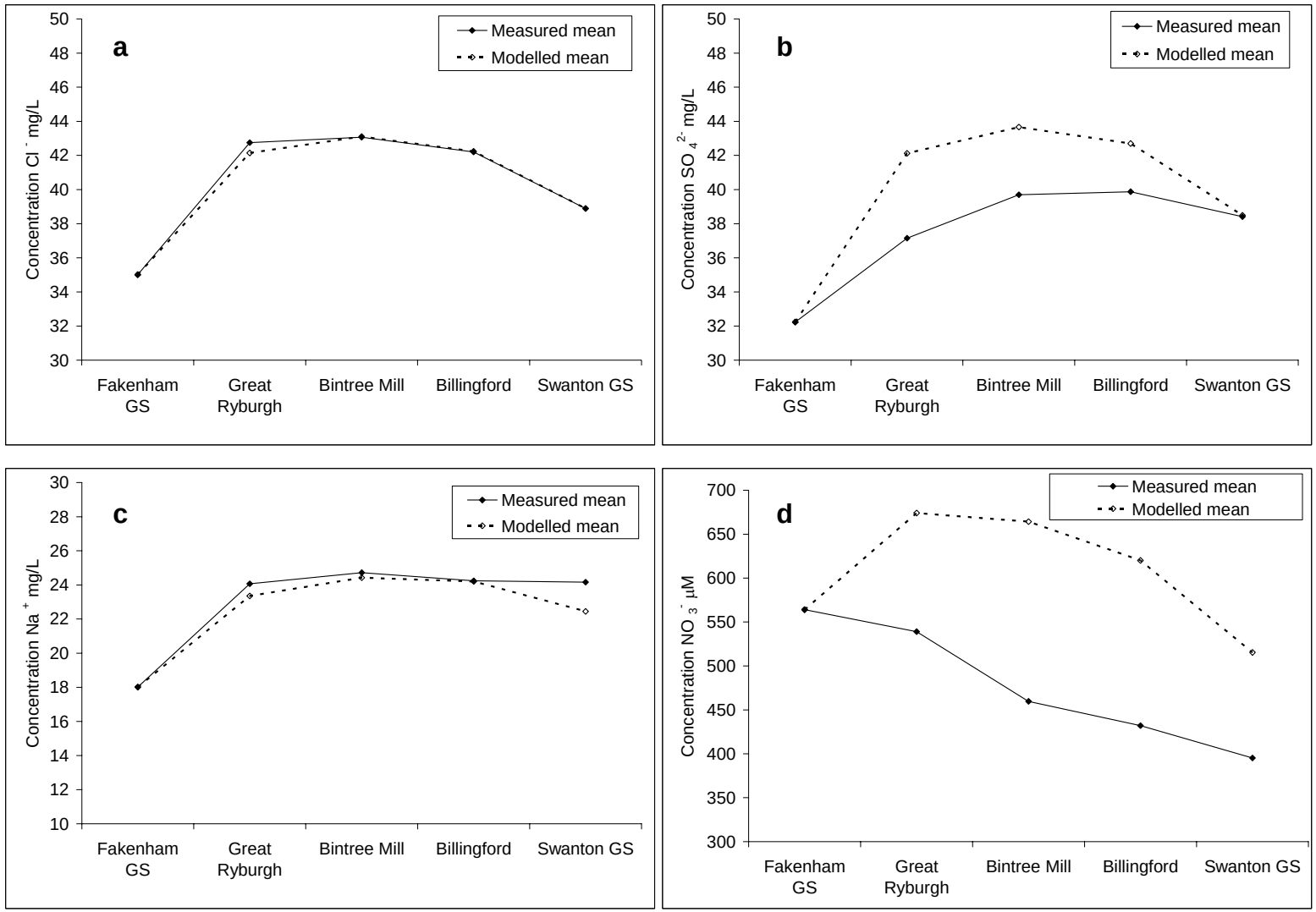

Figure 5.37a-d Four-member mass-balance solute mixing model output for mean data set showing measured (filled line) and modelled (dashed line) concentrations of a) chloride; b) sulphate; c) sodium; and d) nitrate, at the five mid river sampling locations.

The model was run again and the concentration of the valley Chalk groundwater end member was lowered iteratively until a good fit with the measured nitrate concentrations was reached (Figure 5.38). For this, the concentration of valley Chalk groundwater was reduced from 973 to 550 μM NO_3^-, a reduction of 43%, supporting the theory of denitrification of this end member.

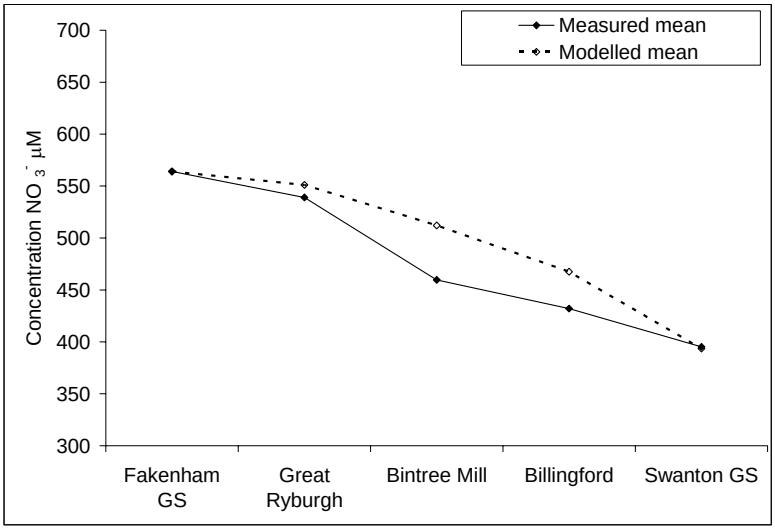

Figure 5.38 Four-member mass-balance solute mixing model output for mean data set showing measured (filled line) and modelled (dashed line) concentrations of nitrate using a valley baseflow concentration of 550 μM NO_3^-.

Model results of potassium concentrations were poor, failing to produce a concentration increase by Swanton gauging station. There is a large degree of variation in concentrations of potassium in the mid river tributaries and drains (4.3 $\pm$ 5.0 mg/L) suggesting that concentrations may be controlled by local point source inputs with a high degree of variability. For this reason potassium was excluded from the model.

The model overestimations of sulphate may indicate the effect of microbial sulphate reduction, either in-stream in the anaerobic layer of the riverbed, or within the sand and gravel sediments as baseflow advects through them. Another explanation is of a source of water which has a lower ratio of sulphate to chloride than that produced by the groundwater mix. A possible source is wastewater effluent. Sulphate to chloride ratios in the two wastewater effluent samples are lower than ratios in both valley Chalk groundwater and interfluve Chalk groundwater (Table 5.6), though it is not known whether these ratios are representative of effluent in general.

Table 5.6 Sulphate to chloride ratios in Wensum catchment waters including the mean ratio from effluent samples.

Water source	Ratio SO_4^{2-}:Cl^-
Valley Chalk groundwater	1.1
Interfluve low-nitrate Chalk groundwater	0.7
Valley edge low-nitrate Chalk groundwater	2.0
Mid river samples	0.9
Mid river tributaries and drains	1.1
Wastewater effluent	0.5

Possible sources of error in the model include the fact that the tributary and drain component is based on a simple mean of measurements, and is not weighted according to proportional contributions from large and small tributaries, or for the spatial distribution of tributaries relative to the locations modelled. Without detailed supplementary data including gauging data for these streams it is not possible to include these factors in the model. In addition, the assumption of no direct effluent discharges to the Wensum is made; in other words, that all effluent is discharged into tributaries, reaching the Wensum indirectly. This is the case for East Dereham works which discharges effluent into the Wendling Beck. Another possible source of error in the model is that there is no attempt to weight mean concentrations of the surface water components for flow condition or season. Notwithstanding these limitations, the solute model performed well for the mean data set.

Following the construction of the four member solute mixing model, isotope mass balance was added, using Equation 3.14 (Chapter 3) in order to model mean $\delta^{15}N_{NO3}$ and $\delta^{18}O_{NO3}$ values in the mid river reach, using the mean measured isotopic composition of the end members, and the model configuration used for solute concentrations (Table 5.7). Interestingly, the mean concentration and isotopic composition of the mid river tributaries and drain used for this end member, and the model target of measured values in the river at Swanton gauging station are very similar, with relatively low nitrate concentration and heavy isotopic composition. In the case of the tributaries and drains this suggests dilute effluent and manure sources which enter the drains in drainage water and runoff, with the effects of denitrification which occurs during flow along the drain and tributaries.

The valley Chalk groundwater component was initially modelled using its measured mean isotopic composition, with the reduced concentration predicted by the solute model ($\delta^{15}N_{NO3}$ 6.7 ‰; $\delta^{18}O_{NO3}$ 1.2 ‰). This produced modelled isotope values lower than measured values (Figure 5.39a and b).

Table 5.7 Four member isotope mass-balance mixing model end members for mean model run.

End member	**$\delta^{15}N_{NO3}$ (‰) vs. AIR**	**$\delta^{15}N_{NO3}$ (‰) vs. VSMOW**	**Concentration NO_3^- (µM)**
River flow at Fakenham	8.4	3.5	564
Mid river tributary and drain mean	10.3	4.9	372
Valley Chalk groundwater mean	6.7	1.2	973
Denitrified valley Chalk groundwater	13.5	6.2	550
Interfluve low-nitrate Chalk groundwater	-	-	-
Target: River flow at Swanton	10.7	4.8	395

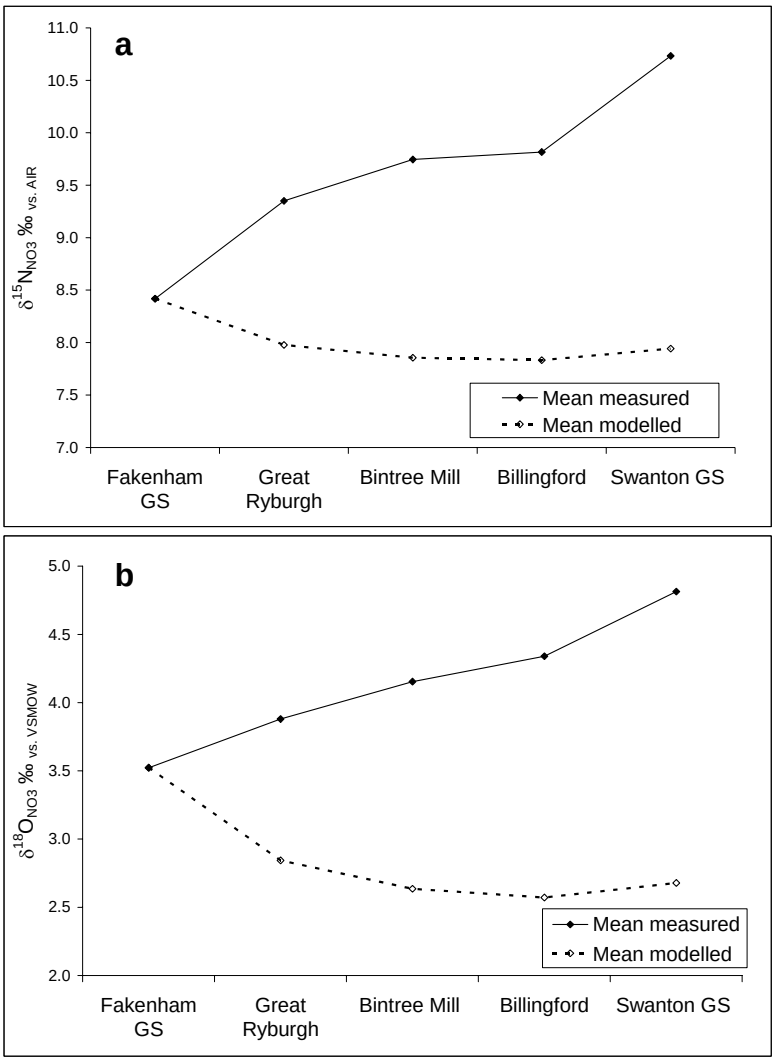

Figure 5.39a and b Four-member isotope mass-balance solute mixing model output for mean data set. $\delta^{15}N_{NO3}$ (‰) a); and $\delta^{18}O_{NO3}$ (‰) b), showing measured (filled line) and modelled (dashed line) isotopic composition using a valley baseflow concentration of 550 µM NO_3^-.

Following this, the isotopic composition of valley Chalk groundwater nitrate was adjusted so the model produced the measured isotopic composition of nitrate at Swanton gauging station. This gave valley Chalk groundwater nitrate values of $\delta^{15}N_{NO3}$ 13.5 ‰ and $\delta^{18}O_{NO3}$ 6.2 ‰. However, although producing a better fit than the previous model run, the isotopic composition of nitrate at the three mid river locations between the gauging stations was heavier than measured values (Figures 5.40a and b).

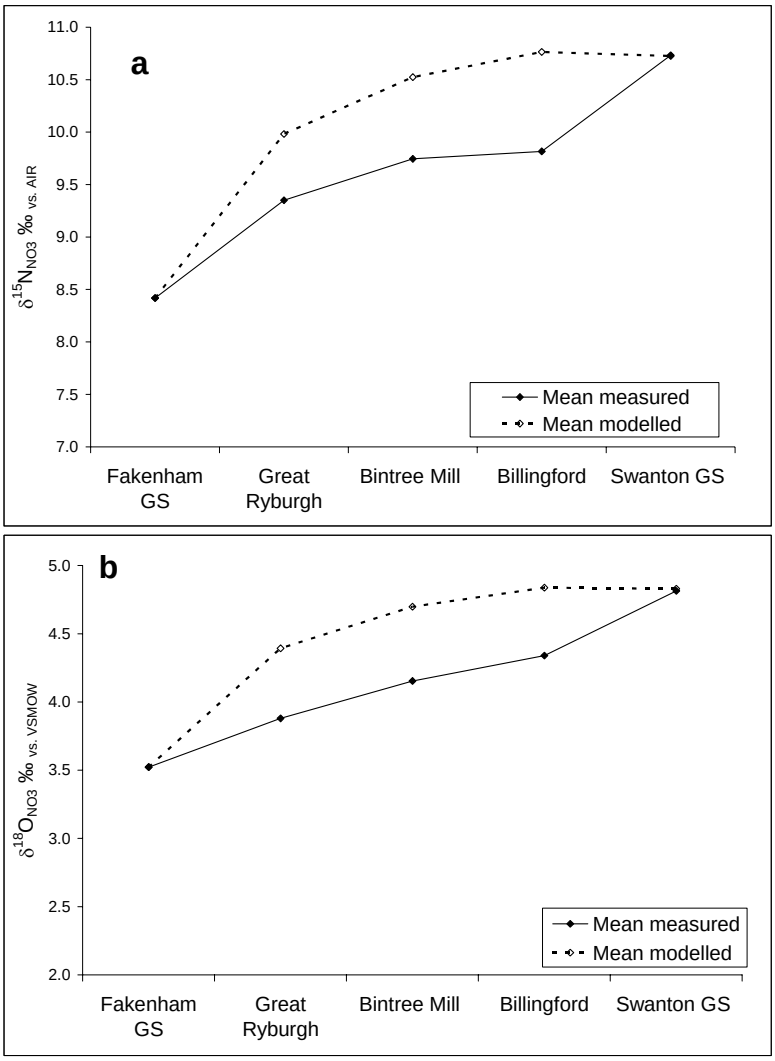

Figure 5.40a and b Four-member isotope mass-balance solute mixing model output for mean data set: a) $\delta^{15}N_{NO3}$ (‰) ; and b) $\delta^{18}O_{NO3}$ (‰), showing measured (filled line) and modelled (dashed line) isotopic composition using a valley baseflow concentration of 550 µM NO_3^-, with an isotopic composition of $\delta^{15}N_{NO3}$ 13.5 ‰; $\delta^{18}O_{NO3}$ 6.2 ‰.

Finally, in order to produce a good fit of isotopic composition, the valley Chalk groundwater end member nitrate isotopic composition was increased incrementally downstream through the mid river locations. The first location beyond Fakenham (Great Ryburgh) showed the greatest increase in isotope values from measured valley Chalk groundwater nitrate values, followed by a minor incremental increase in isotope values, which could suggest additional isotopic fractionation due to further denitrification (Table 5.8; Figures 5.41a and b) (Appendix 3).

Table 5.8 Evolution of isotopic composition of model valley Chalk groundwater end member.

Locations	**$\delta^{15}N_{NO3}$ (‰) vs. AIR**	**$\delta^{15}N_{NO3}$ (‰) vs. VSMOW**
Great Ryburgh	11.30	4.50
Bintree Mill	11.50	4.80
Billingford	11.70	5.10
Swanton GS	13.50	6.20

The isotopic composition estimated by the model for the valley Chalk groundwater end member at Great Ryburgh $\delta^{15}N_{NO3}$ 11.3 ‰ and $\delta^{18}O_{NO3}$ 4.5 ‰ represents this groundwater after partial denitrification in the sands and gravels. The subsequent incremental increase in this end member's isotope values could represent an increased rate of denitrification of valley Chalk groundwater in the sands and gravels further downstream in the catchment, which can occur due to an increase in the rate of advection of groundwater through the sediments (Tsushima *et al.*, 2006). This would imply a higher concentration of nitrate from valley Chalk groundwater at Great Ryburgh than at Swanton. However, an alternative explanation is that the necessity to adjust the isotopic composition of the valley Chalk groundwater end member in the model, in fact, suggests a contribution from in-stream denitrification. If this is the case, the valley Chalk groundwater end member nitrate isotopic composition as represented by the model at Great Ryburgh would remain stable, and its concentration would be higher than the 550 μM NO_3^- predicted by the model, with in-stream denitrification accounting for "additional" removal of nitrate in order to reach the measured concentration at Swanton.

Although it is not possible to verify in-stream denitrification from these data, isotope enrichment factors can be calculated based on the values above. If it is assumed that the concentration of valley Chalk groundwater after partial denitrification in the sediments

is 650 μM NO_3^- (a concentration reduction of 33%), the mixing model output at Swanton gauging station produces a concentration of 424 μM NO_3^-, with an isotopic composition of $\delta^{15}N_{NO3}$ 10.0 ‰ and $\delta^{18}O_{NO3}$ 4.2 ‰. Then, using the mean measured values at Swanton (395 μM NO_3^-; $\delta^{15}N_{NO3}$ 10.7 ‰; $\delta^{18}O_{NO3}$ 4.8 ‰) isotope enrichment factors can be calculated for in-stream denitrification in order to produce the measured nitrate concentration and isotopic composition at Swanton. These are $\varepsilon_{P\text{-}S}{}^{15}N_{NO3}$ -10.8 ‰ and $\varepsilon_{P\text{-}S}{}^{18}O_{NO3}$ of -9.2 ‰, with a fractionation ratio of O:N of 0.85. The nitrogen isotope enrichment factor is similar to that found by Kellman and Hillaire-Marcel (1998) of $\varepsilon_{P\text{-}S}{}^{15}N_{NO3}$ -10.0 ‰, attributable to in-stream denitrification. Iterations with a lower concentration of the groundwater end member after partial denitrification in the sediments produced larger isotope enrichment factors with a smaller fractionation ratio, and those with a higher concentration produced lower enrichment factors with a larger fractionation ratio Thus the hypothesis of a partially denitrified baseflow with in-stream denitrification causing further isotopic enrichment and nitrate removal downstream is feasible. In stream denitrification can occur when river water is diverted from the main channel via the riverbed through flowpaths in the upper layer of the hyporheic zone (Van der Hoven *et al.,* Hinkle *et al.*, 2001, Puckett *et al.*, 2008, Claret and Boulton, 2009, Curie *et al.*, 2009). The hyporheic zone which includes both the upper layer receiving water from the river channel above, and the glacio-fluvial sediments receiving the valley Chalk groundwater at depth, represents an advection dominated system in which suboxic or anoxic conditions are stable, through which nitrate of a high concentration is continuously advected and denitrification can occur continuously (Seitzinger *et al.*, 2006).

Isotope enrichment factors and fractionation ratios were calculated for the mean model valley Chalk groundwater baseflow end member based on the predicted nitrate concentration and isotopic composition at Great Ryburgh (Table 5.9). These are within the literature range where values of $\varepsilon_{P\text{-}S}{}^{15}N_{NO3}$ -4.7 to -30 ‰ have been reported (Mariotti *et al.*, 1981, Vogel *et al.*, 1981, Mariotti *et al.*, 1988). They are greater than enrichment factors found in nitrate sampled from a field drain developing over a six month period, and similar to those found in groundwater nitrate from a multilevel piezometer installation in the Sherwood Sandstone aquifer, Nottingham UK (Fukada *et al.*, 2004, Deutsch *et al.*, 2005).

Table 5.9 Isotope enrichment factors and fractionation ratios calculated for the valley Chalk groundwater component of the four member mixing model, based on measured values and values predicted by the model for mean conditions, with two literature values for comparison (Fukada *et al.*, 2004, Deutsch *et al.*, 2005).

Study	**Environment**	**$\varepsilon_{P\text{-}S}{}^{15}N_{NO3}$**	**$\varepsilon_{P\text{-}S}{}^{18}O_{NO3}$**	**Fractionation ratio O:N**
Fukada *et al.* (2004)	Sherwood sandstone borehole depth samples	-13.7	-6.9	0.50
Deutsch *et al.* (2005)	Tile drain over six-month period	-5.9	-2.0	0.34
Mean model run this study	Valley Chalk groundwater in sand and gravel sediments	-11.4	-8.2	0.74

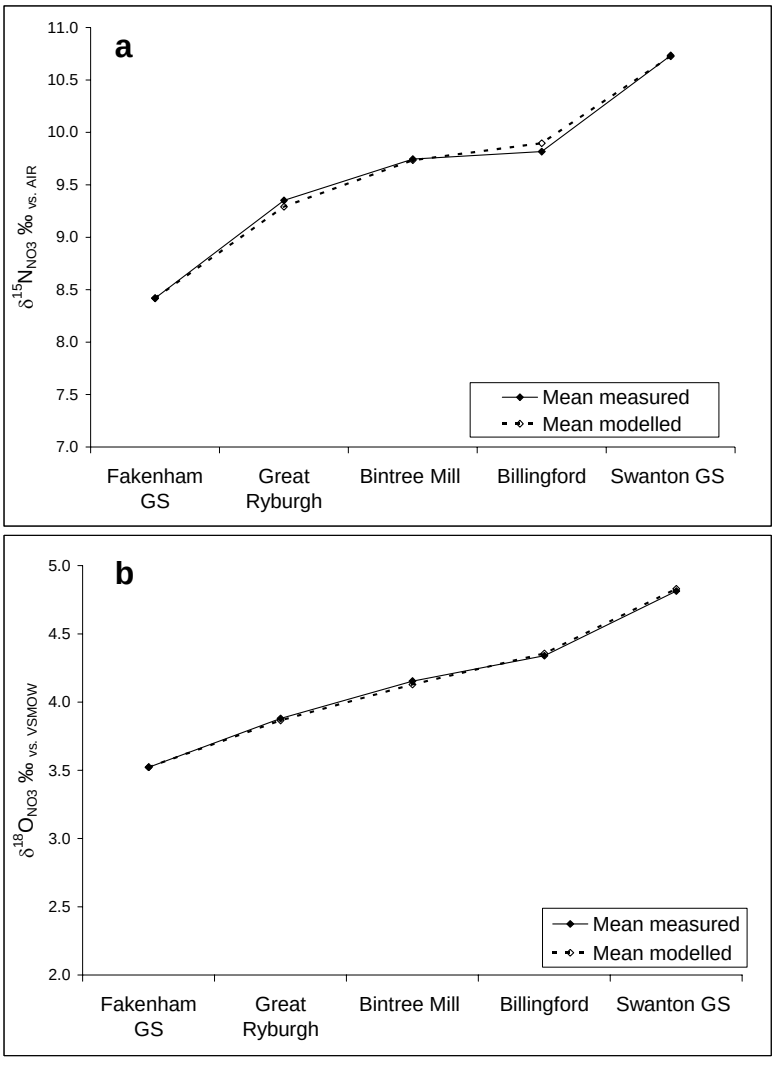

Figures 5.41a and b Four-member isotope mass-balance solute mixing model output for mean data set: $\delta^{15}N_{NO3}$ (‰) a); and $\delta^{18}O_{NO3}$ (‰) b), showing measured (filled line) and modelled (dashed line) isotopic composition using a valley baseflow concentration of 550 µM NO_3^-, with an isotopic composition of $\delta^{15}N_{NO3}$ 13.5 ‰; $\delta^{18}O_{NO3}$ 6.2 ‰ by Swanton gauging station, with an incremental increase in isotopic composition through the mid river locations.

To summarise, the model results suggest that a mass of nitrate-nitrogen is removed by Swanton gauging station, both from the groundwater before it enters the river, and via in-stream denitrification of riverine nitrate. In addition, the nitrate concentration and isotopic composition of the mid river tributaries and drains suggest dilute effluent and manure sources with partial denitrification which may have occurred in-stream or in the soil before the nitrate was flushed in drainage waters to the streams and drains. The model is constrained by mean measured values of solute concentrations, nitrate isotopic composition through the five mid river locations, mean solute concentrations of groundwater samples, and by the baseflow index for the middle catchment to Swanton gauging station. An important factor is the high concentration and light isotopic composition of valley Chalk groundwater, which cannot be successfully incorporated in the model to reproduce measured values in the river at Swanton, despite the fact that valley Chalk groundwater is expected to be one of the main sources of baseflow. In order for nitrate concentrations to be reproduced at Swanton, the valley Chalk groundwater end member concentration must be reduced by 33 %; a figure constrained by the baseflow index, with additional removal attributed to in-stream denitrification. In addition, to model the evolution of nitrate isotopic composition in the river, the valley Chalk groundwater end member must have a heavy isotopic composition.

Next, the mass-balance solute model was used to reproduce concentrations of chloride, sulphate, sodium, and nitrate, and nitrate isotopic composition at Swanton gauging station, for the mean of the three low-flow data sets (17/04/2007; 14/09/2008; 29/05/2009). Solute concentrations under low-flow conditions may give a clearer indication of baseflow mixing. A very good reproduction of measured data was achieved by using the baseflow index as before, of 0.75, with the only alteration in model parameters being a higher proportion of valley Chalk groundwater to interfluve water (low-flow model 0.65: 0.35; mean model 0.55:0.45). This is surprising, as a broader areal groundwater circulation may be expected during low-flow conditions than during high-flows when runoff recharges shallow groundwater and leads to a larger proportion of near-river groundwater baseflow circulation. It is likely that this anomaly reflects a weakness of the model in that the same baseflow index is used for high-flow and low-flow runs. In fact, during high flow there will be a greater proportion of flow originating from surface runoff both via the tributaries and drains, and from shallow groundwater circulation, resulting in a lower baseflow index, and a higher proportion of

flow from surface accretion. If this could be incorporated in the model, it would result in a lower proportion of baseflow overall, with a higher proportion of valley Chalk groundwater to interfluve Chalk groundwater.

In order to fit the measured concentration of nitrate at Swanton, the valley baseflow component concentration was reduced from 973 to 527 μM NO_3^-, a reduction of 46% with an isotopic composition of $\delta^{15}N_{NO3}$ 14.3 ‰; $\delta^{18}O_{NO3}$ 5.8 ‰ (Appendix 3). Due to the fact that the model was only used to reproduce values at Swanton gauging station because of a lack of low-flow samples in the reach, an assessment of the contribution of in-stream denitrification could not be made, nor isotope enrichment factors for the valley Chalk groundwater end member at Great Ryburgh calculated.

To estimate the quantity of nitrate removed via denitrification in this reach, and apportion it to riverine and groundwater processes, it is necessary to predict the hypothetical load without denitrification. This calculation is poorly constrained in comparison to the mixing model, and would ideally require a nitrate budget approach to the catchment. This was not within the scope of this research. However, it is possible to estimate figures for both the mean and low-flow mean data sets for comparison, and also to apportion removal rates for these data sets with respect to groundwater and riverine denitrification, to compare with values in the literature.

Using the mean data set, if all denitrification is attributed to denitrification of valley Chalk groundwater resulting in a reduction its concentration from 973 to 550 μM NO_3^- by Swanton, the calculated removal rate is 499 kg nitrate-nitrogen per day, which is 23% of the mean predicted load. However, if the calculation of in-stream denitrification is included, (responsible for reducing the nitrate concentration by Swanton from 424 to 395 μM NO_3^-), then denitrification of valley Chalk groundwater accounts for removal of 374 kg nitrate-nitrogen per day and in-stream denitrification for 125 kg nitrate-nitrogen per day, a split of 75% to 25% (Appendix 3). It is important to note that the overall removal of 499 kg nitrate-nitrogen per day represents the upper limit of removal, as it is based on the assumption that all nitrate-bearing groundwater comes from the high-concentration valley Chalk groundwater. It is likely that some baseflow is supplied by shallow groundwater, fed directly from recharge runoff. This will have a similar nitrate isotopic composition to valley Chalk groundwater, (as previously discussed), but

could have a lower nitrate concentration, which would reduce the calculated removal rate. This element will be greater during high flows, and may lead to an overestimation from the mean modelled values. The same calculation for the mean low-flow data set, which predicts a concentration reduction for the valley Chalk groundwater end member from 973 to 527 μM NO_3^- by Swanton, gives a removal rate of 372 kg nitrate-nitrogen per day, which is 27% of the mean low-flow predicted load. If it assumed that 25% of this is in fact attributable to in-stream denitrification, then 279 kg nitrate-nitrogen per day is removed from valley Chalk groundwater under low flow, and 93 kg nitrate-nitrogen per day is removed in-stream.

In order to test the sensitivity of the model to the baseflow index, the nitrate-nitrogen removal rate was calculated for the mean data set using a perturbed baseflow index. With BFI+25% (BFI = 0.94) the calculated removal was 1.8% higher, with 508 kg nitrate-nitrogen removed per day, and with BFI-25% (BFI = 0.56), the calculated removal rate was 4.2% lower showing 487 kg nitrate-nitrogen removed per day, indicating that the BFI was not a highly sensitive factor in the model and supporting its use as a controlling parameter.

From these figures a rate of denitrification per volume of hyporheic sediments below the riverbed can be calculated. The Wensum mid river reach is approximately 25 km long, with a mean width of nine metres based on surveying in the field and aerial photography, (Europress, 2003). This gives a riverbed area of 225000 m^2. Assuming a mean depth of sediment with denitrification potential of two and a half metres, the rate of denitrification for the overall mean data sets is 28 mg/m^3/hour, and for the low-flow mean data set, 21 mg/m^3/hour, based on the assumption of 25% removal in-stream. If all removal is assumed to occur in the sediments, the rates are 37 mg/m^3/hour, and 28 mg/m^3/hour respectively. There are few reports in the literature of hyporheic denitrification rates per volume of sediment. However, the rates calculated here are slightly lower than the range reported by Sheibley *et al.* (2003) of 28 to 64 mg/m^3/hour, suggesting that an attribution of 75% of the nitrate removal to denitrification of valley Chalk groundwater is feasible (Appendix 3). Using the calculated volume of the mid river reach hyporheic sediments (562500 m^3), the mean volume of flow at Swanton gauging station under low-flow conditions (2.05 $m^3\ s^{-1}$), the mid river baseflow index (0.75), and the proportion of baseflow attributed to valley Chalk groundwater by the

model (0.65), an estimate of the valley Chalk groundwater residence time there is 6.5 days.

Estimates of riverine denitrification rates based on the assumption that 25% of nitrate removal occurs as a result of in-stream denitrification can be calculated as mg nitrate-nitrogen removed per hour per square metre of riverbed, as denitrification occurs in a thin anaerobic layer immediately below the riverbed surface. In addition to the riverbed area of 225000 m^2, there is likely to be denitrification potential on the channel sides. Using a conservative estimate of the mean river depth of 0.5 metres, the total surface area of the river channel is 250000 m^2. The rate of denitrification for the overall mean data sets is 21 mg/m^2/hour, and 16 mg/m^2/hour for the mean low-flow set (Appendix 3).

There is a wide range of values reported in the literature from a variety of approaches aimed at quantifying riverine denitrification, ranging from around 10 mg nitrate-nitrogen /m^2/hour to 222 mg/m^2/hour, with denitrification rates in wetlands reaching 778 mg/m^2/hour (Table 5.10) (Sjodin *et al.*, 1997, Laursen and Seitzinger, 2002, Kellman, 2004, Royer *et al.*, 2004, Laursen and Seitzinger, 2005, Hernandez and Mitsch, 2006, Pina-Ochoa and Alvarez-Cobelas, 2006). The range represented by these calculations falls within the literature range. Thus it is feasible that 25% of denitrification occurs in-stream.

The percentages of nitrate removal implied by these data, of 23% for the mean data set, and 27% for the low-flow set are in good agreement with estimate of riverine denitrification from the literature, within the range of up to 45% nitrogen removal for streams with a depth < 1 metre predicted by Alexander *et al*. (2000), and up to 40% removal found using the *in situ* acetylene block technique (Kemp and Dodds, 2002), though slightly higher than the upper limit of 20% for within reach nitrate removal estimated by Seitzinger *et al*. in a global model (2006). The higher proportional removal during low-flow conditions is to be expected as riverine denitrification rates are optimised by a high ratio of streambed area to water volume and low flow velocity (Alexander *et al.*, 2000, Mulholland *et al.*, 2008) which occur in this river under low-flow conditions.

Table 5.10 Estimates of in-stream nitrate-nitrogen removal rates from the literature (mg NO3-N/ m^2 riverbed/ hour, for comparison with the range found in this study (Sjodin *et al.*, 1997, Laursen and Seitzinger, 2002, Kellman, 2004, Royer *et al.*, 2004, Laursen and Seitzinger, 2005, Hernandez and Mitsch, 2006, Pina-Ochoa and Alvarez-Cobelas, 2006).

Study	**Approach**	**Rate (mg NO3-N/ m^2 riverbed/ hour)**
Sjodin *et al.* (1997)	Mass-balance	2 - 102
Kellman. (2004)	Field tracers and isotopes/ sediment cores	4-15
Royer *et al.* (2004)	Acetylene block (sediment in laboratory)	5-15
Laursen & Seitzinger, (2002)	N_2: Ar ratios	4 - 222
Laursen & Seitzinger, (2005)	Review of 14 studies various methods	0.01 - 147
Hernandez & Mitsch (2005)	Acetylene bloc *in situ* (wetland)	328-778
Pina-Ochoa & Alvarez-Cobelas, (2006)	Meta analysis	10-16
This study	Isotope and solute mass-balance	16-21

One factor not yet addressed is of the proportion of nitrate removal attributed here to denitrification which is in fact due to in-stream biotic assimilation. Pinardi *et al.* (2009) found near equal proportions of nitrate assimilated by macrophytes and removed via denitrification during spring and summer in river sediments, while Mulholland *et al.* (2008) calculated that on average 84 % of in-stream nitrate removal was attributable to assimilation using ^{15}N tracer experiments. Based on these findings, if a significant proportion of nitrate removal occurs in stream we would expect to see a strong seasonal pattern in the Wensum, with lower concentrations coupled with isotopic enrichment in spring and summer, and a weakening of these markers in winter. In addition, we might expect to see increased concentrations of organic N including DON, correlating inversely with the reduction in nitrate concentration seen downstream, which would indicate the export of nitrate removed via assimilation exported in organic form. However, such a pattern is not seen in the data. This implies that the dominant process is denitrification of groundwater, which occurs all year round, supporting the percentage apportionment suggested by the model. The percentages attributed to in-stream assimilation in the literature suggest that that of the 25% nitrate removal apportioned to in-stream denitrification in the Wensum a significant proportion may be due to assimilation.

Figure 5.42 represents the circulation of runoff and valley Chalk groundwater in the sand and gravel deposits below the river during high-flow and low-flow conditions,

which provide a zone of mixing and denitrification of baseflow to the river, with additional denitrification occurring in-stream.

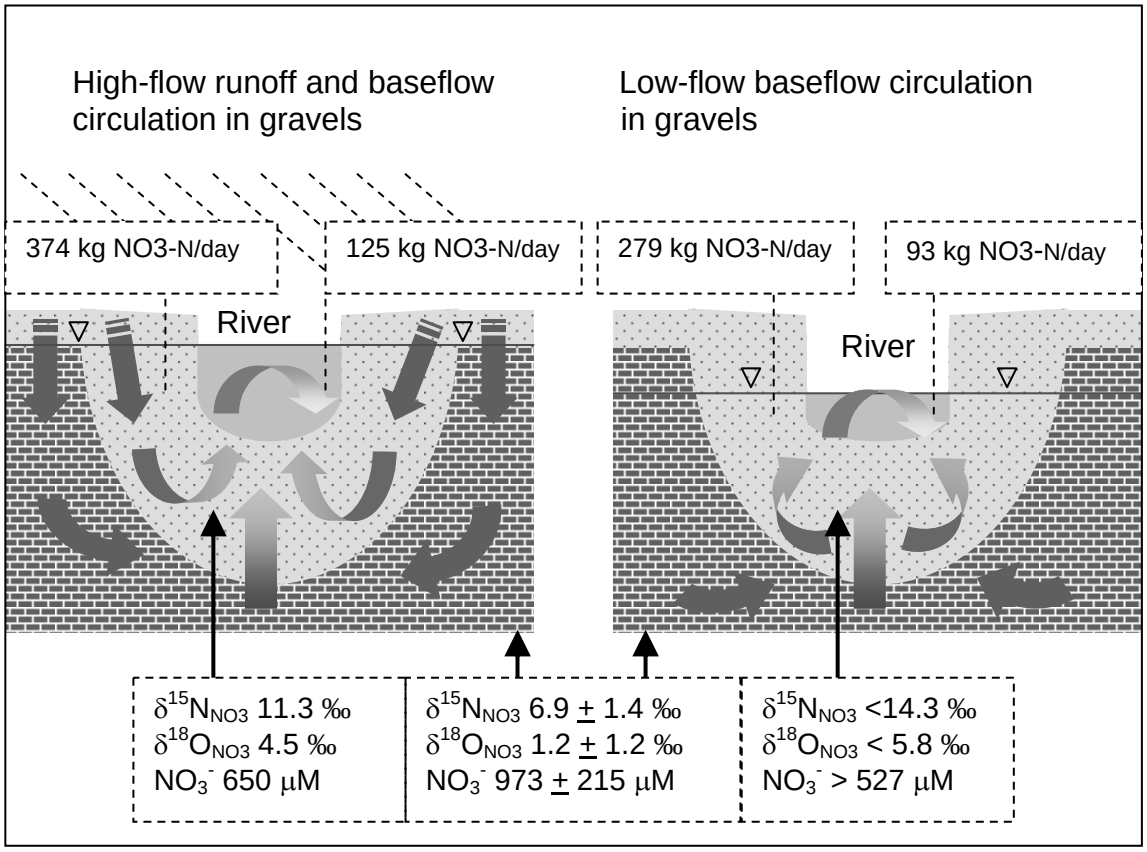

Figure 5.42 Conceptual model of circulation within the sand and gravel hyporheic deposits from runoff and valley Chalk baseflow during high-flow, and valley Chalk baseflow circulation during low-flow conditions in the mid Wensum river, with block arrows denoting in-stream denitrification. Colour gradient from dark to light indicates high to low nitrate concentration resulting from denitrification. Nitrate concentration and isotopic composition of groundwater within sands and gravels is shown, as predicted by model results. Boxes above diagram denote predicted kg NO3-N removal per day in the sands and gravels and the river in the mid river reach.

It is likely that the low-flow calculation provides a more robust estimate of removal rates, as there will be a lower proportional contribution from runoff which may include an element of dilution from the inclusion of high-flow sets in the mean model run. The apportionment between hyporheic groundwater denitrification and riverine denitrification will fall on a mixing line between the low-flow hyporheic and riverine rates (Figure 5.43) with 27% removal of the total nitrate load by Swanton gauging station.

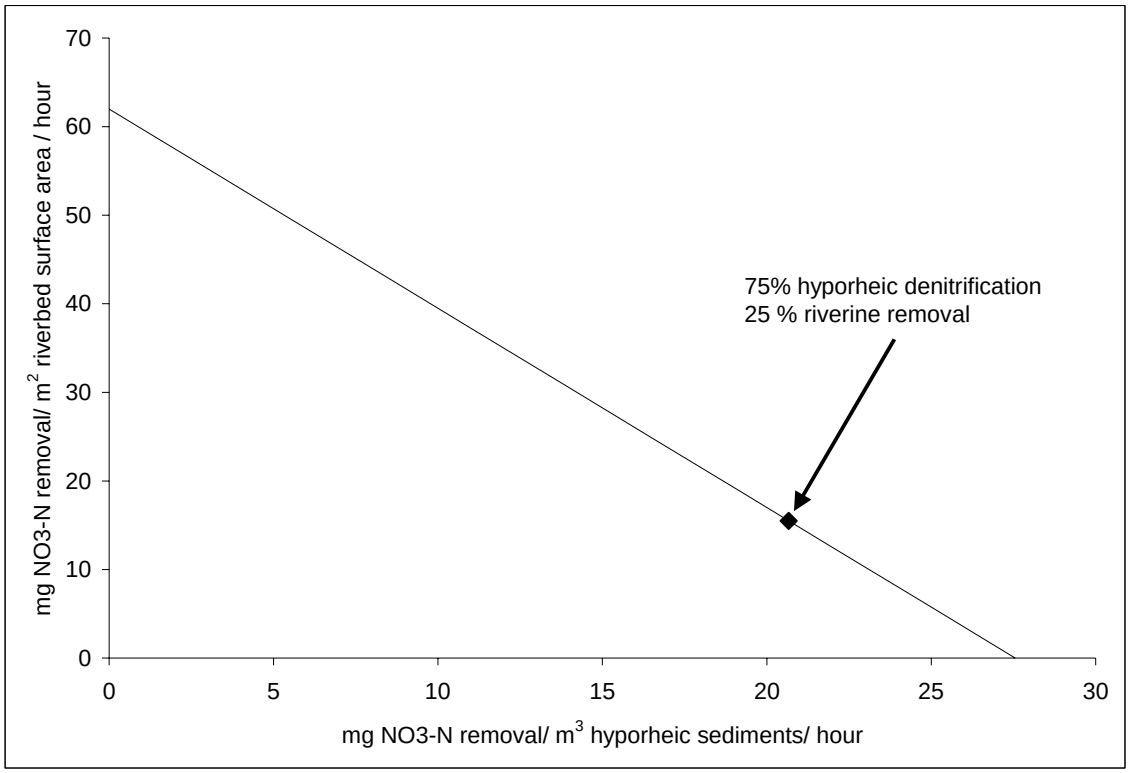

Figure 5.43 Mixing line of estimated denitrification rates from hyporheic denitrification of groundwater (mg NO3-N/m^3/hour) and riverine in-stream removal (mg NO3-N/m^2/hour) under low-flow conditions for the Wensum mid river reach, showing apportionment of 75% to hyporheic and 25% to in-stream removal. 100% in-stream removal gives a rate of 62 mg NO3-N/m^2/hour.

In summary, a four member solute and isotope mass-balance mixing model has elucidated the cause of the decreasing nitrate concentration with isotopic enrichment seen in the Wensum mid river reach. The model suggests that the hydrology of the mid Wensum river comprises a system in which baseflow is supplied from valley Chalk groundwater with high nitrate concentrations, with an increasing proportion of "nitrate free" interfluve Chalk groundwater downstream. Denitrification occurs to the valley Chalk groundwater as it advects up through the deep glacio-fluvial sediments below the riverbed, with additional denitrification in groundwater-fed disused gravel pits adjacent to the river, with an estimated rate of low-flow nitrate-nitrogen removal of 21 mg/m^3/hour and a valley Chalk groundwater residence time in the sediments of 6.5 days. The glacio-fluvial sediments also provide storage and denitrification for runoff during high-flow conditions. Surface accretion from tributaries and drains includes inputs of wastewater effluent, with denitrification along the field-drain-tributary pathway suggested by the concentration and isotopic composition of tributary and drain sample nitrate. Modelled nitrate isotopic composition suggests that denitrification also occurs within the river. The estimated rate of riverine denitrification suggested by the low-flow model is 16 mg/m^2/hour, within the range reported in the literature. The lack

of seasonal differentiation in nitrate removal suggests that a greater proportion of denitrification occurs to the valley Chalk groundwater than that which occurs in-stream, supporting the apportionment of 75% to 25% suggested by the model. Denitrification may be responsible for a reduction in nitrate-nitrogen load of up to 27% by Swanton gauging station during low-flow periods. In all cases, denitrification lowers nitrate concentration and leads to a heavier isotopic composition.

5.4.4 Mid Wensum Individual Sampling Sets

A number of individual data sets from the mid Wensum are worthy of discussion separately. These include samples collected during extreme low-flow conditions in autumn (25/09/2009), the winter data set with mid river reach samples of a high spatial resolution (16/11/2008) and the autosampler data set during winter high-flow conditions (12-13/12/2008).

The extreme low-flow data set (25/09/2009) shows average concentrations of chloride and sulphate at Fakenham followed by very high concentrations at Great Ryburgh and Bintree Mill, dropping off at Billingford and Swanton gauging station, though still at above mean concentrations (Figure 5.44). Nitrate concentrations, in contrast, are very similar to mean concentrations (Figure 5.45). The isotopic composition of nitrate from this data set, however, is slightly differentiated from the mean isotopic composition beyond Fakenham, showing higher $\delta^{15}N_{NO3}$ values than the mean set, causing a lower slope of $\delta^{15}N_{NO3}$ versus $\delta^{18}O_{NO3}$ in the extreme low-flow set between Fakenham and Swanton gauging stations (0.35), than in the mean set (0.57) (Figure 5.46). Together, this suggests a stronger influence of wastewater effluent inputs due to a lower level of dilution within the river than under mean flow conditions, shown in the high concentrations of chloride and sulphate, and the larger than usual difference between $\delta^{15}N_{NO3}$ and $\delta^{18}O_{NO3}$. However, it is interesting that nitrate concentrations are not higher, and that a greater level of isotopic enrichment is not seen downstream which would suggest enhanced in-stream denitrification. This implies a nitrate removal process which does not result in isotopic fractionation. Plant uptake of ammonium appears to result in negligible fractionation (Hubner, 1986), which implies that fractionation from uptake of nitrate may also be negligible. This might account for the nitrate concentration and isotopic composition seen.

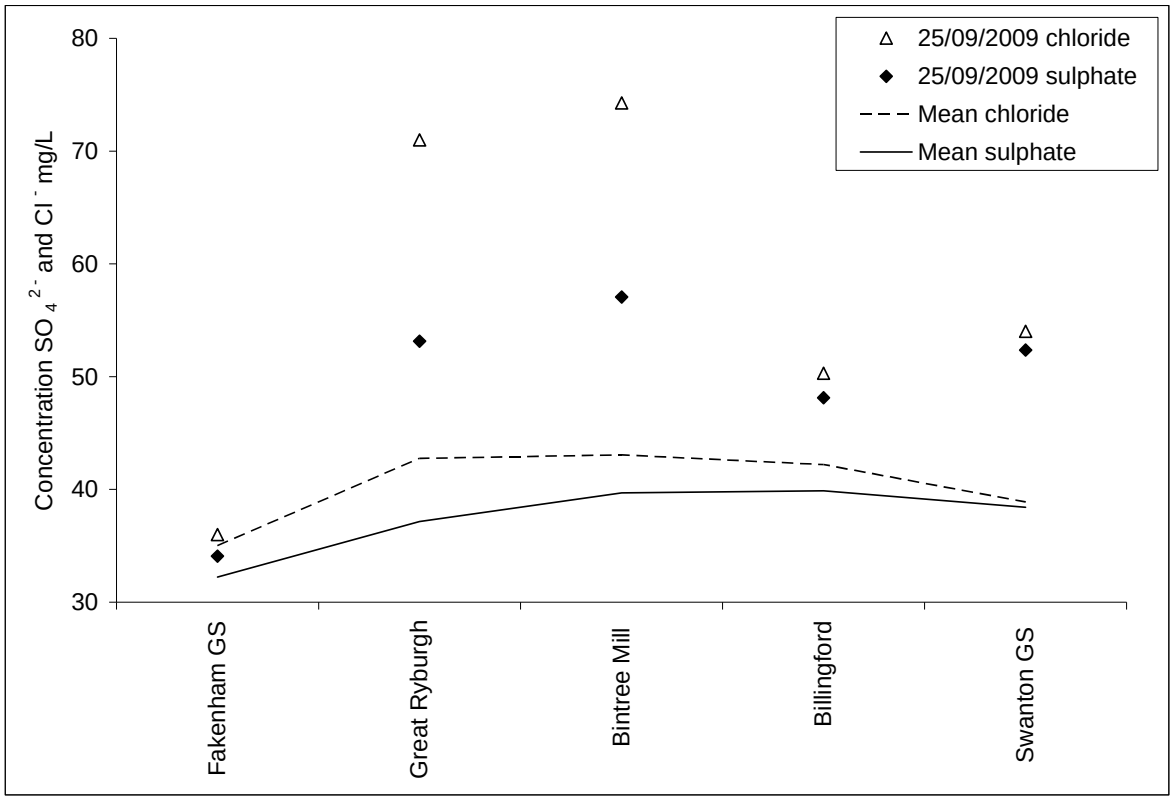

Figure 5.44 Concentration Cl^- and SO_4^{2-} (mg/L) of samples from the mid Wensum river extreme low-flow set (25/09/2009) and mean data set with location.

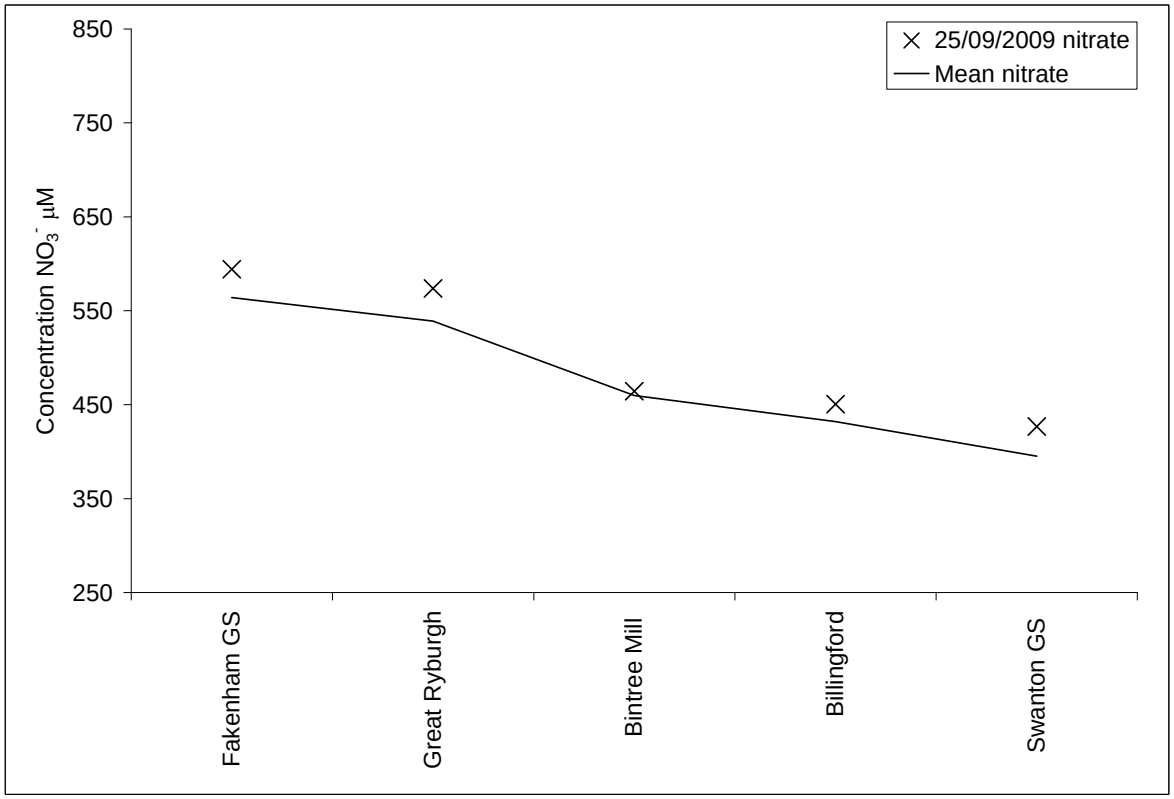

Figure 5.45 Concentration NO_3^- (µM) of samples from the mid Wensum river extreme low-flow set (25/09/2009) and mean data set with location.

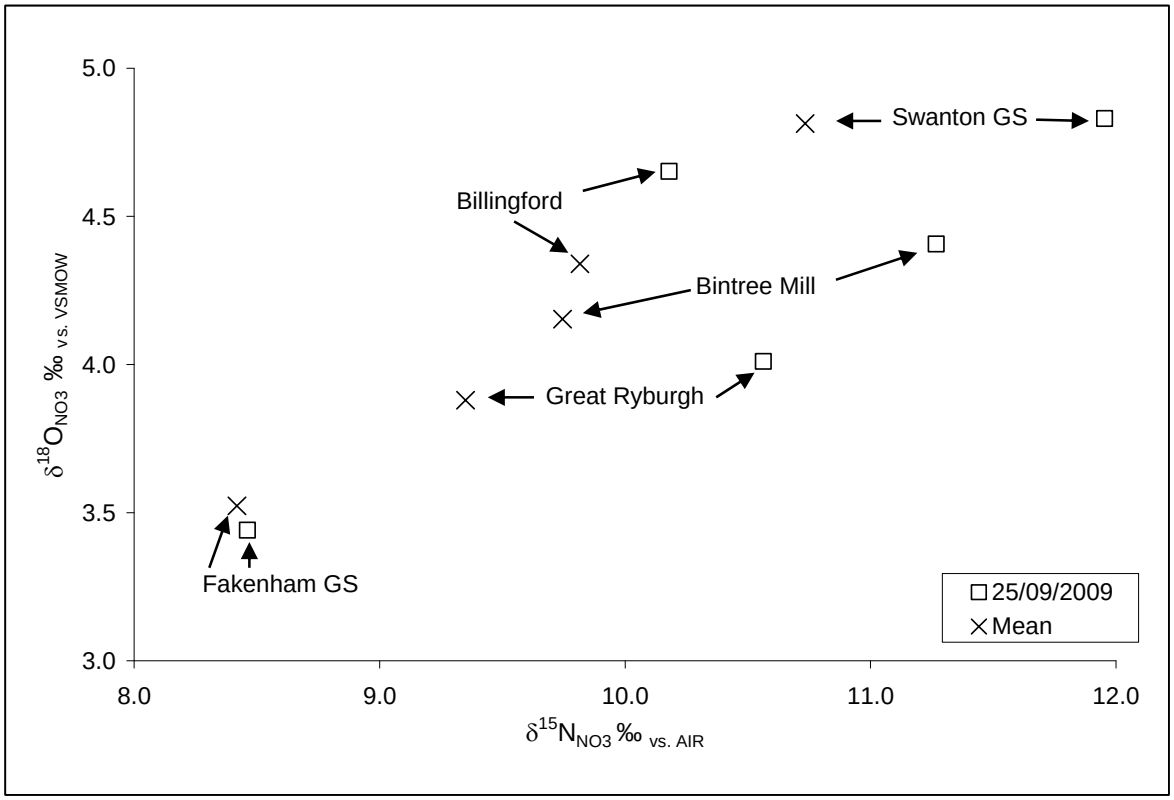

Figure 5.46 $\delta^{18}O_{NO3}$ (‰) versus $\delta^{15}N_{NO3}$ (‰) of samples from the mid Wensum river extreme low-flow set (25/09/2009) and mean data set with arrows indicating location. Error: $\delta^{15}N_{NO3}$ and $\delta^{18}O_{NO3} \pm 0.1$‰.

The mid river reach samples with a high spatial resolution (16/11/2008) include eleven sampling locations from Fakenham to Swanton, as opposed to the five locations sampled in the other data sets (Figure 5.47). Flow conditions on this day had returned to medium flow after a storm peak five days prior to sampling. Concentrations of chloride and sodium show the characteristic large increase between Fakenham and the adjacent sampling location at Fakenham Heath, from valley Chalk groundwater and indirect effluent inputs, as elucidated in the four member solute mixing model (Figure 5.48). This pinpoints more accurately the geographical location of this increase, and therefore, the upstream point at which valley Chalk groundwater baseflow first advects into the river, seen in the other data sets between Fakenham and Great Ryburgh. The ratio of sulphate to chloride at Fakenham Heath gradually changes reaching a ratio at Swanton of 1.1:1, the ratio found in tributary and valley Chalk groundwater samples (Table 5.6).

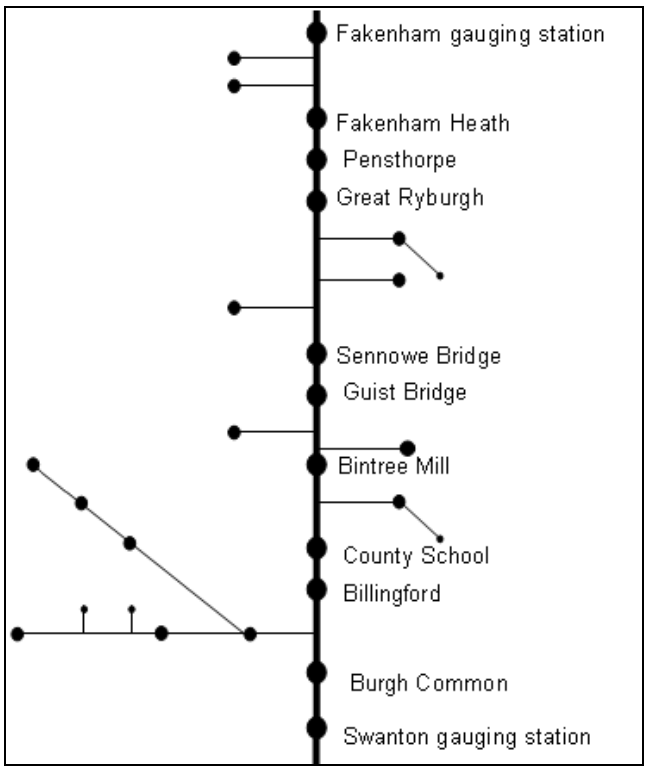

Figure 5.47 Schematic of Wensum mid river sampling locations from 16/11/2008.

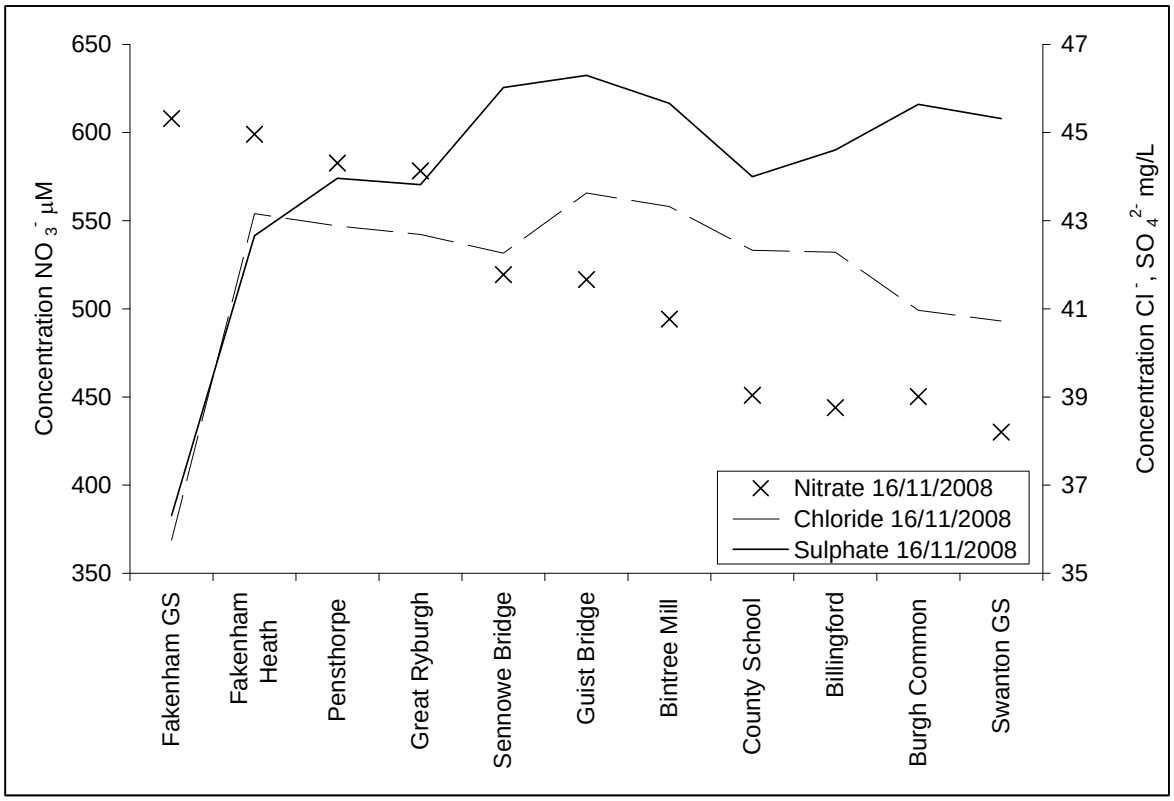

Figure 5.48 Concentration NO_3^- (µM), Cl^- and SO_4^{2-} (mg/L) of samples from the mid Wensum river sampled on 16/11/2008.

Nitrate concentrations through the eleven locations show a stepped rather than incremental decrease, in some locations corresponding increases in concentrations of

chloride which may reflect further valley Chalk groundwater baseflow inputs, for example between Great Ryburgh and Sennowe Bridge. Interestingly, a plot of $\delta^{15}N_{NO3}$ versus $\delta^{18}O_{NO3}$ shows an oscillation between very similar values (some of which are not distinguishable within the measurement error) in two adjacent river reaches; Fakenham Heath to Sennowe Bridge; and Guist Bridge to County School, with clear increases in isotope values from Fakenham gauging station to Fakenham Heath, and from County School through to Swanton gauging station (Figure 5.49). These data shed light on the trend seen in the other data sets, of an incremental decrease in nitrate concentration coupled with an incremental increase in isotope values (Figures 5.29 to 5.31), suggesting here a stronger localised influence of surface water accretion than otherwise seen, which may be due to the effects of the receding storm flow. This is corroborated by evidence of runoff in concentration spikes of phosphate and trace elements seen in river samples on this date (noted in Chapter 4).

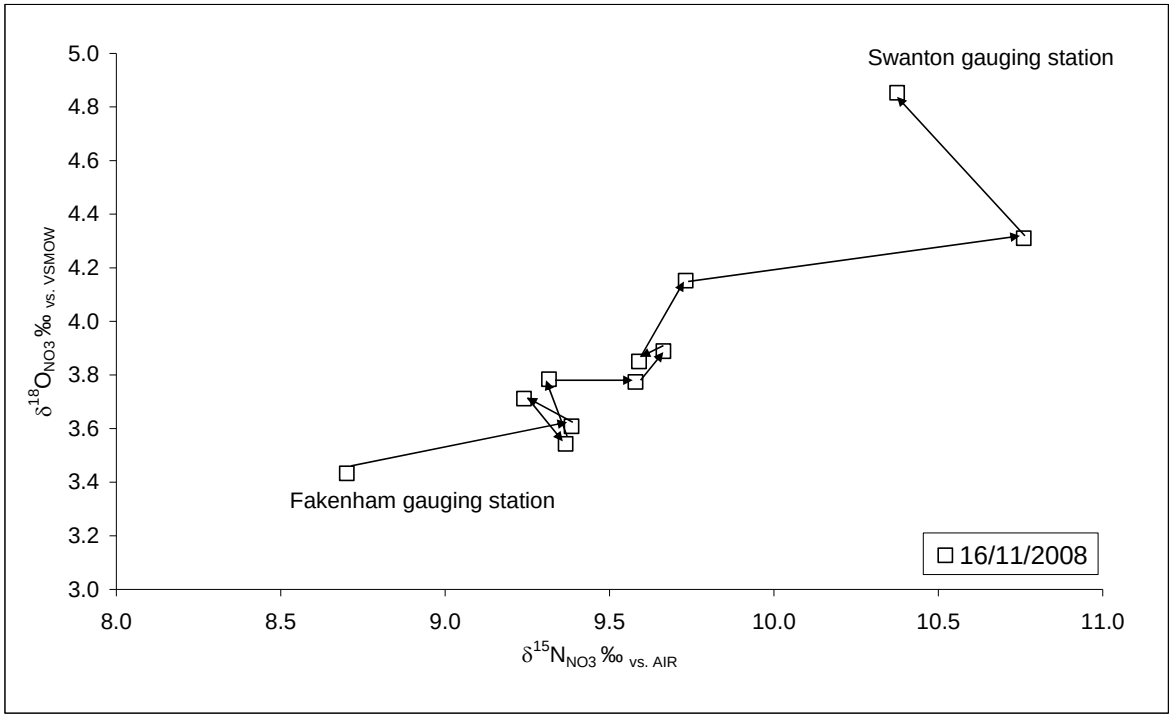

Figure 5.49 $\delta^{18}O_{NO3}$ (‰) versus $\delta^{15}N_{NO3}$ (‰) of samples from the mid Wensum on 16/11/2008 with arrows indicating spatially adjacent samples from Fakenham to Swanton gauging stations. Error: $\delta^{15}N_{NO3}$ and $\delta^{18}O_{NO3}$ $\pm$ 0.1‰.

The autosampler data set collected during winter high-flow conditions (12-13/12/2008) from Fakenham and Swanton gauging stations shows the characteristic overall pattern of higher concentrations of chloride and sulphate at Swanton, with nitrate of a lower concentration and heavier isotopic composition than at Fakenham. The samples from

Fakenham show very stable concentrations of chloride and sulphate over the period, coupled with very stable flow conditions, until the final sample which shows an increase in chloride concentration. Nitrate concentration and isotopic composition also shows very little variation at Fakenham during this period (Figures 5.50 and 5.51). Together this suggests stable sources contributing to flow at Fakenham.

The corresponding samples from Swanton gauging station during the period show a higher variability in solute concentrations and flow, with a higher level of variation in nitrate isotopic composition (Figures 5.52 to 5.54). An increase in concentrations of nitrate and sulphate is seen with a gradual decrease in flow over the first fourteen hours of sampling, with a corresponding decrease in concentrations of chloride. This temporal decoupling of sulphate and chloride is interesting, as the spatial sample sets show them coupled. The pattern seen here shows a gradual change in the ratio of sulphate to chloride, from 0.9 at 20:15 on the 12th December to 1.0 at 12:15 on the 13th, suggesting that during this period there was an alteration in the source of the solutes, and hence, the source of water supplying flow. The ratios suggest a switch from the mean riverine ratio, to that seen in tributaries and drains, and valley Chalk groundwater (Table 5.6). Due to the fact that flow is decreasing at this time, it is more likely that the flow component with an increasing contribution is valley Chalk groundwater, reflecting a stronger influence of baseflow, which here appears to result also in an increase in concentrations of nitrate. This may be due to an element of runoff in the groundwater from the sands and gravel deposits supplying the baseflow leading to an overall higher nitrate concentration. During these hours, the nitrate isotopic composition shows oscillating variation, which may reflect the mix of sources of flow. From 10 a.m. onwards on the 13th, concentrations of the three solutes stabilise, followed by a stabilisation of the nitrate isotopic composition. The final six hours of sampling see a rapid increase in flow which appears to leave solute concentration and nitrate isotopic composition unaffected. This is surprising, as a hydrochemical or isotopic signal from the runoff generating the flow increase might be expected. The fact that this is absent supports the hypothesis of a piston effect during high-flows, of well mixed shallow groundwater sourced from a mix of runoff and valley Chalk groundwater.

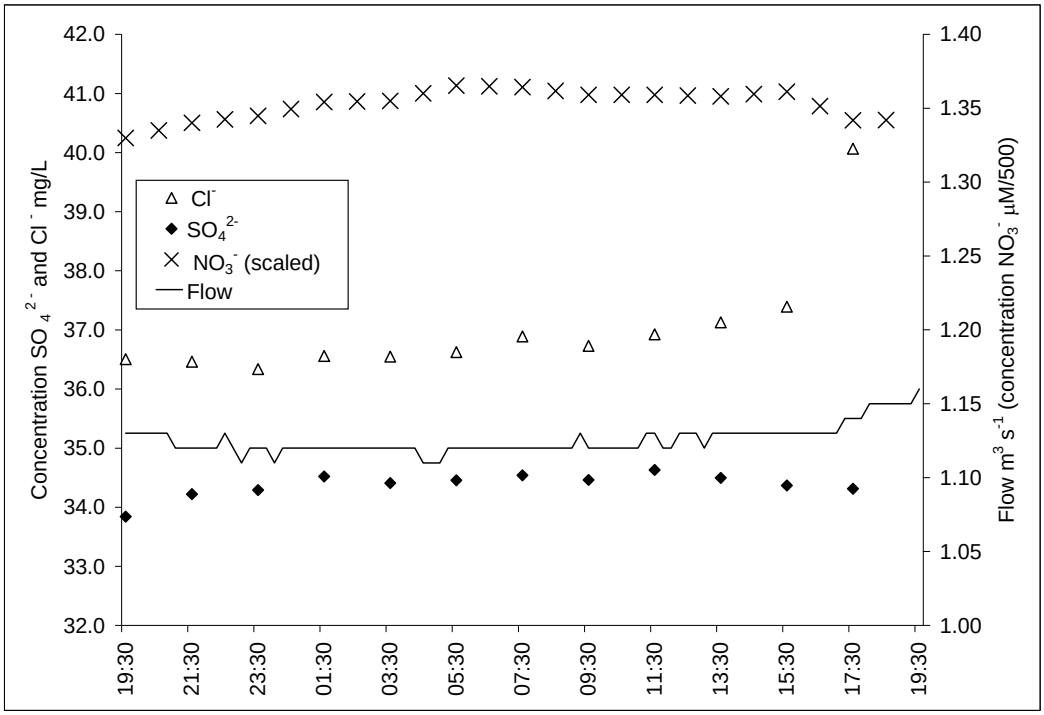

Figure 5.50 Concentration NO_3^- scaled (µM/500), Cl^- and SO_4^{2-} (mg/L) with flow ($m^3\ s^{-1}$) of samples from Fakenham gauging station over a 24 hour period 12-13/12/2008.

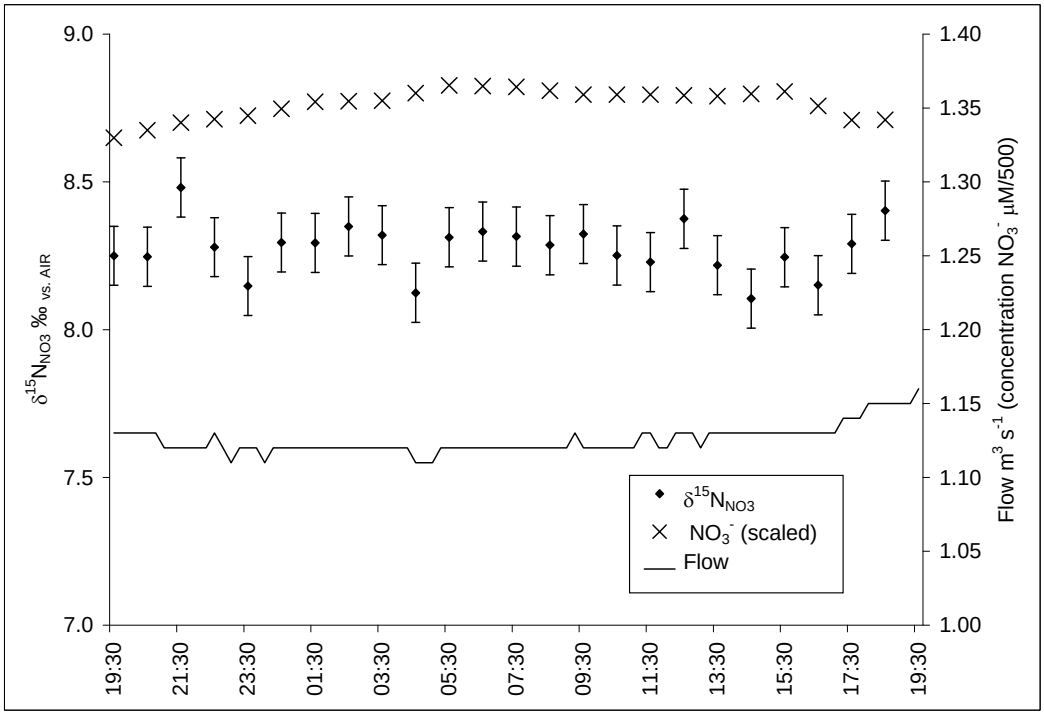

Figure 5.51 $\delta^{15}N_{NO3}$ (‰) and concentration NO_3^- scaled (µM/500), with flow ($m^3\ s^{-1}$) of samples from Fakenham gauging station over a 24 hour period 12-13/12/2008. Error bars show measurement error of $\delta^{15}N_{NO3} \pm 0.1$‰.

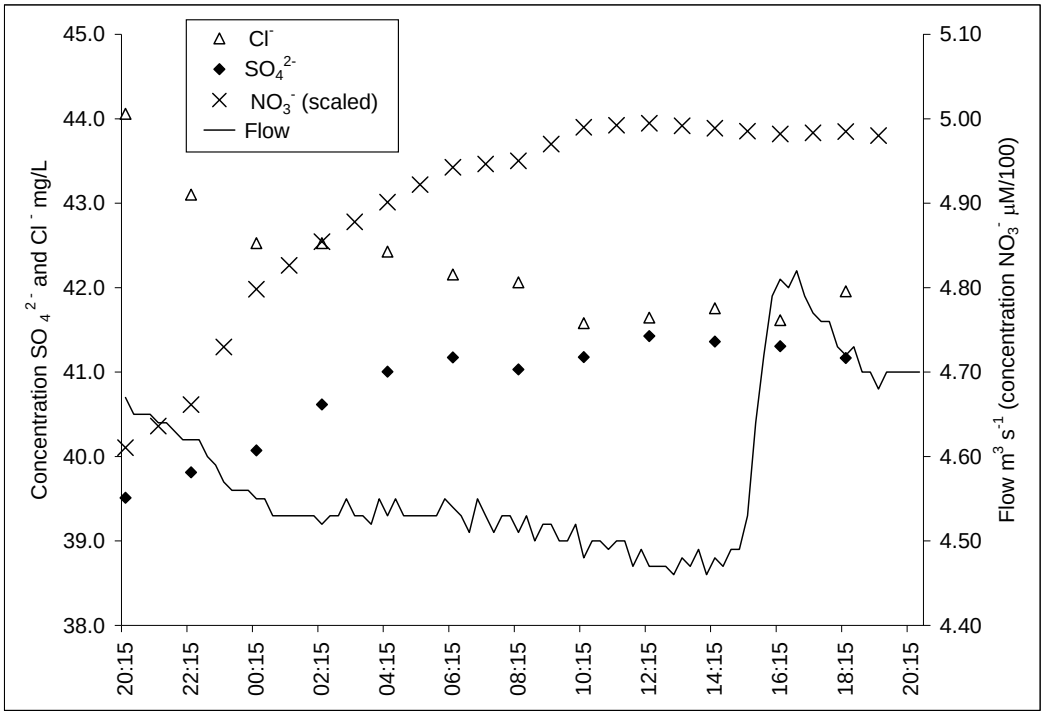

Figure 5.52 Concentration NO_3^- scaled (µM/100), Cl^- and SO_4^{2-} (mg/L) with flow ($m^3\ s^{-1}$) of samples from Swanton gauging station over a 24 hour period 12-13/12/2008.

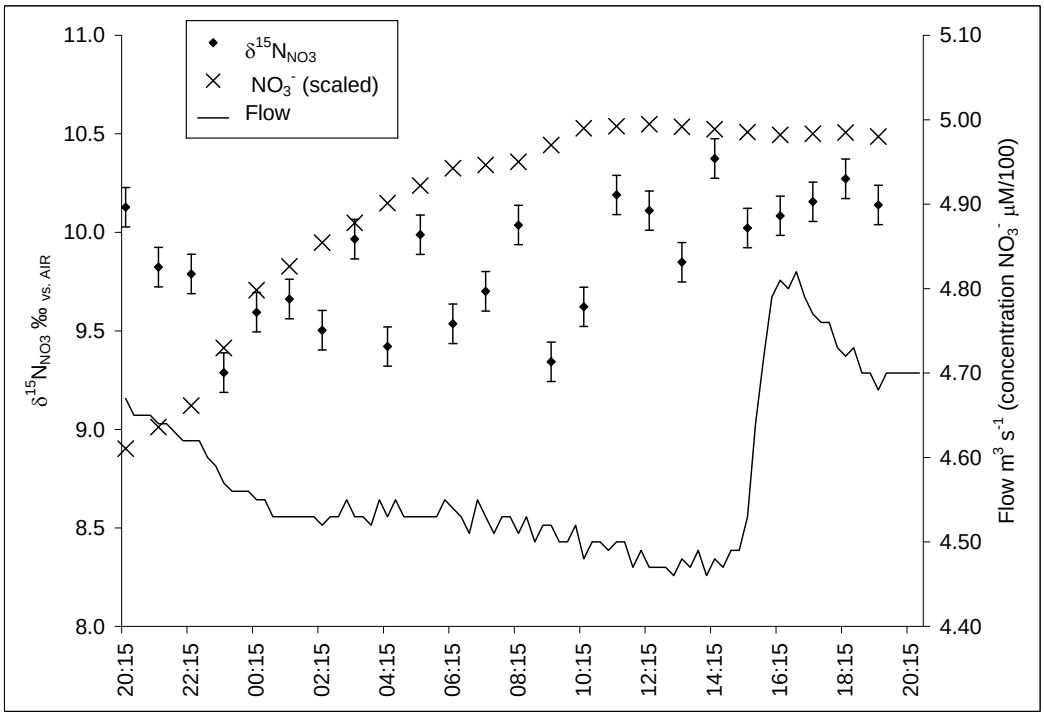

Figure 5.53 $\delta^{15}N_{NO3}$ (‰) and concentration NO_3^- scaled (µM/500), with flow ($m^3\ s^{-1}$) of samples from Swanton gauging station over a 24 hour period 12-13/12/2008. Error bars show measurement error of $\delta^{15}N_{NO3} \pm 0.1$‰.

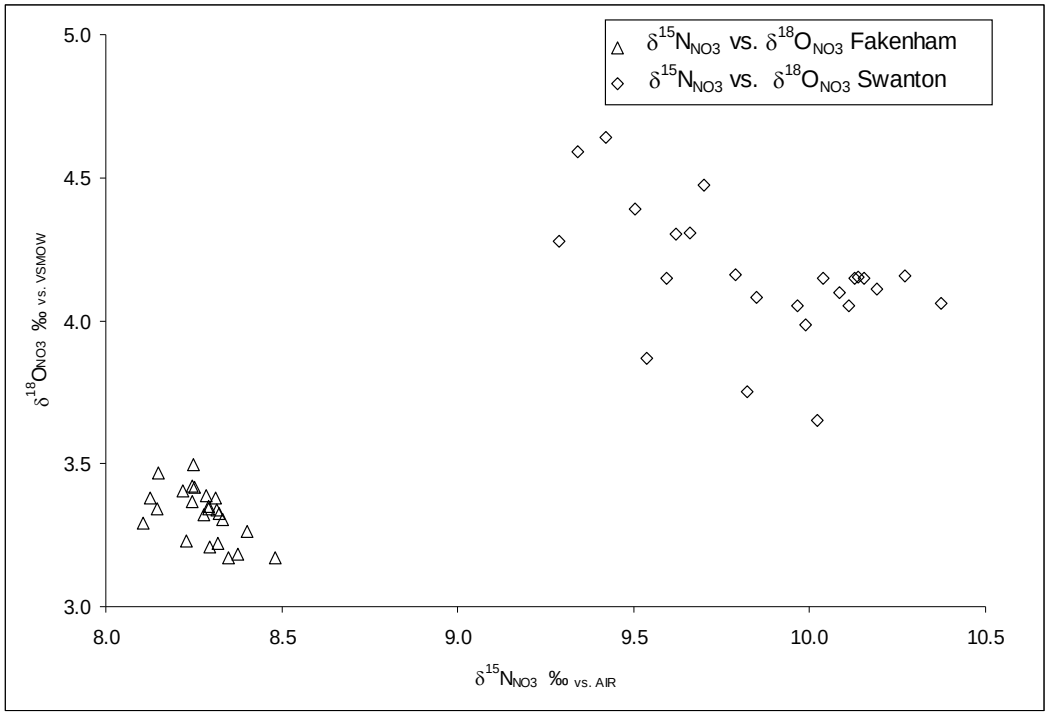

Figure 5.54 $\delta^{18}O_{NO3}$ (‰) versus $\delta^{15}N_{NO3}$ (‰) of hourly samples from Fakenham and Swanton gauging stations 12-13/12/2008. Error $\pm$ 0.1 ‰ for $\delta^{15}N_{NO3}$ and $\delta^{18}O_{NO3}$.

In summary, the sample set from the mid Wensum during extreme low-flow conditions reveals the influence of wastewater effluent in its solute concentrations and nitrate isotopic composition, while the relatively low nitrate concentration might suggest assimilation by aquatic plants. The sample set with a high spatial resolution indicates the uppermost location of valley Chalk groundwater baseflow advection to the river just beyond Fakenham gauging station, and shows a localised influence of surface water accretion in the concentration and isotopic composition of nitrate downstream, which may be due to the effects of receding storm flow. The autosampler data collected from the two mid Wensum gauging stations during high flow show an increase in valley Chalk groundwater as a source of flow to the river at Swanton while flow is decreasing, with a rapid increase in flow not resulting in a change in solute concentrations, indicating a piston effect of well mixed shallow groundwater sourced from a mix of runoff and valley Chalk groundwater.

5.4.5 Mid Wensum Tributaries and Drains

Three tributaries and drains feeding into the mid Wensum were sampled on a number of occasions, enabling a comparison of samples for temporal change with flow condition

or season. These include Fakenham drain, Great Ryburgh drain, and the Wendling Beck at Worthing. In addition, one sample set comprises samples from the southern catchment Wendling Beck and Blackwater tributaries during spring low-flow conditions (27/05/2009).

Fakenham drain was sampled on seven occasions and shows a stable, high nitrate concentration (606 $\pm$ 70 μM NO_3^-) and an isotopic composition which suggests it is the product of nitrification ($\delta^{15}N_{NO3}$ 7.5 $\pm$ 0.2 ‰; $\delta^{18}O_{NO3}$ 3.1 $\pm$ 0.3 ‰). These samples have concentrations of chloride, sulphate and sodium approximately 60% higher than the riverine means. The stream drains a wetland area backing on to an industrial site, and it is possible that high solute concentrations reflect a contaminant source, while the nitrate isotopic composition and homogeneity implies that nitrate inputs to the drain are controlled by nitrogen cycling within the wetlands.

Great Ryburgh drain was sampled on four occasions, showing low to very low nitrate concentrations with heavy isotopic composition (Figure 5.55). This is a small drain which, when the autumn sample was collected, was overgrown with vegetation, although water was still flowing in it. Thus it would be expected that the very low nitrate concentration (38 μM NO_3^-) and isotopic composition ($\delta^{15}N_{NO3}$ 14.0 ‰; $\delta^{18}O_{NO3}$ 3.6 ‰) of this sample reflects nitrate assimilation. In fact, nitrogen and oxygen isotopes do not appear to have been fractionated in tandem, as would be expected during assimilation, as the sample has a heavy $\delta^{15}N_{NO3}$ value with a light $\delta^{18}O_{NO3}$ which is within the range expected for nitrification of ammonium. It is possible that this isotopic composition reflects nitrogen cycling within the drain including remineralisation of organic nitrogen to ammonium and nitrification. The remaining three samples show a coupled isotopic enrichment with relatively low nitrate concentrations which could reflect the effects of nitrate assimilation and denitrification.

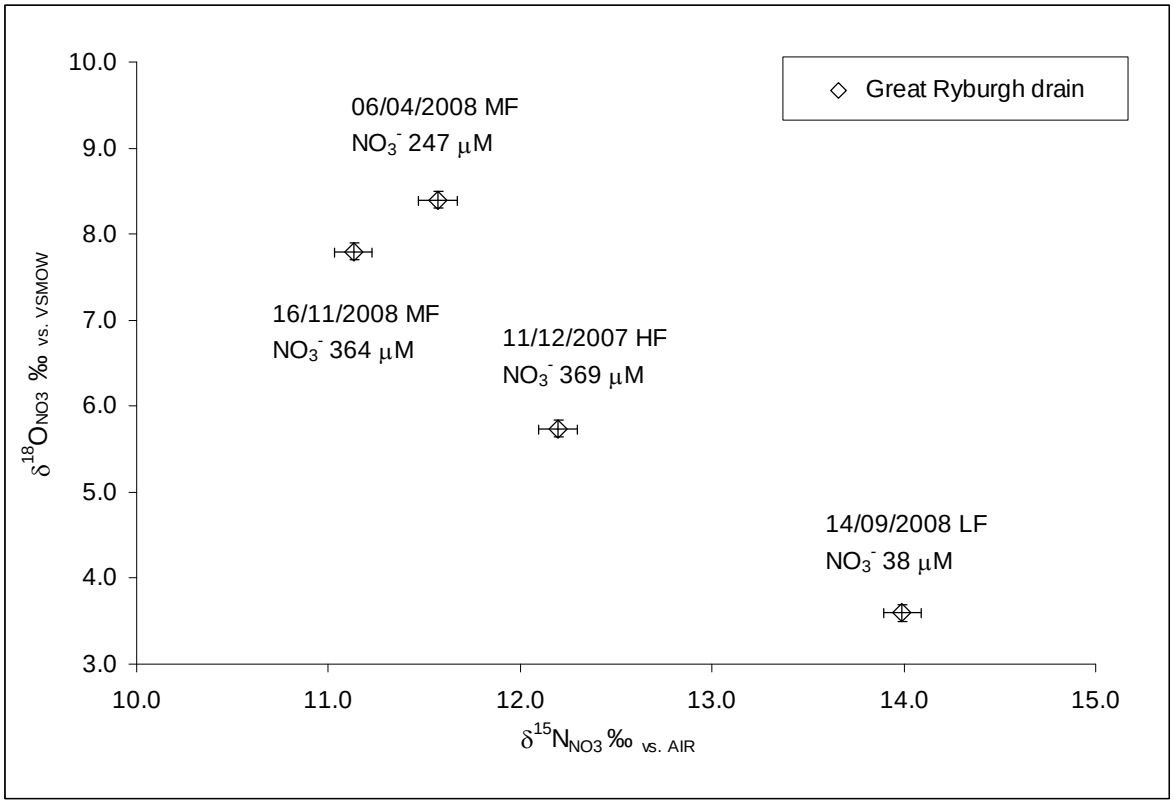

Figure 5.55 $\delta^{18}O_{NO3}$ (‰) versus $\delta^{15}N_{NO3}$ (‰) of samples from the Great Ryburgh drain showing sampling date, flow condition and nitrate concentration. Error bars represent measurement error of $\pm$ 0.1 ‰ for $\delta^{15}N_{NO3}$ and $\delta^{18}O_{NO3}$.

The Wendling Beck carries effluent from the large wastewater works at Dereham to the Wensum river, converging downstream from Worthing at a location upstream of Swanton gauging station. Worthing was sampled seven times. Interestingly, the samples show a mean nitrate concentration slightly lower than the riverine mean (422 versus 475 μM NO_3^-) with a heavy isotopic composition ($\delta^{15}N_{NO3}$ 13.7 $\pm$ 2.0 ‰; $\delta^{18}O_{NO3}$ 5.8 $\pm$ 0.6 ‰). The oxygen isotopic composition of this nitrate is heavier than that expected from nitrification of ammonium in wastewater ($\delta^{18}O_{NO3}$ 2.8 to 3.8 ‰), suggesting that it reflects the effects of uptake and denitrification, which would also explain the relatively low nitrate concentration. Concentrations of chloride, sulphate and sodium in the Wendling Beck samples are only slightly higher than the riverine means, suggesting that in addition to denitrification, some dilution of wastewater effluent has occurred. Denitrification may have occurred in-stream or within the wastewater treatment works after nitrification of ammonium had taken place (Anisfeld *et al.*, 2007). The effluent discharge occurs approximately eight km before the confluence with the Wensum, meaning that dilution from accretion, and in-stream uptake and denitrification are likely. Although all samples have a heavy isotopic composition, there is some flow-related

differentiation (Figure 5.56). The three samples with the heaviest nitrate isotopic composition are from the low and extreme-low-flow sets (spring and autumn), with the two low-flow samples showing a relatively low nitrate concentration. This suggests enhanced uptake and denitrification during low-flow conditions. This is also likely to be the case in the extreme low-flow sample, which may show a higher nitrate concentration due to reduced dilution on that date. In contrast, the three samples with the lightest isotopic composition and highest nitrate concentration are from high and medium flow sets in winter and spring, indicating either a reduced uptake and denitrification efficiency, or the effect of additional nitrate inputs of a high nitrate concentration and lighter isotopic composition from runoff. The high-flow sample from 18/07/2007 collected after a period of flooding shows a lower nitrate concentration, with a relatively high oxygen isotope value, which could indicate both dilution and uptake with denitrification.

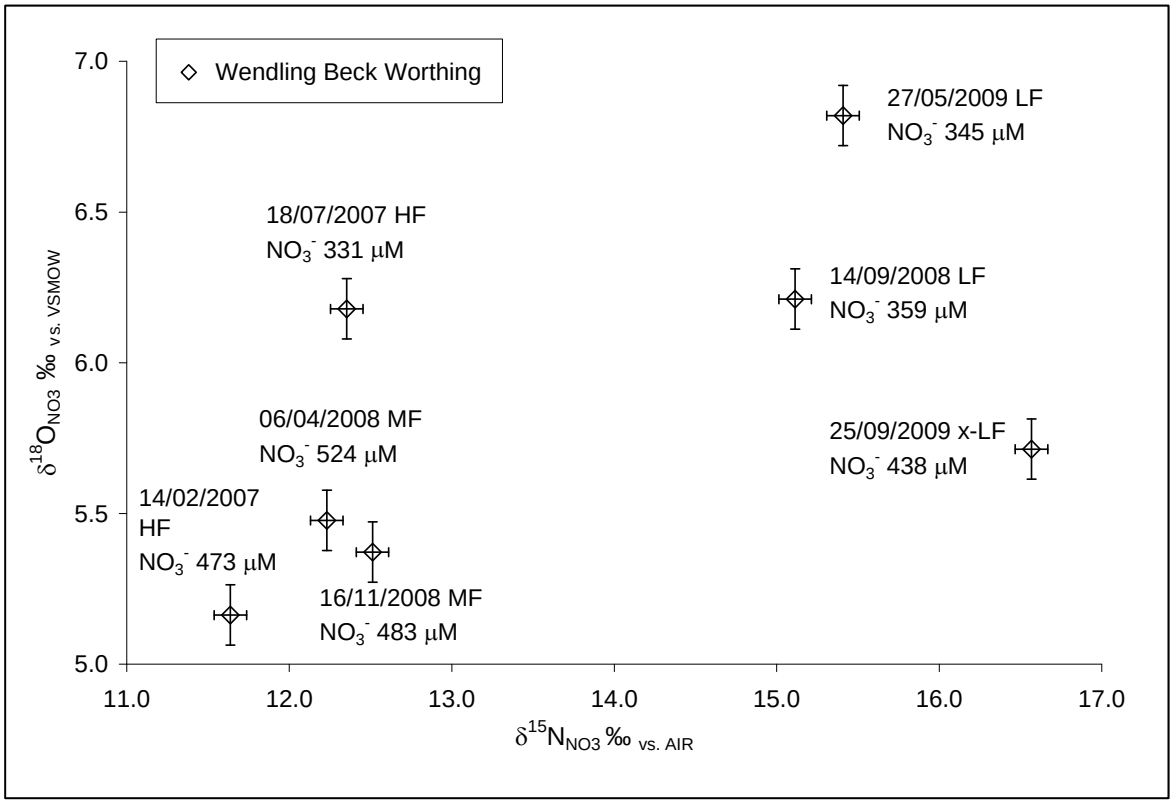

Figure 5.56 $\delta^{18}O_{NO3}$ (‰) versus $\delta^{15}N_{NO3}$ (‰) of samples from the Wendling Beck at Worthing showing sampling date, flow condition and nitrate concentration. Error bars represent measurement error of $\pm$ 0.1 ‰ for $\delta^{15}N_{NO3}$ and $\delta^{18}O_{NO3}$.

The southern catchment samples from three locations upstream from Worthing on the Wendling Beck during spring low-flow conditions (27/05/2009) show a relatively low

nitrate concentration with a heavy isotopic composition (Figure 5.57). This tributary receives the effluent from the Dereham works upstream from the first sampling location at Old Brigg. The heavy nitrogen isotopic composition could result from an effluent source, but if this is the case, the heavy oxygen isotopic composition suggests that subsequent isotopic fractionation from denitrification or assimilation has lead to enrichment of both isotopes. This would also account for the relatively low nitrate concentrations. However, within the reach sampled (approximately seven km) there does not appear to be a downstream trend of removal in the evolution of nitrate concentration and isotopic composition. An alternative explanation is that during these low-flow conditions baseflow is the predominant source of water to Wendling Beck, and that the nitrate isotopic composition and concentration represents that of baseflow, and that the isotopic composition of nitrate here reflects a mix of groundwater and wastewater effluent. This area of the southern catchment has extensive sand and gravel deposits (Moseley *et al.*, 1976) which could provide a large capacity for groundwater storage and denitrification. An effluent source mixing with a partially denitrified baseflow source would have the effect of raising nitrate concentrations and lowering $\delta^{18}O_{NO3}$ values relative to $\delta^{15}N_{NO3}$ values, the level of this effect dependent on the mass balance of the two sources. The overall relationship between $\delta^{18}O_{NO3}$ and $\delta^{15}N_{NO3}$ observed across catchment waters can be used to determine if the $\delta^{18}O_{NO3}$ of Wendling Beck samples is anomalously low, which would indicate the influence of wastewater effluent on its isotopic composition. The equation of the best fit line from the plot of $\delta^{15}N_{NO3}$ versus $\delta^{18}O_{NO3}$ of all Wensum catchment samples (Figure 5.6) used to predict the $\delta^{18}O_{NO3}$ value with a corresponding $\delta^{15}N_{NO3}$ value of $\delta^{15}N_{NO3}$ 15.8 ‰ (seen in the Wendling Beck) gives a value of $\delta^{18}O_{NO3}$ of 7.3 ‰ (non-weighted data) to 8.2 ‰ (equal groundwater and surface water weighted data), indicating that the measured value of $\delta^{18}O_{NO3}$ of 6.6 ‰ is lower than predicted, possibly reflecting the effect of a mixing in of effluent nitrate. The ratio of sulphate to chloride in this reach is close to 1 so does not reflect the expected ratio from an effluent source, though concentrations are approximately 20% higher than mean riverine concentrations which could reflect the influence of wastewater effluent.

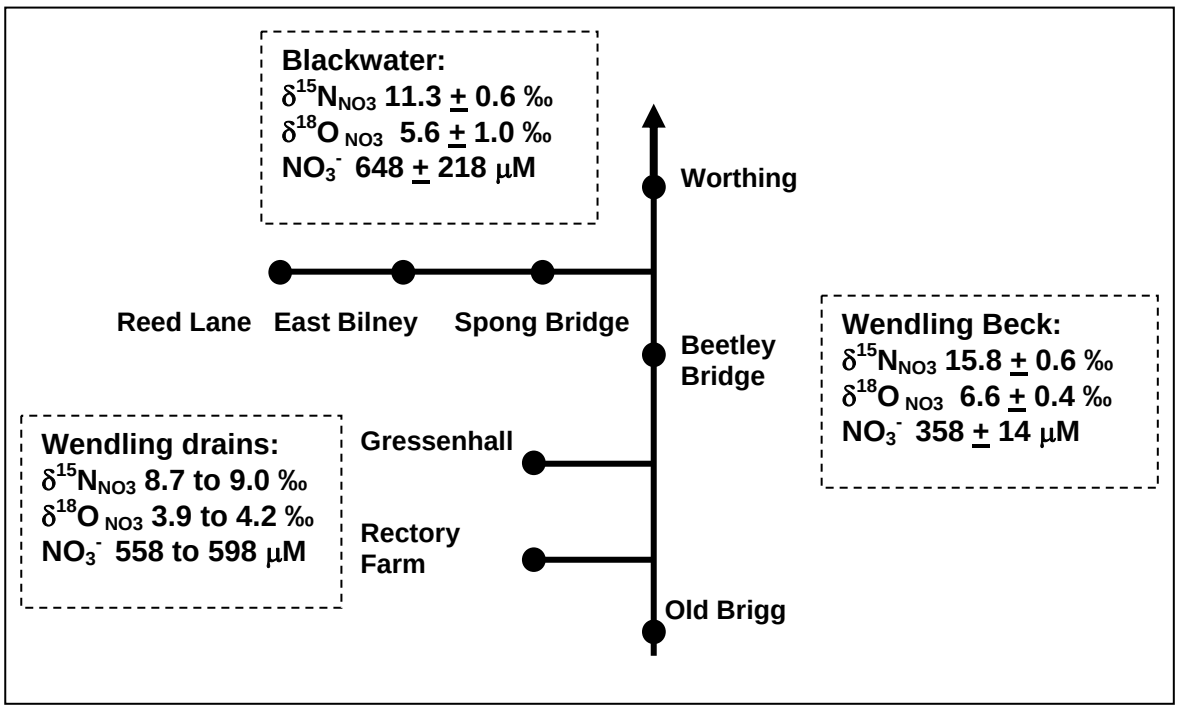

Figure 5.57 Schematic of southern Wensum catchment tributaries and drains with inset boxes showing mean nitrate concentration and isotopic composition of the Wendling Beck, its drains, and the Blackwater.

The two drains feeding into the Wendling Beck between Old Brigg and Beetley Bridge have a higher nitrate concentration with a lower isotopic composition (Figure 5.57). The effect of the mixing in of this nitrate is seen in a slight increase in nitrate concentration between Old Brigg and Beetley Bridge, with a slight lightening of isotopic composition (Old Brigg $\delta^{15}N_{NO3}$ 16.4 ‰; $\delta^{18}O_{NO3}$ 6.9 ‰; 357 μM NO_3^-; Beetley Bridge $\delta^{15}N_{NO3}$ 15.5 ‰; $\delta^{18}O_{NO3}$ of 6.2 ‰; 372 μM NO_3^-).

The Blackwater tributary, which joins the Wendling Beck prior to its convergence with the Wensum, shows a high nitrate concentration with a fairly heavy nitrate isotopic composition. Across the three sampling locations a trend of rapidly decreasing nitrate concentration is seen with a slight lightening of isotopic composition (Figure 5.58), along with increasing concentrations of chloride and sulphate. This suggests a mixing of shallow groundwater. The original high nitrate concentration at Reed Lane is interesting as the isotope values are also high. This implies that isotopic enrichment due to denitrification or assimilation has already occurred, with the implication that the original source of nitrate was of a considerably higher concentration.

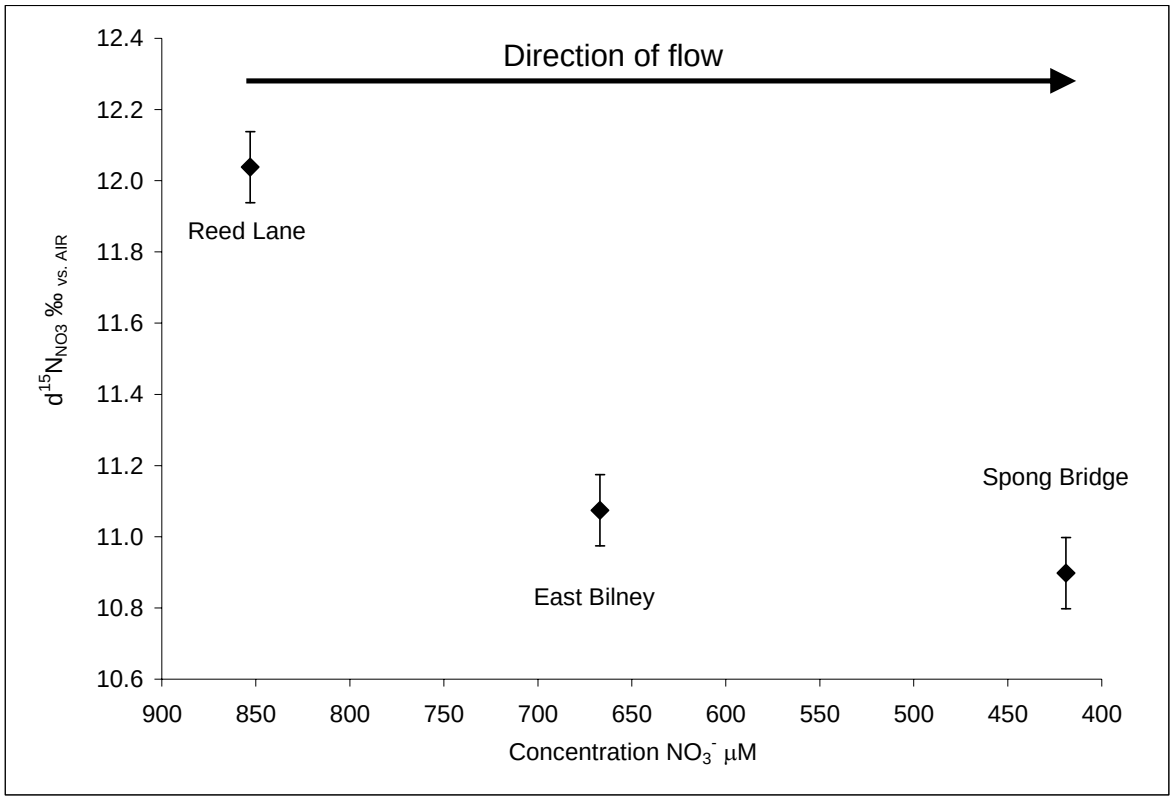

Figure 5.58 $\delta^{15}N_{NO3}$ (‰) versus concentration NO_3^- (µM) of samples from the Blackwater. Note reverse direction of scale of x axis in order that direction of flow can be shown from left to right in agreement with Figure 5.57. Error bars represent measurement error of $\delta^{15}N_{NO3} \pm 0.1$‰.

In summary, there are major differences in the level of variation in nitrate concentration and isotopic composition seen in the tributaries and drains in the mid Wensum. Fakenham drain shows the influence of a wetland area on the stability of nitrate concentration and isotopic composition reaching the drain, while nitrate from Great Ryburgh drain suggests the effects of remineralisation of organic nitrogen and assimilation. The nitrate concentration and isotopic composition in the Wendling Beck reflects the effects of uptake, denitrification and dilution, and the influence of partially denitrified baseflow mixing with effluent from a major wastewater works, while in the Blackwater tributary nitrate concentration and isotopic composition indicate the effects of denitrification or assimilation and mixing of shallow groundwater.

5.4.6 Lower Wensum River

The lower Wensum river reach between Swanton gauging station and Costessey Mill gauging station has a mean proportional flow increase of 60% by Costessey. Of the six data sets containing samples from both gauging stations, three data sets show a concentration decrease between the two locations (extreme low-flow autumn; low-flow

spring; high-flow summer), and three show a minor increase (low-flow autumn; medium flow spring; high-flow winter). Thus there is no clear seasonal or flow related trend in nitrate concentration in this reach (Figure 5.59). Most data sets have a fairly stable nitrate isotopic composition across the lower Wensum locations (Figures 5.60 to 5.62). In the lower river reach, there is no consistent trend in concentrations of chloride, sulphate, and sodium between the two gauging stations (Appendix 3).

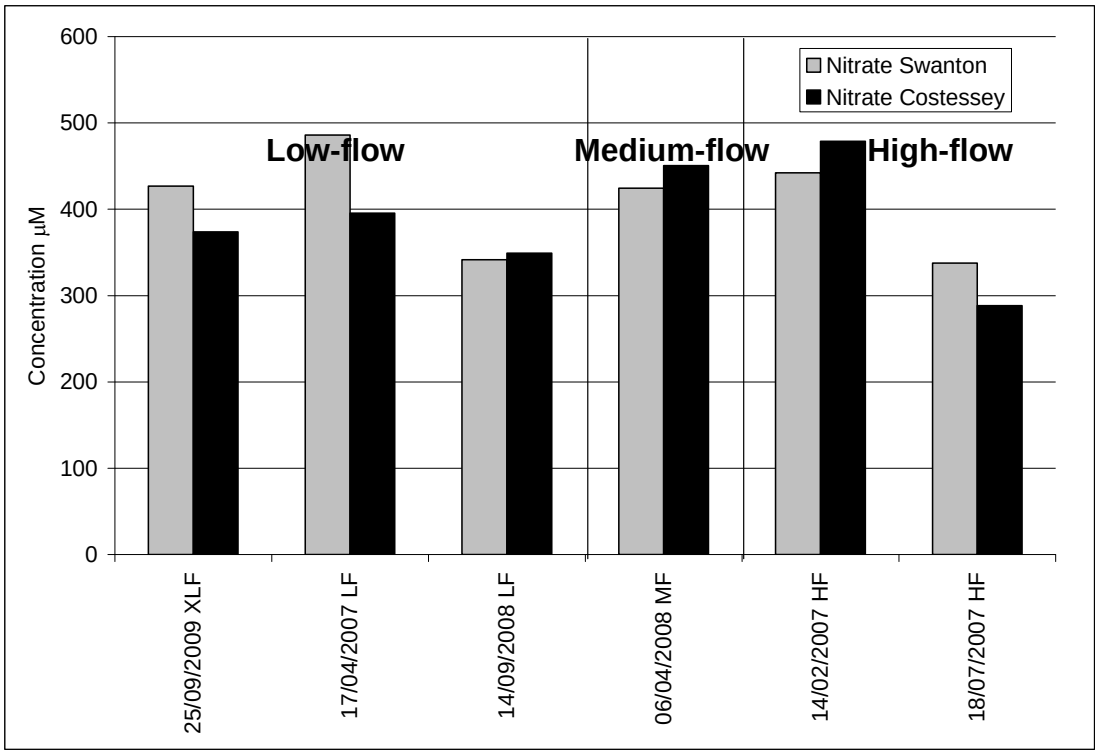

Figure 5.59 Concentration NO_3^- (µM) of samples from the mid Wensum gauging station at Swanton and the lower Wensum gauging station at Costessey for individual data sets. Labels include flow conditions.

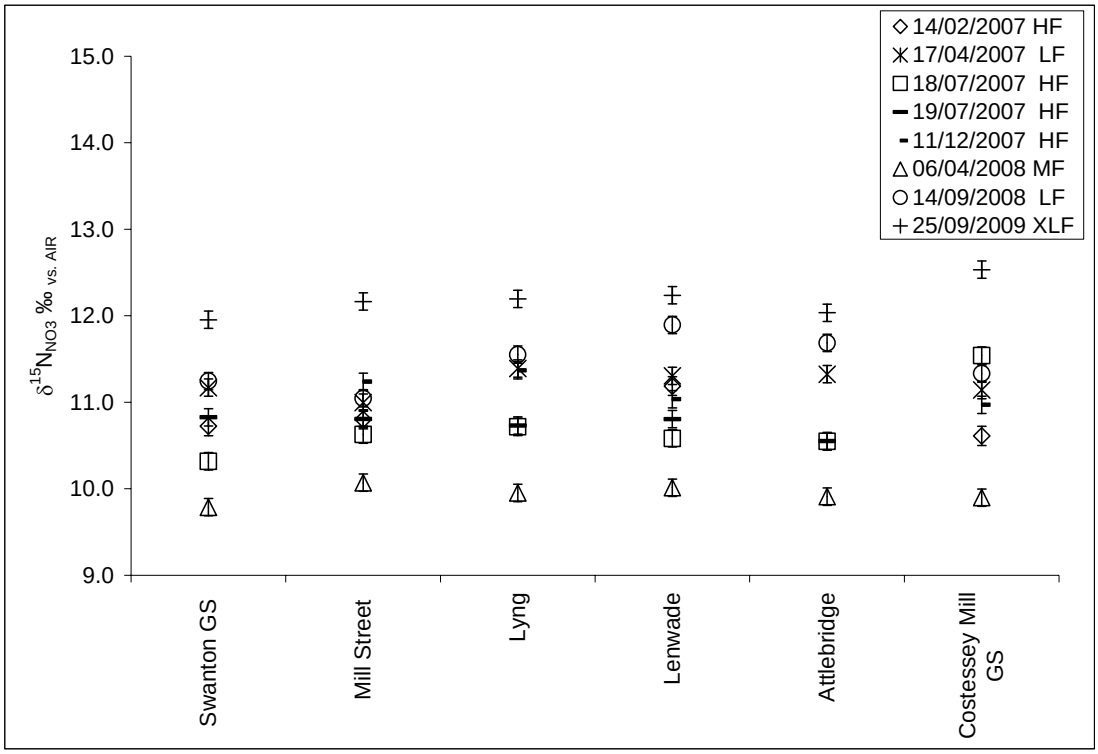

Figure 5.60 $\delta^{15}N_{NO3}$ (‰) of samples from the lower Wensum river showing individual data sets with location. Legend includes flow conditions. Measurement error ($\pm$ 0.1 ‰) is represented by error bars.

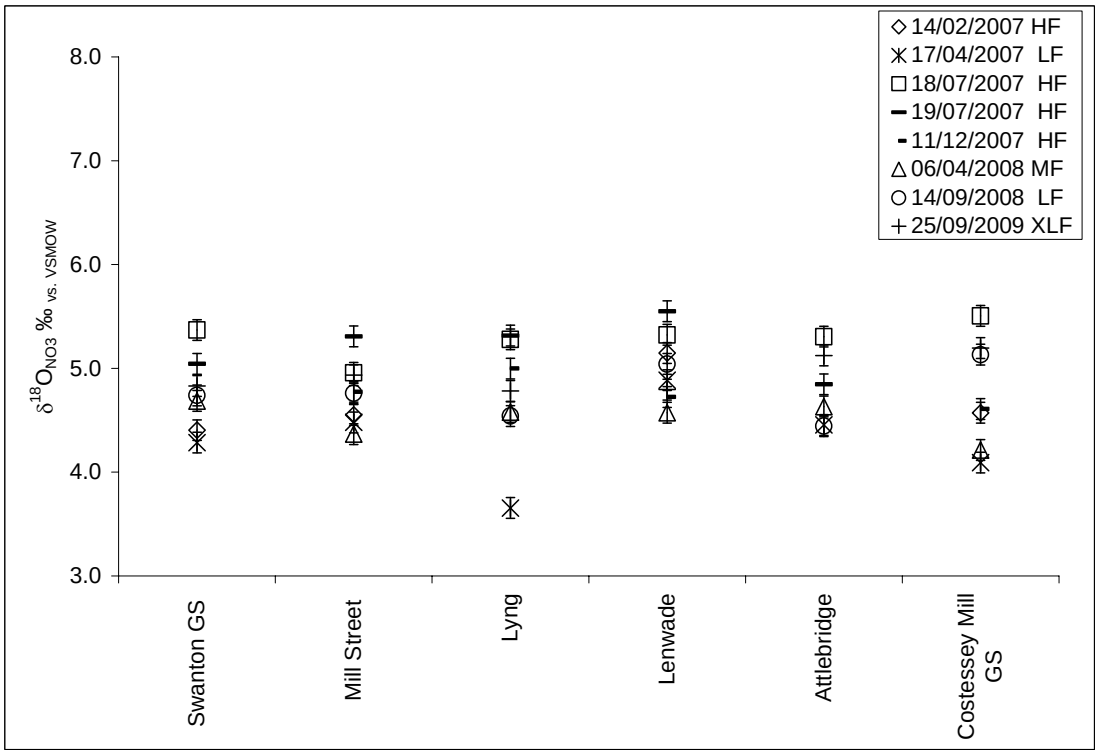

Figure 5.61 $\delta^{18}O_{NO3}$ (‰) of samples from the lower Wensum river showing individual data sets with location. Legend includes flow conditions. Measurement error ($\pm$ 0.1 ‰) is represented by error bars.

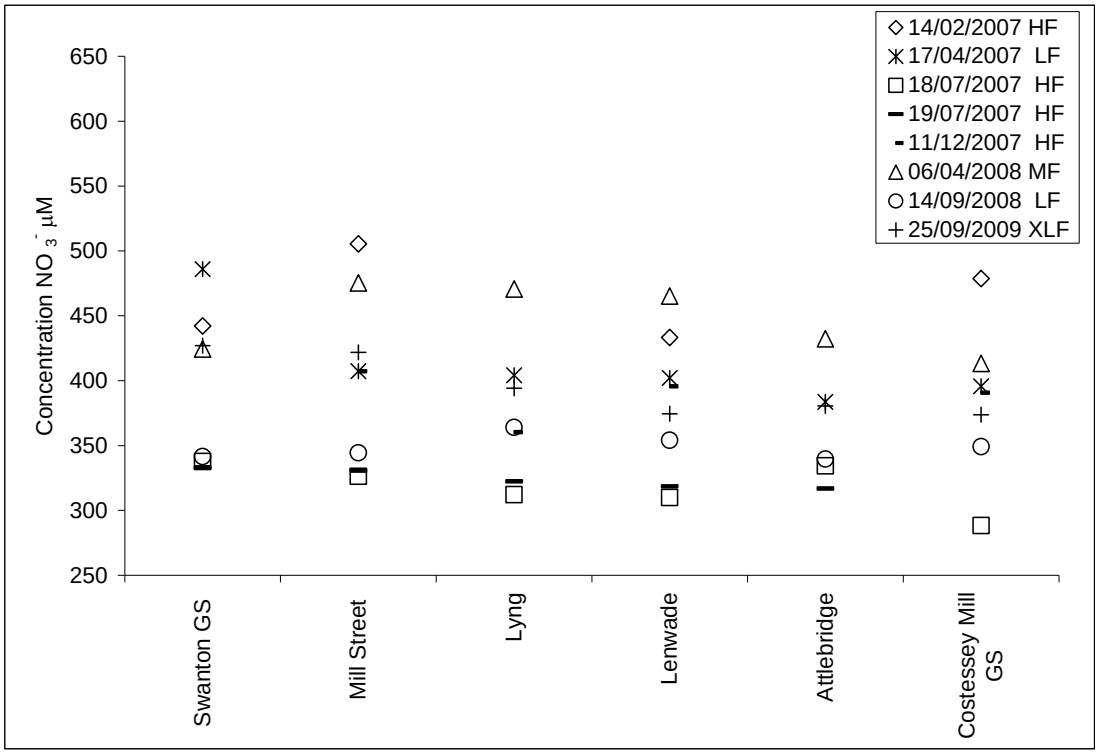

Figure 5.62 Concentration NO_3^- (µM) of samples from the lower Wensum river showing individual data sets with location. Legend includes flow conditions.

The six locations in the lower reach were modelled using the four member mass-balance mixing model adapted to represent the lower Wensum, for mean and mean low-flow conditions. For this, a baseflow index of 0.74 was used to represent the lower Wensum, and the mean tributary and drain solute concentrations and nitrate isotopic composition were recalculated to include the lower river tributaries. The model was calibrated to chloride concentrations by altering the proportion of valley Chalk groundwater to interfluve Chalk groundwater as before. Surprisingly, the relative proportions of valley Chalk groundwater baseflow to interfluve baseflow were 0.95: 0.05 for the mean run, and 0.75: 0.25 for the low-flow mean run. These relative proportions found by the model in the lower Wensum greatly favour valley Chalk groundwater in comparison to the mid river reach which found a ratio of 0.55:0.45 in the mean model run, and 0.65:0.32 in the low-flow model run. A possible explanation could be that the river corridor is wider in the lower Wensum, forming a larger area of exposed Chalk in the valley (Moseley *et al.,* 1976), which results in a greater distance between the river and the interfluves and may lead to an increased valley Chalk groundwater component of baseflow in this reach. Additionally this difference could be an artefact of the model caused by the model's dependence on chloride concentrations which may not be well

represented for the tributary and drain component in the lower Wensum as fewer tributary and drain sampling locations were selected in this reach.

The mean model run for the lower Wensum reproduced concentrations of chloride and sodium well, with a minor overestimation of sulphate at Mill Street and Lyng. This could be attributable to wastewater input from the works at Bylaugh, upstream from Mill Street influencing the sulphate to chloride ratio at these locations. As expected, nitrate concentrations were overestimated when using the mean valley Chalk groundwater nitrate concentration of 973 μM (Figures 5.63a-d). In order for nitrate concentrations to be reproduced, a valley Chalk groundwater nitrate concentration of 360 μM was needed (Figure 5.64).

The mean low-flow model run for the lower Wensum reproduced concentrations of chloride well, with a greater overestimation of sulphate at Mill Street and Lyng, supporting the theory of a wastewater influence here which would be greater under low-flow conditions when dilution is reduced (Figures 5.65a-d). There is an overall underestimation of sodium concentrations by approximately 2 mg/L. This may be due to an increase in concentrations of sodium in the tributaries and drains, due to low-flow conditions, which is not reproduced in the model. In order for nitrate concentrations to be reproduced, a valley Chalk groundwater nitrate concentration of 355 μM was needed.

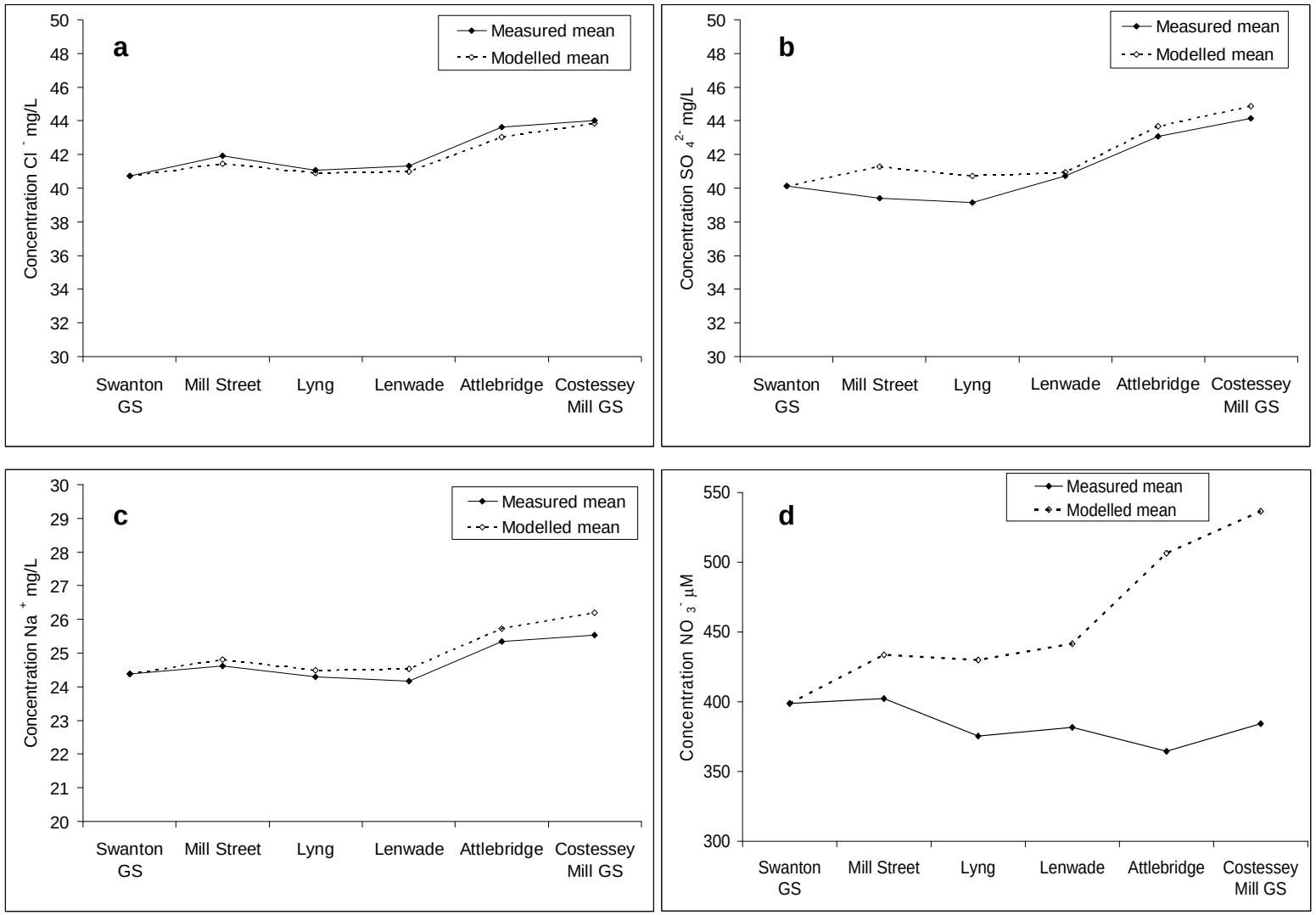

Figure 5.63a-d Lower Wensum four-member mass-balance solute mixing model output for mean data set showing measured (filled line) and modelled (dashed line) concentrations of a) chloride; b) sulphate; c) sodium; and d) nitrate, at the six lower river sampling locations.

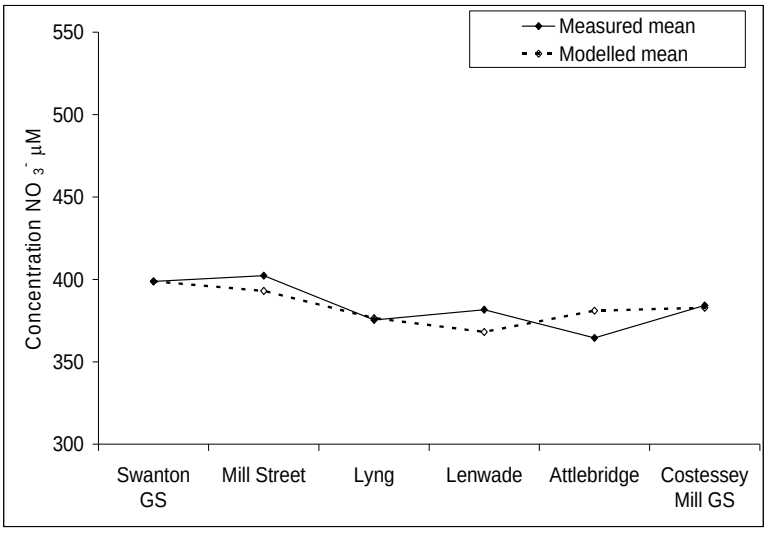

Figure 5.64 Lower Wensum four-member mass-balance solute mixing model output for mean low-flow data set showing measured (filled line) and modelled (dashed line) concentrations of nitrate using a valley baseflow concentration of 360 µM NO_3^-.

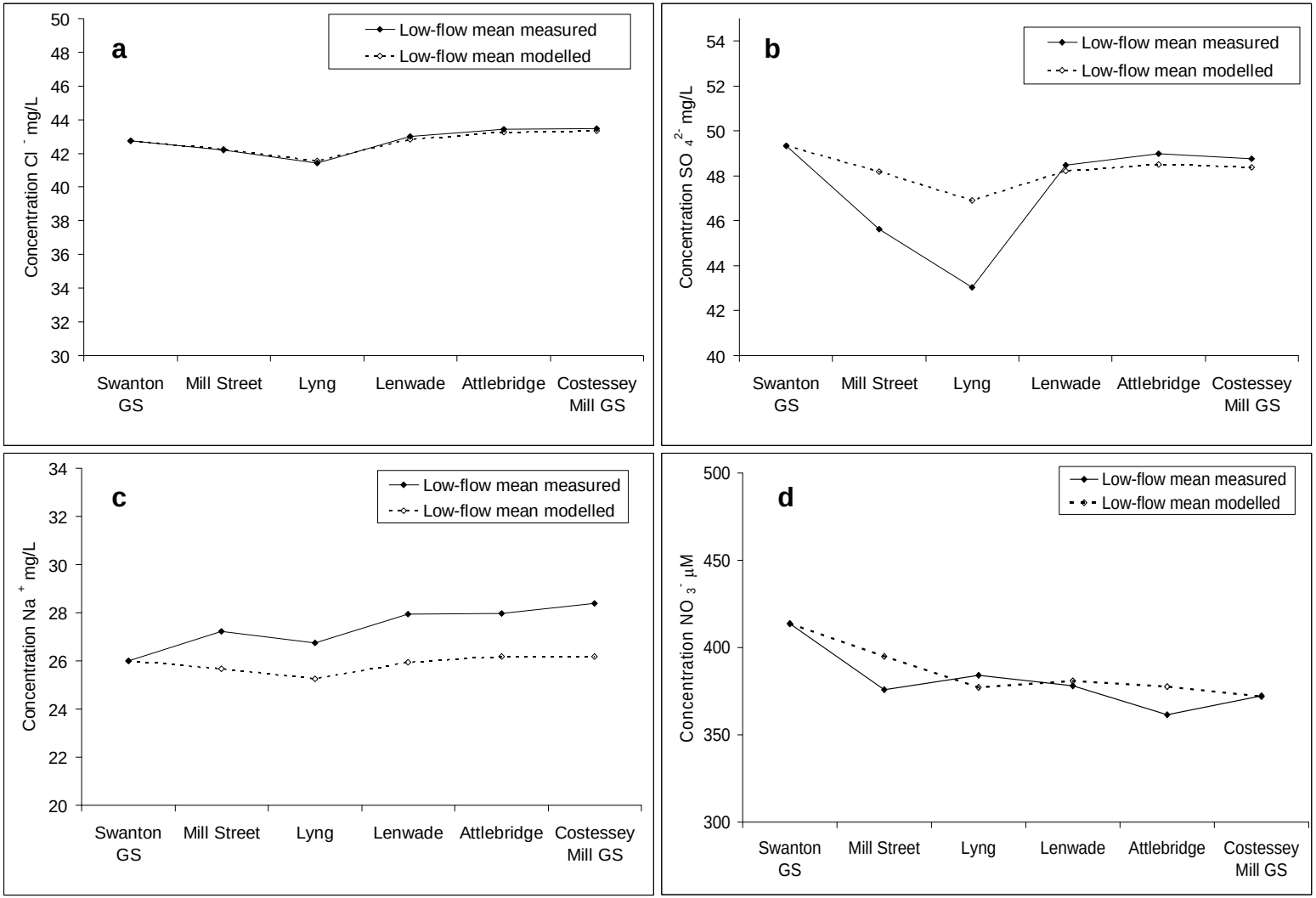

Figure 5.65a-d Lower Wensum four-member mass-balance solute mixing model output for low-flow mean data set showing measured (filled line) and modelled (dashed line) concentrations of a) chloride; b) sulphate; c) sodium; and d) nitrate using a valley Chalk groundwater end member concentration of 355 µM NO_3^-, at the six lower river sampling locations.

As with the mid river reach, in order to model the evolution of nitrate isotopic composition across the six lower river locations, a valley Chalk groundwater baseflow end member with a relatively heavy isotopic composition was needed (mean model: $\delta^{15}N_{NO3}$ 12.0‰; $\delta^{18}O_{NO3}$ 4.7‰; low-flow mean model: $\delta^{15}N_{NO3}$ 11.8‰; $\delta^{18}O_{NO3}$ 4.9‰). The theoretical valley Chalk groundwater end member nitrate concentrations and isotopic compositions for the mean and low-flow mean data produce isotopic enrichment factors within the range reported in the literature for denitrification ($\varepsilon_{P-S}{}^{15}N_{NO3}$ -5.0 to -5.3‰; $\varepsilon_{P-S}{}^{18}O_{NO3}$ -3.5 to -3.6 ‰ fractionation ration O:N 0.67 to 0.73). In order to reproduce the measured isotopic composition in the river through the lower reach sampling locations a minor adjustment to the valley Chalk groundwater end member nitrate isotopic composition was included in the model as in the mid river model run (Appendix 3). However, these represent oscillations in isotopic composition rather than a trend of enrichment as seen in the mid river. This may suggest that in-stream fractionation due to denitrification and assimilation is negligible in this reach, perhaps because of a higher flow velocity than in the mid river reach. It is also possible that the isotopic marker of denitrification in-stream is lost in this reach due to the greater volume of flow. The nitrate concentration predicted by the model for the valley Chalk groundwater end member for the lower river reach (355 to 360 μM NO_3^-) is lower than that predicted for the mid river reach (527 to 550 μM NO_3^-).

The estimated removal rates for the lower Wensum river based on the mean valley Chalk groundwater nitrate concentration are 1039 kg nitrate-nitrogen per day for the mean data, and 511 kg nitrate-nitrogen per day for the low-flow mean data. These removal rates are higher than those estimated for the mid river reach due to the greater flow in the lower reach. Thus, if nitrate concentration were to remain unchanged between Swanton and Costessey gauging stations, kg nitrate-nitrogen export would be higher in the lower reach than in the mid river reach. Therefore a 25% predicted removal of nitrate-nitrogen from the lower reach is a larger amount of nitrogen than that represented by 25% predicted removal of nitrate-nitrogen from the mid river reach. In fact, proportionally the lower river removal rates are similar to the mid river reach, representing a removal of 29% and 26% of the predicted load respectively in comparison to the mid river reach load reductions of 23% and 27%. Again, these percentages are in good agreement with estimate of riverine denitrification from the

literature, within the range of 20% to 45% removal (Alexander *et al.*, 2000, Kemp and Dodds, 2002, Seitzinger *et al.*, 2006). The lower Wensum widens considerably beyond Swanton Morley. Based on an estimated mean width of 30 metres from surveying in the field and aerial photography, (Europress, 2003), and a river depth of 0.75 metres, the estimated hyporheic denitrification rates per volume of sediment are 23 mg nitrate-nitrogen/m^3/hour for the overall mean data, and 11 mg/m^3/hour for the low-flow mean data. Based on the low-flow calculations, valley Chalk groundwater is estimated to have a residence time of 11.9 days in the sediments. If, instead, all the removal is attributed to denitrification in-stream in order to compare with the larger number of studies reported in this way, the rates per square metre river of channel surface are 55 mg nitrate-nitrogen/m^2/hour and 27 mg/m^2/hour respectively. As with the mid river estimates, both the estimates of hyporheic denitrification rates of groundwater and the in-stream denitrification rates of river water are within the ranges reported in the literature (Sjodin *et al.*, 1997, Laursen and Seitzinger, 2002, Sheibley *et al.*, 2003, Kellman, 2004, Royer *et al.*, 2004, Laursen and Seitzinger, 2005, Hernandez and Mitsch, 2006, Pina-Ochoa and Alvarez-Cobelas, 2006).

A notable difference between the mid river model output and the lower river model output is the lower predicted nitrate concentration for the valley Chalk groundwater end member for the lower river reach (lower river: 355 to 360 μM NO_3^-; versus mid river; 527 to 550 μM NO_3). This may be due to the residence time in the glacio-fluvial sediments estimated for the lower river, which is almost double that of the mid river reach (11.9 days versus 6.5 days). In addition, there is a larger number of valley Chalk groundwater fed flooded gravel pits in the lower Wensum adjacent to the river, than in the mid river reach. These are found from Lyng to Lenwade, and downstream of Attlebridge at Ringland, and upstream of Costessey Mill gauging station at Costessey Common, and are likely to contribute to denitrification of valley Chalk groundwater, which then reaches the river in baseflow through shallow flowpaths (Figure 5.32). It is possible that this increased contribution also accounts for the high ratio of valley Chalk groundwater to interfluve Chalk groundwater predicted by the model in the lower reach.

The isotopic mass-balance model of downstream locations may imply that in-stream fractionation due to denitrification and assimilation is minor. There is also a lack of a clear seasonal signal in nitrate concentrations between Swanton and Costessey gauging

stations indicative of seasonal assimilation. Together this suggests that hyporheic denitrification is the dominant process.

In summary, the evolution of solute concentrations and nitrate isotopic composition in the lower Wensum can be represented well by the four member mass-balance mixing model with a modified valley Chalk groundwater end member, showing a continuation of processes elucidated in the mid river reach, though with a probable negligible level of in-stream denitrification, and a greater influence from Chalk groundwater-fed lakes. Estimates of nitrate-nitrogen export show significant removal occurring in the lower Wensum. Interestingly, a trend of decreasing concentration with isotopic enrichment is not seen in this reach, despite the fact that mixing in of pre-denitrified groundwater is occurring. This is because the initial concentration at Swanton gauging station is fairly low and the nitrate isotopic composition already heavy, meaning that subsequent mixing acts to maintain this concentration and isotopic composition.

5.4.7 Lower Wensum Individual Sampling Sets

There are two temporal sample sets from the lower Wensum. The first spans six days during low-flow conditions in spring (19-24/04/2007) when samples were collected twice daily in the morning from lower river locations between Swanton gauging station and Attlebridge. The second, collected from the same locations for comparison, spans two days during high flow in summer (18-19/07/2007), with samples again collected twice daily in the morning. Although there is little differentiation in the isotopic composition of the samples over time, there is one noteworthy feature of the data. The range of $\delta^{15}N_{NO3}$ values of the summer high-flow data set is encompassed by that of the spring low-flow set ($\delta^{15}N_{NO3}$ 10.3 to 10.9‰; $\delta^{15}N_{NO3}$ 10.0 to 11.6‰), but the range of $\delta^{18}O_{NO3}$ values of the summer high-flow data set barely overlaps that of the spring low-flow set ($\delta^{18}O_{NO3}$ 4.6 to 5.7‰; $\delta^{18}O_{NO3}$ 3.3 to 4.8‰) (Figures 5.66 to 5.68).

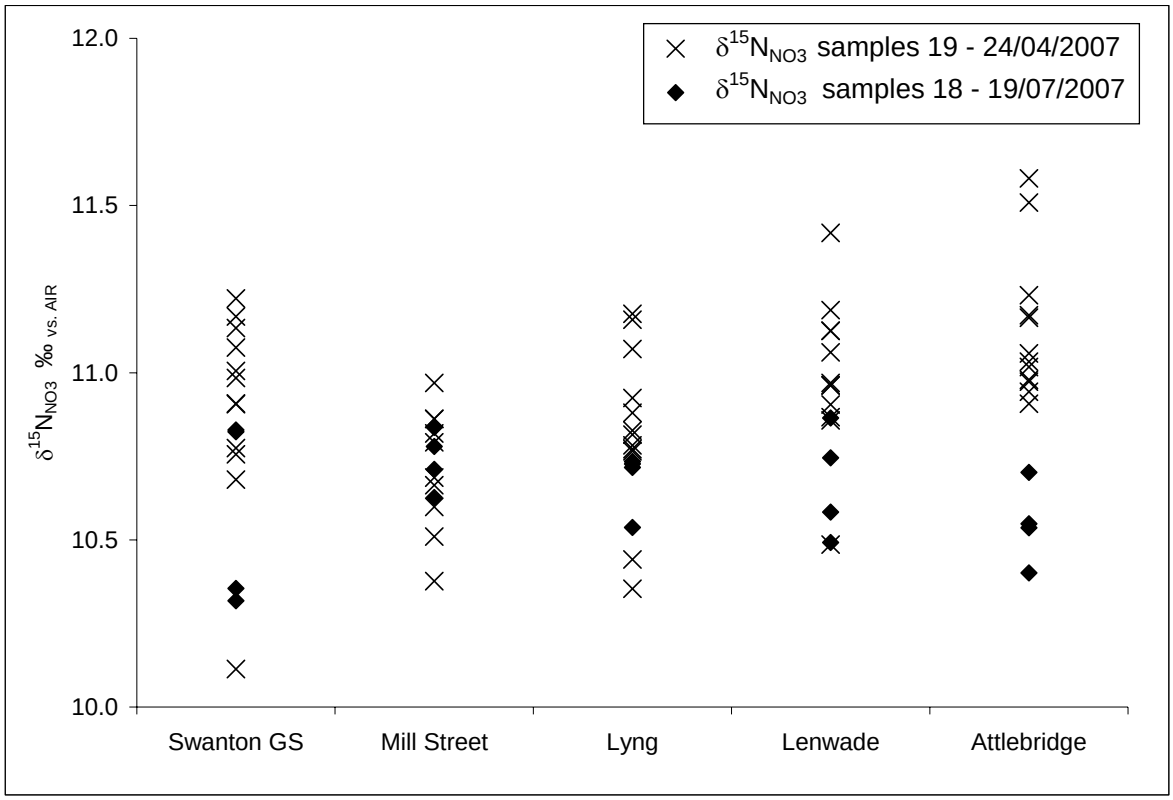

Figure 5.66 $\delta^{15}N_{NO3}$ (‰) of lower river temporal samples collected 19-24/04/2007 and 18-19/07/2007. Measurement error: $\pm$ 0.1‰.

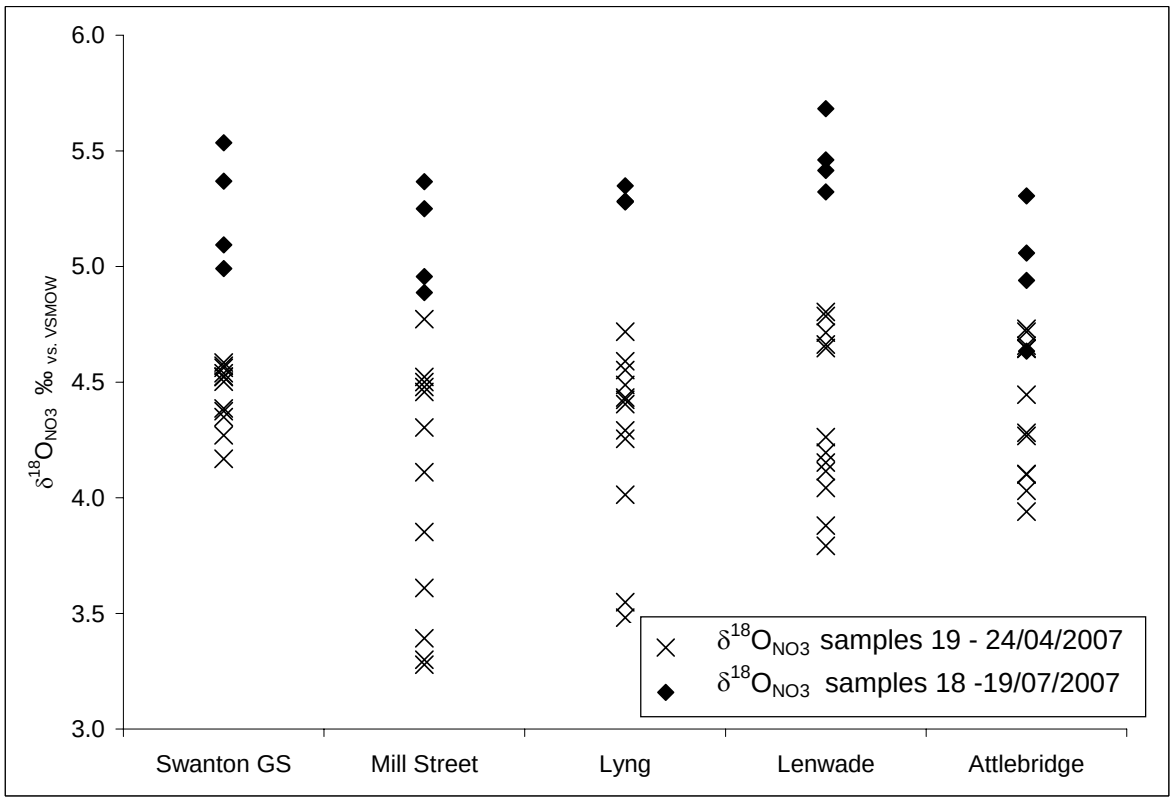

Figure 5.67 $\delta^{18}O_{NO3}$ (‰) of lower river temporal samples collected 19-24/04/2007 and 18-19/07/2007. Measurement error: $\pm$ 0.1‰.

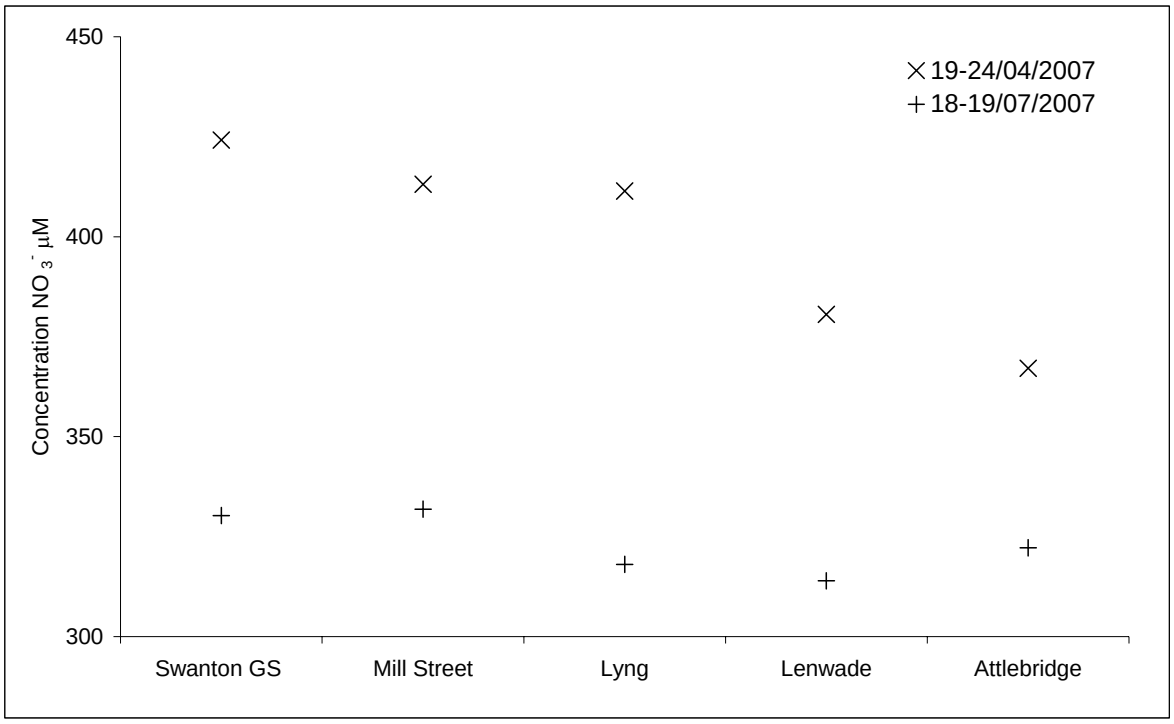

Figure 5.68 Mean concentration NO_3^- (µM) of lower river temporal samples collected 19-24/04/2007 and 18-19/07/2007.

The overall heavy isotopic composition of the nitrate from the low-flow data sets reflects a stronger influence from wastewater and manure inputs during low-flow, which changes the relationship between nitrogen and oxygen isotopic composition in these samples by lowering the oxygen values. The large difference in nitrate concentrations from the two sets of data (Figure 5.68), although in part attributable to enhanced riparian denitrification for the high-flow samples, adds support to this interpretation.

In summary, the isotopic composition of oxygen in nitrate of the temporal sample sets from the lower Wensum river suggest a flow-related influence of wastewater inputs on nitrate concentration and isotopic composition.

5.4.8 Lower Wensum Tributaries and Drains

One tributary and two drains were sampled more than once in the lower Wensum. The stream at Mill Street, which converges with the Wensum before Lyng was sampled on seven occasions, and shows a temporal trend of heavier nitrate isotopic composition with lower concentrations, suggesting denitrification and assimilation fractionations (Figure 5.69). The two samples with the lowest nitrate concentration and heaviest

isotopic composition are from the summer high-flow and autumn low-flow sample sets. Interestingly, the summer high-flow set (18/07/2007) is the sample set for which solute export calculations suggest enhanced denitrification and sulphate reduction after flooding. This is supported by the fact that sulphate concentrations are also anomalously low on this date in this stream (Figure 5.70 contained within oval). The autumn low-flow sample implies that in the stream the effects of denitrification and assimilation kept nitrate concentrations low, despite the low-flow conditions. This is supported by the fact that the concentrations of chloride are not low in this sample as would be expected if dilution accounted for the sample's low nitrate concentration (Figure 5.70 contained within square).

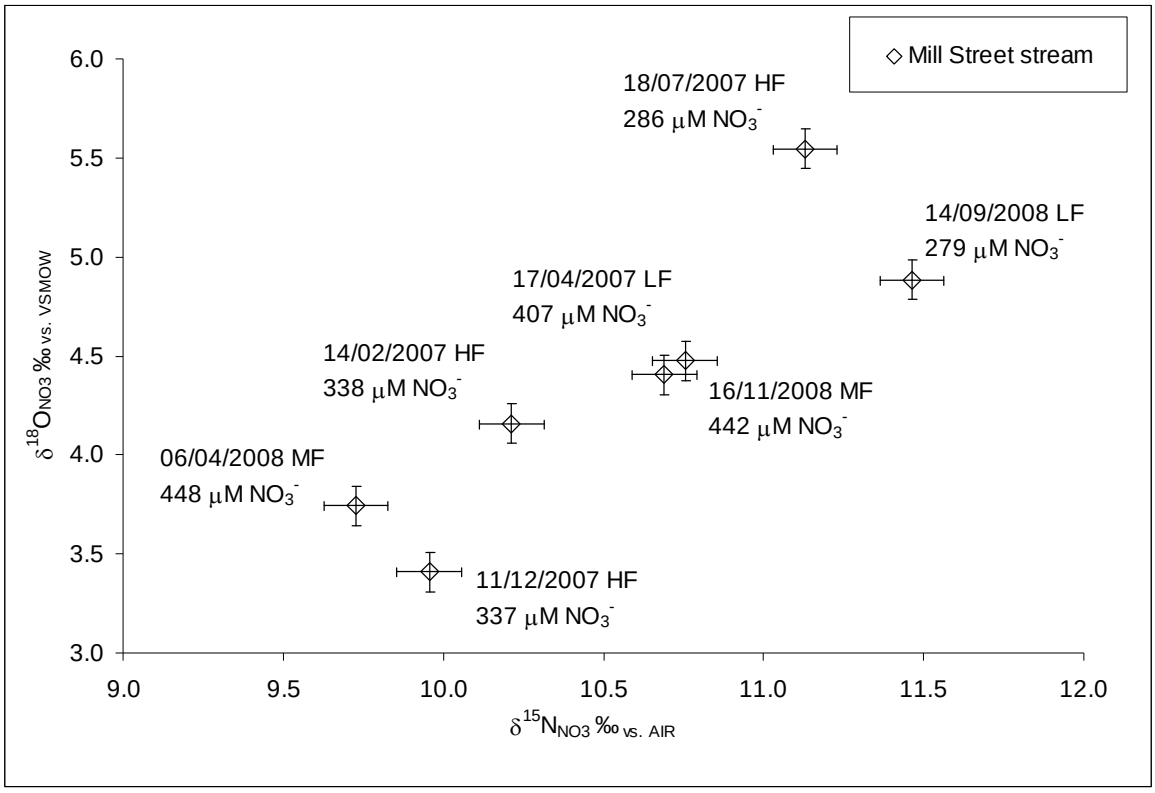

Figure 5.69 $\delta^{18}O_{NO3}$ (‰) versus $\delta^{15}N_{NO3}$ (‰) of samples from Mill Street stream showing sampling date, flow condition and nitrate concentration. Error bars represent measurement error of $\pm$ 0.1 ‰ for $\delta^{15}N_{NO3}$ and $\delta^{18}O_{NO3}$.

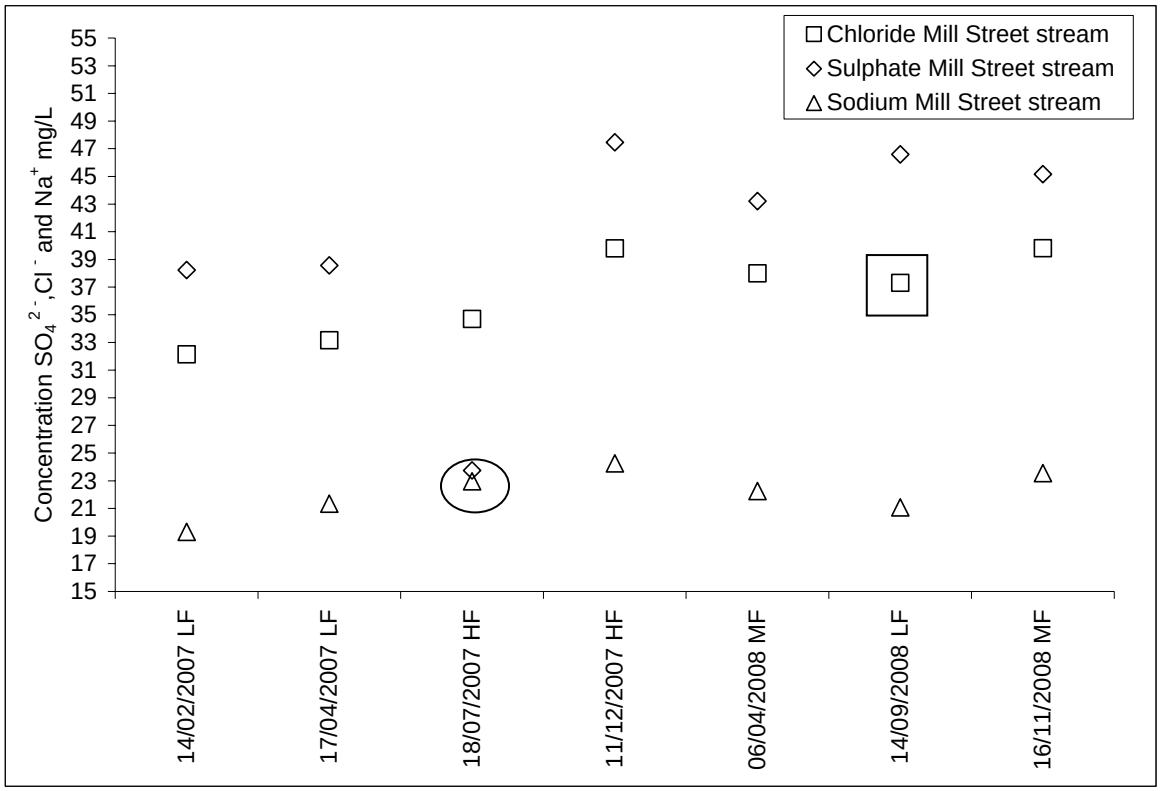

Figure 5.70 Concentration Cl^-, SO_4^{2-}, and Na^+ (mg/L) of samples from Mill Street stream showing sampling data and flow condition. Oval and square show samples referred to in the text.

A similar temporal trend of assimilation and denitrification is seen in the nitrate concentration and isotopic composition of paired samples from Lyng and Lenwade drains (Figures 5.71), although here the concentration range is much greater. The three samples from Lyng drain show a vector of concentration reduction with isotopic enrichment between two samples of high concentration (spring medium flow: 06/04/2008, and autumn low flow: 14/09/2008), to a lower concentration measured during high flow in winter (11/12/2007) (Figure 5.71 contained within oval). This is surprising, as winter high flow would usually be expected to bring runoff of nitrified nitrate from the soil with a high nitrate concentration and lighter isotopic composition. Concentrations of chloride and sulphate in this sample are slightly lower than in the other drain samples, suggesting that an element of dilution is in part responsible for the low nitrate concentration (Figure 5.72 contained within oval). A possible explanation for the heavy nitrate isotopic composition at Lyng on 11/12/2007 is that runoff on this date displaced shallow groundwater into the drain which had already undergone partial denitrification. This would imply that on the other sampling dates when high nitrate concentrations are seen, source nitrate entered the drain directly, for example via field tile drains, and that flow was not augmented by shallow groundwater.

The two corresponding samples from Lenwade drain (which was dry during sampling on 14/09/2008) span a range of nitrate concentration from 498 to 1200 μM NO_3^- (Figure 5.71). The lower concentration sample has an isotopic composition close to those of the higher concentration samples from Lyng drain, suggesting that this isotopic composition represents a "baseline" for nitrate entering these drains of $\delta^{15}N_{NO3}$ 11.3 + 0.2 ‰ and $\delta^{18}O_{NO3}$ 4.2 + 0.1 ‰. This is close to the mean isotopic composition of all tributaries and drains sampled ($\delta^{15}N_{NO3}$ 10.3 + 2.7 ‰ and $\delta^{18}O_{NO3}$ 4.7 + 1.7 ‰), and is likely to reflect manure nitrate sources after some isotopic enrichment from denitrification and assimilation. It is interesting that nitrate concentration shows a much higher level of variation than nitrate isotopic composition across these three samples (662 $\pm$ 207 μM NO_3^-).

The sample from Lenwade drain during spring medium flow (06/04/2008) has very high concentrations of nitrate, with average concentrations of chloride, sulphate, and sodium, with the lowest nitrate isotopic composition of these drain samples ($\delta^{15}N_{NO3}$ 10.7‰; $\delta^{18}O_{NO3}$ 3.6 ‰) (Figures 5.71 and 5.72 contained within rectangle). The oxygen isotopic composition of this sample is within the range predicted for nitrification in East Anglian soils, while the nitrogen isotopic composition is relatively heavy. This suggests a contamination source from nitrate originating from manure entrained in runoff entering the drain during medium flow on this day.

The sample from Lenwade drain during winter high flow (11/12/2007) shows a high NO_3^- concentration and has very high concentrations of chloride and sulphate (Figure 5.72 contained within triangles). The probable source of these solutes is again manure entrained in runoff.

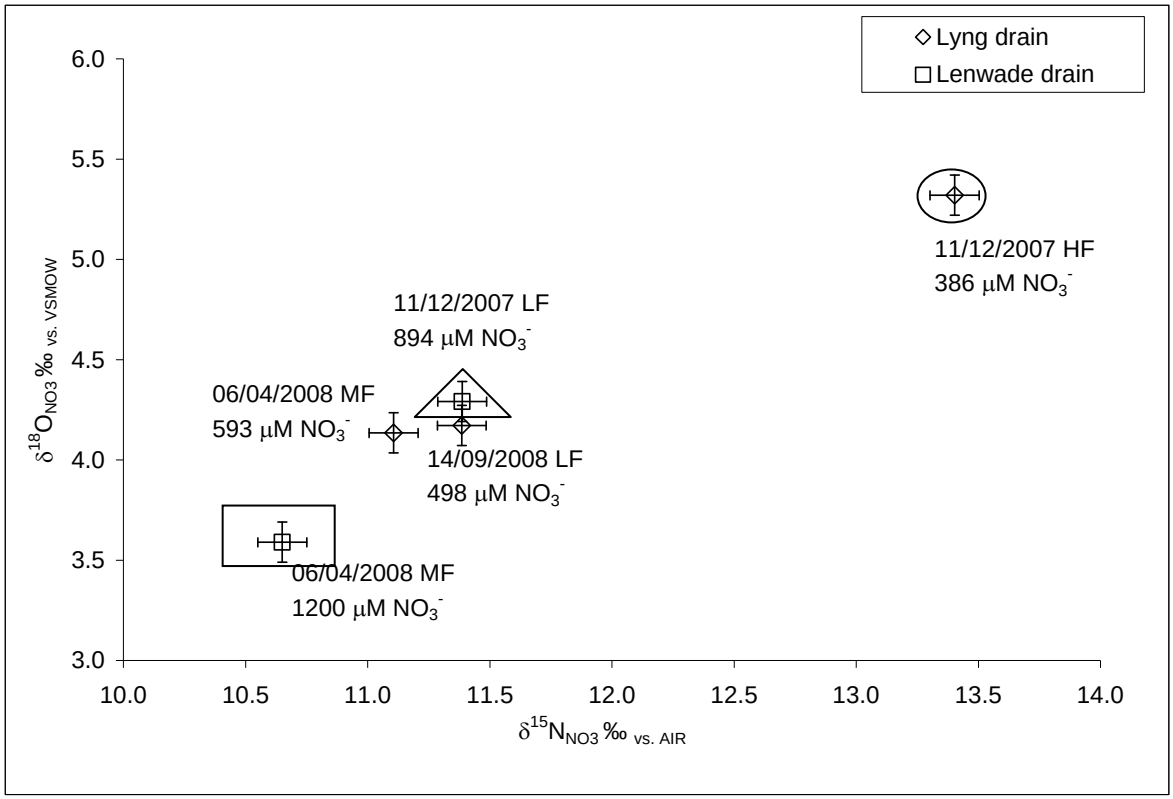

Figure 5.71 $\delta^{18}O_{NO3}$ (‰) versus $\delta^{15}N_{NO3}$ (‰) of samples from Lyng and Lenwade drains showing sampling date, flow condition and nitrate concentration. Error bars represent measurement error of $\pm$ 0.1 ‰ for $\delta^{15}N_{NO3}$ and $\delta^{18}O_{NO3}$. Rectangle and oval show samples referred to in the text.

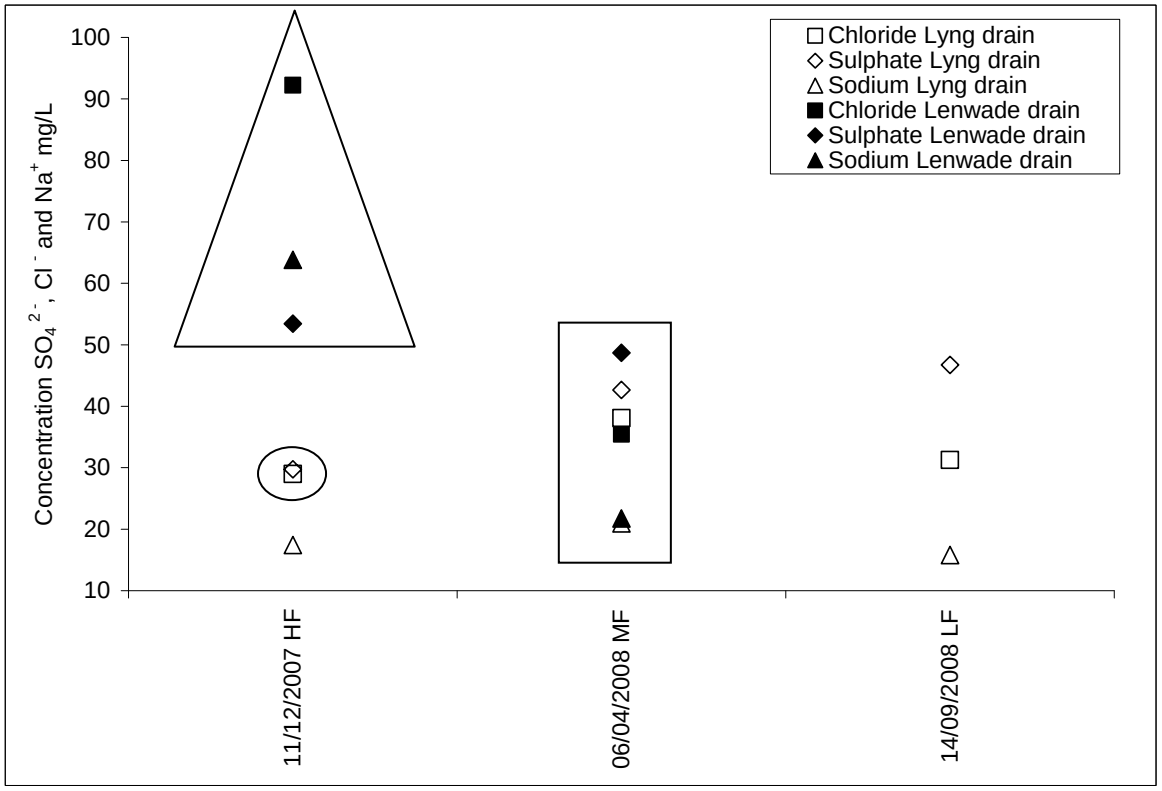

Figure 5.72 Concentration Cl^-, SO_4^{2-}, and Na^+ (mg/L) of samples from Lyng and Lenwade drains showing sampling data and flow condition. Rectangle and oval show samples referred to in the text.

In summary, the nitrate concentration and isotopic composition of the lower Wensum tributaries and drains indicate flow related effects of denitrification and assimilation fractionations over a wide concentration range, in addition to direct source contamination from animal waste during medium and high-flow conditions.

5.5 $\delta^{18}O_{H2O}$ in Wensum River, Tributary and Drain Samples

A trend is seen in samples collected on different dates from the three catchment gauging stations, and from three tributaries and drains spanning the upper, mid and lower catchment which may suggest an increasing influence of catchment drainage water which has undergone evaporative fractionation. The samples show a trend of lighter oxygen isotopic composition in the upper catchment (Fakenham gauging station, Fakenham drain), with a heavier composition in the mid catchment (Swanton gauging station, Wendling Beck), and a greater range of values in the lower catchment (Costessey Mill gauging station, Mill Street stream) (Figures 5.73 and 5.74). The mean value of precipitation in East Anglia ($\delta^{18}O_{H2O}$ -7.1‰) (Eames, 2008), is the same as the mean value at Fakenham gauging station, which suggests that the isotopic composition at Fakenham could represent bulk rainfall, implying that flow there is supplied by rainfall runoff which drains quickly from the soil surface to form shallow and quick circulating groundwater. This supports the hypothesis derived from the two member mixing model for the upper Wensum. In the mid and lower catchment, the heavier isotopic composition might reflect an increasing contribution of soil water drainage via tributaries and drains from a larger land-surface area which has undergone isotopic fractionation at the surface due to evaporation (Darling *et al.*, 2003). The difference between surface water and groundwater mean $\delta^{18}O_{H2O}$ values found in the Wensum catchment (Wensum tributaries and drains -6.7 $\pm$ 0.4‰; river -6.8 + 0.2‰; Chalk groundwater -7.3 $\pm$ 0.2 ‰) suggests an increasingly heavy composition higher up the pathway from precipitation to groundwater recharge, suggesting the influence of surface evaporation in the river and tributary and drain water, with groundwater representing the isotopic composition of bulk recharge with a winter weighting (Hiscock *et al.*, 1996, Darling *et al.*, 2003). Sampling locations which show a wide level of isotopic variation, therefore, such as Costessey gauging station and Mill Street stream, may reflect differences in the relative proportions of runoff to Chalk baseflow across sampling

dates, with the high-flow samples also likely to indicate temporal variations in the isotopic composition of precipitation (Darling *et al.*, 2003).

In summary, Wensum catchment surface water samples show a trend of lighter water oxygen isotopic composition in the upper catchment, with a heavier composition in the mid catchment, and a greater range of values in the lower catchment. This suggests that upper catchment flow is supplied by rainfall runoff in quick-circulating baseflow, with the heavier isotopic composition downstream reflecting the effects of evaporation in surface drainage waters, and the wider isotopic variation reflecting differences in the relative proportions of runoff to Chalk baseflow, as well as temporal variations in the isotopic composition of precipitation.

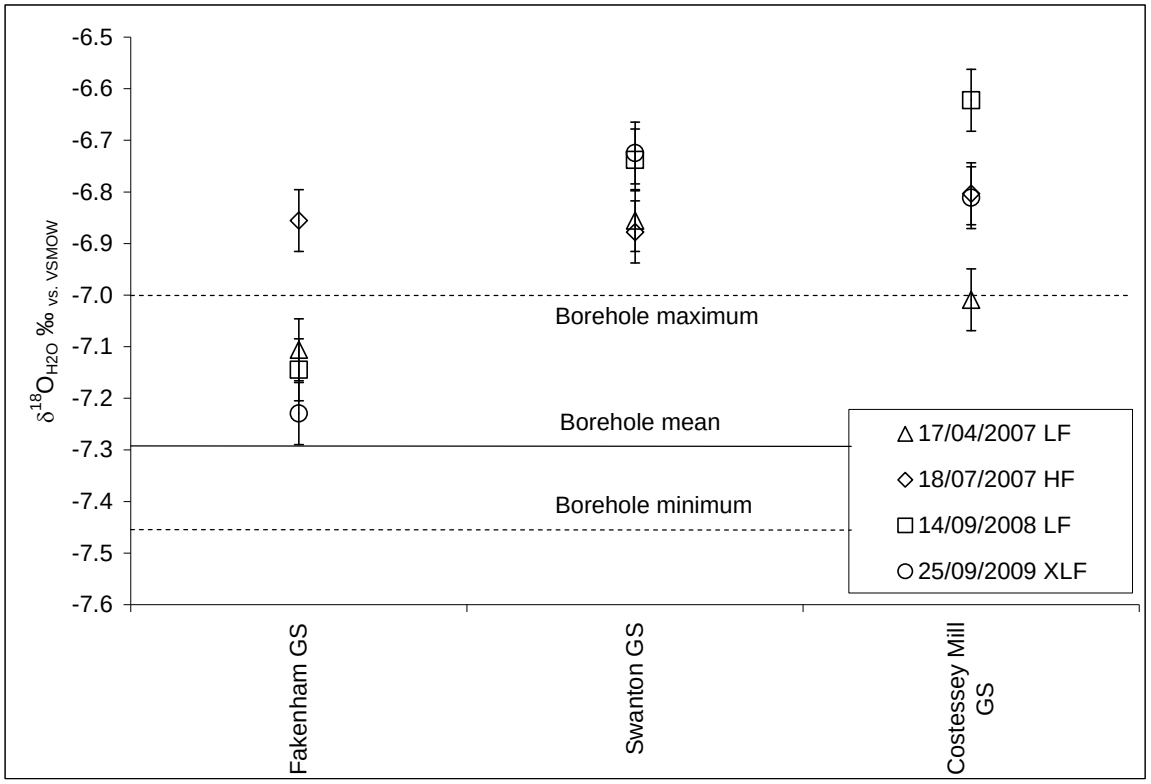

Figure 5.73 $\delta^{18}O_{H2O}$ (‰) of samples from the Wensum river gauging stations showing sampling data and flow condition with mean, maximum and minimum values from Wensum borehole samples marked by lines. Error bars represent measurement error: $\delta^{18}O_{H2O} \pm 0.06$ ‰.

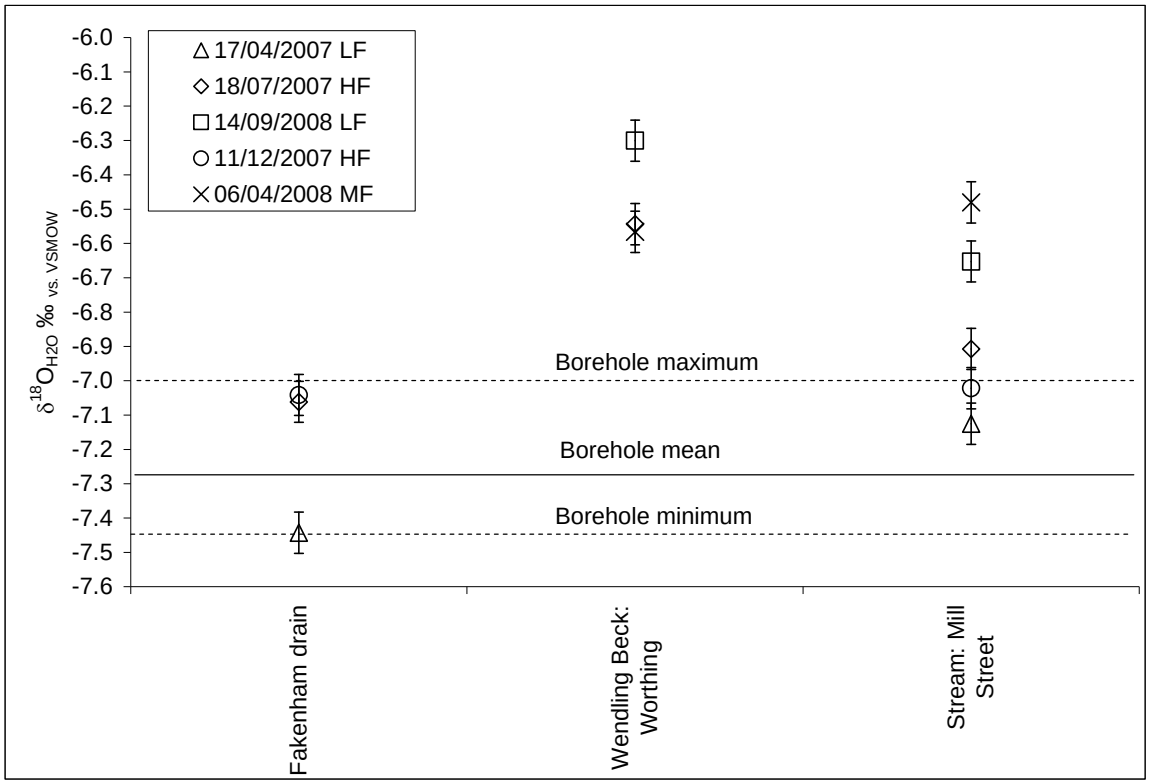

Figure 5.74 $\delta^{18}O_{H2O}$ (‰) of samples from three Wensum tributaries and drains showing sampling data and flow condition with mean, maximum and minimum values from Wensum borehole samples marked by lines. Error bars represent measurement error: $\delta^{18}O_{H2O} \pm 0.06$ ‰.

5.6 SUMMARY

This research has identified sources, cycling, pathways and removal processes of nitrogen contamination in a river draining a lowland agricultural catchment, which cause high concentrations of riverine nitrate that decrease downstream. The research aim has been achieved through the application at the catchment scale of the denitrifier method for the analysis of $\delta^{15}N_{NO3}$ and $\delta^{18}O_{NO3}$. The research has shown that the observed trend of decreasing nitrate concentration in the River Wensum is primarily caused by mixing of partially denitrified baseflow which acts to dilute riverine nitrate concentrations in the mid river and maintain them at a lower level in the lower river. Partially denitrified baseflow derives from the denitrification of high-nitrate-concentration valley Chalk groundwater. Denitrification occurs during baseflow advection through hyporheic glacial sand and gravel deposits below the riverbed.

In summary, in this chapter $\delta^{15}N_{NO3}$ and $\delta^{18}O_{NO3}$ and solute concentrations have been used to investigate removal and cycling of nitrate transported from the Wensum catchment in river water. The isotopic composition of direct nitrate sources and their

overall relationship to catchment water nitrate isotopic composition have been described, with an examination of the isotopic composition of low-nitrate Chalk groundwater and valley Chalk groundwater. The findings show that all the major sources of contemporary nitrate to the catchment undergo cycling and nitrification, with the result that fertiliser and atmospheric inputs cannot be traced using their very heavy oxygen isotopic composition. The isotopic composition of cycled and nitrified source nitrate can be predicted ($\delta^{15}N_{NO3}$ ~ 2.3 to10 ‰; $\delta^{18}O_{NO3}$ 2.8 to 3.8 ‰), and the nitrate isotopic composition of high-concentration valley Chalk groundwater suggests that it originates from this nitrified and cycled source nitrate (973 $\pm$ 215 μM; $\delta^{15}N_{NO3}$ 6.9 $\pm$ 1.4 ‰; $\delta^{18}O_{NO3}$ 1.2 $\pm$ 1.2 ‰). Low-nitrate groundwater may contain very low concentrations of palaeo-nitrate of atmospheric and terrestrial origin, suggested by the heavy oxygen isotopic composition, ($\delta^{18}O_{NO3}$ 21.1 $\pm$ 9.7‰) and lack of an isotopic marker of denitrification.

The use of solute concentrations and water isotopic composition as tracers has been outlined and an overview of Wensum catchment samples has been presented. The results show that high concentrations of nitrate, chloride, sulphate, sodium and potassium can indicate a wastewater effluent source, while precipitation will have a minor diluting effect on river water major ion concentrations. Three hydrochemical groups of Chalk groundwater are identified, from the valley, with high concentrations of nitrate, and medium to high concentrations of the major ions chloride, sulphate, and sodium; from the valley edge, with very low concentrations of nitrate, and medium to high concentrations of the major ions; and from the interfluves, with very low concentrations of nitrate, and low concentrations of the major ions. Groundwater also has a lower mean $\delta^{18}O_{H2O}$ than that of surface water. Catchment surface water nitrate isotopic composition suggests its origins from cycled and nitrified source nitrate, but also shows subsequent isotopic fractionation of $\delta^{15}N_{NO3}$ and $\delta^{18}O_{NO3}$, the relationship of which implies denitrification in the slope of 0.53. Catchment-wide correlations of daily mean flow with solute load indicate increased denitrification in anaerobic riparian soils after flooding in summer which is responsible for removing up to 30% of the expected nitrate-nitrogen load.

Detailed examinations of the upper, mid and lower Wensum river reaches and their tributaries and drains have been made, and mass-balance mixing models have been used

to elucidate the data. Nitrate concentration decrease, flow condition, and season have been considered, using mean and individual data sets, and discussions of the results from temporal sampling have been included. Modelling of the upper Wensum using major ion concentrations and nitrate isotopic composition suggests that in the headwaters flow is initially supplied by shallow groundwater from fluvial deposits, with an increasingly strong influence of baseflow from the exposed Chalk in the western catchment downstream, in which denitrification is absent. The shallow groundwater from fluvial deposits usually has high nitrate concentrations, but undergoes denitrification under low-flow conditions, while the baseflow from the exposed Chalk is expected to have uniformly medium-high nitrate concentrations and a light isotopic composition. This mixing accounts for the decrease in nitrate concentration of approximately 100 μM NO_3^-, seen in the upper Wensum by Fakenham gauging station, which is not associated with flow condition or season. During dry conditions when recharge circulation is reduced, denitrification can occur in the shallow groundwater, and is reflected in a low nitrate concentration and heavy isotopic composition in the Wensum headwaters at Hamrow (298 μM NO_3^- ; $\delta^{15}N_{NO3}$ 14.8‰; $\delta^{18}O_{NO3}$ 7.5‰). The homogeneous nature of nitrate concentration and isotopic composition from the Tat tributary which drains a large area of the western catchment, indicates that it is supported by baseflow from the exposed Chalk containing nitrate from the major sources after cycling and nitrification (600 $\pm$ 28 μM NO_3^-; $\delta^{15}N_{NO3}$ 6.9 $\pm$ 0.6‰; $\delta^{18}O_{NO3}$ 2.4 $\pm$ 0.4‰). Evidence of temporal and localised sources of nitrate contamination and of denitrification is found in concentrations of nitrate and chloride, and nitrate isotopic composition in three upper catchment drains.

In the mid Wensum, a four member mass-balance solute and isotope mixing model suggests removal of 372 kg nitrate-nitrogen per day by Swanton gauging station during low-flow conditions, mainly from valley Chalk groundwater before it enters the river, but also via in-stream denitrification of riverine nitrate. The model is constrained by measured solute concentrations and nitrate isotopic composition of groundwater samples and river samples through five mid river locations, and by the baseflow index of 0.75 for the middle catchment to Swanton gauging station. The hydrology of the mid Wensum river comprises a system in which baseflow is supplied from valley Chalk groundwater with high nitrate concentrations, with an increasing proportion of “nitrate free” interfluve Chalk groundwater downstream. Denitrification occurs to the valley

Chalk groundwater as it advects up through the deep glacio-fluvial sediments below the riverbed and in-stream. The likely apportionment between these two processes is of 75% removal from valley Chalk groundwater before it enters the river, with a calculated low-flow denitrification rate of 21 mg/m^3/hour, and 25% removal in-stream, with a calculated low-flow rate of 16 mg/m^2/hour, within the ranges reported in the literature. The glacio-fluvial sediments also provide storage and denitrification for runoff during high-flow conditions. Surface accretion from tributaries and drains includes inputs of wastewater effluent, with denitrification along the field-drain-tributary pathway suggested by the relatively low concentration and heavy isotopic composition of tributary and drain sample nitrate (372 μM NO_3^-; $\delta^{15}N_{NO3}$ 10.3 ‰; $\delta^{18}O_{NO3}$ 4.9 ‰). The lack of seasonal differentiation in nitrate removal suggests that assimilation plays a minor role, and supports the hypothesis that a greater proportion of denitrification occurs to the valley Chalk groundwater in the sand and gravel sediments than that which occurs in-stream. Denitrification may be responsible for a reduction in nitrate-nitrogen load of up to 27% by Swanton gauging station during low-flow periods. Denitrification lowers nitrate concentration and leads to a heavier isotopic composition, together resulting in the trend of concentration decrease and increase in isotopic values seen between Fakenham and Swanton gauging stations (Fakenham: 573 $\pm$ 76 μM NO_3^-; $\delta^{15}N_{NO3}$ 8.4 + 0.5 ‰; $\delta^{18}O_{NO3}$ 3.5 $\pm$ 0.4 ‰; Swanton: 418 $\pm$ 58 μM NO_3^-; $\delta^{15}N_{NO3}$ 10.7 $\pm$ 0.7 ‰; $\delta^{18}O_{NO3}$ 4.7 $\pm$ 0.4 ‰) .

A conceptual model of the components and processes in the Wensum mid river reach based on the results of the four member mixing model is represented schematically in Figure 5.75, which shows the four end members of upstream flow, tributary accretion fed by runoff, valley Chalk groundwater baseflow and interfluve Chalk groundwater baseflow. High nitrate concentrations are represented by darker greys, with a gradient from dark to light indicating a reduction in nitrate concentration. Nitrate in recharge infiltrating through the soil to valley Chalk groundwater, the tributaries and drains, and to the sands and gravels, (dark grey arrows), reflects a lack of significant denitrification in the soil, as indicated by the high concentration and light isotopic composition of valley Chalk groundwater nitrate which results from this recharge. The reduction of groundwater nitrate concentration through denitrification in the sand and gravel hyporheic deposits below the riverbed and from the mixing of valley and interfluve

Chalk groundwater, is shown by arrows fading to light grey. Denitrification is also shown during flow through the tributaries and drains, and in-stream within the river.

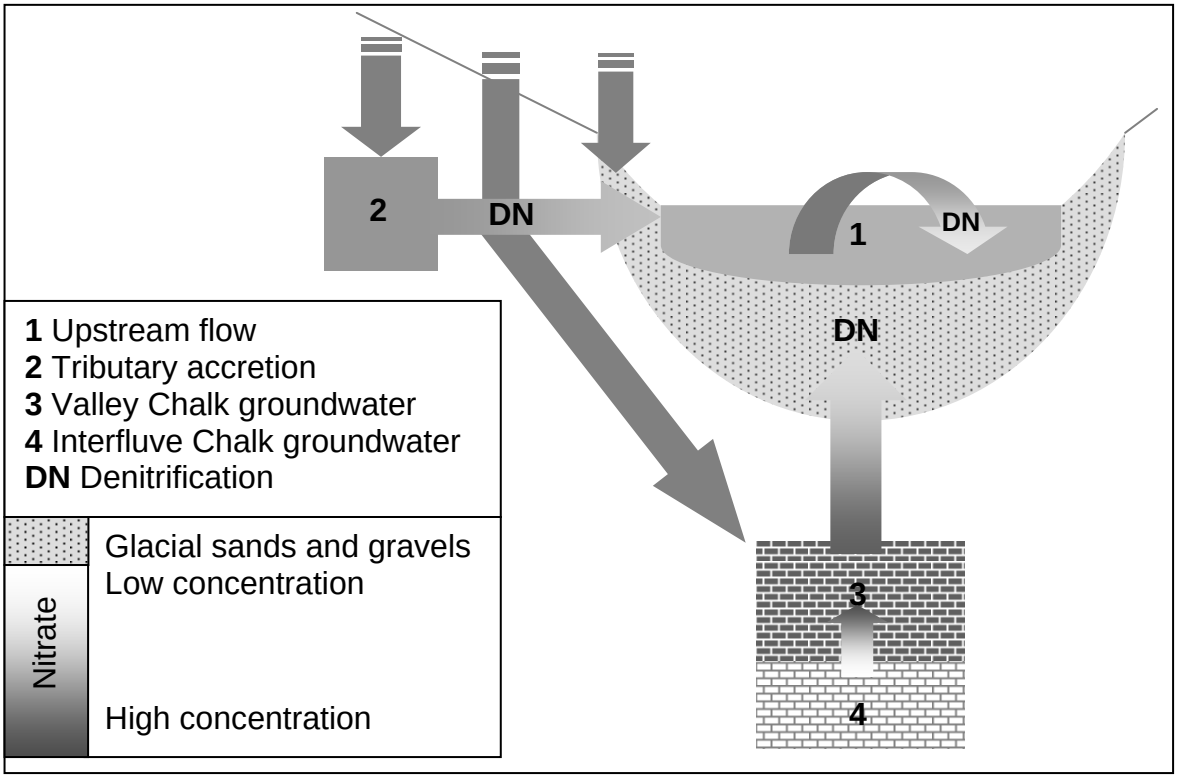

Figure 5.75 Conceptual model of components contributing to flow in the Wensum mid river reach, showing denitrification (DN), with colour gradient from dark to light indicating high to low nitrate concentration.

The evolution of solute concentrations and nitrate isotopic composition in the lower Wensum is also represented by the four member mass-balance mixing model, showing a continuation of processes elucidated in the mid river reach, though here with a negligible level of in-stream denitrification which may be due to higher flow velocities. The removal rates are higher than those estimated for the mid river reach, reflecting the greater flow in the lower river, with removal of 511 kg nitrate-nitrogen per day predicted using the mean low-flow samples in the lower Wensum. A lower concentration of the valley Chalk groundwater end member results from a longer residence time in the glacio-fluvial sediments and may indicate a stronger influence from the many groundwater-fed lakes adjacent to the river, within which denitrification occurs. Estimates of nitrate-nitrogen export show up to 26% removal occurring in the lower Wensum during low-flow periods, with a maximum rate of removal in the glacio-fluvial sediments of 11 mg/m^3/hour during low-flow conditions. Interestingly, a trend of

decreasing concentration with isotopic enrichment is not seen in this reach, despite the fact that mixing in of pre-denitrified groundwater is occurring. This is because the initial concentration at Swanton gauging station is already relatively low and the nitrate isotopic composition already heavy, meaning that subsequent mixing acts to maintain this concentration and isotopic composition.

Individual samples sets from the mid and lower Wensum river and tributaries and drains show the localised influence of surface water accretion in the concentration and isotopic composition of nitrate after a winter storm, direct source contamination from effluent and manure during high and low-flow conditions, and flow related effects of denitrification and assimilation fractionations over a wide concentration range.

Chapter 6 will present conclusions from this Discussion concerning the sources, cycling and attenuation of nitrate within the Wensum catchment, and will consider the implications of this research with respect to land management regulation and policy making.

6. CONCLUSION

The research presented in this thesis has used a catchment scale approach to elucidate the sources, cycling and attenuation of nitrogen contamination which results in decreasing nitrate concentrations downstream in a river draining a lowland agricultural catchment downstream. The research aim has been achieved through the application of the denitrifier method for the analysis of $\delta^{15}N_{NO3}$ and $\delta^{18}O_{NO3}$, with solute and isotope mass-balance modelling, which has enabled the characterisation of the dominant hydrochemical, hydrological and hydrogeological influences on the River Wensum. The importance of microbial nitrogen cycling has been shown in relation to sources of nitrate entering the catchment, and to levels of nitrate exported from the catchment via the river. It is this microbial activity, in the form of denitrification, which is responsible for the trend of decreasing nitrate concentration observed in the river.

Groundwater from the exposed Chalk in the valley is the largest potential source of nitrate to the baseflow-dominated River Wensum. It contains high levels of nitrate originating from soil nitrification, which is flushed from the soil in runoff and reaches the Chalk groundwater in recharge. Denitrification is not significant in the well drained valley soils through which this recharge infiltrates. The nitrate is likely to derive mainly from cycled and nitrified inorganic and organic agricultural sources. The high solubility of nitrate ensures that it is readily carried from the soil to groundwater. Conditions within the Chalk do not support denitrification, with the result that high concentrations of nitrate have built up there. The flowpath which valley Chalk baseflow follows to reach the river as baseflow takes it through a thick layer of glacio-fluvial sediments in the hyporheic zone in the river valley, which provide ideal conditions to support denitrification. During the passage of valley Chalk groundwater through these sediments, denitrification lowers the nitrate concentration of baseflow, significantly reducing the export of nitrogen from the catchment via the river. Denitrification also occurs in groundwater-fed lakes adjacent to the river, with the larger number of lakes in the lower Wensum resulting in a greater influence on baseflow nitrate concentrations there. Baseflow concentrations in the lower river are also affected by a longer residence time in the glacio-fluvial sediments than that in the mid river. In the mid river reach, denitrification also occurs in-stream, optimised by the high ratio of streambed area to

water volume and low flow velocity. On the catchment interfluves denitrification occurring during the slow infiltration of recharge through the Lowestoft Till and Pleistocene deposits effectively protects the underlying interfluve Chalk groundwater from contemporary nitrate contamination, although the isotopic composition of the very low level of nitrate in Chalk groundwater from the interfluves suggests an input of palaeo-nitrate of atmospheric and terrestrial origin, which may have occurred at the end of the last glacial maximum when denitrification was suppressed.

The tributaries and drains feeding into the Wensum present a varied picture of the influence of surface accretion on riverine nitrate loads. Although receiving high levels of nitrogen in field runoff and effluent discharge, overall, the tributaries and drains reflect the effects of denitrification and assimilation within the first-order drainage network, with opposing influences seen under both low and high flows, of increased levels of denitrification with assimilation *and* increased concentrations from agricultural and effluent source inputs due to reduced dilution under low-flow, and increased dilution under high-flow *and* high nitrate concentrations from runoff contamination.

Denitrification is significant in the Wensum catchment. Low-flow conditions are likely to provide the best estimates of nitrate removal within the river valley, due to the lower proportional contribution to river flow of runoff accretion. Microbial nitrate removal, primarily attributed to denitrification in the hyporheic sediments, is estimated to remove 883 kg/day nitrate-nitrogen by the catchment outlet at Costessey gauging station, representing 42% of the nitrate load. Removal rates of 372 kg/day and 511 kg/day for the mid and lower Wensum river represent 27% and 25% of within-reach nitrate-nitrogen removal. If all nitrate removal is attributed to denitrification of valley groundwater as it advects through the hyporheic glacio-fluvial sediments, the estimated removal rates for the mid and lower reaches are 28 mg/m^3/hour and 11 mg/m^3/hour respectively. In the mid Wensum, an isotopic denitrification marker suggests in-stream removal could account for up to a quarter of the within-reach removal, with a rate of 16 mg/m^2/hour in the streambed sediments.

The nitrate removal via hyporheic and in-stream denitrification quantified above, in addition to that in the overlying deposits on the interfluves and within the tributaries and drains, provides a major natural attenuation mechanism containing concentrations of

nitrate in the river Wensum within the legal limits of the EU Drinking Water Directive (98/83/EC: Council of European Communities, 1998). The evidence of major denitrification in the hyporheic sediments of the Wensum catchment contradicts estimations by Smith *et al.* (2009) of very low natural attenuation potential of nitrate at the groundwater-surface water interface in Norfolk. These results from the Wensum reach are in line with findings by Hinkle *et al.* (2001) of major reduction in nitrate concentration in groundwater advecting through the hyporheic zone before reaching the river as baseflow, and of denitrification of riverine nitrate from stream water circulating through the hyporheic zone. Without denitrification in the various environments across the catchment, anthropogenic nitrogen inputs, primarily from agricultural activity, would result in significantly higher concentrations of nitrate within the river, with detrimental impacts on drinking water quality, the health of the river and of downstream ecosystems.

The application of the denitrifier method for the analysis of $\delta^{15}N_{NO3}$ and $\delta^{18}O_{NO3}$ to the Wensum catchment has justified the cost, time, and effort invested in setting up the method. It has enabled a high throughput of samples which has facilitated the identification of stable isotopic trends within the Wensum river across seasons and flow conditions, and differentiated them from ephemeral isotopic signals seen in tributaries and drains. This in turn has enabled the catchment characterisation using a mixing model based on the stable isotopic markers. The high precision and accuracy achieved by the method has lead to robustness of the results. The method has also enabled the analysis of samples with concentrations below 1 μM NO_3^-, revealing a possible palaeo-nitrate in interfluve Chalk groundwater.

Solute and isotope mass-balance mixing modelling to characterise the dominant influences on nitrate concentrations in-stream represents a new approach at the scale of the catchment. In the Wensum catchment, this modelling has been proven to be a simple but effective tool to identify the dominant interactions between groundwater and surface water which result in major natural attenuation of anthropogenic nitrogen inputs.

Although natural attenuation of nitrate contamination within the Wensum catchment is significant and beneficial, the message from this research is not one of complacency as riverine and groundwater nitrate concentrations are high. Moreover, the relationship

between denitrification rate and nitrate concentration is not linear, as the overall efficiency of riverine nitrate removal declines with rising nitrate concentrations (Kemp and Dodds, 2002, Mulholland *et al.*, 2008). This means that optimal rates of denitrification in Wensum catchment waters are not achieved as a result of high nitrate concentrations, and that rising concentrations will not be matched by equal increases in removal through denitrification.

Therefore, there are two messages with respect to nitrogen regulation and control measures from this research. At a local scale, it is important to take into account denitrification when introducing regulatory controls including NVZ designation, as it can reduce the impact of agricultural nitrogen inputs on water quality. In particular, a robust quantification of hyporheic denitrification is essential if an accurate assessment of the riverine export of agricultural nitrogen is to be made. However, in the Wensum catchment, the fact that Chalk groundwater in the valley is only denitrified as baseflow and not within the Chalk aquifer itself, demonstrates the vulnerability of this important groundwater resource to continued inputs of nitrate. Due to the fact that nitrate from the Chalk valley groundwater represents nitrate leached directly from the permeable valley soils without significant attenuation, monitoring of nitrate concentrations in Chalk boreholes in the valley may give the best indication of current nitrate contamination trends, rather than riverine concentrations, which represent levels of nitrate after significant attenuation.

Further work should focus on demonstrating the wider applicability of the isotope and solute mass-balance mixing model approach to agricultural catchments. If its usefulness can be demonstrated across a range of hydrological environments it could prove to be a cost-effective method to aid the calibration of nitrogen regulation and control measures at the catchment scale.

It would be useful to confirm the findings of significant denitrification of Chalk valley groundwater in the hyporheic zone of the Wensum river. This could be achieved by using a temperature probe to identify areas in the riverbed where groundwater is advecting (identifiable because groundwater is warmer than river water in winter and cooler in summer). Then multilevel piezometers could be used in the riverbed to sample hyporheic waters at different depths for analysis of $\delta^{15}N_{NO3}$ and $\delta^{18}O_{NO3}$ and solute concentrations to look for a denitrification gradient in the isotopic composition and

concentration of nitrate, and for hydrochemical tracers of Chalk groundwater within the hyporheic zone. In addition riverbed collection chambers could be used to collect dissolved gases useful for the identification of denitrification (N_2, Ar, N_2O).

It would be of great interest to the scientific community to build upon the finding of significant hyporheic denitrification using isotopomers of nitrous oxide to differentiate and apportion nitrous oxide produced via denitrification from that produced through nitrification (Toyoda and Yoshida, 1999, Perez *et al.*, 2006, Sutka *et al.*, 2006, Koba *et al.*, 2009). The mid river reach of the Wensum would provide an ideal environment for this, as significant nitrous oxide production from denitrification is expected, along with nitrous oxide produced from nitrification in the surface layer of the riverbed sediments. This would enhance our understanding of riverine nitrogen cycling, and nitrous oxide emission from indirect sources.

REFERENCES

Aleem, M. I. H., Hoch, G. E. & Varner, J. E. (1965) Water as the source of oxidant and reductant in bacterial chemosynthesis. *Biochemistry,* 54**,** 869-873.

Alexander, R. B., Smith, R. A. & Schwarz, G. E. (2000) Effect of stream channel size on the delivery of nitrogen to the Gulf of Mexico. *Nature,* 403**,** 758-761.

Amberger, A. & Schmidt, H. L. (1987) Naturliche Isotopengehalte von nitrat als indikatoren fur dessen herkunft. *Geochimica et Cosmochimica Acta,* 51**,** 2699-2705.

Andersson, K. K. & Hooper, A. B. (1983) O_2 and H_2O are each the source of one O in NO_2^- produced from NH_3 by *Nitrosomonas*: ^{15}N-NMR evidence. *Federation of European Biochemical Societies Letters,* 164**,** 236-240.

Anisfeld, C. S., Barnes, R. T., Altabet, M. A. & Wu, T. (2007) Isotopic apportionment of atmospheric and sewage nitrogen sources in two Connecticut rivers. *Environmental Science and Technology,* 41**,** 6363-6369.

Aravena, R. & Robertson, W. D. (1998) Use of multiple isotope tracers to evaluate denitrification in ground water: study of nitrate from a large-flux septic system plume. *Ground Water,* 36**,** 975-982.

Arthurton, R. S., Booth, S. J., Morigi, A. N., Abbott, M. A. W. & Wood, C. J. (1994) *Geology of the country around Great Yarmouth. Memoir for 1: 50 000 geological sheet 162 (England and Wales),* British Geological Survey.

Baker, A. R. (2004) Inorganic iodine speciation in Tropical Atlantic aerosol. *Geophysical Research Letters,* 31**,** 4pp.

Baker, A. R., Weston, K., Kelly, S. D., Voss, M., Streu, P. & Cape, J. N. (2007) Dry and wet deposition of nutrients from the tropical Atlantic atmosphere: Links to primary productivity and nitrogen fixation. *Deep-Sea Research,* 1**,** 1704-1720.

Baker, M. A. & Vervier, P. (2004) Hydrological variability, organic matter supply and denitrification in the Garonne River ecosystem. *Freshwater Biology,* 49**,** 181-190.

Barkan, E. & Luz, B. (2005) High precision measurements of $^{17}O/^{16}O$ and $^{18}O/^{16}O$ ratios in H_2O. *Rapid Communications in Mass Spectrometry,* 19**,** 3737-3742.

Battaglin, W. A., Kendall, C., Chang, C., C.Y., Silva, S., R. & Cambell, D., H. (2001) Chemical and isotopic evidence of nitrogen transformation in the Mississippi River, 1997-98. *Hydrological Processes,* 15**,** 1285-1300.

Black, A. S. & Waring, S. A. (1977) The natural abundance of $\delta^{15}N$ in the soil water system of a small catchment area. *Australian Journal of Soil Research,* 15**,** 51-57.

Bohlke, J. K., Mroczkowski, S. J. & Coplen, T. B. (2003) Oxygen isotopes in nitrate: new reference materials for $^{18}O:^{17}O:^{16}O$ measurements and observations on nitrate-water equilibration. *Rapid Communications in Mass Spectrometry,* 17**,** 1835-1846.

Böttcher, J., Strebel, O., Voerkelius, S. & Schmidt, H. L. (1990) Using isotope fractionation of nitrate-nitrogen and nitrate-oxygen for evaluation of microbial denitrification in a sandy aquifer. *Journal of Hydrology,* 114**,** 413-424.

Boulton, A. J., Findlay, S., Marmonier, P., Stanley, E. H. & Valett, H. M. (1998) The functional significance of the hyporheic zone in streams and rivers. *Annual Review of Ecology and Systematics,* 29**,** 59-81.

Boyer, E., W., Goodale, C., Jaworski, N., A. & Howarth, R., W. (2002) Anthropogenic nitrogen sources and relationships to riverine nitrogen export in the northeastern U.S.A. *Biogeochemistry,* 57-58**,** 137-169.

Buda, A. R. & DeWalle, D. R. (2009) Dynamics of stream nitrate sources and flow pathways during stormflows on urban, forest and agricultural watersheds in central Pennsylvania, USA. *Hydrological Processes,* 23**,** 3292-3305.

Burger, M. & Jackson, L. E. (2004) Plant and microbial nitrogen use and turnover: Rapid conversion of nitrate to ammonium in soil with roots. *Plant and Soil,* 266**,** 289-301.

Burns, D., A. & Kendall, C. (2002) Analysis of $\delta^{15}N$ and $\delta^{18}O$ to differentiate NO_3^- sources in runoff at two watersheds in the Catskill Mountains of New York. *Water Resources Research,* 38.

Buss, S., Cai, Z., Cardenas, B., Fleckenstein, J., Hannah, D., Happel, K., Hulme, P. & Ibrahim, Y. (2009) The Hyporheic Handbook: A handbook on the groundwater-surface water interface and hyporheic zone for environmental managers. In Environment Agency (Ed.) *Integrated catchment science programme.* Bristol, Environment Agency.

Cambell, D., H., Kendall, C., Chang, C., C.Y., Silva, S., R. & Tonnessen, K., A. (2002) Pathways for nitrate release from an alpine watershed: Determination using $\delta^{15}N$ and $\delta^{18}O$. *Water Resources Research,* 38**,** 9pp.

Casciotti, K. L. & McIlvin, M. R. (2007) Isotopic analyses of nitrate and nitrite from reference mixtures and application to Eastern Tropical North Pacific waters. *Marine Chemistry,* 107**,** 184-201.

Casciotti, K. L., Sigman, D. M., Galanter Hastings, M., Bohlke, J. K. & Hilkert, A. (2002) Measurement of the oxygen isotopic composition of nitrate in seawater and freshwater using the denitrifier method. *Analytical Chemistry,* 74**,** 4905-4912.

Centre for Ecology and Hydrology (2009) National River Flow Archive. Natural Environment Research Council.

Cey, E., E., Rudolph, D., L., Aravena, R. & Parkin, G. (1999) Role of the riparian zone in controlling the distribution and fate of agricultural nitrogen near a small stream in southern Ontario. *Journal of Contaminant Hydrology,* 37**,** 45-67.

Chang, C., C.Y., Kendall, C., Silva, S., R., Battaglin, W., A. & Cambell, D., H. (2002) Nitrate stable isotopes: tools for determining nitrate sources among different land uses in the Mississippi River Basin. *Canadian journal of Fishery and Aquatic Science,* 56**,** 1856-1864.

Chang, C. C. Y., Langston, J., Riggs, M., Cambell, D. H., Silva, S. R. & Kendall, C. (1999) A method for nitrate collection for $\delta^{15}N$ and $\delta^{18}O$ analysis from waters with low nitrate concentrations. *Canadian journal of Fishery and Aquatic Science,* 56**,** 1856-1864.

Chatwin, C. P. (1961) *East Anglia and Adjoining Areas, 4th edition,* London, Her Majesty's Stationery Office.

Claret, C. & Boulton, A. J. (2009) Integrating hydraulic conductivity with biogeochemical gradients and microbial activity along river–groundwater exchange zones in a subtropical stream. *Hydrogeology Journal,* 17**,** 151-160.

Clement, J. C., Holmes, R. M., Peterson, B. J. & G., P. (2003) Isotopic investigation of denitrification in a riparian ecosystem in western France. *Journal of Applied Ecology,* 40**,** 1035-1048.

Cole, M. L., Kroeger, K. D., McClelland, J. W. & Valiela, I. (2006) Effects of watershed land use on nitrogen concentrations and δ^{15} nitrogen in groundwater. *Biogeochemistry***,** 199-215.

Coplen, T. B. (2008) Explanatory Glossary of Terms used in Expression of Relative Isotope ratios and Gas Ratios (Provisional Recommendations). Reston, International Union of Pure and Applied Chemistry Inorganic Chemistry Division Commission on Isotopic Abundances and Atomic Weights.

Coplen, T. B., Bohlke, J. K. & Casciotti, K. L. (2004) Using dual-bacterial denitrification to improve $\delta^{15}N$ determinations of nitrates containing mass-independent ^{17}O. *Rapid Communications in Mass Spectrometry,* 18**,** 245-250.

Coplen, T.B., Herczeg, A.L. & Barnes, C. (2000) Isotope engineering-using stable isotopes of the water molecule to solve practical problems; in: *Environmental Tracers in Subsurface Hydrology* (Cook, P.G. & Herczeg, A.L.eds.) Kluwer Academic Publishers, Boston.

Coplen, T. B., Kendall, C. & Hopple, J. (1983) Comparison of stable isotope reference samples. *Nature,* 302**,** 236-238.

Council of European Communities (1991) Directive Concerning the Protection of Waters against Pollution Caused by Nitrates from Agricultural Sources (91/676/EEC).

Council of European Communities (1998) Directive Relating to the Quality of Water Intended for Human Consumption (98/83/EC).

Council of European Communities (2000) Directive of the European Parliament and of the Council establishing a framework for the Community action in the field of water policy (2000/60/EC).

Craig, H. (1957) Isotopic standards for carbon and oxygen and correction factors for mass-spectrometric analysis of carbon dioxide. *Geochimica et Cosmochimica Acta,* 12**,** 133-149.

Craig, H. (1961) Isotopic variations in meteoric waters. *Science,* 133**,** 1702-1703.

Curie, F., Ducharne, A., Sebilo, M. & Bendjoudi, H. (2009) Denitrification in a hyporheic riparian zone controlled by river regulation in the Seine river basin (France). *Hydrological Processes,* 23**,** 655-664.

Dansgaard, W. (1964) Stable istotopes in precipitation. *Tellus,* 16**,** 436-468.

Darling, W. G., Bath, A. H. & Talbot, J. C. (2003) The O & H stable isotopic composition of fresh waters in the British Isles. 2. Surface waters and groundwater. *Hydrology and Earth System Sciences,* 7**,** 183-195.

Darling, W. G. & Talbot, J. C. (2003) The O and H stable isotope composition of fresh waters in the British Isles. 1. Rainfall. *Hydrology and Earth System Sciences,* 7**,** 163-181.

De Laeter, J. R., Bohlke, J. K., De Bievre, P., Hidaka, H., Peiser, H. S., Rosman, K. J. R. & Taylor, P. D. P. (2003) Atomic weights of the elements: review 2000, IUPAC Technical Report. *Pure and Applied Chemistry,* 75**,** 683-800.

Defra (2006) Final Results of the June 2005 Agricultural and Horticultural Census for England. Department for Environment, Food and Rural Affairs.

Defra (2009a) Guidance for Farmers in Nitrate Vulnerable Zones: Summary of the guidance for farmers in NVZs. In Defra (Ed.), Department for Environment, Food and Rural Affairs.

Defra (2009b) Farming: Single Payment Scheme. Department for Environment, Food and Rural Affairs, http://www.defra.gov.uk/foodfarm/farmmanage/singlepay/index.htm Last accessed 12/2009.

Defra: Water Quality Division (2008) Implementation of the Nitrates Directive (91/676/EEC): Description of the methodology applied in identifying waters and designating Nitrates Vulnerable Zones in England (2008). Department for Environment, Food and Rural Affairs.

Delwiche, C. C. & Steyn, P. L. (1970) Nitrogen isotope fractionation in soils and microbial reactions. *Environmental Science and Technology,* 4**,** 927-935.

Deutsch, B., Liskow, I., Kahle, P. & Voss, M. (2005) Variations of the $\delta^{15}N$ and $\delta^{18}O$ values of nitrate in drainage water of two fertilized fields in Mecklenburg-Vorpommern (Germany). *Aquatic Sciences,* 67**,** 156-165.

Deutsch, B., Mewes, M., Liskow, I. & Voss, M. (2006) Quantification of diffuse nitrate inputs into a small river system using stable isotopes of oxygen and nitrogen in nitrate. *Organic Geochemistry,* 37**,** 1333-1342.

DiSpirito, A. A. & Hooper, A. B. (1986) Oxygen exchange between nitrate molecules during nitrite oxidation by Nitrobacter. *Journal of Biological Chemistry,* 261**,** 10534-10537.

Drapcho, D. L., Sisterton, D. & Kumar, R. (1983) Nitrogen fixation by lightening activity in a thunderstorm. *Atmospheric Environment,* 17**,** 729-734.

Driscoll, C. T., Lawrence, G. B., Bulger, A. J., Butler, T. J., Cronan, C. S., Eager, C., Lambert, K. F., Likens, G. E., Stoddard, J. L. & Weathers, K. C. (2001) Acid Rain Revisited: Advances in Scientific Understanding since the Passage of the 1970 and 1990 Clean Air Act Amendments. *Science Links Publication.* Hubbard Brook Research Foundation.

Duan, S., Bianchi, T. S., Shiller, A. M., Dria, K., Hatcher, P. G. & Carman, K. R. (2007) Variability in the bulk composition and abundance of dissolved organic matter in the lower Mississippi and Pearl rivers. *Journal of Geophysical Research,* 112**,** G02024.

Eames, K. (2008) A Lagrangian trajectory and isotopic fractionation (FLEXPART-MCIM) approach to modelling the isotopic composition of Western European precipitation. PhD Thesis. School of Environmental Sciences, University of East Anglia UK.

Edwards, A. M. C. (1973) The variation of dissolved constituents with discharge in some Norfolk rivers. *Journal of Hydrology* 18**,** 219-242.

Entec (2007) Phase 3 Project Report for the Yare and North Norfolk Groundwater Resource Investigation Area. Wensum and Tud Reporting Area, Volume 1: Characterisation of Catchment Behaviour. Peterborough, Environment Agency.

Environment Agency (2006) Broadland Rivers Catchment Flood Management Plan - Draft Report, June 2006. Environment Agency.

Environment Agency (2009a) Water for livelihoods: River Basin Management Plan Anglian River Basin District. Bristol, Environment Agency.

Environment Agency (2009b) What's in your backyard? river quality nutrient concentrations. Environment Agency, http://maps.environment-agency.gov.uk/wiyby Last accessed 10/2009.

Environment Agency (2009c) Catchment sensitive farming. Environment Agency.

Environment Agency (2009d) What's in your backyard? urban wastewater treatment. Environment Agency, http://maps.environment-agency.gov.uk/wiyby Last accessed 11/2009.

Environment Agency (2009e) HiFlows-UK. Environment Agency http://www.environment-agency.gov.uk/hiflows/91727.aspx Last accessed 10/2009.

Epstein, S. & Mayeda, T. (1953) Variations of ^{18}O content of waters from natural sources. *Geochimica et Cosmochimica Acta,* 4**,** 213-224.

Europress (2003) High in the sky, get mapping aerial photography: Norfolk *The Millennium Map.*

Feast, N. A., Hiscock, K. M., Dennis, P. F. & Andrews, J. N. (1998) Nitrogen isotope hydrochemistry and denitrification within the Chalk aquifer system of north Norfolk, UK. *Journal of Hydrology,* 211**,** 233-252.

Feast, N. A., Hiscock, K. M., Dennis, P. F. & Bottrell, S. H. (1997) Controls on stable isotope profiles in the Chalk aquifer of north-east Norfolk, UK, with special reference to dissolved sulphate. *Applied Geochemistry,* 12**,** 803-812.

Fegin, A., Shearer, G., Kohl, D. H. & Commoner, B. (1974) The amount and N15-content of nitrate in soil profiles from two central Illinois fields in a corn-soybean rotation. *Soil Science Society of America Proceedings,* 38**,** 465-471.

Fogel, M. L. & Cifuentes, L. A. (1993) Isotope fractionation during primary production. In Engel, M. H. & Macko, S. A. (Eds.) *Organic Chemistry.* New York, Plenium Press.

Fogg, G. E., Rolston, D. E., Decker, D. L., Louie, D. T. & Grismer, M. E. (1998) Spatial variation in nitrogen isotope values beneath nitrate contamination sources. *Ground Water,* 36**,** 418-426.

Fukada, T., Hiscock, K. M. & Dennis, P. F. (2004) A dual-isotope approach to the nitrogen hydrochemistry of an urban aquifer. *Applied Geochemistry,* 19**,** 709-719.

Galloway, J. N., Aber, J. D., Erisman, J. W., Seitzinger, S. P., Howarth, R. W., Cowling, E. B. & Cosby, J. (2003) The nitrogen cascade. *BioScience,* 53**,** 341-356.

Gooseff, M. N. (2010) Defining hyporheic zones – advancing our conceptual and operational definitions of where stream water and groundwater meet. *Geography Compass,* 4**,** 945-955.

Granger, J., Sigman, D. M., Lehmann, M. F. & Tortell, P. D. (2008) Nitrogen and oxygen isotope fractionation during dissimilatory nitrate reduction by denitrifying bacteria. *Limnology and Oceanography,* 53**,** 2533-2545.

Granger, J., Sigman, D. M., Needoba, J. A. & Harrison, P. J. (2004) Coupled nitrogen and oxygen isotope fractionation of nitrate during assimilation by cultures of marine phytoplankton. *Limnology and Oceanography,* 49**,** 1763-1773.

Granger, J., Sigman, D. M., Prokopenko, M. G., Lehmann, M. F. & Tortell, P. D. (2006) A method for nitrite removal in nitrate N and O isotope analyses. *Limnology and Oceanography: Methods,* 4**,** 205-212.

Green, P. A., Vorosmarty, C. J., Meybeck, M., Galloway, J. N., Peterson, B. J. & Boyer, E. W. (2004) Pre-industrial and contemporary fluxes of nitrogen through rivers: a global assessment based on typology. *Biochemistry,* 68**,** 71-105.

Harvey, B. I., Langston, M. J., Hughes, M. D. A., Whalley, H. A. & Cripps, A. C. (1973) Records of wells in the area around Norwich: Inventory for one-inch geological sheet 161, new series. In NERC (Ed.) *Well Inventory Service.* Institute of Geological Sciences.

Harvey, B. I., Langston, M. J., Hughes, M. D. A., Whalley, H. A. & Cripps, A. C. (1974) Records of wells in the area around Fakenham: Inventory for one-inch geological sheet 146, new series. In NERC (Ed.) *Well Inventory Service.* Institute of Geological Sciences.

Heaton, T. H. E. (1986) Isotopic studies of nitrogen pollution in the hydrosphere and atmosphere: a review. *Chemical Geology (Isotope Geosciences Section),* 59**,** 87-102.

Heaton, T. H. E., Spiro, B., Madeline, S. & Robertson, C. (1997) Potential canopy influences on the isotopic composition of nitrogen and sulphur in atmospheric deposition. *Oceologia,* 109**,** 600-607.

Heaton, T. H. E., Talma, A. S. & Vogel, J. C. (1983) Origin and history of nitrate in confined groundwater in the western Kalahari. *Journal of Hydrology,* 62**,** 243-262.

Hedin, L. O., von Fischer, J. C., Ostrom, N. E., Kennedy, B. P., Brown, M. G. & Robertson, G. P. (1998) Thermodynamic constraints on nitrogen transformations and other biogeochemical processes at soil-stream interfaces. *Ecology,* 79**,** 684-703.

Hem, J. D. (1985) *Study and Interpretation of the Chemical Characterstics of Natural Water,* United States Geological Survey.

Hernandez, M. E. & Mitsch, W. J. (2006) Denitrification in created riverine wetlands: influence of hydrology and season. *Annual Report: Olentangy River Wetland Research Park.* Ohio, Ohio State Knowledge Bank.

Hinkle, S. R., Duff, J. H., Triska, F. J., Laenen, A., Gates, E. B., Bencala, K. E., Wentz, D. A. & Silva, S. R. (2001) Linking hyporheic flow and nitrogen cycling near the Willamette River-a large river in Oregon, USA. *Journal of Hydrology,* 244**,** 157-180.

Hiscock, K. M. (1993) the influence of pre-Devensian glacial deposits on the hydrogeochemistry of the Chalk aquifer system of north Norfolk, UK. *Journal of Hydrology***,** 335-369.

Hiscock, K. M. (2005) *Hydrogeology Principles and Practice,* Oxford, Blackwell Publishing.

Hiscock, K. M., Dennis, P. F., Saynor, P. R. & Thomas, M. O. (1996) Hydrochemical and stable isotope evidence for the extent and nature of the effective Chalk aquifer of north Norfolk, UK. *Journal of Hydrology,* 180**,** 79-107.

Hoefs, J. (2004) *Stable Isotope Geochemistry,* Berlin, Springer-Verlag.

Hogberg, P. (1997) Tansley Review No. 95. ^{15}N Natural Abundance in Soil-Plant Systems. *New Phytologist,* 137**,** 179 - 203.

Hollocher, T. C. (1984) Source of the oxygen atoms of nitrate in the oxidation of nitrite by *Nitrobacter agilis* and evidence against a P-O-N anhydride mechanism in oxidative phosphorylation. *Archives of Biochemistry and Biophysics,* 233**,** 721-727.

Hollocher, T. C., Tate, M. E. & Nicholas, D. J. D. (1981) Oxidation of ammonia by *Nitrosomonas europaea*: definitive ^{18}O tracer evidence that hydroxylamine formation involves a monooxygenase. *The Journal of Biological Chemistry,* 262**,** 10834-10836.

Holtan-Hartwig, L., Dorsch, P. & Bakken, L. R. (2002) Low temperature control of soil denitrifying communities: kinetics of N_2O production and reduction. *Soil Biology & Biochemistry,* 34**,** 1797-1806.

Hopson, P. M. (2005) A stratigraphical framework for the Upper Cretaceous Chalk of England and Scotland, with statements on the Chalk of Northern Ireland and the UK Offshore Sector: Geological Survey Research Report. Keyworth, Nottingham, British Geological Survey.

Hornung, M. (1999) The Role of Nitrates in the Eutrophication and Acidification of Surface Waters. In Wilson, W. S., Ball, A. S. & Hinton, R. H. (Eds.) *Managing Risks of Nitrates to Humans and the Environment.* Cambridge, The Royal Society of Chemistry.

Hubner, H. (1986) Isotope Effects of Nitrogen in the Soil and Biosphere. In Fritz, P. & Fontes, J. C. (Eds.) *Handbook of Environmental Isotope Geochemistry.* New York, Elsevier.

Hudson, F. (2004) Sample Preparation and Calculations for Dissolved Gas Analysis in Water Samples Using a GC Headspace Equilibration Technique. United States Environmental Protection Agency.

Inoue, H. Y. & Mook, W. G. (1994) Equilibrium and kinetic nitrogen and oxygen isotope fractionations between dissolved and gaseous N_2O. *Chemical Geology (Isotope Geosciences Section),* 113**,** 135-148.

Johannsen, A., Dahnke, K. & Emeis, K. (2008) Isotopic composition of nitrate in five German rivers discharging into the North Sea. *Organic Geochemistry,* 39**,** 1678-1689.

Johnson, M. (2004) The air sea flux of ammonia. PhD Thesis. School of Environmental Sciences, University of East Anglia UK.

Kaiser, J., Hastings, M. G., Houlton, B. Z., Rockmann, T. & Sigman, D. M. (2007) Triple oxygen isotope analysis of nitrate using the denitrifier method and thermal decomposition of N_2O. *Analytical Chemistry,* 79**,** 599-607.

Karamanos, R. E. & Rennie, D. A. (1978) N isotope fractionation during NH_4^+ exchange reactions with soil clay. *Canadian journal of Soil Science,* 58**,** 53-60.

Kellman, L. M. (2004) Nitrate removal in a first-order stream: reconciling laboratory and field measurements. *Biogeochemistry,* 71**,** 89-105.

Kellman, L. M. & Hillaire-Marcel, C. (1998) Nitrate cycling in streams: using natural abundances of NO_3-$\delta^{15}N$ to measure *in-situ* denitrification. *Biogeochemistry,* 43**,** 273-292.

Kellman, L. M. & Hillaire-Marcel, C. (2003) Evaluation of nitrogen isotopes as indicators of nitrate contamination sources in an agricultural watershed. *Agriculture, Ecosystems and Environment,* 95**,** 87-102.

Kemp, M. J. & Dodds, W. K. (2002) Comparison of nitrification and denitrification in prairie and agriculturally influenced streams. *Ecological Applications,* 12**,** 998-1009.

Kendall, C. (1998) Tracing nitrogen sources and cycling in catchments. In Kendall, C. & McDonnell, J. J. (Eds.) *Isotope Tracers in Catchment Hydrology.* New York, Elsevier Science.

Kendall, C., Elliott, E. M. & Wankel, S. D. (2007) Tracing Anthropogenic Inputs of Nitrogen to Ecosystems. In Lajtha, K. & Michener, R. (Eds.) *Stable Isotopes in Ecology and Environmental Science (2nd Edition).* Blackwell.

Kendall, C., Silva, S. R. & Kelly, V. J. (2001) Carbon and nitrogen isotopic compositions of particulate organic matter in four large river systems across the United States. *Hydrological Processes,* 15**,** 1301-1346.

Khalil, M. A. K., Rasmussen, R. A. & Shearer, M. J. (2002) Atmospheric nitrous oxide: patterns of global change during recent decades and centuries. *Chemosphere,* 47**,** 807-821.

Killham, K. (1994) *Soil Ecology,* Cambridge University Press.

Koba, K., Osaka, K., Tobari, Y., Toyoda, S., Ohte, N., Katsuyama, M., Suzuki, N., Itoh, M., Yamagishi, H., Kawasaki, I. M., Kim, S. J., Yoshida, N. & Nakajima, T. (2009) Biogeochemistry of nitrous oxide in groundwater in a forested ecosystem elucidated by nitrous oxide isotopomer measurements. *Geochimica et Cosmochimica Acta,* 73**,** 3115-3133.

Kohl, D. H., Shearer, G. B. & Commoner, B. (1971) Fertilizer nitrogen: contribution to nitrate in surface water in a corn belt watershed. *Science,* 174**,** 1331-1334.

Kool, D. M., Wrage, N., Oenema, O., Dolfing, J. & Van Groenigen, J. W. (2007) Oxygen exchange between (de)nitrification intermediates and H_2O and its implications for source determination of NO_3^- and N_2O: a review. *Rapid Communications in Mass Spectrometry,* 21**,** 3569-3578.

Kreitler, C. W. (1979) Nitrogen-isotope ratio studies of soils and groundwater nitrate from alluvial fan aquifers in Texas. *Journal of Hydrology,* 42**,** 147-170.

Kroopnick, P. & Craig, H. (1972) Atmospheric Oxygen: Isotopic Composition and Solubility Fractionation. *Science,* 175**,** 54-55.

Kumar, S., Nicholas, D. J. D. & Williams, E. H. (1983) Definitive ^{15}N NMR evidence that water serves as a source of "O" during nitrite oxidation by *Nitrobacter agilis*. *Federation of European Biochemical Societies Letters,* 152**,** 71-74.

Laursen, A. E. & Seitzinger, P. S. (2002) Measurement of denitrification in rivers: an integrated, whole reach approach. *Hydrobiologia,* 485**,** 67-81.

Laursen, A. E. & Seitzinger, P. S. (2005) Limitations to measuring riverine denitrification at the whole reach scale: effects of channel geometry, wind velocity, sampling interval, and temperature inputs of N_2-enriched groundwater. *Hydrobiologia,* 545**,** 225-236.

Lehmann, M. F., Reichert, P., Bernasconi, S. M., Barbieri, A. & McKenzie, J. A. (2003) Modelling nitrogen and oxygen isotope fractionation during denitrification in a lacustrine redox-transition zone. *Geochimica et Cosmochimica Acta,* 67**,** 2529-2543.

Leininger, S., Urich, T., Schloter, M., Schwark, L., Qi, J., Nicol, G. W., Prosser, J. I., Schuster, S. C. & Schleper, C. (2006) Archaea predominate among ammonia-oxidizing prokaryotes in soils. *Nature,* 442**,** 806-809.

Lloyd, J. & Taylor, J. A. (1994) On the temperature dependence of soil respiration. *Functional Ecology,* 8**,** 315-323.

Lloyd, J. R., Klessa, D. A., Parry, D. L., Buck, P. & Brown, N. L. (2004) Stimulation of microbial sulphate reduction in a constructed wetland: microbiological and geochemical analysis. *Water Research,* 38**,** 1822-1830.

Mackney, D., Hodgson, J. M., Hollis, J. M. & Staines, S. J. (1983) Soil Map of England and Wales 1: 250 000 Sheet 4: Eastern England. Soil Survey of England and Wales.

Mariotti, A., Germon, J. C., Hubert, P., Kaiser, P., Letolle, R., Tardieux, A. & Tardieux, P. (1981) Experimental determination of nitrogen kinetic isotope fractionation: some principles; illustration for the denitrification and nitrification processes. *Plant and Soil,* 62**,** 413-430.

Mariotti, A., Landreau, A. & Simon, B. (1988) ^{15}N isotope biogeochemistry and natural denitrification process in groundwater: Application to the chalk aquifer of northern France. *Geochimica et Cosmochimica Acta,* 52**,** 1869 -1878.

Mariotti, A., Mariotti, F., Armarger, N., Pizelle, G., Ngambi, J. M., Champigny, M. L. & Moyse, A. (1980) Fractionnements isotopiques de l'azote lors processus d'absorption de nitrates et de fixation de l'azote atmospherique par les plantes. *Physiologie Vegetale,* 18**,** 163-181.

Marsh, T. J. & Hannaford, J. (Eds.) (2008) *UK Hydrometric Register*, Centre for Ecology and Hydrology.

Mayer, B., Bollwerk, S. M., Mansfeldt, T., Hutter, B. & Veizer, J. (2001) The oxygen isotope composition of nitrate generated by nitrification in acid forest floors. *Geochimica et Cosmochimica Acta,* 65**,** 2743-2756.

Mayer, B., Boyer, E., W., Goodale, C., Jaworski, N., A., Van Breemen, N., Howarth, R., W., Seitzinger, S., Billen, G., Lajtha, K., Nadelhoffer, K., Van Dam, douwe, hetling, L., j., Nosal, M. & Paustian, K. (2002) Sources of nitrates in rivers draining sixteen watersheds in northeastern U.S.: Isotopic constraints. *Biogeochemistry,* 57/58**,** 171-197.

McCulloch, I., Pettman, I. & Talling, J. (2007) Interrelated contributions to freshwater science over 78 years: a guide to published works from The Freshwater Biological Association, Institute of Freshwater Ecology, and Centre for Ecology and Hydrology, 1929-2006. *Freshwater Forum,* 27**,** 27-46.

McIlvin, M. R. & Altabet, M. A. (2005) Chemical conversion of nitrate and nitrite to nitrous oxide for nitrogen and oxygen isotopi analysis in freshwater and seawater. *Analytical Chemistry,* 77**,** 5589-5595.

Met Office (2009) East Anglia 1961-1990 climate averages. Met Office, http://www.metoffice.gov.uk/climate/uk/averages/19611990/areal/east_anglia Last accesses 10/2009.

Michalski, W. P. & Nicholas, D. J. D. (1984) The adaptation of *Rhodopseudomonas sphaeroides* f. sp. *denitrificans* for growth under denitrifying conditions. *Journal of General Microbiology,* 130**,** 155-165.

Michalski, W. P. & Xu, F. (2010) Isotope modeling of nitric acid formation in the atmosphere using ISO-RACM: testing the importance of NO oxidation, heterogeneous reactions, and trace gas chemistry. *Atmospheric Chemistry and Physics Discussions,* 10**,** 6829-6869.

Millennium Ecosystem Assessment (2005) Ecosystems and Human Well-Being: findings of the Condition and Trends Working Group. Volume 1: Current State and Trends, Millennium Ecosystem Assessment. In Hassan, H., Scholes, R. & Ash, N. (Eds.) *Millenium Ecosystem Assessment.* Island Press.

Moorlock, B. S. P., Booth, S. J., Fish, S. J., Hamblin, R. J. O., Kessler, H., Riding, J. B., Rose, J. & Whiteman, C. A. (2000) A revised glacial stratigraphy of Norfolk. In Lewis, S. G., Whiteman, C. A. & Preece, R. C. (Eds.) *The Quaternary of Norfolk and Suffolk; Field guide.* London, Quaternary Research Association.

Moorlock, B. S. P., Hamblin, R. J. O., Booth, S. J., Kessler, H., Woods, M. A. & Hobbs, P. R. N. (2002) Geology of the Cromer district - a brief explanation of the geological map. Sheet explanation of the British Geological Survey, 1: 50 000, Sheet 131, Cromer (England and Wales). Keyworth, Nottingham, British Geological Survey.

Morkved, P. T., Dorsch, P., Sovik, A. K. & Bakken, L. R. (2007) Simplified preparation for the δ^{15}N-analysis in soil NO_3^- by the denitrifier method. *Soil Biology & Biochemistry,* 39**,** 1907-1915.

Moseley, R., Woodward, C. M., Day, J. B. W. & Langston, M. J. (1976) Hydrogeological map of northern East Anglia sheet 1. Institute of Geological Sciences.

Mulholland, P. J., Helton, A. M., Poole, G. C., Hall, R. O., Hamilton, S. K., Peterson, B. J., Tank, J. L., Ashkenas, L. R., Cooper, L. W., Dahm, C. N., Dodds, W. K., Findlay, S. E. G., Gregory, S. V., Grimm, N. B., Johnson, S. L., McDowell, W. H., Meyer, J. L., Valett, H. M., Webster, J. R., Arango, C. P., Beaulieu, J. J., Bernot, M. J., Burgin, A. J., Crenshaw, C. L., Johnson, L. T., Niederlehner, B. R., O'Brien, J. M., Potter, J. D., Sheibley, R. W., Sobota, D. J. & Thomas, S. M. (2008) Stream denitrification across biomes and its response to anthropogenic nitrate loading. *Nature,* 452**,** 202-206.

National Soil Resources Institute (2009) LandIS Soilscapes 1: 250 000. Cranfield University, http://www.landis.org.uk/soilscapes/ Last accessed 11/2009.

Office for National Statistics (2005) Census 2001. Population Statistics Unit, Office for National Statistics.

Pardo, L. H., Kendall, C., Pett-Ridge, J. & Chang, C. C. Y. (2004) Evaluating the source of streamwater nitrate using δ^{15}N and δ^{18}O in nitrate in two watersheds in New Hampshire, USA. *Hydrological Processes,* 18**,** 2699-2712.

Perez, T., Garcia-Montiel, D., Trumbore, S., Tyler, S., de Carmargio, P., Moreira, M., Piccolo, M. & Cerri, C. (2006) Nitrous oxide nitrification and denitrification ^{15}N enrichment factors from Amazon forest soils. *Ecological Applications,* 16**,** 2153-2167.

Petitta, M., Fracchiolla, D., Aravena, R. & Barbieri, M. (2009) Application of isotopic and geochemical tools for the evaluation of nitrogen cycling in an agricultural basin, the Fucino Plain, central Italy. *Journal of Hydrology,* 372**,** 124-135.

Pina-Ochoa, E. & Alvarez-Cobelas, M. (2006) Denitrification in aquatic environments: a cross-system analysis. *Biochemistry,* 81**,** 111-130.

Pinardi, M., Bartoli, M., Longhi, D., Marzocchi, U., Laini, A., Ribaudo, C. & Viaroli, P. (2009) Benthic metabolism and denitrification in a river reach: a comparison between vegetated and bare sediments. *Journal of Liminology,* 68**,** 133-145.

Puckett, L. J., Zamora, C., Essaid, H., Wilson, J. T., Johnson, H. M., Brayton, M. J. & Vogel, J. R. (2008) Transport and fate of nitrate at the ground-water/surface-water interface. *Jounal of Environmental Quality,* 37**,** 1034-1050.

Ravishankara, A. R., Daniel, J. S. & Portmann, R. W. (2009) Nitrous Oxide (N_2O): The Dominant Ozone-Depleting Substance Emitted in the 21st Century. *Science,* 326**,** 123-125.

Rekacewicz, P., Bournay, E. & UNEP/GRID-Arendal (2005) Reactive nitrogen on earth by human activity, with projection to 2050. Millennium Ecosystem Assessment.

Revesz, K. & Bohlke, J. K. (2002) Comparison of $\delta^{18}O$ measurements in nitrate by different combustion techniques. *Analytical Chemistry,* 74**,** 5410-5413.

Rockmann, T., Kaiser, J., Brenninkmeijer, C. A. M. & Brand, W. A. (2003) Gas chromatography/isotope-ratio mass spectrometry method for high-precision position-dependent ^{15}N and ^{18}O measurements of atmospheric nitrous oxide. *Rapid Communications in Mass Spectrometry,* 17**,** 1897-1908.

Royal Society (1983) The Nitrogen Cycle of the United Kingdom - A Study Group Report. London, The Royal Society.

Royer, T. V., Tank, J. L. & David, M. B. (2004) Transport and fate of nitrate in headwater agricultural streams in Illinois. *Journal of Environmental Quality***,** 1296-1304.

Schleper, C., Jurgens, G. & Jonuscheit, M. (2005) Genomic studies of uncultivated archaea. *Nature Reviews: Microbiology,* 3**,** 479-488.

Sear, D. A., Newson, M., Old, J. C. & Hill, C. (2006) Geomorphological Appraisal of the River Wensum Special Area of Conservation. English Nature Research Reports, No 685. English Nature.

Sebilo, M., Billen, G., Grably, M. & Mariotti, A. (2003) Isotopic composition of nitrate-nitrogen as a marker of riparian and benthic denitrification at the scale of the whole Seine River system. *Biogeochemistry,* 63**,** 35-51.

Seitzinger, S., Harrison, J. A., Bohlke, J. K., Bouwman, A. F., Lowrance, R., Peterson, B. J., Tobias, C. & Van Drecht, G. (2006) Denitrification across landscapes and waterscapes: a synthesis. *Ecological Applications,* 16**,** 2064-2090.

Shaw, E.M. (1994) *Hydrology in Practice,* Chapman Hall.

Shearer, G. B., Kohl, D. H. & Commoner, B. (1974a) The precision of determinations of the natural abundance of nitrogen-15 in soils, fertilizers, and shelf chemicals. *Soil Science* 118**,** 308-316.

Sheibley, R. W., Jackman, A. P., Duff, J. H. & Triska, F. J. (2003) Numerical modeling of coupled nitrification–denitrification in sediment perfusion cores from the hyporheic zone of the Shingobee River, MN. *Advances in Water Resources,* 26**,** 977-983.

Sickman, J., O., Leydecker, A., Chang, C. C. Y., Kendall, C., Melack, J., M., Lucero, D., M. & Schimel, J. (2003) Mechanisms underlying export on N from high-elevation catchments during seasonal transitions. *Biogeochemistry,* 64**,** 1-24.

Sigman, D. M., Casciotti, K. L., Andreani, M., Barford, C., M., G. & Bohlke, J. K. (2001) A bacterial method for the nitrogen isotopic analysis of nitrate in seawater and freshwater. *Analytical Chemistry,* 73**,** 4145-4153.

Silva, S. R., Ging, P. B., Lee, R. W., Ebbert, J. C., Tesoriero, A. J. & Inkpen, E. L. (2002) Forensic applications of nitrogen and oxygen isotopes in tracing nitrate sources in urban environments. *Environmental Forensics,* 3**,** 125-130.

Silva, S. R., Kendall, C., Wilkinson, D. H., Ziegler, A. C., Chang, C. C. Y. & Avanzino, R. J. (2000) A new method for collection of nitrate from fresh water and the analysis of nitrogen and oxygen isotope ratios. *Journal of Hydrology,* 228**,** 22-36.

Sjodin, A. L., Lewis, W. M. & Saunders, J. F. (1997) Denitrification as a component of the nitrogen budget for a large plains river. *Biochemistry,* 39**,** 327-342.

Smith, J. W. N., Surridge, B. W. J., Haxton, T. H. & Lerner, D. N. (2009) Pollutant attenuation at the groundwater–surface water interface: A classification scheme and statistical analysis using national-scale nitrate data. *Journal of Hydrology,* 369**,** 392-402.

Spoelestra, J., Schiff, S. L., Hazlett, P. W., Jeffries, D. S. & R.G., S. (2007) The isotopic composition of nitrate produced from nitrification in a hardwood forest floor. *Geochimica et Cosmochimica Acta,* 71**,** 3757-3771.

Sutka, R. L., Ostrom, N. E., Ostrom, P. H., Breznak, J. A., Ghandi, H., Pitt, A. J. & Li, F. (2006) Distinguishing nitrous oxide production from nitrification and denitrification on the basis of isotopomer abundances. *Applied and Environmental Microbiology,* 72**,** 638-644.

Tiedje, J. M. (1988) Ecology of denitrification and dissimilatory reduction of nitrate to ammonium. In Zehnder, A. J. B. (Ed.) *Biology of Anaerobic Organisms.* New York, Wiley.

Toynton, R. (1979) Waste disposal hydrogeology with special reference to the Chalk of East Anglia. PhD Thesis. School of Environmental Sciences, University of East Anglia UK.

Toyoda, S. & Yoshida, N. (1999) Determination of nitrogen isotopomers of nitrous oxide on a modified isotope ratio mass spectrometer. *Analytical Chemistry,* 71**,** 4711-4718.

Tsushima, K., Ueda, S., Ohno, H., Ogura, N., Katase, T. & Watanabe, K. (2006) Nitrate decrease with isotopic fractionation in riverside sediment column during infiltration experiment. *Water, Air, and Soil Pollution,* 174**,** 47-61.

UK Meteorological Office (2010) MIDAS Land Surface Stations data (1853-current). British Atmospheric Data Centre.

Van der Hoven, S. J., Fromm, N. J. & Peterson, E. W. Quantifying nitrogen cycling beneath a meander of a low gradient, N-impacted, agricultural stream using tracers and numerical modelling. *Hydrological Processes,* 22**,** 1206-1215.

Vitousek, P. M., Aber, J. D., Howarth, R. W., Likens, G. E., Matson, P. A., Schindler, D. W., Schlesinger, W. H. & Tilman, D. G. (1997) Human alteration of the global nitrogen cycle: sources and consequences. *Ecological Applications,* 7**,** 737-750.

Vogel, J. C., Talma, A. S. & Heaton, T. H. E. (1981) Gaseous nitrogen as evidence for denitrification in groundwater. *Journal of Hydrology,* 50**,** 191-200.

Wade, A. J., Neal, C., Whitehead, P. G. & Flynn, N. J. (2005) Modelling nitrogen fluxes from the land to the coastal zone in European systems: a perspective from the INCA project. *Journal of Hydrology,* 304**,** 413-429.

Ward, M. H., deKok, T. M., Levallois, P., Brender, J., Gulis, G., Nolan, B. T. & VanDerslice, J. (2005) Workgroup report: drinking-water nitrate and health—recent findings and research needs. *Environmental Health Perspectives,* 113**,** 1607–1614.

Warnecke-Eberz, U. & Friedrich, B. (1993) Three nitrate reductase activities in *Alcaligenes eutrophus*. *Archives of Microbiology,* 159**,** 405-409.

Wassenaar, L. I. (1995) Evaluation of the origin and fate of nitrate in the Abbotsford Aquifer using the isotopes of ^{15}N and ^{18}O in NO_3^-. *Applied Geochemistry,* 10**,** 391-405.

Weisse, T. (1991) The annual cycle of heterotrophic freshwater nanoflagellates: role of botton-up versus top-down control. *Journal of Plankton Research,* 13**,** 167-185.

Wilhelm, E., Battino, R. & Wilcock, R. J. (1977) Low-pressure solubility of gases in liquid water. *Chemical Reviews,* 77**,** 219-262.

Wolfe, A. & Patz, J. A. (2002) Reactive nitrogen and human health: acute and long-term implications. *Ambio,* 31**,** 120-125.

Wrage, N., Velthof, G. L., van Beusichem, M. L. & Oenema, O. (2001) Role of nitrifier denitrification in the production of nitrous oxide. *Soil Biology and Biochemistry*, 33**,** 1723-1732.

Yang, Z., Niimi, H., Kanda, K. & Suga, Y. (2003) Measurement of ammonia volatilization from a field, in upland Japan, spread with cattle slurry. *Environmental Pollution,* 121**,** 463-467.

Yusoff, I., Hiscock, K. M. & Conway, D. (2002) Simulation of the impacts of climate change on groundwater resources in eastern England. In Hiscock, K. M., Rivett, M. O. & Davison, R. M. (Eds.) *Sustainable Groundwater Development.* London, Geological Society Special Publications N^{o} 193.

Zumft, W. G. (1997) Cell biology and molecular basis of denitrification. *Microbiology and Molecular Biology Reviews,* 61**,** 533-616.

APPENDICES

APPENDIX 1 METHODS

A 1.1 Denitrifier Method SOP:
Pseudomonas aureofaciens culturing protocol adapted from Frank Yi Wang SOP, 2006 (Danny Sigman's group) and Matt McIlvin personal communication, Oct 2007 (Karen Casciotti's group).

General Information
Always swab surface before and after use with ethanol, and rub gloves in ethanol to sterilise before and after handling bacteria and when dealing with autoclaved items which are to remain sterile.
Any item which has not been in contact with bacteria can be disposed of as general waste. Bacterially contaminated items must be autoclaved prior to disposal.
Wear a mask when weighing out Tryptic Soy agar and broth powder as it tends to become airborne.

1 Preparing Media:

- Media bottles are filled with 445 ml of media. Quantities here will make enough medium to fill four bottles.
- To 1800 ml deionised water (DI) add 1.8 g KNO_3, 0.45 g $(NH4)_2SO_4$, 11.7 g K_2HPO_4, and 54 g Tryptic Soy Broth
- Stir with magnetic stirrer until the liquid is clear (15-30 minutes).
- Transfer 445ml medium into 500ml serum bottles, using a glass funnel and a measuring cylinder.
- Wrap stoppers and bottle tops separately in foil and autoclave for 1½ hours on a liquid cycle.
- Wearing sterilised gloves place stoppers on the bottles immediately after opening the autoclave then crimp seal them on to bottles.
- Mark the bottles with the date and store in the dark at room temperature for up to one year. If any bottles become cloudy at any time discard.
- Use the same recipe to make media for 15 ml centrifuge tubes. Autoclave the media in duran bottles (leave lids resting on top of duran bottle and screw tight after autoclaving). Media can be stored in this way and used to fill new sterile 15 ml centrifuge tubes with 9 ml per tube.

2 Nitrate free medium (NFM):

- Prepare using the same recipe as for media but exclude the KNO_3.
- Pour 200ml NFM into 250ml duran bottles and autoclave for ½ hour on a liquid cycle.
- Remove from autoclave wearing sterilised gloves, tighten lids and label bottles.
- Store the duran bottles at room temperature in the dark. If the liquid becomes cloudy at anytime discard.

3 Preparing agar plates:

- Add 30g Triptych Soy Agar granules to 500 ml of media (made according to above recipe).
- Stir with magnetic stirrer and heat until dissolved (do not boil).
- Pour into duran bottles (half fill) and autoclave on a 30 minute liquid cycle.
- Remove from autoclave, tighten lid and label, and leave to cool.
- When side of bottle feels slightly hotter than blood temperature it is ready to pour. This needs to be done quickly before the agar cools further and sets.
- In laminar flow hood remove a stack of plates from their wrapping, leaving them stacked.
- Lift the whole stack except for the base of the bottom most plate. Pour the agar into the base so it is ¾ filled. Replace the stack and swirl round so that agar covers whole plate. Work your way quickly up the stack in this way.
- Leave plates to dry overnight or for longer, until most evidence of condensation on the lids has gone. (The agar sets quickly but if condensation remains it can encourage fungal growth. if the plates are poured too hot there will be a lot of condensation which will not disperse).
- While still in laminar flow hood, seal side of plates with parafilm and place in labelled polythene bags.
- Mark date on bag.
- Store in the dark at room temperature. Dispose of plates if culture growth appears during storage.

4 Rehydrating the bacteria (*Pseudomonas aureofaciens* ATCC #13985):

- Heat tip of outer vial in Bunsen flame, squirt the tip with a few drops of cold water to make it brittle then strike it with a file or pencil to remove tip.
- Use tweezers to take out inner vial then gently remove cotton plug.
- Take a 15ml centrifuge tube containing 9ml of autoclaved medium (hereafter referred to as a 9 ml medium tube).
- Pipette 0.5 to 1.0 ml of medium from the tube into the inner vial to rehydrate the bacterial pellet.
- Pipette the mixture slowly back into the broth tube being careful not to get the pellet jammed in the pipette tip.
- Repeatedly use pipette to agitate suspension and encourage rehydration.
- Inoculate two agar plates (see below for agar plate preparation) from the original tube by dipping flamed or sterile inoculation loop into the rehydrated bacteria. If using a flamed inoculating loop, hold loop in flame until it glows red, then touch it on the edge of the new plate to cool it down before culturing with it.
- To help you see where you are on the plate, draw an inoculating point on the plate underside and touch loop here first, then streak. Return loop to flame after each set of zig-zag lines so that new set of lines spreads a smaller number of cells, picked up from drawing the loop through the previous zig-zag once:

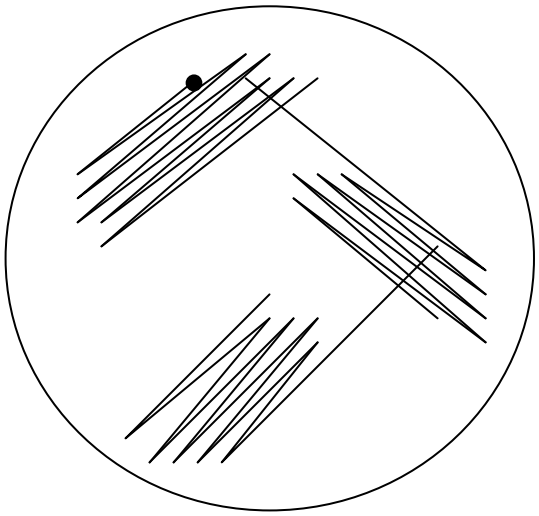

- When culturing for the first time on a plate, also inoculate two 9ml medium tubes with 100 µl of the rehydrated bacteria from the original tube in case the plates don't grow. If the culture grows in the medium but not on the first plates inoculate plates on from this.
- Seal plates and tubes with parafilm, and label. Incubate at room temperature for 1-5 days (individual colonies should be clearly visibly when the plate is ready, and large enough to touch with a loop).
- Culture growth on plates becomes dark orange with time; tubes become cloudy.
- Keep the rest of the original rehydrated bacteria at 4^{o}C for up to a month. Within this time prepare bacterial super stock and working stock for long-term storage and use.

5 Preparing the bacterial super stock and working stock:

- Prepare a 50% by weight dilute solution of glycerol with deionised water and autoclave it (glycerol weighs 1.261 g/ cm^3).
- Identify two single colonies from the incubated plates (i.e. discrete dots which have not yet joined with neighbouring dots).
- Using a sterile inoculation loop, touch one colony then dip loop into a 9 ml medium tube and stir medium to ensure inoculation. Repeat with the other colony and a second tube. Seal tubes with parafilm and label A and B.
- Incubate overnight at room temperature on a shaker table.
- For the working stock, inoculate a further two plates each from tubes A and B and incubate until single colonies are visible.
- With the remainder of the contents of tubes A and B, prepare the super-stock:
- Pipette 400µl from these tubes into 2.5 ml eppendorfs.
- Add 600µl of the 50% glycerol to each eppendorf.
- Label with date, species, and colony A or B.
- Snap freeze eppendorfs by placing in liquid nitrogen.
- Store vials at - 80^{o}C in a labelled cryogenic storage box.
- For the working stock, inoculate a number of 9 ml media tubes (depending on freezer storage capacity), with single colonies from the plates (sterilising loop each

time) and incubate overnight at room temperature, then prepare for freezing as for the super stock.

6 Reviving culture from working stock and growing on plates:

- Label plate with species, date and draw inoculating point on underside.
- Using a sterilised toothpick or sterile pipette tip remove a small amount of frozen cells from one of the frozen 2.5 ml working stock eppendorfs and drop it onto the inoculating point. Close eppendorf immediately and return it to freezer.
- Streak plates with a loop, put lids on, and seal with parafilm.
- Incubate in the dark at room temperature for 3-5 days until single colonies are easily discernable.
- Identify a single colony from one of the plates and use this to inoculate a new plate (label #2).
- Repeat with second colony and plate in case the first does not grow.
- Reseal the old plate and keep all plates in the dark at room temperature for 3-4 days. (The old plate is always resealed and kept for a further four days in case there is a problem with the new plates)
- After three to five days repeat the process so that the culture is maintained, and dispose of #1 plate.
- Return to frozen stock every 4 plates.

7 Inoculation of *Pseudomonas aureofaciens*:

- Do this about a week before you need to use the cells to prepare samples for the IRMS (the exact timing depend on how long the culture is left on the shaker table).
- Take enough 9ml medium tubes to ensure there will be sufficient liquid to inoculate the required number of media bottles (2.7 ml per bottle), plus one or two reserve tubes in case they don't all grow. One media bottle will supply cells for approximately 21 analysis vials based on concentrating cells 7 fold and using 3 ml of cells per vial. To prepare 40 to 45 3 ml vials per day, two media bottles are needed, for 60 to 65 3 ml vials per day, 3 media bottles are needed.
- Using a loop transfer a single colony from a freshly grown current plate to the medium (only use plates 2, 3, or 4). Repeat for all tubes.
- Cap tubes and seal with parafilm.
- Incubate at room temperature overnight on shaker.
- Set out the media bottles to be inoculated and label with species, plate number, and inoculation date.
- Inject 2.7 ml the freshly incubated bacterial medium into each bottle through stopper with disposable syringe.
- Put bottles in a box to keep them dark on a shaker for 6-10 days.

8 Centrifuging and concentrating the bacteria:

- Ensure the 250 ml centrifuge bottles have been autoclaved prior to use.
- Divide the culture evenly between 4 or 6 centrifuge bottles.
- Centrifuge for 10 minutes at 4950 rpm.
- Check for clumps of pink bacterial cells lying at the bottom of the centrifuge bottles.

- From all bottles gently pour off all the liquid above cells leaving the cells in the bottle.
- To the first centrifuge bottle add the correct volume of nitrate free medium for the number of vials you are preparing (3 ml per vial) plus 10 to 15 ml extra in case some gets spilt, then pour back and forth into the next centrifuge bottle to resuspend the cells. Continue until the nitrate free medium contains all the resuspended cells.
- Using a sterile Pasteur pipette add 1.5 ml antifoam to the liquid containing the cells and swirl the centrifuge bottle to mix.

9 Preparing sample vials:

- Pipette 3 ml of the cell concentrate into each 20 ml vial and immediately close vial with an autoclaved stopper.
- Put crimps on and crimp seal the whole batch of vials, and label.
- Insert long blue venting needles through the stopper of each vial ready for purging.

10 Setting up and using purge system:

- Mounting and removing needles: Wearing gloves, place short brown purge needle still in its plastic cover firmly onto luer mount on purge system manifold, and twist to lock it in place. Twist needle cover to remove, leaving mounted needle behind. Do not remove individual needle covers until each particular needle is to be used (retain cover as it is needed for needle removal). To remove needle place cover over it and twist until needle comes loose then remove it in its cover. For safety reasons never handle uncovered purge needles when mounted on purge system, and leave needles covered until use. Dispose of used needles in a sharps bin for incineration.
- With He cylinder turned off, attach the correct number of purge needles to the manifold ports with and cap any remaining ports with leur caps. Loosen needle caps so they are no longer air tight. Mount one vial upside-down onto a brown purge needle.
- Turn on He gas cylinder and set flow rate so that bubbles can be seen in vial but are not travelling up the side of the vial.
- Mount the other vials on the manifold.
- Set flow rate at 60-70 ml/ min using a bubble meter attached to the venting needle from a vial. Do not use a flow meter as bacterial solution may be sucked into it and cause damage.
- Check all vials are bubbling and that none are leaking.
- Purge vials for 30 minutes.
- Remove vials from purge system by lifting vial off purge needle and quickly removing venting needle, then cover purge needle with needle cap so it is not air tight. This avoids pressurising vials which may lead to leaking, and building up pressure in purge system when last vials are removed.
- Close He gas cylinder.
- Place vials on shaker table in the dark for 5 hours.
- Return them to the purge system and purge for another hour.

11 Injecting vials with samples:

- Label purged vials with sample, standard, or blank ID.
- Injection volumes of samples and standards are calculated based on known concentration of nitrate + nitrite. The injection volume should contain 20 nanomoles. Rinse syringe in DI 10 times then 3 times with the sample, then fill syringe to correct injection volume and inject through vial cap. Shake and invert vial. If the injection volume is greater than 1 ml put a venting needle in the cap at the same time to avoid pressurising the vial. Remove it after injecting.
- Standards used are IAEA N3, USGS 34 and 35 and a laboratory standard TF. These are made up to concentrations of 400 μM and stored frozen in 1.5 ml eppendorfs and require an injection volume of 50 μL. If high volume injections are needed due to low concentrations of samples, dilute standards with DI 24 hours before use.
- Blanks are bacterial solution only so no injection is required.
- Incubate vials at room temperature overnight in inverted position to prevent headspace gas leakage.
- The following morning inject 0.1 to 0.2 ml of 6M NaOH into each vial and shake the vial to lyse the bacterial cells, and stop the reaction.
- Analyse on the Geo 20: 20 GCIRMS within a week.

Denitrifier method images:

Pseudomonas aureofaciens culture growing on plate.

Media bottle.

Pipetting concentrated bacterial solution into analysis vials.

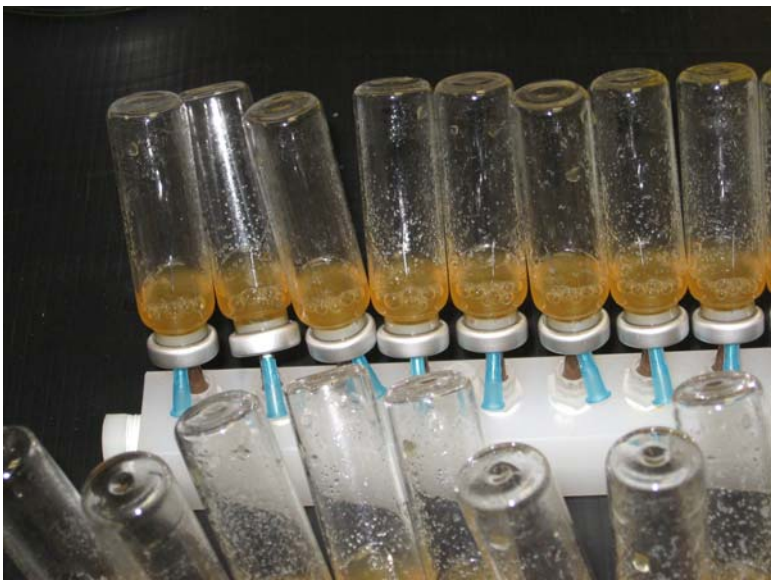

Purging analysis vials with helium.

Injecting analysis vials with sample water.

TG II prep system and autosampler.

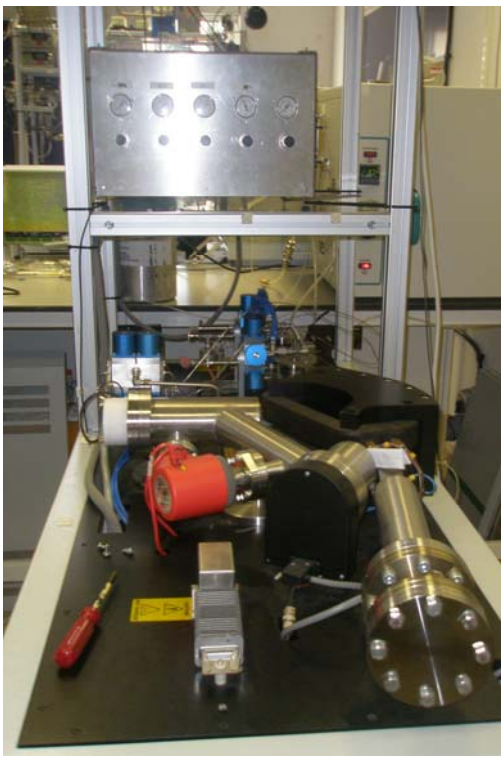

Geo 20:20 GCIRMS.

A 1.2 Freezing and Boiling Points for GEO Purge and Trap Line:

Compounds relevant to the purging and trapping extraction and purification line of the Geo GCIRMS

Table A 1.1 Melting and boiling points of N_2O, H_2O, CO_2, N_2 and He.

Compound	**Freezing point (^{0}C)**	**Boiling point (^{0}C)**
N_2O	- 90.9	- 88.5
H_2O	0.0	100.0
CO_2	- 55.6	- 78.5
N_2	- 209.9	- 195.8
He	- 272.1	- 268.8

A 1.3 $\delta^{15}N_{NO3}$ and $\delta^{18}O_{NO3}$ Example Calibration data

Data from one analysis batch after drift correction to reference gas and ^{17}O correction showing measured values and error (± one standard deviation n = 4 for each standard) for the three international nitrate standards and the internal laboratory standard, including the calibration equations generated from these data which were used to calibrate the measured values of samples to 'true' values (Table A1.2).

Table A1.2 Measured and accepted isotopic composition of NO_3^- standards used with the denitrifier method and example calibration equations. SIL-TF 'accepted' values are italicised as they have not been independently verified.

Reference standard measurements				
Measured values N_2O (ref) ‰			**Accepted values NO_3^- ‰**	
	$\delta^{15}N_{N2O}$	± 1 standard deviation (n=4)		$\delta^{15}N_{NO3}$‰ vs. AIR
IAEA N3	5.82	0.07	IAEA N3	4.70
USGS 34	-0.78	0.06	USGS 34	-1.80
USGS 35	3.82	0.01	USGS 35	2.70
SIL-TF	14.46	0.12	*SIL-TF*	*13.31*
	$\delta^{18}O_{N2O}$	± 1 standard deviation (n=4)		$\delta^{18}O_{NO3}$‰ vs. VSMOW
IAEA N3	22.12	0.09	IAEA N3	25.61
USGS 34	-29.68	0.06	USGS 34	-27.93
USGS 35	53.11	0.06	USGS 35	57.50
SIL-TF	25.73	0.14	*SIL-TF*	*29.23*
Calibration equations				
$\delta^{15}N_{NO3}$ ‰	$d^{15}N_{NO3}$-true = ($\delta^{15}N_{N2O}$-measured -1.05578947)/ 1.01654135			
$\delta^{18}O_{NO3}$ ‰	$\delta^{18}O_{NO3}$-true = ($\delta^{18}O_{N2O}$-measured - -2.63988624)/ 0.96893321			

Data from an analysis batch showing mean beam area of standards and blanks, relative beam area of blank and percentage oxygen exchange (Table A1.3).

Table A1.3 Example of beam area (C), % blank and oxygen exchange for calibration standards.

Beam areas, blank and oxygen exchange	
Mean beam area of standards (C)	4.17×10^{-8}
$\pm$ 1 standard deviation (n=16)	1.37×10^{-8}
Mean beam area of blanks (C) (n=2)	4.64×10^{-10}
Blank beam area as % of mean standard beam area	1.1 %
% oxygen retained calculated with USGS 34 and USGS 35	97 %
Equation to calculate % oxygen retained =(((1+($\delta^{18}O_{N2O}$-USGS35/1000))/(1+($\delta^{18}O_{N2O}$-USGS34/1000)))-1)/(((1+($\delta^{18}O_{NO3}$USGS35/1000))/(1+($\delta^{18}O_{NO3}$USGS34/1000)))-1) (Coplen *et al*., 2004).	
% oxygen retained =(((1+($\delta^{18}O_{N2O}$ 53.11/1000))/(1+($\delta^{18}O_{N2O}$ -29.68/1000)))-1)/(((1+($\delta^{18}O_{NO3}$ 57.50/1000))/(1+($\delta^{18}O_{NO3}$ -27.93/1000)))-1)	

A 1.4 N_2O Partitioning Between Headspace and Liquid in Sample Vial:

Calculation:

Using calculations from Hudson (2004) which were developed to determine concentrations of N_2O in a water sample by equilibrating the sample in a closed vessel with He filled headspace at atmospheric pressure, then sampling the headspace concentration and using this to calculate the total concentration (i.e. that of the original water sample).

The method uses the mass balance equation:

$$TC\ (mg/L) = C_{AH} + C_A$$

where TC = Aqueous concentration of N_2O if it were all dissolved in the water
C_{AH} = Gaseous concentration at equilibrium in the headspace
C_A = Aqueous concentration at equilibrium in the water

For this research, based on the assumption of complete conversion of 20 nanomoles of nitrate to 10 nanomoles of nitrous oxide and the known volume of liquid in the vial, TC, the "total concentration" was known (i.e. the concentration if all the nitrous oxide were dissolved in the liquid fraction only), and the calculations were carried out iteratively until the mass balance agreed, with the following parameters:

Vial volume: 21 ml
Liquid volume: 3 ml
Headspace volume: 18 ml
Temperature: 293.15 K
Pressure: 101.325 kPa
TC = 0.147 mg/L N_2O

The temperature dependent Henry's Law constant for N_2O was calculated using the following equation using and coefficients from Wilhelm et al. (1977):

$$H_{N2O} \text{ (atmosphere/ mole fraction)} = 1/ e^{[(A + B / T + C \times \ln T + D \times T)/ R]}$$
$$= 1964.4597 \text{ (atmosphere/ mole fraction)}$$

where:
$A = 180.950 \text{ cal } K^{-1} \text{ mol}^{-1}$
$B = 13205.8 \text{ cal mol}^{-1}$
$C = 20.0399 \text{ cal } K^{-1} \text{ mol}^{-1}$
$D = 0.0238554 \text{ cal } K^{-2} \text{ mol}^{-1}$
$R = 1.98719 \text{ cal } K^{-1} \text{ mol}^{-1}$

$$C_{AH} = [(M_{H2O}) \times (Pg/H) \times (MW_{N2O}) \times 1000]$$

$$C_A = [(Vh/(Vv-Vh)) \times Cg \times (MW \text{ (g/mol)}/ Vm_{STP} \text{ L/mol}) \times (273.15/(T\ ^oC+273.15)) \times 1000]$$

⇨ TC (mg N_2O/ L water) $= [(M_{H2O}) \times (Pg/H) \times (MW_{N2O}) \times 1000] +$
$[(Vh/(Vv-Vh)) \times Cg \times (MW \text{ (g/mol)}/ Vm_{STP} \text{ L/mol}) \times (273.15/(T\ ^oC+273.15)) \times 1000]$

where:
M_{H2O} = molarity of water = 55.5 mol/L
MW_{N2O} = molecular weight of N_2O = 44.01 g/ mol
Vm_{STP} = Standard molar volume of an ideal gas at STP = 22.4 L/mol
Vh = volume of headspace = 18×10^{-6} m^3
Vv = volume of vial = 21×10^{-6} m^3

Cg = decimal equivalent of volumetric concentration of gas in headspace
= concentration ppm x 10^{-6}, solved iteratively as 1.2 x 10^{-5}
Pg = partial pressure of N_2O in headspace atm
= Cg x P_{total},
and P_{total} = 1 atm,
⇨ Pg = 1.2 x 10^{-5} atm

For the sample vial at equilibrium:

C_{AH} = [55.5 x (1.2 x 10^{-5} /1964.4597) x 44.01 x 1000] = 0.132 mg/L N_2O

C_A = [(18 x 10^{-6} /(21 x 10^{-6} - 18 x 10^{-6})) x 1.2 x 10^{-5} x (44.01 / 22.4) x (273.15/(20 +273.15)) x 1000]
= 0.0149 mg/L N_2O

TC = 0.147 mg/L = [55.5 x (1.2 x 10^{-5} /1964.4597) x 44.01 x 1000] +
[(18 x 10^{-6} /(21 x 10^{-6} - 18 x 10^{-6})) x 1.2 x 10^{-5} x (44.01 / 22.4) x (273.15/(20 +273.15)) x 1000]

This gives a ratio of N_2O in the liquid to that in the headspace of 0.11, and the percentages of N_2O in the liquid and in the headspace of 10 % and 90 % respectively.

The calculation was checked against the Ostwald coefficient for N_2O at 20 ^oC (0.6788), which describes the proportion of N_2O in the water to that in headspace at equilibrium in a closed system where the volume of headspace and liquid are equal (Wilhelm *et al*., 1977) (Figure A1.1).

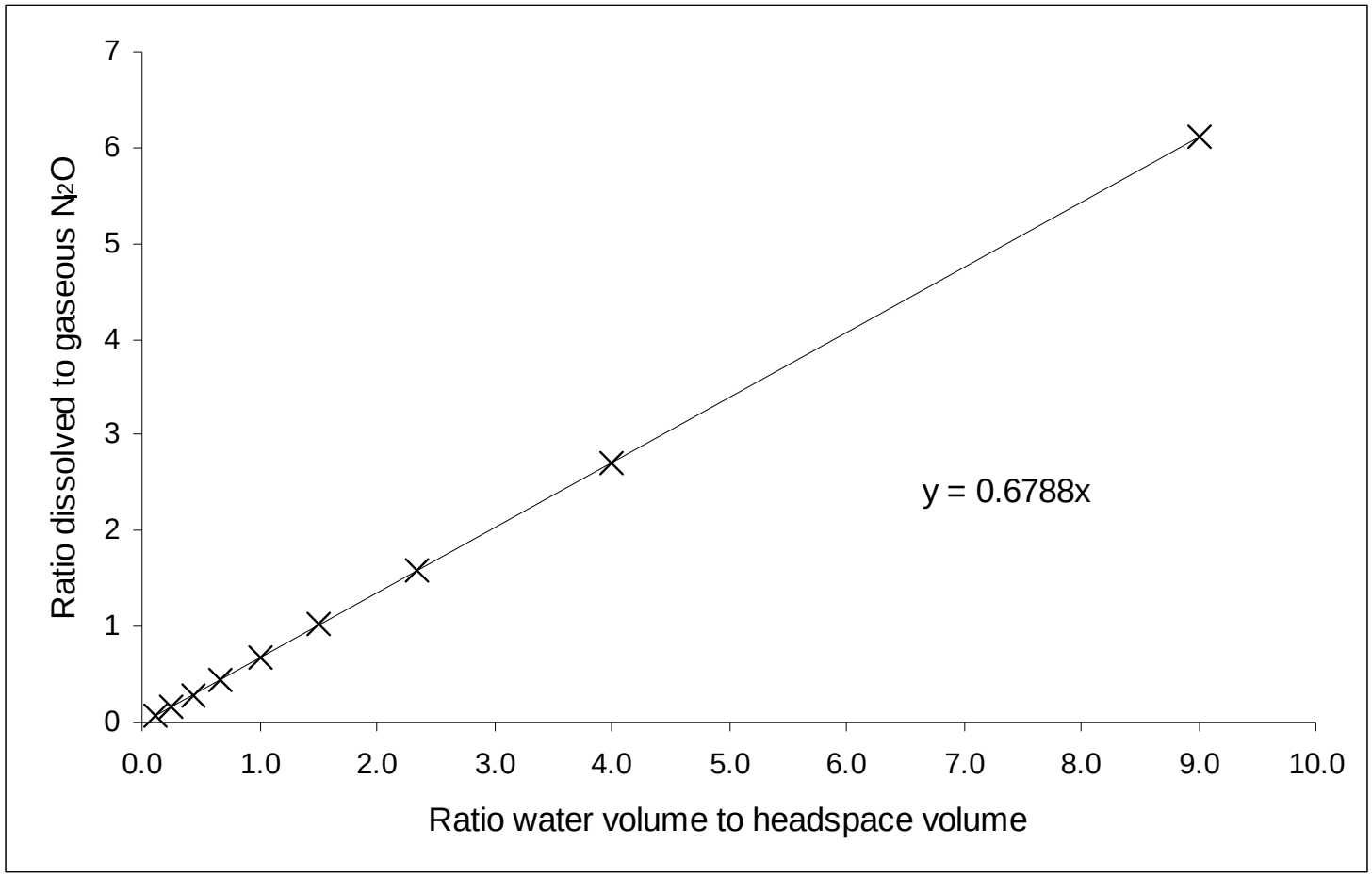

Figure A1.1 Ostwald coefficient shown as slope of the ratio of water volume to headspace volume versus the ratio of dissolved to gaseous N_2O in a closed system at equilibrium calculated using the above method (Wilhelm *et al.*, 1977).

A 1.5 Isotopic Composition of N_2O Partitioned Between Headspace and Liquid:

Using the mass balance equation:

$$\delta_{totalN2O} = ((\ mol_{hsN2O}\ x\ \delta_{hsN2O}) + (\ mol_{lqN2O}\ x\ \delta_{lqN2O})) / (mol_{hsN2O} + mol_{lqN2O})$$

Setting the reference N_2O isotopic composition for $\delta^{15}N_{totalN2O}$ and $\delta^{18}O_{totalN2O}$ to 0.00 ‰, if:
total N_2O = 1 mol
mol_{hsN2O} = 0.90 mol
mol_{lqN2O} = 0.10 mol

and

$\delta^{15}N_{totalN2O}$ = 0.00 ‰
$\delta^{18}O_{totalN2O}$ = 0.00 ‰

with

$\Delta^{15}N_{lqN2O}$ and $^{15}N_{hsN2O}$ = -0.75 ‰
$\Delta^{18}O_{lqN2O}$ and $^{18}O_{hsN2O}$ = - 1.06 ‰

then

$$\delta^{15}N_{totalN2O} = 0.00\ ‰ = ((\ 0.9\ x\ -\ 0.075) + (\ 0.1\ x\ 0.675)) / (0.9 + 0.1)$$

and

$$\delta^{18}O_{totalN2O} = 0.00\ ‰ = ((\ 0.9\ x\ -\ 0.106) + (\ 0.1\ x\ 0.954)) / (0.9 + 0.1)$$

A 1.6 $\delta^{15}N_{N2O}$ of the Bacterial Blank:

Calculation:

For the international standard IAEA N3:

Mean measured value with respect to reference gas of 3 ml standards: $\delta^{15}N_{N2OS3ml}$ = 5.54 ‰

Mean beam area of 3 ml blanks = 2.67 x 10^{-10} (C)

Mean beam area of 3 ml standards = 4.04 x 10^{-8} (C) = total N_2O of 3 ml standards (including blank)

Mean beam area of 3 ml blanks/ mean beam area of 3 ml standards = 0.007

Mean measured value with respect to reference gas of 13 ml standards: $\delta^{15}N_{N2OS13ml}$ = 8.43 ‰

Mean beam area of 13 ml blanks = 1.70 x 10^{-9} (C)

Mean beam area of 13 ml standards = 7.71 x 10^{-9} (C) = total N_2O of 13 ml standards (including blank)

Mean beam area of 13 ml blanks/ mean beam area of 13 ml standards = 0.22

Working on the assumption that the difference between $\delta^{15}N_{N2OS3ml}$ and $\delta^{15}N_{N2OS13ml}$ of $\Delta^{15}N_{N2O}$ 2.89 ‰ is solely attributable to the *additional* blank N_2O contribution in the higher volume standards, and calculating the percentage of additional N_2O relative to total N_2O of 13 ml standards from the relative proportions of the beam areas of the blanks to the standards, gives an additional blank equivalent to:

22 % - 0.7 % = 21.35 % of total N_2O of 13 ml standards

Assuming that without this additional 21.35 % of blank, the measured value with respect to reference gas of 13 ml standards would be the same as the measured value with respect to reference gas of 3 ml standards an isotopic mass balance equation can be used to express the relative proportions of N_2O derived from the standards and the blank which make up the measured value of the 13 ml standards:

$$\delta^{15}N_{N2OIAEAmeasured\ \mathbf{13ml}} = ((\delta^{15}N_{N2OSIAEAmeasured\ \mathbf{3ml}} \times (1- 0.213)) + (\delta^{15}N_{N2O\mathbf{blank}} \times 0.213))$$

Rearranging the equation for $\delta^{15}N_{N2O\mathbf{blank}}$:

$$\delta^{15}N_{N2O\mathbf{blank}} = \frac{\delta^{15}N_{N2OIAEAmeasured\ \mathbf{13ml}} - ((\delta^{15}N_{N2OSIAEAmeasured\ \mathbf{3ml}} \times (1 - 0.213))}{0.213}$$

$$\delta^{15}N_{N2O\mathbf{blank}} = \frac{8.43 - (5.54 \times (1 - 0.213))}{0.213} = 19.1\ ‰$$

For the international standard USGS 34:
Mean measured value with respect to reference gas of 3 ml standards: $\delta^{15}N_{N2OS3ml} = -0.94$ ‰
Mean measured value with respect to reference gas of 13 ml standards: $\delta^{15}N_{N2OS13ml} = 2.70$ ‰

$$\delta^{15}N_{N2O\mathbf{blank}} = \frac{2.70 - (-0.94 \times (1 - 0.213))}{0.213} = 16.15\ ‰$$

For the international standard USGS 35:
Mean measured value with respect to reference gas of 3 ml standards: $\delta^{15}N_{N2OS3ml} = 3.57$ ‰
Mean measured value with respect to reference gas of 13 ml standards: $\delta^{15}N_{N2OS13ml} = 6.85$ ‰

$$\delta^{15}N_{N2O\mathbf{blank}} = \frac{6.85 - (3.57 \times (1 - 0.213))}{0.213} = 18.97\ ‰$$

Therefore, the calculated $\delta^{15}N_{N2O\mathbf{blank}} = 18.1 \pm 1.7$ ‰ with respect to the reference gas. Calibration to the 13 ml standard set gives a value of $\delta^{15}N_{NO3}$ 15.4 ± 1.7 ‰.

A 1.7 Liquid Ion Chromatography

The Dionex ICS 2000 was used to analyse anion concentrations. The column is a 2 mm AS182 with a 2mm AG18 guard column, and a 2 mm ASRS Ultra II suppressor and potassium hydroxide (KOH) as the eluent. The injection volume was 25 μL. Initially a 25 minute cycle was used but this was later changed to a 45 minute cycle to enable better peak separation.

The Dionex DX600 was used to analyse ammonium. The cation column is a 3 mm CS16 with a 3mm CG16 guard column, and methanesulfonic acid (MSA) as the cation eluant. The injection volume was 1000 μL. The analysis cycle was 48 minutes.

A 1.7.1 ICS 2000 Precision

Example of in-run precision:
A single sample was analysed ten times (scattered throughout the run) during a 40-hour analysis on the Dionex ICS 2000 liquid ion chromatograph, to test within-run precision. Nitrite concentration in the sample was below the limit of detection. One standard deviation is presented as a measure of precision. The standard deviation is also expressed as a percentage of the concentration (Table A1.4, Figure A1.2).

Table A1.4 Concentrations of anions (mg/L) measured ten times from a single sample within a 40 hour run on the Dionex ICS 2000 liquid ion chromatograph, showing mean, standard deviation (SD) and standard deviation as a percentage of the sample concentration.

Analysis number	**Cl^- mg/L**	**NO_2^- mg/L**	**NO_3^- mg/L**	**SO_4^{2-} mg/L**	**PO_4^{3-} mg/L**
1	18.0	<LOD	11.6	11.7	0.091
2	18.3	<LOD	11.7	11.8	0.090
3	18.6	<LOD	11.8	11.9	0.093
4	18.0	<LOD	11.7	11.8	0.089
5	17.5	<LOD	11.4	11.4	0.088
6	18.1	<LOD	11.6	11.6	0.080
7	18.9	<LOD	11.6	11.8	0.095
8	18.2	<LOD	11.7	11.8	0.090
9	18.7	<LOD	12.1	12.2	0.090
10	17.3	<LOD	11.2	11.5	0.091
Mean	18.2	\	11.6	11.7	0.090
SD	0.5	\	0.2	0.2	0.004
SD as %	3%	\	2%	2%	4%

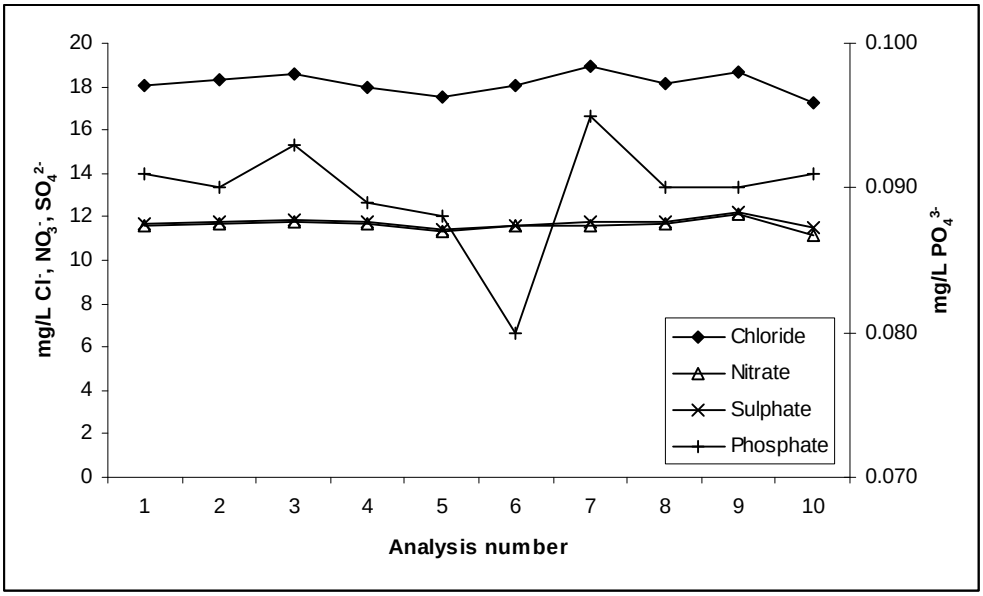

Figure A1.2 Concentrations of anions (mg/L) measured ten times from a single sample within a 40 hour run on the Dionex ICS 2000 liquid ion chromatograph.

A 1.7.2 ICS 2000 Limit of Detection

Example of in-run limit of detection:

A single blank of deionised water was analysed after every 5th sample, for a total of eighteen times over a 40 hour analysis on the Dionex ICS 2000 liquid ion chromatograph. Concentrations of nitrite and phosphate in the blank were below the limit of detection. Mean concentration, one standard deviation and limits of detection (three times the standard deviation) for the other anions are presented (Table A1.5, Figure A1.3).

Table A1.5 Concentrations of anions (mg/L) measured eighteen times from a single deionised water blank through a 40 hour run on the Dionex ICS 2000 liquid ion chromatograph, showing mean, standard deviation (SD) and limit of detection (LOD).

Blank analysis number	**Cl^- mg/L**	**NO_2^- mg/L**	**NO_3^- mg/L**	**SO_4^{2-} mg/L**	**PO_4^{3-} mg/L**
1	0.012	<LOD	\	\	<LOD
2	0.013	<LOD	\	\	<LOD
3	0.024	<LOD	0.007	0.006	<LOD
4	0.015	<LOD	0.007	\	<LOD
5	0.010	<LOD	\		<LOD
6	0.016	<LOD	0.021	0.008	<LOD
7	0.012	<LOD	0.007	\	<LOD
8	0.014	<LOD	0.002	0.002	<LOD
9	0.013	<LOD	0.011	0.002	<LOD
10	0.015	<LOD	0.013	0.002	<LOD
11	0.014	<LOD	0.001	0.002	<LOD
12	0.017	<LOD	0.002	0.001	<LOD
13	0.015	<LOD	0.012	0.002	<LOD
14	0.017	<LOD	0.010	0.002	<LOD
15	0.018	<LOD	0.008	0.002	<LOD
16	0.024	<LOD	0.009	0.001	<LOD
17	0.021	<LOD	0.011	\	<LOD
18	0.020	<LOD	\	\	<LOD
Mean	0.016	\	0.009	0.003	\
SD	0.004	\	0.005	0.002	\
SD * 3 (LOD)	0.012	\	0.015	0.006	\

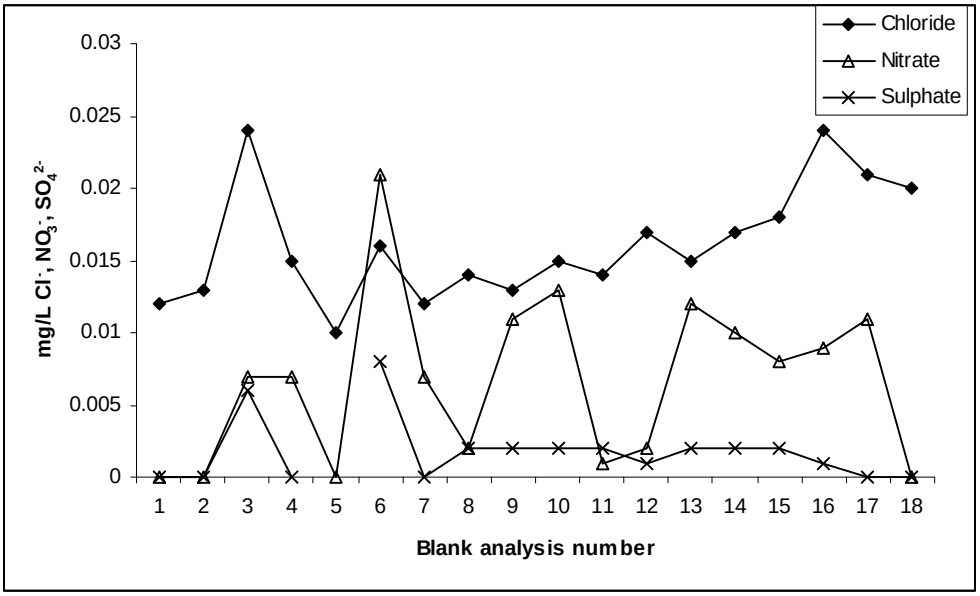

Figure A1.3 Concentrations of anions (mg/L) measured eighteen times from a single deionised water blank through a 40 hour run on the Dionex ICS 2000 liquid ion chromatograph.

A 1.7.3 ICS 2000 Anion Calibration

Example of mixed anion standard calibration:

Mixed anion standards were routinely used to calibrate concentrations of chloride, sulphate and phosphate on the Dionex ICS 2000 liquid ion chromatograph. The concentration ranges of were set to encompass the usual concentration ranges found in samples. Each standard was measured at least three times during a run, at the beginning, in the middle and at the end. A slight positive drift was regularly seen during analysis on this instrument but was not consistent enough to allow drift correction (Table A1.6, Figure A1.4 a-d). In order to standardise the calibration, samples were calibrated to the mean peak areas of standards. Although this does not fully correct for drift the potential error due to drift was not significant to the precision requirements of this research.

Table A1.6 Concentration mean and standard deviation (mg/L) of mixed anion standard calibration (triplicate analysis) on the Dionex ICS 2000 liquid ion chromatograph, with numbers 1, 2 and 3 denoting the beginning, middle and end of run positions respectively.

Anion					
Cl^-	*Intended concentration (mg/L)*	*10*	*20*	*30*	*40*
	1	9.97	19.93	29.47	39.35
	2	10.19	20.32	30.20	40.15
	3	10.30	20.46	30.27	40.07
	Mean measured concentration (mg/L)	10.15	20.24	29.98	39.86
	Standard deviation	0.17	0.28	0.44	0.44
SO_4^{2-}	*Intended concentration (mg/L)*	*10*	*20*	*30*	*40*
	1	10.03	20.29	30.05	38.86
	2	10.03	20.70	30.67	39.68
	3	10.26	20.75	30.59	39.52
	Mean measured concentration (mg/L)	10.10	20.58	30.44	39.36
	Standard deviation	0.13	0.26	0.34	0.43
PO_4^{3-}	*Intended concentration (mg/L)*	*0.5*	*1.0*	*2.5*	*5.0*
	1	044	0.88	2.36	5.11
	2	0.36	081	2.22	4.99
	3	0.41	0.92	2.39	5.08
	Mean measured concentration (mg/L)	0.41	0.87	2.32	5.06
	Standard deviation	0.04	0.06	0.09	0.06

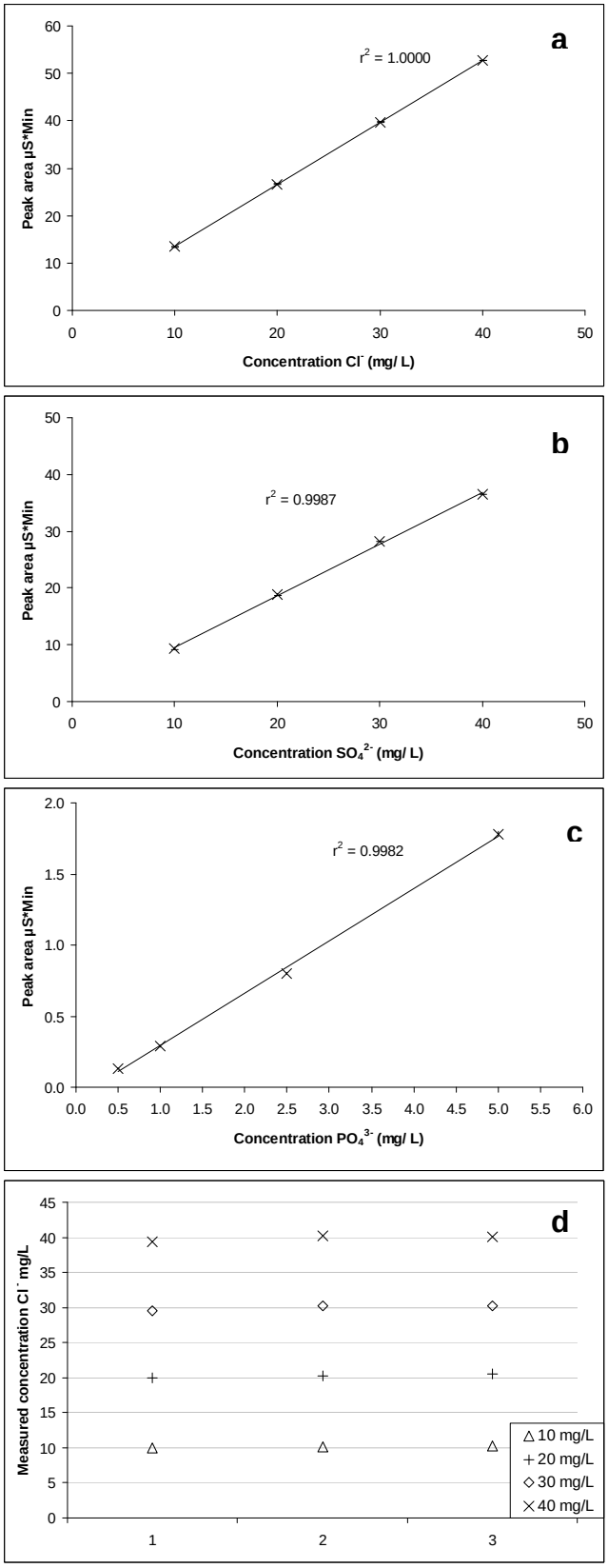

Figure A1.4 Calibration curves for Cl^- (a), SO_4^{2-} (b) and PO_4^{3-} (c), (mg/L) with error bars representing $\pm$ one standard deviation from the mean of the triplicate analysis, and individual analyses of Cl^- (d) from the beginning middle and end of the run to show drift on the Dionex ICS 2000 liquid ion chromatograph.

A 1.7.4 ICS 2000 Nitrite and Nitrate Calibration

Example of nitrite and nitrate standard calibration:

Mixed dissolved inorganic nitrogen (DIN) standards were routinely used to measure nitrite and nitrate on the Dionex ICS 2000 liquid ion chromatograph. The concentration ranges of were set to encompass the usual concentration ranges found in samples. Each standard was measured at least three times during a run, at the beginning, in the middle and at the end. No significant drift was seen (Table A1.7, Figure A1.5a and b).

Table A1.7 Concentration, mean and standard deviation of mixed DIN standard calibration (μM) (triplicate analysis) on the Dionex ICS 2000 liquid ion chromatograph, with numbers 1, 2 and 3 denoting the beginning, middle and end of run positions respectively.

Anion					
NO_2^-	*Intended concentration (μM)*	*1*	*2*	*3*	*4*
	1	0.97	2.00	3.02	4.04
	2	0.87	1.92	3.00	4.02
	3	0.85	1.96	2.95	3.99
	Mean measured concentration (μM)	0.90	1.96	2.99	4.02
	Standard deviation	0.06	0.04	0.04	0.03
NO_3^-	*Intended concentration (μM)*	*100*	*250*	*500*	*750*
	1	101	248	501	749
	2	99	248	501	751
	3	98	247	495	749
	Mean measured concentration (μM)	99	248	499	750
	Standard deviation	1.4	1.0	3.5	0.8

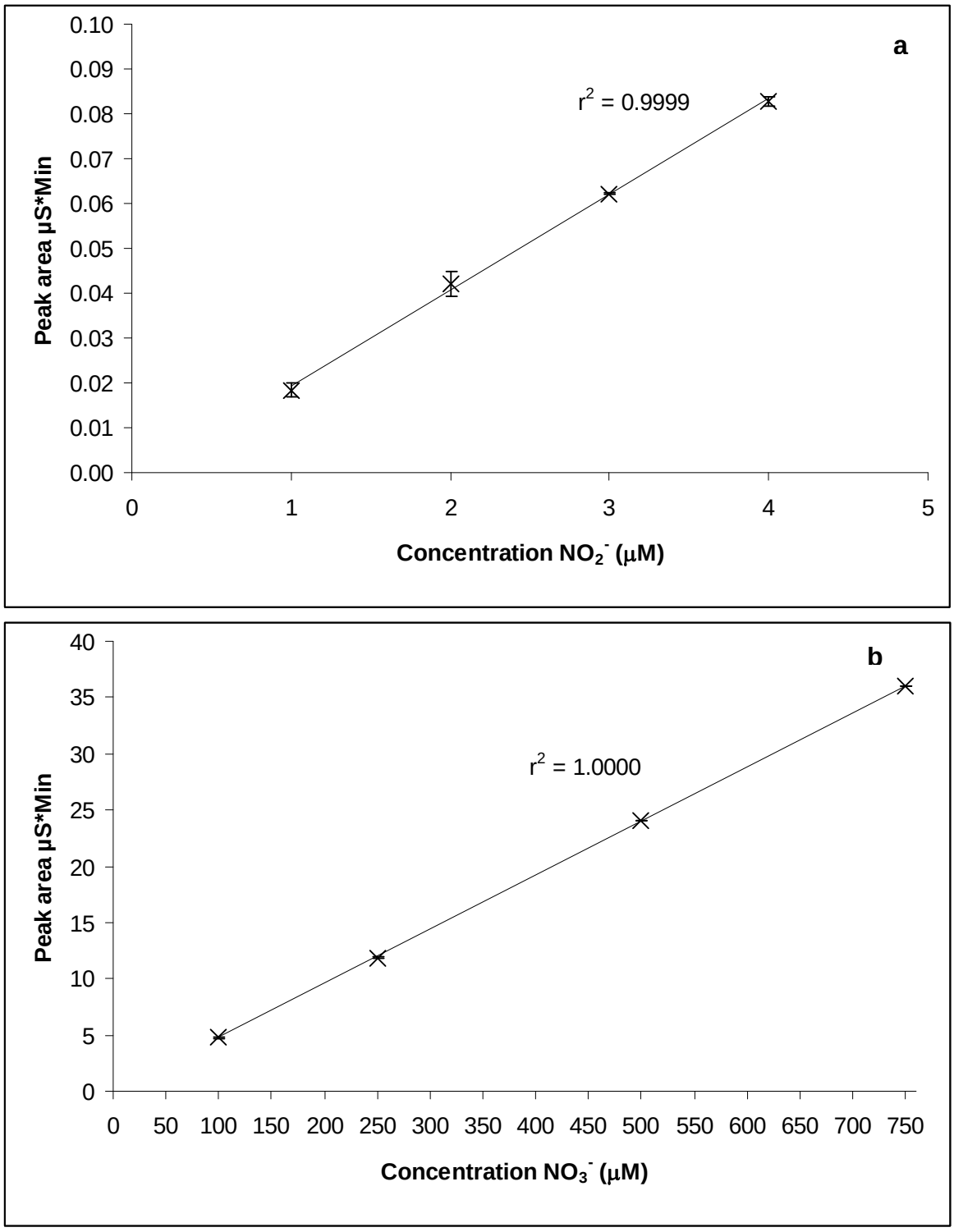

Figure A1.5 Calibration curves for NO_2^-(a), and NO_3^-(b) (µM) with error bars representing ± one standard deviation from the mean of the triplicate analysis, from the beginning middle and end of the run to show drift on the Dionex ICS 2000 liquid ion chromatograph.

A 1.7.5 DX 600 Ammonium Precision

Example of in-run precision:

Three samples were analysed in triplicate for concentrations of ammonium scattered throughout the run during a 30-hour analysis on the Dionex DX 600 liquid ion chromatograph to test within-run precision. One standard deviation is presented as a measure of precision. The standard deviation is also expressed as a percentage of the concentration (Table A1.8, Figure A1.6).

.

Table A1.8 Concentrations of ammonium measured in triplicate from three samples within a 30 hour run on the Dionex DX 600 liquid ion chromatograph, showing mean, standard deviation (SD) and standard deviation as a percentage of the sample concentration.

	Analysis number	NH_4^+ µM		Analysis number	NH_4^+ µM		Analysis number	NH_4^+ µM
Sample A	1	11.9	Sample B	1	3.5	Sample C	1	7.4
	2	11.2		2	3.6		2	6.7
	3	11.5		3	3.3		3	8.0
	Mean	11.5		Mean	3.5		Mean	7.4
	SD	0.4		SD	0.1		SD	0.7
	SD as %	3.1		SD as %	3.9		SD as %	8.8

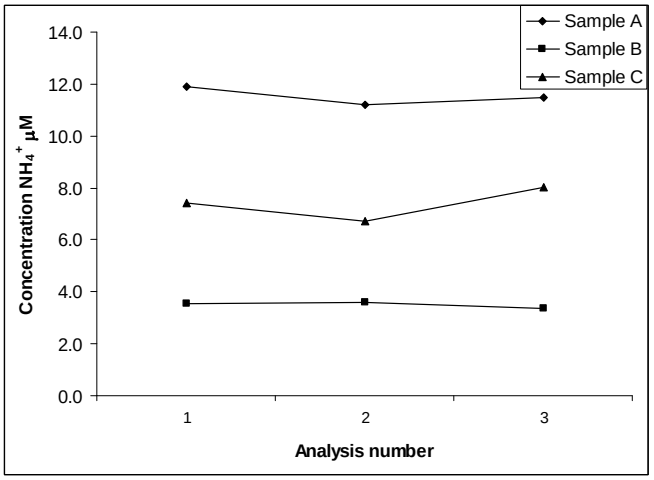

Figure A1.6 Concentrations of ammonium (µM) measured in triplicate from a three samples within a 30 hour run on the Dionex DX 600 liquid ion chromatograph.

A 1.7.6 DX 600 Ammonium Limit of Detection

Example of in-run limit of detection:

A single blank of deionised water was analysed after every 5th position in run for a total of seven times over a 28 hour analysis on the Dionex DX 600 liquid ion chromatograph. Mean concentration of ammonium, one standard deviation and limit of detection (three times the standard deviation) are presented (Table A1.9, Figure A1.7).

Table A 1.9 Concentrations of ammonium (μM) measured seven times from a single deionised water blank through a 28 hour run on the Dionex DX 600 liquid ion chromatograph, showing mean, standard deviation (SD) and limit of detection (LOD).

Blank analysis number	NH_4^+ μM
1	0.12
2	0.08
3	0.04
4	0.44
5	0.07
6	0.17
7	0.05
Mean	0.14
SD	0.14
SD*3 (LOD)	0.42

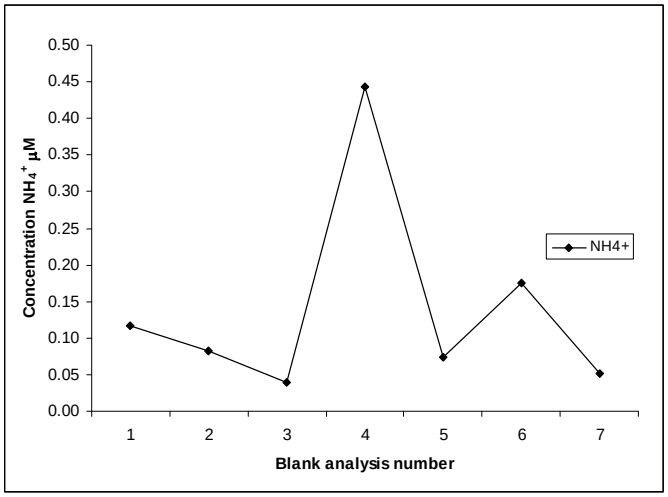

Figure A1.7 Concentrations of ammonium (μM) measured seven times from a single deionised water blank through a 28 hour run on the Dionex DX 600 liquid ion chromatograph.

A 1.7.7 DX 600 Ammonium Calibration

Example of ammonium standard calibration:

NH_4Cl standards of concentrations 1 to 25 μM were used calibrate of ammonium concentrations in samples run on the Dionex DX 600 liquid ion chromatograph. There was no consistent trend of drift on this instrument (Figure A1.8).

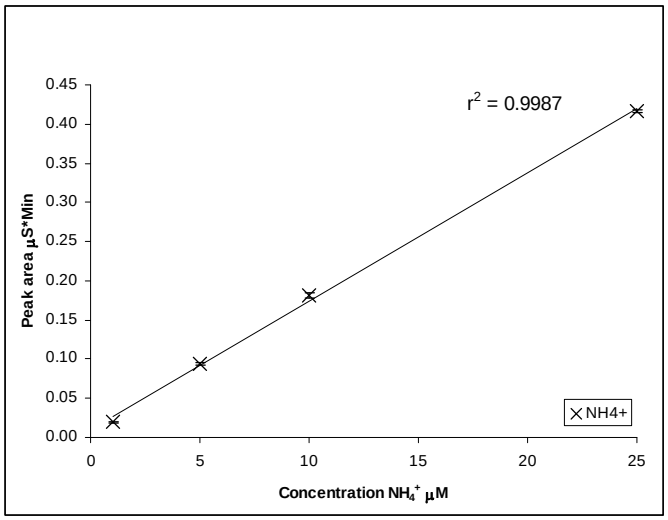

Figure A1.8 Calibration curve for ammonium (µM) from analysis on Dionex DX 600 liquid ion chromatograph (concentration range 1 - 25 µM), with error bars representing ± one standard deviation from the mean of the triplicate analysis.

A 1.8 Total Nitrogen and Liquid Ion Chromatography DIN

A 1.8.1 ICS 2000 DX 600 and Thermalox Cross Calibration

Example of nitrate, nitrite and ammonium cross calibration between ICS 2000, DX 600 and Thermalox:

To enable the use of the difference method for DON measurement of filtered samples, a mixed dissolved inorganic nitrogen (DIN) standard set comprising KNO_3, $NaNO_2$ and NH_4Cl was routinely used on the Dionex ICS 2000 (NO_2^-, NO_3^-) and DX 600 (NH_4^+) and the Thermalox (TN) instruments. The concentration ranges of each DIN species was set to encompass the expected concentration ranges found in samples (Table A1.10, Figure A1.9a-d). Later in the research the concentration range of the NH_4Cl standard was reduced to 1 - 25 µM.

Table A1.10 Concentrations of standard sets used for cross calibration of the Dionex ICS 2000 and DX 600 instruments with the Thermalox. The mixed DIN set comprised KNO_3 + $NaNO_2$ + NH_4Cl.

	Standard species			
Concentrations (µM N)	**KNO_3**	**$NaNO_2$**	**NH_4Cl**	**Mixed DIN**
Blank	0	0	0	0
Standard 2	100	1	10	111
Standard 3	250	2	20	272
Standard 4	500	3	30	533
Standard 5	750	4	40	794
Standard 6	1000	5	50	155

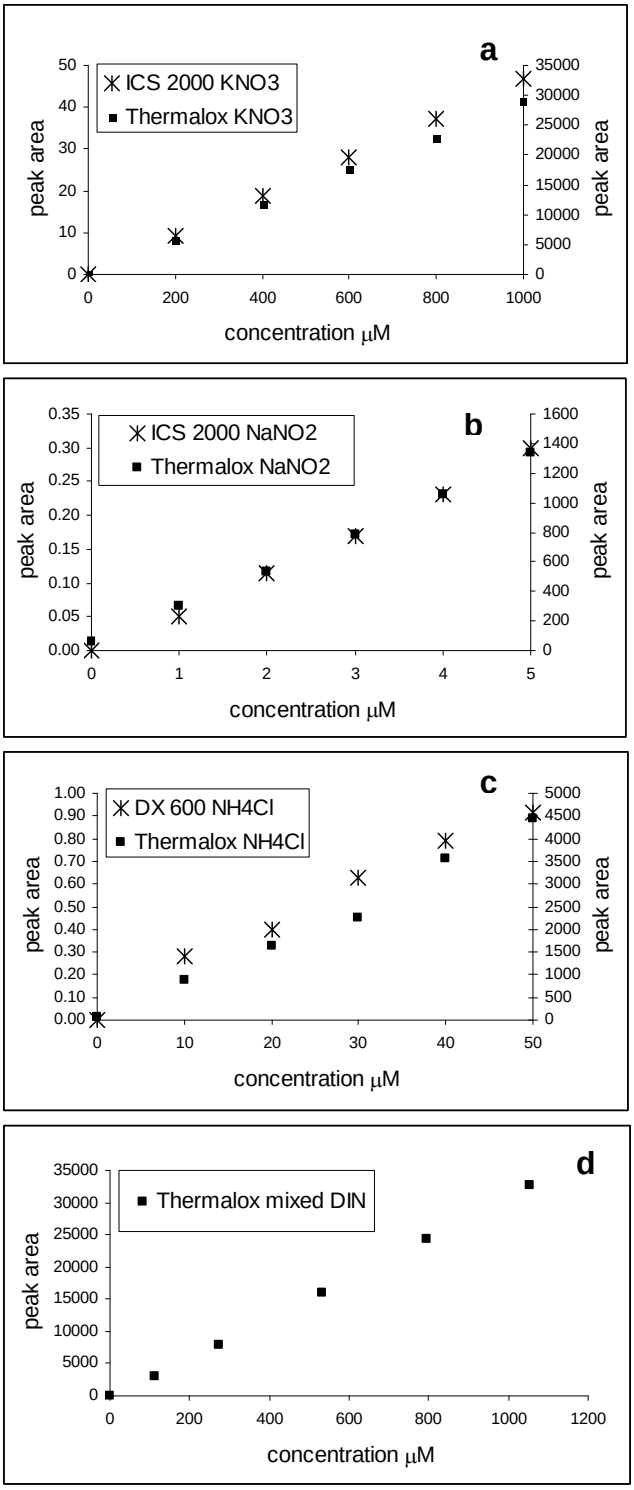

Figure A1.9 Calibration curves for KNO_3 (a), $NaNO_2$ (b), NH_4Cl(c) and mixed DIN(d) standards (μM) on the Dionex ICS 2000 (KNO_3 and $NaNO_2$), Dionex DX600 (NH_4Cl) and all standards on the Thermalox.

A 1.9 Cations and Trace Elements ICP-AES

The Varian Vista Pro ICP-AES (inductively coupled plasma atom emission spectrometer) burns diluted, acidified aspirated sample in argon plasma at very high temperatures. Each trace element produces a different wavelength on combustion in the argon plasma, enabling the concurrent analysis of multiple trace elements. Concentration is measured by intensity, calibrated to standards of a known concentration.

A 1.9.1 ICP-AES Example Calibrations:

Mixed standards were used on the ICP-AES. Example calibrations for the trace elements aluminium, boron, iron and manganese are presented (Figure A1.10a-d).

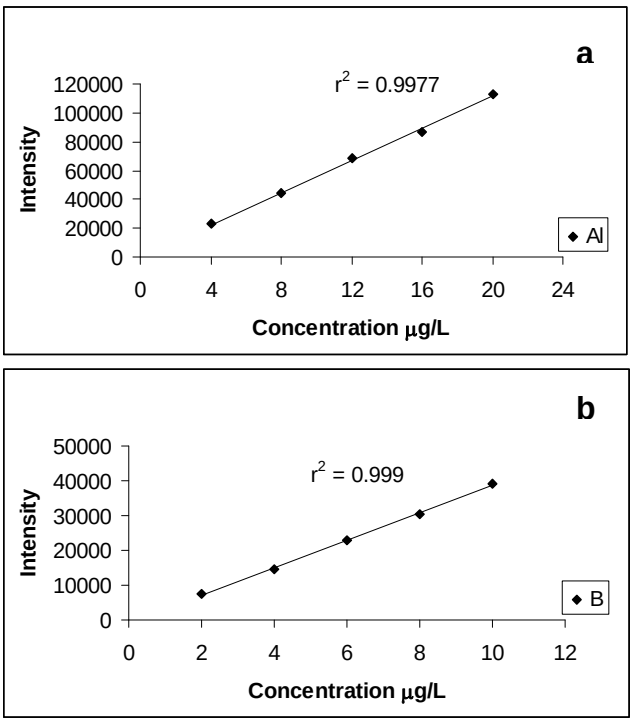

Figure A1.10 ICP-AES trace element calibration curves for Al (a), and B (b) (µg/L).

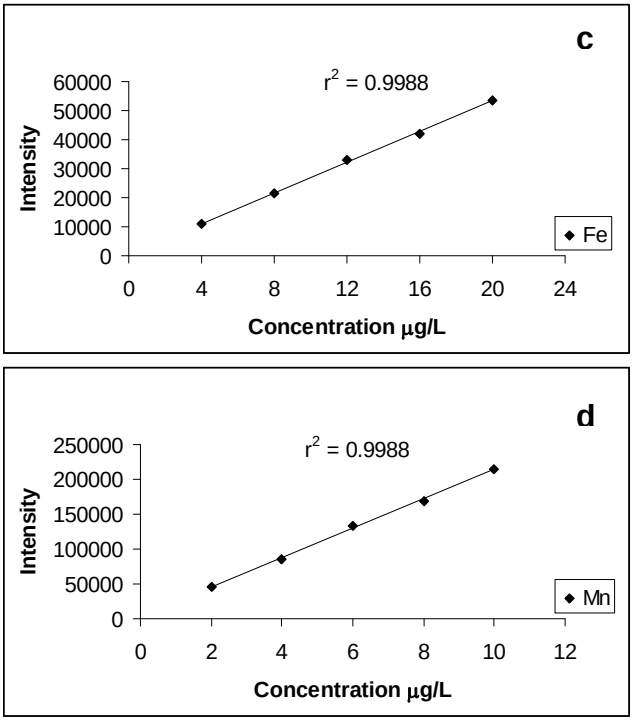

Figure A1.10cont. ICP-AES trace element calibration curves for Fe (c), and Mn (d) (µg/L).

.

A 1.10 Ion Standard Protocols

MIXED ANION STANDARD PROTOCOL (FOR USE WTH LIQUID ION CHROMATOGRAPH DIONEX ICS 2000)

Method: A) dilute the superstocks down to stock concentrations then B) combine the stocks with DIW to make the final mixed standard concentrations.

A)	Superstock concentration	Volume superstock	Volume DIW	Dilution factor	Final stock volume	Final stock concentration
Anion						
Cl^- (NaCl)	1000 mg/L	2 ml	8 ml	1 to 4	10 ml	200 mg/L
SO_4^{2-} (K_2SO_4)	500 mg/L	4 ml	6 ml	2 to 3	10 ml	200 mg/L
PO_4^{3-} (KH_2PO_4)	50 mg/L	4 ml	6 ml	2 to 3	10 ml	20 mg/L
B)	Cl^- stock + DIW	SO_4^{2-} stock + DIW	PO_4^{3-} stock + DIW		Total DIW	Final volume
ANION MXD 1	1.0 ml + 4.0 ml DIW	1.0 ml + 4.0 ml DIW	0.5 ml + 4.5 ml DIW		17.5 ml	20 ml
ANION MXD 2	2.0 ml + 3.0 ml DIW	2.0 ml + 3.0ml DIW	1.0 ml + 4.0 ml DIW		15.0 ml	20 ml
ANION MXD 3	3.0 ml + 2.0 ml DIW	3.0 ml + 2.0 ml DIW	2.5 ml + 2.5 ml DIW		11.5 ml	20 ml
ANION MXD 4	5.0 ml	5.0 ml	5.0 ml		5.0 ml	20 ml
	Final concentrations					
Standard	Cl^- mg/L	SO_4^{2-} mg/L	PO_4^{3-} mg/L			
ANION MXD 1	10	10	0.5			
ANION MXD 2	20	20	1.0			
ANION MXD 3	30	30	2.5			
ANION MXD 4	50	50	5.0			

DIN STANDARD PROTOCOL (FOR USE WTH LIQUID ION CHROMATOGRAPH DIONEX ICS 2000 AND DX 600, AND THERMALOX TN)

Method: A) dilute the superstocks down to stock concentrations then B) combine the stocks with DIW to make the final mixed standard concentrations.

A)	Superstock concentration	Volume superstock	Volume DIW	Dilution factor	Final stock volume	Final stock concentration
Anion						
NO_3^- (KNO_3)	8000 μM	5.0 ml	5.0 ml	1 to 1	10 ml	4000 μM
NH_4^+ (NH_4Cl)	400 μM	2.5 ml	7.5 ml	1 to 3	10 ml	100 μM
NO_2^- ($NaNO_2$)	40 μM	10.0 ml	-	-	10 ml	40 μM
B)	NO_3^- stock + DIW	NH_4^+ stock + DIW	NO_2^- stock + DIW		Total DIW	Final volume
DIN MXD 1	0.5 ml + 4.5 ml DIW	0.2 ml + 4.8 ml DIW	0.5 ml + 4.5 ml DIW		18.8 ml	20 ml
DIN MXD 2	1.25 ml + 3.75 ml DIW	1.0 ml + 4.0 ml DIW	1.0 ml + 4.0 ml DIW		16.75 ml	20 ml
DIN MXD 3	2.50 ml + 2.50 ml DIW	2.0 ml + 3.0 ml DIW	1.5 ml + 3.5 ml DIW		14.0 ml	20 ml
DIN MXD 4	3.75 ml + 1.25 ml DIW	5.0 ml	2.0 ml + 3.0 ml		9.25 ml	20 ml
	Final concentrations					
Standard	NO_3^- μM	NH_4^+ μM	NO_2^- μM			
DIN MXD 1	100	1	1			
DIN MXD 2	250	5	2			
DIN MXD 3	500	10	3			
DIN MXD 4	750	25	4			

A 1.11 Alkalinity Titration

Sample pH fell within the range pH 6.9 to 7.6, below the range at which carbonate forms, so alkalinity was assumed to be virtually all attributable to bicarbonate. Bicarbonate concentration was calculated from the volume of 0.01 M HCl used to titrate 10 ml of unfiltered sample with BDH 4.5 indicator, using the following calculation:

1. Calculate the volume HCl needed to titrate one litre from volume used to titrate 10 ml sample:

   Volume HCl (ml) x 100

2. Convert this volume to moles HCl:

   Volume HCl for one litre (ml) x molarity (0.01)

3. This gives milliequivalents of alkalinity in one litre of sample. To convert this to concentration HCO_3^-, (based on the assumption that all alkalinity is attributable to bicarbonate), multiply the milliequivalents by the molecular mass of HCO_3^-:

   Milliequivalents in one litre of sample x 61 = concentration HCO_3^- (mg/L)

A 1.12 Fieldwork Instruments

pH meter:	Hanna HI 9025 with A BDH Gelplas multipurpose probe, calibrated with pH 4 and pH 7 buffer solutions
Eh meter:	Hanna HI 9025 with A BDH Gelplas redox probe and a temperature probe calibrated with Zobells solution
Dissolved oxygen meter:	Jenway DO_2 9200 calibrated with sodium sulphite
EC meter:	PHOX meter

A 1.13 Fieldwork Protocol

On the day of sampling:

1. Prepare pre-acidified tubes for ICP-AES samples: 9 ml DIW + 0.8 ml nitric acid

2. Calibrate DO, pH, Eh, EC meters

3. Pick up frozen cool packs and put in cool boxes

4. Load van: DO, pH, Eh + T, EC meters, thermometer, cool boxes and cool packs, sample tubes, filter units, vinyl gloves, syringes, clip board with printed sampling grid and spare pencils, GPS unit, maps, blue roll, sampling buckets with rope, hazard triangle, high visibility jacket, mobile phone.

In Field:

1. Wearing gloves, fill bucket on rope from bridge mid stream on downstream side of bridge (avoid disturbing stream bed sediment and scraping bridge when pulling up) and rinse onto bank three times. On fourth filling carry back to van avoiding contamination from rope in bucket.

2. Rinse the sub-sampling bucket three times and fill on fourth. Place probes in large bucket (pH, Eh +T, EC, DO, thermometer) and rinse syringe and filter unit and tubes, then filter sample into tubes. (2 x 50 ml leave 15 ml → freezer, 2 x 15 ml → cold store, 1 x 50 ml not filtered → titration).

3. Put sample tubes into cool box.

4. If at new sampling location take a GPS reading.

5. Note sample ID (location code), location, meter readings, any other comments (e.g flow conditions, weather).

On return:

6. put 50 ml tubes for nitrate isotope analysis in - 20^{o}C freezer, subsample 200 μL from the anion tubes into the pre-prepared acidified tubes (for ICP-AES analysis) and tape the tops of the second set of 15 ml tubes with parafilm (for water isotope analysis) and place three sets in cold store (water isotope tubes upside-down), then carry out titrations on the 50 ml tubes of unfiltered water.

A 1.14 Example Fieldwork Sampling Grid:

WENSUM Date	ID	Time	Mileage	pH	Eh	EC	DO	T ^{0}C	Comments
1 Horningtoft									
2 Hamrow									
3 West Raynham									
4 Helhoughton									
5 Tat									
6 Shereford									
7 Fakenham GS									
8 Fakenham stream									
9 Great Ryburgh									
10 Bintree Mill									
11 Billingford									
12 Swanton GS									
13 Mill Street									
14 Lenwade									
15 Attlebridge									
16 Costessey Mill GS									

A 1.15 Wensum Sampling Location Images

West Raynham 25/09/2009 (downstream). Eastings: 58788; northings: 32538.

Helhoughton 25/09/2009 (downstream). Eastings: 58722; northings: 32690.

Helhoughton 25/09/2009 (downstream). Eastings: 58722; northings: 32690.

Shereford 25/09/2009 (upstream). Eastings: 58824; northings: 32912.

Fakenham gauging station 16/11/2008 (upstream). Eastings: 59192; northings: 32931.

Great Ryburgh 25/09/2009 (downstream). Eastings: 59637; northings: 32730.

Bintree Mill 25/09/2009 (downstream). Eastings: 59991; northings: 32550.

County School 25/09/2009 (downstream). Eastings: 59926; northings: 32273.

Wendling Beck: Worthing 25/09/2009 (downstream). Eastings: 59985; northings: 32007.

Swanton Morley gauging station 25/09/2009 (upstream). Eastings: 60212; northings: 31858.

Lyng 25/09/2009 (downstream). Eastings: 60720; northings: 31795.

Lenwade 25/09/2009 (downstream). Eastings: 61082; northings: 31878.

Attlebridge 25/09/2009 (upstream). Eastings: 61278; northings: 31667.

Costessey gauging station 25/09/2009 (downstream). Eastings: 61774; northings: 31271.

APPENDIX 2 RESULTS

A 2.1 National Grid References for Wensum Catchment Sampling Locations and Borehole Logs:

Wensum river	NGR	
Hamrow	59178	32377
West Raynham	58788	32538
Helhoughton	58722	32690
Shereford Common	58824	32912
Fakenham GS	59192	32931
Fakenham Heath	59365	32917
Pensthorpe	59441	32881
Great Ryburgh	59637	32730
Sennowe Bridge	59750	32610
Guist Bridge	59960	32500
Bintree Mill	59991	32550
County School	59926	32273
Billingford	60055	32020
Burgh Common	60128	31930
Swanton GS	60212	31858
Mill Street	60512	31784
Lyng	60720	31795
Lenwade	61082	31878
Attlebridge	61278	31667
Costessey Mill GS	61774	31271

Wensum tributaries and drains	NGR	
Horningtoft drain	59352	32338
East Raynham drain	58940	32524
Helhoughton drain	58693	32689
Tat: Tatterford	58671	32794
Shereford drain	58820	32915
Fakenham drain	59238	32920
Fakenham heath drain	59382	32911
The Carr: Langor Bridge	59612	32919
Meadowcote stream: Stibbard	59845	32892
Great Ryburgh bridge drain	59965	32500
Great Ryburgh drain	59618	32718
Stream: Guist	59970	32512
Guist Carr: Twyford	60158	32468
Bintree west drain	59960	32449
Bintree east drain	59975	32447
Blackwater drain Reed Lane	59330	31972
Blackwater: East Bilney	59554	31932
Blackwater: Spong Bridge	59834	31910
Wendling Beck: Old Brigg	59658	31518
Wendling drain Rectory Farm	59648	31618
Wendling drain Gressenhall	59712	31662
Wendling Beck: Beetley Bridge	59772	31690
Wendling Beck: Worthing	59985	32007
Stream: Mill Street	60508	31788
Lyng drain	60718	31778
Lenwade drain	61029	31785

Wensum boreholes	NGR	
Hamrow west	59174	32415
Hamrow east	59194	32415
Wellingham	58752	32303
Great Ryburgh A & B	59565	32748
Bylaugh A& B	60296	31845
Cawston	61411	32557
Weston Longville	61083	31433
Taverham	61650	31422
Hellesdon	61635	31382
Costessey west	62056	31003
Costessey east	62064	31027

Borehole logs from Harvey *et al.* (1974, , 1973)

Borehole name	NGR		Aquifer	Strata	Thickness	Depth
Hamrow west	59174	32415	Upper Chalk	Lowestoft Till	22.55	22.55
				Upper Chalk	46.63	69.18
Hamrow east	59194	32415	Upper Chalk	Lowestoft Till	26.51	26.51
				Upper Chalk	13.10	39.62
Wellingham	58752	32303	Upper Chalk	Lowestoft Till	22.55	22.55
				Sands and gravels	10.05	32.61
				Upper Chalk	43.58	76.19
Great Ryburgh	59565	32748	Upper Chalk	Lowestoft Till	4.57	4.57
				Sands and gravels	12.19	16.76
				Upper Chalk	27.43	44.19
Bylaugh	60296	31845	Upper Chalk	Superficial deposits	2.04	2.04
				Upper Chalk	28.44	30.48
Cawston	61411	32557	Upper Chalk	Lowestoft Till	20.08	20.08
				Upper Chalk	46.98	67.06
Weston Longville	61083	31433	Upper Chalk	Sands and gravels	10.16	10.16
				Upper Chalk	24.28	34.44
Taverham	61650	31422	Upper Chalk	Sands and gravels	13.10	13.10
				Lowestoft Till	5.48	18.59
				Sands and gravels	6.40	24.99
				Upper Chalk	26.21	51.20
Hellesdon	61635	31382	Upper Chalk	Superficial deposits	1.52	1.52
				Sands and gravels	6.09	7.61
				Upper Chalk	20.42	28.04
Costessey west	62056	31003	Upper Chalk	Superficial deposits	4.26	4.26
				Upper Chalk	117.65	121.91
Costessey east	62064	31027	Upper Chalk	Superficial deposits	5.18	5.18
				Upper Chalk	116.73	121.91

A 2.2 Wensum Spatial Sample Data:

Boxes indicate that a sample was taken from this location on this date. Where the sample was analysed for a determinand but was below the limit of detection, the box is filled with the symbol <LOD. Where a sample was not analysed for a determinand, the box is filled with the symbol /.

Wensum river spatial samples

$\delta^{15}N_{NO3}$ ‰ vs. AIR	14/02/2007	17/04/2007	18/07/2007	11/12/2007	06/04/2008	14/09/2008	16/11/2008	27/05/2009	25/09/2009
Hamrow	10.7		9.9		10.6	14.8			
West Raynham	9.9		9.3		9.0	9.2			9.2
Helhoughton	9.9		9.4		9.1	9.4			9.6
Shereford Common				9.9	7.9	8.4			8.2
Fakenham GS	8.8	8.0	8.6	9.5	7.8	8.2	8.7	7.9	8.5
Fakenham Heath							9.4		
Pensthorpe							9.2		
Great Ryburgh	9.3		9.4	9.6	8.4	9.0	9.4		10.6
Sennowe Bridge							9.3		
Guist Bridge							9.6		
Bintree Mill	9.8		9.6	9.8	8.7	9.5	9.7		11.3
County School						9.9	9.6		10.6
Billingford	10.1		9.3		9.0	10.6	9.7		10.2
Burgh Common							10.8		
Swanton GS	10.7	11.2	10.3		9.8	11.2	10.4	10.9	12.0
Mill Street	10.8	11.0	10.6	11.2	10.1	11.0	10.3		12.2
Lyng		11.4	10.7	11.4	10.0	11.6			12.2
Lenwade	11.2	11.3	10.6	11.0	10.0	11.9			12.2
Attlebridge		11.3	10.5		9.9	11.7			12.0
Costessey Mill GS	10.6	11.1	11.5	11.0	9.9	11.3			12.5

$\delta^{18}O_{NO3}$ ‰ vs. VSMOW	14/02/2007	17/04/2007	18/07/2007	11/12/2007	06/04/2008	14/09/2008	16/11/2008	27/05/2009	25/09/2009
Hamrow	5.0		6.4		5.7	7.5			

West Raynham	4.1		4.9		4.1	3.9			3.8
Helhoughton	4.3		4.9		4.2	4.0			4.0
Shereford Common				4.5	3.4	3.3			3.2
Fakenham GS	3.7	3.0	4.1	4.1	3.0	3.5	3.4	3.6	3.4
Fakenham Heath							3.6		
Pensthorpe							3.7		
Great Ryburgh	3.6		4.9	4.3	3.4	3.8	3.5		4.0
Sennowe Bridge							3.8		
Guist Bridge							3.8		
Bintree Mill	3.8		5.1	4.3	3.9	3.8	3.9		4.4
County School						4.0	3.9		4.4
Billingford	4.0		5.1		3.8	4.4	4.2		4.7
Burgh Common							4.3		
Swanton GS	4.4	4.3	5.4		4.7	4.7	4.9	4.9	4.8
Mill Street	4.6	4.5	5.0	4.8	4.4	4.8	3.7		4.9
Lyng		3.7	5.3	5.0	4.6	4.5			4.8
Lenwade	5.1	4.9	5.3	4.7	4.6	5.0			4.8
Attlebridge		4.5	5.3		4.6	4.4			5.1
Costessey Mill GS	4.6	4.1	5.5	4.6	4.2	5.1			5.2

NO_3^- µM	14/02/2007	17/04/2007	18/07/2007	11/12/2007	06/04/2008	14/09/2008	16/11/2008	27/05/2009	25/09/2009
Hamrow	694		591		587	298			
West Raynham	757		565		665	654			722
Helhoughton	663		553		604	611			677
Shereford Common				476	618	565			625
Fakenham GS	618	599	456	455	587	551	608	499	594
Fakenham Heath							599		
Pensthorpe							583		
Great Ryburgh	572		420	436	590	535	578		574
Sennowe Bridge							519		
Guist Bridge							517		
Bintree Mill	519		352	394	494	439	494		464

County School						420	451		444
Billingford	492		347		489	388	444		451
Burgh Common							450		
Swanton GS	442	486	338		424	342	430	410	427
Mill Street	505	407	326	407	475	344	392		422
Lyng		404	312	360	471	364			394
Lenwade	433	402	310	396	465	354			375
Attlebridge		384	334		432	340			380
Costessey Mill GS	479	396	288	391	413	349			374

NO_2^- µM	14/02/2007	17/04/2007	18/07/2007	11/12/2007	06/04/2008	14/09/2008	16/11/2008	27/05/2009	25/09/2009
Hamrow	1.1		1.6		0.8	0.8			
West Raynham	<LOD		0.7			0.9			1.0
Helhoughton	0.7		1.7		<LOD	1.1			1.0
Shereford Common					0.5	0.9			0.8
Fakenham GS	<LOD		4.0			1.0	1.5	1.8	1.7
Fakenham Heath							1.8		
Pensthorpe							1.9		
Great Ryburgh	<LOD		3.6	<LOD	<LOD	1.0	1.7		1.2
Sennowe Bridge							2.2		
Guist Bridge							2.2		
Bintree Mill	0.7		7.4	0.5	0.6	1.4	2.2		1.1
County School						1.3	2.0		1.4
Billingford	0.8		2.6		<LOD	0.8	2.3		1.4
Burgh Common							3.2		
Swanton GS	1.1	0.5	5.7		0.7	0.8	2.9	1.2	0.7
Mill Street	1.0	0.6	4.6		0.9	1.6	6.8		2.1
Lyng		0.5	5.1	0.5	0.8	1.1			1.6
Lenwade	1.1		5.2	0.5	0.7	0.7			1.0
Attlebridge		0.5	3.3		0.8	0.8			1.0
Costessey Mill GS	0.7	<LOD	6.7	0.6	0.7	1.4			0.9

NH_4^+ µM	14/02/2007	17/04/2007	18/07/2007	11/12/2007	06/04/2008	14/09/2008	16/11/2008	27/05/2009	25/09/2009
Hamrow	<LOD		<LOD		<LOD	<LOD			
West Raynham	<LOD		1.9		<LOD	0.6			/
Helhoughton	<LOD		21.4		<LOD	0.9			/
Shereford Common			<LOD	3.6	<LOD	1.4			/
Fakenham GS	<LOD		<LOD	0.8	<LOD	0.9	<LOD	/	/
Fakenham Heath							<LOD		
Pensthorpe							<LOD		
Great Ryburgh	<LOD		<LOD	4.9	<LOD	1.0	<LOD		/
Sennowe Bridge							<LOD		
Guist Bridge							<LOD		
Bintree Mill	<LOD		1.9	<LOD	<LOD	0.9	<LOD		/
County School						1.0	<LOD		/
Billingford	<LOD		2.1		<LOD	0.6	<LOD		/
Burgh Common						<LOD	<LOD		/
Swanton GS	<LOD	<LOD	<LOD		<LOD	<LOD	<LOD	/	/
Mill Street	<LOD	<LOD	<LOD	5.6	<LOD	1.1	<LOD		/
Lyng			<LOD	2.3	<LOD	0.6			/
Lenwade	<LOD	<LOD	<LOD	2.7	<LOD	0.4			/
Attlebridge		<LOD	1.9		<LOD	<LOD			/
Costessey Mill GS	<LOD	<LOD	2.6	5.1	<LOD	<LOD			/

DON µM	14/02/2007	17/04/2007	18/07/2007	11/12/2007	06/04/2008	14/09/2008	16/11/2008	27/05/2009	25/09/2009
Hamrow	195		117		/	80			
West Raynham	117		<LOD		/	52			/
Helhoughton	181		<LOD		/	88			/
Shereford Common				<LOD	/	60			/
Fakenham GS	<LOD		102	<LOD	/	62	/	/	/
Fakenham Heath							/		
Pensthorpe							/		
Great Ryburgh	180		<LOD	<LOD	/	51	/		/

Sennowe Bridge							/		
Guist Bridge							/		
Bintree Mill	147		<LOD	<LOD	/	74	/		/
County School						84	/		/
Billingford	150		<LOD		/	91	/		/
Burgh Common							/		
Swanton GS	187	115	64		/	59	/		/
Mill Street	176	143		<LOD	/	84	/		/
Lyng		152		<LOD	/	51			/
Lenwade	136	139	<LOD	<LOD	/	65			/
Attlebridge				<LOD	/	66			/
Costessey Mill GS	141	156	94	<LOD	/	56			/

PO_4^{3-} mg/L	14/02/2007	17/04/2007	18/07/2007	11/12/2007	06/04/2008	14/09/2008	16/11/2008	27/05/2009	25/09/2009
Hamrow	<LOD		<LOD		<LOD	0.06			
West Raynham	<LOD		<LOD		<LOD	0.04			0.08
Helhoughton	<LOD		<LOD		<LOD	0.02			0.06
Shereford Common				<LOD	<LOD	0.12			0.14
Fakenham GS	<LOD	<LOD	<LOD	<LOD	<LOD	0.05	0.10	<LOD	0.10
Fakenham Heath							0.12		
Pensthorpe							0.11		
Great Ryburgh	<LOD		<LOD	<LOD	<LOD	0.06	0.12		0.12
Sennowe Bridge							0.11		
Guist Bridge							0.14		
Bintree Mill	<LOD		<LOD	<LOD	<LOD	0.34	0.08		0.19
County School							0.12		
Billingford	<LOD		<LOD		<LOD	0.20	0.15		0.18
Burgh Common							0.12		
Swanton GS	<LOD	<LOD	<LOD		<LOD	0.17	0.15		0.12
Mill Street	<LOD	<LOD	<LOD	<LOD	<LOD	0.21	0.04		0.26
Lyng						0.19			0.24
Lenwade	<LOD	<LOD	<LOD	<LOD	<LOD	0.20			0.18

Attlebridge		<LOD	<LOD	<LOD	<LOD	0.19			0.10
Costessey Mill GS	<LOD	<LOD	<LOD	<LOD	<LOD	0.16			0.15

SO_4^{2-} mg/L	14/02/2007	17/04/2007	18/07/2007	11/12/2007	06/04/2008	14/09/2008	16/11/2008	27/05/2009	25/09/2009
Hamrow	24.2		22.8		38.7	33.4			
West Raynham	31.2		27.7		38.3	41.8			44.0
Helhoughton	30.1		29.3		36.7	41.3			43.3
Shereford Common				29.3	34.0	32.8			33.4
Fakenham GS	33.2	35.7	26.0	27.7	32.9	32.7	36.3	28.0	34.1
Fakenham Heath							42.7		
Pensthorpe							44.0		
Great Ryburgh	37.2		22.2	32.4	40.0	42.5	43.8		53.1
Sennowe Bridge							46.0		
Guist Bridge							46.3		
Bintree Mill	39.6		26.7	35.6	41.0	45.5	45.7		57.1
County School						44.6	44.0		53.2
Billingford	41.2		28.0		43.0	42.5	44.6		48.1
Burgh Common							45.6		
Swanton GS	33.8	53.1	27.3		40.1	45.6	45.3	43.0	52.4
Mill Street	40.4	50.0	22.2	38.6	45.4	41.3	42.7		54.1
Lyng		48.5	23.6	37.4	45.2	37.6			54.4
Lenwade	33.8	50.2	24.6	41.6	45.9	46.7			51.4
Attlebridge		51.5	35.2		44.2	46.5			52.8
Costessey Mill GS	41.8	51.2	33.2	40.9	42.6	46.3			52.9

Cl^- mg/L	14/02/2007	17/04/2007	18/07/2007	11/12/2007	06/04/2008	14/09/2008	16/11/2008	27/05/2009	25/09/2009
Hamrow	43.3		32.5		44.9	37.9			
West Raynham	38.6		32.4		39.4	36.4			36.1
Helhoughton	37.0		34.2		36.4	35.5			35.6
Shereford Common				37.4	37.3	34.3			34.5
Fakenham GS	36.0	31.4	31.7	35.2	36.4	35.2	35.7	32.0	36.0
Fakenham Heath							43.2		

Pensthorpe							42.9		
Great Ryburgh	46.3		36.5	41.4	43.9	44.4	42.7		71.0
Sennowe Bridge							42.3		
Guist Bridge							43.6		
Bintree Mill	45.2		35.5	41.7	44.2	47.1	43.3		74.3
County School						46.5	42.3		62.2
Billingford	44.1		36.0		43.8	44.9	42.3		50.3
Burgh Common							41.0		
Swanton GS	37.1	41.5	34.7		37.9	44.0	40.7	43.0	54.0
Mill Street	42.6	40.5	34.1	41.1	44.4	43.9	36.8		53.4
Lyng		37.7	33.9	39.1	44.5	45.1			52.9
Lenwade	37.2	41.2	34.4	42.5	44.0	44.8			52.0
Attlebridge		43.4	37.3		42.5	43.5			58.9
Costessey Mill GS	43.1	42.4	38.7	40.6	39.6	44.6			58.9

HCO_3^- mg /L	14/02/2007	17/04/2007	18/07/2007	11/12/2007	06/04/2008	14/09/2008	16/11/2008	27/05/2009	25/09/2009
Hamrow	340		/		/	/			
West Raynham	401		/		/	/			/
Helhoughton	329		/		/	/			/
Shereford Common				302	/	/			/
Fakenham GS	401	313	/	302	/	/	/	332	/
Fakenham Heath							/		
Pensthorpe									
Great Ryburgh	340		/	307	/	/	/		/
Sennowe Bridge							/		
Guist Bridge							/		
Bintree Mill	373		/	329	/	/	/		/
County School							/		/
Billingford	329		/			/	/		/
Burgh Common							/		
Swanton GS	362	307	/		/	/	/	312	/
Mill Street	390	313	/	318	/	/	/		/

Lyng		329	/		/	/			/
Lenwade	384	307	/	324	/	/			/
Attlebridge		307	/		/	/			/
Costessey Mill GS	346	313	/	302	/	/			/

Ca mg/L	14/02/2007	17/04/2007	18/07/2007	11/12/2007	06/04/2008	14/09/2008	16/11/2008	27/05/2009	25/09/2009
Hamrow	150		147		126	126			
West Raynham	136		133		124	120			/
Helhoughton	146		144		121	124			/
Shereford Common				121	115	109			/
Fakenham GS	149	123	126	119	112	109	124	106	/
Fakenham Heath							128		
Pensthorpe							130		
Great Ryburgh	162		129	122	114	113	128		/
Sennowe Bridge							126		
Guist Bridge							123		
Bintree Mill	143		126	122	114	116	126		/
County School						115	123		/
Billingford	147		115		114	108	119		/
Burgh Common							120		
Swanton GS	142	117	116		111	108	122	112	/
Mill Street	140	125	108	122	116	106	109		/
Lyng		121	105	122	111	108			/
Lenwade	129	128	117	125	110	108			/
Attlebridge		122	114		110	109			/
Costessey Mill GS	135	126	118	130	111	111			/

Na mg/L	14/02/2007	17/04/2007	18/07/2007	11/12/2007	06/04/2008	14/09/2008	16/11/2008	27/05/2009	25/09/2009
Hamrow	19.2		20.8		23.4	20.2			
West Raynham	15.9		23.2		20.1	17.7			/
Helhoughton	17.3		19.4		18.9	18.3			/
Shereford Common				19.3	19.3	16.9			/

Fakenham GS	17.7	17.8	18.1	19.8	19.2	17.4	17.7	15.5	/
Fakenham Heath							24.3		
Pensthorpe							23.7		
Great Ryburgh	27.0		23.2	24.3	23.9	23.1	23.1		/
Sennowe Bridge							22.4		
Guist Bridge							23.0		
Bintree Mill	24.8		23.4	25.6	24.6	26.9	23.8		/
County School						27.3	23.7		/
Billingford	25.1				24.8	25.2	23.3		/
Burgh Common							23.5		
Swanton GS	23.9	25.7	22.0		24.7	26.3	23.9	25.4	/
Mill Street	22.3	28.7	20.6	24.8	26.4	25.8	21.5		/
Lyng		26.6	20.5	24.9	24.9	26.9			/
Lenwade	19.2	30.2	22.9	25.5	23.8	25.7			/
Attlebridge		30.2	22.7		24.5	25.7			/
Costessey Mill GS	21.0	30.9	24.5	25.9	25.0	25.8			/

Mg mg/L	14/02/2007	17/04/2007	18/07/2007	11/12/2007	06/04/2008	14/09/2008	16/11/2008	27/05/2009	25/09/2009
Hamrow	3.0		2.8		2.8	2.6			
West Raynham	2.9		2.7		2.9	2.9			/
Helhoughton	3.1		2.9		3.0	3.0			/
Shereford Common				2.6	2.7	2.6			/
Fakenham GS	3.3	2.6	2.7	2.7	2.8	2.6	2.8	2.4	/
Fakenham Heath							3.0		
Pensthorpe							3.1		
Great Ryburgh	3.9		3.0	2.9	3.0	2.9	3.1		/
Sennowe Bridge							3.4		
Guist Bridge							3.3		
Bintree Mill	3.8		3.3	3.2	3.5	3.6	3.5		/
County School						3.8	3.6		/
Billingford	4.1		3.2		3.5	3.5	3.5		/
Burgh Common							3.5		

Swanton GS	4.1	3.5	3.2		3.6	3.7	3.7	3.5	/
Mill Street	3.9	3.8	3.0	3.3	3.7	3.6	5.8		/
Lyng		3.8	3.1	3.4	3.6	3.7			/
Lenwade	3.7	4.1	3.3	3.5	3.6	3.8			/
Attlebridge		4.2	3.5		3.8	4.2			/
Costessey Mill GS	4.3	4.4	3.8	3.9	4.0	4.0			/

K mg/L	14/02/2007	17/04/2007	18/07/2007	11/12/2007	06/04/2008	14/09/2008	16/11/2008	27/05/2009	25/09/2009
Hamrow	2.7		1.8		1.3	1.5			
West Raynham	3.0		4.8		1.6	1.6			/
Helhoughton	3.4		2.0		2.7	1.8			/
Shereford Common				3.9	1.5	1.4			/
Fakenham GS	3.3	1.3	2.2	4.6	1.5	1.5	1.7	1.8	/
Fakenham Heath							2.3		
Pensthorpe							2.3		
Great Ryburgh	5.0		3.1	5.4	2.1	1.9	2.2		/
Sennowe Bridge							2.6		
Guist Bridge							2.7		
Bintree Mill	5.0		4.6	6.4	4.0	4.6	3.0		/
County School						5.3	3.2		/
Billingford	7.7		4.1		2.9	3.4	3.7		/
Burgh Common							3.6		
Swanton GS	6.2	3.7	3.7		3.0	3.8	3.7	3.1	/
Mill Street	6.4	4.7	3.3	6.5	3.3	3.8	2.5		/
Lyng		3.8	3.4	6.3	3.2	3.4			/
Lenwade	5.2	4.8	3.9	6.7	3.1	3.7			/
Attlebridge		4.2	3.6		3.0	3.5			/
Costessey Mill GS	6.0	3.7	4.0	6.6	3.0	3.5			/

Si mg /L	14/02/2007	17/04/2007	18/07/2007	11/12/2007	06/04/2008	14/09/2008	16/11/2008	27/05/2009	25/09/2009
Hamrow	1.4		3.5		0.9	1.8			
West Raynham	1.5		3.5		1.3	1.7			/

Helhoughton	1.7		3.9		1.3	1.7			/
Shereford Common				1.8	1.4	1.8			/
Fakenham GS	2.0	1.1	4.0	1.8	1.2	1.8	1.9	1.2	/
Fakenham Heath							2.0		
Pensthorpe							2.0		
Great Ryburgh	2.2		4.2	1.9	1.3	1.8	2.0		/
Sennowe Bridge							2.0		
Guist Bridge							2.0		
Bintree Mill	1.7		4.4	1.9	1.3	2.0	2.1		/
County School						2.1	2.0		/
Billingford	2.2		4.0		1.3	2.0	2.0		/
Burgh Common							2.0		
Swanton GS	2.0	0.6	3.8		1.3	2.0	2.0	1.3	/
Mill Street	2.0	0.7	3.6	1.9	1.3	1.9	3.1		/
Lyng		0.7	3.8	1.9	1.3	1.9			/
Lenwade	1.9	0.8	4.1	2.0	1.3	1.9			/
Attlebridge		0.8	3.9		1.4	2.1			/
Costessey Mill GS	2.2	0.7	4.3	2.2	1.4	2.0			/

Fe µg/L	14/02/2007	17/04/2007	18/07/2007	11/12/2007	06/04/2008	14/09/2008	16/11/2008	27/05/2009	25/09/2009
Hamrow	<LOD		<LOD		1.2	0.6			
West Raynham			<LOD		0.8	0.6			/
Helhoughton	1.9		<LOD		0.8	0.8			/
Shereford Common			1.0	1.0	1.1	0.8			/
Fakenham GS	<LOD	<LOD	0.9	0.9	0.7	0.9	<LOD	0.7	/
Fakenham Heath							0.7		
Pensthorpe							2.1		
Great Ryburgh	1.1		1.1	1.1	2.1	0.8	<LOD		/
Sennowe Bridge							<LOD		
Guist Bridge							<LOD		
Bintree Mill	<LOD		0.8	0.8	0.9	1.1	<LOD		/
County School						1.8	<LOD		/

Billingford	<LOD		<LOD		0.9	0.9	<LOD		/
Burgh Common							<LOD		
Swanton GS	<LOD	<LOD	<LOD		<LOD	1.0	<LOD	<LOD	/
Mill Street	<LOD	<LOD	0.8	0.8	0.9	0.9	<LOD		/
Lyng		<LOD	0.7	0.7	0.9	0.9			/
Lenwade	<LOD	<LOD	0.8	0.8	0.8	0.9			/
Attlebridge		<LOD	<LOD		0.8	0.9			/
Costessey Mill GS	<LOD	<LOD	0.9	0.9	0.9	0.9			/

Al µg/L	14/02/2007	17/04/2007	18/07/2007	11/12/2007	06/04/2008	14/09/2008	16/11/2008	27/05/2009	25/09/2009
Hamrow	1.3		1.1		1.3	0.9			
West Raynham	1.4		1.0		0.9	0.8			/
Helhoughton	1.6		1.0		1.0	1.1			/
Shereford Common				1.0	0.8	0.8			/
Fakenham GS	<LOD	<LOD	1.0	1.0	1.3	0.8	<LOD	<LOD	/
Fakenham Heath							<LOD		
Pensthorpe							<LOD		
Great Ryburgh	<LOD		0.9	1.0	1.0	0.8	<LOD		/
Sennowe Bridge							<LOD		
Guist Bridge							<LOD		
Bintree Mill	<LOD		1.0	0.9	1.0	0.8	<LOD		/
County School						0.8	<LOD		/
Billingford	<LOD		1.0		0.9	0.8	<LOD		/
Burgh Common							<LOD		
Swanton GS	<LOD	<LOD	0.9		4.2	0.8	<LOD	<LOD	/
Mill Street	1.1	<LOD	0.9	0.9	1.4	0.8	<LOD		/
Lyng		<LOD	1.6	0.9	0.9	0.7			/
Lenwade	<LOD	<LOD	0.9	0.9	1.0	0.8			/
Attlebridge		<LOD	0.9		0.9	0.7			/
Costessey Mill GS	<LOD	<LOD	1.0	0.9	0.9	0.7			/

Zn µg/L	14/02/2007	17/04/2007	18/07/2007	11/12/2007	06/04/2008	14/09/2008	16/11/2008	27/05/2009	25/09/2009
Hamrow	1.7		0.6		1.1	<LOD			
West Raynham	1.7		0.5		0.5	<LOD			/
Helhoughton	1.7		0.5		0.5	0.3			/
Shereford Common				0.7	0.7	<LOD			/
Fakenham GS	2.2	0.6	0.7	0.4	0.6	<LOD	0.7	0.3	/
Fakenham Heath									
Pensthorpe							22.5		
Great Ryburgh	1.6		0.5	0.7	0.6	<LOD	<LOD		/
Sennowe Bridge							<LOD		
Guist Bridge							<LOD		
Bintree Mill	1.7		0.6	0.5	0.5	<LOD	<LOD		/
County School							0.3		/
Billingford	1.5		0.7		0.6	0.3	<LOD		/
Burgh Common							<LOD		
Swanton GS	1.4	<LOD	0.6		0.7	<LOD	<LOD	<LOD	/
Mill Street	1.5	<LOD	0.7	0.4	0.6	<LOD	<LOD		/
Lyng		<LOD	0.8	0.5	0.5	<LOD			/
Lenwade	1.3	0.6	1.0	0.5	0.6	<LOD			/
Attlebridge		<LOD	0.5		0.7	0.4			/
Costessey Mill GS	1.5	0.8	0.6	0.5	0.5	<LOD			/

Mn µg/L	14/02/2007	17/04/2007	18/07/2007	11/12/2007	06/04/2008	14/09/2008	16/11/2008	27/05/2009	25/09/2009
Hamrow	0.11		0.12		0.11	0.05			
West Raynham	0.08		0.14		0.11	0.06			/
Helhoughton	0.12		0.19		0.13	0.07			/
Shereford Common				0.11	0.16	0.08			/
Fakenham GS	0.14	0.08	0.11	0.12	0.19	0.09	0.21	0.19	/
Fakenham Heath							0.19		
Pensthorpe							0.20		
Great Ryburgh	0.16		0.08	0.12	0.18	0.10	0.15		/

Sennowe Bridge							0.17		
Guist Bridge							0.18		
Bintree Mill	0.21		0.25	0.12	0.23	0.17	0.21		/
County School						0.13	0.19		/
Billingford	0.24		0.21		0.22	0.09	0.19		/
Burgh Common							0.18		
Swanton GS	0.19	0.10	0.16		0.26	0.12	0.17	0.14	/
Mill Street	0.19	0.08	0.13	0.11	0.21	0.08	0.70		/
Lyng		0.08	0.09	0.18	0.20	0.05			/
Lenwade	0.16	0.11	0.08	0.11	0.21	0.07			/
Attlebridge		0.13	0.13		0.24	0.08			/
Costessey Mill GS	0.17	0.13	0.36	0.13	0.25	0.11			/

Sr mg/L	14/02/2007	17/04/2007	18/07/2007	11/12/2007	06/04/2008	14/09/2008	16/11/2008	27/05/2009	25/09/2009
Hamrow	/		/		/	/			
West Raynham	/		/		/	/			/
Helhoughton	/		/		/	/			/
Shereford Common				/	/	/			/
Fakenham GS	/	/	/	/	/	/	0.26	0.23	/
Fakenham Heath							0.27		
Pensthorpe							0.28		
Great Ryburgh	/		/	/	/	/	0.27		/
Sennowe Bridge							0.28		
Guist Bridge							0.27		
Bintree Mill	/		/	/	/	/	0.28		/
County School							0.28		/
Billingford	/		/		/	/	0.28		/
Burgh Common							0.28		
Swanton GS	/	/	/		/	/	0.29	0.27	/
Mill Street	/	/	/	/	/	/	0.55		/
Lyng		/	/	/	/	/			/
Lenwade	/	/	/	/	/	/			/

Attlebridge		/	/		/	/			/
Costessey Mill GS	/	/	/	/	/	/			/

Cu µg/L	14/02/2007	17/04/2007	18/07/2007	11/12/2007	06/04/2008	14/09/2008	16/11/2008	27/05/2009	25/09/2009
Hamrow	/		/		0.13	0.04			
West Raynham	/		/		0.09				/
Helhoughton	0.30		/		0.09	0.03			/
Shereford Common				0.09	0.08	0.02			/
Fakenham GS	/	0.14	/	0.12	0.12		0.05	0.03	/
Fakenham Heath							0.05		
Pensthorpe							0.22		
Great Ryburgh	0.28		/	0.08	0.16	0.03	0.04		/
Sennowe Bridge							0.02		
Guist Bridge							0.04		
Bintree Mill	/		/	0.10	0.06	0.04	/		/
County School						0.04	/		/
Billingford	/		/		0.12	0.03	0.03		/
Burgh Common							/		
Swanton GS	/	0.18	/		0.15	0.05	/	0.03	/
Mill Street	/	0.15	/	0.12	0.11		/		/
Lyng		0.11	/	0.10	0.09	0.03			/
Lenwade	/	0.19	/	0.10	0.09	0.03			/
Attlebridge		0.11	/		0.09	0.03			/
Costessey Mill GS	/	0.10	/	0.14	0.10	0.03			/

B µg/L	14/02/2007	17/04/2007	18/07/2007	11/12/2007	06/04/2008	14/09/2008	16/11/2008	27/05/2009	25/09/2009
Hamrow	1.68		0.80		0.28	0.55			
West Raynham	0.94		0.81		0.62	0.36			/
Helhoughton	1.64		1.73		0.48	0.43			/
Shereford Common				0.58	0.28	0.33			/
Fakenham GS	1.22	0.59	0.60	0.29	0.19	0.30	2.09	0.77	/
Fakenham Heath							3.58		

Pensthorpe							6.36		
Great Ryburgh	1.21		1.07	0.45	1.97	0.31	0.53		/
Sennowe Bridge							0.64		
Guist Bridge							0.51		
Bintree Mill	1.73		1.95	0.36	0.25	0.37	0.53		/
County School						0.38	0.49		/
Billingford	1.66		0.64		0.23	0.35	0.45		/
Burgh Common							0.44		
Swanton GS	1.73	0.54	1.13		0.36	0.41	0.49	0.63	/
Mill Street	1.87	0.84	0.61	0.47	1.05	0.40	0.66		/
Lyng		0.35	0.60	0.39	0.90	0.39			/
Lenwade	1.05	0.87	0.55	0.65	0.35	0.41			/
Attlebridge		0.48	0.53		0.28	0.40			/
Costessey Mill GS	1.12	0.59	1.38	1.50	0.29	0.40			/

Wensum tributary and drain spatial samples

$\delta^{15}N_{NO3}$ ‰ vs. AIR	14/02/2007	17/04/2007	18/07/2007	11/12/2007	06/04/2008	14/09/2008	16/11/2008	27/05/2009	25/09/2009
Horningtoft drain	7.3	8.7	9.6		7.2				
East Raynham drain					7.3				
Helhoughton drain					7.6	7.3			
Tat: Tatterford	6.9		6.3		6.3	7.3			7.6
Shereford drain				17.5	14.4	7.5			
Fakenham drain	7.4	7.7	7.9	7.5	7.6	7.1	7.4		
Fakenham Heath drain							8.3		
The Carr: Langor							7.9		
Meadowcote stream: Stibbard							7.3		
Great Ryburgh bridge drain						9.2	8.3		
Great Ryburgh drain				12.2	11.6	14.0	11.1		
Stream: Guist							14.4		
Guist Carr: Twyford							9.1		

Bintree west drain				11.9	10.0	8.6	8.6		
Bintree east drain							8.8		
Blackwater: Reed Lane								12.0	
Blackwater: East Bilney								11.1	
Blackwater: Spong Bridge								10.9	
Wendling Beck: Old Brigg								16.4	
Wendling drain: Rectory Farm								9.0	
Wendling drain: Gressenhall								8.7	
Wendling Beck: Beetley Bridge								15.5	
Wendling Beck: Worthing	11.6		12.4		12.2	15.1	12.5	15.4	16.6
Stream: Mill Street	10.2	10.8	11.1	10.0	9.7	11.5	10.7		
Lyng drain				13.4	11.1	11.4			
Lenwade drain				11.4	10.7				

$\delta^{18}O_{NO3}$ ‰ vs. VSMOW	14/02/2007	17/04/2007	18/07/2007	11/12/2007	06/04/2008	14/09/2008	16/11/2008	27/05/2009	25/09/2009
Horningtoft drain	2.4	3.3	4.4		2.4				
East Raynham drain					1.6				
Helhoughton drain					2.7	2.2			
Tat: Tatterford	2.3		2.3		1.9	2.5			3.1
Shereford drain				9.6	7.4	2.8			
Fakenham drain	3.3	2.9	3.5	2.9	3.1	2.7	3.2		
Fakenham Heath drain							4.0		
The Carr: Langor							4.2		
Meadowcote stream: Stibbard							3.6		
Great Ryburgh bridge drain						3.8	4.3		
Great Ryburgh drain				5.7	8.4	3.6	7.8		
Stream: Guist							9.4		
Guist Carr: Twyford							4.9		
Bintree west drain				4.4	6.8	4.0	4.8		
Bintree east drain							4.7		
Blackwater: Reed Lane								6.6	
Blackwater: East Bilney								4.6	

Blackwater: Spong Bridge								5.5	
Wendling Beck: Old Brigg								6.9	
Wendling drain: Rectory Farm								4.1	
Wendling drain: Gressenhall								3.9	
Wendling Beck: Beetley Bridge								6.2	
Wendling Beck: Worthing	5.2		6.2		5.5	6.2	5.4	6.8	5.7
Stream: Mill Street	4.2	4.5	5.5	3.4	3.7	4.9	4.4		
Lyng drain				5.3	4.1	4.2			
Lenwade drain				4.3	3.6				

NO_3^- µM	14/02/2007	17/04/2007	18/07/2007	11/12/2007	06/04/2008	14/09/2008	16/11/2008	27/05/2009	25/09/2009
Horningtoft drain	1279	845	640		703				
East Raynham drain					1365				
Helhoughton drain					728	671			
Tat: Tatterford	616		576		636	570			604
Shereford drain				20	521	585			
Fakenham drain	527	662	509	565	657	658	661		
Fakenham Heath drain							407		
The Carr: Langor							375		
Meadowcote stream: Stibbard							674		
Great Ryburgh bridge drain						259	292		
Great Ryburgh drain				369	247	38	364		
Stream: Guist							265		
Guist Carr: Twyford							330		
Bintree west drain				98	266	22	49		
Bintree east drain							378		
Blackwater: Reed Lane								853	
Blackwater: East Bilney								667	
Blackwater: Spong Bridge								419	
Wendling Beck: Old Brigg								357	
Wendling drain: Rectory Farm								558	
Wendling drain: Gressenhall								598	

Wendling Beck: Beetley Bridge								372	
Wendling Beck: Worthing	473		331		524	359	483	345	438
Stream: Mill Street	338	407	286	337	448	279	442		
Lyng drain				386	593	498			
Lenwade drain				894	1200				

NO_2^- µM	14/02/2007	17/04/2007	18/07/2007	11/12/2007	06/04/2008	14/09/2008	16/11/2008	27/05/2009	25/09/2009
Horningtoft drain	<LOD	4.8	7.4		<LOD				
East Raynham drain					<LOD				
Helhoughton drain					0.9	4.8			
Tat: Tatterford	<LOD		3.6		0.5	1.5			1.8
Shereford drain				<LOD	0.7	1.4			
Fakenham drain	<LOD	<LOD	1.9	<LOD	<LOD	0.6	0.9	5.0	
Fakenham heath drain							4.0		
The Carr: Langor Bridge							2.6		
Meadowcote stream: Stibbard									
Great Ryburgh bridge drain						6.1	4.9		
Great Ryburgh drain				<LOD	<LOD	<LOD			
Stream: Guist							3.7		
Guist Carr: Twyford							2.9		
Bintree west drain				<LOD	0.8	<LOD	0.6		
Bintree east drain							1.3		
Blackwater drain Reed Lane								0.7	
Blackwater: East Bilney								<LOD	
Blackwater: Spong Bridge								<LOD	
Wendling Beck: Old Brigg								2.7	
Wendling drain Rectory Farm								0.7	
Wendling drain Gressenhall								<LOD	
Wendling Beck: Beetley Bridge								1.9	
Wendling Beck: Worthing	<LOD		3.5		1.3	1.0	4.9	5.0	0.9
Stream: Mill Street	<LOD	1.0	14.7	1.1	1.4	5.9	2.1		
Lyng drain					1.2	1.9			

Lenwade drain				0.7	1.0				

NH_4^+ µM	14/02/2007	17/04/2007	18/07/2007	11/12/2007	06/04/2008	14/09/2008	16/11/2008	27/05/2009	25/09/2009
Horningtoft drain	<LOD	<LOD	1.5		<LOD				
East Raynham drain					0.8				
Helhoughton drain					7.0	5.8			
Tat: Tatterford	<LOD		<LOD		<LOD	1.4			/
Shereford drain				21.4	<LOD	0.8			
Fakenham drain	<LOD	<LOD	<LOD	3.9	<LOD	1.5	<LOD		
Fakenham heath drain							<LOD		
The Carr: Langor Bridge							<LOD		
Meadowcote stream: Stibbard							<LOD		
Great Ryburgh bridge drain						15.5	<LOD		
Great Ryburgh drain				3.6	<LOD	2.7	<LOD		
Stream: Guist							<LOD		
Guist Carr: Twyford							<LOD		
Bintree west drain				5.5	<LOD	1.1	<LOD		
Bintree east drain							<LOD		
Blackwater drain Reed Lane								/	
Blackwater: East Bilney								/	
Blackwater: Spong Bridge								/	
Wendling Beck: Old Brigg								/	
Wendling drain Rectory Farm								/	
Wendling drain Gressenhall								/	
Wendling Beck: Beetley Bridge								/	
Wendling Beck: Worthing	<LOD		2.6		1.8	1.6	<LOD	/	/
Stream: Mill Street	<LOD	<LOD	3.9	15.6	<LOD	3.1	<LOD		
Lyng drain				2.8	<LOD	3.3			
Lenwade drain				3.3	<LOD				

DON µM	14/02/2007	17/04/2007	18/07/2007	11/12/2007	06/04/2008	14/09/2008	16/11/2008	27/05/2009	25/09/2009
Horningtoft drain	73	/	/		/				

East Raynham drain					/					
Helhoughton drain					/	/				
Tat: Tatterford	174		/		/	/				/
Shereford drain				83	/	30				
Fakenham drain	151	171	86	81	/	55	/			
Fakenham heath drain							/			
The Carr: Langor Bridge							/			
Meadowcote stream: Stibbard							/			
Great Ryburgh bridge drain						130	/			
Great Ryburgh drain				80	/	55	/			
Stream: Guist							/			
Guist Carr: Twyford							/			
Bintree west drain				54	/	45	/			
Bintree east drain							/			
Blackwater drain Reed Lane								/		
Blackwater: East Bilney								/		
Blackwater: Spong Bridge								/		
Wendling Beck: Old Brigg								/		
Wendling drain Rectory Farm								/		
Wendling drain Gressenhall								/		
Wendling Beck: Beetley Bridge								/		
Wendling Beck: Worthing	467		/		/	55	/	/	/	
Stream: Mill Street		155	/	84	/	73	/			
Lyng drain				132	/	84				
Lenwade drain				151	/					

PO_4^{3-} mg/L	14/02/2007	17/04/2007	18/07/2007	11/12/2007	06/04/2008	14/09/2008	16/11/2008	27/05/2009	25/09/2009
Horningtoft drain	<LOD	<LOD	<LOD		<LOD				
East Raynham drain					<LOD				
Helhoughton drain					<LOD	0.10			
Tat: Tatterford	<LOD		<LOD		<LOD	0.38			<LOD
Shereford drain					<LOD	0.07			

Fakenham drain	<LOD	<LOD	<LOD		<LOD	<LOD	0.06			
Fakenham heath drain							0.14			
The Carr: Langor Bridge							0.05			
Meadowcote stream: Stibbard							0.01			
Great Ryburgh bridge drain						1.81	0.70			
Great Ryburgh drain				<LOD	<LOD	0.02	0.03			
Stream: Guist							0.03			
Guist Carr: Twyford							0.29			
Bintree west drain				<LOD	<LOD	0.04	0.02			
Bintree east drain							0.04			
Blackwater drain Reed Lane								<LOD		
Blackwater: East Bilney								<LOD		
Blackwater: Spong Bridge								<LOD		
Wendling Beck: Old Brigg								<LOD		
Wendling drain Rectory Farm								<LOD		
Wendling drain Gressenhall								<LOD		
Wendling Beck: Beetley Bridge								<LOD		
Wendling Beck: Worthing	<LOD		<LOD		<LOD	0.10	0.08	<LOD	<LOD	
Stream: Mill Street	<LOD	<LOD	<LOD	<LOD	<LOD	<LOD	0.14			
Lyng drain				<LOD	<LOD	0.28				
Lenwade drain				<LOD	<LOD					

SO_4^{2-} mg/L	14/02/2007	17/04/2007	18/07/2007	11/12/2007	06/04/2008	14/09/2008	16/11/2008	27/05/2009	25/09/2009
Horningtoft drain	33.1	33.6	37.1		29.9				
East Raynham drain					35.8				
Helhoughton drain					33.9	32.6			
Tat: Tatterford	36.0		22.7		28.4	27.3			25.6
Shereford drain				56.9	53.8	32.5			
Fakenham drain	55.1	68.8	38.7	67.0	62.5	69.4	64.4		
Fakenham heath drain							78.6		
The Carr: Langor Bridge							53.0		
Meadowcote stream: Stibbard							43.9		

Great Ryburgh bridge drain						57.5	56.3		
Great Ryburgh drain				28.6	44.1	25.1	34.1		
Stream: Guist							38.4		
Guist Carr: Twyford							39.9		
Bintree west drain				35.8	37.3	19.7	25.6		
Bintree east drain							44.4		
Blackwater drain Reed Lane								48.3	
Blackwater: East Bilney								45.0	
Blackwater: Spong Bridge								51.1	
Wendling Beck: Old Brigg								51.6	
Wendling drain Rectory Farm								37.3	
Wendling drain Gressenhall								41.3	
Wendling Beck: Beetley Bridge								39.7	
Wendling Beck: Worthing	34.8		29.4		49.6	48.2	48.5	49.9	68.9
Stream: Mill Street	38.2	38.6	23.7	47.5	43.2	46.6	45.2		
Lyng drain				29.7	42.6	46.7			
Lenwade drain				53.4	48.7				

Cl^- mg/L	14/02/2007	17/04/2007	18/07/2007	11/12/2007	06/04/2008	14/09/2008	16/11/2008	27/05/2009	25/09/2009
Horningtoft drain	47.5	39.8	35.3		40.7				
East Raynham drain					58.5				
Helhoughton drain					37.5	32.1			
Tat: Tatterford	38.7		34.1		34.5	33.4			32.9
Shereford drain				43.2	44.7	35.7			
Fakenham drain	73.3	61.8	62.3	73.8	75.0	60.0	72.3		
Fakenham heath drain							64.2		
The Carr: Langor Bridge							42.1		
Meadowcote stream: Stibbard							40.0		
Great Ryburgh bridge drain						52.0	42.9		
Great Ryburgh drain				29.2	42.8	28.5	27.0		
Stream: Guist							42.8		
Guist Carr: Twyford							37.1		

Bintree west drain				33.5	35.8	34.6	29.6		
Bintree east drain							43.9		
Blackwater drain Reed Lane								43.8	
Blackwater: East Bilney								47.1	
Blackwater: Spong Bridge								50.0	
Wendling Beck: Old Brigg								50.8	
Wendling drain Rectory Farm								35.2	
Wendling drain Gressenhall								39.7	
Wendling Beck: Beetley Bridge								43.2	
Wendling Beck: Worthing	39.7		29.2		44.0	42.1	39.0	48.1	62.0
Stream: Mill Street	32.1	33.2	34.7	39.8	38.0	37.3	39.8		
Lyng drain				29.0	38.1	31.3			
Lenwade drain				92.2	35.5				

HCO_3^- mg /L	14/02/2007	17/04/2007	18/07/2007	11/12/2007	06/04/2008	14/09/2008	16/11/2008	27/05/2009	25/09/2009
Horningtoft drain	384	384	/		/				
East Raynham drain					/				
Helhoughton drain					/	/			
Tat: Tatterford	329		/		/	/			/
Shereford drain				379	/	/			
Fakenham drain	401	335	/	/	/	/	/		
Fakenham heath drain							/		
The Carr: Langor Bridge							/		
Meadowcote stream: Stibbard							/		
Great Ryburgh bridge drain						/	/		
Great Ryburgh drain				324	/	/	/		
Stream: Guist							/		
Guist Carr: Twyford							/		
Bintree west drain				/	/	/	/		
Bintree east drain							/		
Blackwater drain Reed Lane								/	
Blackwater: East Bilney								351	

Blackwater: Spong Bridge								390	
Wendling Beck: Old Brigg								234	
Wendling drain Rectory Farm								/	
Wendling drain Gressenhall								/	
Wendling Beck: Beetley Bridge								312	
Wendling Beck: Worthing	351		/		/	/	/	322	/
Stream: Mill Street	324	297	/	/	/	/	/		
Lyng drain				/	/	/			
Lenwade drain				351	/				

Ca mg/L	14/02/2007	17/04/2007	18/07/2007	11/12/2007	06/04/2008	14/09/2008	16/11/2008	27/05/2009	25/09/2009
Horningtoft drain	157	144	149		131				
East Raynham drain					111				
Helhoughton drain					124	121			
Tat: Tatterford	136		124		102	103			/
Shereford drain				144	112	107			
Fakenham drain	157	143	148	150	128	128	138		
Fakenham heath drain							139		
The Carr: Langor Bridge							128		
Meadowcote stream: Stibbard							137		
Great Ryburgh bridge drain						107	117		
Great Ryburgh drain				133	117	120	130		
Stream: Guist							117		
Guist Carr: Twyford							126		
Bintree west drain				113	91	36	57		
Bintree east drain							120		
Blackwater drain Reed Lane								154	
Blackwater: East Bilney								133	
Blackwater: Spong Bridge								134	
Wendling Beck: Old Brigg								104	
Wendling drain Rectory Farm								112	
Wendling drain Gressenhall								106	

Wendling Beck: Beetley Bridge								97	
Wendling Beck: Worthing	136		116		111	107	124	111	/
Stream: Mill Street	125	107	115	115	99	99	125		
Lyng drain				100	89	85			
Lenwade drain				145	127				

Na mg/L	14/02/2007	17/04/2007	18/07/2007	11/12/2007	06/04/2008	14/09/2008	16/11/2008	27/05/2009	25/09/2009
Horningtoft drain	18.6	19.7	22.0		20.8				
East Raynham drain					30.5				
Helhoughton drain					19.7	16.9			
Tat: Tatterford	19.6		19.4		19.0	17.5			/
Shereford drain				26.3	29.2	16.6			
Fakenham drain	38.5	33.2	37.7	41.2	39.5	27.8	37.2		
Fakenham heath drain							41.2		
The Carr: Langor Bridge							21.9		
Meadowcote stream: Stibbard							20.7		
Great Ryburgh bridge drain						23.9	21.7		
Great Ryburgh drain				14.2	22.5	16.5	13.5		
Stream: Guist							20.9		
Guist Carr: Twyford							22.9		
Bintree west drain				21.9	23.9	17.6	16.4		
Bintree east drain							21.9		
Blackwater drain Reed Lane								26.0	
Blackwater: East Bilney								28.1	
Blackwater: Spong Bridge								27.9	
Wendling Beck: Old Brigg								39.2	
Wendling drain Rectory Farm								19.1	
Wendling drain Gressenhall								22.6	
Wendling Beck: Beetley Bridge								32.6	
Wendling Beck: Worthing	21.2		22.1		27.4	27.0	24.7	36.2	/
Stream: Mill Street	19.3	21.3	23.0	24.3	22.3	21.1	23.6		
Lyng drain				17.4	20.9	15.8			

Lenwade drain				63.8	21.7				
Mg mg/L	14/02/2007	17/04/2007	18/07/2007	11/12/2007	06/04/2008	14/09/2008	16/11/2008	27/05/2009	25/09/2009
Horningtoft drain	3.7	2.7	3.6		3.0				
East Raynham drain					8.1				
Helhoughton drain					2.9	2.5			
Tat: Tatterford	3.3		2.7		2.5	2.4			/
Shereford drain				5.5	7.1	2.6			
Fakenham drain	4.7	3.8	4.1	4.2	4.0	3.8	4.0		
Fakenham heath drain							4.1		
The Carr: Langor Bridge							4.9		
Meadowcote stream: Stibbard							3.6		
Great Ryburgh bridge drain						5.5	4.7		
Great Ryburgh drain				2.6	2.9	3.0	2.7		
Stream: Guist							4.2		
Guist Carr: Twyford							4.3		
Bintree west drain				3.2	3.4	2.6	2.7		
Bintree east drain							4.8		
Blackwater drain Reed Lane								4.0	
Blackwater: East Bilney								3.8	
Blackwater: Spong Bridge								3.7	
Wendling Beck: Old Brigg								4.2	
Wendling drain Rectory Farm								3.6	
Wendling drain Gressenhall								3.9	
Wendling Beck: Beetley Bridge								3.6	
Wendling Beck: Worthing	3.8		3.2		3.7	3.7	3.7	4.1	/
Stream: Mill Street	6.6	5.3	3.8	5.7	5.7	5.5	3.7		
Lyng drain				3.3	3.8	3.3			
Lenwade drain				4.3	4.1				

K mg/L	14/02/2007	17/04/2007	18/07/2007	11/12/2007	06/04/2008	14/09/2008	16/11/2008	27/05/2009	25/09/2009
Horningtoft drain	3.0	0.6	3.4		1.1				
East Raynham drain					12.1				
Helhoughton drain					1.6	1.5			
Tat: Tatterford	3.7		1.5		1.4	1.4			/
Shereford drain				14.4	12.9	1.1			
Fakenham drain	7.1	3.1	3.7	7.1	3.7	2.6	3.7		
Fakenham heath drain							2.1		
The Carr: Langor Bridge							2.4		
Meadowcote stream: Stibbard							1.2		
Great Ryburgh bridge drain						27.8	10.4		
Great Ryburgh drain				2.4	1.3	2.0	1.3		
Stream: Guist							1.7		
Guist Carr: Twyford							3.2		
Bintree west drain				6.1	2.8	0.9	1.7		
Bintree east drain							2.6		
Blackwater drain Reed Lane								4.7	
Blackwater: East Bilney								2.5	
Blackwater: Spong Bridge								2.1	
Wendling Beck: Old Brigg								5.2	
Wendling drain Rectory Farm								1.5	
Wendling drain Gressenhall								3.1	
Wendling Beck: Beetley Bridge								4.0	
Wendling Beck: Worthing	7.3		3.3		2.9	3.3	3.2	4.4	/
Stream: Mill Street	4.8	2.2	3.7	5.0	2.4	2.0	3.2		
Lyng drain				6.4	2.4	3.2			
Lenwade drain				7.2	2.8				

Si mg /L	14/02/2007	17/04/2007	18/07/2007	11/12/2007	06/04/2008	14/09/2008	16/11/2008	27/05/2009	25/09/2009
Horningtoft drain	2.2	2.1	6.1		1.7				
East Raynham drain					2.5				
Helhoughton drain					1.8	1.7			

Tat: Tatterford	2.2		4.3		1.4	2.0			/
Shereford drain				3.6	1.6	1.8			
Fakenham drain	2.3	3.0	4.3	2.0	1.7	1.7	1.9		
Fakenham heath drain							2.3		
The Carr: Langor Bridge							2.3		
Meadowcote stream: Stibbard							1.6		
Great Ryburgh bridge drain						2.2	2.2		
Great Ryburgh drain				1.5	0.7	2.5	1.5		
Stream: Guist							2.6		
Guist Carr: Twyford							2.2		
Bintree west drain				2.4	0.2	1.2	0.8		
Bintree east drain							2.7		
Blackwater drain Reed Lane								1.2	
Blackwater: East Bilney								1.6	
Blackwater: Spong Bridge								1.6	
Wendling Beck: Old Brigg								1.9	
Wendling drain Rectory Farm								1.3	
Wendling drain Gressenhall								1.5	
Wendling Beck: Beetley Bridge								1.5	
Wendling Beck: Worthing	2.0		3.6		1.3	1.9	1.8	1.7	/
Stream: Mill Street	2.9	2.8	4.1	3.0	1.8	2.7	2.0		
Lyng drain				1.8	0.2	1.4			
Lenwade drain				1.9	1.5				

Fe µg/L	14/02/2007	17/04/2007	18/07/2007	11/12/2007	06/04/2008	14/09/2008	16/11/2008	27/05/2009	25/09/2009
Horningtoft drain	1.6	<LOD	1.0		0.7				
East Raynham drain					3.0				
Helhoughton drain					0.8	0.6			
Tat: Tatterford	<LOD		1.5		1.1	1.0			/
Shereford drain				1.6	1.3	0.8			
Fakenham drain	<LOD	<LOD	0.9	0.7	0.9	0.7	<LOD		
Fakenham heath drain							1.1		

The Carr: Langor Bridge							<LOD		
Meadowcote stream: Stibbard							<LOD		
Great Ryburgh bridge drain						1.9	0.8		
Great Ryburgh drain				0.8	2.0	1.1	<LOD		
Stream: Guist							<LOD		
Guist Carr: Twyford							<LOD		
Bintree west drain				0.8	3.8	1.4	0.7		
Bintree east drain							<LOD		
Blackwater drain Reed Lane								<LOD	
Blackwater: East Bilney								<LOD	
Blackwater: Spong Bridge								0.7	
Wendling Beck: Old Brigg								0.7	
Wendling drain Rectory Farm								0.7	
Wendling drain Gressenhall								1.0	
Wendling Beck: Beetley Bridge								0.9	
Wendling Beck: Worthing	0.9		1.1		0.9	0.9	<LOD	0.6	/
Stream: Mill Street	<LOD	<LOD	1.6	0.8	1.4	1.3	<LOD		
Lyng drain				0.9	0.8	1.3			
Lenwade drain				0.7	1.8				

Al µg/L	14/02/2007	17/04/2007	18/07/2007	11/12/2007	06/04/2008	14/09/2008	16/11/2008	27/05/2009	25/09/2009
Horningtoft drain	1.2	<LOD	1.1		0.8				
East Raynham drain					1.1				
Helhoughton drain					0.8	0.8			
Tat: Tatterford	1.2		0.9		0.9	0.8			/
Shereford drain				0.9	0.9	0.8			
Fakenham drain	1.2	<LOD	0.8	0.9	0.8	0.8	<LOD		
Fakenham heath drain							<LOD		
The Carr: Langor Bridge							<LOD		
Meadowcote stream: Stibbard							<LOD		
Great Ryburgh bridge drain						<LOD	<LOD		
Great Ryburgh drain				0.9	0.9	0.8	<LOD		

Stream: Guist							<LOD		
Guist Carr: Twyford							<LOD		
Bintree west drain				0.9	4.7	0.7	<LOD		
Bintree east drain							<LOD		
Blackwater drain Reed Lane								<LOD	
Blackwater: East Bilney								<LOD	
Blackwater: Spong Bridge								<LOD	
Wendling Beck: Old Brigg								<LOD	
Wendling drain Rectory Farm								<LOD	
Wendling drain Gressenhall								<LOD	
Wendling Beck: Beetley Bridge								<LOD	
Wendling Beck: Worthing	1.0		1.0		0.8	0.7	<LOD	<LOD	/
Stream: Mill Street	1.2	<LOD	0.8	0.8	0.9	0.7	<LOD		
Lyng drain				0.9	1.0	1.0			
Lenwade drain				0.9	1.2				

Zn µg/L	14/02/2007	17/04/2007	18/07/2007	11/12/2007	06/04/2008	14/09/2008	16/11/2008	27/05/2009	25/09/2009
Horningtoft drain	2.3	0.9	1.0		0.6				
East Raynham drain									
Helhoughton drain					0.5	<LOD			
Tat: Tatterford	1.7		0.6		0.5	<LOD			/
Shereford drain				0.8	0.6	<LOD			
Fakenham drain	2.1	1.7	0.3	0.6	0.5	<LOD	<LOD		
Fakenham heath drain							<LOD		
The Carr: Langor Bridge							0.4		
Meadowcote stream: Stibbard							0.3		
Great Ryburgh bridge drain						<LOD	<LOD		
Great Ryburgh drain				0.6	0.7	<LOD	0.7		
Stream: Guist							0.4		
Guist Carr: Twyford							0.4		
Bintree west drain				0.6	5.3	<LOD	<LOD		
Bintree east drain							<LOD		

Blackwater drain Reed Lane								0.5	
Blackwater: East Bilney								0.5	
Blackwater: Spong Bridge								<LOD	
Wendling Beck: Old Brigg								0.3	
Wendling drain Rectory Farm								0.3	
Wendling drain Gressenhall								0.3	
Wendling Beck: Beetley Bridge								0.4	
Wendling Beck: Worthing	1.3		0.6		0.5	<LOD	0.3	<LOD	/
Stream: Mill Street	1.9	1.7	1.7	0.6	0.9	<LOD	<LOD		
Lyng drain				0.6	1.0	<LOD			
Lenwade drain				0.7	0.5				

Mn µg/L	14/02/2007	17/04/2007	18/07/2007	11/12/2007	06/04/2008	14/09/2008	16/11/2008	27/05/2009	25/09/2009
Horningtoft drain	0.07	0.10	0.48		0.11				
East Raynham drain					2.05				
Helhoughton drain					0.14	0.06			
Tat: Tatterford	0.13		0.22		0.15	0.16			/
Shereford drain				4.78	0.47	0.13			
Fakenham drain	0.25	0.10	0.14	0.20	0.16	0.07	0.11		
Fakenham heath drain							0.27		
The Carr: Langor Bridge							0.38		
Meadowcote stream: Stibbard							0.13		
Great Ryburgh bridge drain						0.21	0.42		
Great Ryburgh drain				0.08	0.15	0.41	0.16		
Stream: Guist							0.10		
Guist Carr: Twyford							0.30		
Bintree west drain				0.15	0.28	0.08	0.06		
Bintree east drain							0.23		
Blackwater drain Reed Lane								0.03	
Blackwater: East Bilney								0.16	
Blackwater: Spong Bridge								0.14	
Wendling Beck: Old Brigg								0.32	

Wendling drain Rectory Farm								0.10	
Wendling drain Gressenhall								0.22	
Wendling Beck: Beetley Bridge								0.27	
Wendling Beck: Worthing	0.19		0.05		0.22	0.10	0.19	0.20	/
Stream: Mill Street	0.91	0.82	0.29	1.00	0.92	0.63	0.15		
Lyng drain				0.31	0.79	0.26			
Lenwade drain				0.18	0.13				

Sr mg/L	14/02/2007	17/04/2007	18/07/2007	11/12/2007	06/04/2008	14/09/2008	16/11/2008	27/05/2009	25/09/2009
Horningtoft drain	/	/	/		/				
East Raynham drain					/				
Helhoughton drain					/	/			
Tat: Tatterford	/		/		/	/			/
Shereford drain				/	/	/			
Fakenham drain	/	/	/	/	/	/	0.30		
Fakenham heath drain							0.31		
The Carr: Langor Bridge							0.34		
Meadowcote stream: Stibbard							0.34		
Great Ryburgh bridge drain						/	0.30		
Great Ryburgh drain				/	/	/	0.28		
Stream: Guist							0.30		
Guist Carr: Twyford							0.32		
Bintree west drain				/	/	/	0.17		
Bintree east drain							0.32		
Blackwater drain Reed Lane								0.32	
Blackwater: East Bilney								0.28	
Blackwater: Spong Bridge								0.29	
Wendling Beck: Old Brigg								0.29	
Wendling drain Rectory Farm								0.25	
Wendling drain Gressenhall								0.24	
Wendling Beck: Beetley Bridge								0.26	
Wendling Beck: Worthing	/		/		/	/	0.30	0.29	/

Stream: Mill Street	/	/	/	/	/	/	0.29		
Lyng drain				/	/	/			
Lenwade drain				/	/				

Cu µg/L	14/02/2007	17/04/2007	18/07/2007	11/12/2007	06/04/2008	14/09/2008	16/11/2008	27/05/2009	25/09/2009
Horningtoft drain	0.32	0.27	<LOD		0.09				
East Raynham drain					<LOD				
Helhoughton drain					0.09	0.02			
Tat: Tatterford	<LOD		<LOD		0.08	0.03			/
Shereford drain				0.11	0.10	0.02			
Fakenham drain	<LOD	0.17	<LOD	0.10	0.09	0.02	0.04		
Fakenham heath drain							0.05		
The Carr: Langor Bridge							0.02		
Meadowcote stream: Stibbard							0.02		
Great Ryburgh bridge drain						<LOD	0.02		
Great Ryburgh drain				0.08	0.10	0.09	0.04		
Stream: Guist							0.03		
Guist Carr: Twyford							0.03		
Bintree west drain				0.10	0.23	0.03	<LOD		
Bintree east drain							<LOD		
Blackwater drain Reed Lane								0.03	
Blackwater: East Bilney								0.02	
Blackwater: Spong Bridge								0.03	
Wendling Beck: Old Brigg								0.04	
Wendling drain Rectory Farm								0.05	
Wendling drain Gressenhall								0.04	
Wendling Beck: Beetley Bridge								0.03	
Wendling Beck: Worthing	0.25		<LOD		0.11	0.04	0.03	0.04	/
Stream: Mill Street	<LOD	0.14	<LOD	0.10	0.10	<LOD	0.05		
Lyng drain				0.09	0.07	0.05			
Lenwade drain				0.11	0.20				

B µg/L	14/02/2007	17/04/2007	18/07/2007	11/12/2007	06/04/2008	14/09/2008	16/11/2008	27/05/2009	25/09/2009
Horningtoft drain	3.05	0.67	1.07		0.58				
East Raynham drain					<LOD				
Helhoughton drain					0.20	0.46			
Tat: Tatterford	6.89		0.40		0.19	0.27			/
Shereford drain				0.75	0.94	0.27			
Fakenham drain	1.07	0.74	0.64	0.39	0.60	0.34	2.45		
Fakenham heath drain							4.62		
The Carr: Langor Bridge							0.56		
Meadowcote stream: Stibbard							0.63		
Great Ryburgh bridge drain						<LOD	0.54		
Great Ryburgh drain				0.39	0.60	0.48	0.59		
Stream: Guist							0.43		
Guist Carr: Twyford							0.58		
Bintree west drain				0.35	0.29	0.33	0.47		
Bintree east drain							0.42		
Blackwater drain Reed Lane								0.74	
Blackwater: East Bilney								0.51	
Blackwater: Spong Bridge								0.52	
Wendling Beck: Old Brigg								0.87	
Wendling drain Rectory Farm								0.84	
Wendling drain Gressenhall								0.53	
Wendling Beck: Beetley Bridge								0.54	
Wendling Beck: Worthing	0.99		0.69		0.30	0.43	0.53	0.66	/
Stream: Mill Street	1.64	0.45	0.92	0.46	0.32	0.37	0.65		
Lyng drain				0.33	0.30	0.41			
Lenwade drain				0.40	2.20				

A 2.3 Tributary and Drain Samples $\delta^{15}N_{NO3}$ Median and Range versus Mean and Standard Deviation

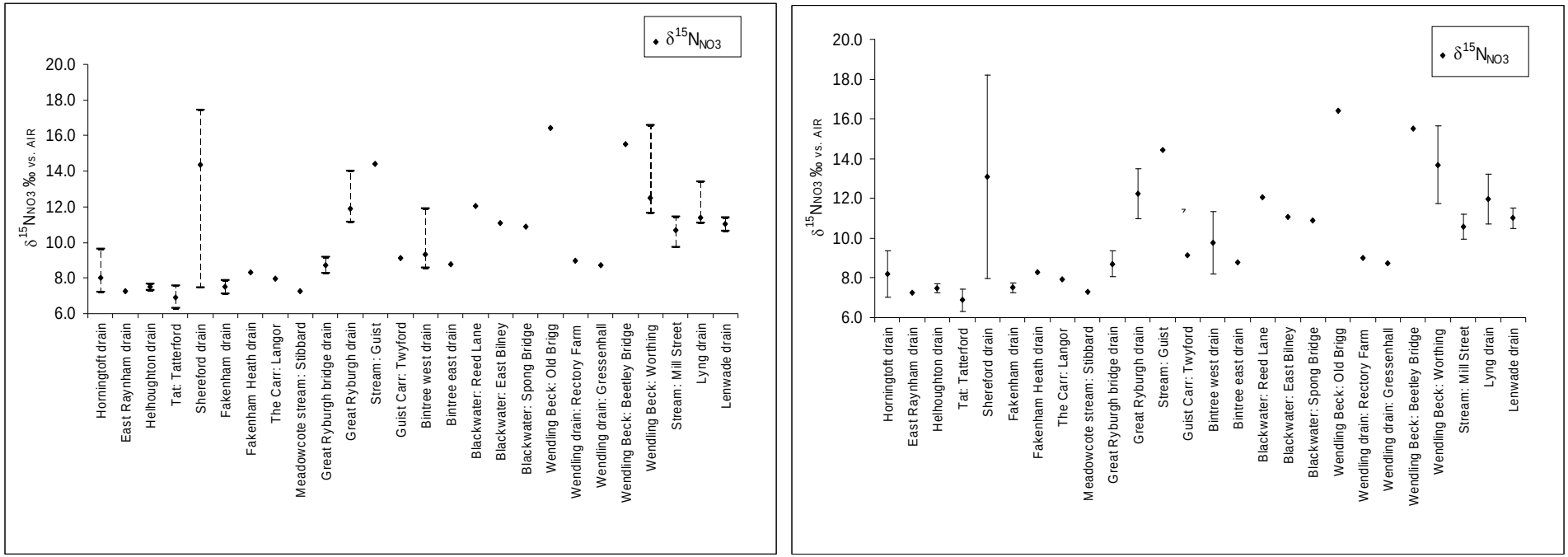

Tributary and drain samples a) $\delta^{15}N_{NO3}$ median and range, b) mean and standard deviation.

A 2.4 Wensum Temporal Sample Data:

Wensum lower river temporal samples 19-24/04/2007

Sampling location	Date	Time	$\delta^{15}N_{NO3}$ ‰ AIR	$\delta^{18}O_{NO3}$ ‰ VSMOW	NO_3^- µM	NO_2^- µM	NH_4^+ µM	DON µM	Cl^- mg/L	SO_4^{2-} mg/L	PO_4^{3-} mg/L
Swanton GS	19/04/2007	8.20	11.2	4.3	438	<LOD	/	/	43.3	52.4	<LOD
Mill Street	19/04/2007	8.45	11.0	4.5	404	<LOD	/	/	39.7	48.3	<LOD
Lyng	19/04/2007	9.00	11.1	4.6	409	<LOD	/	/	40.4	50.9	<LOD
Lenwade	19/04/2007	9.25	11.4	4.8	362	<LOD	/	/	37.9	46.8	<LOD
Attlebridge	19/04/2007	9.40	11.5	4.6	382	<LOD	/	/	43.3	52.0	<LOD
Swanton GS	19/04/2007	10.15	11.2	4.6	437	<LOD	/	/	42.5	52.1	<LOD
Mill Street	19/04/2007	10.25	10.9	4.8	419	<LOD	/	/	40.4	52.5	<LOD
Lyng	19/04/2007	10.40	11.2	4.7	408	<LOD	/	/	39.3	49.6	<LOD
Lenwade	19/04/2007	10.55	11.2	4.8	386	<LOD	/	/	39.9	50.0	<LOD
Attlebridge	19/04/2007	11.05	11.6	4.6	371	<LOD	/	/	42.4	49.5	<LOD
Swanton GS	20/04/2007	9.20	10.8	4.6	429	/	/	/	/	/	/
Mill Street	20/04/2007	9.30	10.0	4.1	418	<LOD	/	/	41.5	51.8	<LOD
Lyng	20/04/2007	9.45	10.4	4.3	419	<LOD	/	/	43.3	53.2	<LOD
Lenwade	20/04/2007	10.02	10.9	4.6	383	<LOD	/	/	40.5	50.8	<LOD
Attlebridge	20/04/2007	10.15	10.9	4.7	367	<LOD	/	/	41.8	50.4	<LOD
Swanton GS	20/04/2007	10.35	10.1	4.3	427	<LOD	/	/	42.7	52.6	<LOD
Mill Street	20/04/2007	10.50	10.0	3.9	412	<LOD	/	/	40.8	51.9	<LOD
Lyng	20/04/2007	11.00	10.4	4.3	409	<LOD	/	/	41.7	51.7	<LOD
Lenwade	20/04/2007	11.10	10.5	4.2	383	<LOD	/	/	40.4	51.1	<LOD
Attlebridge	20/04/2007	11.25	11.0	4.4	368	<LOD	/	/	43.2	51.1	<LOD
Swanton GS	21/04/2007	10.00	10.9	4.2	426	<LOD	/	/	43.6	52.0	<LOD
Mill Street	21/04/2007	10.15	10.8	4.5	405	<LOD	/	/	40.6	50.0	<LOD
Lyng	21/04/2007	10.25	10.9	4.0	401	<LOD	/	/	41.8	50.1	<LOD
Lenwade	21/04/2007	10.50	11.0	4.1	378	<LOD	/	/	41.0	48.9	<LOD
Attlebridge	21/04/2007	11.05	11.0	4.3	374	<LOD	/	/	44.3	51.4	<LOD
Swanton GS	21/04/2007	11.25	10.9	4.5	412	<LOD	/	/	42.1	50.4	<LOD

Mill Street	21/04/2007	11.40	10.9	4.5	411	<LOD	/	/	41.2	51.3	<LOD
Lyng	21/04/2007	11.50	11.2	4.6	406	<LOD	/	/	41.7	50.4	<LOD
Lenwade	21/04/2007	12.05	11.0	4.3	380	<LOD	/	/	40.2	49.5	<LOD
Attlebridge	21/04/2007	12.15	11.2	4.3	373	<LOD	/	/	43.5	51.4	<LOD
Swanton GS	22/04/2007	8.30	10.8	4.6	422	<LOD	/	/	43.1	52.1	<LOD
Mill Street	22/04/2007	8.45	10.7	4.3	419	<LOD	/	/	39.8	50.7	<LOD
Lyng	22/04/2007	9.00	10.8	4.4	416	<LOD	/	/	44.2	52.7	<LOD
Lenwade	22/04/2007	9.20	11.0	4.7	374	<LOD	/	/	40.5	50.0	<LOD
Attlebridge	22/04/2007	9.35	11.2	4.7	370	<LOD	/	/	42.5	50.7	<LOD
Swanton GS	22/04/2007	9.55	10.7	4.4	412	<LOD	/	/	43.0	51.1	<LOD
Mill Street	22/04/2007	10.05	10.6	4.5	407	<LOD	/	/	40.8	50.1	<LOD
Lyng	22/04/2007	10.15	10.8	4.5	405	<LOD	/	/	42.1	51.1	<LOD
Lenwade	22/04/2007	10.30	11.1	4.7	342	<LOD	/	/	37.5	45.6	<LOD
Attlebridge	22/04/2007	10.40	11.0	4.7	372	<LOD	/	/	43.3	51.5	<LOD
Swanton GS	23/04/2007	8.20	11.1	4.5	427	<LOD	/	/	42.6	52.3	<LOD
Mill Street	23/04/2007	8.40	10.7	3.4	422	<LOD	/	/	42.0	51.7	<LOD
Lyng	23/04/2007	8.55	10.8	3.5	414	<LOD	/	/	44.3	52.3	<LOD
Lenwade	23/04/2007	9.15	10.9	3.8	383	<LOD	/	/	42.4	50.6	<LOD
Attlebridge	23/04/2007	9.30	11.0	4.1	370	<LOD	/	/	43.9	50.4	<LOD
Swanton GS	23/04/2007	9.50	11.0	4.4	427	<LOD	/	/	42.7	52.3	<LOD
Mill Street	23/04/2007	10.05	10.5	3.3	386	<LOD	/	/	42.5	51.5	<LOD
Lyng	23/04/2007	10.15	10.8	3.5	410	<LOD	/	/	43.1	51.9	<LOD
Lenwade	23/04/2007	10.30	11.1	4.2	424	<LOD	/	/	42.1	51.6	<LOD
Attlebridge	23/04/2007	10.40	11.1	4.1	333	<LOD	/	/	40.1	46.1	<LOD
Swanton GS	24/04/2007	8.05	11.1	4.5	430	<LOD	/	/	42.3	53.0	<LOD
Mill Street	24/04/2007	8.20	10.4	3.3	434	<LOD	/	/	41.3	52.6	<LOD
Lyng	24/04/2007	8.35	10.8	4.4	421	<LOD	/	/	41.7	52.0	<LOD
Lenwade	24/04/2007	8.50	10.9	4.0	393	<LOD	/	/	42.2	51.1	<LOD
Attlebridge	24/04/2007	9.05	10.9	4.0	378	<LOD	/	/	44.0	50.9	<LOD
Swanton GS	24/04/2007	9.30	11.0	4.5	403	<LOD	/	/	40.8	48.8	<LOD
Mill Street	24/04/2007	9.40	10.8	4.6	421	<LOD	/	/	41.1	50.7	<LOD
Lyng	24/04/2007	9.50	10.9	4.4	418	<LOD	/	/	42.3	51.5	<LOD
Lenwade	24/04/2007	10.00	11.1	4.7	378	<LOD	/	/	40.0	49.4	<LOD

Attlebridge	24/04/2007	10.10	11.2	4.7	348	<LOD	/	/	39.5	47.7	<LOD

Wensum lower river temporal samples 19-24/04/2007 continued.

Sampling location	Date	Time	Na mg/L	K mg/L	Mg mg/L	Ca mg/L	Si mg /L	Sr mg/L	Fe µg/L	Al µg/L	Zn µg/L	Mn µg/L	Cu µg/L	B µg/L	HCO_3^- mg /L
Swanton GS	19/04/2007	8.20	29.5	4.7	3.7	122	0.6	/	0.2	<LOD	0.6	0.11	0.29	0.92	329
Mill Street	19/04/2007	8.45	26.5	3.7	3.7	119	0.7	/	0.3	<LOD	0.5	0.08	0.26	0.62	318
Lyng	19/04/2007	9.00	27.1	4.3	3.8	119	0.6	/	2.2	<LOD	0.7	0.09	0.54	2.88	324
Lenwade	19/04/2007	9.25	25.9	3.6	3.7	114	0.7	/	0.3	<LOD	0.6	0.09	0.27	0.45	329
Attlebridge	19/04/2007	9.40	27.1	3.5	3.9	115	0.7	/	0.4	<LOD	0.4	0.13	0.29	0.60	313
Swanton GS	19/04/2007	10.15	28.0	4.4	3.6	118	0.6	/	0.4	<LOD	0.3	0.12	0.26	0.29	/
Mill Street	19/04/2007	10.25	27.1	3.6	3.7	121	0.6	/	0.5	1.0	0.9	0.09	0.32	1.57	/
Lyng	19/04/2007	10.40	27.0	4.0	3.7	119	0.7	/	0.2	<LOD	0.8	0.08	0.20	1.39	/
Lenwade	19/04/2007	10.55	25.9	3.7	3.7	116	0.6	/	0.5	<LOD	0.3	0.10	0.22	0.26	/
Attlebridge	19/04/2007	11.05	27.7	3.7	4.0	117	0.7	/	0.4	<LOD	<LOD	0.13	0.20	0.19	/
Swanton GS	20/04/2007	9.20	/	/	/	/	/	/	/	/	/	/	/	/	/
Mill Street	20/04/2007	9.30	27.8	3.6	3.8	122	0.6	/	<LOD	<LOD	0.6	0.08	0.31	0.51	307
Lyng	20/04/2007	9.45	28.2	4.2	3.8	120	0.6	/	<LOD	<LOD	0.6	0.09	0.18	0.68	313
Lenwade	20/04/2007	10.02	26.5	3.9	3.7	114	0.6	/	<LOD	<LOD	0.5	0.08	0.21	0.44	302
Attlebridge	20/04/2007	10.15	28.3	3.7	3.9	116	0.7	/	<LOD	<LOD	0.4	0.13	0.21	0.48	329
Swanton GS	20/04/2007	10.35	28.0	4.0	3.6	117	0.6	/	0.6	<LOD	0.8	0.16	0.25	1.19	/
Mill Street	20/04/2007	10.50	27.3	3.6	3.6	117	0.6	/	<LOD	<LOD	0.8	0.07	0.18	1.36	/
Lyng	20/04/2007	11.00	28.0	4.0	3.7	120	0.6	/	<LOD	<LOD	0.9	0.08	0.17	0.64	/
Lenwade	20/04/2007	11.10	26.1	3.8	3.6	112	0.6	/	0.6	<LOD	0.9	0.11	0.20	0.63	/
Attlebridge	20/04/2007	11.25	28.2	3.7	3.9	113	0.6	/	0.6	<LOD	0.9	0.13	0.27	1.62	/
Swanton GS	21/04/2007	10.00	27.7	4.0	3.5	114	0.6	/	<LOD	<LOD	0.7	0.16	0.18	0.44	297
Mill Street	21/04/2007	10.15	27.2	3.8	3.6	115	0.5	/	<LOD	<LOD	0.5	0.08	0.26	0.92	318
Lyng	21/04/2007	10.25	27.4	4.0	3.6	115	0.5	/	<LOD	<LOD	0.6	0.09	0.22	0.76	307
Lenwade	21/04/2007	10.50	27.3	3.9	3.8	115	0.6	/	<LOD	0.7	0.6	0.10	0.26	0.69	335
Attlebridge	21/04/2007	11.05	30.0	3.8	4.1	118	0.6	/	<LOD	<LOD	0.6	0.14	0.30	0.42	313
Swanton GS	21/04/2007	11.25	28.1	3.7	3.6	116	0.6	/	<LOD	<LOD	0.9	0.15	0.10	0.62	/
Mill Street	21/04/2007	11.40	28.7	4.3	3.7	118	0.5	/	<LOD	<LOD	0.9	0.07	0.12	0.78	/
Lyng	21/04/2007	11.50	30.1	4.2	4.0	125	0.6	/	<LOD	<LOD	0.8	0.09	0.10	0.74	/

Lenwade	21/04/2007	12.05	27.4	3.9	3.8	115	0.6	/	<LOD	<LOD	0.9	0.09	0.13	1.24	/
Attlebridge	21/04/2007	12.15	30.8	3.9	4.1	119	0.8	/	<LOD	<LOD	0.8	0.13	0.09	0.66	/
Swanton GS	22/04/2007	8.30	30.7	4.3	3.8	122	0.6	/	0.8	<LOD	0.6	0.17	0.28	0.45	302
Mill Street	22/04/2007	8.45	28.9	3.7	3.8	122	0.6	/	<LOD	<LOD	0.6	0.07	0.16	0.70	297
Lyng	22/04/2007	9.00	29.8	4.3	3.8	120	0.5	/	0.6	<LOD	0.5	0.09	0.23	1.84	313
Lenwade	22/04/2007	9.20	26.9	4.3	3.7	113	0.6	/	<LOD	<LOD	0.5	0.08	0.15	0.47	297
Attlebridge	22/04/2007	9.35	28.5	4.0	4.0	116	0.6	/	<LOD	<LOD	0.3	0.12	0.27	0.46	307
Swanton GS	22/04/2007	9.55	29.7	4.1	3.7	119	0.5	/	<LOD	<LOD	0.5	0.16	0.26	0.27	/
Mill Street	22/04/2007	10.05	27.6	3.6	3.6	116	0.5	/	<LOD	<LOD	0.3	0.07	0.28	0.28	/
Lyng	22/04/2007	10.15	29.3	4.2	3.8	119	0.5	/	<LOD	<LOD	<LOD	0.08	0.23	0.23	/
Lenwade	22/04/2007	10.30	28.0	4.4	3.8	116	0.6	/	<LOD	<LOD	0.3	0.09	0.18	0.51	/
Attlebridge	22/04/2007	10.40	31.8	4.6	4.4	125	0.6	/	<LOD	<LOD	0.3	0.13	0.20	0.47	/
Swanton GS	23/04/2007	8.20	33.0	5.1	4.2	133	0.6	/	<LOD	<LOD	0.3	0.19	0.25	0.29	307
Mill Street	23/04/2007	8.40	27.2	3.5	3.6	117	0.5	/	<LOD	<LOD	<LOD	0.07	0.18	0.29	313
Lyng	23/04/2007	8.55	29.0	4.1	3.7	116	0.5	/	<LOD	<LOD	0.3	0.08	0.23	0.31	318
Lenwade	23/04/2007	9.15	29.0	4.2	3.9	117	0.6	/	1.6	<LOD	0.3	0.09	0.24	0.28	302
Attlebridge	23/04/2007	9.30	29.9	3.8	4.1	120	0.6	/	<LOD	<LOD	<LOD	0.12	0.20	0.36	297
Swanton GS	23/04/2007	9.50	28.6	4.2	3.7	118	0.5	/	<LOD	<LOD	0.3	0.17	0.27	0.39	/
Mill Street	23/04/2007	10.05	27.8	3.5	3.7	118	0.5	/	<LOD	<LOD	<LOD	0.06	0.16	0.32	/
Lyng	23/04/2007	10.15	29.4	4.1	3.8	118	0.5	/	0.6	<LOD	0.4	0.08	0.36	0.34	/
Lenwade	23/04/2007	10.30	28.6	4.2	3.9	117	0.6	/	<LOD	<LOD	0.4	0.09	0.22	0.37	/
Attlebridge	23/04/2007	10.40	30.7	4.4	4.1	119	0.6	/	<LOD	<LOD	0.6	0.12	0.21	0.39	/
Swanton GS	24/04/2007	8.05	28.9	4.6	3.8	122	0.5	/	<LOD	<LOD	<LOD	0.15	0.18	0.41	291
Mill Street	24/04/2007	8.20	27.4	3.6	3.8	120	0.5	/	<LOD	1.6	0.6	0.08	0.23	0.80	318
Lyng	24/04/2007	8.35	29.5	4.5	3.9	122	0.5	/	<LOD	<LOD	0.8	0.08	0.38	0.61	324
Lenwade	24/04/2007	8.50	27.3	3.9	3.8	115	0.6	/	<LOD	<LOD	0.2	0.09	0.24	0.32	286
Attlebridge	24/04/2007	9.05	30.4	3.6	4.2	123	0.7	/	<LOD	1.1	0.7	0.14	0.38	0.58	340
Swanton GS	24/04/2007	9.30	28.0	4.2	3.7	118	0.5	/	<LOD	<LOD	0.3	0.16	0.18	0.29	/
Mill Street	24/04/2007	9.40	26.7	3.4	3.6	117	0.5	/	<LOD	<LOD	<LOD	0.07	0.21	0.39	/
Lyng	24/04/2007	9.50	28.3	4.0	3.7	118	0.5	/	<LOD	<LOD	1.4	0.08	0.80	1.14	/
Lenwade	24/04/2007	10.00	27.2	3.9	3.7	113	0.6	/	<LOD	<LOD	0.9	0.09	0.16	0.55	/
Attlebridge	24/04/2007	10.10	29.0	3.6	4.0	116	0.7	/	<LOD	<LOD	<LOD	0.12	0.18	0.30	/

Wensum lower river temporal samples 18-19/07/2007

Sampling location	Date	Time	$\delta^{15}N_{NO3}$ ‰ AIR	$\delta^{18}O_{NO3}$ ‰ VSMOW	NO_3^- µM	NO_2^- µM	NH_4^+ µM	DON µM	Cl^- mg/L	SO_4^{2-} mg/L	PO_4^{3-} mg/L
Swanton GS	18/07/2007	15:00	10.3	5.4	338	5.7	<LOD	/	34.7	27.3	<LOD
Mill Street	18/07/2007	15:20	10.6	5.0	326	4.6	<LOD	/	34.1	22.2	<LOD
Lyng	18/07/2007	15:50	10.7	5.3	312	5.1	<LOD	/	33.9	23.6	<LOD
Lenwade	18/07/2007	16:10	10.6	5.3	310	5.2	<LOD	/	34.4	24.6	<LOD
Attlebridge	18/07/2007	16:20	10.5	5.3	334	3.3	1.9	/	37.3	35.2	<LOD
Swanton weir	18/07/2007	16:40	10.4	5.5	317	4.9	2.4	/	33.9	24.3	<LOD
Mill Street	18/07/2007	16:55	10.7	4.9	340	9.3	<LOD	/	35.1	24.4	<LOD
Lyng	18/07/2007	17:00	10.5	5.3	315	3.5	<LOD	/	33.3	30.0	<LOD
Lenwade	18/07/2007	17:10	10.5	5.5	309	2.8	<LOD	/	33.8	28.2	<LOD
Attlebridge	18/07/2007	17:20	10.5	4.9	321	3.9	<LOD	/	36.5	25.0	<LOD
Swanton GS	19/07/2007	10:05	10.8	5.0	339	8.0	1.9	/	35.6	33.8	<LOD
Mill Street	20/07/2007	10:30	10.8	5.2	324	2.1	<LOD	/	35.1	22.5	<LOD
Lyng	21/07/2007	10:50	10.7	5.3	318	6.4	<LOD	/	34.0	24.8	<LOD
Lenwade	22/07/2007	11:05	10.7	5.4	319	2.7	2.8	/	34.3	30.8	<LOD
Attlebridge	23/07/2007	11:20	10.4	4.6	315	6.0	1.5	/	36.7	25.3	<LOD
Swanton GS	24/07/2007	11:40	10.8	5.1	327	3.3	<LOD	/	36.2	23.5	<LOD
Mill Street	25/07/2007	11:50	10.8	5.4	337	4.5	<LOD	/	35.6	23.9	<LOD
Lyng	26/07/2007	12:00	10.7	5.3	327		1.3	/	34.6	30.1	<LOD
Lenwade	27/07/2007	12:15	10.9	5.7	318	2.5	2.4	/	34.3	32.3	<LOD
Attlebridge	28/07/2007	12:25	10.7	5.1	318	2.2	1.4	/	35.9	30.9	<LOD

Wensum lower river temporal samples 18-19/07/2007 continued.

Sampling location	Date	Time	Na mg/L	K mg/L	Mg mg/L	Ca mg/L	Si mg /L	Sr mg/L	Fe µg/L	Al µg/L	Zn µg/L	Mn µg/L	Cu µg/L	B µg/L	HCO_3^- mg /L
Swanton GS	18/07/2007	15:00	22.0	3.7	3.2	116	3.8	/	1.2	0.9	0.6	0.16	<LOD	1.13	/
Mill Street	18/07/2007	15:20	20.6	3.3	3.0	108	3.6	/	1.1	0.9	0.7	0.13	<LOD	0.61	/
Lyng	18/07/2007	15:50	20.5	3.4	3.1	105	4.1	/	1.2	0.9	1.0	0.08	<LOD	0.55	/
Lenwade	18/07/2007	16:10	22.9	3.9	3.3	117	3.9	/	1.4	0.9	0.5	0.13	<LOD	0.53	/
Attlebridge	18/07/2007	16:20	22.7	3.6	3.5	114	4.3	/	1.6	1.0	0.6	0.36	<LOD	1.38	/
Swanton weir	18/07/2007	16:40	21.9	3.6	3.2	112	3.8	/	1.3	0.9	0.9	0.11	<LOD	0.75	/
Mill Street	18/07/2007	16:55	22.2	3.4	3.2	115	4.0	/	1.5	1.1	0.6	0.11	<LOD	0.70	/
Lyng	18/07/2007	17:00	22.5	3.7	3.3	115	3.9	/	1.3	1.0	0.7	0.10	<LOD	0.66	/
Lenwade	18/07/2007	17:10	21.6	3.5	3.2	112	3.9	/	1.3	0.9	0.7	0.13	<LOD	0.64	/
Attlebridge	18/07/2007	17:20	24.2	3.8	3.6	121	4.2	/	4.5	1.1	0.6	0.15	<LOD	0.51	/
Swanton GS	19/07/2007	10:05	/	/	/	/	/	/	/	/	/	/	/	/	/
Mill Street	20/07/2007	10:30	22.9	3.7	3.4	125	4.1	/	1.4	0.9	1.6	0.18	<LOD	0.47	/
Lyng	21/07/2007	10:50	21.9	3.7	3.3	119	3.9	/	1.4	0.9	0.3	0.13	<LOD	0.47	/
Lenwade	22/07/2007	11:05	22.0	3.7	3.3	115	3.9	/	1.3	1.1	0.5	0.14	<LOD	0.45	/
Attlebridge	23/07/2007	11:20	24.0	3.7	3.5	117	4.1	/	1.5	1.2	0.7	0.19	<LOD	0.46	/
Swanton GS	24/07/2007	11:40	23.7	3.6	3.5	126	4.0	/	2.0	1.0	0.6	0.26	<LOD	0.44	/
Mill Street	25/07/2007	11:50	24.7	4.6	3.3	122	3.9	/	2.2	1.1	0.8	0.22	<LOD	0.64	/
Lyng	26/07/2007	12:00	22.1	3.7	3.3	119	4.0	/	1.4	1.0	1.1	0.15	<LOD	0.47	/
Lenwade	27/07/2007	12:15	21.8	3.7	3.3	115	3.8	/	1.3	0.9	0.3	0.15	<LOD	0.44	/
Attlebridge	28/07/2007	12:25	23.2	3.8	3.5	117	4.0	/	1.4	1.0	0.6	0.19	<LOD	0.42	/

Wensum mid river gauging station temporal samples 12-13/12/2008

Sampling location	Date	time	$\delta^{15}N_{NO3}$ ‰ AIR	$\delta^{18}O_{NO3}$ ‰ VSMOW	NO_3^- µM	NO_2^- µM	NH_4^+ µM	DON µM	Cl^- mg/L	SO_4^{2-} mg/L	PO_4^{3-} mg/L
Fakenham GS	12/12/2008	19:30	8.3	3.5	665	1.6	/	/	36.5	33.8	0.02
Fakenham GS	12/12/2008	20:30	8.2	3.4	667	/	/	/	/	/	/
Fakenham GS	12/12/2008	21:30	8.5	3.2	670	1.1	/	/	36.5	34.2	0.08
Fakenham GS	12/12/2008	22:30	8.3	3.3	671	/	/	/	/	/	/
Fakenham GS	12/12/2008	23:30	8.1	3.3	672	1.0	/	/	36.3	34.3	0.07
Fakenham GS	13/12/2008	00:30	8.3	3.2	675	/	/	/	/	/	/
Fakenham GS	13/12/2008	01:30	8.3	3.3	677	1.1	/	/	36.6	34.5	0.07
Fakenham GS	13/12/2008	02:30	8.3	3.2	677	/	/	/	/	/	/
Fakenham GS	13/12/2008	03:30	8.3	3.2	677	1.0	/	/	36.5	34.4	0.05
Fakenham GS	13/12/2008	04:30	8.1	3.4	680	/	/	/	/	/	/
Fakenham GS	13/12/2008	05:30	8.3	3.4	683	1.1	/	/	36.6	34.5	0.04
Fakenham GS	13/12/2008	06:30	8.3	3.3	682	/	/	/	/	/	/
Fakenham GS	13/12/2008	07:30	8.3	3.3	682	1.1	/	/	36.9	34.5	0.03
Fakenham GS	13/12/2008	08:30	8.3	3.4	681	/	/	/	/	/	/
Fakenham GS	13/12/2008	09:30	8.3	3.3	680	1.1	/	/	36.7	34.5	0.06
Fakenham GS	13/12/2008	10:30	8.3	3.4	680	/	/	/	/	/	/
Fakenham GS	13/12/2008	11:30	8.2	3.2	680	1.1	/	/	36.9	34.6	0.08
Fakenham GS	13/12/2008	12:30	8.4	3.2	679	/	/	/	/	/	/
Fakenham GS	13/12/2008	13:30	8.2	3.4	679	1.2	/	/	37.1	34.5	0.06
Fakenham GS	13/12/2008	14:30	8.1	3.3	680	/	/	/	/	/	/
Fakenham GS	13/12/2008	15:30	8.2	3.4	681	1.2	/	/	37.4	34.4	0.03
Fakenham GS	13/12/2008	16:30	8.2	3.5	676	/	/	/	/	/	/
Fakenham GS	13/12/2008	17:30	8.3	3.3	671	1.3	/	/	40.1	34.3	0.04
Fakenham GS	13/12/2008	18:30	8.4	3.3	671	/	/	/	/	/	/
Swanton GS	12/12/2008	20:15	10.1	4.1	461	2.6	/	/	44.1	39.5	<LOD
Swanton GS	12/12/2008	21:15	9.8	3.7	464	/	/	/	/	/	/
Swanton GS	12/12/2008	22:15	9.8	4.2	466	1.6	/	/	43.1	39.8	<LOD
Swanton GS	12/12/2008	23:15	9.3	4.3	473	/	/	/	/	/	/

Swanton GS	13/12/2008	00:15	9.6	4.1	480	2.3	/	/	42.5	40.1	0.04
Swanton GS	13/12/2008	01:15	9.7	4.3	483	/	/	/	/	/	/
Swanton GS	13/12/2008	02:15	9.5	4.4	485	2.2	/	/	42.5	40.6	<LOD
Swanton GS	13/12/2008	03:15	10.0	4.1	488	/	/	/	/	/	/
Swanton GS	13/12/2008	04:15	9.4	4.6	490	1.9	/	/	42.4	41.0	<LOD
Swanton GS	13/12/2008	05:15	10.0	4.0	492	/	/	/	/	/	/
Swanton GS	13/12/2008	06:15	9.5	3.9	494	0.3	/	/	42.2	41.2	<LOD
Swanton GS	13/12/2008	07:15	9.7	4.5	495	/	/	/	/	/	/
Swanton GS	13/12/2008	08:15	10.0	4.1	495	2.3	/	/	42.1	41.0	<LOD
Swanton GS	13/12/2008	09:15	9.3	4.6	497	/	/	/	/	/	/
Swanton GS	13/12/2008	10:15	9.6	4.3	499	2.2	/	/	41.6	41.2	0.03
Swanton GS	13/12/2008	11:15	10.2	4.1	499	/	/	/	/	/	/
Swanton GS	13/12/2008	12:15	10.1	4.1	499	2.2	/	/	41.6	41.4	0.05
Swanton GS	13/12/2008	13:15	9.8	4.1	499	/	/	/	/	/	/
Swanton GS	13/12/2008	14:15	10.4	4.1	499	2.3	/	/	41.8	41.4	0.04
Swanton GS	13/12/2008	15:15	10.0	3.7	499	/	/	/	/	/	/
Swanton GS	13/12/2008	16:15	10.1	4.1	498	2.0	/	/	41.6	41.3	0.03
Swanton GS	13/12/2008	17:15	10.2	4.1	498	/	/	/	/	/	/
Swanton GS	13/12/2008	18:15	10.3	4.2	498	2.0	/	/	42.0	41.2	<LOD
Swanton GS	13/12/2008	19:15	10.1	4.2	498	/	/	/	/	/	/

Wensum mid river gauging station temporal samples 12-13/12/2008 continued.

Sampling location	Date	time	Na mg/L	K mg/L	Mg mg/L	Ca mg/L	Si mg /L	Sr mg/L	Fe µg/L	Al µg/L	Zn µg/L	Mn µg/L	Cu µg/L	B µg/L	HCO_3^- mg /L
Fakenham GS	12/12/2008	19:30	18.2	1.5	2.7	127	1.6	0.26	<LOD	<LOD	0.6	0.22	0.06	0.26	/
Fakenham GS	12/12/2008	20:30	/	/	/	/	/	/	/	/	/	/	/	/	/
Fakenham GS	12/12/2008	21:30	18.3	1.5	2.6	126	1.6	0.26	1.8	1.5	0.5	0.18	0.07	0.20	/
Fakenham GS	12/12/2008	22:30	/	/	/	/	/	/	/	/	/	/	/	/	/
Fakenham GS	12/12/2008	23:30	18.1	1.5	2.6	127	1.6	0.26	0.6		0.5	0.13	0.04	0.19	/
Fakenham GS	13/12/2008	00:30	/	/	/	/	/	/	/	/	/	/	/	/	/
Fakenham GS	13/12/2008	01:30	18.4	1.6	2.7	129	1.6	0.26	2.6	1.4	0.5	0.15	0.07	0.23	/
Fakenham GS	13/12/2008	02:30	/	/	/	/	/	/	/	/	/	/	/	/	/

Fakenham GS	13/12/2008	03:30	18.7	1.6	2.7	129	1.6	0.27	6.9	0.9	0.8	0.20	0.07	0.26	/
Fakenham GS	13/12/2008	04:30	/	/	/	/	/	/	/	/	/	/	/	/	/
Fakenham GS	13/12/2008	05:30	19.0	1.5	2.7	131	1.6	0.27	<LOD	<LOD	<LOD	0.12	0.02	0.25	/
Fakenham GS	13/12/2008	06:30	/	/	/	/	/	/	/	/	/	/	/	/	/
Fakenham GS	13/12/2008	07:30	18.9	1.5	2.7	131	1.6	0.27	<LOD	<LOD	<LOD	0.12	0.04	0.26	/
Fakenham GS	13/12/2008	08:30	/	/	/	/	/	/	/	/	/	/	/	/	/
Fakenham GS	13/12/2008	09:30	18.6	1.5	2.7	130	1.6	0.27			0.4	0.11	0.03	0.19	/
Fakenham GS	13/12/2008	10:30	/	/	/	/	/	/	/	/	/	/	/	/	/
Fakenham GS	13/12/2008	11:30	18.6	1.5	2.6	128	1.6	0.27	<LOD	<LOD	<LOD	0.11	<LOD	0.21	/
Fakenham GS	13/12/2008	12:30	/	/	/	/	/	/	/	/	/	/	/	/	/
Fakenham GS	13/12/2008	13:30	18.9	1.5	2.7	129	1.6	0.27	<LOD	<LOD	0.5	0.12	0.13	0.25	/
Fakenham GS	13/12/2008	14:30	/	/	/	/	/	/	/	/	/	/	/	/	/
Fakenham GS	13/12/2008	15:30	18.7	1.5	2.6	128	1.6	0.27	<LOD	<LOD	<LOD	0.13	0.06	0.31	/
Fakenham GS	13/12/2008	16:30	/	/	/	/	/	/	/	/	/	/	/	/	/
Fakenham GS	13/12/2008	17:30	21.4	1.5	2.7	130	1.6	0.27	<LOD	<LOD	0.3	0.13	0.07	0.30	/
Fakenham GS	13/12/2008	18:30	/	/	/	/	/	/	/	/	/	/	/	/	/
Swanton GS	12/12/2008	20:15	26.0	2.7	3.5	123	1.7	0.28			0.4	0.18	0.11	0.45	/
Swanton GS	12/12/2008	21:15	/	/	/	/	/	/	/	/	/	/	/	/	/
Swanton GS	12/12/2008	22:15	24.9	2.5	3.3	121	1.6	0.28	<LOD	<LOD	<LOD	0.15	0.03	0.34	/
Swanton GS	12/12/2008	23:15	/	/	/	/	/	/	/	/	/	/	/	/	/
Swanton GS	13/12/2008	00:15	24.6	2.4	3.3	121	1.6	0.28	<LOD	<LOD	0.4	0.14	0.06	0.28	/
Swanton GS	13/12/2008	01:15	/	/	/	/	/	/	/	/	/	/	/	/	/
Swanton GS	13/12/2008	02:15	25.1	2.5	3.4	123	1.7	0.28	<LOD	<LOD	<LOD	0.14	0.03	0.28	/
Swanton GS	13/12/2008	03:15	/	/	/	/	/	/	/	/	/	/	/	/	/
Swanton GS	13/12/2008	04:15	25.0	2.5	3.4	124	1.7	0.28	<LOD	<LOD	<LOD	0.14	0.02	0.32	/
Swanton GS	13/12/2008	05:15	/	/	/	/	/	/	/	/	/	/	/	/	/
Swanton GS	13/12/2008	06:15	25.5	2.6	3.5	127	1.7	0.29	<LOD	<LOD	<LOD	0.14	0.08	0.40	/
Swanton GS	13/12/2008	07:15	/	/	/	/	/	/	/	/	/	/	/	/	/
Swanton GS	13/12/2008	08:15	24.2	2.5	3.3	123	1.7	0.28	<LOD	<LOD	0.3	0.14	0.07	0.40	/
Swanton GS	13/12/2008	09:15	/	/	/	/	/	/	/	/	/	/	/	/	/
Swanton GS	13/12/2008	10:15	24.5	2.5	3.4	124	1.7	0.28				0.13	0.04	0.34	/
Swanton GS	13/12/2008	11:15	/	/	/	/	/	/	/	/	/	/	/	/	/
Swanton GS	13/12/2008	12:15	25.0	2.8	3.4	126	1.7	0.29	<LOD	<LOD	<LOD	0.14	0.05	0.36	/

Swanton GS	13/12/2008	13:15	/	/	/	/	/	/	/	/	/	/	/	/	/
Swanton GS	13/12/2008	14:15	25.1	3.4	3.5	125	1.7	0.29	<LOD	<LOD	<LOD	0.15	0.04	0.33	/
Swanton GS	13/12/2008	15:15	/	/	/	/	/	/	/	/	/	/	/	/	/
Swanton GS	13/12/2008	16:15	18.7	1.5	2.6	128	1.6	0.27	<LOD	<LOD	0.5	0.13	0.06	0.31	/
Swanton GS	13/12/2008	17:15	/	/	/	/	/	/	/	/	/	/	/	/	/
Swanton GS	13/12/2008	18:15	25.4	3.3	3.5	127	1.8	0.29	<LOD	<LOD	<LOD	0.14	0.06	0.45	/
Swanton GS	13/12/2008	19:15	/	/	/	/	/	/	/	/	/	/	/	/	/

A 2.5 Wensum Chalk Borehole Sample Data:

Wensum Chalk boreholes

	$\delta^{15}N_{NO3}$ ‰ AIR	$\delta^{18}O_{NO3}$ ‰ VSMOW	NO_3^- µM	NO_2^- µM	NH_4^+ µM	DON µM	Cl^- mg/L	SO_4^{2-} mg/L	PO_4^{3-} mg/L
Hamrow west	8.27	29.68	<LOD	<LOD	<LOD	<LOD	17.8	8.1	<LOD
Hamrow east	2.46	13.83	<LOD	<LOD	<LOD	<LOD	17.0	7.7	<LOD
Wellingham	<LOD	<LOD	<LOD	<LOD	<LOD	<LOD	16.5	11.8	<LOD
Great Ryburgh A	8.34	24.05	<LOD	<LOD	<LOD	<LOD	36.2	75.8	<LOD
Great Ryburgh B	<LOD	<LOD	<LOD	<LOD	<LOD	<LOD	36.9	74.3	<LOD
Bylaugh A	5.77	1.23	1011	<LOD	<LOD	<LOD	40.0	44.3	<LOD
Bylaugh B	5.84	1.31	1027	<LOD	<LOD	16	41.2	46.3	<LOD
Cawston	5.37	8.22	0.50	<LOD	<LOD	<LOD	26.6	26.9	<LOD
Weston Longville	9.23	3.27	1314	<LOD	<LOD	16	40.1	66.9	<LOD
Taverham	5.39	29.95	0.50	<LOD	<LOD	<LOD	26.6	46.2	<LOD
Hellesdon	7.19	0.82	874	<LOD	<LOD	13	59.9	77.7	<LOD
Costessey west	6.16	0.31	786	<LOD	<LOD	<LOD	72.9	59.2	<LOD
Costessey east	6.10	0.26	823	<LOD	<LOD	<LOD	74.9	60.8	<LOD

Wensum Chalk boreholes

	Na mg/L	K mg/L	Mg mg/L	Ca mg/L	Si mg /L	Sr mg/L	Fe µg/L	Al µg/L	Zn µg/L	Mn µg/L	Cu µg/L	B µg/L	HCO_3^- mg /L
Hamrow west	12.4	0.6	2.1	101	2.35	0.24	5.81	0.83	1.58	0.52	0.08	0.31	327
Hamrow east	12.0	0.6	2.3	105	2.58	0.25	0.85	0.82	0.71	0.65	0.10	1.08	347
Wellingham	11.1	0.5	3.1	96	2.10	0.26	<LOD	0.71	0.37	0.45	0.02	0.26	308
Great Ryburgh A	18.0	1.5	4.3	124	2.64	0.38	9.72	0.85	0.67	0.65	0.09	0.36	312
Great Ryburgh B	16.9	1.4	4.1	119	2.31	0.40	1.69	0.69	<LOD	0.59	<LOD	0.67	317
Bylaugh A	20.0	2.0	4.8	97	2.82	0.30	<LOD	0.81	3.91	0.08	0.19	0.25	220
Bylaugh B	19.8	1.9	4.8	99	2.58	0.30	<LOD	0.76	3.34	0.08	0.02	0.57	219
Cawston	15.0	0.9	3.8	67	3.08	0.19	0.98	0.75	0.77	0.31	0.05	<LOD	215
Weston Longville	21.8	3.1	4.5	129	2.29	0.32	<LOD	0.80	0.63	0.02	0.04	0.43	286
Taverham	16.2	2.1	4.2	75	2.99	4.04	1.21	0.74	0.25	0.26	<LOD	0.43	220
Hellesdon	40.5	2.9	7.7	109	2.63	1.06	0.62	0.71	0.40	0.02	0.02	0.54	264
Costessey west	46.9	2.5	6.6	107	2.39	0.79	1.11	0.72	0.53	0.02	0.05	0.43	268
Costessey east	49.3	2.6	6.8	113	2.39	0.72	<LOD	0.80	0.30	0.02	<LOD	0.57	293

A 2.6 Wensum Field Parameters:

Parameters of pH, redox potential (Eh mV), % saturation dissolved oxygen (DO %), temperature (T ^oC), and electrical conductivity (EC µS min^{-1}).

Field parameters: Wensum river

14/02/2007	pH	Eh mV	DO %	T ^oC	EC µS min^{-1}
Hamrow	7.9	153	100	8.5	
West Raynham	7.7	147	93	8	
Helhoughton	7.8	167	85	8	
Shereford common					
Fakenham GS	7.9	142	84	7.5	
Fakenham heath					
Pensthorpe					
Great Ryburgh	7.8	171	100	7.75	
Sennowe Bridge					
Guist Bridge					

17/04/2007	pH	Eh mV	DO %	T ^oC	EC µS min^{-1}
Hamrow					
West Raynham					
Helhoughton					
Shereford common					
Fakenham GS	6.7	238	79	12.0	700
Fakenham heath					
Pensthorpe					
Great Ryburgh					
Sennowe Bridge					
Guist Bridge					

Bintree Mill	7.8	164	89	7.5	
County School					
Billingford	8.0	180	84	8	
Burgh Common					
Swanton GS	8.0	163	91	8	
Mill Street					
Lyng					
Lenwade					
Attlebridge					
Costessey GS	8.0	177	88	8	

Bintree Mill					
County School					
Billingford					
Burgh Common					
Swanton GS	6.5	256	85	11.0	800
Mill Street	7.0	236	94	12.0	800
Lyng	7.1	239	100	12.5	800
Lenwade	6.9	230	108	13.0	800
Attlebridge	7.1	233	106	13.0	700
Costessey GS	6.8	230	100	13.5	500

19/04/2007	**pH**	**Eh mV**	**DO %**	**T ^{o}C**	**EC µS min^{-1}**
Hamrow					
West Raynham					
Helhoughton					
Shereford common					
Fakenham GS	6.8	188	93	10.0	800
Fakenham heath					
Pensthorpe					
Great Ryburgh					
Sennowe Bridge					
Guist Bridge					
Bintree Mill					
County School					
Billingford					
Burgh Common					
Swanton GS					
Mill Street	6.6	198	103	11.0	800
Lyng	6.9	201	99	13.0	800
Lenwade	6.8	191	92	12.0	800
Attlebridge	6.9	193	107	12.0	800
Costessey GS					

20/04/2007	**pH**	**Eh mV**	**DO %**	**T ^{o}C**	**EC µS min^{-1}**
Hamrow					
West Raynham					
Helhoughton					
Shereford common					
Fakenham GS	6.7	169	100	11.0	800
Fakenham heath					
Pensthorpe					
Great Ryburgh					
Sennowe Bridge					
Guist Bridge					
Bintree Mill					
County School					
Billingford					
Burgh Common					
Swanton GS					
Mill Street	6.8	182	101	11.0	800
Lyng	6.8	191	98	11.0	800
Lenwade	6.8	186	104	11.5	800
Attlebridge	6.7	191	93	11.5	800
Costessey GS					

21/04/2007	pH	Eh mV	DO %	T °C	EC µS min^{-1}
Hamrow					
West Raynham					
Helhoughton					
Shereford common					
Fakenham GS	6.8	163	95	11.0	800
Fakenham heath					
Pensthorpe					
Great Ryburgh					
Sennowe Bridge					
Guist Bridge					
Bintree Mill					
County School					
Billingford					
Burgh Common					
Swanton GS					
Mill Street	7.1	182	104	12.0	800
Lyng	7.0	191	99	12.0	800
Lenwade	7.2	185	103	12.0	800
Attlebridge	7.1	185	106	12.5	800
Costessey GS					

22/04/2007	pH	Eh mV	DO %	T °C	EC µS min^{-1}
Hamrow					
West Raynham					
Helhoughton					
Shereford common					
Fakenham GS	6.7	182	105	11.5	800
Fakenham heath					
Pensthorpe					
Great Ryburgh					
Sennowe Bridge					
Guist Bridge					
Bintree Mill					
County School					
Billingford					
Burgh Common					
Swanton GS					
Mill Street	7.0	186	100	12.0	800
Lyng	7.0	199	94	12.0	800
Lenwade	6.9	191	95	12.5	800
Attlebridge	6.9	193	102	12.0	800
Costessey GS					

23/04/2007	pH	Eh mV	DO %	T °C	EC µS min^{-1}
Hamrow					
West Raynham					
Helhoughton					
Shereford common					
Fakenham GS	6.9	159.0	91.0	12.0	800
Fakenham heath					
Pensthorpe					
Great Ryburgh					

24/04/2007	pH	Eh mV	DO %	T °C	EC µS min^{-1}
Hamrow					
West Raynham					
Helhoughton					
Shereford common					
Fakenham GS	7.2	161.0	81.0	13.5	800
Fakenham heath					
Pensthorpe					
Great Ryburgh					

Sennowe Bridge					
Guist Bridge					
Bintree Mill					
County School					
Billingford					
Burgh Common					
Swanton GS					
Mill Street	6.9	184.0	105.0	12.5	800
Lyng	6.9	180.0	100.0	12.5	800
Lenwade	6.8	204.0	102.0	12.5	800
Attlebridge	7.1	190.0	100.0	13.0	800
Costessey GS					

Sennowe Bridge					
Guist Bridge					
Bintree Mill					
County School					
Billingford					
Burgh Common					
Swanton GS					
Mill Street	7.0	172.0	96.0	14.0	800
Lyng	7.1	190.0	96.0	14.0	800
Lenwade	7.1	193.0	91.0	14.0	800
Attlebridge	7.1	193.0	91.0	14.0	800
Costessey GS					

18/07/2007	**pH**	**Eh mV**	**DO %**	**T ^{o}C**	**EC µS min^{-1}**
Hamrow	7.5	179	90	15	700
West Raynham				15	700
Helhoughton	7.5	192	98	15	700
Shereford common					
Fakenham GS	7.6	176	98	15	700
Fakenham heath					
Pensthorpe					
Great Ryburgh	7.4	182	94	15	700
Sennowe Bridge					
Guist Bridge					
Bintree Mill	7.6	172	87	15	700
County School					
Billingford	7.5	173	100	15	700
Burgh Common					
Swanton GS	7.6	171	92	15	700
Mill Street	7.5	181	96	15	700
Lyng	7.5	187	90	15	700
Lenwade	7.5	190	99	15	700

19/07/2007	**pH**	**Eh mV**	**DO %**	**T ^{o}C**	**EC µS min^{-1}**
Hamrow					
West Raynham					
Helhoughton					
Shereford common					
Fakenham GS					
Fakenham heath					
Pensthorpe					
Great Ryburgh					
Sennowe Bridge					
Guist Bridge					
Bintree Mill					
County School					
Billingford					
Burgh Common					
Swanton GS	7.4	180	89	15	700
Mill Street	7.3	172	90	15	700
Lyng	7.2	180	96	15	700
Lenwade	7.2	181	93	15	700

Attlebridge	7.6	198	103	15	700
Costessey GS	7.6	172	84	15	700

11/12/2007	pH	Eh mV	DO %	T °C	EC µS min^{-1}
Hamrow					
West Raynham					
Helhoughton					
Shereford common	7.3	127	98	11	600
Fakenham GS	7.5	146	114		500
Fakenham heath					
Pensthorpe					
Great Ryburgh	7.0	176	101	11	700
Sennowe Bridge					
Guist Bridge					
Bintree Mill	7.8	109	112		500
County School					
Billingford					
Burgh Common					
Swanton GS					
Mill Street	7.5	130	112		500
Lyng	7.0	108	114		600
Lenwade	7.5	104	112		600
Attlebridge					
Costessey GS					

Attlebridge	7.4	177	89	15	700
Costessey GS					

06/04/2008	pH	Eh mV	DO %	T °C	EC µS min^{-1}
Hamrow	7.2	200			600
West Raynham	7.3	217			600
Helhoughton	7.3	194			650
Shereford common	7.3	214			600
Fakenham GS	7.3	222			600
Fakenham heath					
Pensthorpe					
Great Ryburgh	7.2	194			600
Sennowe Bridge					
Guist Bridge					
Bintree Mill	6.9	178			600
County School					
Billingford	7.3	194			600
Burgh Common					
Swanton GS	7.0	192			600
Mill Street	7.4	208			600
Lyng	7.2	193			600
Lenwade	7.3	210			600
Attlebridge	7.2	208			600
Costessey GS	7.3	185			600

Field parameters: Wensum tributaries and drains

14/02/2007	pH	Eh mV	DO %	T °C	EC µS min^{-1}
Horningtoft drain	7.2	71	61	7	
East Raynham drain					
Helhoughton drain					
Tat: Tatterford	7.7	170	76	7	
Shereford drain					
Fakenham drain	7.7	157	91	6	
Fakenham heath drain					
The Carr: Langor Bridge					
Meadowcote stream: Stibbard					
Great Ryburgh bridge drain					
Great Ryburgh drain					
Stream: Guist					
Bintree west drain					
Bintree east drain					
Blackwater drain Reed Lane					
Blackwater: East Bilney					
Blackwater: Spong Bridge					
Wendling Beck: Old Brigg					
Wendling drain Rectory Farm					
Wendling drain Gressenhall					
Wendling Beck: Beetley Bridge					
Wendling Beck: Worthing	8.0	169	97	8.2	
Stream: Mill Street	7.5	132	63	6.5	
Stream: Twyford					
Lyng drain					
Lenwade drain					

17-24/04/2007	pH	Eh mV	DO %	T °C	EC µS min^{-1}
Horningtoft drain	6.0	236	48	12.0	650
East Raynham drain					
Helhoughton drain					
Tat: Tatterford					
Shereford drain					
Fakenham drain	6.0	245	93	10.0	700
Fakenham heath drain					
The Carr: Langor Bridge					
Meadowcote stream: Stibbard					
Great Ryburgh bridge drain					
Great Ryburgh drain					
Stream: Guist					
Bintree west drain					
Bintree east drain					
Blackwater drain Reed Lane					
Blackwater: East Bilney					
Blackwater: Spong Bridge					
Wendling Beck: Old Brigg					

Wendling drain Rectory Farm					
Wendling drain Gressenhall					
Wendling Beck: Beetley Bridge					
Wendling Beck: Worthing					
Stream: Mill Street					
Stream: Twyford					
Lyng drain					
Lenwade drain					

18/07/2007	pH	Eh mV	DO %	T ^{o}C	EC µS min^{-1}
Horningtoft drain	7.2	179	83	15	700
East Raynham drain					
Helhoughton drain					
Tat: Tatterford	7.6	174	80	15	700
Shereford drain					
Fakenham drain	7.5	174	88	15	700
Fakenham heath drain					
The Carr: Langor Bridge					
Meadowcote stream: Stibbard					
Great Ryburgh bridge drain					
Great Ryburgh drain					
Stream: Guist					
Bintree west drain					
Bintree east drain					
Blackwater drain Reed Lane					
Blackwater: East Bilney					
Blackwater: Spong Bridge					
Wendling Beck: Old Brigg					
Wendling drain Rectory Farm					
Wendling drain Gressenhall					
Wendling Beck: Beetley Bridge					
Wendling Beck: Worthing	7.5	192	92	15	700
Stream: Mill Street	7.5	176	90	15	700
Stream: Twyford					
Lyng drain					
Lenwade drain					

11/12/2007	pH	Eh mV	DO %	T ^{o}C	EC µS min^{-1}
Horningtoft drain					
East Raynham drain					
Helhoughton drain					
Tat: Tatterford					
Shereford drain	7.4	162	96		800
Fakenham drain	7.0	124	86		800
Fakenham heath drain					
The Carr: Langor Bridge					
Meadowcote stream: Stibbard					
Great Ryburgh bridge drain					
Great Ryburgh drain					

Stream: Guist				
Bintree west drain	7.2	133	118	500
Bintree east drain				
Blackwater drain Reed Lane				
Blackwater: East Bilney				
Blackwater: Spong Bridge				
Wendling Beck: Old Brigg				
Wendling drain Rectory Farm				
Wendling drain Gressenhall				
Wendling Beck: Beetley Bridge				
Wendling Beck: Worthing				
Stream: Mill Street	6.9	112	115	600
Stream: Twyford				
Lyng drain	7.4	104	116	500
Lenwade drain	7.3	112	113	800

06/04/2008	**pH**	**Eh mV**	**DO %**	**T ^{o}C**	**EC µS min^{-1}**
Horningtoft drain	7.1	207			700
East Raynham drain	6.9	191			700
Helhoughton drain	7.3	196			600
Tat: Tatterford	7.3	196			600
Shereford drain	7.3	208			600
Fakenham drain	6.9	189			900
Fakenham heath drain					
The Carr: Langor Bridge					
Meadowcote stream: Stibbard					
Great Ryburgh bridge drain					
Great Ryburgh drain	7.1	183			700
Stream: Guist					
Bintree west drain	7.3	209			500
Bintree east drain					
Blackwater drain Reed Lane					
Blackwater: East Bilney					
Blackwater: Spong Bridge					
Wendling Beck: Old Brigg					
Wendling drain Rectory Farm					
Wendling drain Gressenhall					
Wendling Beck: Beetley Bridge					
Wendling Beck: Worthing	7.3	211			600
Stream: Mill Street	7.5	208			500
Stream: Twyford					
Lyng drain	7.5	200			600
Lenwade drain	7.4	204			600

A 2.7 Wensum Catchment $\delta^{18}O_{H2O}$:

Wensum river

$^{18}O_{H2O}$ ‰ vs. VSMOW	17/04/2007	19/04/2007	24/04/2007	18/07/2007	19/07/2007	11/12/2007	14/09/2008	16/11/2008	25/09/2009
Hamrow				-6.52			-6.4		
West Raynham				-6.82			-6.9		-6.8
Helhoughton				-6.84			-6.9		-6.8
Shereford Common						-6.30			-7.0
Fakenham GS	-7.11			-6.86		-6.48	-7.14	-6.7	-7.2
Fakenham Heath								-6.9	
Pensthorpe									
Great Ryburgh				-7.04		-6.56	-7.14	-6.6	-7.2
Sennowe Bridge								-6.8	
Guist Bridge								-6.8	
Bintree Mill				-7.02		-6.59	-7.1	-6.5	-7.1
County School							-7.1	-6.90	-7.1
Billingford				-7.00			-6.9	-7.03	-7.0
Burgh Common								-6.5	
Swanton GS	-6.86	-7.10	-6.85	-6.84	-6.72		-6.74	-6.6	-6.7
Mill Street	-6.92		-6.87	-6.95	-6.82	-6.49	-6.7	-6.5	-6.6
Lyng	-7.03	-6.81	-6.92	-6.98	-6.89	-6.55	-6.4		-6.8
Lenwade	-6.93		-6.86	-6.93	-6.88	-6.56	-6.5		-6.8
Attlebridge	-6.87	-6.89	-6.75	-6.90	-6.92		-6.6		-6.7
Costessey Mill GS	-7.01			-6.80		-6.59	-6.6		-6.8

Wensum tributaries and drains

$^{18}O_{H2O}$ ‰ vs. VSMOW	17/04/2007	18/07/2007	11/12/2007	06/04/2008	14/09/2008	16/11/2008	25/09/2009
Horningtoft drain	-6.94	-6.67					
East Raynham drain							
Helhoughton drain							
Tat: Tatterford		-7.29					-7.4
Shereford drain			-6.78				
Fakenham drain	-7.44	-7.06	-7.04				
Fakenham Heath drain							
The Carr: Langor							
Meadowcote stream: Stibbard							
Great Ryburgh bridge drain							
Great Ryburgh drain			-6.15				
Stream: Guist							
Guist Carr: Twyford							
Bintree west drain			-6.21				
Bintree east drain							
Blackwater: Reed Lane							
Blackwater: East Bilney							
Blackwater: Spong Bridge							
Wendling Beck: Old Brigg							
Wendling drain: Rectory Farm							
Wendling drain: Gressenhall							
Wendling Beck: Beetley Bridge							
Wendling Beck: Worthing		-6.54		-6.6	-6.30	-6.5	
Stream: Mill Street	-7.13	-6.91	-7.02	-6.5	-6.7		
Lyng drain			-6.03				
Lenwade drain			-6.54				

Wensum Chalk groundwater

$^{18}O_{H2O}$ ‰ vs. VSMOW	
Hamrow west	-7.02
Hamrow east	-7.01
Wellingham	-7.00
Great Ryburgh A	-7.25
Great Ryburgh B	-7.14
Bylaugh A	-7.40
Bylaugh B	-7.29
Cawston	-7.43
Weston Longville	-7.32
Taverham	-7.41
Hellesdon	-7.38
Costessey west	-7.46
Costessey east	-7.36

A 2.8 Wensum Catchment δ^2H_{H2O}:

Wensum river

δ^2H‰ V-SMOW	14/09/2008
Hamrow	-44.3
Fakenham GS	-48.6
Great Ryburgh	-49.4
Bintree Mill	-48.7
Billingford	-48.1
Swanton GS	-47.4
County School	-48.4

Wensum tributaries and drains

δ^2H‰ V-SMOW	14/09/2008
Wendling Beck: Worthing	-45.5

Wensum Chalk groundwater

δ^2H‰ V-SMOW	
Hamrow west	-50.9
Hamrow east	-50.9
Wellingham	-49.9
Great Ryburgh A	-50.9
Great Ryburgh B	-50.6
Bylaugh A	-50.5
Bylaugh B	-51.6
Cawston	-50.8
Weston Longville	-50.8
Taverham	-50.5
Hellesdon	-51.8
Costessey west	-50.4
Costessey east	-51.4

A 2.9 Nitrate Sources:

Ammonium nitrate fertiliser from local suppliers

	$\delta^{15}N_{NO3}$ ‰ vs. AIR	$\delta^{18}O_{NO3}$ ‰ vs. VSMOW
1	4.3	23.3
2	2.6	24.4

Manure

	$\delta^{15}N_{NO3}$ ‰ vs. AIR	$\delta^{18}O_{NO3}$ ‰ vs. VSMOW
Chicken manure	7.0	32.3
Cattle manure	7.3	29.2

Aerosol samples: roof of University of East Anglia School of Environmental Sciences

Date	Filter	$\delta^{15}N_{NO3}$ ‰ vs. AIR	$\delta^{18}O_{NO3}$ ‰ vs. VSMOW
17/07/2008	back up	6.4	71.9
17/07/2008	3	4.0	70.0
18/07/2008	back up	5.7	71.9
18/07/2008	3	3.0	70.2
19/07/2008	back up	6.8	76.7
19/07/2008	3	3.8	67.0
20/07/2008	back up	9.5	70.0
20/07/2008	3	4.3	63.9
21/07/2008	back up	9.4	68.0
21/07/2008	3	5.7	65.5
22/07/2008	back up	0.8	69.2
22/07/2008	3	3.9	67.1
23/07/2008	back up	6.7	82.6
23/07/2008	3	6.3	79.1
23/07/2008	4	4.7	71.3
24/07/2008	back up	4.6	85.3
24/07/2008	3	4.8	82.4
24/07/2008	4	4.9	83.5
25/07/2008	back up	1.5	74.4
25/07/2008	3	-2.4	60.5
25/07/2008	4	0.4	72.5
26/07/2008	back up	-1.9	75.0
26/07/2008	3	-2.0	73.8
26/07/2008	4	-1.8	73.0
27/07/2008	back up	-2.4	76.3
27/07/2008	3	-4.5	78.2
27/07/2008	4	-3.0	76.0

Sewage effluent	Date	Time	$\delta^{15}N_{NO3}$ ‰ vs. AIR	$\delta^{18}O_{NO3}$ ‰ vs. VSMOW	NO_3^- µM	NO_2^- µM	NH_4^+ µM	DON µM	SO_4^{2-} mg/L	Cl^- mg/L	PO_4^{3-} mg/L	$^{18}O_{H2O}$ ‰ vs. VSMOW
Bylaugh	19/07/2007	10:20	10.1	-0.7	1928	41	1	<LOD	96	258	<LOD	-7.2
North Walsham	01/08/2008	14:45	14.0	2.7	1644	34	61	<LOD	94	128	20.4	/

Precipitation		Time	$\delta^{15}N_{NO3}$ ‰ vs. AIR	$\delta^{18}O_{NO3}$ ‰ vs. VSMOW	NO_3^- µM	NO_2^- µM	NH_4^+ µM	DON µM	SO_4^{2-} mg/L	Cl^- mg/L	PO_4^{3-} mg/L	$^{18}O_{H2O}$ ‰ vs. VSMOW
Norwich	16/07/2007	06:00	0.6	58.3	28	0.9	<LOD	<LOD	1.5	1.5	<LOD	-6.4
Norwich	17/07/2007	17:00	0.5	61.0	16	<LOD	0.5	<LOD	1.0	1.2	<LOD	-3.4
Norwich	10/12/2007	16:30	5.3	37.5	14	1.24	21.0	11	1.4	3.9	<LOD	-4.8
Burnham market	06/04/2008 (snow)	06:30	1.8	53.1	10	0.23	25.0	<LOD	3.2	13.4	<LOD	/
Norwich	31/07/2008	17:30	-7.3	66.5	146	2.07	117.2	151	4.3	1.4	0.4	/
Norwich	01/08/2008	06:30	-5.9	66.1	56	1.51	29.9	43	1.9	1.1	<LOD	/

Sewage effluent	Date	Time	Ca mg/L	Na mg/L	Mg mg/L	K mg/L	Si mg /L	Fe µg/L	Al µg/L	Zn µg/L	Mn µg/L	Cu µg/L	B µg/L
Bylaugh	19/07/2007	10:20	123	200	5.7	17.5	7.5	1.1	1.0	0.6	0.16	<LOD	1.53
North Walsham	01/08/2008	14:45	97	85	9.7	15.7	3.0	1.1	0.8	0.3	0.08	0.15	2.28

Precipitation		Time	Ca mg/L	Na mg/L	Mg mg/L	K mg/L	Si mg /L	Fe µg/L	Al µg/L	Zn µg/L	Mn µg/L	Cu µg/L	B µg/L
Norwich	16/07/2007	06:00	1.0	1.2	0.1	0.5	<LOD	<LOD	<LOD	0.6	0.02	<LOD	0.33
Norwich	17/07/2007	17:00	1.4	0.9	0.1	0.3	0.1	0.8	0.9	1.7	0.03	<LOD	1.35
Norwich	10/12/2007	16:30	6.0	2.0	0.1	0.4	<LOD	<LOD	<LOD	<LOD	<LOD	0.07	0.04
Burnham market	06/04/2008 (snow)	06:30	1.0	5.4	0.9	0.2	<LOD	1.0	0.8	0.8	0.05	0.08	<LOD
Norwich	31/07/2008	17:30	5.6	1.9	0.2	1.4	<LOD	0.9	0.7	0.6	0.06	0.15	1.84
Norwich	01/08/2008	06:30	3.6	1.0	0.1	0.5	<LOD	<LOD	<LOD	<LOD	<LOD	<LOD	<LOD

APPENDIX 3 DISCUSSION

A3.1 Predicting $\delta^{18}O_{NO3}$ After Nitrification East Anglian Soils:

Calculation of predicted $\delta^{18}O_{NO3}$ originating from fertiliser and atmospheric sources after nitrification East Anglian soil using a range of $\delta^{18}O_{H2O}$ from local catchment water of $\delta^{18}O_{H2O}$ -7.5 to -6 ‰, and the accepted value for $\delta^{18}O_{O2}$ of air of 23.5‰:

$\delta^{18}O_{NO3} = {}^{2}/_{3} (\delta^{18}O_{H2O}) + {}^{1}/_{3} (\delta^{18}O_{O2})$

Upper limit $= {}^{2}/_{3} (-6.0) + {}^{1}/_{3} (23.5) \quad = \delta^{18}O_{NO3}$ 3.8 ‰

Lower limit $= {}^{2}/_{3} (-7.5) + {}^{1}/_{3} (23.5) = \delta^{18}O_{NO3}$ 2.8 ‰

Range of predicted $\delta^{18}O_{NO3}$ of nitrified ammonium (East Anglia): $\delta^{18}O_{NO3}$ 2.8 to 3.8 ‰

A3.2 Mixing of Interfluve Water With Valley Groundwater:

Calculated effect on nitrate isotopic composition and concentration of mixing three parts of interfluve water with one part valley groundwater:

Interfluve end member mean: $\delta^{15}N_{NO3}$ 5.97 ‰ $\delta^{18}O_{NO3}$ 21.14 ‰ µM NO_3^-, 0.5

Valley groundwater mean: $\delta^{15}N_{NO3}$ 6.72 ‰ $\delta^{18}O_{NO3}$ 1.20 ‰ µM NO_3^-, 972.5

Mixing 3 parts interfluve groundwater to 1 part valley groundwater:

$$\delta_{mixed} = \frac{(C_a \times v_a \times \delta_a) + (C_b \times v_b \times \delta_b)}{(C_a \times v_a) + (C_b \times v_b)}$$

$\delta^{15}N_{NO3\ mixed} = ((0.5 \times 3 \times 5.97)+(972.5 \times 1 \times 6.72))/((0.5 \times 3)+(972.5 \times 1)) = 6.72$ ‰

$\delta^{18}O_{NO3\ mixed} = ((0.5 \times 3 \times 21.14)+(972.5 \times 1 \times 1.20))/((0.5 \times 3)+(972.5 \times 1))=1.23$ ‰

Concentration $NO_3^-{}_{mixed}$ µM $= ((0.5 \times 3)+(972.5 \times 1))/(3+1) = 243.5$ µM NO_3^-

A3.3 Calculated Export of Nitrate, Chloride, and Sulphate (kg/day):

Calculated for each Wensum sampling date:
Example export calculation for NO3-N at Fakenham gauging station on 14/02/2007:

Daily mean flow 1.38 ($m^3 s^{-1}$), nitrate concentration at Fakenham 618 μM NO_3^-
Load NO_3^- in moles per day
= (618/1000000) x (1.38 x 1000 x 60x60x24) = 73685 mol/day
Load NO3-N kg d^{-1} = (34313 x 14.01) / 1000 = 1032 NO3-N kg/day

Daily mean flow ($m^3 s^{-1}$), and export of nitrate-nitrogen, chloride and sulphate (kg d^{-1}) at Fakenham, Swanton and Costessey gauging stations

	Daily mean flow ($m^3 s^{-1}$)	**NO3-N export (kg/day)**	**Cl^- export (kg/day)**	**SO_4^{2-} export (kg/day)**
Fakenham gauging station				
14/02/2007 winter high flow	1.38	1032	4291	3964
17/04/2007 spring low flow	0.66	481	1800	2043
18/07/2007 summer high flow	1.85	1021	5070	4157
06/04/2008 spring high flow	1.72	1332	5416	4882
14/09/2008 autumn low flow	0.57	382	1738	1618
16/11/2008 winter medium flow	0.61	450	1887	1900
12-13/12/2008 winter high flow	1.21	990	3868	3554
27/05/2009 spring low flow	0.66	396	1811	1585
25/09/2009 autumn x low flow	0.19	137	591	559
Swanton gauging station				
14/02/2007 winter high flow	5.46	2921	17503	15927
17/04/2007 spring low flow	2.08	1224	7455	9543
18/07/2007 summer high flow	4.96	2029	14870	11704
06/04/2008 spring medium flow	3.96	2219	12964	13713
14/09/2008 autumn low flow	2.07	857	7871	7947
16/11/2008 winter medium flow	3.12	1624	12131	12131
12-13/12/2008 winter high flow	5.05	2989	18325	17889
27/05/2009 spring low flow	1.99	988	7393	7393
25/09/2009 autumn x low flow	0.88	455	4107	3981
Costessey gauging station				
14/02/2007 winter high flow	8.31	4818	30968	29983
17/04/2007 spring low flow	2.95	1414	10805	13055
18/07/2007 summer high flow	7.27	2534	24327	20835
06/04/2008 spring medium flow	6.22	3388	21300	22894
14/09/2008 autumn low flow	3.64	1538	14022	14557
16/11/2008 winter medium flow	5.34	/	/	/
12-13/12/2008 winter high flow	8.29	/	/	/
27/05/2009 spring low flow	3.24	/	/	/
25/09/2009 autumn x low flow	1.55	684	7688	6908

A3.4 Calculation of $\varepsilon_{P\text{-}S}{}^{15}N_{NO3}$ and $\varepsilon_{P\text{-}S}{}^{18}O_{NO3}$ at Hamrow, Upper Wensum:
With fractionation ratio O:N for 14/09/2008:

The calculation uses the equation (Mariotti, 1988):

$$\varepsilon_{P\text{-}S} = \delta_t - \delta_0 / \ln (Ct/C_0)$$

where δ_t refers to the isotopic composition of the nitrate at time t (after the effects of denitrification, so the measurement at Hamrow on 14/09/2008), δ_0 refers to the initial isotopic composition of the nitrate (before the effects of denitrification, taken as the mean values from the other three sample sets from 14/02/2007, 18/07/2007, and 06/04/2008), C is the concentration of the nitrate at time t (after the effects of denitrification, so the measurement at Hamrow on 14/09/2008), C_0 is the original nitrate concentration (before the effects of denitrification, taken as the mean values from the other three sample sets from 14/02/2007, 18/07/2007, and 06/04/2008).
Table A3.1

Variables:

$\delta^{15}N_{NO3}$ ‰ vs. AIR							
	14/02/2007	18/07/2007	06/04/2008				14/09/2008
Hamrow	10.7	9.9	10.6	mean = $\delta^{15}N_0$ ‰	10.4	$\delta^{15}N_t$ ‰	14.8
$\delta^{18}O_{NO3}$ ‰ vs. VSMOW							
	14/02/2007	18/07/2007	06/04/2008				14/09/2008
Hamrow	5.0	6.4	5.7	mean= $\delta^{18}O_0$ ‰	5.7	$\delta^{18}O_t$ ‰	7.5
NO_3^- µM							
	14/02/07	18/07/07	06/04/08				14/09/08
Hamrow	694	591	640	mean =C_0 µM	642	C_t µM	298

$\varepsilon_{P\text{-}S}{}^{15}N_{NO3}$ = (14.8 -10.4) / ln (298/ 642) = - 5.8 ‰
$\varepsilon_{P\text{-}S}{}^{18}O_{NO3}$ = (7.5 - 5.7) / ln (298/ 642) = - 2.4 ‰
$\varepsilon_{P\text{-}S}{}^{18}O_{NO3}$ / $\varepsilon_{P\text{-}S}{}^{15}N_{NO3}$ = -2.4/ -5.8 = 0.41

A3.5 Upper Wensum Isotope Mass Balance Mixing Model

Model output data for the sample set 06/04/2008 (presented in figure form in Chapter 5), for sampling locations on the upper Wensum using the following mass balance mixing equation:

$$\delta_{mixed} = \frac{(C_a \times v_a \times \delta_a) + (C_b \times v_b \times \delta_b)}{(C_a \times v_a) + (C_b \times v_b)}$$

End member 'a' uses the measured values at Hamrow; end member 'b' uses the measured values from the Tat. For concentration mixing, the equation is used omitting the isotopic variables. Solute concentrations at each location were modelled using the following multiplication factors: West Raynham: 1.1; Helhoughton: 1.01; Shereford Common: 1.09; Fakenham GS: 1.0.

	SO_4^{2-} mg/L		Cl^- mg/L		Na^+ mg/L	
End members	Measured		Measured		Measured	
Tat: Tatterford	28.4		34.5		19.0	
Hamrow	38.7		44.9		23.4	
	SO_4^{2-} mg/L		Cl^- mg/L		Na^+ mg/L	
	Measured	Modelled	Measured	Modelled	Measured	Modelled
West Raynham	38.3	40.1	39.4	46.8	20.1	24.6
Helhoughton	36.7	34.9	36.4	41.0	18.9	21.8
Shereford Common	34.0	33.8	37.3	40.1	19.3	21.6
Fakenham GS	32.9	31.7	36.4	37.9	19.2	20.4
	NO_3^- μM		$\delta^{15}N_{NO3}$ ‰ vs. AIR		$\delta^{18}O_{NO3}$ ‰ vs. VSMOW	
End members	Measured		Measured		Measured	
Tat: Tatterford	636		6.3		2.0	
Hamrow	640		10.6		5.7	
	NO_3^- μM		$\delta^{15}N_{NO3}$ ‰ vs. AIR		$\delta^{18}O_{NO3}$ ‰ vs. VSMOW	
	Measured	Modelled	Measured	Modelled	Measured	Modelled
West Raynham	665	648	9.0	8.9	4.1	4.5
Helhoughton	604	419	9.1	8.9	4.2	4.2
Shereford Common	618	226	7.9	7.7	3.4	3.3
Fakenham GS	587	627	7.8	7.7	3.0	3.2

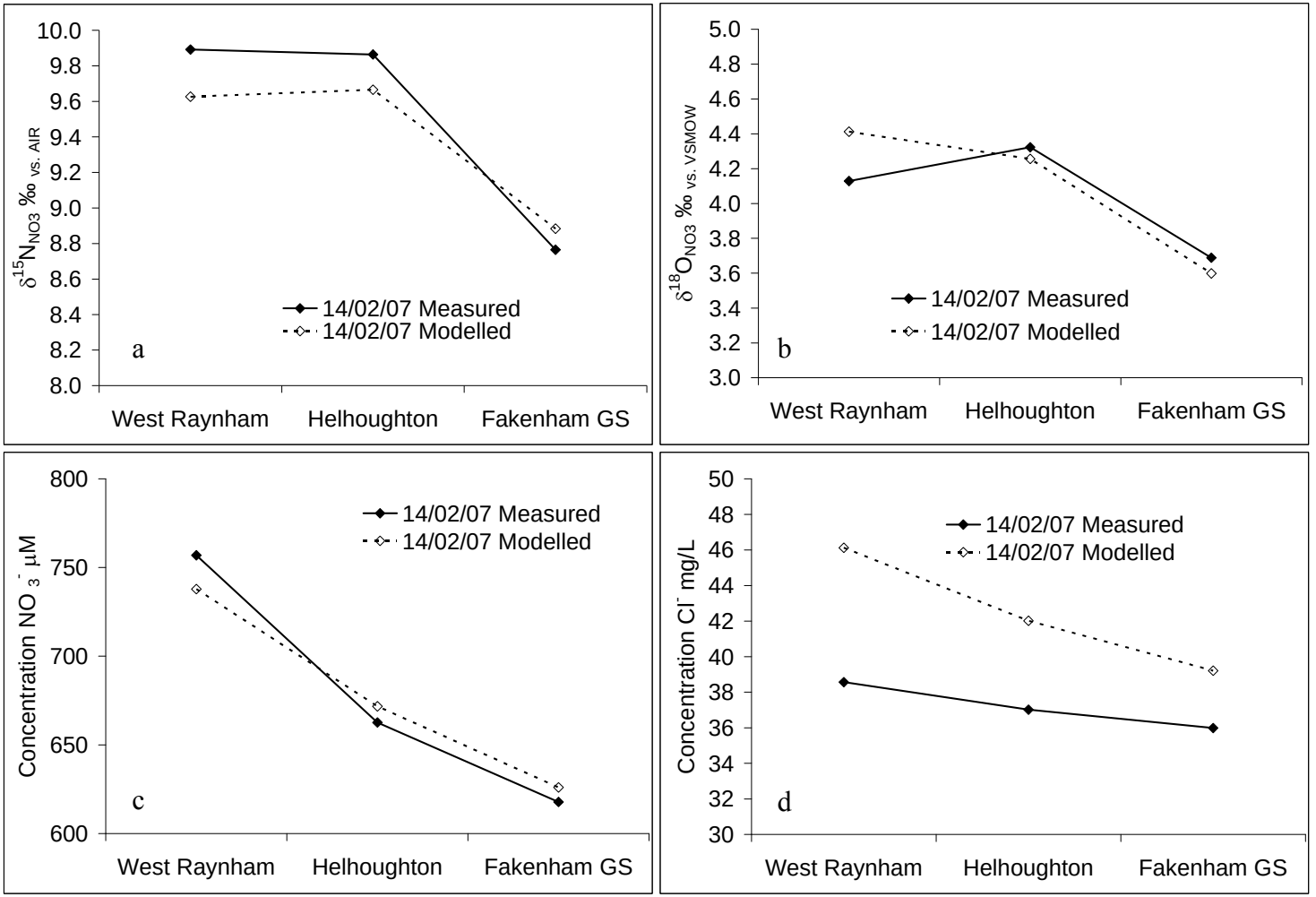

Figure A3.1a-d Model outputs from upper Wensum mixing model for data set A: 14/02/2007 showing measured and modelled values of: a) $\delta^{15}N_{NO3}$ (‰); b) $\delta^{18}O_{NO3}$ (‰); c) concentration NO_3^- (µM); and d) concentration Cl^- (mg/L).

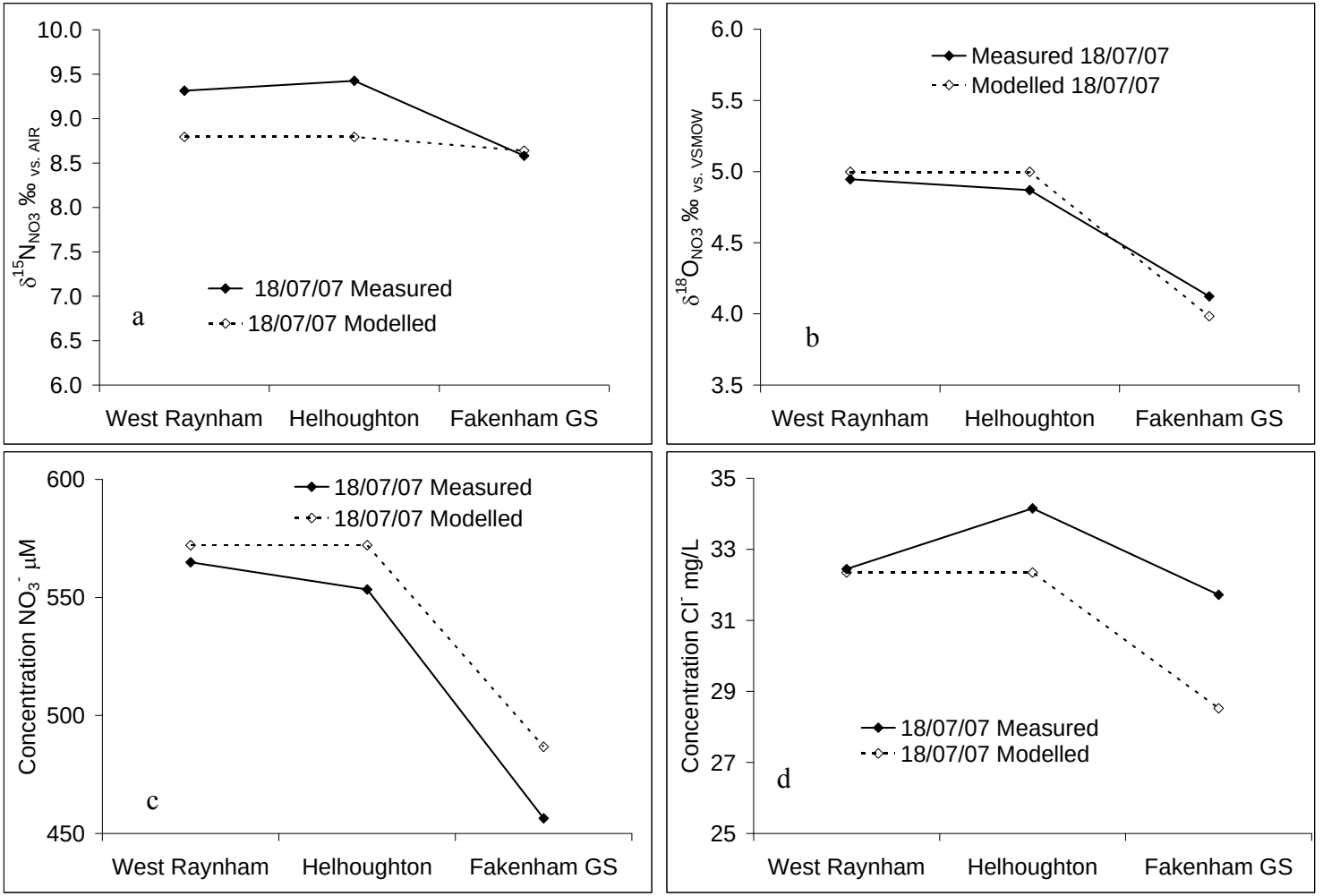

Figure A3.2a-d Model outputs from upper Wensum mixing model for data set B: 18/07/2007 showing measured and modelled values of: a) $\delta^{15}N_{NO3}$ (‰); b) $\delta^{18}O_{NO3}$ (‰), c) concentration NO_3^- (µM); and d) concentration Cl^- (mg/L).

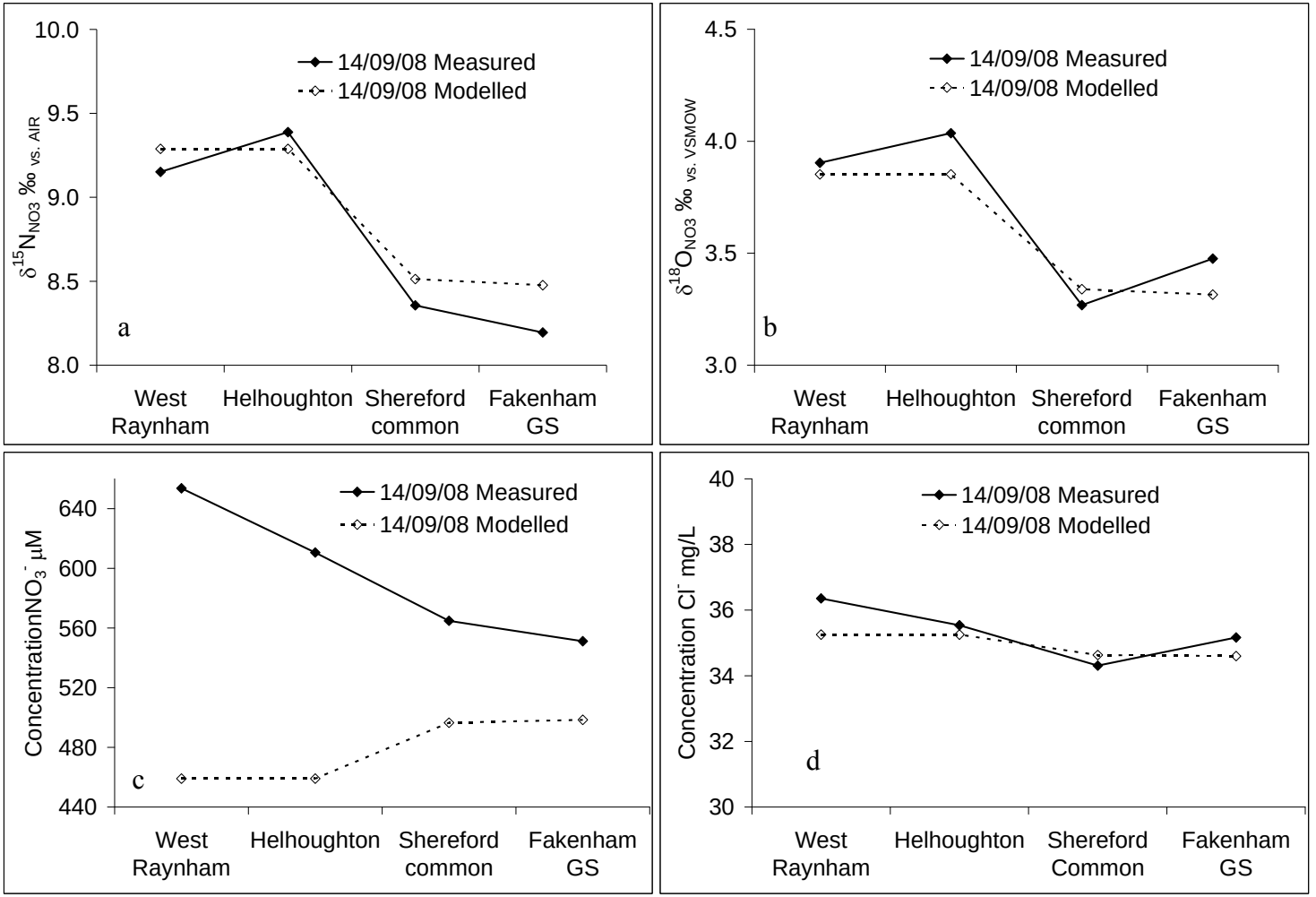

Figure A3.3a-d Model outputs from upper Wensum mixing model for data set C: 14/09/2008 showing measured and modelled values of: a) $\delta^{15}N_{NO3}$ (‰); b) $\delta^{18}O_{NO3}$ (‰); c) concentration NO_3^- (µM); and d) concentration Cl^- (mg/L).

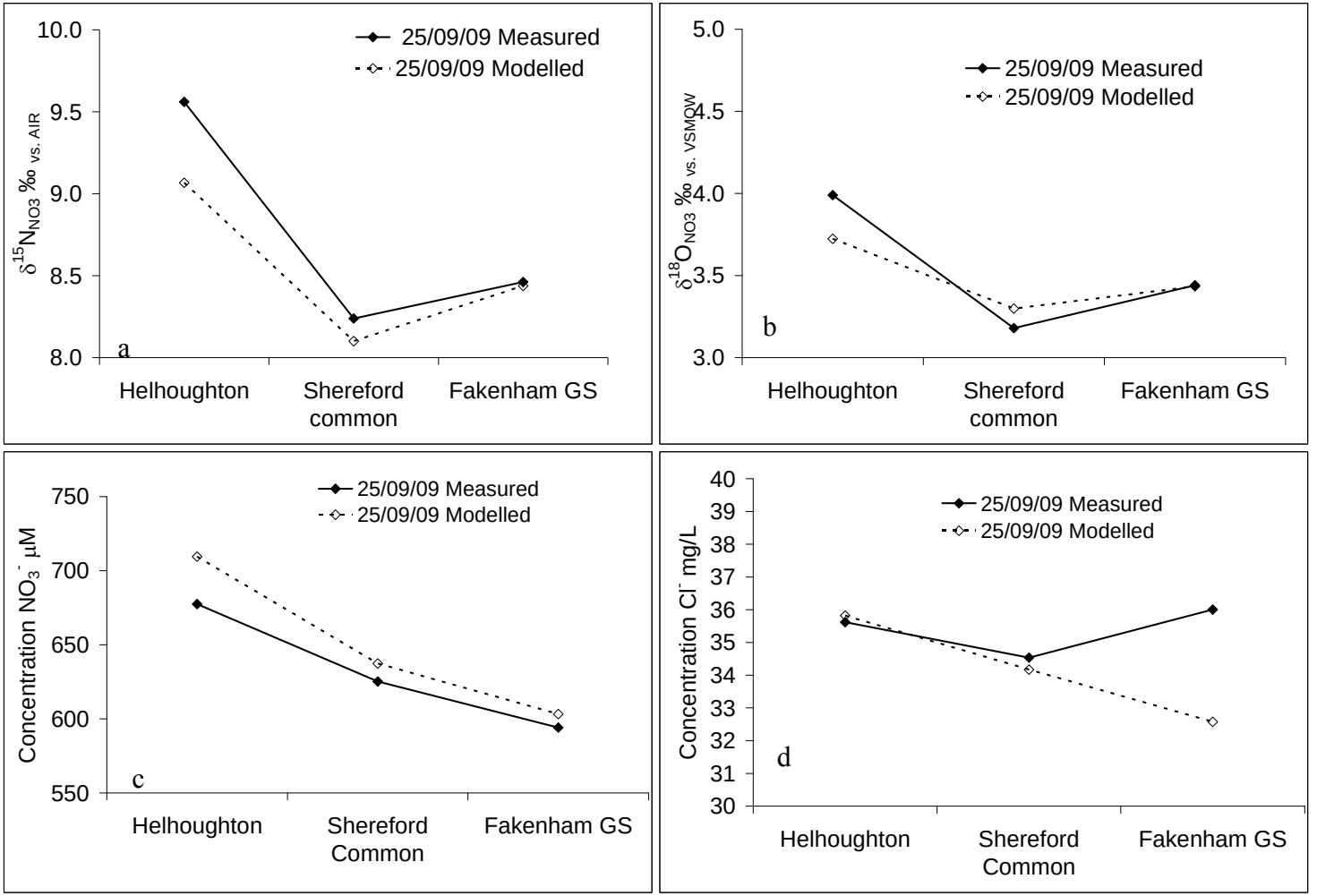

Figure A3.4a-d Model outputs from upper Wensum mixing model for data sets D: 25/09/2009, showing measured and modelled values of: a) $\delta^{15}N_{NO3}$ (‰); b) $\delta^{18}O_{NO3}$ (‰); c) concentration NO_3^- (µM); and d) concentration Cl^- (mg/L).

A3.6 Upper Wensum Two-Member Model Concentration Variations:
Concentration variations used in two member mass balance mixing model to represent measured data from the upper Wensum.

Data set and location	Fluvial deposits end member concentration NO_3^- (μM)	Fluvial deposits end member concentration Cl^- (mg/L)
06/04/2008		
Hamrow	640 (measured)	44.9 (measured)
West Raynham	710	49.8
Helhoughton	645	45.3
Shereford Common	700	49.1
Fakenham GS	640	44.9
14/02/2007		
Hamrow	694 (measured)	43.3 (measured)
West Raynham	750	46.1
Helhoughton	694	42.0
Fakenham GS	640	39.2
18/07/2007		
Hamrow	591 (measured)	32.5 (measured)
West Raynham	570	32.3
Helhoughton	570	32.3
Fakenham GS	220	28.5
14/09/2008		
Hamrow	298 (measured)	37.9 (measured)
West Raynham	298	35.3
Helhoughton	298	35.3
Shereford Common	298	34.6
Fakenham GS	298	34.6
25/09/2009		
West Raynham	722 (measured)	36.1 (measured)
Helhoughton	720	35.8
Shereford Common	720	34.2
Fakenham GS	600	32.6

A.3.7 Upper Wensum Solute Model Output at Fakenham:

Model output data at Fakenham for solute concentrations using two and three member mass-balance mixing model of upper Wensum:

The following equation was used:

$$C_{mixed} = \frac{(C_a \times v_a)+(C_b \times v_b)+(C_c \times v_c)}{(C_a + C_b + v_c)}$$

Sampling date		**14/02/2007**	**18/07/2007**	**06/04/2008**	**14/09/2008**	**25/09/2009**
2 member ratios Tat: Hamrow		1.1:1	1.1:1	2.1:1	2.8:1	0.9:1
3 member ratios Tat: Interfluve: Hamrow		1.1:0.6:1	1.1:0.6:1	2.1:0.6:1	2.8:0.6:1	0.9:0.6:1
Fakenham 2 member model	*NO_3^- µM*	*663*	*583*	*637*	*420*	*666*
Fakenham 3 member model		*526*	*462*	*541*	*367*	*517*
Fakenham measured		618	456	640	551	594
Fakenham 2 member model	*SO_4^{2-} mg/L*	*30.4*	*22.7*	*31.7*	*28.9*	*35.3*
Fakenham 3 member model		*26.0*	*19.9*	*28.3*	*26.4*	*29.4*
Fakenham measured		33.2	26.0	32.9	32.7	34.1
Fakenham 2 member model	*Cl^- mg/L*	*40.9*	*33.3*	*37.9*	*34.6*	*34.5*
Fakenham 3 member model		*36.0*	*30.0*	*34.7*	*32.4*	*30.6*
Fakenham measured		36.0	31.7	36.4	35.2	36.0
Fakenham 2 member model	*Na^+ mg/L*	*19.4*	*19.9*	*20.4*	*18.2*	not analysed
Fakenham 3 member model		*17.8*	*18.2*	*19.1*	*17.4*	not analysed
Fakenham measured		17.7	18.1	19.2	17.4	not analysed
Fakenham 2 member model	*K^+ mg/L*	*3.3*	*1.6*	*1.4*	*1.4*	not analysed
Fakenham 3 member model		*2.7*	*1.4*	*1.2*	*1.3*	not analysed
Fakenham measured		3.3	2.2	1.5	1.5	not analysed
Fakenham 2 member model	*Mn^{2+} µg/L*	*0.12*	*0.17*	*0.13*	*0.13*	not analysed
Fakenham 3 member model		*0.20*	*0.25*	*0.20*	*0.18*	not analysed
Fakenham measured		0.14	0.11	0.19	0.09	not analysed

A3.8 $\delta^{15}N_{NO3}$ Versus the Natural Log and Reciprocal of Concentration:

r^2 Values for $\delta^{15}N_{NO3}$ versus the natural log of nitrate concentration and the reciprocal of concentration calculated for each data set for the five sampling locations between the Wensum gauging stations at Fakenham and Swanton.

Sampling date	**$\delta^{15}N_{NO3}$ (‰) vs. ln concentration NO_3^- (μM) linear regression r^2 values**	**$\delta^{15}N_{NO3}$ (‰) vs. 1/ concentration NO_3^- (μM) linear regression r^2 values**
14/02/2007	0.86	0.89
18/07/2007	0.81	0.80
06/04/2008	0.86	0.84
14/09/2008	0.88	0.91
16/11/2008	0.84	0.85
25/09/2009	0.91	0.91

A3.9 Wensum Mid River Mean Solute Model End Members:

Model end members for Wensum mid river mean solute and isotopic four member mass-balance mixing model:

Solute	Measured concentrations Swanton GS	Modelled concentrations Swanton GS	End member measured concentrations	Fakenham GS	Tributaries and drains	Interfluve groundwater	Valley groundwater no denitrification	Valley groundwater with denitrification (Swanton)
NO_3^-	395	395* (516#)	NO_3^-	564	372	0	973	550
Cl^-	38.9	38.8	Cl^-	35.0	45.0	19.5	54.8	54.8
SO_4^{2-}	38.4	38.3	SO_4^{2-}	32.2	47.8	13.6	59.2	59.2
Na^+	24.2	22.2	Na^+	18.0	24.7	12.6	33.1	33.1
$\delta^{15}N_{NO3}$ (‰)	10.7	10.7*	$\delta^{15}N_{NO3}$ (‰)	8.4	10.3	-	6.7	13.5
$\delta^{18}O_{NO3}$ (‰)	4.8	4.8*	$\delta^{18}O_{NO3}$ (‰)	3..5	4.9	-	1.2	6.2
$\delta^{15}N_{NO3}$ (‰)		7.7#						
$\delta^{18}O_{NO3}$ (‰)		2.4#						
* Using denitrified valley groundwater end member			Contribution to flow					
# Using measured valley groundwater end member			increase $m^3 s^{-1}$	1.05	0.59	0.80	0.97	0.97
Flow increase by Swanton GS $m^3 s^{-1}$			2.36					
Total flow by Swanton GS $m^3 s^{-1}$			3.41					
Baseflow index			0.75					
Proportion of valley to interfluve baseflow			0.55:0.45					

A3.10 Wensum Mid River Low-Flow Mean Solute Model End Members:

Model end members for Wensum mid river low-flow mean solute and isotopic four member mass-balance mixing model:

Solute	Measured concentrations Swanton GS	Modelled concentrations Swanton GS	End member measured concentrations	Fakenham GS	Tributaries and drains	Interfluve groundwater	Valley groundwater no denitrification	Valley groundwater with denitrification (Swanton)
NO_3^-	412	412* (562#)	NO_3^-	550	372	0	973	527
Cl^-	42.8	43.0	Cl^-	42.8	45.0	19.5	54.8	54.8
SO_4^{2-}	47.2	45.2	SO_4^{2-}	47.2	47.8	13.6	59.2	59.2
Na^+	25.8	25.7	Na^+	25.8	24.7	12.6	33.1	33.1
$\delta^{15}N_{NO3}$ (‰)	11.10	11.09*	$\delta^{15}N_{NO3}$ (‰)	8.0	10.3	-	6.7	14.3
$\delta^{18}O_{NO3}$ (‰)	4.63	4.64*	$\delta^{18}O_{NO3}$ (‰)	3.4	4.9	-	1.2	5.8
$\delta^{15}N_{NO3}$ (‰)		7.5#						
$\delta^{18}O_{NO3}$ (‰)		2.3#	Contribution to flow					
* Using denitrified valley groundwater end member # Using measured valley groundwater end member			increase $m^3 s^{-1}$	0.63	0.35	0.69	0.37	0.37
Flow increase by Swanton GS $m^3 s^{-1}$			1.42					
Total flow by Swanton GS $m^3 s^{-1}$			2.05					
Baseflow index			0.75					
Proportion of valley to interfluve baseflow			0.65:0.35					

A3.11 Mean Nitrate-Nitrogen Load Reduction and Denitrification:
Rates calculated using mean data set:

Measured nitrate concentrations Swanton GS: 395 μM NO_3^-

Predicted nitrate concentration Swanton GS using above model with measured valley groundwater (no denitrification component), using end member flow contribution and nitrate concentration from mean run model end member table above and denoted by subscripts:

Predicted nitrate concentration Swanton GS =
$((564_{FGS} \times 1.05 \times 1000) + (372_{TD} \times 0.59 \times 1000) + (973_{VGW} \times 0.97 \times 1000) + (0_{IFGW} \times 0.80 \times 1000) /((1.05 \times 1000) + (0.59 \times 1000) + (0.97 \times 1000) + (0.80 \times 1000)) = 516$ μM NO_3^-

Predicted mean daily nitrate load Swanton GS = (((516 / 1000000) x (3.41 x 1000 x 60 x 60 x 24)) x 14.01)/ 1000 = 2130 kg NO3-N/day
Measured low-flow daily nitrate load Swanton GS = (((395 / 1000000) x (3.41 x 1000 x 60 x 60 x 24)) x 14.01)/ 1000 = 1631 kg NO3-N/day

Nitrate-nitrogen load reduction = 2130 - 1631 = 499 kg NO3-N/day

NO3-N removal rate per m^3 hyporheic sediment volume = (499/ (25 x 1000 x 9 x 2.5)) x 1000000 / 24 = 37.0 mg/m^3/hour
NO3-N removal rate per m^2 riverbed surface = (499/ ((25 x 1000 x 9)+(2 x (25 x 1000 x 0.5)))) x 1000000 / 24 = 83.2 mg/m^2/hour

Based on 75%:25% apportionment:
NO3-N removal rate per m^3 hyporheic sediment volume = (374.25/ (25 x 1000 x 9 x 2.5)) x 1000000 / 24 = 27.8 mg/m^3/hour
NO3-N removal rate per m^2 riverbed surface = (124.75/ ((25 x 1000 x 9)+(2 x (25 x 1000 x 0.5)))) x 1000000 / 24 = 20.8 mg/m^2/hour

A3.12 Low-Flow Mean Nitrate-Nitrogen Load Reduction and Denitrification:
Rates calculated using low-flow mean data set:

Measured nitrate concentrations Swanton GS: 412 μM NO_3^-

Predicted nitrate concentration Swanton GS using above model with measured valley groundwater (no denitrification component), using end member flow contribution and nitrate concentration from mean run model end member table above and denoted by subscripts:

Predicted nitrate concentration Swanton GS =
$((550_{FGS} \times 0.63 \times 1000) + (372_{TD} \times 0.35 \times 1000) + (973_{VGW} \times 0.69 \times 1000) + (0.37_{IFGW} \times 1000)) / ((0.63 \times 1000) + (0.35 \times 1000) + (0.69 \times 1000) + (0.37 \times 1000))$
= 562 μM NO_3^-

Predicted low-flow daily nitrate load Swanton GS = (((562 / 1000000) x (2.05 x 1000 x 60 x 60 x 24)) x 14.01)/ 1000 = 1393 kg NO3-N/day

Measured low-flow daily nitrate load Swanton GS = (((412 / 1000000) x (2.05 x 1000 x 60 x 60 x 24)) x 14.01)/ 1000 = 1021 kg NO3-N/day

Nitrate-nitrogen load reduction = 1393 - 1021 = 372 kg NO3-N/day

NO3-N removal rate per m^3 hyporheic sediment volume = (372/ (25 x 1000 x 9 x 2.5)) x 1000000 / 24 = 27.6 mg/m^3/hour
NO3-N removal rate per m^2 riverbed surface = (372/ ((25 x 1000 x 9)+(2 x (25 x 1000 x 0.5)))) x 1000000 / 24 = 62.0 mg/m^2/hour

Based on 75%:25% apportionment:
NO3-N removal rate per m^3 hyporheic sediment volume = (279/ (25 x 1000 x 9 x 2.5)) x 1000000 / 24 = 20.7 mg/m^3/hour
NO3-N removal rate per m^2 riverbed surface = (93/ ((25 x 1000 x 9)+(2 x (25 x 1000 x 0.5)))) x 1000000 / 24 = 15.5 mg/m^2/hour

A3.13 Concentrations of Chloride, Sulphate and Sodium with Flow Condition:
Swanton and Costessey Gauging Stations for individual data sets:

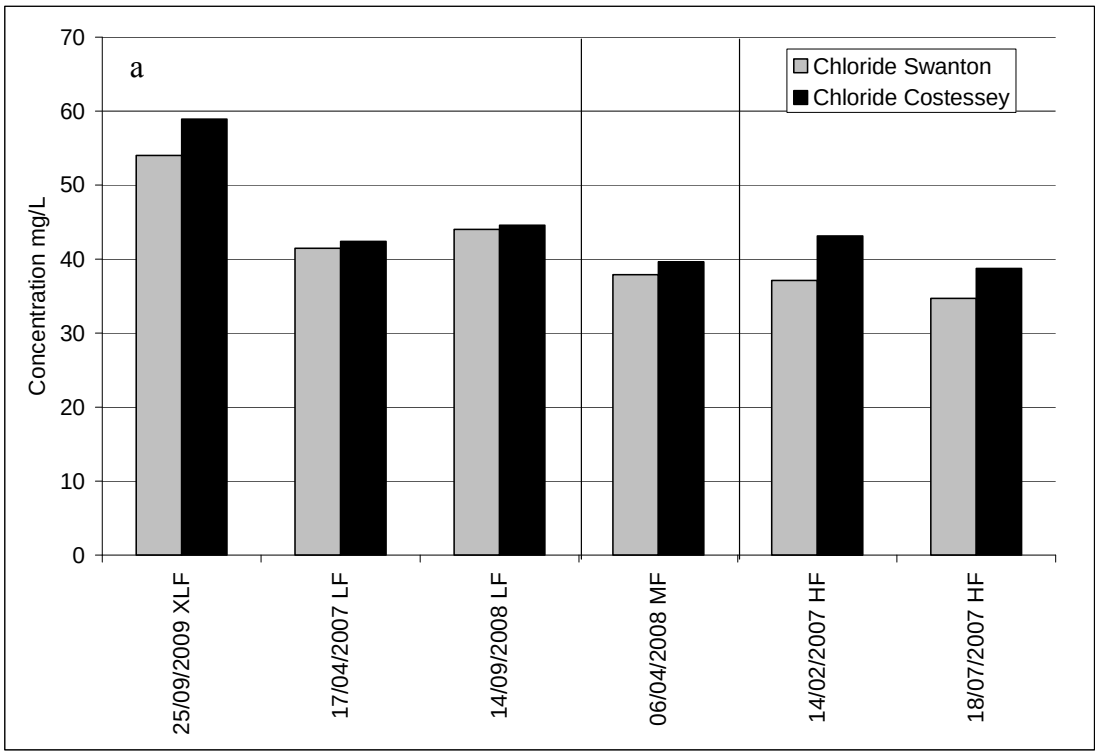

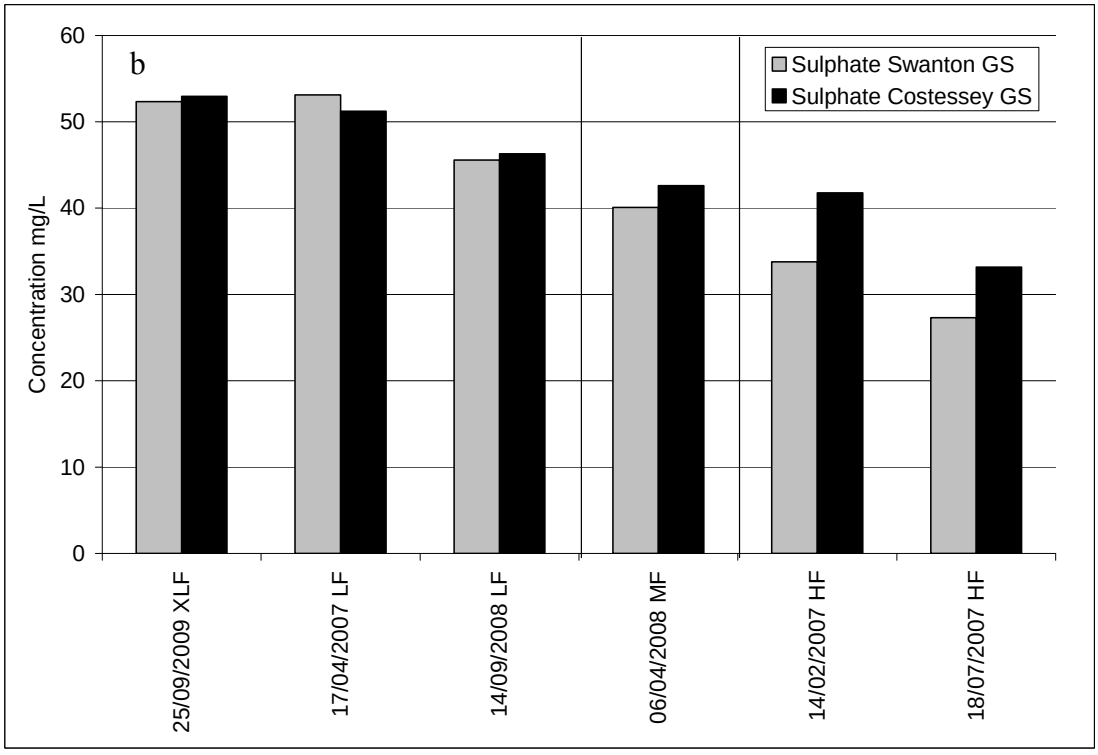

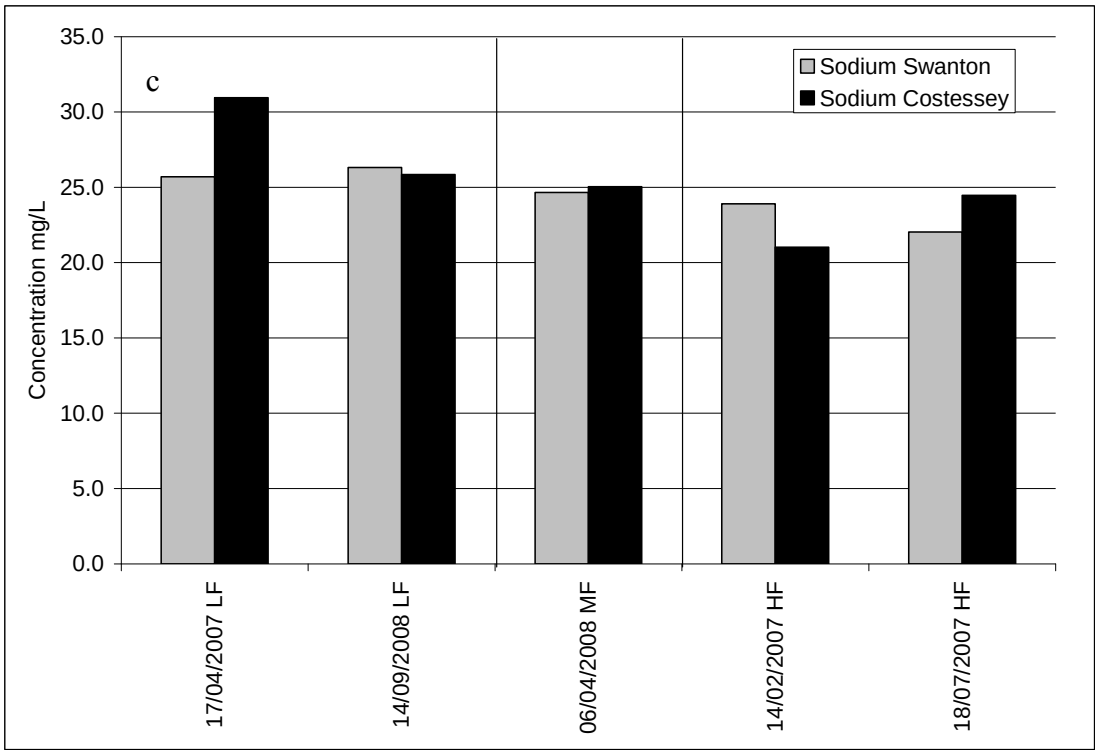

Figure A3.5a-c Concentrations of chloride, sulphate and sodium (mg/L) at Swanton and Costessey gauging stations for individual data sets showing flow condition.

A3.14 Wensum Lower River Mean Solute Model End Members:

Model end members for Wensum mid river mean solute and isotopic four member mass-balance mixing model:

Solute	Measured concentrations Costessey GS	Modelled concentrations Costessey GS	End member measured concentrations	Swanton GS	Tributaries and drains	Interfluve groundwater	Valley groundwater no denitrification	Valley groundwater with denitrification (Costessey)
NO_3^-	384	384	NO_3^-	399	400	0	973	360
Cl^-	44.0	43.8	Cl^-	40.7	39.7	19.5	54.8	54.8
SO_4^{2-}	44.1	44.8	SO_4^{2-}	40.1	43.9	13.6	59.2	59.2
Na^+	25.5	26.2	Na^+	24.4	22.4	12.6	33.1	33.1
$\delta^{15}N_{NO3}$ (‰)	11.15	11.15*	$\delta^{15}N_{NO3}$ (‰)	10.97	10.47	-	6.7	11.95
$\delta^{18}O_{NO3}$ (‰)	4.76	4.76*	$\delta^{18}O_{NO3}$ (‰)	4.77	4.83	-	1.2	4.70
* Using denitrified valley groundwater end member			Contribution to flow increase $m^3 s^{-1}$	3.62	0.52	0.07	1.40	1.40
Flow increase by Costessey GS $m^3 s^{-1}$			1.99					
Total flow by Costessey GS $m^3 s^{-1}$			5.61					
Baseflow index			0.74					
Proportion of valley to interfluve baseflow			0.95:0.05					

A3.15 Wensum Lower River Low-Flow Mean Solute Model End Members:

Model end members for Wensum mid river low-flow mean solute and isotopic four member mass-balance mixing model:

Solute	Measured concentrations Costessey GS	Modelled concentrations Costessey GS	End member measured concentrations	Swanton GS	Tributaries and drains	Interfluve groundwater	Valley groundwater no denitrification	Valley groundwater with denitrification (Costessey)
NO_3^-	372	372	NO_3^-	414	400	0	973	355
Cl^-	43.5	43.3	Cl^-	42.7	39.7	19.5	54.8	54.8
SO_4^{2-}	48.8	48.4	SO_4^{2-}	49.3	43.9	13.6	59.2	59.2
Na^+	28.4	26.2	Na^+	26.0	22.4	12.6	33.1	33.1
$\delta^{15}N_{NO3}$ (‰)	11.24	11.24*	$\delta^{15}N_{NO3}$ (‰)	11.21	10.47	-	6.7	11.75
$\delta^{18}O_{NO3}$ (‰)	4.61	4.61*	$\delta^{18}O_{NO3}$ (‰)	4.51	4.83	-	1.2	4.85
* Using denitrified valley groundwater end member			Contribution to flow increase $m^3 s^{-1}$	2.08	0.32	0.23	0.68	0.68
Flow increase by Costessey GS $m^3 s^{-1}$			0.90					
Total flow by Costessey GS $m^3 s^{-1}$			3.30					
Baseflow index			0.74					
Proportion of valley to interfluve baseflow			0.75:0.25					

A3.16 Lower Wensum Isotope Mass Balance Mixing Model:

Isotope mass balance four member mixing model output for the lower Wensum river mean model run:

The model was run using a valley groundwater end member nitrate concentration of 360 μM, with an isotopic composition of $\delta^{15}N_{NO3}$ 12.0 ‰; $\delta^{18}O_{NO3}$ 4.7 ‰, and an incremental adjustment in the isotopic composition of the valley groundwater end member shown in the table.

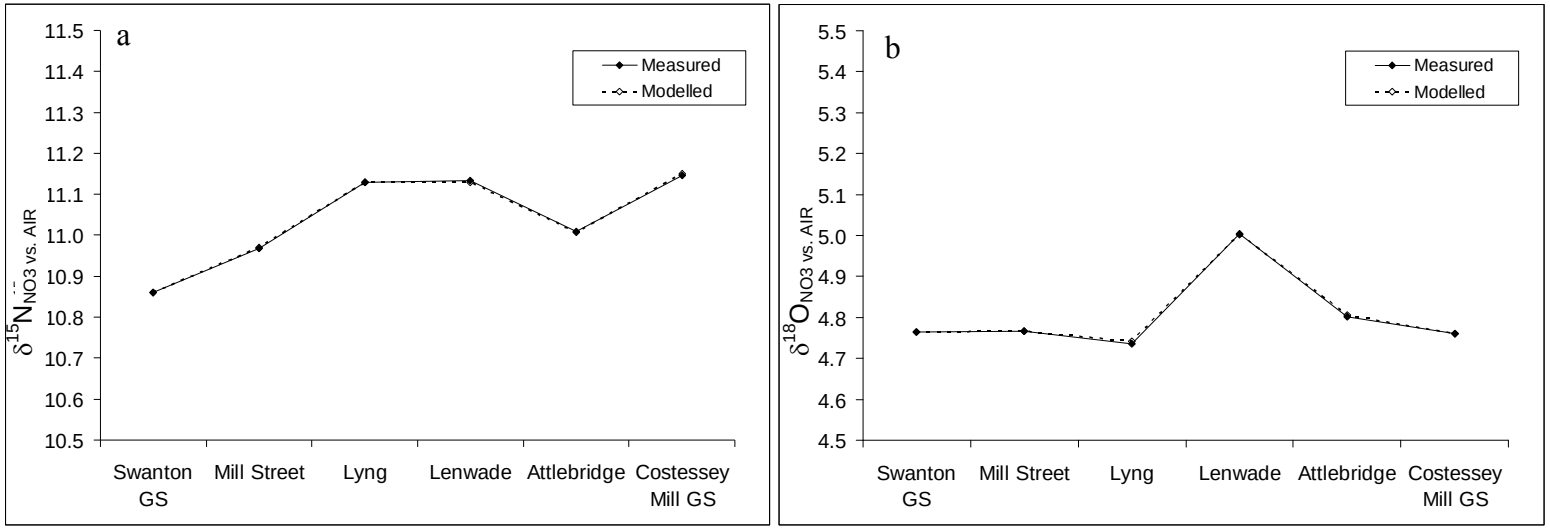

Figure A3.6a and b Isotope mass balance four member mixing model output for $^{15}N_{NO3}$ (‰) and $\delta^{18}O_{NO3}$ (‰) for the lower Wensum river mean model run

		$\delta^{15}N_{NO3}$ (‰) vs. AIR	$\delta^{18}O_{NO3}$ (‰) vs. VSMOW
Isotopic composition of valley groundwater end member used at each lower river location:	Mill Street	11.00	4.77
	Lyng	11.30	4.40
	Lenwade	11.30	4.90
	Attlebridge	11.10	4.90
	Costessey Mill GS	11.95	4.70